

Elseragy, Ahmed A.B. (2004) Architectural and solar potential of curved and flat roofs in hot arid regions (with reference to Egypt). PhD thesis, University of Nottingham.

Access from the University of Nottingham repository:

<http://eprints.nottingham.ac.uk/12383/1/404052.pdf>

Copyright and reuse:

The Nottingham ePrints service makes this work by researchers of the University of Nottingham available open access under the following conditions.

This article is made available under the University of Nottingham End User licence and may be reused according to the conditions of the licence. For more details see:
http://eprints.nottingham.ac.uk/end_user_agreement.pdf

A note on versions:

The version presented here may differ from the published version or from the version of record. If you wish to cite this item you are advised to consult the publisher's version. Please see the repository url above for details on accessing the published version and note that access may require a subscription.

For more information, please contact eprints@nottingham.ac.uk

The University of Nottingham
School of The Built Environment
Institute of Building Technology
Sustainable Architectural Environments



The University of
Nottingham

**ARCHITECTURAL AND SOLAR POTENTIAL
OF CURVED AND FLAT ROOFS
IN HOT ARID REGIONS**
(With Reference To Egypt)



By

Ahmed A. B. ELSERAGY
BSc., MSc. in Architecture

**Thesis Submitted to the University of Nottingham for the Degree of
DOCTOR OF PHILOSOPHY**

December 2003
Nottingham, United Kingdom

**The Best introduction to this work is the first five
verses revealed of the Glorious Quran:**

“Read in the name of thy Lord who created
Created man out of a clot of congealed blood*
Read! And thy Lord is Most Bountiful*
He Who taught (the use of) the Pen*
Taught man that which he knew not.”*

Verses 1-5, Chapter 96

*To My Mother & Father,
To Amira & Farida; My Wife & Daughter
With my Gratitude for all their Support
That Made me Succeed*

THE AUTHOR

The author has graduated from Alexandria University – Egypt, where he got his B.Sc. (*Hons*) in Architecture and Architectural Engineering, in 1993. The author then got his M.Sc. in Environmental studies and Architecture from the same University in 1997. In 1996, the author has been appointed to work as Assistant-Lecturer in the Department of Architectural Engineering and Environmental Design - Arab Academy for Science and Technology (AAST) www.aast.edu. The AAST has offered the author a partial scholarship to carry out his Doctoral Degree in the United Kingdom (the University of Nottingham – the School of the Built Environment). The author is a licensed architect since 1993. He is also a working member of The Egyptian Architectural Engineers Syndicate (EES) since July 1993. Different research interests of the author including the research project presented in this thesis have been disseminated through number of publications (*Bibliography*). A Number of online articles and links have depicted the author and his research work;

- **Tilting at windmills, Al-Ahram Weekly Online, 28 March - 3 April 2002, Issue No.579**
<http://www.ahram.org.eg/weekly/2002/579/economy.htm>
- **The Perfect Curve, ArchNet Online, News - 9 May 2002,**
http://archnet.org/news/view.tcl?news_id=2622
- http://archnet.org/shared/community-member.tcl?user_id=5254
- <http://www.nottingham.ac.uk/sbe/research/projects/c35.htm>

ACKNOWLEDGMENTS

Firstly, I would like to gratefully acknowledge the effort of my supervisor Dr. M. Gadi, who has been an endless source of motivation and advice, and from whom I have learnt a great deal of experience throughout the progress of this research. During the crucial period of writing up he whole-heartedly supported me. I wish to thank him not only for reading and correcting errors in earlier drafts, but also for the valuable suggestions on my entire work, and especially for all the efforts he exerted during the submission period of this thesis.

I wish also to thank and express my deep gratitude to *The Arab Academy for Science and Technology (AAST)*, www.aast.edu, for supporting my living expenses during the period of my PhD study in the UK, and also to the School of the Built Environment and the International Office at the University of Nottingham for awarding me a partial tuition fees scholarship.

I am deeply indebted to Amira, my wife and colleague, for her sincere moral support. She constructively supported me throughout my studies and in the editing and sewing of this thesis. Doubtlessly, I could not have survived the period of my study without her patient support. I cannot thank her adequately enough for all her love, help and support; her role throughout this period cannot be expressed in words.

I would like to address my great appreciations to my father for his continuous encouragement, help, advice and financial-support. All thanks and respects go to my mother for her moral support and love; her phone calls from Egypt have relieved hard-times and have produced motivation and enthusiasm. They both have shown great understanding, patience and support during the course of my PhD study, without which I could not have approached my aim. I hope that I would be able to repay them some of their favors and to fulfill my obligations towards them. Special thanks go to Lamya, my sister, and all my family who gave me every possible support and help.

I have to acknowledge that without the love of my daughter Farida, and her continuous unintentional encouragements for me to finish my PhD in time and have my “big exam” to “be doctor” and “to be good boy” as she says. I hope that my daughter and my wife would forgive that I was not able to fulfill all my obligations towards them during this period.

Thanks are due to Professor J. Chilton, Head of School of Architecture, University of Lincoln, for his continuous encouragement, unlimited support and assistance throughout my stay in the UK. He has always been of great help to my family and me, for which I whole-heartedly appreciate. Finally, I wish to express my sincere thanks and gratitude to Professor S. B. Riffat, Head of School of the Built Environment, University of Nottingham, for his invaluable help, encouragement and guidance.

Ahmed Elseragy.....

ABSTRACT

This thesis investigates the effect of various vaulted and domed roof geometries on their solar behaviour under given summer and winter conditions. Roof is the building-envelope element that is most exposed to the sun as it receives a high amount of solar radiation, which is the main cause of summer overheating in hot-arid climates. In addition, to other climatic and physical factors, indoor thermal comfort in hot-arid climates is also influenced by the intensity of solar radiation received by roof surfaces. Therefore, roof form and geometry should be designed with careful consideration to insolation parameters. Domed, vaulted, and curved roofs have been used for a long time in hot-arid regions for historical, cultural, climatic, and structural reasons. The review of previous research work showed that different explanations have been given to the climatic effects of their forms and the environmental behaviour of their enclosed spaces.

The research explores the previous attempts that discussed the relevant principles of solar radiation and solar geometry on horizontal and tilted surfaces with different orientations. The previous work that applied these principles and theories to evaluate the solar behaviour of architectural elements with arbitrary forms was also investigated. In order to evaluate the solar performance of flat and curved roofs geometrical configurations, a parametric study testing the received solar radiation intensity (W/m^2) on flat, vaulted, and domed roofs with different span-to-height ratios and orientations was carried out using a published solar computer model. The results of this model were followed by validation tests using other two commercially available computer tools to carry out a brief solar and thermal analysis of selected curved-roof geometries. The evaluated curved-roofs solar performance and main findings of the present research have been compared with recently published independent research.

It is believed that this research establishes a sound theoretical basis for the validity of various claims of the climatic advantages of different curved-roof forms in hot-arid regions. As part of this research outcome, solar and architectural design-guidelines for curved-roofs are introduced. The research concludes with a discussion of the architectural and solar potential of curved-roof forms, which is believed to be novel contribution to the knowledge and the understanding of curved-roofs solar behaviour and architectural applications in hot-arid climates.

THESIS CONTENTS *(List of Main Chapters)*

Chapter 1.
Introduction

Chapter 2.
Energy Resources and Indoor Thermal Comfort in Hot Arid Climates
(With Reference To Egypt)

Chapter 3.
Traditional and Modern Passive Cooling Techniques in Hot Arid Regions

Chapter 4.
Energy Conscious Roof Design in Hot-Arid Climates

Chapter 5.
Solar Radiation on Different Surface Geometries

Chapter 6.
Solar Behaviour of Flat and Semicircular Vaulted Roofs with Different Orientations

Chapter 7.
Solar Behaviour of Flat and Vaulted Roofs with Different Curvatures and Orientations

Chapter 8.
Solar Behaviour of Flat and Domed Roofs with Different Curvatures

Chapter 9.
Conclusions, Validation and Further Developments

THESIS CONTENTS (Full List of Chapters and Sections)

ACKNOWLEDGEMENTS.....	i
ABSTRACT.....	ii
THESIS CONTENTS (List of Main Chapters).....	iii
THESIS CONTENTS (Full List of Chapters and Sections).....	iv
LIST OF FIGURES.....	ix
LIST OF TABLES.....	xviii
ABBREVIATIONS.....	xix
NOMENCLATURE.....	xx
CHAPTER 1: INTRODUCTION.....	1
1.1 RESEARCH PROBLEM	1
1.2. RESEARCH AIMS	3
1.3. EMPIRICAL RESEARCH METHODOLOGY	4
1.4. OUTLINE OF THE THESIS.....	5
1.5 CONCLUSIONS.....	6
REFERENCE LIST.....	8
CHAPTER 2: ENERGY RESOURCES AND INDOOR THERMAL COMFORT IN HOT-ARID CLIMATES (with reference to Egypt).....	9
2.1 ENERGY, NATURAL RESOURCES AND POPULATION GROWTH.....	12
2.1.1 World's Population Growth and Energy Consumption Rates.....	13
2.1.2 African Continent Population Growth and Energy-Consumption Rates.....	14
2.1.3 Egypt Population Growth and Energy-Consumption Rates	14
2.2 ENERGY EFFICIENT BUILDINGS AND SUSTAINABILITY.....	16
2.2.1 Global Environmental Impact From Current Energy Use.....	18
2.2.2 Sustainability in Architecture and Buildings.....	20
2.2.3 Climate Conscious Design in Sustainable Buildings.....	21
2.2.4 BIOCLIMATIC Architecture.....	23
2.3 CLIMATIC DESIGN AND INDOOR THERMAL COMFORT.....	24
2.3.1 Hot-Arid Zones; Climatic Characteristics & Geographical Locations.....	26
2.3.1.1 African Continent Climatic Regions & The Selected Hot-Arid Zone.....	27
2.3.1.2 Egypt Climate & Geography.....	28
2.3.1.4 Egypt Geographic and Climatic Classifications.....	30
2.3.2 Indoor Thermal Comfort And Human Requirements.....	34
2.3.2.1 The Main Factors and Variables Affecting Indoor Thermal Comfort.....	35
2.3.2.2 The Thermal Body's Balance.....	36
2.3.2.3 The Bio-Climatic Chart and The Comfort Zone	38
2.4 CONCLUSION.....	40
REFERENCE LIST.....	42
CHAPTER 3: TRADITIONAL AND MODERN PASSIVE COOLING TECHNIQUES IN HOT ARID REGIONS.....	44
3.1 PRINCIPLES OF PASSIVE COOLING TECHNIQUES IN BUILDINGS.....	45
3.1.1 Cooling by Ventilation.....	45
3.1.2 Cooling by Dehumidification.....	46
3.1.3 Cooling by Evaporation.....	46
3.1.4 Cooling By Convection and Conduction Heat Loss	46
3.1.4.1 Cooling by Radiation.....	47
3.1.4.2 Mass-effect Cooling.....	47

3.2 TRADITIONAL PASSIVE COOLING TECHNIQUES AND MATERIALS.....	48
3.2.1 Preliminary Investigations and Historical Overview.....	48
3.2.1.1 Ancient Passive Cooling Techniques (<i>Egyptian & Mesopotamian Civilisations</i>)..	49
3.2.1.2 Exemplary Techniques of Traditional Passive Cooling in Hot Regions...	51
3.2.2 Traditional Passive Cooling Techniques in Contemporary Architecture.....	63
3.2.2.1 TUWAIQ Palace, Riyadh, Saudi Arabia, 1985.....	64
3.2.2.2 KASR ALHOKM; Justice Palace & Mosque, Riyadh, Saudi Arabia.....	66
3.2.2.3 National Commercial Bank, Jeddah, Saudi Arabia, 1982-84.....	68
3.3 CONCLUSIONS.....	71
REFERENCE LIST.....	73

CHAPTER 4: ENERGY CONSCIOUS ROOF DESIGN IN HOT-ARID CLIMATES.....75

4.1 CLIMATE AND BUILDING DESIGN.....	76
4.1.1 Roof Design in Hot-arid Climates.....	76
4.1.2 Thermal Performance of Roofs Form and Geometry.....	77
4.1.3 Roofing Construction Materials.....	79
4.2 TRADITIONAL CURVED ROOFS CONSTRUCTIONS (Vaults and Domes)	79
4.2.1 Curved Roofs Geometrical Forms and Types.....	80
4.2.2 Curved Roofs Construction Technologies and Materials.....	82
4.2.2.1 Curved Roofs, Vaults, and Domes Construction Materials.....	82
4.2.2.2 Woodless Construction Techniques (<i>Vaulted and Domed Mud Constructions</i>).....	82
4.2.2.3 Nubian Vaults and Domes.....	85
4.2.2.4 Afghan and Persian Domes.....	92
4.3 REINTRODUCING TRADITIONAL CURVED ROOFS.....	93
4.3.1 Persuasive Introduction and Successive Publicity.....	93
4.3.2 Training And Practical Skills Development Programs.....	94
4.3.3 Technical Future Update and Training for Architects and Building Designers.....	95
4.4 REVITALISATION OF TRADITIONAL CURVED ROOFS.....	96
4.4.1 Hassan Fathy And Other Egyptian Architects.....	97
4.4.1.1 Hassan Fathy Architectural Philosophies, Efforts, and Attempts.....	97
4.4.1.2 Hassan Fathy Development Housing Projects.....	98
4.4.1.3 Hassan Fathy Residential Designs.....	102
4.4.1.4 Ramses Wissa Wassef (1911 – 1974)	105
4.4.1.5 Abdel Wahid El-Wakil.....	107
4.4.2 Other Regional Architects Works.....	109
4.4.3 Socio-cultural and Technical Development Workshops.....	110
4.4.3.1 ADAUA Organisation and Two Successful Projects in Africa.....	110
4.4.3.2 The Agricultural Training Centre.....	113
4.4.4 Research and Development Projects.....	114
4.5 CONCLUSIONS.....	116
REFERENCE LIST.....	118

CHAPTER 5: SOLAR RADIATION ON DIFFERENT SURFACE GEOMETRIES 120

5.1 SOLAR AND ARCHITECTURAL DESIGN.....	120
5.1.1 Solar Radiation and Earth Thermal Balance	122
5.1.2 Solar Geometry.....	123
5.1.2.1 Earth-Sun Geometrical Relationships.....	123
5.1.2.2 Sun Path and Position	125
5.2 ESTIMATION OF SOLAR RADIATION INTENSITY ON HORIZONTAL AND OBLIQUE SURFACES.....	127
5.2.1 Solar Radiation Intensity and Geographical Latitudes.....	128
5.2.2 Solar Radiation Intensity and Recipient Surface Geometry (Solar Geometry of Sloped Surfaces).....	131
5.2.3 Ratio of Beam Radiation on Tilted Surface to that on Horizontal Surface...133	
5.2.4 Solar Radiation on Sloping Surfaces and on Curved Forms.....	134

5.2.5 Previous Applications of Sloped Solar Irradiance On Curved Forms	135
5.2.5.1 Irradiation on an Inclined Planar Surface (Skylight Domes)	135
5.2.5.2 Geometric Forms and Insolation Compared with Horizontal Surfaces.....	137
5.3 DESCRIPTION OF THE SOLAR RADIATION SIMULATION MODEL SRSM.....	139
5.4 CALCULATION OF THE EXTERNAL SURFACE SOLAR RADIATION.....	143
5.4.1 The Orientation of Curved Roof and Solar Radiation Intensity.....	143
5.4.1.1 The Curved Roof Curvature Faces North and South Directions (Extended CCS - Vaulted Roof).....	146
5.4.1.2 The Curved Roof Curvature Faces East and West Directions.....	147
5.4.2 The Geometrical Resemblance of Curved Roofs.....	148
5.4.2.1 Definition of Curved-roof Curvature.....	149
5.4.3 Calculating <i>The Total Received Solar Radiation Intensity (W/m^2)</i> on a CCS	153
5.5 CONCLUSIONS.....	154
REFERENCE LIST.....	157

CHAPTER 6: SOLAR BEHAVIOUR OF FLAT AND SEMICIRCULAR VAULTED ROOFS WITH DIFFERENT ORIENTATIONS159

6.1 DATA INPUT AND CCS(std) GEOMETRY RESEMBLANCE.....	159
6.2 THE SOLAR PERFORMANCE OF SEMICIRCULAR CURVED ROOF (The CCS _(std) Curvature Faces Principal Directions) (N-S) & (E-W)	162
6.2.1 CCS _(std) Curvature Faces NORTH and SOUTH.....	163
6.2.1.1 CCS _(std) Faces (N-S) During June.....	163
6.2.1.2 CCS _(std) Faces (N-S) During December.....	165
6.2.2 CCS _(std) Curvature Faces EAST and WEST.....	167
6.2.2.1 CCS _(std) Faces (E-W) During June.....	167
6.2.2.2 CCS _(std) Faces (E-W) During December.....	169
6.2.3 The Calculated Difference Between $I_{(HTCS)}$ on Flat Roof and $I_{(HTCS)}$ on CCS _(std) Faces Principal Directions (N-S) & (E-W)	173
6.3 THE SOLAR PERFORMANCE OF SEMICIRCULAR CURVED ROOF (CCS _(std) Curvature Faces Secondary Directions) (NW-SE) & (NE-SW)	173
6.3.1 CCS _(std) Curvature Faces NORTHWEST and SOUTHEAST.....	174
6.3.1.1 CCS _(std) Faces (NW-SE) During June.....	174
6.3.1.2 CCS _(std) Faces (NW-SE) During December.....	177
6.3.2 CCS _(std) Curvature Faces NORTHEAST and SOUTHWEST.....	180
6.3.2.1 CCS _(std) Faces (NE-SW) During June.....	180
6.3.2.2 CCS _(std) Faces (NE-SW) During December.....	181
6.3.3 The Calculated Difference Between $I_{(HTCS)}$ on Flat Roof and $I_{(HTCS)}$ on CCS _(std) Faces Secondary-Directions (NW-SE) & (NE-SW)	182
6.4 FORM SEASONAL RATIO.....	183
6.5 THE HOURLY RATIO BETWEEN $I_{(HTCS)}$ on CCS _(std) AND FLAT ROOF.....	185
6.6 THE SOLAR PERFORMANCE OF A HALF CURVED ROOF (Half-CCS _(std))	187
6.7 CONCLUSIONS.....	189
REFERENCE LIST.....	191

CHAPTER 7: SOLAR BEHAVIOUR OF FLAT AND VAULTED ROOFS WITH DIFFERENT CURVATURES AND ORIENTATIONS.....192

7.1 DATA INPUT AND CURVED ROOFS GEOMETRICAL RESEMBLANCE.....	193
7.2 THE SOLAR PERFORMANCE OF SEVEN CURVED ROOFS.....	197
7.2.1 CCS Curvatures Face NORTH and SOUTH during June.....	197
7.2.2 CCS Curvatures Face NORTH and SOUTH during December.....	200
7.2.3 CCS Curvatures Face EAST and WEST during June.....	203
7.2.4 CCS Curvatures Face EAST and WEST during December.....	206

7.3 THE SOLAR PERFORMANCE OF SEVEN CURVED ROOFS.....	209
7.3.1 CCS Curvatures Face NORTHWEST and SOUTHEAST during June.....	209
7.3.2 CCS Curvatures Face NORTHWEST and SOUTHEAST during December.	212
7.3.3 CCS Curvatures Face NORTHEAST and SOUTHWEST during June.....	215
7.3.4 CCS Curvatures Face NORTHEAST and SOUTHWEST during December.	216
7.4 FORM SEASONAL RATIOS.....	217
7.5 DATA INPUT AND CURVED ROOFS GEOMETRICAL RESEMBLANCE.....	221
7.6 COMPARISON BETWEEN THE RECEIVED $I_{(HRCs)}$ on 19 and 37 Joint-segments CCS	222
7.7 CONCLUSIONS.....	224
REFERENCE LIST.....	228

CHAPTER 8: SOLAR BEHAVIOUR OF FLAT AND DOMED ROOFS WITH DIFFERENT CURVATURES.....229

8.1 DATA INPUT AND DOMED FORMS GEOMETRICAL RESEMBLANCE	230
8.2 THE SOLAR PERFORMANCE OF DIFFERENT DOMED ROOF CURVATURES.	233
8.2.1 The Solar Performance on Dome _{1 (std)} (A=B)	233
8.2.2 The Solar Performance on Dome ₂ A= 0.5B.....	239
8.2.3 The Solar Performance on Dome ₃ A= 2B.....	245
8.2. The Solar Performance of The Three Dome Geometries and Flat Roof.....	251
8.3 DOMED ROOFS SHADE-ANALYSIS.....	252
8.3.1 The Ratios of Self-Shaded and Exposed Areas Above Domed Roofs.....	258
8.4 CONCLUSIONS.....	261
REFERENCE LIST.....	264

CHAPTER 9: CONCLUSIONS, VALIDATION AND FURTHER DEVELOPMENTS265

9.1 TRADITIONAL PASSIVE COOLING TECHNIQUES AND THE NEED FOR ENERGY EFFICIENT CONTEMPORARY ARCHITECTURE.....	265
9.1.1 Architectural Proposals of The Tested Curved Roofs Different Building Types	266
9.1.1.1 Different Architectural Masses and Compositions	267
9.1.1.2 Different Building Types (Inner-Spaces Functional Suitability).....	271
9.2 SOLAR RADIATION INTENSITY AND THE RECEIVER SURFACE GEOMETRY	276
9.3 VALIDATION OF RESEARCH TOOLS	277
9.3.1 Self-Shaded Areas on Domed Roof Surfaces.....	277
9.3.2 ECOTECH Solar Radiation Intensity Modelling	278
9.3.2.1 Solar Radiation Intensity on Flat Roof	280
9.3.2.2 ECOTECH Solar Intensity Simulation on Semicircular Domed-roof .	282
9.3.2.3 Comparison Between the Solar Performances Semicircular domed Using Two Different Computer simulation Tools	284
9.3.3 Curved-Roofs Indoor Thermal Analysis	287
9.4 VALIDATION OF THE RESEARCH WORK AND MAIN FINDINGS	289
9.5 NOVEL CONTRIBUTION AND AIMS FULFILLMENT	292
9.5.1 Solar Performance of Flat and Curved-roofs with Different Forms, Curvatures, and Orientations	293
9.5.2 Design Guidelines of Solar Performance of Flat and Curved Roofs Form and Orientation in Hot-arid Regions	295
9.5.2.1 Flat and Vaulted Roofs in Summer and Winter	295
9.5.2.2 Flat and Domed Roofs in Summer & Winter	297
9.6 RECOMMENDATIONS FOR FURTHER RESEARCH WORK	298
9.6.1 Computer Simulation and Modelling	298
9.6.2 Monitoring of Full-Scale Models	399
REFERENCE LIST	303

BIBLIOGRAPHY

APPENDIX A

Solar Radiation Simulation Model (Inputs and Outputs) SRSM.....(Appendix- 1)
Example Spreadsheets (Vaults).....(Appendix- 3)
Example Spreadsheets (Domes).....(Appendix- 6)
Tables for Vaulted Roofs with different Curvatures and Orientations..... (Appendix- 14)

APPENDIX B

Integrated Environmental Solutions (IES)(Appendix- 22)

LIST OF FIGURES

FIGURES OF CHAPTER 2

Figure 2-1 Buildings, Environment and Non-Renewable Resources	10
Figure 2-2 World's Population Growth (<i>Developed & Developing Countries</i>)	13
Figure 2-3 Map of the African Continent Map and Regional Parts	14
Figure 2-4 Population Growth Projections for Egypt 1990-2035	15
Figure 2-5 Egypt's Energy Consumption and Resources	16
Figure 2-6 A Sustainable Design Process.....	22
Figure 2-7 Africa Climatic Regions & the Selected Hot-Arid Zone.....	27
Figure 2-8 Middle East and North Africa Region.....	28
Figure 2-9 Map of Egypt and Geographical Location.....	28
Figure 2-10 The Inhabited Areas Along The Nile Narrow Valley.....	29
Figure 2-11 The Main Two Climatic Regions & Egypt Geographical Regions.....	30
Figure 2-12 Monthly Average Temperature and Humidity Distribution Forms throughout the Year At Different Cities and Latitudes In Egypt.....	32
Figure 2-13 Monthly Average Temperature And Humidity Distribution Forms Throughout The Year At Different Cities And Latitudes In Egypt.....	33
Figure 2-14 Future Extensions Towards The Uninhabited-Desert New Regions.....	34
Figure 2-15 Physical and Physiological Factors for the State of Thermal Comfort.....	35
Figure 2-16 Body Heat Exchange.....	37
Figure 2-17 BIO-CLIMATIC Chart and The Comfort Zone.....	38

FIGURES OF CHAPTER 3

Figure 3-1 (I) Ancient Egypt Triangle Wind Catcher.....	50
Figure 3-2 (1) Surfaces Area in Flat & Curved Roofs (2) Exposed & Self Shaded Areas in Flat & Curved Roofs.....	52
Figure 3-3 Different Shapes of Contemporary Curved Roofs.....	52
Figure 3-4 Different Types of Domes with Lighting and Ventilation Vents	53
Figure 3-5 Schematic Sketch for A Doubled Roof with Air Gap.....	54
Figure 3-6 Photos Depicting Doubled Roof & Roofs Vents.....	54
Figure 3-7 External Thick Walls, Roughness and Irregularity of Outer Walls Surface Earth Fully and Partially Covering and Shading Devices.....	55

Figure 3-8 Photos Depicting Thick and Massive Walls with Different Construction Materials.....	56
Figure 3-9 Air Patterns Through Different Courtyards Typologies.....	57
Figure 3-10 Photos Depict Different Types of Courtyards.....	58
Figure 3-11 Openings Sizes and Locations.....	59
Figure 3-12 Different Arched Openings.....	59
Figure 3-13 Schematic Sketch for A Traditional Wind Catcher (Malqaf).....	60
Figure 3-14 Contemporary Ideas For the Ancient Wind-Catcher	61
Figure 3-15 Traditional Wind Catchers (Malqaf).....	61
Figure 3-16 The Traditional Window (Mashrabiya)	62
Figure 3-17 Mashrabiya Wooden Meshes.....	62
Figure 3-18 The Project Layout Shows The Windowless External Walls and Inner Walls With Small Openings View The Main Courtyard	65
Figure 3-19 Tuwaiq Palace Photos.....	65
Figure 3-20 Analytical Sketches of Number of Passive Cooling Techniques.....	66
Figure 3-21 Traditional Najdi Typology Photos.....	67
Figure 3-22 The Three Sky-Courtyards Locations and The Tower Exteriors Photos.....	69
Figure 3-23 Sketches of NCB Environmental Control Techniques.....	70

FIGURES OF CHAPTER 4

Figure 4-1 Geometric Forms of Different Vaults.....	80
Figure 4-2 Forms and Types of Traditional Domes and Domes on Pendentives.....	81
Figure 4-3 Traditional Buildings and Mud Constructions, Siwa & Upper Egypt	83
Figure 4-4 Different Types of Dried Mud and Earth Bricks	84
Figure 4-5 The Nubian Way for Erecting Vaults	85
Figure 4-6 Modification of Nubian Dome with Eccentric Guide.....	86
Figure 4-7 The traditional Process of Erecting Woodless Mud Bricks' Domes	87
Figure 4-8 Vault Woodless Construction Methods.....	88
Figure 4-9 Mobile Guide for Erecting Woodless Mud Bricks' Domes.....	89
Figure 4-10 Different Woodless Mud Bricks Domes Covering Different Plans	90
Figure 4-11 Woodless Stones and Mud Bricks Domes on Pendentives	90
Figure 4-12 Woodless Bricks and Stones Constructions in Southern Part of Egypt	91
Figure 4-13 Training Programs and Small Houses Provide Good Training For Local Beginner Masons.....	91

Figure 4-14 Bell-shaped Domes with Reclining Arches.....	92
Figure 4-15 Photos of Sidi Kreer Housing Project, Egypt	99
Figure 4-16 Analytical Sketch of Courtyard Typology (New BARIS Village-Egypt).....	100
Figure 4-17 Photos of New BARIS Village (Houses & Market).....	101
Figure 4-18 Fouad Riad House Roofing Systems.....	102
Figure 4-19 Akil Sami House, Egypt.....	102
Figure 4-20 Casaroni House (Exterior).....	103
Figure 4-21 Casaroni House (Interior & Courtyard).....	104
Figure 4-22 El-Haraneya Arts Centre, Egypt	105
Figure 4-23 Halwa House, Agamy, Egypt.....	107
Figure 4-24 Architectural Drawings and Masonry Work of Halawa House	108
Figure 4-25 Sanganth, India	109
Figure 4-26 Satara Zone Housing, Mauritania.....	111
Figure 4-27 The Regional Hospital, Mauritania.....	112
Figure 4-28 Plan & Cross Section of The Regional Hospital, Mauritania	112
Figure 4-29 Drawings of The Structural System Developed by BREDA / Dakar.....	113
Figure 4-30 Vault and Dome Structures At The Indian Institute of Technology.....	114
Figure 4-31 New Projects	115
Figure 4-32 Agni Jata Building by Ray Meeker 1988.....	115

FIGURES OF CHAPTER 5

Figure 5-1 Beam and Diffuse Solar Radiation.....	121
Figure 5-2 Solar Radiation Passage through the Atmosphere.....	122
Figure 5-3 Heat Releases From the Ground & the Atmosphere.....	122
Figure 5-4 Earth -Sun Movement and Distance.....	123
Figure 5-5 The Earth Axis of Rotation & The Earth Movement Around The Sun.....	124
Figure 5-6 Earth -Sun Geometrical Relationship.....	124
Figure 5-7 Sun Path Three Dimensional Diagram.....	125
Figure 5-8 Solar Geometry (Altitude & Azimuth Angles).....	125
Figure 5-9 The Wall Azimuth in Relation to Its Orientation.....	126
Figure 5-10 Vertical and Horizontal Shadow Angles.....	126
Figure 5-11 Direct Solar Radiation Intensity on Horizontal Surfaces at Different Latitudes.....	128

Figure 5-12 Solar Radiation Peaks on Horizontal Surfaces throughout the Year at Different Latitudes.....	129
Figure 5-13 The Difference Between Peaks Due to Seasonal Variation.....	130
Figure 5-14 Solar Geometry.....	131
Figure 5-15 Solar Radiation Intensity is A Function of The Tilted Angle of The Receiver Surface and The Solar Angle of Incidence.....	132
Figure 5-16 Direct Solar Radiation Received by Different Surfaces at 30°N.....	132
Figure 5-17 Beam Radiation on Horizontal and Tilted Surfaces	133
Figure 5-18 Geometrical Relations for Defining the Tilted Surface Geometry	142
Figure 5-19 The Tested Principal Directions and Secondary Directions.....	144
Figure 5-20 SRSM Numerical Identification for Curved-roof Curvature Facing-Direction.....	145
Figure 5-21 The CCS and Its Tilted Segments North and South aspects.....	146
Figure 5-22 The CCS and Its Tilted Segments East and West Aspects.....	147
Figure 5-23 CAD Drawings and 2D and 3D Illustrations for Curved Forms.....	148
Figure 5-24 The Two Proposed Planar Segment Resembling Techniques.....	149
Figure 5-25 Circles and Ellipses Algebraic-Equations-Form	149
Figure 5-26 The Geometrical Resemblance of Curved Roof Cross Sections.....	150
Figure 5-27 The Slope Angle and Length of Planar Segments.....	151
Figure 5-28 The Resemblance Techniques of Curved Roofs and Segments Slopes.....	152

FIGURES OF CHAPTER 6

Figure 6-1 $CCS_{(std)}$ Geometrical Resemblance (<i>Tangent Segment Technique</i>) (37segments)....	160
Figure 6-2 Numerical Definition For The Principal Facing-Direction (N-S) & (E-W).....	162
Figure 6-3 $I_{(HTCS)}$ (W/m^2) on Flat Roof and $CCS_{(std)}$	163
Figure 6-4 $I_{(HTCS)}(CCS_{(std)}) / I_{(HTCS)}(flat\ roof) \%$	164
Figure 6-5 $I_{(HTCS)}$ (W/m^2) on Flat Roof and $CCS_{(std)}$	165
Figure 6-6 $I_{(HTCS)}(CCS_{(std)}) / I_{(HTCS)}(flat\ roof) \%$	166
Figure 6-7 $I_{(HTCS)}$ (W/m^2) on Flat Roof and $CCS_{(std)}$	167
Figure 6-8 $I_{(HTCS)}(CCS_{(std)}) / I_{(HTCS)}(flat\ roof) \%$	168
Figure 6-9 $I_{(HTCS)}$ (W/m^2) on Flat Roof and $CCS_{(std)}$	169
Figure 6-10 $I_{(HTCS)}(CCS_{(std)}) / I_{(HTCS)}(flat\ roof) \%$	171
Figure 6-11 The Difference Between $I_{(HTCS)}$ on Flat Roof and $CCS_{(std)}$	172
Figure 6-12 Numerical Identification of the Secondary Facing-Directions.....	173
Figure 6-13 $I_{(HTCS)}$ (W/m^2) on Flat Roof and $CCS_{(std)}$	174

Figure 6-14 $I_{(HTCS)} (CCS_{(std)}) / I_{(HTCS)} (flat\ roof) \%$	176
Figure 6-15 $I_{(HTCS)} (W/m^2)$ on Flat Roof and $CCS_{(std)}$	177
Figure 6-16 $I_{(HTCS)} (CCS_{(std)}) / I_{(HTCS)} (flat\ roof) \%$	178
Figure 6-17 $I_{(HTCS)} (W/m^2)$ on Flat Roof and $CCS_{(std)}$	180
Figure 6-18 $I_{(HTCS)} (W/m^2)$ on Flat Roof and $CCS_{(std)}$	181
Figure 6-19 The Difference Between $I_{(HTCS)}$ on Flat Roof and $CCS_{(std)}$	182
Figure 6-20 The received $I_{(HTCS)}$ Day Average on the $CCS_{(std)}$ and The Flat Roof at Different Orientations.....	184
Figure 6-21 $I_{(HTCS)} (CCS_{(std)}) / I_{(HTCS)} (flat\ roof)$ Hourly Ratios (<i>Principle Directions</i>).....	185
Figure 6-22 $I_{(HTCS)} (CCS_{(std)}) / I_{(HTCS)} (flat\ roof)$ Hourly Ratios (<i>Secondary Directions</i>)....	186

FIGURES OF CHAPTER 7

Figure 7-1 Tangent Segment is not Applicable For The Ellipse CCSR (where $A \neq B$).....	193
Figure 7-2 Geometrical Resemblance of CCS_1 ($CCSR: A = B$).....	193
Figure 7-3 Geometrical Resemblance of $CCS_2, CCS_3, \& CCS_4$ ($CCSR: A < B$).....	194
Figure 7-4 Geometrical Resemblance of $CCS_5 \& CCS_6$ ($CCSR: A > B$).....	195
Figure 7-5 Geometrical Resemblance of CCS_7 ($CCSR: A > B$).....	196
Figure 7-6 $I_{(HTCS)} (W/m^2)$ on The CCS_{1-7} , The $CCS_{(std)}$, and The Flat Roof.....	197
Figure 7-7 The Received $I_{(HTCS)}$ on CCS_{1-4} , The Flat Roof, and The $CCS_{(std)}$	198
Figure 7-8 The Received $I_{(HTCS)}$ on CCS_{5-7} , The Flat Roof, and The $CCS_{(std)}$	199
Figure 7-9 Alternated Arrangements of The Received $I_{(HTCS)}$ on The Tested Roofs.....	199
Figure 7-10 $I_{(HTCS)} (W/m^2)$ on The CCS_{1-7} , The $CCS_{(std)}$, and The Flat Roof.....	200
Figure 7-11 The Received $I_{(HTCS)}$ on CCS_{1-4} , The Flat Roof, and The $CCS_{(std)}$	201
Figure 7-12 The Received $I_{(HTCS)}$ on CCS_{5-7} , The Flat Roof, and The $CCS_{(std)}$	202
Figure 7-13 Alternated Arrangements of The Received $I_{(HTCS)}$ on The Tested Roofs.....	202
Figure 7-14 $I_{(HTCS)} (W/m^2)$ on The CCS_{1-7} , The $CCS_{(std)}$, and The Flat Roof.....	203
Figure 7-15 The Received $I_{(HTCS)}$ on CCS_{1-4} , The Flat Roof, and The $CCS_{(std)}$	204
Figure 7-16 The Received $I_{(HTCS)}$ on CCS_{5-7} , The Flat Roof, and The $CCS_{(std)}$	205
Figure 7-17 Alternated Arrangements of The Received $I_{(HTCS)}$ on The Tested Roofs.....	205
Figure 7-18 $I_{(HTCS)} (W/m^2)$ on The CCS_{1-7} , The $CCS_{(std)}$, and The Flat Roof.....	206
Figure 7-19 The Received $I_{(HTCS)}$ on CCS_{1-4} , The Flat Roof, and The $CCS_{(std)}$	207
Figure 7-20 The Received $I_{(HTCS)}$ on CCS_{5-7} , The Flat Roof, and The $CCS_{(std)}$	208
Figure 7-21 Alternated Arrangements of The Received $I_{(HTCS)}$ on The Tested Roofs.....	208

Figure 7-22 $I_{(HTCS)}$ (W/m^2) on The CCS ₁₋₇ , The CCS(std), and The Flat Roof.....	209
Figure 7-23 The Received $I_{(HTCS)}$ on CCS ₁₋₄ , The Flat Roof, and The CCS _(std)	210
Figure 7-24 The Received $I_{(HTCS)}$ on CCS ₅₋₇ , The Flat Roof, and The CCS _(std)	211
Figure 7-25 Alternated Arrangements of The Received $I_{(HTCS)}$ on The Tested Roofs.....	212
Figure 7-26 $I_{(HTCS)}$ (W/m^2) on The CCS ₁₋₇ , The CCS(std), and The Flat Roof.....	212
Figure 7-27 The Received $I_{(HTCS)}$ on CCS ₁₋₄ , The Flat Roof, and The CCS _(std)	213
Figure 7-28 The Received $I_{(HTCS)}$ on CCS ₅₋₇ , The Flat Roof, and The CCS _(std)	214
Figure 7-29 Alternated Arrangements of The Received $I_{(HTCS)}$ on The Tested Roofs.....	214
Figure 7-30 $I_{(HTCS)}$ (W/m^2) on The CCS ₁₋₇ , The CCS _(std) , and The Flat Roof.....	215
Figure 7-31 $I_{(HTCS)}$ (W/m^2) on The CCS ₁₋₇ , The CCS _(std) , and The Flat Roof.....	216
Figure 7-32 The Maximum Received $I_{(HTCS)}$ on Different Forms of Roofs.....	218
Figure 7-33 The Day Average Received $I_{(HTCS)}$ on Different Forms of Roofs.....	218
Figure 7-34 The Maximum Received $I_{(HTCS)}$ on Different Forms of Roofs.....	219
Figure 7-35 The Day Average Received $I_{(HTCS)}$ on Different Forms of Roofs.....	219
Figure 7-36 The Maximum Received $I_{(HTCS)}$ on Different Forms of Roofs.....	220
Figure 7-37 The Day Average Received $I_{(HTCS)}$ on Different Forms of Roofs.....	220
Figure 7-38 The Geometrical Resemblance (37 Joint Segments).....	221
Figure 7-39 Comparison Between the Received $I_{(HTCS)}$ on 19 and 37 joint segment Curved Roofs (Principle Directions)	222
Figure 7-40 Comparison Between the Received $I_{(HTCS)}$ on 19 & 37 joint segment (<i>Secondary Directions</i>).....	223

FIGURES OF CHAPTER 8

Figure 8-1 Dome Geometrical Resemblance (Each ring has different slope angle).....	229
Figure 8-2 The Three CCSR of the Tested Domed Roofs.....	230
Figure 8-3 Rings and Planar Segment Orientations & Section a-a for Dome1 (A=B).....	231
Figure 8-4 Section a-a for Dome ₂ (A=0.5B) and Dome ₃ (A=2B)	232
Figure 8-5 $I_{(HTCS)}$ (W/m^2) on Dome ₁ Rings in Summer (CCSR (A=B)).....	233
Figure 8-6 $I_{(HTCS)}$ (W/m^2) on Dome ₁ Rings in Summer (CCSR (A=B)).....	234
Figure 8-7 $I_{(HTCS)}$ (W/m^2) on Dome ₁ Rings in Winter (CCSR (A=B)).....	236
Figure 8-8 $I_{(HTCS)}$ (W/m^2) on Dome ₁ Rings in Winter (CCSR (A=B)).....	237
Figure 8-9 $I_{(HTCS)}$ (W/m^2) on Dome ₂ Rings in Summer (CCSR (A=0.5B)).....	239
Figure 8-10 $I_{(HTCS)}$ (W/m^2) on Dome ₂ Rings in Summer (CCSR (A=0.5B)).....	240
Figure 8-11 $I_{(HTCS)}$ (W/m^2) on Dome ₂ Rings in Winter (CCSR (A=0.5B))	242

Figure 8-12 $I_{(HTCS)}$ (W/m^2) on Dome ₂ Rings in Winter (CCSR (A=0.5B))	243
Figure 8-13 $I_{(HTCS)}$ (W/m^2) on Dome ₃ Rings in Summer (CCSR (A=2B))	245
Figure 8-14 $I_{(HTCS)}$ (W/m^2) on Dome ₃ Rings in Summer (CCSR (A=2B)).....	246
Figure 8-15 $I_{(HTCS)}$ (W/m^2) on Dome ₃ Rings in Winter (CCSR (A=2B)).....	248
Figure 8-16 $I_{(HTCS)}$ (W/m^2) on Dome ₃ Rings in Winter (CCSR (A=2B)).....	249
Figure 8-17 $I_{(HTCS)}$ (W/m^2) Day Average on The Three Domes and The Flat Roof in Summer and Winter.....	251
Figure 8-18 The Self-shaded and Exposed Areas Patterns and Ratios in Summer.....	252
Figure 8-19 The Self-shaded and Exposed Areas Patterns and Ratios in Winter.....	253
Figure 8-20 The Self-shaded and Exposed Areas Patterns and Ratios in Summer.....	254
Figure 8-21 The Self-shaded and Exposed Areas Patterns and Ratios in Winter.....	255
Figure 8-22 The Self-shaded and Exposed Areas Patterns and Ratios in Summer.....	256
Figure 8-23 The Self-shaded and Exposed Areas Patterns and Ratios in Winter.....	257

FIGURES OF CHAPTER 9

Figure 9-1 Diagram Illustrating Different Ways of Combing Vaults and Domes on Principle Single Spaces	267
Figure 9-2 A Layout of The Possible Use of Composite of Vaults and Domes in a Single Storey Building	268
Figure 9-3 Different Proposals of a Domed House	268
Figure 9-4 Composition, Orientation and Curvatures of Curved Roofs in Architectural Applications (Layout, Plans And Elevations).....	269
Figure 9-5 Plan, Section and Elevation of an Architectural Proposal for a Nursery, Primary School, or Multicultural Community Centre.....	270
Figure 9-6 Modern Applications of Domed Domestic Housing.....	271
Figure 9-7 Application of Monolithic Domes in Schools.....	272
Figure 9-8 Curved-roofs in Commercial and Public Buildings.....	272
Figure 9-9 Domes and Vaults in Mosques and Churches.....	273
Figure 9-10 Domes for Multipurpose and Sports Halls.....	274
Figure 9-11 Geometrical Models for ECOTECT Solar Tests.....	279
Figure 9-12 ECOECT Solar Intensity Distribution.....	280
Figure 9-13 (a) ECORECT v5.01 (b) ECOTECT v5.20.....	282

Figure 9-14 $I_{(HTCS)}$ W/m ² on Semicircular Dome and Flat Roofs In Summer & Winter (ECOTECH v5.20 Results)	284
Figure 9-15 $I_{(HTCS)}$ W/m ² on Three Domes and Flat Roof In Summer & Winter.	286
Figure 9-16 Day-average inner-surface temperature of Domed and Flat Roofs.....	288
Figure 9-17 Geometrical Methodology (<i>Gomez-Munoz</i>)	289
Figure 9-18 Graphical Comparison Between The Main Findings.....	290
Figure 9-19 The Average Daily Received $I_{(HTCS)}$ on Different Curved Roof Forms.....	295
Figure 9-20 The Average Daily Received $I_{(HTCS)}$ on Different Curved Roof Forms.....	296
Figure 9-21 The Day-average Received $I_{(HTCS)}$ on Different Domed-roofs.....	297
Figure 9-22 Full-scale Model Sketches.....	300
Figure 9-23 Schematic Sketches for some Ideas to be investigated in Further Research.....	301

LIST OF TABLES

TABLES OF CHAPTER 2

Table 2-1 Tropical Climatic Classification Zones.....	25
Table 2-2 The Annual Main Seasons of Egypt Climate.....	31
Table 2-3 Monthly Global Solar Radiation on Horizontal Surface at Different Cities and Latitudes in Egypt.....	31
Table 2-4 Monthly Average Temperature and Humidity Values at Different Cities and Latitudes in Egypt.....	32
Table 2-5 Monthly Average Temperature and Humidity Values at Different Cities and Latitudes in Egypt.....	33

TABLES OF CHAPTER 5

Table 5-1 A Seasonal Comparison of Sun Altitude Angles.....	130
--	-----

TABLES OF CHAPTER 6

Table 6-1 The Seasonal Ratios of A Flat Roof & Different Orientated $CCS_{(std)}$	183
Table 6-2 $I_{(HTCS)}$ on North-facing half and South-facing half of $CCS_{(std)}$	187
Table 6-3 $I_{(HTCS)}$ on East-facing half and West-facing half of $CCS_{(std)}$	187
Table 6-4 $I_{(HTCS)}$ on Northwest-facing half and Southeast-facing half of $CCS_{(std)}$	188
Table 6-5 $I_{(HTCS)}$ on Northeast-facing half and Southwest-facing half of $CCS_{(std)}$	188
Table 6-6 The Ratio Between The Received $I_{(HTCS)}$ on $CCS_{(std)}$ and Flat Roof.....	190

TABLES OF CHAPTER 7

Table 7-1 Radial Lines Slopes from The Horizontal and Planar Segments Slopes.....	196
Table 7-2 Radiuses Slopes from The Horizontal and Planar Segments Slopes.....	221
Table 7-3 The Ratio Between The Received $I_{(HTCS)}$ on Different CCS	225
Table 7-4 The Ratio Between The Received $I_{(HTCS)}$ on Different CCS.....	226

TABLES OF CHAPTER 8

Table 8-1 Rings and Planar Segments Slopes (<i>Angles from the Horizontal</i>).....	230
Table 8-2 The Received $I_{(HTCS)}$ on Each Ring of Dome ₁ in Summer.....	235
Table 8-3 The Received $I_{(HTCS)}$ on Each Ring of Dome ₁ in Winter.....	238
Table 8-4 The Received $I_{(HTCS)}$ on Each Ring of Dome ₂ in Summer.....	241
Table 8-5 The Received $I_{(HTCS)}$ on Each Ring of Dome ₂ in Winter.....	244
Table 8-6 The Received $I_{(HTCS)}$ on Each Ring of Dome ₃ in Summer.....	247

Table 8-7 The Received $I_{(HTCS)}$ on Each Ring of Dome ₃ in Winter.....	250
Table 8-8 The Self-shaded and The Exposed Segments and Areas on Dome ₁	258
Table 8-9 The Self-shaded and The Exposed Segments and Areas on Dome ₂ &3.....	259
Table 8-10 The Day Average of The Received $I_{(HTCS)}$ on Different Dome Curvatures and Their Ratios To That on The Flat Roof.....	261

TABLES OF CHAPTER 9

Table 9-1 Curved- roofs Main Geometric Profiles (<i>Curvatures</i>) and Their Architectural Proposals	275
Table 9-2 Solar Radiation Intensity W/m^2 on Flat Roof in Summer (<i>Riyadh, Saudi Arabia</i>).....	281
Table 9-3 Solar Radiation Intensity W/m^2 on Flat Roof in Winter(<i>Riyadh, Saudi Arabia</i>).....	281
Table 9-4 Solar Radiation Intensity W/m^2 on Domed-roof in Summer (<i>Riyadh, Saudi Arabia</i>) ...	283
Table 9-5 Solar Radiation Intensity W/m^2 Domed-roof in Winter (<i>Riyadh, Saudi Arabia</i>)... ..	283
Table 9-6 Two Construction Materials For Domed and Flat roofs.....	287
Table 9-7 The Average Daily Received $I_{(HTCS)}$ on Different Curved Roof Forms and Curvatures in Summer and Winter and Their Ratios % to that on Flat Roof	293

ABBREVIATIONS

$I_{(HTCS)}$ Hourly Total Clear Sky Irradiation (W/m^2)

CCS..... Curved-roof Cross Section (*For Vaults and domes*)

CCSR..... Curved-roof Cross Section Ratio (height-to-span ratio) (*For Vaults and domes*)

CCS *(std)*Semicircular Curved roof Cross Section (*For Vaults and domes*)

SRSMSolar Radiation Simulation Model

NOMENCLATURE

Chapter 4

- T_{sa}** : Sol-air temperature [$^{\circ}\text{C}$]
 T_o : Outside air temperature in [$^{\circ}\text{C}$]
 R_o : External surface resistance [m^2]
 I : Intensity of direct plus diffuse solar radiation on the outer surface [W/m^2]
 I_1 : Intensity of long-wave radiation from a black surface at the ambient temperature [W/m^2]
 a : Absorption coefficient which varies from 0.5 for brick to 0.9 for a black surface
 e : Emissivity of the outer surface for long wave radiation

Chapter 5

- R_b** : A geometric factor represents the ratio of beam radiation on the tilted surface to that on horizontal surfaces at any time
 G_{bT} : Total radiation on tilted surface [W/m^2]
 G_b : Beam radiation [W/m^2]
 G_{bn} : Total radiation on horizontal surface [W/m^2]
 $I_{b,\beta}$: Beam irradiance incident on an inclined surface [W/m^2]
 $I_{d,\beta}$: Diffuse irradiance incident on an inclined surface [W/m^2]
 I_b : Beam solar radiation [W/m^2]
 I_d : Sky diffuse solar radiation on a horizontal surface [W/m^2]
 $I_{d,t}$: Total diffuse radiation on an inclined surface [W/m^2]

Greek

- ϕ** : Latitude, that is, the angular location north or south of the equator
 δ : Sun declination angle
 β : Surface slope angle (*the angle between the surface and the horizontal*)
 γ : Surface azimuth angle, (*the projection on a horizontal plane of the normal to the surface*)
 ω : Hour angle
 θ : Angle of incidence, (*the angle between the beam radiation on a surface and the normal to that surface*)

 θ_z : Angle of incident on Horizontal surface
 θ : Angle of incident on tilted surface

 θ_β : Incidence angle on an inclined surface for beam radiation
 β : Inclination angle of the surface with respect to the horizontal
 θ_z : Sun zenith angle (*or the incidence angle on a horizontal planar surface*)
 ψ_s : Sun azimuth angle
 ψ_f : Surface azimuth angle (*surface orientation with the respect to south direction*)

Chapter 9

- G** : Absorbed radiation [W/m^2]
 q : The heat transfer from the roof per unit area [W/m^2]
 q_c : The heat transfer from the roof per unit area by convection [W/m^2]
 q_r : The heat transfer from the roof per unit area by radiation [W/m^2]
 q_k : The heat transfer from the roof per unit area by conduction [W/m^2]

CHAPTER 1

INTRODUCTION

1. INTRODUCTION

In early times, traditional architecture was mainly made of locally available materials to provide indoor thermal comfort. Design dealing with climatic constraints has been introduced since ancient Egyptian and Greek times, where many traditional and vernacular buildings employed passive cooling techniques. These techniques successfully helped to provide indoor thermal comfort particularly in hot-arid areas. However, contemporary modern living-styles, economic growth and advanced technologies have resulted in a clear abandonment of most of those techniques.

Nowadays, after the introduction of air-conditioning systems and despite the shortage of non-renewable energy resources together with the increase in the number of environmental pollution problems, in many parts of the world, buildings still consume lots of energy for heating and cooling [1]. This has dictated the intervention of the architectural and built-environment communities. Consequently, during the last two decades, a considerable amount of research work has been carried out into the problems of energy conservation, sustainability and energy efficiency in buildings [2].

Increasingly in hot-arid regions (*e.g. Arabian Peninsula and Egypt*), where the difference between unbearable outdoor and desirable indoor climatic conditions is large, the concern is to establish systems, which make use of *Natural Passive Cooling* to ensure sustainability of resources [3]. However, many modern buildings in those regions neither reflect their local climatic conditions nor architectural identity. Consequently, modern towns and cities start to embody modern forms and shapes and lose their regional and traditional architecture that have made use of many available resources to provide indoor thermal comfort.

Moreover, modern buildings are becoming increasingly complex; involving technologically advanced building materials and mechanical systems for controlling indoor air quality, thermal comfort, lighting and acoustics. Furthermore, those systems, which mostly rely on non-renewable energy resources, are often expensive and produce environmental pollutants.

For creating a desirable indoor environment with minimal energy consumption, energy conscious design of buildings requires an understanding of the local climatic conditions and the proper use of one or more traditional passive strategies [3]. Despite their abilities to harness passive and renewable energies, the success of such strategies depends on their level of integration into contemporary buildings and designs from one side and their satisfaction to users lifestyle and needs from the other.

The concept of passive indoor thermal comfort and energy efficient buildings in developing countries that forms a larger part of the hot-arid zone has yet to be widely and properly addressed. In this context, urban designers, planners, architects, clients and the regulatory authorities of modern buildings have a key role to play.

In order to abate the rapid spread of the western-international architectural style, architects have started making use of some traditional solutions in an effort to regain and revive the missed architectural identity and to seek an environmentally, culturally and socially adapted architecture. However, they have often used traditional forms and features without delving into the scientific facts behind their potential for climate control.

Building envelopes and roofs in particular have a major influence on indoor thermal conditions in hot-arid regions. For detached single storied building, the roof is the most exposed element of the building envelope, which often receives the greatest amount of solar radiation and consequently it is the main cause of heat gain (around 50% of the heat load in buildings) [4] and indoor thermal discomfort during summer in hot-arid regions [5].

The use of vaulted, domed and curved surfaces for the passive cooling of buildings can be traced back to as early as the 3rd millennium BC. Those roof-forms, which met the needs of public and private building programs, low-cost or quality housing and religious buildings, were widely used in Egypt, Iraq, India and their surrounding hot-arid regions.

This research reviews a number of traditional building technologies in order to facilitate better understanding of their solar and thermal characteristics with special reference to the new communities in Egypt.

1.1 RESEARCH PROBLEM

Domes, vaults and curved roofs in general have been used for a long time to roof both large and small buildings in the hot arid region of Egypt and in the neighbouring arid zone. Among the initial interpretations for their frequent use was the shortage of timber in that area to build flat roofs, thus adobe and other resources were used [6]. Other justifications cited it to climatic aspects, aesthetic issues and cultural and historical preferences [7].

Prominent among these interpretations is the climate related claim that buildings with curved roof surfaces generally maintain lower temperatures during the summer months than others with flat roofs [7-9]. On the contrary, other researches believe that the use of domes or curved surfaces have no effect at all on the environmental behavior of the enclosed space and sometimes increases solar gain of roofs [10].

Climate-related performance of curved-roof forms has been investigated by different researches to evaluate their influences on the indoor environments [6,11,12]. Olgyay suggested that the radiation of high sun positions is “diluted” on a rounded surface, resulting in lower surface temperatures [12]. A comparable suggestion was that “the intensity of solar radiation is spread over a larger area and the average heat transmission to the internal enclosed spaces is reduced [11]. Chapter 3 in this thesis analyses the ratio between curved-roof and flat roof surface areas. For a semicircular vaulted-roof this “dilution factor” equals 1.6, whereas it equals 2.0 for semicircular dome (*hemisphere*) (see Chapter 3, page no. 52). These and other climate-related explanations were argued to be incomplete [13].

It is obvious from the literature that there is a clear conflict of views on the climate related explanations and indoor thermal effect of curved-roof forms (domes and vaults). Thus, it is the aim of this research to investigate the architectural and solar potential of flat and curved roofs in hot-arid regions in order to establish architectural perception and understanding of their effect on solar gain and indoor environmental conditions.

1.2 RESEARCH AIMS

The overall purpose of the research presented in this thesis is to provide a sound theoretical base from which investigations into the solar and thermal behaviour of spaces enclosed by curved roofs could be undertaken with confidence. Research was carried out with the practical goal of exploring the architectural and solar potential of curved roofs (domes and vaults) in hot arid regions. Other aims are:

- To offer a better understanding of the traditional passive cooling and roofing techniques for enhancing indoor thermal comfort in hot-arid regions.
- To investigate the solar behavior of external roof surface through the calculations of the solar radiation intensities on different forms, curvatures and orientations.
- To develop a better understanding of the suitability of various roof forms for different architectural applications, through a comparison between solar behavior of flat and curved roofs.
- To find out the patterns of the exposed and self shaded areas above selected dome geometries.
- To develop design guidelines for curved-roofs architecture in hot-arid regions.

1.3 RESEARCH METHODOLOGY

A literature research was carried to review the various methods of calculating the intensity of solar radiation on different surface geometries. This was important to be aware of the theory behind the mathematical equations appropriate for studying the intensity of the received solar radiation on sloped surfaces. A number of these equations has been applied for different architectural applications and for improving buildings environmental performances [14-16].

Accordingly, a computer model, which was developed by Exell in 1986 [17], has been chosen. This model calculates the solar radiation on sloped surfaces with any orientation for particular geographical latitudes.

A geometrical resemblance technique was used to identify the curved roof cross section as a group of planar segments; each segment has a different slope and azimuth angle. For higher accuracy more planar segments were generated. This is viable regardless of the type of the curved forms tested parameters and performances.

A series of calculations was carried out on planar segments with different slopes and orientations that resemble flat and curved roofs using this computer model. A comparative analysis of the solar behaviour of flat and curved roofs (with different cross section ratios and orientations) was carried out. Along side with using the model results for sloped surfaces, the author has developed a large number of Microsoft Excel Spreadsheets in order to supplement the evaluation of the solar behaviour of different curved-roof, forms, curvatures and orientations.

The results were validated using two commercially available computer tools. These tools were also used to achieve a comprehensive investigation into the solar performance of the curved roofs, thus shade analysis and other solar radiation intensity calculations were carried out. To create a more useful perception of energy consciousness of curved roofs, indoor thermal calculations were briefly introduced for flat and semicircular domed roofs.

1.4 OUTLINE OF THE THESIS

The work in this research can be classified into two parts, the first of which (*the first four chapters*) acts as an approach to this research in which the research problem, objectives and necessity are described. This part dwells on energy crisis and the non-renewable energy limited resources and environmental problems in order to prompt for more energy efficient buildings and passive cooling technologies in developing countries with hot climatic conditions.

Part two (the empirical study chapters) represents the main core of this research. It carried out extensive solar investigations and calculations for the solar radiation intensity received by different roof forms and orientations. Therefore, the research has generated different graphical illustrations in order to discuss the solar behaviour of roofs outer surfaces due to their geometries variation. This part of the thesis have pointed out that both curved-roof forms (*vault and dome*) facilitate a significant decrease in the received solar radiation intensity above roof outer-surface.

Chapter 2 presents an introduction to the world population growth and its effect on energy demand, (known as the world energy crisis). The chapter concludes that there is a need for energy efficient architecture, sustainable buildings and climatic conscious designs in hot-arid regions of the developing countries.

Chapter 3 introduces the principles of passive cooling strategies and related aspects along with classifying different traditional passive cooling techniques. The chapter concludes with a discussion of the potentials of employing passive cooling techniques to be appropriately applicable in contemporary buildings in hot-arid regions.

Chapter 4 reviews different types of woodless construction techniques for erecting traditional curved roofs including their advantages and disadvantages along with their use in both traditional and contemporary architecture. The chapter concludes that besides their environmental, cultural and social issues, curved-roofs are also stated to have high-energy conscious potentials.

Chapter 5 discusses the principles of solar radiation and solar geometry. The chapter reviews previous research applications, which investigated the received solar radiation on sloped surfaces and their architectural applications. The empirical research methodology employed in the present research is discussed in this chapter. The chapter highlights the influence of curved-roof geometrical configurations on the received solar radiation intensity above roof surfaces.

Chapters 6 to 8 present the procedures and the results of a parametric study into the solar behaviour of flat, vaulted and domed roofs. Based on the outcomes of the solar behaviour investigations on different curved roofs, forms, curvatures and orientations, a comprehensive list of conclusions is presented at the end of each chapter.

Chapter 9 discusses the overall conclusions of the research presented in this thesis. Conclusions are drawn on the results from the empirical investigations with regard to the research aims stated in **Chapter 1** and the unresolved issues in **Chapter 2** and **Chapter 5**. In this chapter an overall validation of the empirical results presented in **Chapters 6 to 8** was carried out through employing other commercially available computer tools and other recent published research work. A number of design guidelines for the application of curved roofs in hot-arid regions are presented in this chapter. The opportunities for further research work in this field are also discussed.

1.5 CONCLUSIONS

In conclusion, the aim of this research is to emphasize and evaluate the solar and architectural potentials of different curved-roof forms. The work in this research can be classified as continuing research aiming to investigate the received solar radiation intensity above roof surfaces with different geometrical configurations. The thesis seeks a better architectural understanding of the solar and thermal performance of curved-roofs forms and geometries to be effectively employed in hot-arid regions where the passive controlling of indoor climatic conditions is crucial. Therefore, the present research provides architects and building designers with architectural and solar design-guidelines of curved-roofs applications in hot-arid climates.

Reference List

1. Sophia and Stefan Behhling in Collaboration with Bruno Schindler Foreword by Norman Foster. *Solar Power The Evolution of Sustainable Architecture* 2000.
2. Al-Sanea, S. A. Thermal Performance of Building Roof Elements, *Building and Environment* Vol. 37: pp. 665-75.
3. Fathy, H. Architecture and Environment, *Arid Land News Letter 1994 Fall-1994 Winter; ALN No. 36*.
4. Nini, G. Thermal Effect of Roof on Comfort in Classrooms in Constantine. *World Renewable Energy Congress VII (WREC 2002)*, Elsevier Science Ltd 2002; ElSayigh, A. A. M ed.
5. Zakaria, N. Z., Woods P. Roof Design and Thermal Performance of houses in Equatorial Climates, *World Renewable Energy Congress VII (WREC 2002)*, Elsevier Science Ltd. 2002; ElSayigh, A. A. M. ed.
6. Runsheng, T., Meir, I. A. and Etzion, Y. An Analysis of Absorbed Radiation by Domed and Vaulted Roofs as Compared with Flat Roofs. *Energy and Buildings* 2003; Vol. 35: pp: 539-48.
7. Fathy, H. Architecture for the poor *An Experiment in Rural Egypt* [Web Page], (1973).
8. Konya, A. A. Design Primer for Hot Climates. The Architectural Press, London 1980.
9. Bahadori, M. N. Passive Cooling Systems in Iranian Architecture. *Scientific American* 1978 Feb; Vol. 238(No. 2): pp: 144-54.
10. Fekry, A. A. and Elzafarani, A. M. Quantitative Evaluation of Shading Patterns of Domes and its Impact on Roof Solar Gain, Urban Development and Building Problems in Desert Areas, conference Proceedings, Vol. 2: Desert Architecture, Ministry of housing and public affairs, 2002, Riyadh, Saudi Arabia
11. Fathy, H. Natural Energy and Vernacular Architecture, *principles and examples with reference to hot -arid climates*, Chicago & London: Published for United Nations University by the university of Chicago press , 1986. (Edited by Walter Shearer, Abdel-Rahman, Ahmed Sultan.
12. Olygyay, V. Design with Climate. Princeton: Princeton University Press, 1973.
13. Pearlmutter, D. Roof Geometry as a Determinant of Thermal Behaviour: A Comparative Study of Vaulted and Flat Surfaces in a Hot-Arid Zone. *Architectural Science Review* 1993 Jun; Vol. 36: pp: 75-86.
14. Laouadi, A. , Atif, M. R. Natural convection heat transfer within multi-layer domes. *International Journal of Heat and Mass Transfer* 2001; Vol. 44: pp 1973-81.
15. Laouadi, A. and Atif, M. R. Transparent Domed Skylights: *Optical Model for Predicting Transmittance, Absorptance and Reflectance*. *International Journal of Lighting Research and Technology* 1998; Vol. 30(No. 3): pp. 111-18.
16. Stasinopoulos, T. N. Form Insolation Form Index; *notes on the relation of geometric shape and solar irradiation*. *Environmentally Friendly Cities - Proceedings of PLEA 98 Passive and Low Energy Architecture*. Lisbon, Portugal. 1998.
17. Exell, R. H. B. A program in BASIC for calculating solar radiation in tropical climates on small computers. *Renewable Energy Review Journal*, 1986 Dec; Vol. 8(No. 2).

CHAPTER 2

ENERGY RESOURCES AND INDOOR THERMAL COMFORT IN HOT-ARID CLIMATES WITH REFERENCE TO EGYPT

2. ENERGY RESOURCES AND INDOOR THERMAL COMFORT IN HOT ARID CLIMATES (With Reference to Egypt)

During the 18th century, which witnessed the *Industrial Revolution*, many natural energy resources, such as firewood, wind, waterfalls and sun were replaced by coal. It is well known that the way energy has been used or misused has played an important role in the development of different communities. The accelerated intensity of sophisticated and advanced activities and the way that energy is unconsciously consumed in general are currently contributing to damage of the global environment. The inappropriate use of energy resources in all its forms has been the common behaviour of most human activities through history. All this has provoked, especially during the last fifty years, severe damage to the ecosystem of the natural habitat [1]. This chapter discusses the indirect proportional relationship between non-renewable energy and natural resources on the one hand and population growth and buildings on the other.

The chapter clarifies the influence of the world's overpopulation growth on non-renewable energy resources production and their consumption in buildings. It also discusses the need for establishing sustainable and energy efficient systems to overcome the current situation in buildings, save the environment and to sustain energy and natural resources. The meaning of sustainability in buildings and sustainable architecture and its principles are also discussed throughout this chapter.

Generally, the chapter overviews the conflict between climate and architecture in hot-arid regions. It also explains the bio-climatic architecture and other different architectural concepts intended to be suitable and practical solutions that can effectively lessen the world's environmental damage and contribute to finding answers to the global energy crisis. The chapter also illustrates that sustainable architecture can lead to reviving the missing architectural character and identity of such regions, which traditionally were able to cope with the harsh climatic conditions of tropical and hot-arid areas. The chapter reviews Egypt's climate in general and its southern part new communities in particular, which is classified as a hot-arid and desert climate.

Due to their limited resources, developing countries need to construct most of their new communities' taking into account scarce energy resources and environmental sustainability. Energy efficient buildings, which provide indoor thermal comfort mainly by effectively applying a number of passive techniques, can contribute to achieving this goal.

Finally, the chapter as a starting point explores the different aspects of the research problem and discusses the necessity of handling such topics. Moreover, it proposes the possible practical solutions of relying on passive techniques to provide indoor thermal comfort in buildings.

Thereby, lowering consumption of non-renewable energy resources and consequently lessening the outcome pollutants, which are both major causes of the existing environmental situation. Many of today's buildings **MUST** be considered environmental destroyers as shown in Figure (2-1).

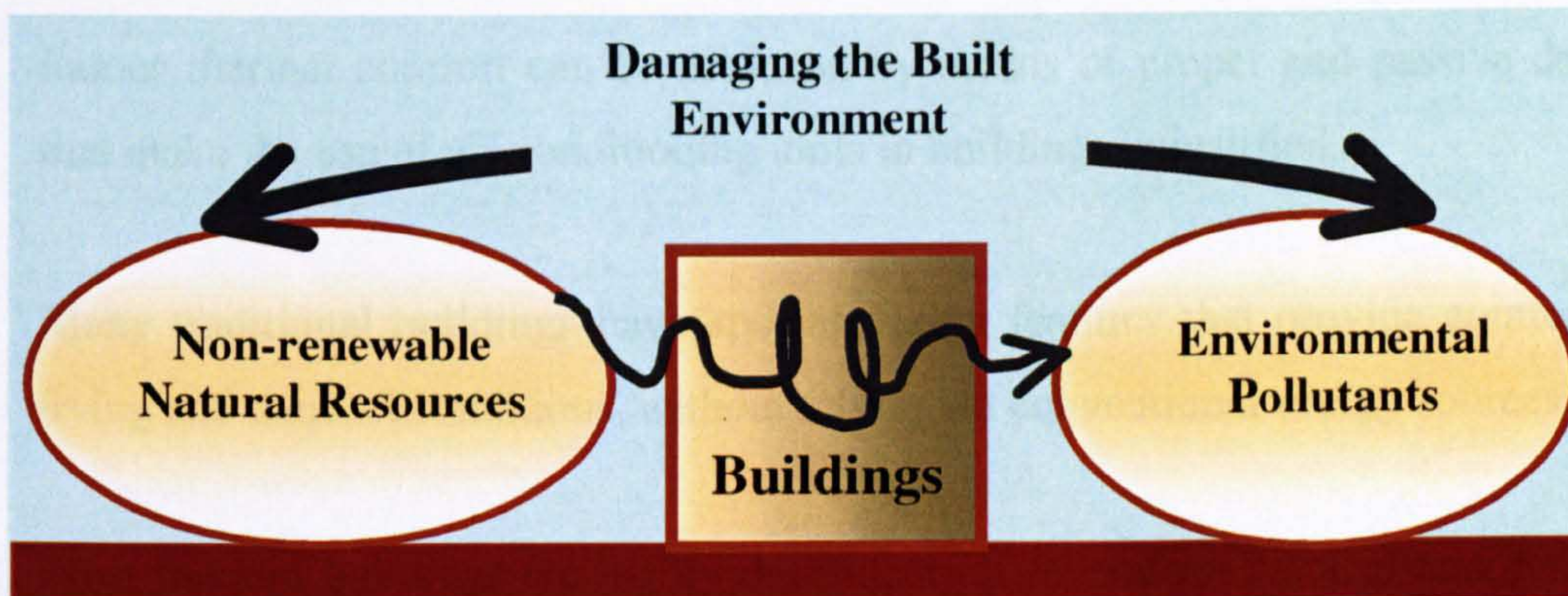


Figure 2-1 Buildings, Environment and Non-Renewable Resources

Passive cooling and heating strategies in buildings should be seriously considered in both hot and cold climatic conditions, as relying upon artificial systems to provide indoor thermal comfort year round demands high-energy consumption. The following sections show that the required and consumed energies for climatic conditions controllers and providing thermal comfort in buildings, are quantitatively and qualitatively the mutual responsibility of building designers and users.

Among many other fundamentals that prove the research potentialities, the following six aspects can clearly summarise the importance of creating sustainable and energy efficient architecture.

1. The required energy for heating and cooling in buildings represents high ratios of many parts of the world energy consumption [2].
2. By proper environmental design, at least 2.35% of world energy output can be saved [2].
3. In general, cooling systems are more expensive and less efficient comparing to heating. However, the annual needed energy for cooling in hot climate regions is two or three times that for heating.
4. Indoor thermal comfort can be achieved by means of proper and passive designs that make the use of air-conditioning units in buildings unjustified.
5. Many traditional buildings have special design features that provide comfortable living and thermal conditions, without relying on conventional energy sources.
6. Most modern buildings are highly dependent on several mechanical and electrical systems to control indoor environments and consume large quantities of fossil fuels that cause a severe negative impact on the environment in order to achieve this.

2.1 ENERGY, NATURAL RESOURCES AND POPULATION GROWTH

The earth is rapidly becoming a more crowded place. Therefore, current concerns regarding environmental crisis on both local and global levels reflect a general acceptance that the present form and degree of resources exploitation and the associated consumption practices are unsustainable. Rapid population growth and people lifestyles, due to rapid urbanisation, have led to deterioration of natural energy resources on both a world basis and a developing country-basis [3].

Urban population in developing countries is growing at 3.5% per year; while in the developed countries the rate is less than 1%. In 1990, 43% of the world's population was urbanized. United Nations studies indicate that the total global population reached 6.5 billion persons by year 2000. Cities have reached tremendous sizes that have placed strains on natural resources and negatively affected the environment [3].

Since 1945, exponential growth has led to a rapid expansion of numbers on an ever-increasing population base. Whilst the rate of population growth has declined and stabilized at very low levels in a number of developed countries, the high birth rates in developing countries has ensured this rapid expansion of global population. In other words, within the next decades, more than half of the world's population will be living in urban areas [3].

In many developing parts of the world, remote rural settlements have to seek an affordable better standard of living without much relying on either migration to urban settlements or non-renewable energy resources. The application of natural renewable energy resources and passive thermal comfort techniques is an energy conscious and efficient concept, which proposes more sustainability with suitable scales and norms in both existing and new communities.

2.1.1 World's Population Growth and Energy Consumption Rates

During the 1950s and 60s world energy consumption increased at a vast rate, and has grown 52% in the last two decades. In 1800 when about 1000 million people lived on earth, energy consumption was stated as 10 million tons of oil equivalent/ year (1 million tons of equivalent oil generate 4 billion kilowatt-hours of electricity) [3]. After 100 years, in 1900, the population had grown to about 1700 million people, who consumed 800 million ton/year.

In 1998, the world's population reached about 5800 million people with 8800 million ton/year of energy consumption. Over 90 % of global energy production comes from fossil fuels (coal, oil and gas), which in turn are responsible for the great majority of the world's severe environmental damage [1]. The world population increased from 3600 million people in 1970 to 5800 million people during 1998; it reached more than 6000 million people in 2000. The World's population is estimated to reach over 9000 million people by the year 2050 [3].

The average of the annual growth rate during the period (2000-2050) in the developing part of the world is about 1.7%, while it is 0.1% in the developed part. Figure (2-2) shows the total world population size in 2000 and its projections at 2025 and 2050 in both developing and developed parts of the world [4].

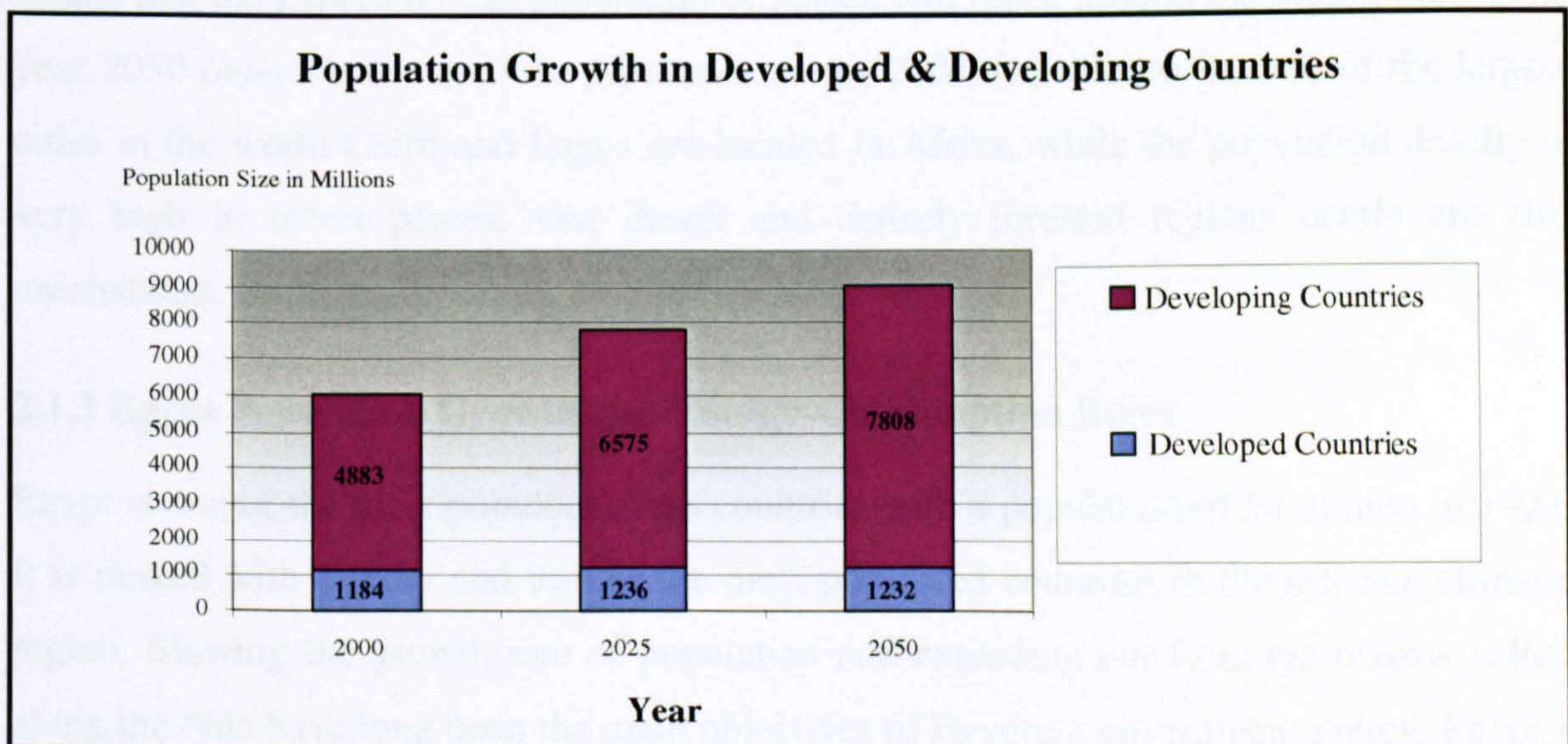


Figure 2-2 World's Population Growth (*Developed & Developing Countries*) [4]

2.1.2 African Continent Population Growth and Energy-Consumption Rates

Africa is home to around 800 million people (over 13% of the world's total population). About 29% live in West Africa, 27% in East Africa, 18% in North Africa and 10% in Central Africa; Fig. (2-3).

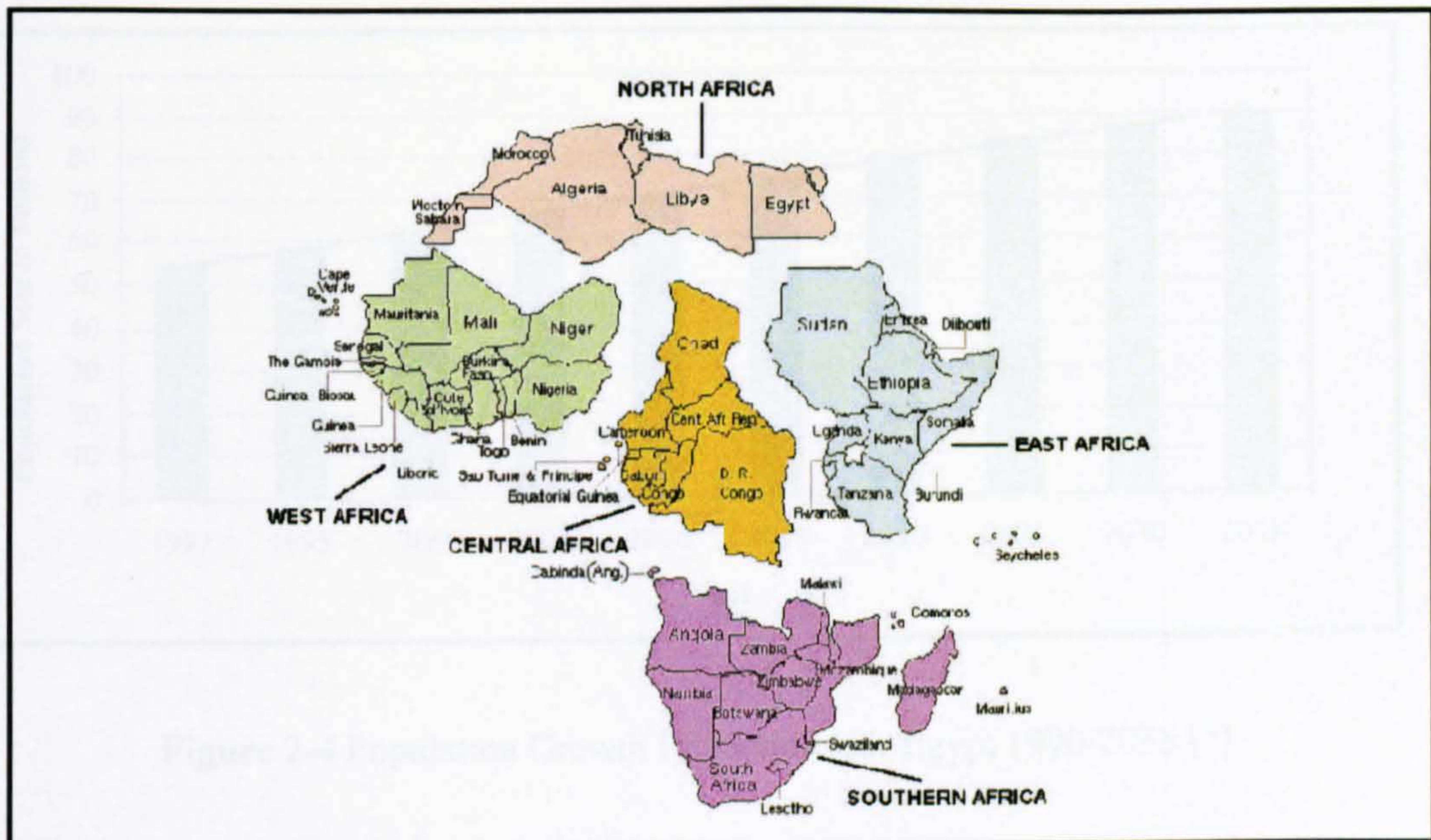


Figure 2-3 Map of African Continent Map and Regional Parts [5]

Population in Africa is growing rapidly. It has more than doubled since 1970. The yearly growth rate is about 2.7%, which is considered as the fastest growth rate in the world [4]. Population growth rates are expected to slow to reach around 2% through 2020, which means that the expected total population of Africa will reach around 1.8 billion during the year 2050 (*more than twofold the population during 2000*) [6]. Moreover, two of the largest cities in the world Cairo and Lagos are located in Africa, while the population density is very high in urban places, vast desert and densely forested regions nearly are still uninhabited.

2.1.3 Egypt Population Growth and Energy-Consumption Rates

Egypt is one of the most populous Arab countries with a population of 54 million in 1992. It is ranked with Turkey and Iran as the most populated countries in the selected climatic region. Slowing the growth rate of population and extending out from the narrow valley along the Nile have long been the main objectives of Egyptian government policy. Egypt's population was 10 million in 1897, increased by almost six times since the beginning of the 20th century and by almost three times from 1950 to the present as shown in Fig. (2-4).

Approximately 95% of Egypt's area forms desert, it depends mainly on the Nile River for all its life activities [7]. In addition to their sociological behaviours and attitudes, this geographical distribution continuously leads most of the Egyptian population to live in the narrow bands of the Nile valley, which represents only 5% of Egypt's total area [8].

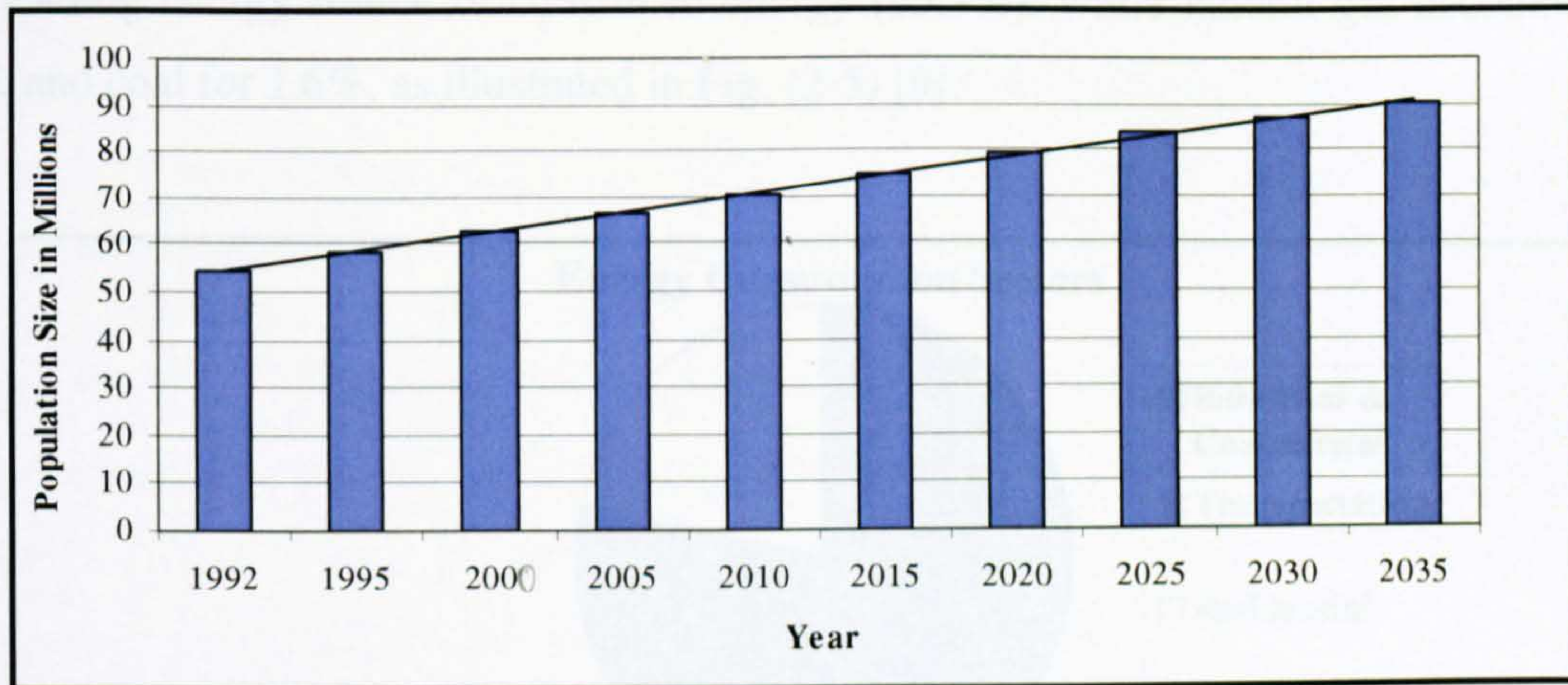


Figure 2-4 Population Growth Projections for Egypt 1990-2035 [7]

The population grew slowly at an average rate 1.3% per annum from 1897 to 1947, but accelerated greatly after World War II. The growth rate was around 2.5 % between 1950 and 1970. It dropped to 2.2% during the period from 1970 to 1975, reached 2.6% during the period from 1980 to 1985. Since 1985 the growth rate has begun decreasing to reach 2% in 1993 and 1.9% in 2000. The present population size is about 68 million.

Modern development has placed great stress on Egypt's environment, as well as the world's environments. The need for better environmental protection in the world generally and Egypt particularly, is clear. In 1994 Egypt passed the "Environmental Protection Law", as a result of its rising level of energy consumption, which is also a major factor behind the country's environmental damage. Over the last 20 years, Egyptian energy consumption has risen 171% [7].

Egypt's increasing energy consumption is still comparatively below other countries in the region. Egypt's energy consumption per capita is significantly lower than other developed countries. Fig. (2-5) shows that industry and commercial activities accounted for 53.6% of all energy consumed in Egypt, with transportation (24.7%) and residential (22.1%). Oil is the leading energy source of consumed energy (63.7%), while natural gas accounted for 28% and coal for 1.6%, as illustrated in Fig. (2-5) [9].

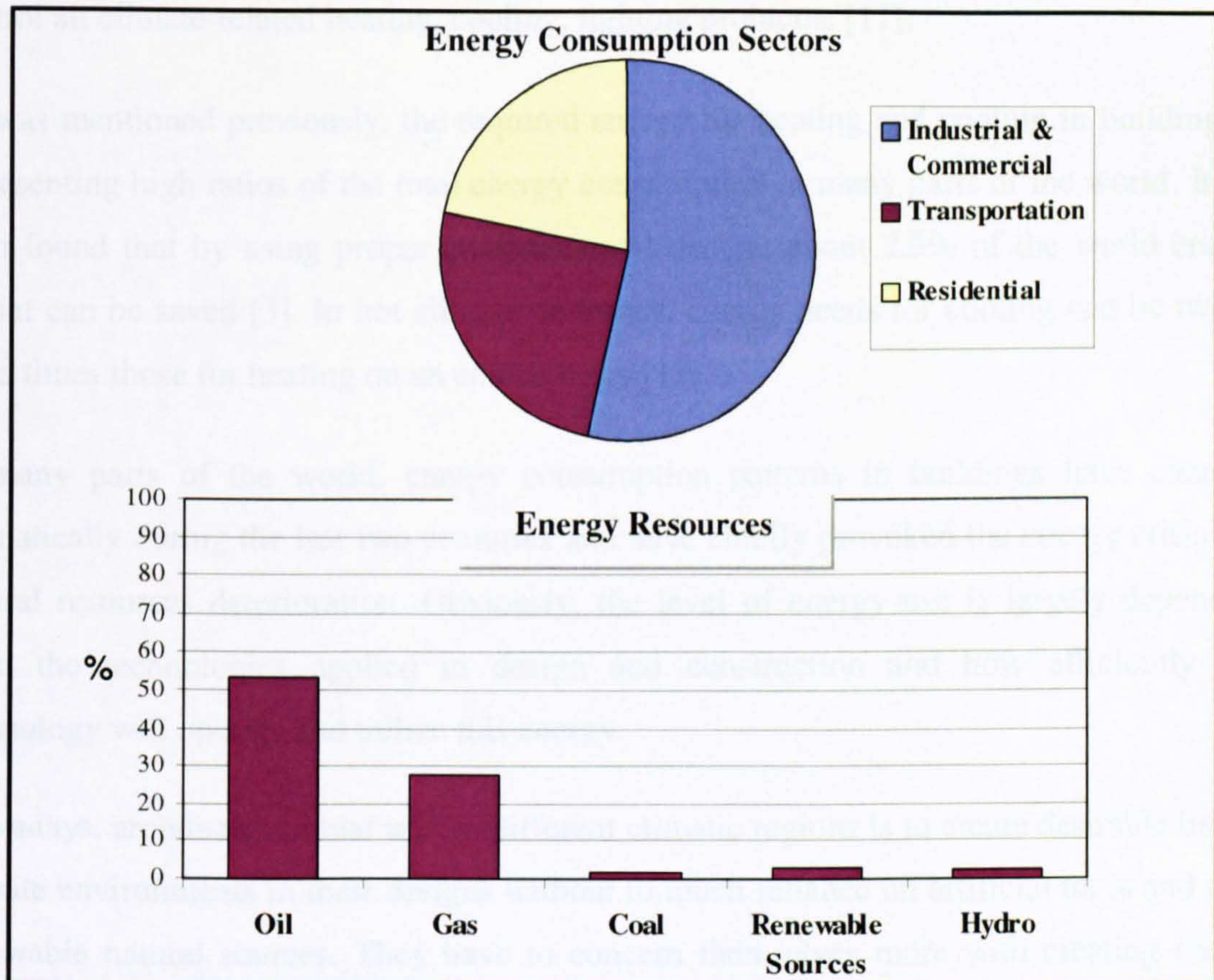


Figure 2-5 Egypt's Energy Consumption and Resources
(Up to 75% of the total energy consumption occurs in Buildings) [9]

2.2 ENERGY EFFICIENT BUILDINGS AND SUSTAINABILITY

Sustainability as a term related to resources, became widely used with the publications of the International Union of Conservation of Nature "World Conservation Strategy" in 1980. It describes a state where renewable resources are used in a safe manner that does not eliminate and degrade them or their usefulness for future generations [10].

The energy crisis has not disappeared yet, but rather important technological developments in architectural design have taken into consideration for design and construction detailing. It is becoming obvious that architecture in general and buildings in particular, are contributing significantly in all recent environmental problems. This situation is a continuous one because owners, users, architects, designers and decision-makers are still looking to solve their energy needs mechanically. They are not well prepared to integrate with such systems and nowadays' building designs are reliant on mechanical systems to control all climate-related heating, cooling, lighting problems [11].

As was mentioned previously, the required energy for heating and cooling in buildings is representing high ratios of the total energy consumption in many parts of the world. It has been found that by using proper environmental design, about 2.5% of the world energy output can be saved [3]. In hot climate countries, energy needs for cooling can be two or three times those for heating on an annual basis [12].

In many parts of the world, energy consumption patterns in buildings have changed dramatically during the last two centuries and have chiefly provoked the energy crisis and natural resources deterioration. Obviously, the level of energy use is largely dependent upon the technologies applied in design and construction and how efficiently this technology will operate and utilize this energy.

Nowadays, architects' crucial task in different climatic regions is to create desirable indoor climate environments in their designs without to much reliance on artificial tools and non-renewable natural sources. They have to concern themselves more with creating energy efficient designs, which are compatible with occupants' life styles and also addressing more environmentally friendly designs that form a real sustainable environment.

2.2.1 Global Environmental Impact From Current Energy Use

According to the World Energy Council, global CO₂ fossil emissions rose 6.4% between 1990 and 1996 and by 2.7% during 1996 alone [1]. Greenhouse gas emissions have caused an increase in air temperature [12]. Several studies confirm that in fact, the world's average air temperature has risen between 0.3 and 0.6 °C since the late 19th century [1]. It means that the dry bulb temperature of the air has increased about 0.5°C in the last 100 years. This clearly indicates a global climatic change. In records, the last 10 years have been the warmest since the 1880s [1].

These environmental conditions place the world in a hazardous situation and have also caused other several environmental changes such as the increasing of sea levels of between 10 and 25 cm during the last 100 years. Nowadays the global potential of natural renewable energies and improving energy efficiency through buildings are very important factors to reduce recent environmental damage, also to save our future [13].

In Cairo, which is the home to one-fourth of Egypt's population, air pollution is a serious environmental problem due to the rising energy consumption levels [7]. The concentration of total suspended particulate matter in Cairo is 5-10 times higher than World Health Organisation (*WHO*) guidelines, and on average, sulphur dioxide is four times higher, smoke and lead are three times higher, and nitrogen oxides are two times higher [7]. The increasing demand of using air-conditioning units in the hot-arid climates causes many environmental problems, which can be summarised in four main problems:

1. **Energy Consumption Problem**, wide use of air-conditioning units has caused a shift in electrical energy consumption during the summer season, increasing electricity demand. Peak electric loads impose an additional strain on national grids, which can only be covered by development of extra new power plants.
2. **Environmental Problems**,
 - Increased electrical energy production contributes to exploitation of the finite fossil fuels, to atmospheric pollution and to global climatic changes [12].
 - During the production process (fuel conversion), CO₂ is released which is one of the main causes of the greenhouse effect [12].
 - Heat rejection during operation of air-conditioning units increases the phenomenon of "Urban Heat Island" [12].

- CFC and HCFC (the most common refrigerants of currently used air-conditioning units) can cause ozone-layer depletion from a possible leakage during manufacture or system maintenance.
3. **Indoor Air Quality Problem**, people working in air-conditioned buildings report increased cases of illness symptoms (lethargy, Headache, Blocked or runny nose, dry or sore eyes, dry throat and sometimes dry skin and asthma), known as “sick building syndrome”[2,12].
 4. **Economic Problems**, economic and political dependence of countries with limited natural resources on other countries, richer in natural resources [12]. Installation of air-conditioning units presents an extra cost in the construction of a building, followed by an additional operation and maintenance cost, in addition to its transport expenses.

2.2.2 Sustainability in Architecture and Buildings

The term "sustainable" communicates slightly different meanings to various audiences and it seems as a complicated term to others. This part passes through some relevant definitions to establish an adequate understanding for this term and also to make the concept of sustainable architecture clearer. The verb “sustains” means to support, to keep alive, or to keep going continuously. “Sustenance” is the process of sustaining life and the adjective “sustainable” is used to describe an object that gives continuous support and relief. [10].

Sustainability in architecture is not a “topic” but an “attitude”. It is a process of responsible consumption, wherein waste is minimised, buildings interact in balanced ways with natural environments, balancing the desires and activities of humankind and finally, achieving a stable long-term relationship within the limits of their local and global environments [4,14].

After those definitions and even after further discussions, which are included in this part and the following parts, numerous questions are still in need of definitive answers. What are the most practical and most effective means to begin with? What strategies are most critical for architects and their designs? What strategies are most suitable to provide energy efficient designs and buildings? What do architects have to do? What should be done to promote sustainability in architecture? The research presented in this thesis and other related research attempts are serious trials to answer such questions.

Sustainable architecture as an approach is the practice of designing buildings that create more desirable living environments with the minimum use of non-renewable energy and natural resources. It is very important to address the issue of sustainability in modern architecture and buildings. Sustainable architecture is an operating concept that provides "sustenance" to users through healthy and environmentally friendly built environments, thus improving the life quality towards a long-term survivability of human generations and their natural resources.

Building materials and designs, and post-operating systems, (*such as heating, cooling and power*) have a great role towards providing such buildings. "Sustainable" from an environmental aspect is the processes of maintaining an ecological balance, exploiting natural resources without destroying the ecological balance of a particular region.

Before sustainable architecture, the term "solar architecture" expressed the architectural approach to reducing the consumption of natural resources and fuels by using solar energy. Sustainable architecture is a broader concept and it expands the scope of the issue involved. It includes water use, climate control, food production, solid waste materials, emphasising the use of local materials and renewable energy resources. Moreover, it includes the mental and physical comfort of building's inhabitants. In other words, designing a building that harmonises with its environment and surroundings as naturally as possible is sustainable architecture.

Steven Strong stated, "The term is intellectually dishonest", and the society does not know exactly how to build a sustainable architecture, Dick Levine went further and stated that the term "sustainable architecture" is an oxymoron"[15]. The term popularly understood is inadequate. The appropriate uses and aims of the term are not clear enough, which consequently forms negative influences on the expansion of the sustainable architecture movement in developing countries.

Hunter and Amory Lovins, determine that the purpose of sustainable architecture is to "meet the needs of the present without compromising the ability of future generations to meet their own needs" [16]. It applies to design buildings that can provide indoor thermal comfort by more dependence upon renewable resources to reduce energy consumption and environment pollutants.

John Tillman Lyle described sustainable architecture in terms of a “Regenerative Design for Sustainable Development”, or “Regenerative Architecture”. Others simply explain it as an approach to making buildings less consumptive of natural resources [17].

The United Nations lists the main principles of sustainable architecture as the following [18]:

1. Healthful Interior Environment
2. Resources Efficiency
3. Ecologically Benign Materials
4. Environmental Form
5. Proper Design

Finally, the better architects understand and implement their stewardship of the built environment, the better the quality of life that present and future generations will enjoy. Such a movement needs environmentally sensitive architects who are able to integrate different environmental-responsive concepts into their final designs effectively.

2.2.3 Climate Conscious Design in Sustainable Buildings

The current attempts and practices of creating sustainable designs work within a range of green strategies including and not limited to, passive or active solar design, wind technologies and passive cooling or heating designs. Architects should learn to generate new sustainable typologies from the climate formed from traditional vernacular buildings. Many modern passive design technologies have learned to build upon the climatic responsive methodology that was found in vernacular and traditional buildings.

The sought approach is not only towards more sustainable architecture and environment, but also to create an architectural identity, which is recently missed. *Charles Correa* said: "We have to know from where we are coming to know where we are going" [19]. Climate conscious design is considered as one of the sustainable architecture promoters. Fig (2-6) clarifies a schematic diagram of the sequence of a sustainable design process.

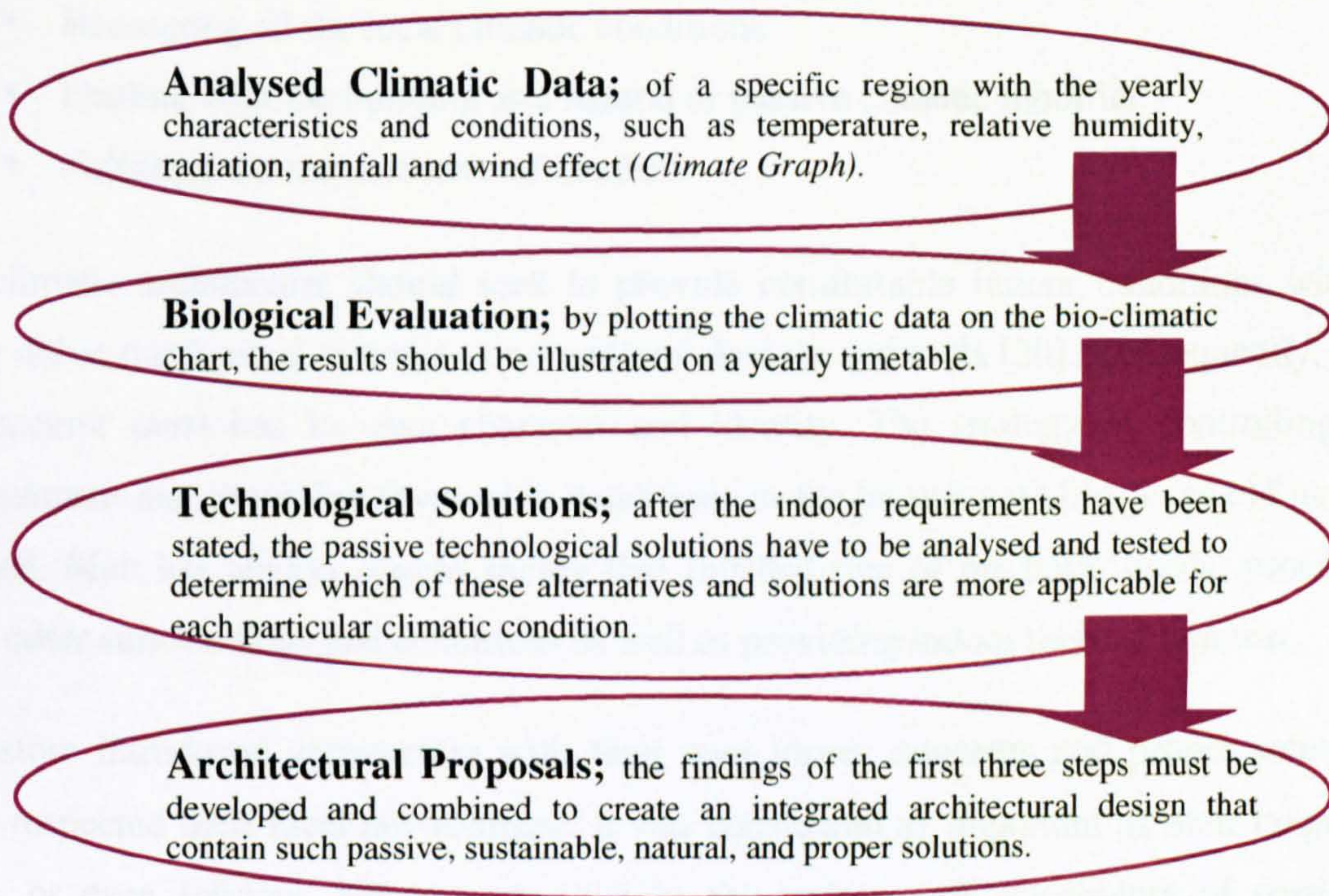


Figure 2-6 A Sustainable Design Process

Finally, no rigid recommendation can be produced, because there are many architectural alternatives to approach the goal of indoor thermal human comfort at each particular location [20]. Site selection, building orientation according to the sun's path and its solar radiation could be the right solution for a particular case, whilst shading devices may also be the right one.

Building forms and shapes, or roofing systems may be the only successful solution for the solar radiation problems for a specific location. Air movement and natural ventilation tools such as openings location, arrangement, sizes and the ratio between inlet and outlet sizes and other special architectural vocabularies are capable of providing indoor thermal comfort passively in another location.

2.2.4 BIOCLIMATIC Architecture

(An approach towards reviving the missing architectural character)

It seems advisable to define the *Bio-climatic* architecture, which is not a newly known architectural style or approach. It is an old well-known approach that provides one or more of the following objectives [20]:

- Respecting all the local climatic conditions
- Dealing with the building as a natural or passive climatic modifier
- Fulfilling the requirements of comfort.

Bio-climatic architecture should seek to provide comfortable indoor conditions without using either mechanical systems or non-natural devices and tools [20]. Consequently, such architecture must have its own character and identity. The strategy of controlling the environment and providing favourable conditions to the human activities is as old as man himself. Man has always sought shelter that fulfilled two of his basic needs; protection from outer surroundings and conditions as well as providing indoor thermal comfort.

Ancestors introduced architecture with their own forms, concepts and proper solutions. They respected their local environment. It was considered as important as their language, dress, or even folklore. No one can mistake the architectural vocabulary of particular region, or fail to recognise its signature.

Yet many architectural graduates in the developing world believe that they should design with a different style. But which style are they going to choose in their designs? As if they imagine that buildings can change their style according to the architects' morals, or as a man changes his clothes [8]. Therefore, *Middle East, Egypt and North Africa Region* cities and villages are becoming ugly and are lacking harmony with built form, culture, place and climate. This situation can be improved by architecture take into account both local climate and indigenous people.

2.3 CLIMATIC DESIGN AND INDOOR THERMAL COMFORT

Boundaries of climatic zones are very difficult to determine or to be accurately mapped. The zones gradually merge and almost overlap into each other. Tropical climates are those where heat is the main problem when designing for *Human Thermal Comfort in Buildings*. The main emphasis is placed upon building design that provides desirable indoor environments and serves to keep occupants thermally comfortable throughout the year.

The annual mean temperature in such regions is not less than 22°C. G.A. Atkinson[21] suggested the classification in Table (2-1), in 1953. It was classified according to air temperature and humidity as the main factors influencing the human thermal comfort. The table divides the tropical zone climatically into three major zones and three other sub-zones [21].

Basically, climate is defined by the Oxford dictionary as “region with certain conditions of temperature, dryness, wind, light, etc”. Another scientific definition is the integration in time of the physical states of the atmospheric environment, characteristic of a certain geographical location [21]. The comparative analysis of traditional architecture along the tropics with their different climatic conditions, suggests that climate always has a significant influence on building design, form, orientation and materials. Egypt, Yemen, Turkey, Greece and Spain are good examples for such climatic influence on architectural products [21].

In general, the properties of energy efficient and sustainable architecture must be considered in order to fully understand the local climatic conditions. In a changing climates environment, the architect has to place a fixed building. Such a rigid structure is intended to provide a comfortable internal environment over a wide range of these external variables. Two factors facilitate this task: first, in temperate and subtropical zones, ordinary buildings offer fair protection from climatic extremes, and, second, the human body has a considerable margin of tolerance for these variables. However, special treatment is required, particularly in tropical zones [22].

Table 2-1 Tropical Climatic Classification Zones [21]

CLIMATE	EXAMPLES	Air Temperature (°C) in the hot seasons			Humidity RH%	Precipitation Annual Rainfall	Winds	Vegetation
		Day Time In Shade °C	Day Time °C	Night °C				
WARM-HUMID	Legos, Jakarta, Dar El salaam	27-32	Over 32	21-27	75 55 - 100	2000-5000mm	Low velocities, frequently calm, Strong during rains	Soil are generally poor for agriculture
<i>Warm-humid island</i>	Caribbean islands	29-32	Over 32	18-24	55 - 100	1250-1800mm	6-7m/s provides relief from heat & humidity, (45-70m/s hazardous tropical hurricanes)	Soil is often dry with low water table
HOT-DRY	Arizona, Cairo Aswan	34-38	43-49	24-30	10 - 55	50-150mm	Local hot, carrying dust & sand (dust storms)	Sparse and difficult because the lack of rain and low humidity
<i>Hot-dry maritime</i>	Kuwait, Karachi	38	Over 38	24-30	50 - 90	Very Low	Local coastal	Sparse & Dry grass
COMPOSITE	Lahore, Kano, New Delhi		(1)	(2)	Dry 20-50 Wet 55-95	500-1300mm	Hot dusty during (1), Strong steady humid wind from the sea during (2)	Sparse in (1), Green and grow quickly with the rain in (2)
		Daytime max.	32-43	27-32				
		Night min.	21-27	24-27				
		Diurnal range	11-22 deg C	3-6 deg C				
<i>Tropical upland</i>	Nairobi, Mexico City, Addis Ababa	Day time 24-30 Night 10-13	45-99	Less than 1000mm	45-99	Less than 1000mm	More than 15m/s varies according to the topography	Green, the soil damp in rain and then quickly dries.

The composite climates usually occur in large land near tropics of Cancer and Capricorn, two-thirds of the year is hot-dry (1), and the other third is warm-humid (2)

In the past, there was no doubt that climate has had its impact on a number of design and construction elements and techniques, such as internal circulation, external orientation of buildings, roofs forms and thickness and the use of materials. Nowadays, the relationship between climate and architecture in most tropical countries in general, and in *Middle East, Egypt and North Africa Region* in particular, has been misunderstood. Many of the traditional architecture elements in such countries are being replaced by international modern designs, which are often not in harmony with the built form, culture, place and climate. The principle climatic elements in general, and the climatic characteristics of the studied area Egypt and its southern parts as hot-arid regions in particular, are discussed throughout the following sections of this chapter.

2.3.1 Hot-Arid Zones; Climatic Characteristics & Geographical Locations

Hot -Arid climate zones are found in the sub-tropical regions of Africa, central and western Asia, north western and southern America, and in central and Western Australia. In all these cases the climatic conditions are caused by the trade winds, blowing southwest and northwest towards the equator, losing most of their water vapour. Due to the pressure and down-flow in these regions the air becomes heated and dried [23].

The geographical latitude influences climatic conditions and their annual ranges. Direct solar radiation intensity is up to 814-930 W/m² on the horizontal surfaces, the low humidity and the absence of cloud result in a very wide temperature range. In summer the unobstructed solar rays heat the land surface up to 70°C at midday, while at night the rapid loss of this heat by long-wave radiation cools the surfaces to 15°C or below [21]. The summer maximum temperatures during the day are around 40-50°C, and the mean minimum night temperature within the range 27-32°C.

The diurnal range is about 15-25 deg C. The maximum day temperature is between 24-30°C and the minimum night temperature is between 10-20°C in winter [21]. The relative humidity in these areas fluctuates with the air temperature, ranging from below 20% in the afternoon to over 40% at night. Sometimes the wind direction changes and brings air from the sea, which can raise the humidity.

Rains are few, and precipitation sometimes starts at high altitude that means the water evaporates before reaching the ground. Shortage of vegetation causes low-level winds. The wind speed is generally low in the morning, rising towards noon to reach the maximum in the afternoon; frequently it is accompanied with sand and dust. As it is considered the main causal factor for overheating problems in tropical and hot-arid regions, solar radiation will be discussed in more details in the following chapters.

Solar geometry (*Sun path and position*), and earth-sun geometrical relation also will be discussed to find out the solar radiation influences on indoor thermal comfort in buildings at different latitudes. This chapter identifies the requirements of indoor thermal comfort in such climatic conditions. It also illustrates the different factors that can affect the thermal human comfort in buildings.

2.3.1.1 African Continent Climatic Regions & The Selected Hot-Arid Zone

According to the previous climatic zone criteria, the African continent is classified geographically as shown in Fig. (2-7) by three main climatic regions and other three sub-regions.

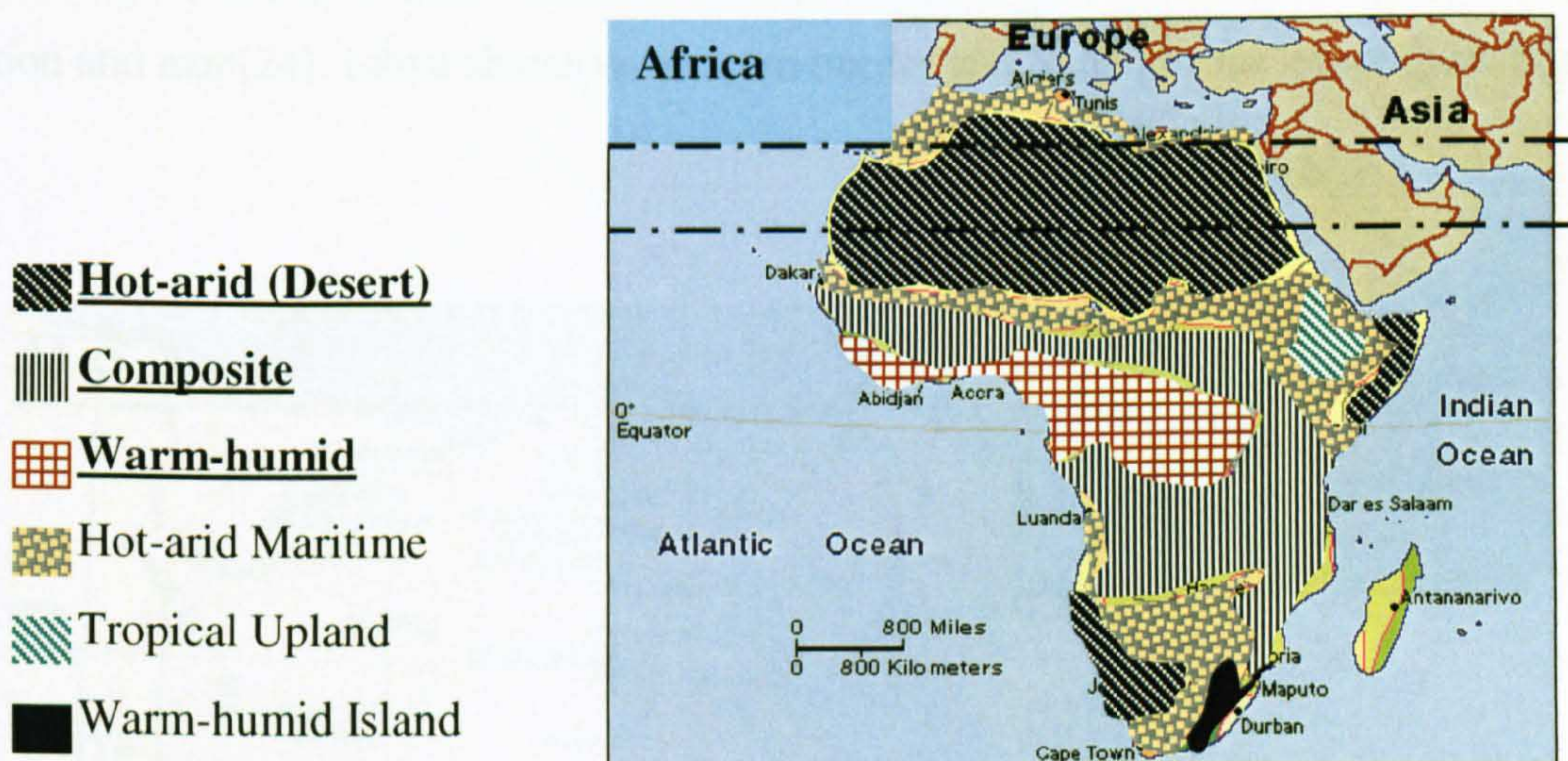


Figure 2-7 Africa Climatic Regions & the Selected Hot-Arid Zone (After Hamdy [24])

The North-African and Arab countries are considered hot-arid countries that lie in the greatest hot -arid zone in the world. This zone extends from the Atlantic coast across North Africa and the Arabian Peninsula to the Indian subcontinent, Fig. (2-8).



Figure 2-8 Middle East and North Africa Region [5]

2.3.1.2 Egypt Climate & Geography

Egypt is located in the northeaster corner of the North African hot-arid zone, it is situated between latitude 22° N and 31.5° N. Egypt’s coastline prolongs the Mediterranean Sea from the north, and its eastern coastline extends along the Red Sea. Fig. (2-9) shows Egypt location and map[24]. Libya shares its western border and Sudan forms its southern border,



Figure 2-9 Map of Egypt and Geographical Location [5]

Egypt's climate in general is a hot-arid climate, classified as extremely arid. It is hot and dry in summer with cold and mild days during the winter[25]. Rainfall occurs only during the winter months. It varies from a trace in the southern part "Upper Egypt" (due to the flow of Nile south to north). to less than 7 inches in Alexandria on the Mediterranean coast. In Cairo rain rarely exceeds 2 inches a year and the humidity level is relatively low[25].

Egypt covers an area of approximately 1,001,450 sq. km [26], but the inhabited and cultivated area is less than 40'000 km², which is about 5% of Egypt's total area. The population density in those inhabited areas is about 1800 capita/Km² [8]. Most of those cultivated settlements are grouped along the Nile. As shown in Fig. (2-9), the Nile emanates from Sudan flowing north through the country for 1,545km, emptying into the Mediterranean Sea and all along its course provides Egypt and her people with life and sustenance.

Fig. (2-10) illustrates Egypt's map, which mostly is desert. It is bisected by the Nile-river. Yet, over 90% of its land area is desert, the Libyan Desert to the west, the Sahara and Nubian deserts to the south and the Arabian Desert to the east.



Figure 2-10 The Inhabited Areas Along the Nile Narrow Valley [5]

2.3.1.4 Egypt Geographic and Climatic Classifications

Throughout history the Egyptian Nile valley has been defined geographically as two distinct regions. The first is Upper Egypt, which extends south of Cairo to the Sudanese border, and the second is Lower Egypt, which encompasses the Nile Delta north of Cairo[7], Fig. (2-11).

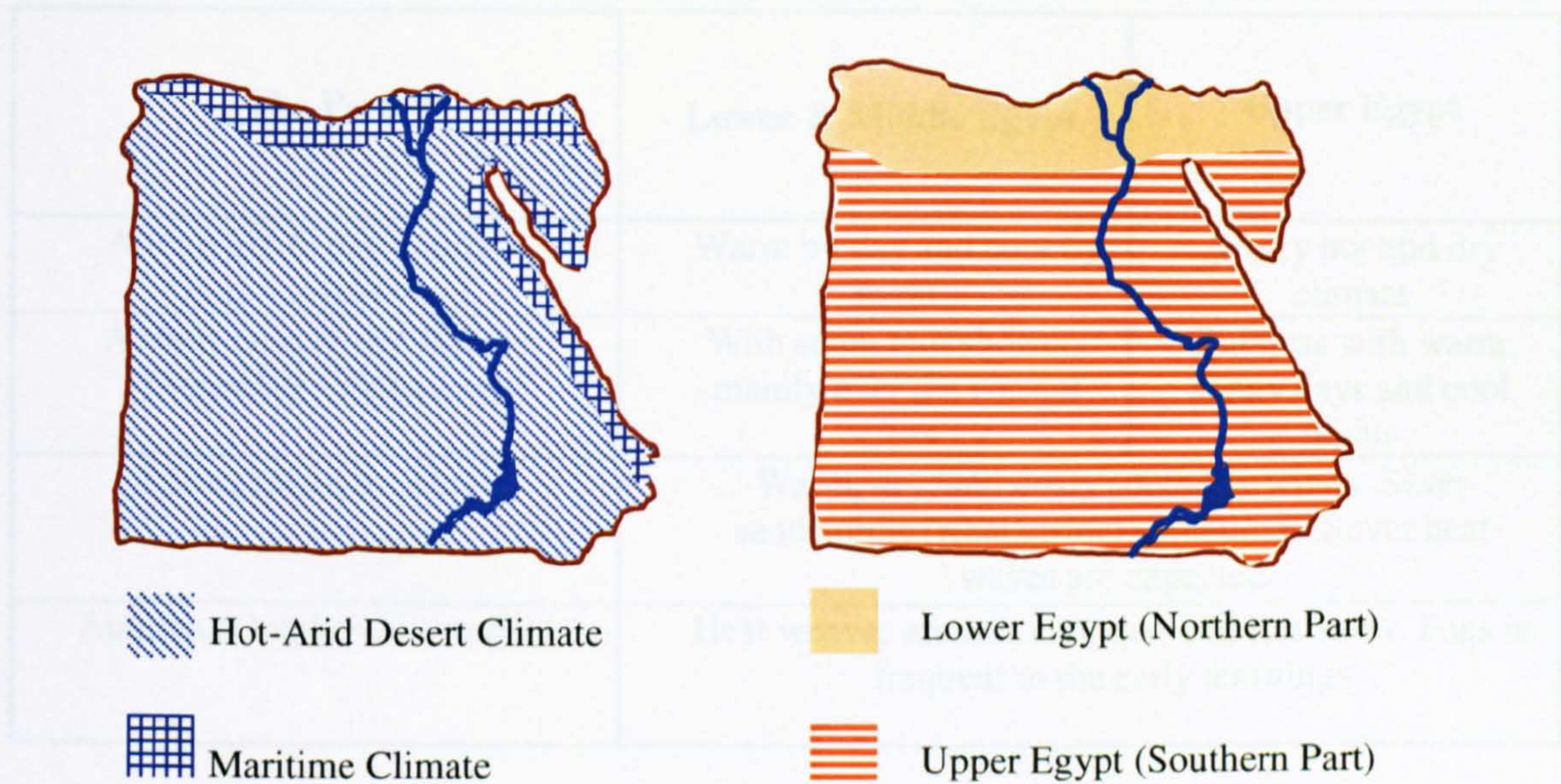


Figure 2-11 The Main Two Climatic Regions and Egypt Geographical Regions

As shown in Fig. (2-11) Egypt falls into two main climatic regions. The first is Lower Egypt region, which is represented by the northern part (north of 28°N). This is a maritime climate (*Mediterranean climate*) with mild winter and relative humidity more than 45% in average [24]. It covers the narrow strip (40km width) along the Mediterranean coastline. This climatic region includes also the Nile delta and the Red Sea coastline. It is characterised as a temperate humid climate with mild winters and summers.

The second is the Upper Egypt region, a hot-arid desert climate, which covers the rest of Egypt's area that extends from the Sudanese border towards the Nile delta. It is classified as a hot-arid zone with a very wide difference between day and night temperatures. Because of the absence of cloud screening, the ground by day receives a great amount of solar radiation [8]. So, any surface exposed to direct sunshine, such as the ground or the walls and roofs of a building, heats up during the day.

Consequently, the annual climate of Egypt can be divided into two main seasons and two transitional periods, which leads to marked clear difference between the upper and lower geographical regions as shown in Table (2-2),[24].

Table 2-2 The Annual Main Seasons of Egypt Climate

The Period	Lower & Middle Egypt	Upper Egypt
A long hot & dry Summer (June - September)	Warm by day and cool by night	A very hot and dry climate
A short mild & dry Winter (December - February)	With some rain showers mainly over the coastal areas	Rainless with warm sunny days and cool nights
Spring (March - May)	Warm, dry, and dusty southerly winds. Sever sandstorms (Khamasine) sometimes. Sever heat waves are expected	
Autumn (October-November)	Heat weaves are less common and less sever. Fogs is frequent in the early mornings	

Table (2-3) displays monthly solar radiation on horizontal surface in kWh/m²/day at different cities and geographical latitudes in Egypt [26].

Table 2-3 Global Solar Radiation on Horizontal Surface in KhW/m²/day [26]

	Jan.	Feb.	Mar	Apr.	May	June	July	Aug.	Sep.	Oct.	Nov.	Dec.
Cairo (Lat. 30.05°N)	3.04	3.70	5.04	6.05	6.96	7.45	7.25	6.64	5.71	4.49	3.29	2.85
Asyout (Lat. 27.03°N)	3.88	4.91	5.98	6.91	7.47	7.93	7.82	7.29	6.48	5.37	4.18	3.60
Khargah (Lat. 25.27°N)	4.43	5.43	6.38	7.17	7.66	8.02	7.90	7.45	6.70	5.64	4.68	4.13
Aswan (Lat. 23.58°N)	4.70	5.65	6.61	7.41	7.68	8.02	7.94	7.45	6.76	5.81	4.96	4.39

Monthly average temperature and humidity distributions at different cities and latitudes in Egypt are graphically illustrated in Fig. (2-12), (2-13). Temperature and humidity values are displayed in Tables (2-4) and (2-5) [26,27].

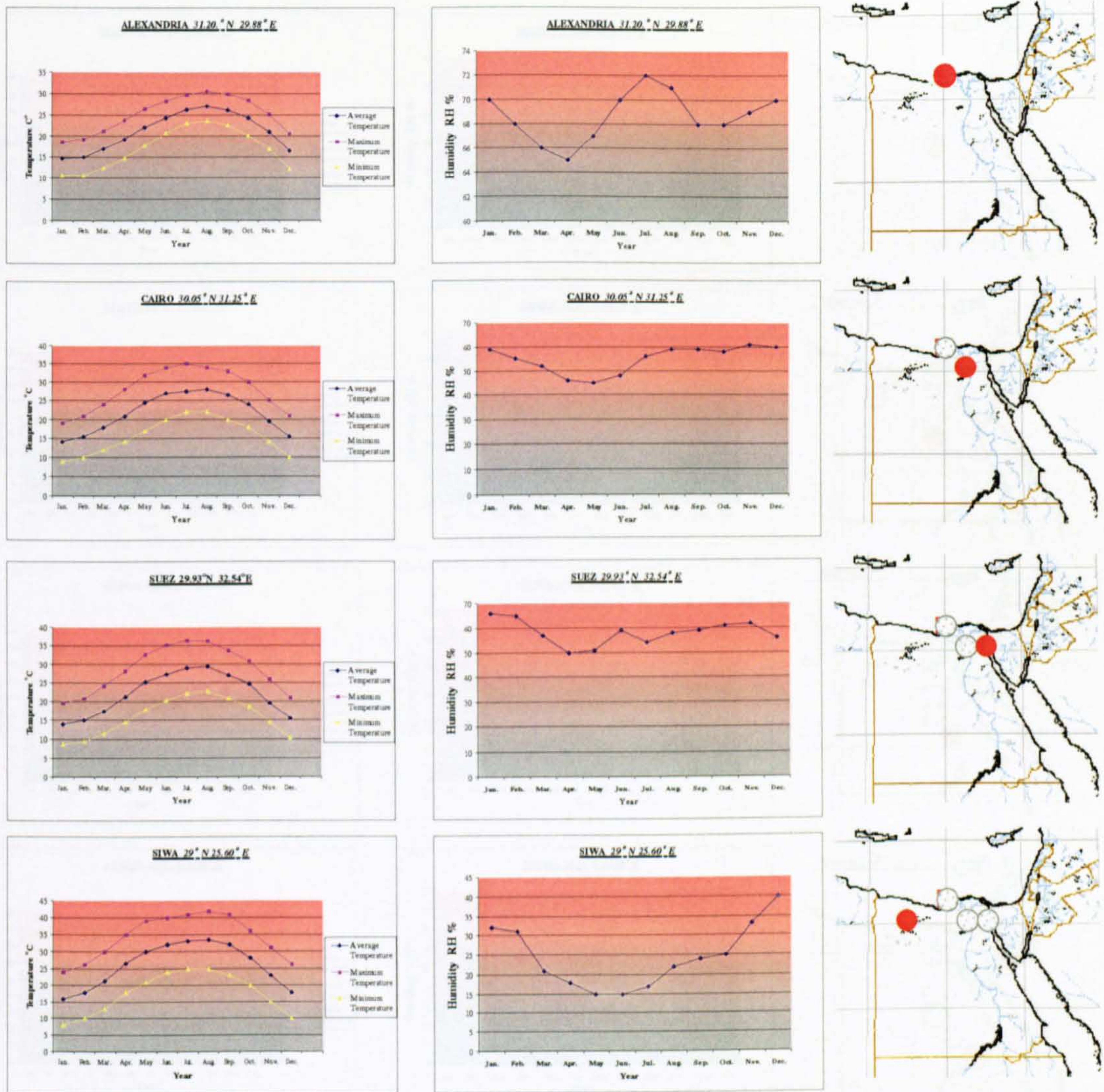


Figure 2-12 Monthly Average Temperature and Humidity Distribution Forms at Different Cities in Egypt

Table 2-4 Monthly Average Temperature and Humidity Values

Month	Alexandria 31°N 29.92°E			Cairo 30.05°N 31.25°E			Suez 29.98°N 32.55°E			Siwa 29°N 25.60°E		
	Max °C	Min °C.	RH %	Max °C	Min. °C.	RH %	Max °C	Min. °C.	RH %	Max °C	Min. °C.	RH %
Jan.	19	09	70	19	09	59	20	8	66	24	8	32
Feb.	19	09	68	21	10	55	21	9	65	26	10	30
Mar.	21	11	66	24	12	52	24	11	57	30	13	21
April	24	14	65	28	14	46	28	14	50	35	18	18
May	24	14	65	26	14	46	32	17	51	39	21	15
June	27	17	67	32	17	45	35	20	59	40	24	15
July	30	23	72	32	22	56	36	21	54	41	25	17
Aug.	31	23	71	34	22	59	36	22	58	42	25	22
Sept.	30	21	68	33	20	59	33	20	59	41	23	24
Oct.	28	18	68	30	18	58	30	18	61	36	20	25
Nov.	24	15	69	25	14	61	26	14	62	31	15	33
Dec.	21	11	70	21	10	60	21	9	56	26	10	40

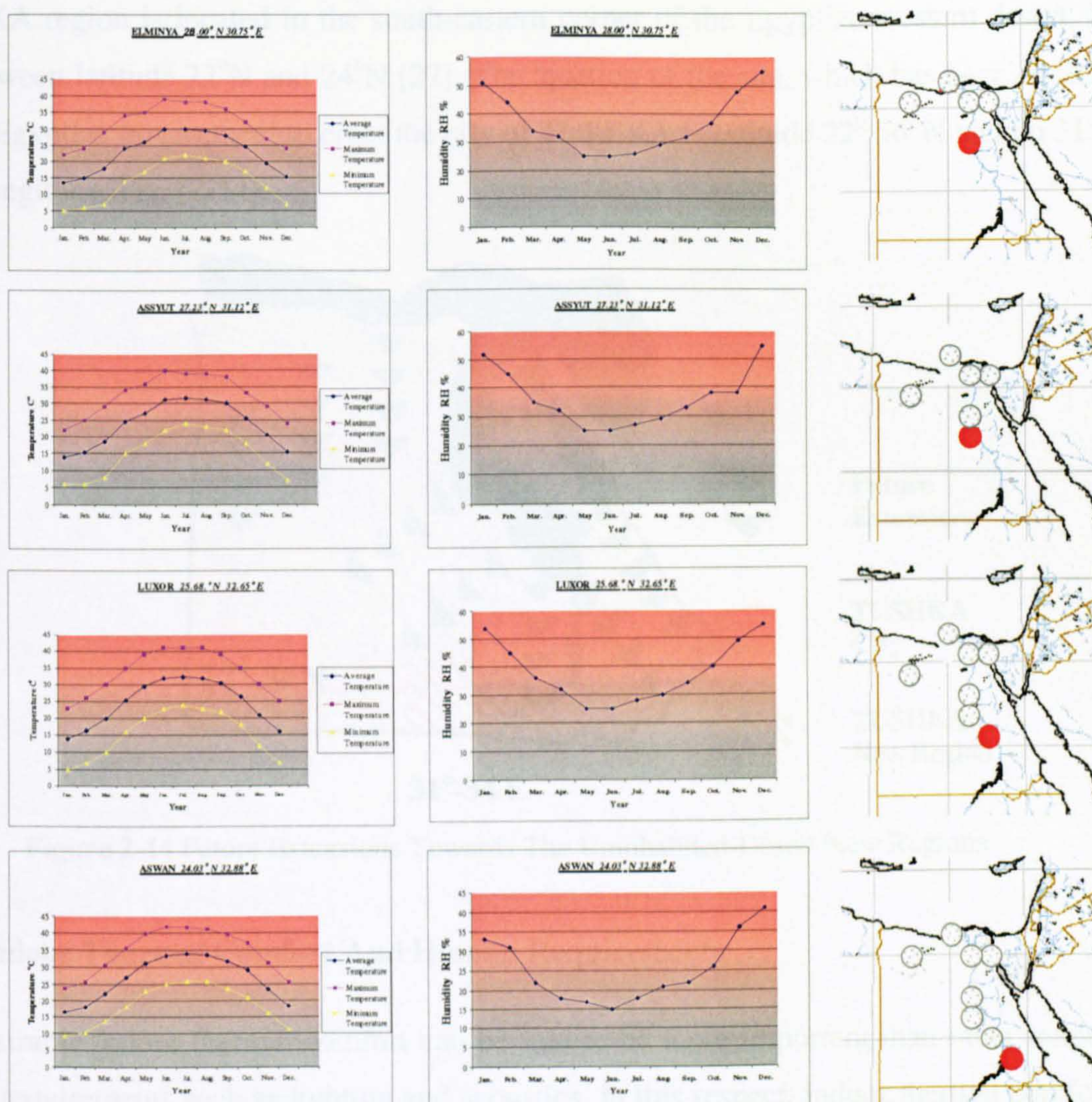


Figure 2-13 Monthly Average Temperature and Humidity Distribution Forms at Different Cities in Egypt

Table 2-5 Monthly Average Temperature and Humidity Values

Month	Elminya 28°N 30.75°E			Assyut 27.23°N 31.12°E			Luxor 25.681°N 32.65°E			Aswan 24.08°N 32.93°E		
	Max. °C	Min. °C	RH %	Max. °C	Min. °C	RH %	Max. °C	Min. °C	RH %	Max. °C	Min. °C	RH %
Jan.	22	5	51	22	6	52	23	5	54	24	8	33
Feb.	24	6	44	25	6	45	26	7	45	26	10	31
Mar.	29	7	34	29	8	35	30	10	36	31	14	22
April	34	14	32	34	15	32	35	16	32	35	18	18
May	35	17	25	36	18	25	39	20	25	39	22	17
June	39	21	25	40	22	25	41	23	25	42	25	15
July	38	22	26	39	24	27	41	24	28	41	26	18
Aug.	38	21	29	39	23	29	41	23	30	41	25	21
Sept.	36	20	32	38	22	33	39	22	34	40	23	22
Oct.	32	17	37	33	18	38	35	18	40	36	21	26
Nov.	27	12	48	29	12	38	30	12	49	31	16	36
Dec.	24	7	55	24	7	55	25	7	55	26	11	41

TUSHKA region is located in the south-eastern corner of the Egyptian western desert. It lies between latitude 22°N and 24°N [27]. The location of the site, which has been chosen by the Egyptian government to erect the city of TUSHKA is latitude $22^{\circ} 56' \text{N}$ and on $31^{\circ}-34^{\circ} \text{E}$ longitude, Fig. (2-14).

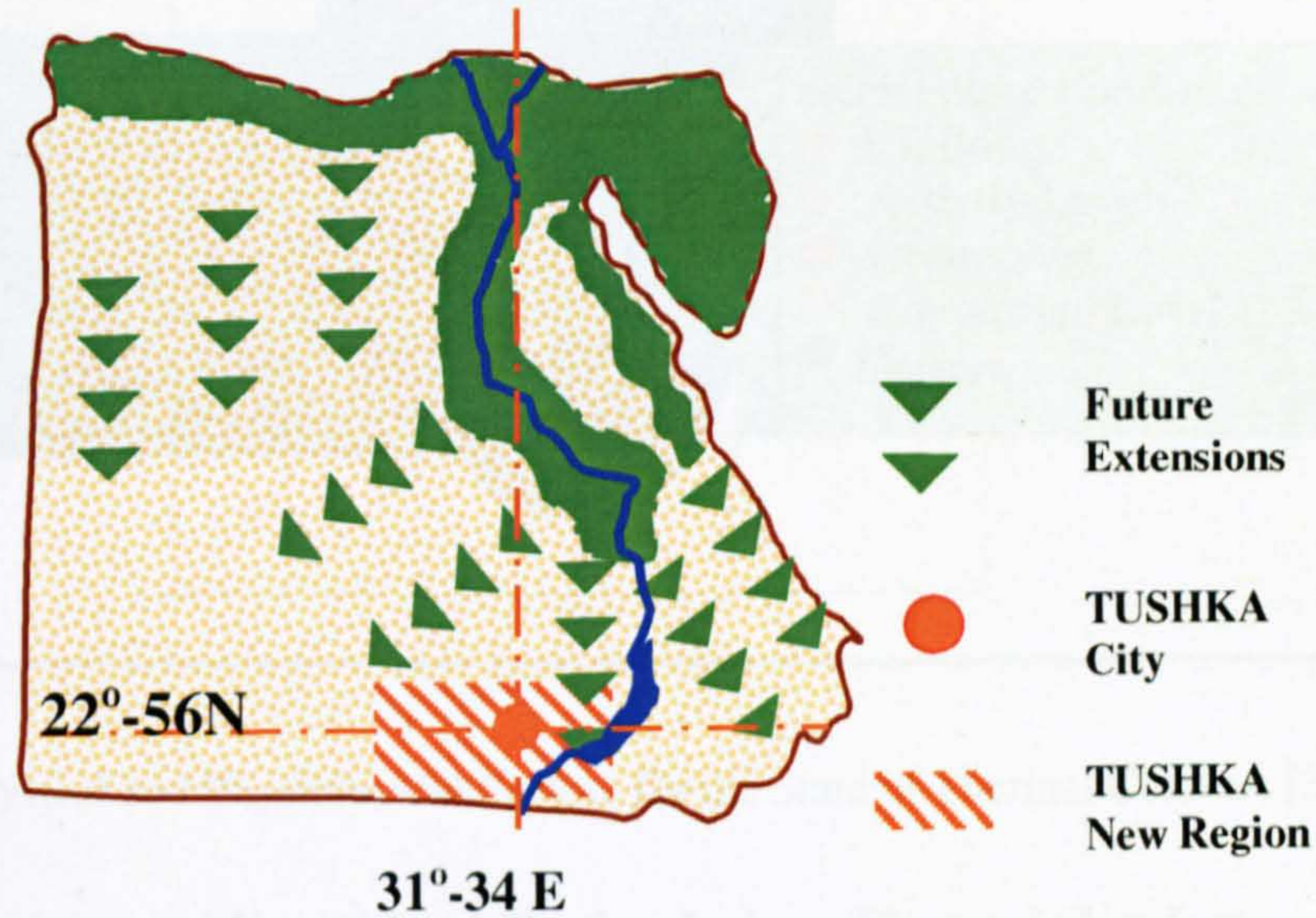


Figure 2-14 Future Extensions Towards The Uninhabited-Desert New Regions

2.3.2 Indoor Thermal Comfort And Human Requirements

The desirable indoor thermal comfort can be said to be more important than other indoor human requirements such as lighting and acoustics. In this respect, indoor thermal comfort can be provided through building designs and construction materials that respect local climatic conditions. Thermal comfort in building is compelled by the incident solar radiation, which influences the mean radiant temperature and other climatic factors such as air temperature humidity and airflow[2]. Large numbers of physical and physiological factors affect the feelings of thermal comfort and its indoor maintenance. Fig. (2-15) illustrates these factors.

The thermal balance between the human body and its environment, in other words, the balance between heat gains and heat losses of the body to the surrounding environment, must be considered as one of the primary requirements for the health, well-being and comfort of the occupants. The thermal comfort has been defined by ASHRAE (*American Society of Heating, Refrigerating and Air-conditioning Engineers*) [28] as the condition of mind, which expresses satisfaction with the thermal environment [2].

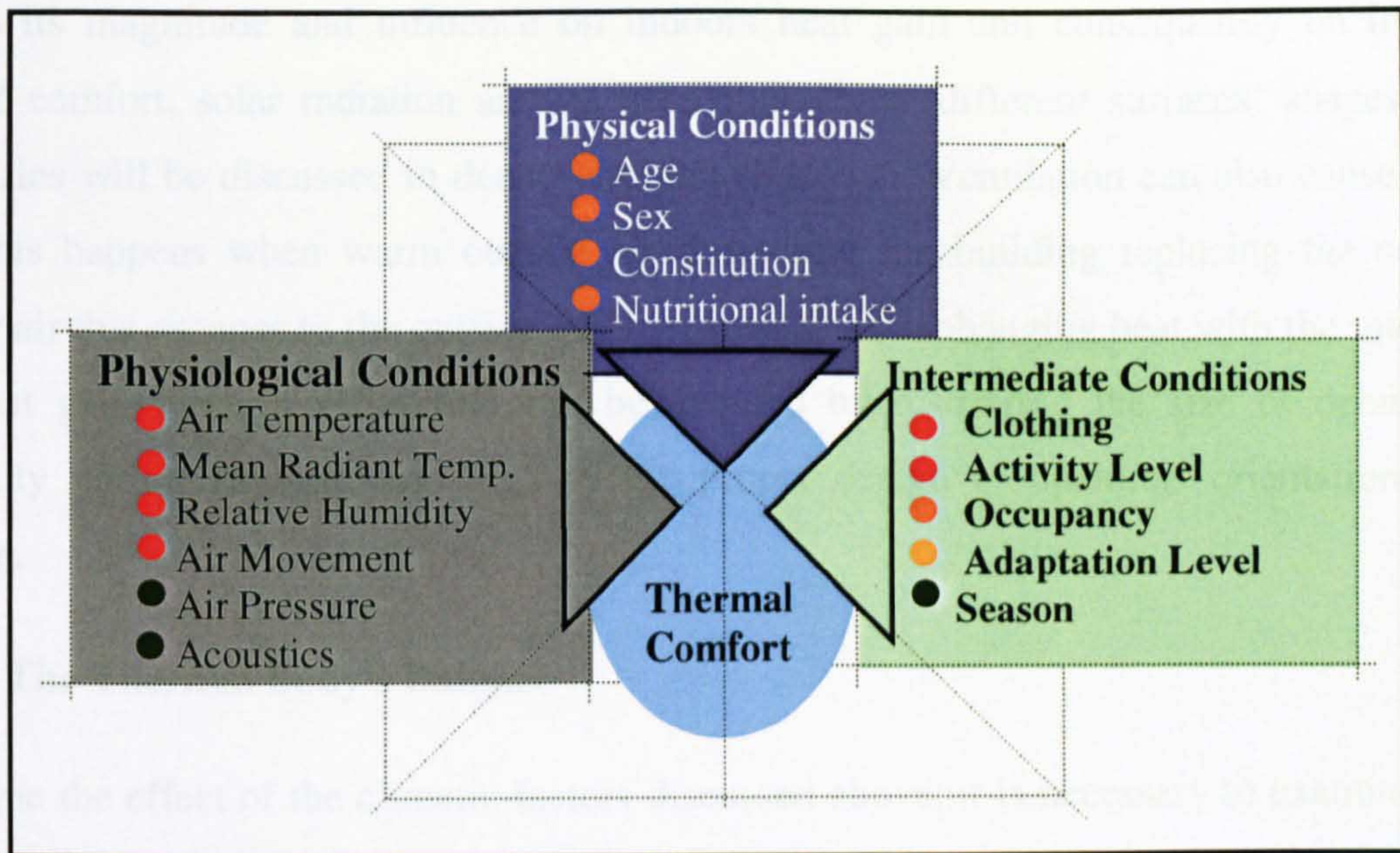


Figure 2-15 Physical and Physiological Factors for the State of Thermal Comfort [2]

2.3.2.1 The Main Factors and Variables Affecting Indoor Thermal Comfort

Solar radiation is the principle source of heat in hot arid climates. Heat can be transmitted to the indoor environments through various ways in which heat gain occurs without internal heating devices throughout the daytime. Conduction of the absorbed solar radiation through walls and roof has a great effect on indoor heat gain. The conduction rate depends on the thermal conductance or thermal resistivity of the used construction materials, the area of the solar radiation receiver surface and its properties (*colour, texture and thickness*).

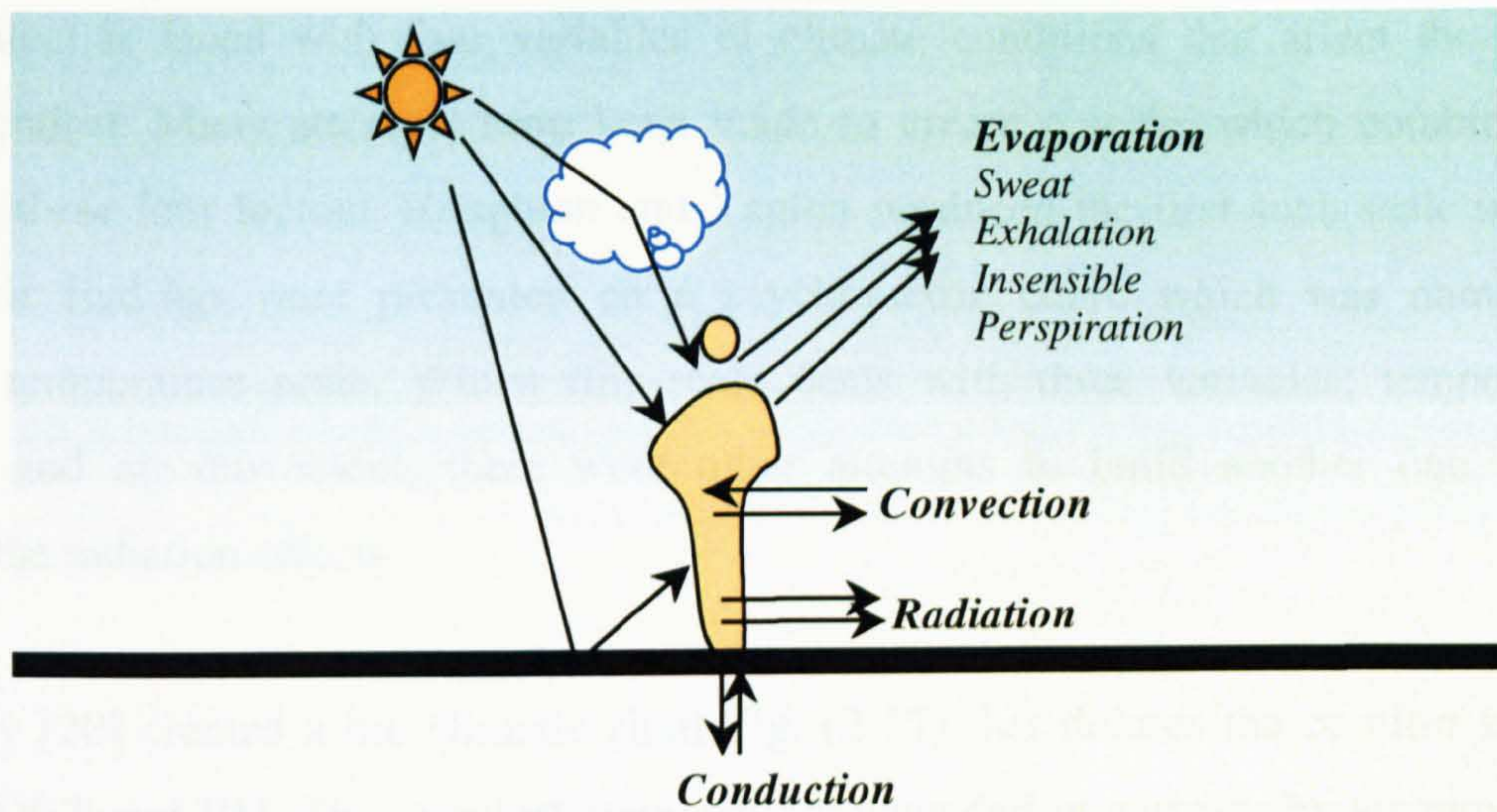
The direct and reflected solar radiation, absorbed and reemitted heat and heat gain are differently responsible for heat gain. About 3% of incident energy is transformed into heating the structure. Shading can be used to prevent solar radiation from directly falling on building surfaces. Building's envelope and roof shapes, geometry, colour and construction materials' thermal properties can effectively provide passive indoor thermal comfort.

Due to its magnitude and influence on indoors heat gain and consequently on indoor thermal comfort, solar radiation and its behaviour above different surfaces' shapes and geometries will be discussed in details through chapter 5. Ventilation can also cause heat gain, this happens when warm outside air flows into the building replacing the cooler interior air that escapes to the outside and by external air exchanging heat with the internal air. Heat gain through ventilation can be avoided by restricting the size of openings, especially during daytime, and also by the proper design of openings orientation and location.

2.3.2.2 The Thermal Body's Balance

To define the effect of the climatic factors discussed above, it is necessary to examine the basic thermal processes of the human body. The human body's biochemical processes, such as tissue building, energy conversion and muscular work, are heat producers. The total heat production is divided into Basal Metabolism and Muscular Metabolism. Only 20% of the energy produced is utilised and the remaining must be dissipated to the environment. This heat production varies according to the activity [21].

The deep body temperature must remain balanced and constant around 37.5°C. To maintain this steady temperature all surplus heat gained from solar radiation or warm air, must be dissipated to the surrounding environment. The human body can gain and release heat from the environment by one or more of the ways that are shown in Fig. (2-16). The body's thermal balance can be expressed geographically or mathematically as shown in Fig. (2-16) [21].



$$\text{Met} - \text{Evp} + \text{Cnd} + \text{Cnv} + \text{Rad} = 0.0$$

Gain: Met = metabolism (basal & muscular)

Cnd = conduction (contact with warm bodies)

Cnv = convection (if the air is warmer than the skin)

Rad = radiation (from the sun, the sky and hot bodies)

Loss: Cnd = conduction (contact with cold bodies)

Cnv = convection (if the air is cooler than the skin)

Rad = radiation (to night sky and cold bodies)

Evp = evaporation (of moisture and sweat if the air humidity allows)

Figure 2-16 Body Heat Exchange: After Koenisberger [21]

On the other hand, human response to the thermal environment does not only depend on solar radiation and other climatic factors such as air temperature, humidity and air movement, as there are other factors and variables that produce thermal effects. These variable factors can be divided into two groups, the primarily climatic factors group and the subjective variables group. These factors must be taken into considerations during any building design process intended to provide for natural indoor thermal comfort.

Finally, the sensation of comfort or discomfort depends primarily on the four main climatic variables; temperature, solar radiation, humidity and air movement. These variables cause a kind of cooling sensation due to the heat loss by convection and increasing evaporation from the body. In addition to the climatic elements and the level of activities, thermal performance is also influenced by other subjective factors, such as type of clothing, age and sex, state of health and skin colour.

2.3.2.3 The Bio-Climatic Chart and The Comfort Zone

The architect is faced with four variables of climate conditions that affect the indoor human comfort. Many attempts have been made to create a scale, which combines the effects of these four factors. Houghton and Yaglou produced the first such scale in 1923 [20]. Their findings were presented on a psychometric chart, which was named the effective temperature scale. Whilst this scale deals with three variables; temperature, humidity and air movement, there were other attempts to build another one, which included the radiation effects.

V. Olgyay [20] created a bio-climatic chart Fig. (2-17) that defines the comfort zone in terms of DBT and RH. This comfort zone can be expanded in summer by air movement and in winter by solar radiation and in winter by solar radiation [20].

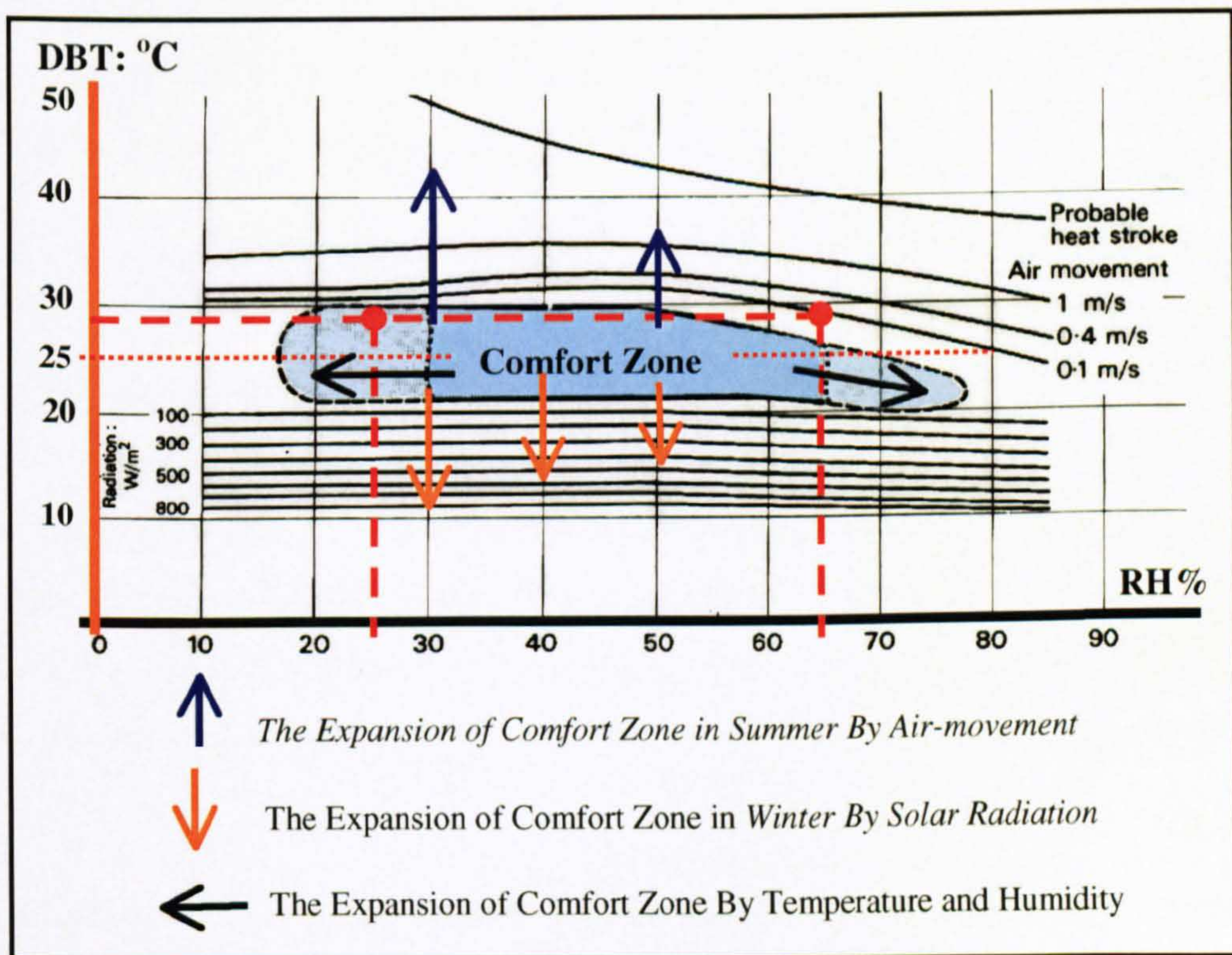


Figure 2-17 BIO-CLIMATIC Chart and the Comfort Zone [20]

If sunstroke or heat stroke can be considered as the upper temperature limit for human existence, the freezing point can be taken as its lower limit. The ideal air temperature may be assumed to be midway between these extremes. Therefore, comfort zones do not have fixed boundaries but differ individually due to types of clothing worn, nature of activity, sex and age.

The British Department of Scientific and Industrial Research concluded that the ideal temperature with slight air movement (0.25 m/s or less) is 18.9 °C in summer and 16.7 °C in winter [20]. It gave the ideal indoor air temperature as 18.1 °C, and defined the comfort zone ranges as being from 14 to 22.5 °C. Others suggested that the standard is 20.8 °C with 50% relative humidity [20].

S. F. Markham proposes a temperature range from 21 to 24.5 °C with relative humidity varying from 40 to 70%. C. E. P. Brooks shows that the British comfort zone lies between 14.5 and 21 °C; the comfort zone in the USA lies between 20.5 and 26 °C [20]. In the tropics it is between 23 and 28 °C with relative humidity between 30 and 70 % [20].

2.4 CONCLUSIONS

This chapter concludes that there is a need for a rethinking and rearguing of recent architectural approaches. Sustainability seems to be the new "archi-environmental" catchword of this decade. Recently, the phrase "sustainable Environment" seems as prevalent as the phrase "Energy Crisis" was in the 1970's. The architectural concerns over energy efficient architecture were replaced by concentration on design style, building form and masses. Energy conscious design courses have shown a marked decline, and architectural theory and history have increased in most architectural schools, especially, those which are located in most developing countries[14].

Cultural, social and regional considerations are realistic approaches to climatic control designs. Identifying cultural, social and regional differences and requirements helps to define the technological content, which is suitable for a particular region. Architecture that respects the cultural, social and regional influence is a sustainable architecture that takes account of local cultural, social and regional identities.

Many international development plans are involved in most of the developing countries plans. These plans impose their point of views on the choice of settlement patterns, building type, technologies and norms of production. Based on this situation the issue of global design "globalisation" becomes more observable in such traditional regions. Architecture is shaped by these development strategies and architects appear to be obsessed with the desire of following-up these plans. This social and cultural alienation associated the production of unsuitable building forms, materials and concepts in a great number and part of developing countries with a wider loss of local cultural, social and regional identities [11].

In the *Middle East, Egypt and North Africa* most modern buildings lack *architectural* style and character. The signature is often missed and buildings are almost always similar and without a local accent. The gap between continuity and modernity has been misunderstood. For example, modern Egyptian architects believe that Ancient Egyptian architecture is represented by temples with their *pylons and cornice* and Arab architecture by clustered stalactites, whereas the domestic architecture in both is quite different from the Egyptian temple or the Arab mosque[8].

The aim of sustainable architecture is to improve the quality of human life and environment; its intention is not only to save resources but also to reorder them properly to serve the people. Therefore, there is a need to establish a proper integration of several sustainable technologies, which are more passive, natural and environmentally friendly, into both architectural design and the building construction industry. Bio-climatic architecture is the proper approach towards reviving the missing architectural, cultural, social and regional characters in most of the developing countries in the hot-arid region.

Finally, modifying the architectural education syllabus in order for it to be focused on the new applied sciences as well as the architectural theories, is necessary as many architectural schools are dealing and studying the history of such architectural periods by the accidents of styles and the main features only, without searching through the scientific reasons that resulted in creating these styles.

The next chapter, a number of traditional passive cooling techniques, which have been employed in hot arid regions will be discussed in a way that explains the passive-cooling strategy of each technique. Chapter 3 also discusses a number of the exemplary techniques of traditional passive cooling in hot regions, such as domed and vaulted roofs, doubled roofs with air gap, the use of massive walls and earth direct contact, courtyard (*Inner Patio*), wind watcher towers (*Malqaf*) and doubled screen window (*Mashrabyya*).

Reference List

1. Garcia-Chavez, J. R. Towards a new sustainable ecological community, *Principles, Strategies, and Applications (Integration of sustainable technology into architectural design and regional planning)*, Environmentally Friendly Cities, *Proceedings of PLEA 98, Passive and Low Energy Architecture* 1998 Jun; Lisbon, Portugal.
2. Bansal, N. K. *Passive Building Design, A Hand of Natural Climatic Control*, Amsterdam, The Netherlands: Elsevier Science B.V.; (1994).
3. Sophia and Stefan Behhling in Collaboration with Bruno Schindler Foreword by Norman Foster. *Solar Power The Evolution of Sustainable Architecture* 2000.
4. Cook, J. Sustainable suburbs for the American desert, *goals and models-Environmentally Friendly Cities - Proceedings of PLEA 98 Passive and Low Energy Architecture; Lisbon, Portugal*. 1998.
5. Online World Atlas, (2003 Maps.com). [Web Page]; www.maps.com/explore/atlas/. [Accessed 8 Aug 2002].
6. Mosquera, G. Energy Performance and traditional neighbourhood design, *Environmentally Friendly Cities, Proceedings of PLEA 98, Passive and Low Energy Architecture* 1998 Jun; Lisbon, Portugal.
7. Urban Settlements Authorisation. *Urban Structural and Texture planning for the Toshka Region*. 1st Edition ed. Cairo, Egypt: Ministry of Housing, Infrastructure and Urban Settlements; 1999.
8. Fathy, H. *Architecture for the poor An Experiment in Rural Egypt* [Web Page] (1973).
9. Ozdeniz, M. B. Bekleyen A., Gonul I. A. Vernacular Domed Houses of Harran in Turkey. *Habitat International* 1998; Vol. 22 (No. 4): pp 477-85.
10. Boake, M. T. Passive Versus Active Solar Design: Opposing Strategies in Support of a New Sustainable Vernacular. *Architronic: In Support of a New Sustainable Vernacular* Vol. 4(NO. 3):p. 2.
11. Abel, C. *Architecture and Identity: Responses to Cultural and Technological Change with a foreword by Suha Ozkan*. 2nd ed. Oxford: Architectural Press; 1994.
12. Edited by Santamouris, M., Asimakopoulos, D. *Passive Cooling of Buildings*. European Commission (Directorate General xvii for Energy); (1996).
13. Littlefair, P. J. *Environmental site layout planning: solar access, microclimate and passive cooling in urban areas*. London: construction Research Communications; 2000.
14. Boake, M. T. *Sustainability & Construction Technology: An Attitude in Support of Quality*. *Architronic* Vol. 5(No. 2).
15. Kremers, J. " *Defining sustainable Architecture*" *Architronic*. [Web Page] (1995); <http://www.saed.kent.edu/v4n3/v4n3.02.html>.
16. Barnett, D. and Browing, W. *A primer on Sustainable Building*", A report Colorado. Rocky Mountain Institute.

17. Tillman Lyle, J. Regenerative Design for Sustainable Development. New York, Wiley & Sons Inc.; (1994).
18. World resources Institute "Dimensions of Sustainable Development", Washington, Dc: Report, WRI. (1990).
19. Pearson, D. Earth to Spirit - *In Search of Natural Architecture*. Gaia books Ltd; 1994.
20. Olgyay, V. Design with climate: Bioclimatic Approach to architectural Regionalism. New York: Some chapters based on cooperative research with Aladar Olgyay, Van Nostr and Reinhold; 1992.
21. Koenigsberger, O. H., et al. Manual of Tropical housing and Building - *Part one: Climatic Design*. (1973) .
22. Fathy, H. Natural Energy and Vernacular Architecture, *principles and examples with reference to hot -arid climates Chicago & London: Published for United Nations University by the university of Chicago press; 1986. (EDITED BY WALTER SHEARER; Abdel-Rahman; Ahmed Sultan.*
23. Givoni and Brauch, M. Climate & Architecture. London; (1976).
24. Hamdy, I. F. Architectural Approach to The Energy Performance of Buildings in a hot-dry climate, with special reference to Egypt, Bath: University of Bath; (1986), Ph.D. Thesis.
25. Nohad, A. T. Climatic Considerations in the Design of Urban Housing in Egypt. Housing in Arid Lands - *Design and Planning*. London: The Architectural Press; 1984. (GOLANY, G.
26. The International American Agency for Development, Solar Radiation Atlas for Egypt, Renewable Energy Authorisation - Ministry of Electricity and Energy, Cairo; 1990.
27. Salah El Din, O. and Abdul Hamid, A. A., et al. The Usage of Efficient Construction Techniques in Urban Settlements in the Desert areas. Cairo, Egypt: Institute of Urban and Building Research, Ministry of Housing, Infrastructure and Urban Settlements; 1999 Dec. Report No.: Report no. 1.
28. ASHRAE Handbook 2000. Heating, ventilating, and air-conditioning systems and equipment. SI ed. Atlanta, American Society of Heating, Refrigeration and Air-Conditioning Engineers; 2000.

CHAPTER 3

TRADITIONAL AND MODERN PASSIVE COOLING TECHNIQUES IN HOT-ARID REGIONS

3. TRADITIONAL AND MODERN PASSIVE COOLING TECHNIQUES IN HOT ARID REGIONS

In the previous chapter, the world energy crisis and developing communities limited non-renewable resources have been highlighted with the problem of high population densities in many parts of the world. Also, the need for more sustainable buildings and approaches to reduce the required energy in buildings in developing communities has been illustrated. Many years ago, the use of climate sensitive design strategies has become an essential starting point for architects in order to design energy efficient buildings in hot-arid regions generally, and the developing countries in particular. Passive cooling techniques have a much longer history of theory and application in indigenous and traditional buildings. However, few of these principles are widely found in a large number of traditional and vernacular buildings [1].

This chapter analyses and evaluates a number of traditional passive cooling techniques, which have succeeded in providing indoor thermal comfort in the tropical climatic region contemporary architecture (*Middle East, Egypt and other developing countries*). The chapter analysis and evaluation procedures of these techniques aim at providing a better understanding of their technical aspects and traditional approaches in order to employ them in today's contemporary buildings.

Passive as a word means not actively taking part, or tending not to participate actively, and usually letting others make decisions and actions. Passive cooling strategy in such overheated climates means defensive. It includes techniques that can avoid the over-heat sources or minimise the building heat gain, therefore protect the indoor thermal environments from the outside hot climatic conditions without using artificial means. For example they avoid heat gains due to solar radiation by shading and reflective barriers, and buildings envelope form and orientation. Therefore, stop heat transfer through the building's envelope, proper insulation and construction materials. Passive cooling strategies may take place through one or more of the following [2]:

- An energy consciousness design approach that reduces the use of electricity and general energy consumption
- The use of natural and renewable resources to produce energy in buildings versus high tech systems

- Different design concepts that avoid the heat gain or reduce heat loads by non-environmental destroyer means
- The emulation of vernacular constructions successes for cooling
- An architecture that responds suitably to local climatic conditions
- .Finally, a romantic view that returns to the rustic and nature, and simplifies the occupants' lifestyle.

Many publications have suggested a return to the use of natural renewable materials, and a lower technology lifestyle. The influence of the traditional passive cooling designs, in which they cannot provide the desirable thermal comfort, depends on the changing level of the occupants' lifestyle and their ability to diminish their expectations of convenience and comfort. John Reynolds (*University of Oregon*) studied the temperature pattern in a vernacular Spanish house in Cordoba, he found no artificial dependent systems were employed to achieve indoor thermal comfort but natural cooling means [2].

3.1 PRINCIPLES OF PASSIVE COOLING TECHNIQUES IN BUILDINGS

Basically, passive-cooling strategies aims at avoiding overheating, which is chiefly generated by the sun. Therefore, using proper building designs, construction materials and techniques can possibly control the indoor comfort conditions. This is may be achieved by avoiding heat gain and protecting the indoor environments from the climatic conditions, which are extremely hot during summer. The following sections of this chapter review number of passive cooling principles, which have been applied through different traditional design techniques and successfully have been employed in buildings in hot-arid regions.

3.1.1 Cooling by Ventilation

Ventilation means the circulation of air and the supplying of fresh air to an enclosed space. It is the process of replacing the exhausted warm indoor air with cooler outdoor air by bringing in the outdoor air. The movement of fresh air over occupants' skin produces a cooling effect by both convection and evaporation. Appropriate ventilation and air movement that drives fresh air in and circulates warm air out can be provided passively in enclosed spaces through the proper design of the openings size and position. A high position opening helps to create a stack effect (*traditional domes*), which helps to evacuate warm air (*see sketches Fig. (3-4) in this chapter and Fig. (9-23) in Chapter 9*). Ventilation can be also considered as another mode of heat loss, which occurs when hot air escapes through an opening in roof or wall, to be replaced by cooler air from outside [3].

3.1.2 Cooling by Dehumidification

Cooling by dehumidification is the contradictory process of humidification; it means the removal of water vapour from room air by dilution with dryer air, condensation or desiccation. In the case of condensation and desiccation, dehumidification is the exchange of latent heat in air for the sensible heat of water droplets on surfaces; both these methods are the reverse of evaporative cooling. Dehumidification can be achieved in buildings through a substance that absorbs water and removes moisture, (*known as desiccant dehumidification*), or by condensation on passively cooled surfaces [2].

3.1.3 Cooling by Evaporation

Physically, evaporation means the process of changing the liquidity phase of a liquid to vapour without its temperature reaching the boiling point. In buildings, cool water droplets catch the indoor warm air's sensible heat to evaporate and make it fresher, which is known as evaporative cooling. Water in buildings can be provided by many means such as, water clay-jars, fountains or other wetted surfaces. Water evaporates from a wet surface if it is exposed to air with a dew point lower than the surface temperature [4]. The rate at which water evaporates from the surface depends on the relative humidity of the ambient air, the surface temperature and the velocity of air movement. Thus, for a wet surface at a given temperature, a reduction in relative humidity or an increase in air velocity can both increase evaporation [4].

Energy is needed to convert water from liquid to vapour. The latent heat for evaporation must be supplied by the wet surface, which thus loses heat or absorbs heat from the ambient air and cools it. Evaporation from the surface of the building or from objects within the interior can produce a cooling effect on the building, which acts as a source of heat loss. In hot arid climates, this can be a particularly effective cooling mechanism since the rate of evaporation in dry air is very high [4].

3.1.4 Cooling By Convection and Conduction Heat Loss

In general, the concepts of thermal conduction and resistance are important for providing a comfortable indoor environment in hot-arid regions. The heat-flow concept is based on the movement of a quantity of heat. Conduction is the process by which heat flows through a material, or from one material to another with which it is in contact. Some materials, such as metals, are good thermal conductors, while others, like air, are poor thermal conductors [2].

Thermal conductivity is a specific property of a material, and is a measure of the rate at which heat will flow through a material when a difference in temperature exists between its surfaces. It is defined as the quantity of heat that will flow through a unit area in a unit time, or equivalently, as the rate of heat flow through a unit area, when a unit of temperature difference exists between the faces of the material of unit thickness [4].

Conduction through the building envelope, roof and walls can cause heat loss, similar to the process of gaining heat by direct solar radiation. Once gained heat has been absorbed by the envelope surfaces, or through the roof by a combination of convection and conduction, it can cause heat loss, which can positively provide indoor thermal comfort. Heat may be also transferred naturally by convection between a surface and a liquid or a gas. When the surface is at a temperature above that of the air, heat is transferred from the surface to the adjacent air by convection. Even if the air is still, the convection can occur due to temperature differences. Obviously, the rate of heat transfer by natural convection depends on the temperature difference between the surface and the ambient air [4].

3.1.4.1 Cooling by Radiation

Warm building surfaces radiate heat to cooler sky, this is called cooling by radiation. It is the loss of heat through the heat transfer from warmer surface to a cooler surrounding surface (*the sky or the outer air*). Also it cools people, while the warm skin radiates heat to cooler surrounding room. This strategy can be achieved by passive means, such as skytherm, cool pool, or roof pond systems [1].

3.1.4.2 Mass-effect Cooling

Mass-effect cooling is also a way of heat loss in building through conduction and convection. It depends on delaying the transmission of absorbed heat from solar radiation or the gained heat from the ambient outer air to be transferred to less temperature indoor spaces by employing massive and thick walls, and bad-conductors construction materials. Due to their thermal storage, these walls and roofs can absorb heat during the warmest part of the day to be released later to both cooler sky and outer air [4]. Mass-effect cooling can be achieved through employing different architectural elements as explained later in this chapter.

3.2 TRADITIONAL PASSIVE COOLING TECHNIQUES AND MATERIALS

In the past, people (*the natural architects*) have had some reasons for what they built and erected. Their architecture was more than just natural or organic materials, shapes, forms and traditions. It was derived from a real understanding of their local environmental and climatic conditions and materials. The accumulated misunderstanding of these architectural techniques, means and strategies broke the real knowledge that is supposed to be passed down from one generation to another. Nowadays, traditional passive cooling techniques are missed in most hot-arid region modern architecture.

The new importance of such traditional architecture is that the proper experimenting, modifying, and developing of their architectural principles and climatic control abilities will make them more applicable as energy efficient means in buildings and adaptable with contemporary architecture, new building materials and technologies. From what has been discussed in Chapter 2, required-energy in buildings is approximately 50 % of the world's total energy consumption [5]. This affects the economical and environmental situation in many countries with limited natural and non-renewable resources. Therefore, in developing countries, learning from traditional passive cooling technologies must be considered as a crucial strategy for a sustainable environmentally friendly future.

3.2.1 Preliminary Investigations and Historical Overview

As previously mentioned, the main problem that designers have to deal with in most of the hot-arid regions is the outdoor overheated conditions. All passive cooling techniques in traditional architecture were concerned with avoiding the outdoor overheat, which is chiefly generated by the sun. Moreover, traditional architecture depended mainly on defensive strategies, which can avoid or reduce solar heat gain in order to minimise the required cooling loads for providing affordable, desirable and thermally comfortable indoor environments.

Due to the rapid decrease of natural non-renewable resources, there is a necessity to give more attention to traditional and vernacular architecture [6]. These architecture styles not only have their own special characteristics for passive cooling, but the influence of their architectural identity is also very viable for sustainable future.

Most of those passive cooling techniques, which traditionally have provided indoor thermal comfort, were related to the occupants' needs, culture and local climatic conditions. It has been found that analysing such ecological lessons and signifying their role to build sustainable architecture in the past is very valuable to the empirical study presented in this thesis.

Tradition means a long-established custom or belief that has often been handed down from generation to generation. Tradition is not necessarily old-fashioned or from a long time ago and may have begun quite recently. If someone thought how to overcome a working problem, this trial to solve the problem is considered as the first step to establish a tradition. When another person decides to modify or adopt the same previous solution, the tradition is moving, and by the time a third person has followed the first two solutions and added contributions, the tradition has been well established.

Vernacular in language means an ordinary language, or a language of particular group, it is a common spoken language of people as opposed to a formal written or literary language. Vernacular architecture is that ordinary building style of a particular place or group of people, particularly the used architectural style for ordinary buildings as opposed to the large official and neat architecture.

Architecture is one of the most traditional arts, and one of the main signs of civilisation. Therefore, the architect should respect the work of his predecessors and public sensibility. Finally, architects should not ignore the tradition of their own countries, districts and regions nor should they let their minds become attracted to alien modernism at the expense of traditions. As recent initiatives that should be followed, this chapter illustrates some modern architectural examples that have effectively employed traditional techniques in terms of providing indoor thermal comfort in hot climates.

3.2.1.1 Ancient Passive Cooling Techniques (*Egyptian & Mesopotamian Civilisations*)

The greatest arid zone in the world extends from the Atlantic coast across North Africa and Arabian Peninsula to the Indian subcontinent [7]. The arid zone lies between latitudes 15 and 30 north or south of the equator, which consists mostly of desert or semi-desert. The first three civilisations have been established along sides of the three great rivers; *The Nile, Indus and the Tigris-Euphrates* [7].

Egypt's ancestors left many descriptions of towns, country houses, temples, funeral architecture, gardens, palaces and even other architectural vocabularies for different types of buildings. These vocabularies have been developed through to the new generations.

The typical ancient Egyptian house was a paradigm of its era. It was designed in a tripartite plan: the porch leading to a public reception court, then to a semi-private area, and finally an inner private area [4]. This plan concept was followed in larger houses and even palaces. A north-facing high wall or other buildings have surrounded the court in order to keep it in shade and catching the cool north breeze. Similar to the ancient Egyptian Malkaf, number of the contemporary houses has used triangle wind catchers facing the north, Fig. (3-1) [4].

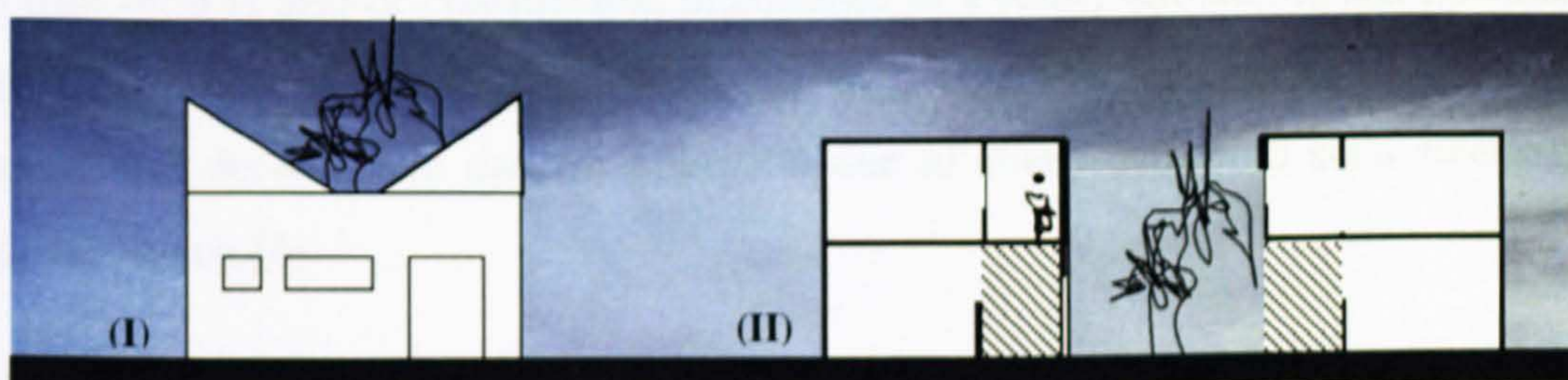


Figure 3-1 (I) Ancient Egypt Triangle Wind Catcher
(II) Mesopotamian Courtyard [4]

Mesopotamian buildings were less elegant inside and very dull outside. Houses comprised two or three stories set around inner courtyards with galleries around the courts to shade the ground floor rooms, Fig. (1-3). There were no windows facing the exterior and the court doors and windows were the main ventilation devices. Different types of wind-towers (*wind-catchers*) were found in a number of large houses and palaces.

Briefly, these two cultures built around shaded courts or patios, their buildings oriented to the prevailing winds, and apparently had several devices to both reduce solar gain while bringing wind in through the shaded courtyards. Geographically, there is a wide sandy desert between Egypt and Mesopotamia, which was the home of nomad people and Arabs who have adopted these local architectural styles and techniques in different applications, such as the compact Arab houses in Yemen and cave dwellings in North Africa [4].

3.2.1.2 Exemplary Techniques of Traditional Passive Cooling in Hot Regions

1. Domed and Vaulted Roofs (Roof Geometry);

Passive Cooling by Ventilation, Radiation and Convection Heat Loss

For natural passive cooling in buildings, the roof has a major influence on thermal indoor conditions. Approximately 50% of the heat load in buildings comes from the roof, because it is the most exposed element to the sky [8]. Traditional roofing systems enabled to reduce the received solar gain [8]. Thus, their thermal properties, forms and geometries have proved energy-efficient performances. Dome, vault and curved roofs in general are the most noticeable forms of traditional roofs and architecture.

The roof form is also of considerable importance in a sunny climate. A flat roof receives solar radiation continuously throughout the day, at a rate that increases in the early morning and decreases in the late afternoon due to changes in both solar intensity and angle of the sun [4].

In general, curved roof form has several advantages compared with the flat one. Firstly, the curved-roof shape increases part of the interior height; thereby it provides a space far above the heads of the inhabitants for warm air to rise [6]. Secondly, the total surface area of a curved-roof increases by its shape-curvature, which apparently can reduce the intensity of the received solar radiation above roof's surface and increase its heat loss factors. Thirdly, except at midday when the sun is directly overhead, part of any curved-roof is always shaded from the sun, which is called the self-shaded part [4]. Different climatic-related explanations of curved-roofs have been investigated by number of previous and recent research attempts, which has been discussed in chapter 9 of this thesis.

On the other hand, the area of the shaded part is significantly affected by the roof curvature. Therefore, the shaded part acts as a radiator, which absorbs heat from both warm internal air and the sunlit outer part and reemits the absorbed heat to the cooler outside air.

In terms of surface areas, a semicircular vaulted- roof has less than twice surface area of flat one; it will receive less solar radiation per unit area, Fig. (3-2). Semicircular dome (*hemisphere*) creates up to twice the surface area of flat one.

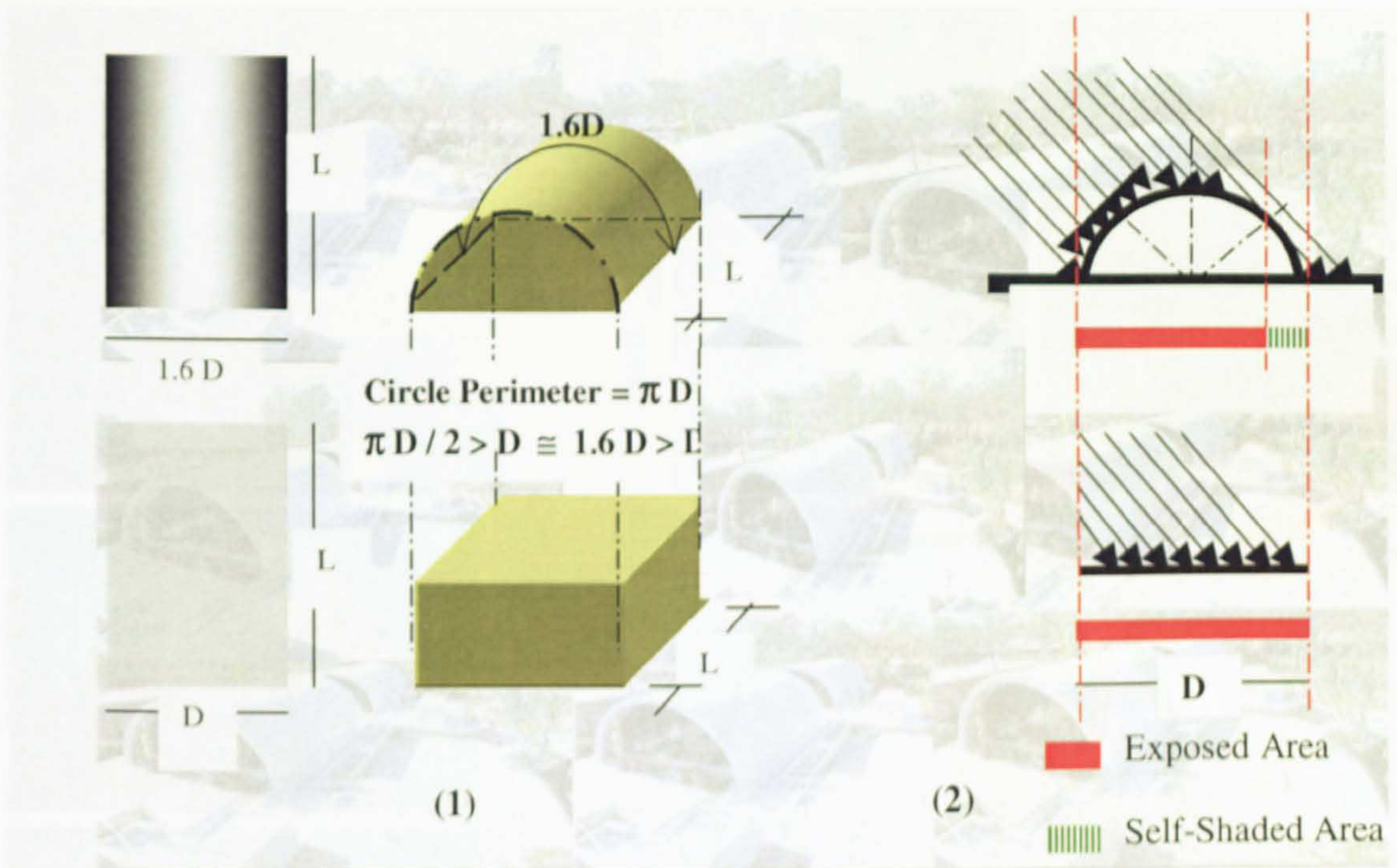


Figure 3-2 (1) Surfaces Area in Flat and Curved Roofs (2) Exposed and Self Shaded Areas in Flat and Curved Roofs

Despite the positive effect of their shapes to speed the flowing-air over their outer surfaces, domed roofs have also been employed to enhance natural lighting and ventilation by allocating vent and oculus to let air and light as in Fig. (3-3).



Figure 3-3 Different Shapes of Contemporary Curved Roofs

Source: ArchNet Digital Library [9]

As shown from the schematic sketch in Fig. (3-4), the dome enlarges the volume of the inner-space. This effectively increases indoor air movements, in which warm air rises and escapes from the top vent, therefore, allowing fresh air to replace the escaped warm air.

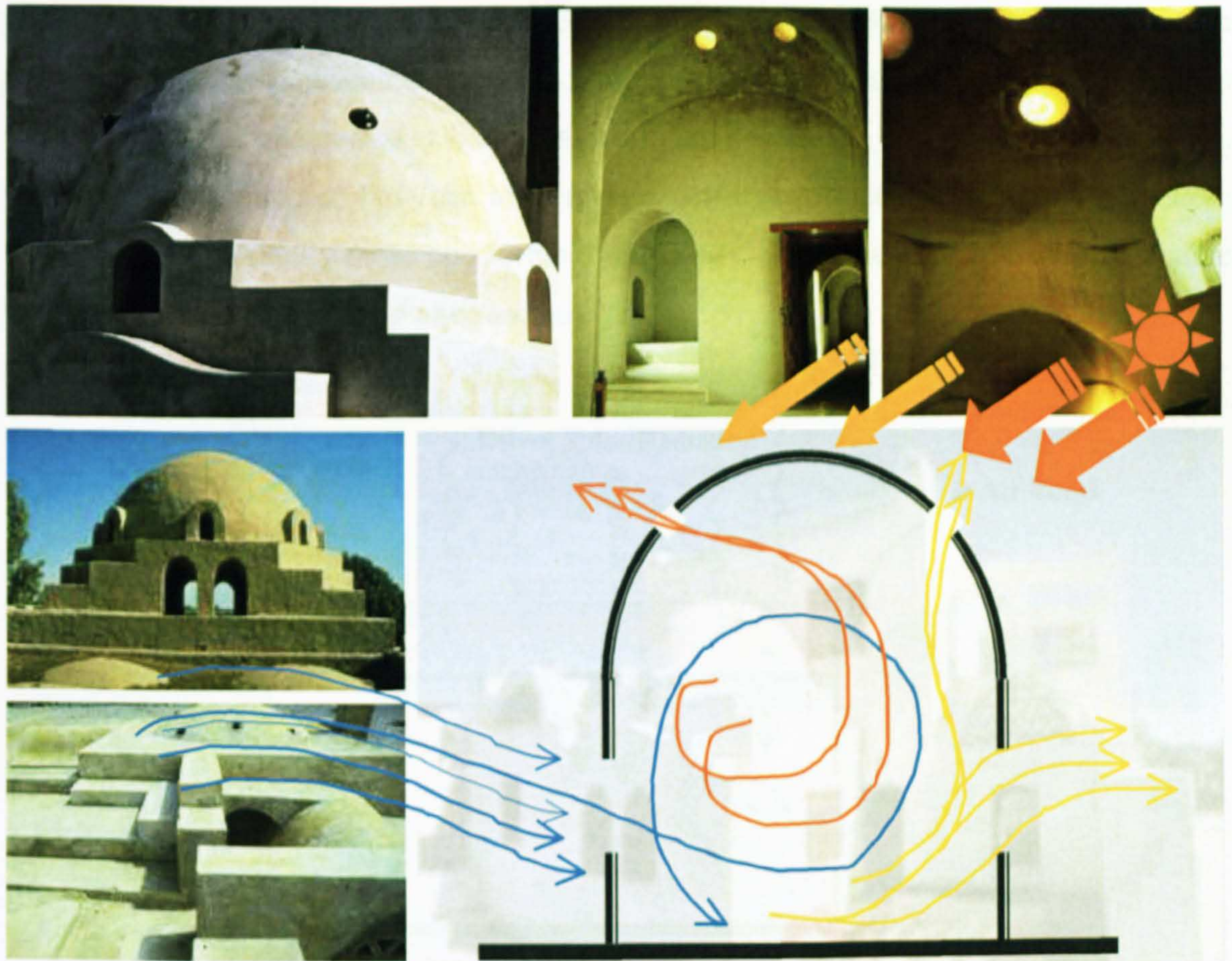


Figure 3-4 Different Types of Domes with Lighting and Ventilation Vents,
Source: ArchNet Digital Library [9]

2. Doubled Roofs with Air Gap and Roofs Top Vents

Passive Cooling by Ventilation and Conduction

Double roofing with air gaps was one of the old methods of sun radiation and heat protection by air gaps between the upper and lower roofs. Small openings (holes) can provide continuous replacement of the hot air with fresh air between the roof's two layers, which may be considered as a bad heat conductor layer. Fig. (3-5) illustrates fresh and warm air behaviour and how the roof air-gap performs effectively in terms of keeping indoor spaces thermally more comfortable. Fig. (3-6) shows number of different doubled roofs applications in contemporary architecture.

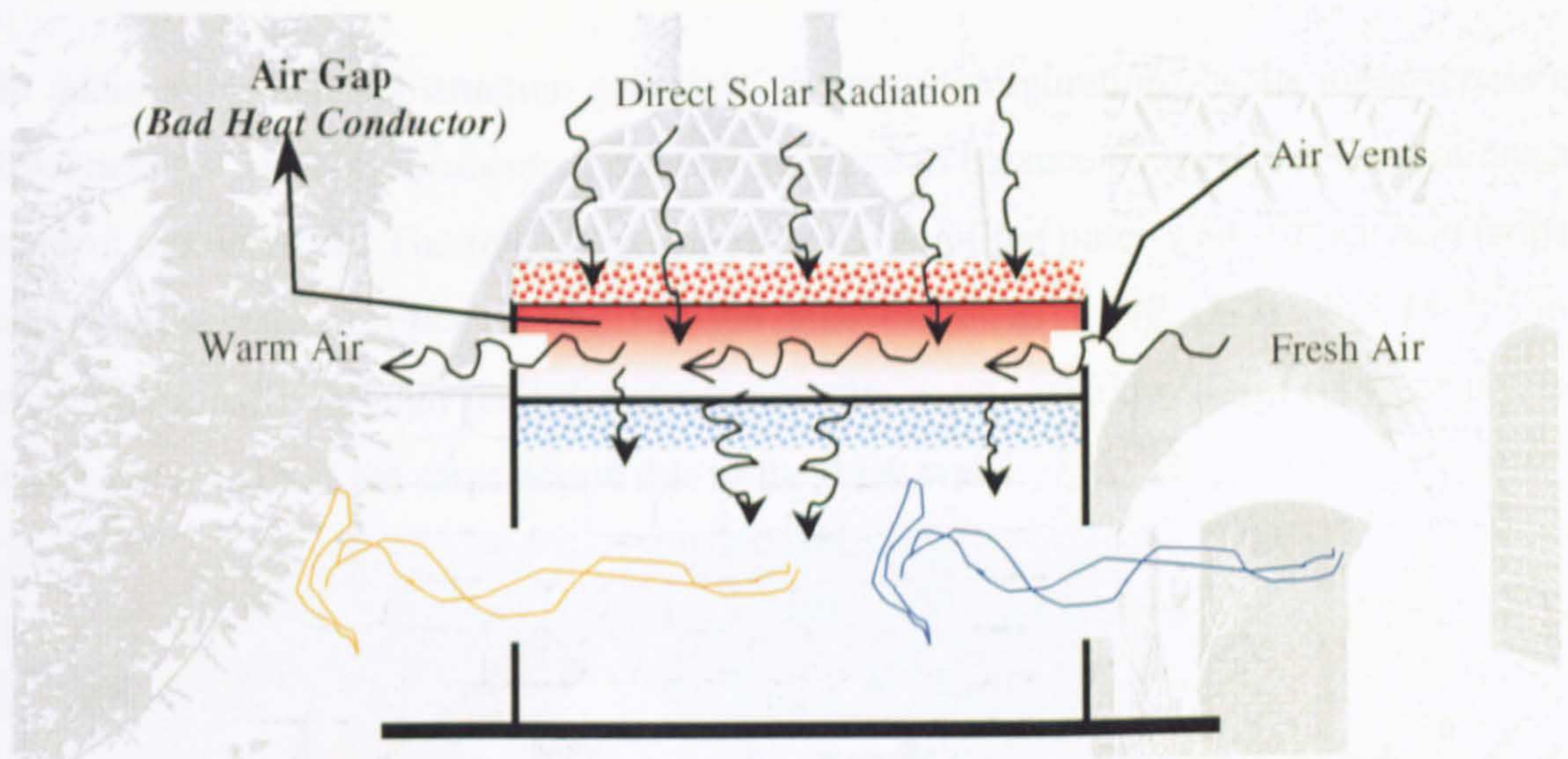


Figure 3-5 Schematic Sketch for A Doubled Roof with Air Gap



Figure 3-6 Photos Depicting Doubled Roof and Roofs Vents

Source: ArchNet Digital Library [9]

3. The Use of Massive Walls and Earth Direct Contact;

Passive Cooling by Conduction and Mass Effect (Mud Constructions)

The transfer of heat from a warmer surface to a cooler surrounding surface (*or outer space*) may be used to cool the building (*warm building surfaces radiate heat to the sky*) or to cool people (*warm skin radiates heat to cooler surrounding room*) Fig. (3-7). This strategy can be classified also as radiation passive cooling. The adobe and thick mud walls have properties of storing heat and transmitting it slowly, this produces what is called “lag”, which delays the time when one side of the wall is getting heated till the other side feels the effects (*being heated*).

In addition to their construction materials’ thermal configurations, walls massiveness and thickness (*as bad heat conductors*), effectively serve to balance temperature fluctuations and control humidity [1]. The roughness and irregularity of the outer-wall surface also helps to increase the ratio of reflected and diffused solar beams as in Fig. (3-7). Fig. (3-7) shows that traditionally through their direct contact with earth, cave dwellings (*fully or partially earth-covered*) had the same action due to the thick walls.

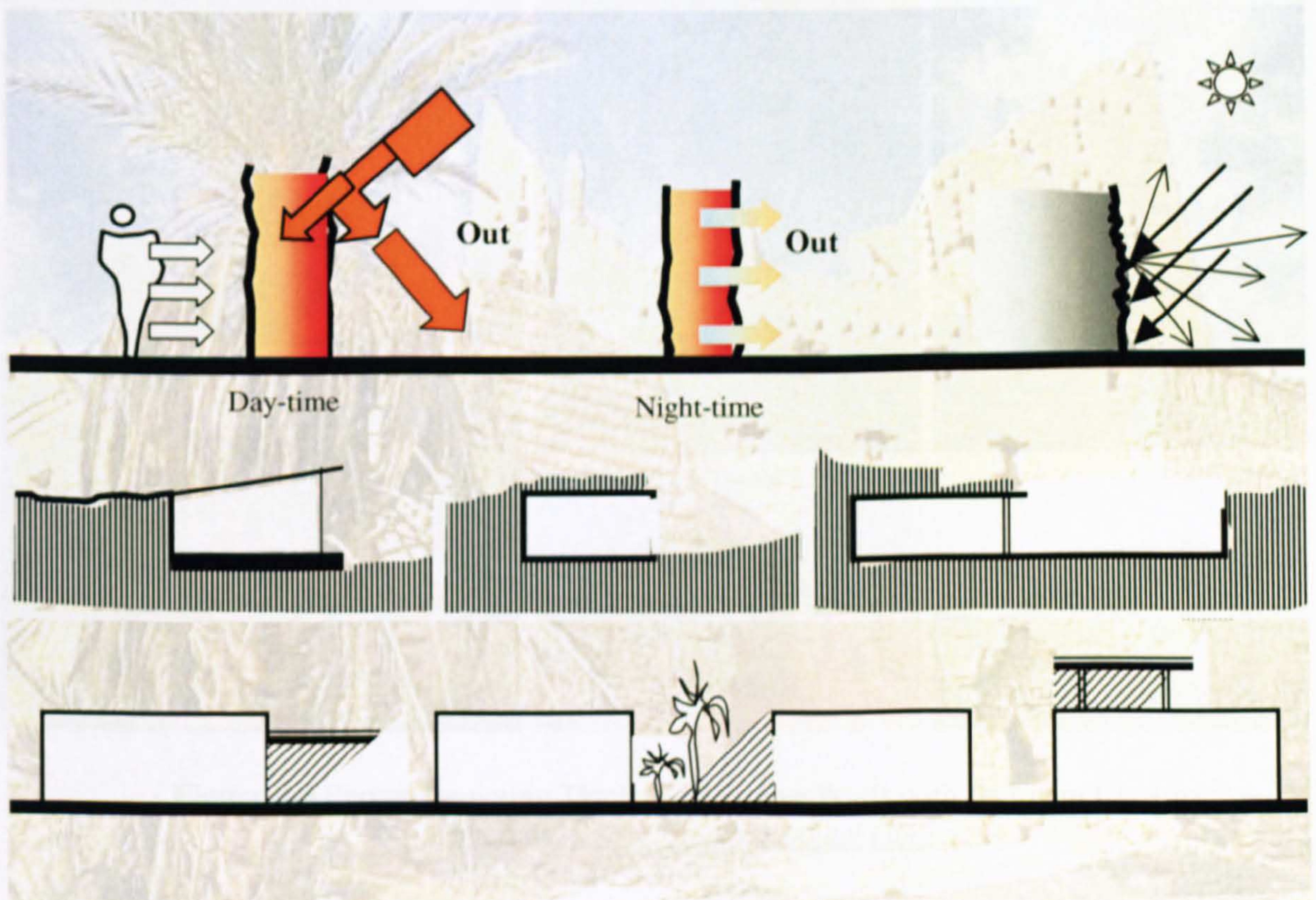


Figure 3-7 External Thick Walls, Roughness and Irregularity of Outer Walls Surface Earth Fully and Partially Covering and Shading Devices

On the other hand, there were other devices that succeeded to reduce solar heat gain such using high-density structures fabric with a lot of vegetation and overhangs louvers for shading the building surfaces and openings from the sun, as shown in Fig. (3-7). Also using limited opening sizes and placing the kitchen outdoors or at the leeward helped to reduce the internal heat gains.

As depicted in the photos Fig. (3-8), in addition to their structural necessity because of the weakness of traditional construction materials, thick walls have been widely used in hot climates' buildings to provide desirable indoor thermal comfort. The mass-effect cooling process is defined as the use of thermal storage to absorb heat during the warmest period of the day (*daytime*) to be released later during a cooler period (*night-time*).

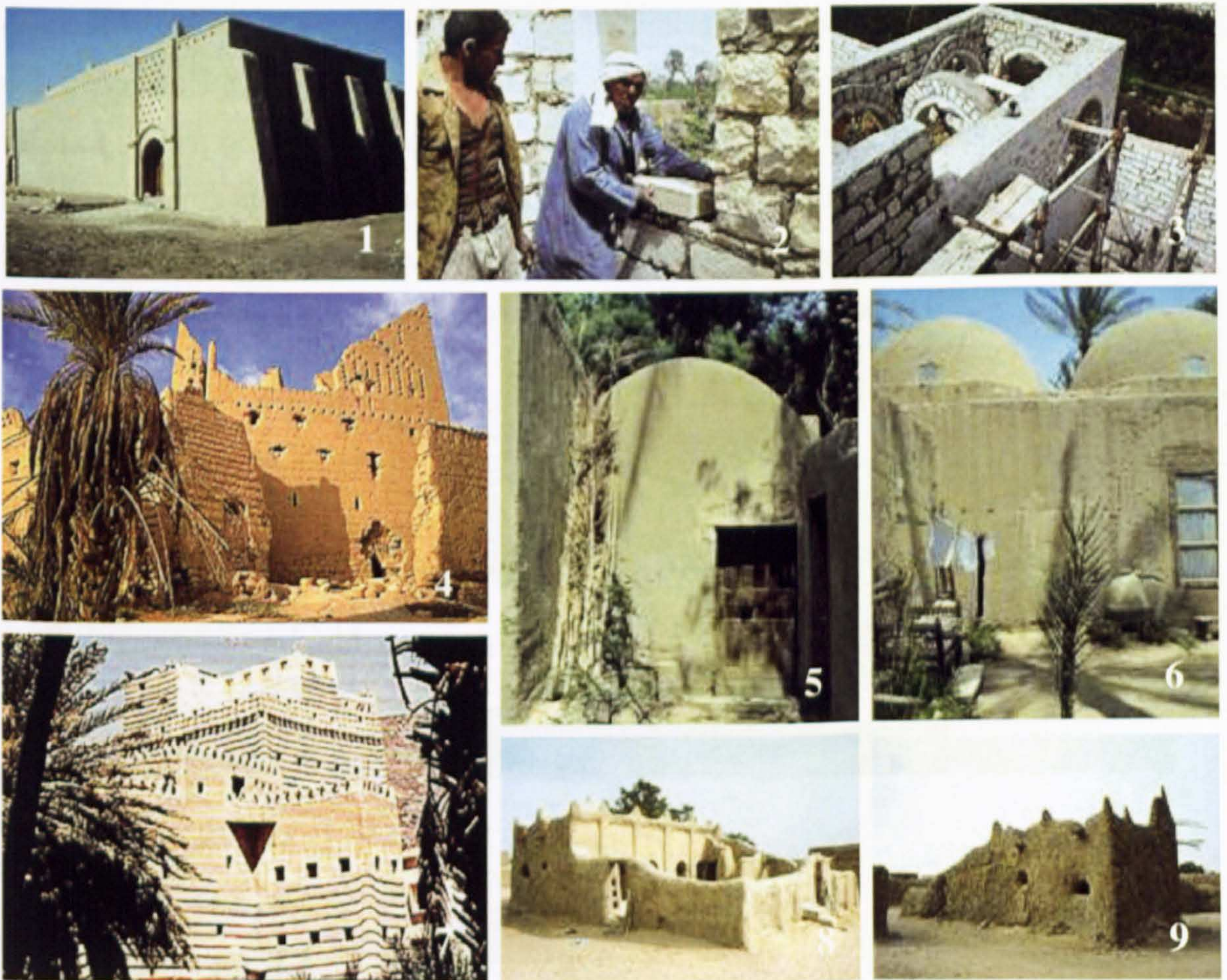


Figure 3-8 Photos Depicting Thick and Massive Walls with Different Construction Materials, *Source: ArchNet Digital Library* [9]

4. Courtyard (Inner Patio);

Air Movement by Convection

Under some circumstances, traditional designs have used the sun factor to take advantage for maintaining air movement, which is exactly what the traditional courtyard (*Inner Patio*) successfully provided by convection. Warm air is less dense than cool air and therefore will rise in an environment of cool air. This movement is called convection and can lead to the phenomenon called the stack effect. As the warm air rises, it must be replaced by cooler air from the surroundings [4]. Fig. (3-9) shows air patterns through this process.

Traditionally, courtyards have been designed to be in shade all day, so the airflow passes through them and stays cool throughout the daytime, Fig. (3-9). On the other hand, courtyards employed evaporation and dehumidification as passive cooling principles by water fountains in the middle. Evaporative cooling is the exchange from sensible heat in the air to latent heat of water droplets on wetted surfaces. While using courtyards as cool breathing spaces, they may also be used to cool the building itself (where wetted surfaces are cooled by evaporation), and the air flows through it (*cooled either directly by evaporation or indirectly by contact with a surface previously cooled by evaporation*) [1].

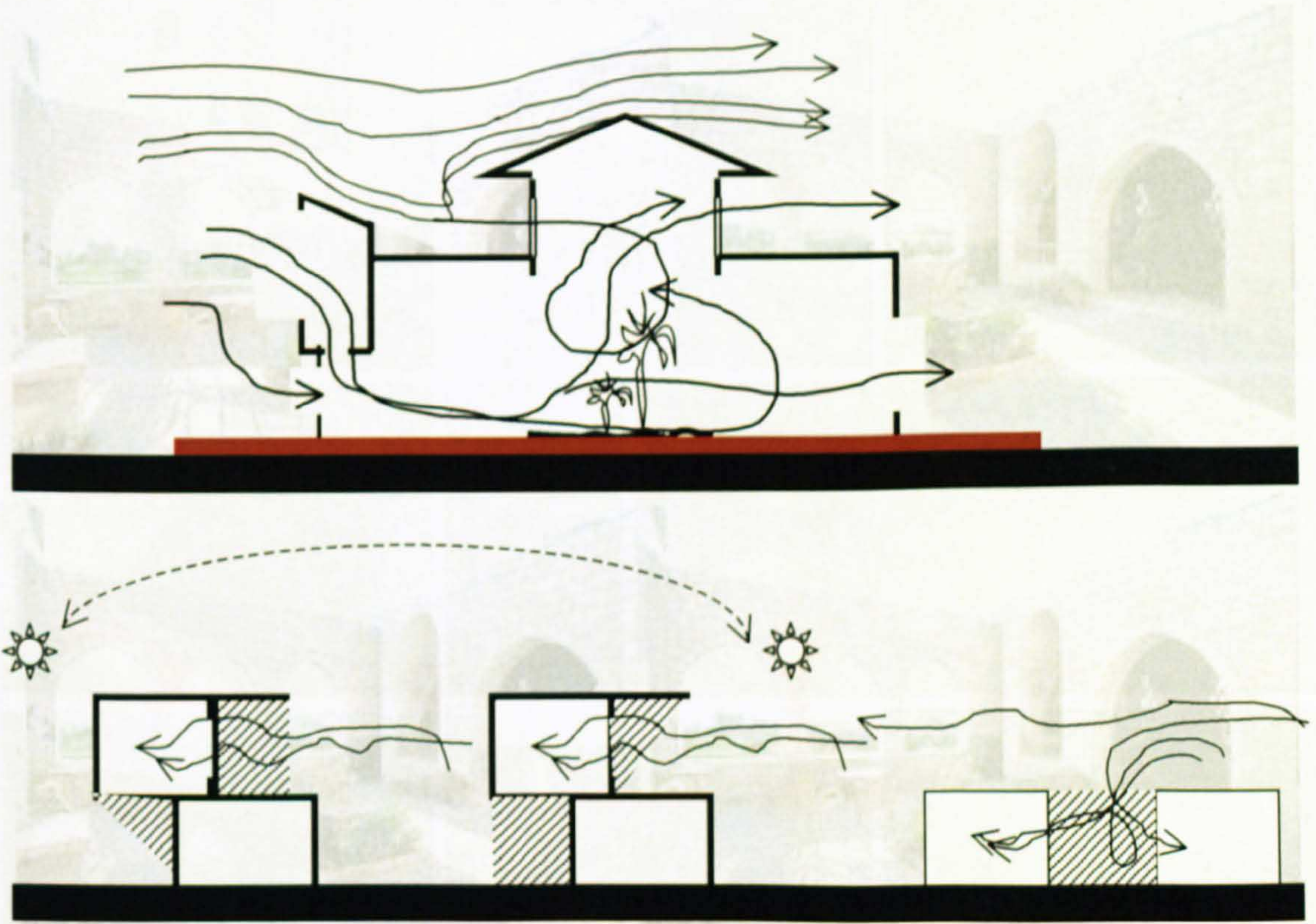


Figure 3-9 Air Patterns Through Different Courtyards Typologies

The used cooling system in a courtyard house can generate sufficient air movement by convection. In general, this phenomenon has been employed through different types of contemporary courtyards, as in Fig. (3-9). Therefore, enhancing the thermal comfort of both indoor and the courtyard space.

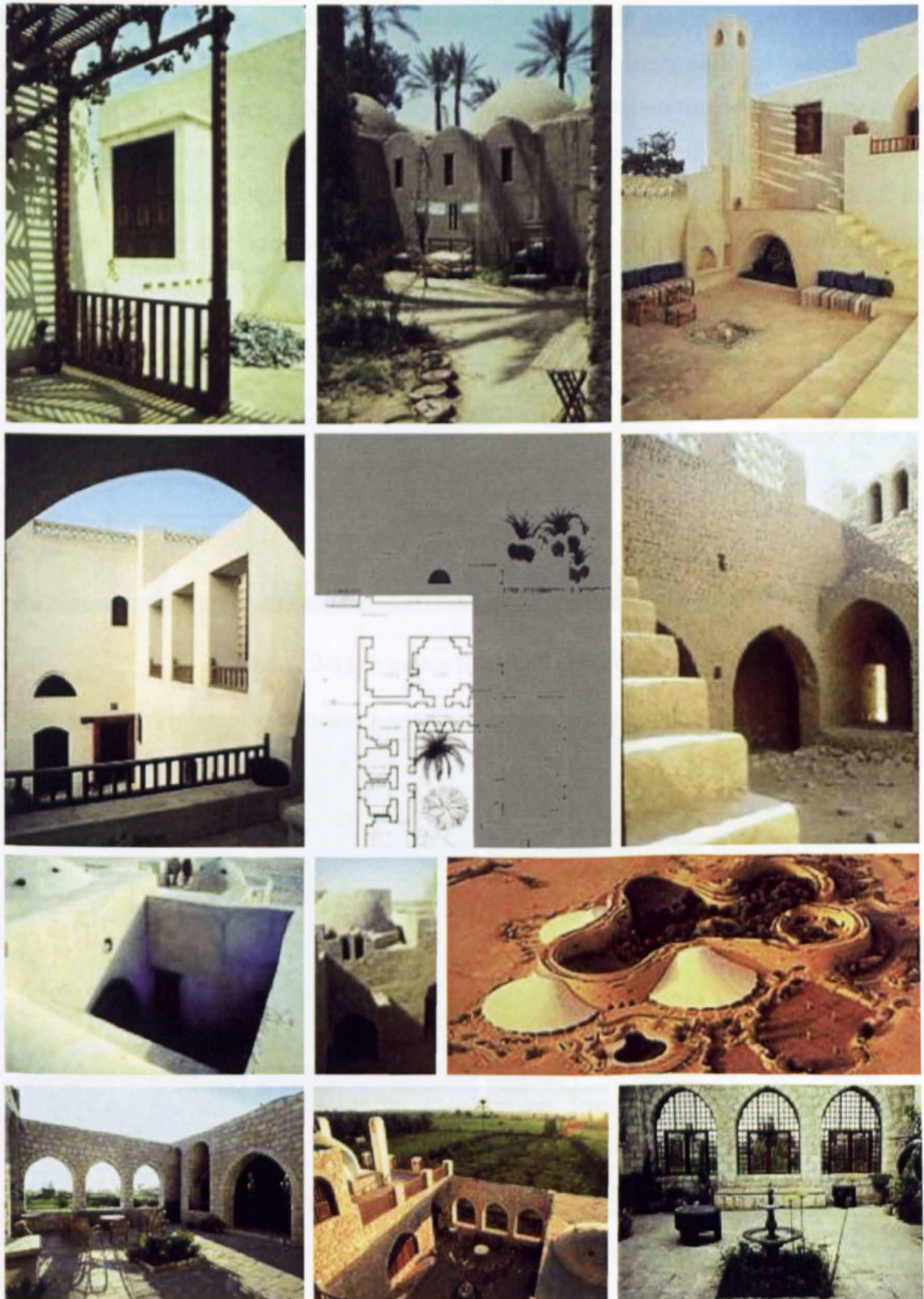


Figure 3-10 Photos Depict Different Types of Courtyards

Source: ArchNet Digital Library [9]

5. Openings;

Passive Cooling by Air Movement and Ventilation

As mentioned previously, proper design of air inlets and outlets shape, size and location provides fresh airflow and natural ventilation in buildings. It has been found traditionally that a proper natural ventilation system increases natural heat loss. Moreover, outlet-inlet size ratio has a great effect on indoor airflow. Furthermore, the traditional openings were only small at the windward. Consequently, a low pressure within the opening is generated due to the airflow over and around it. This low pressure helps to pull in the air with nearly a steady stream. Hassan Fathy implied that the greater the ratio of outlet to inlet area, the greater the airflow through the building [10], Fig. (3-11). Fig. (3-12) shows different arched openings used in some traditional buildings.

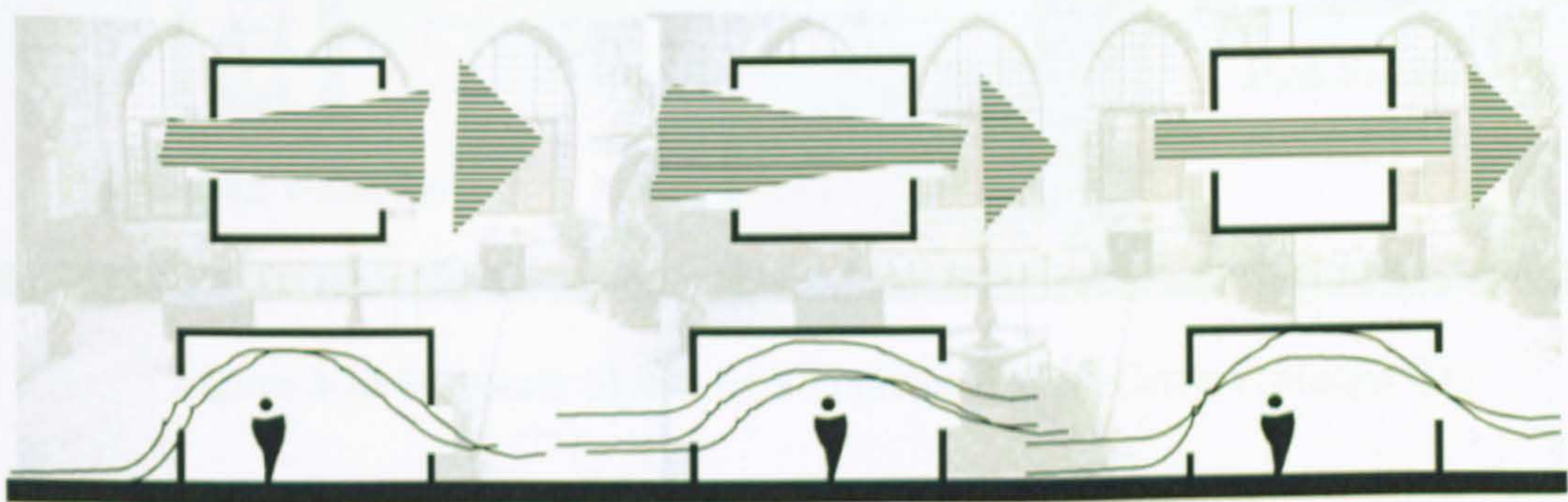


Figure 3-11 Openings Sizes and Locations [1]

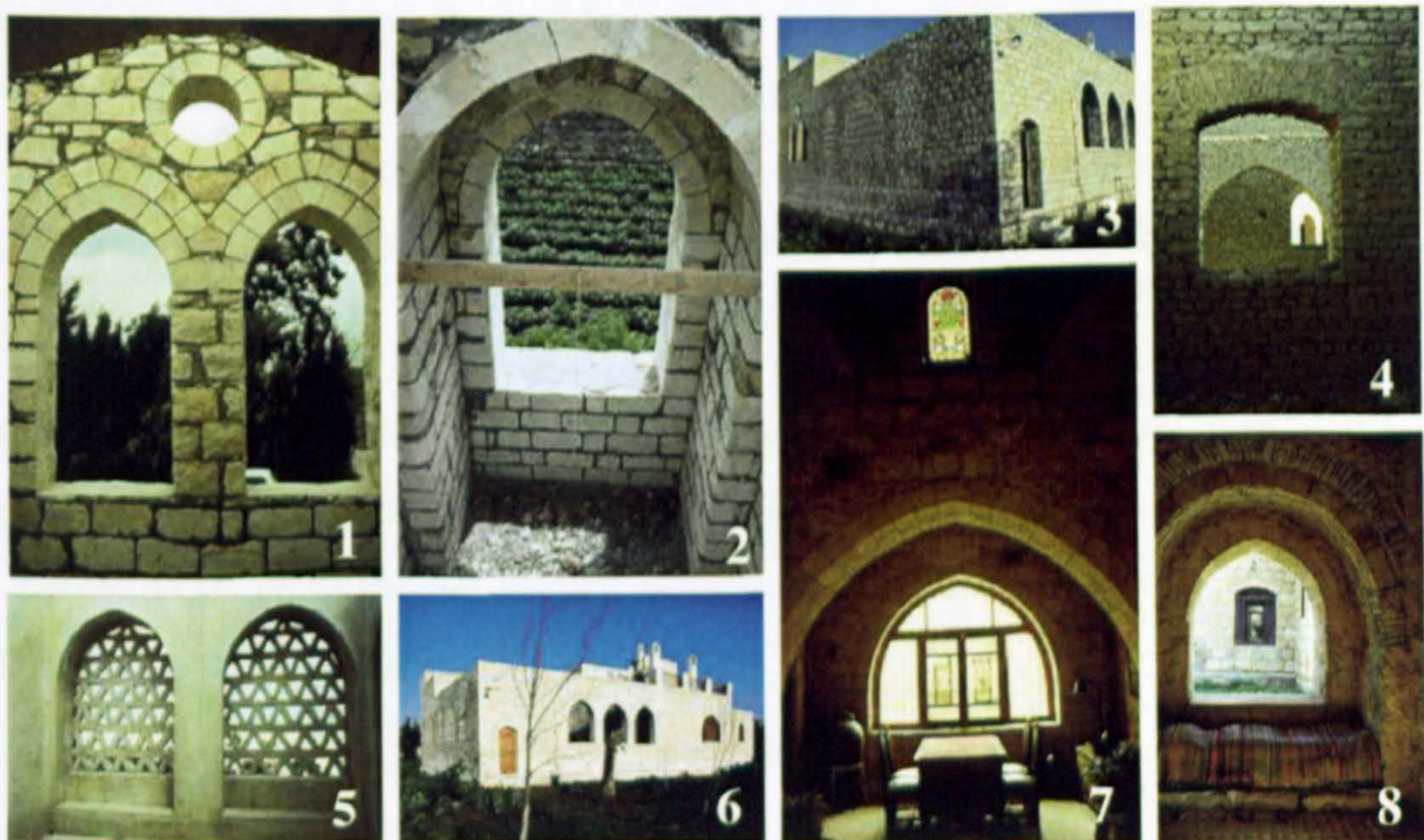


Figure 3-12 Different Arched Openings, *Source: ArchNet Digital Library* [9]

6. Wind Catcher Towers (Malqaf);

Passive Cooling by Ventilation (Air Movement by Pressure Differential)

Fig. (3-13), illustrates a schematic sketch for the typical concept of traditional wind-catchers. The wind-catcher, or *Malqaf* in Arabic, is a tall tower with an opening at the top. This opening is directed to catch the cool north winds and run down to cool the interior rooms of the house. Wind catcher will be discussed in detail later through one of Hassan Fathy's designs.

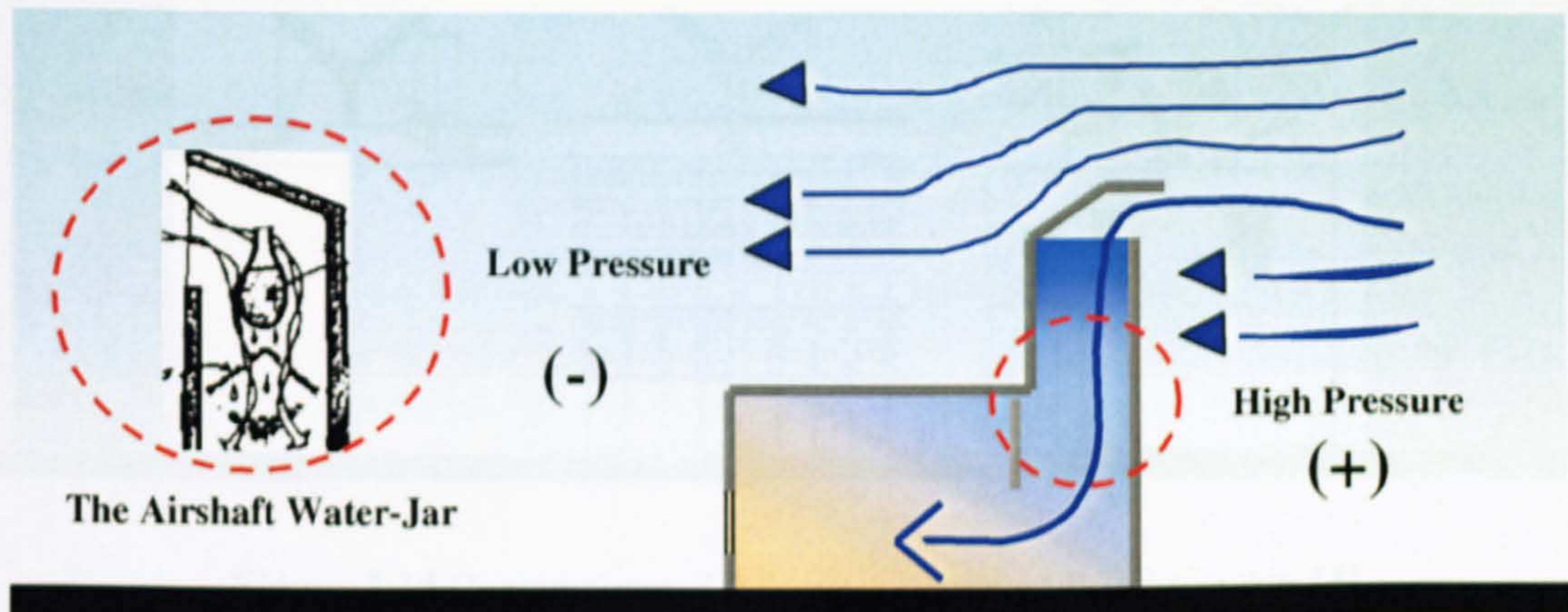


Figure 3-13 Schematic Sketch for a Traditional Wind Catcher (*Malqaf*) [1]

Chiefly, the concept of a typical wind-catcher depends on a shaft device that rises high above the building with a top opening facing the prevailing wind [11]. This device catches the wind from high above the building where it is available and cooler. This lets the air down into the interior of the building. The influence of the *Malqaf* is more obvious in dense urban communities of hot regions where indoor thermal comfort depends significantly on air movement and where the ordinary window is inadequate for ventilation [12].

The idea of the *Malqaf* dates back to very early historical times. It was used by the ancient Egyptians in the houses of *Tal Al-Amarna* and is represented in wall paintings of the tombs of Thebes [11]. In Egypt the *Malqaf* is well developed and has long been a feature of vernacular architecture. Refer to Fig. (3-1)

Fig. (3-14) shows the Egyptian ancient *Malqaf*, which has two openings, one facing windward and the other leeward, to evacuate the air by suction. It shows that the same concept has been applied in the design of the workshop at the *University of Science and Technology in Kumasi, Ghana*, Fig. (3-14), where a Y-beam system is used for routing the air circulation.

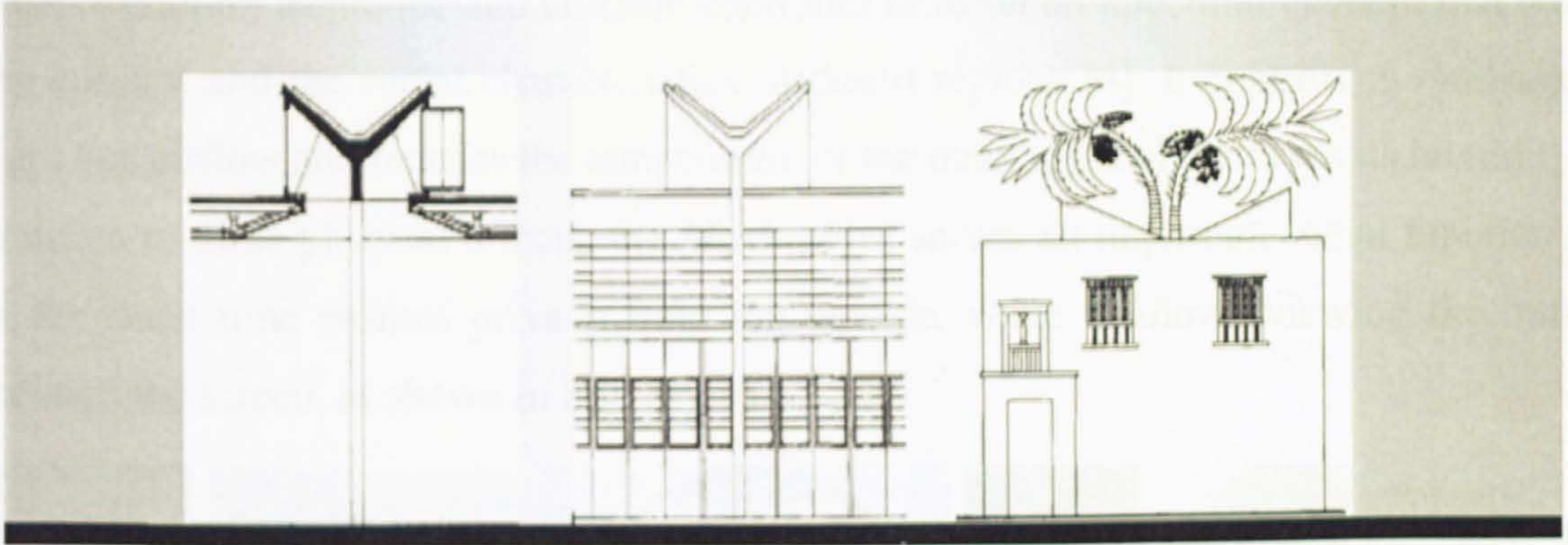


Figure 3-14 Contemporary Ideas for the Ancient Wind-Catcher [4]

In Iraq, where the air temperature in summer rises to 45°C (113°F), the typical *Malqaf* shaft is very narrow [7]. It is placed in the northern wall with a small inlet allowing the air to cool before it flows into the interior. In some hot areas in Iraq, where air temperature is very high in summer, people used to live in basements ventilated by small holes in the ceiling and a *Malqaf* with very small inlets [7].

Examples of wind-catchers placed directly over roofs or in ground floors of courtyards are shown in Fig. (3-15). The photos also depict how the *Malqaf's* principle can be incorporated into contemporary architectural designs. Further contemporary examples of different types of *Malqafs* will be discussed in detail within Hassan Fathy's and other projects in Chapter 4.



Figure 3-15 Traditional Wind Catchers (*Malqaf*)

Source: ArchNet Digital Library [9]

7. Doubled Screen Window with Porous Jar of Water (Mashrabiya);

Passive Cooling by Ventilation, Evaporation and Humidification

The traditional double screen window is a cantilevered space, which contains a lattice opening, Fig. (3-16). Small jars used to be placed beneath the wind catchers airshaft or behind the double screen windows to be cooled by evaporative cooling [4]. Traditionally, the *Mashrabiya* (the Arabic name of the double screen window) has been acting either as a passive cooling technique and climatic controller or as an architectural element that adapts the cultural and the social characteristics of desert regions [4]. It controls the passage of light and airflow and reduces the temperature of the outer air, and increases its humidity. In addition to these physical effects, the *Mashrabiya* serves an important social function and at the same time ensures privacy from the outside, while it allows viewing the outside through the screen, as shown in Fig. (3-16).

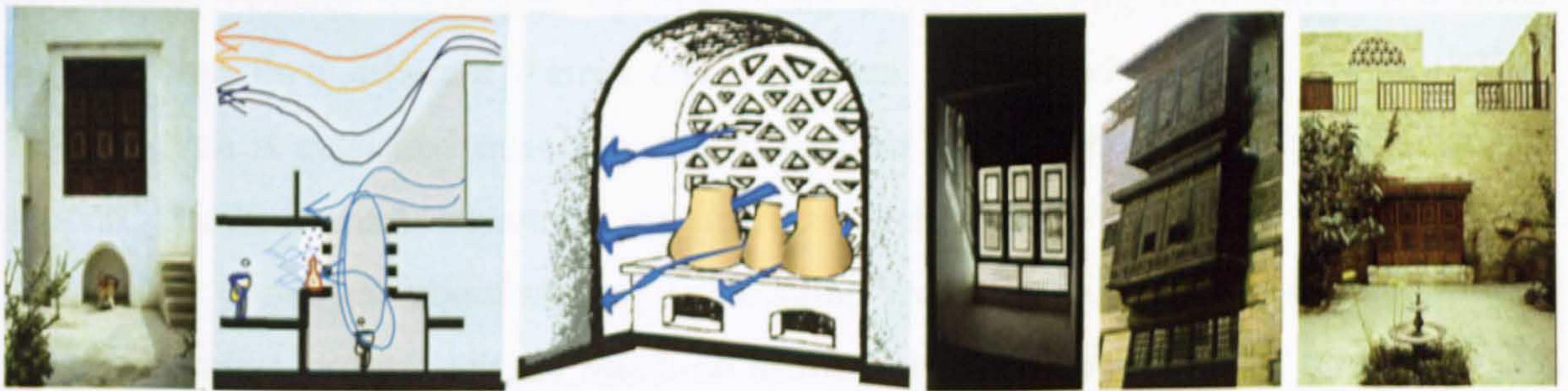


Figure 3-16 The Traditional Window (*Mashrabiya*), Source: ArchNet Digital Library [9]

Mashrabiya needs large interstices to provide airflow into a room. But in hot-arid climates, sunlight considerations require small interstices and thus sufficient airflow is not provided. For this reason, a typical *Mashrabiya* is composed of two parts; a lower section with fine close mesh, and an upper section filled with a wide mesh grill of turned wood in a pattern called *Sahrigi* [4], as shown in Fig. (3-17). The *Mashrabiya* concept has been universally used in hot arid areas, particularly throughout the Middle East and North Africa.

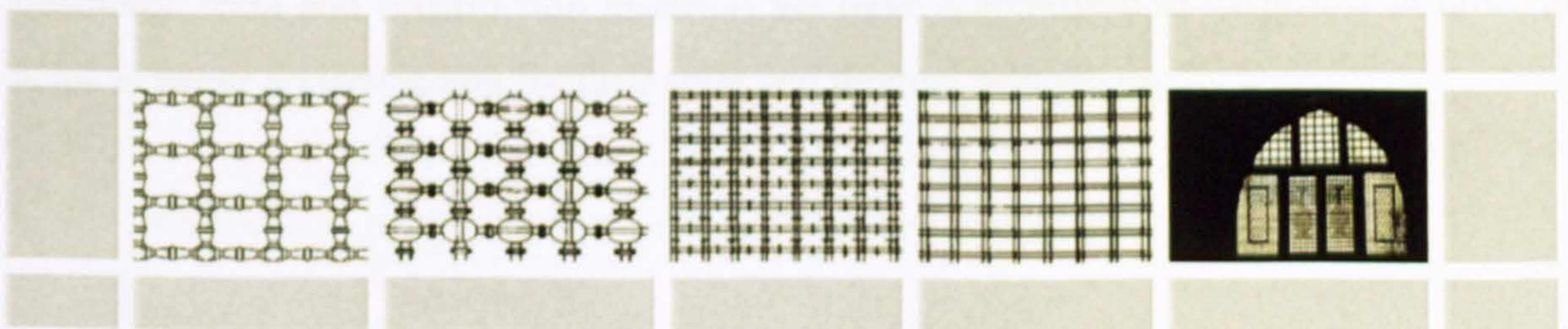


Figure 3-17 *Mashrabiya* Wooden Meshes [4]

The *Mashrabiya* cooling and humidifying functions are closely related. All organic fibres, such as the wood of a *Mashrabiya* readily absorb, retain and release considerable quantities of water. Wood fibres retain this ability even after they are cut from the tree and used in buildings, as long as the pores are not covered by an impervious paint. Wind passing through the interstices of the porous-wooden *Mashrabiya* will give up some of its humidity to the wooden balusters if they are cool, as at night [12]. When the *Mashrabiya* is directly heated by sunlight, this humidity is released to any air that may be flowing through the interstices. This technique can be used to increase the humidity of dry air in the heat of the day, cooling and humidifying the air at a time when most needed [4].

3.2.2 Traditional Passive Cooling Techniques in Contemporary Architecture

This part discusses three contemporary designs, which have tackled the issue of controlling the outside climatic conditions by employing passive cooling techniques. The three projects with their different themes and characters are located at Saudi Arabia (22°N-28°N), which is classified extremely hot in summer. Due to the availability of financial support, facilities and advanced construction technologies, the three designs have deliberately employed traditional passive cooling techniques in order to provide indoor thermal comfort without relying much on artificial tools and means. The internationally known architects intended to create a link between tradition and modernity in landmark buildings with international and milestone pieces of architecture.

In this context, the discussed examples in this chapter are different than those in Chapter 4, where employing such energy efficient and passive cooling techniques is essential. Chapter 4 examples, which have been designed by local and regional architects aim to reduce the required energy for providing the desired indoor thermal comfort in developing communities. Therefore, save their limited resources and environment. Furthermore, roof geometry, form and construction materials are more emphasised in Chapter 4 in order to achieve better understanding for their solar and thermal behaviours.

3.2.2.1 TUWAIQ Palace, Riyadh, Saudi Arabia, 1985

Architects: Frei Otto (Germany) and Omrania (Saudi Arabia)
Aga Khan Award for Architecture 1996 - 1998



Tuwaiq Palace is a recreational and cultural centre for the diplomatic quarter in Riyadh. The building stands on a high limestone plateau and looks towards the desert. In 1980, the Arriyadh Development Authority organised a competition for the Tuwaiq Palace design. Frei Otto (*Germany*) and Omrania (*Saudi Arabia*) designs have attracted attention, for the use of tents in Otto's design, and for the terraced building that engaged the landscape in Omrania's.

The two initial designs have been merged and modified in a new design on January 1983, which formed a snaking 800-metre-long wall that wraps around and protects an inner courtyard with a green garden oasis. Other facilities (*restaurants and swimming pool*) have been accommodated in three tent structures fanning out from the wall [9,13]. The architects successfully employed a number of traditional passive cooling techniques such thick exterior and stone- cladding walls that wrapped the courtyards, which are concealed from the outside harsh climatic conditions.

The white *Teflon* tents with their fan shapes reflect the direct sunlight and reduce the solar heat gain. The large building mass controls the outdoor climatic conditions passively and produces more desirable indoor thermal environment [13]. The main courtyard also contains another blue tent that shades the building entrance. The following photos, schematic sketches and drawings illustrate some of the environmental climatic controllers, which are inspired from number of the region traditional passive cooling techniques. These techniques have showed a positive contribution for accomplishing the indoor thermal comfort in this project, which the surrounding environment and the architectural heritage of central Arabia were the key design.

Fig. (3-18) shows the Tuwaiq Palace layout, which appears as well-integrated masses with the surrounding built environment and the site natural curves and slopes. The building expresses the confrontation between tradition, landscape and high technology.



Figure 3-18 The Project Layout Shows the Windowless External Walls and Inner Walls with Small Openings View the Main Courtyard [13]

Photos in Fig. (3-19) depict that the design followed two local and traditional archetypes without clear imitations of the original elements. The first one is the massive and curved thick walls constructed irregularly by limestone with small openings towards the outside. The second is the main courtyard with inner oasis and outer membrane tents.

Finally, Frei Otto's innovations in form, materials, structure and testing techniques have been recognised by numerous awards, including the Aga Khan Award for Architecture in 1980. His design showed a successful combination trial that fittingly used traditional techniques and introduced a new building typology with a strong relationship to its local region.



Figure 3-19 Tuwaiq Palace Photos, *Source: ArchNet Digital Library* [9]

3.2.2.2 KASR ALHOKM; Justice Palace & Mosque, Riyadh, Saudi Arabia, 1992

Architect: Rasem Badran
Aga Khan Award for Architecture 1993 - 1995



The growth of Riyadh, from a town of 25,000 inhabitants in 1950 to a city of over 3 million people today, has virtually obliterated the traditional building style of Saudi Arabia's Najd province, characterised by mud brick, flat roofs and a distinctive decorative style. The Arriyadh Development Authority (ADA) project for the development of the old town as the core of the new city represents a powerful alternative. It has brought the new construction into balance with the traditional architectural idiom and spatial relationships.

Fig. (3-20) shows some schematic sketches for the project's traditional style, which clearly matches traditional Saudi Arabia's Najd buildings. Rows of towers placed above the roof have been used to provide natural lighting and ventilation. While it reduced heat gain by creating shaded areas above the main roof [14]. The rows of towers also served as a double roof with air gaps, Fig. (3-20) [9]. Rasem Badran defined the central core of Riyadh through a series of open spaces, including plazas, fountains and courtyards, that connect the building to its surroundings [15]. His approach combines a reinterpretation of traditional Najdi architecture with an innovative yet unobtrusive use of modern materials and technologies.

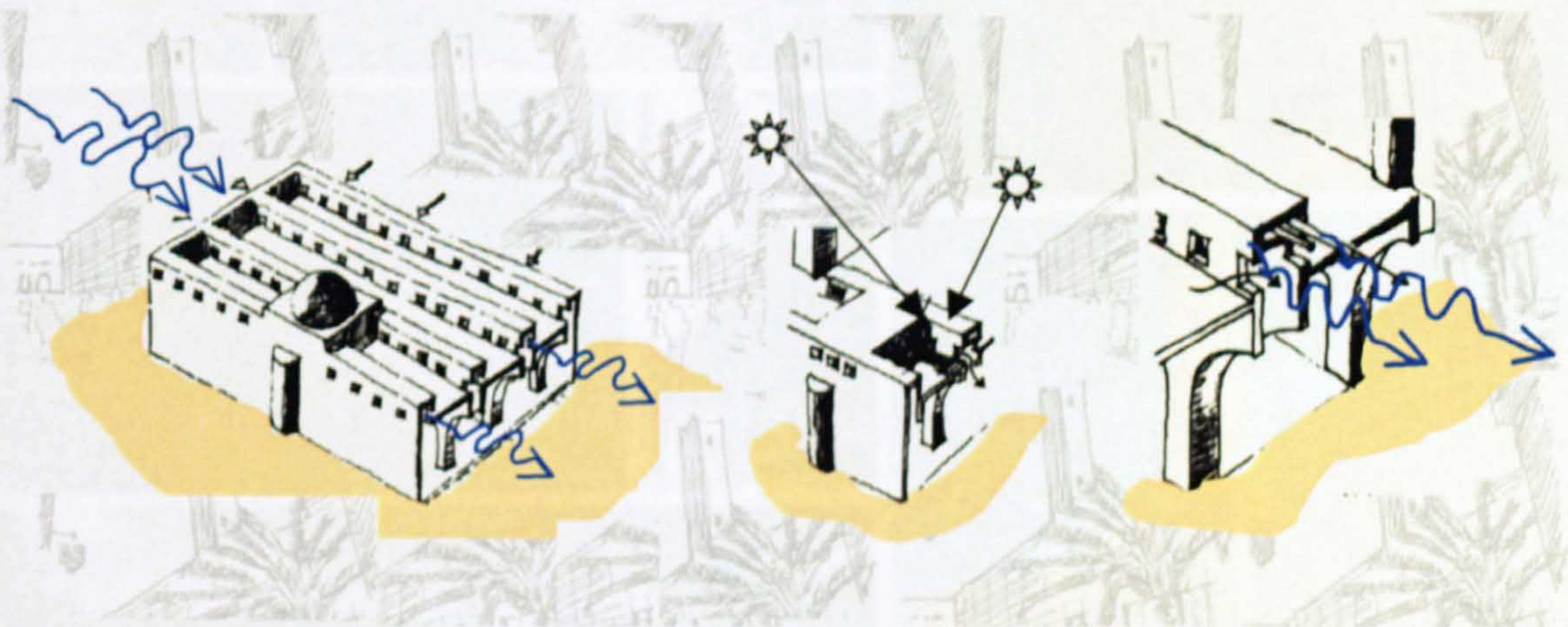


Figure 3-20 Analytical Sketches of Number of Passive Cooling Techniques
 (After R. Badran), Source: ArchNet Digital Library [9]

As is shown from the photos on Fig. (3-21), mud brick, flat roofs and a distinctive decorative were the main characteristics of that traditional building style. Other traditional strategies were adopted in which the building elements and materials were used positively in response to the harsh climatic conditions. Ventilation towers provide indirect lighting, which eliminates the need for external wall windows to save the indoor environment from outdoor heat [14]. The use of thick and massive windowless walls increases thermal mass effect as well as privacy and security.

On the other hand, the minaret, rather than following its function (*calling public for praying*), is treated as a traditional wind catcher (Malqaf) with its climatic and symbolic power, Fig (3-21). Finally, the architect was able to confirm typological proportions without mindlessly copying the past Najdi forms. He dealt with the problem as a planning issue, in direct contrast to the current trend toward lightweight detached structures. The created pattern of massiveness and clustering successfully reduces heat gain (*the thick mud brick walls with its small opening-holes significantly helped in this respect*) [15].



Figure 3-21 Traditional Najdi Typology Photos [16]

3.2.2.3 National Commercial Bank, Jeddah, Saudi Arabia, 1982-84

Architect: SOM (Skidmore, Owings and Merrill)



Skidmore, Owings and Merrill (SOM) design of the **National Commercial Bank (NCB)** is set in a three-acre plaza on the edge of the Red Sea. The project geometry consists of a triangular form rising 27 floors [17]. The building stands 122 meters tall.

The National Commercial Bank is the headquarters office building for the largest privately owned bank in Saudi Arabia. The design is a response to both the shape of the site and the harsh desert climate of Jeddah (*latitude 21°N and 39°E longitude*) with high humidity rates around the year, which strongly generated the need for an inward looking building (*Islamic Traditional Typology*). It expresses traditional indigenous architectural identity and Arab culture.

The design attitude in terms of controlling outdoor harsh climatic conditions lets the tower turn its back towards the outside. The design also keeps the rooms shielded from direct sunlight, thus the exhausted warm air is allowed to escape through the three large façade openings. External surfaces are covered with a well-treated stone cladding to serve efficiently as mass effect cooling [17].

The three sky-courts form one triangle courtyard, which extends vertically through the building providing natural ventilation. The stacked courtyards, combined with the windowless exterior, ward-off direct sunlight, but also allow diffuse daylight in the office spaces. The verticality of the 400 feet bank tower is interrupted by these three dramatic triangular courtyards chiselled into the building's facade[17].

Two of the courtyards face southward and view the old portion of the city and the Red Sea, (each contains seven stories, 95 feet high and 97 feet wide). The third nine-story courtyard (125 feet high and 97 feet wide) is located in the middle of the Northeast façade, and provides a thermal buffer for all the glazing, which is more than 20% of vertical surface area [17], as shown in Fig. (3-22).

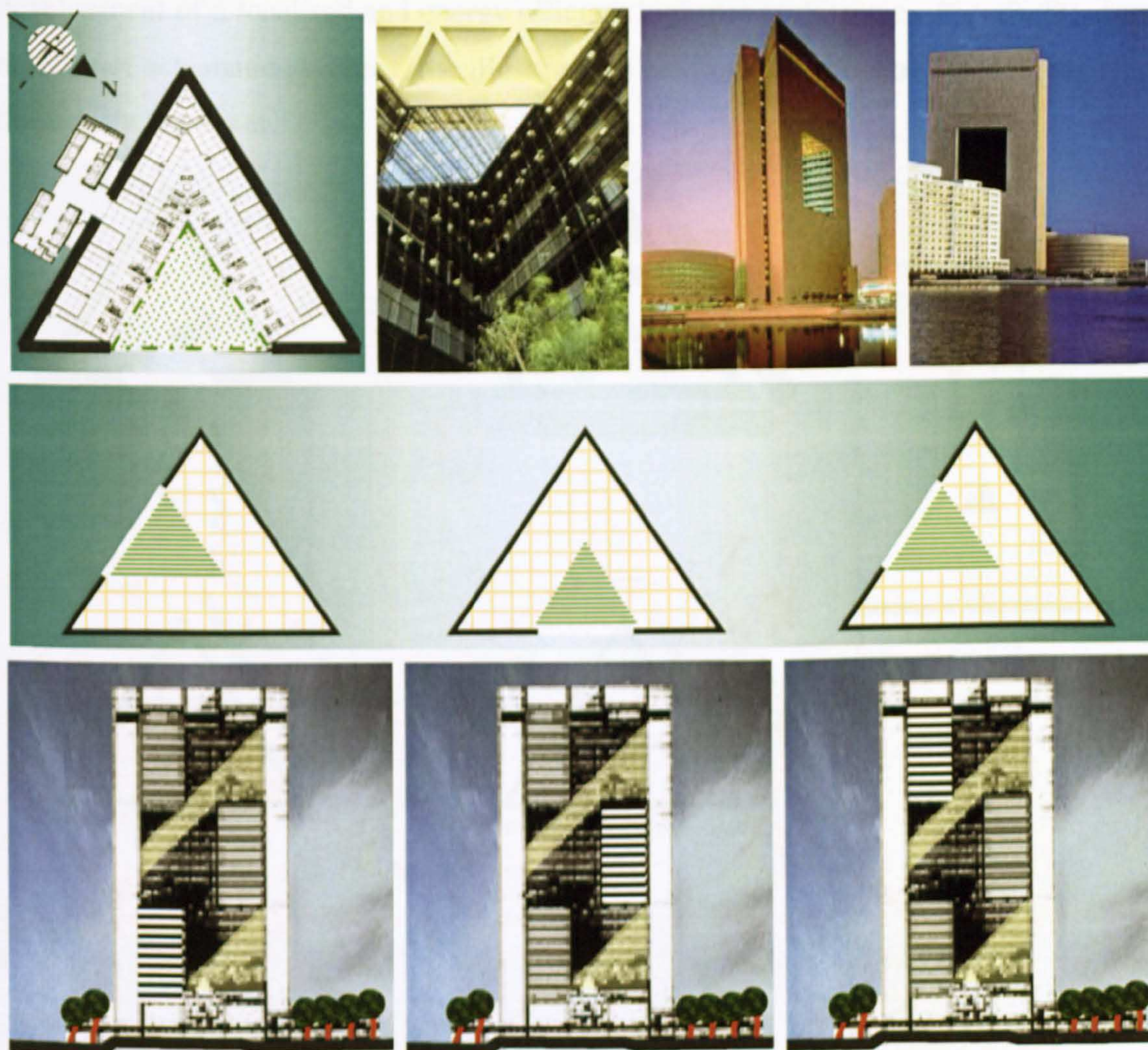


Figure 3-22 The Three Sky-Courtyards Locations and The Tower Exteriors Photos *Source: ArchNet Digital Library* [9]

The northwest side of the triangle is abutted by vertical circulation and service core (*lifts, staircases and public services*). Similar to Islamic traditional design, the office windows open directly onto these courtyards with an inward orientation. All glazed surfaces are recessed and face into three shaded sky-courts or the hanging gardens, making deep incisions into the otherwise monolithic block, two on one side, one on the other, alternating vertically in a spiral arrangement.

There is no doubt that the effectiveness of this project's design and solutions can be considered as a simple and modern climatic control design, and a sheltered recreational space, which is also a traditional courtyard. As shown previously in Fig. (3-22), the design represents a radical shift in modern architecture, which opens the way towards a more regional modernism. Therefore, the tower represents a significant step towards the development of a localised and energy efficient high-rise architecture. Fig. (3-23) shows a number of schematic sketches that illustrate the environmental control techniques applied throughout the tower.

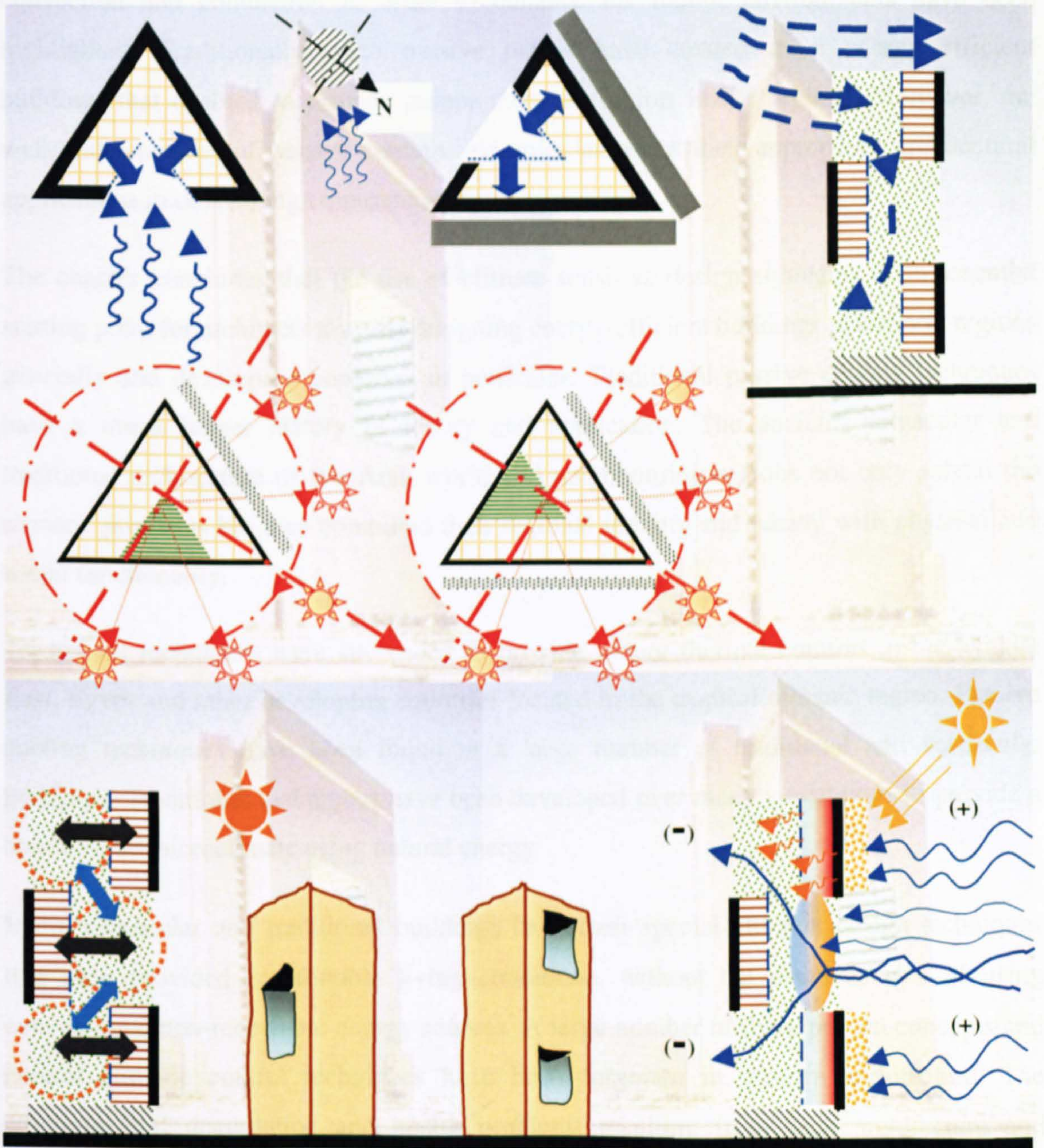


Figure 3-23 Sketches of NCB Environmental Control Techniques

3.3 CONCLUSIONS

The maintenance of indoor thermal comfort in contemporary buildings by heating, cooling, humidification, or dehumidification, is often achieved by consuming non-renewable energy. This is one of the rapid depletion causes of the fossil fuel reserves of the earth, and the emission of harmful substances and CO₂ [18]. Contemporary buildings in hot-arid climates must widely employ passive cooling principles, such as cooling by ventilation, evaporation, or dehumidification. Also the thermal concepts of losing heat through natural convection and conduction in order to enhance the indoor environments have been highlighted. Traditionally, such passive means have created more energy efficient buildings that enabled to provide indoor thermal comfort in hot regions. Moreover, the well understanding of passive cooling principles increases their appropriate architectural applications in developing communities.

The chapter concludes that the use of climate sensitive design strategies is an essential starting point for architects towards designing energy-efficient buildings in hot-arid regions generally and developing countries in particular. Traditional passive cooling techniques have a much longer history of theory and application. The ancient, vernacular and traditional architecture of the Arab world and neighbouring regions not only solved the climatic problems but also combined their regional identity and beauty with physical and social functionality.

Traditional techniques have succeeded to provide indoor thermal comfort in the Middle East, Egypt and other developing countries located in the tropical climatic region. Passive cooling techniques have been found in a large number of traditional and vernacular buildings. Traditional techniques have been developed over many generations to provide a comfortable microclimate using natural energy.

Many vernacular and traditional buildings have their special climatic design techniques that have provided comfortable living conditions, without the disadvantages of using conventional non-renewable energy sources. A large number of these proven concepts and natural climatic control techniques have been forgotten in modern architecture. The environmental degradation and health problems resulting from such architecture and modern buildings " *sick building syndrome*" have led to an obvious interest in building designs that can provide indoor thermal comfort mainly by natural and passive means.

The chapter has represented a trial for analysing and evaluating a number of traditional passive cooling techniques to be effectively employed in contemporary designs. Domed and vaulted roofs, massive walls, courtyards, openings, wind catcher (*Malqaf*), and doubled window (*Mashrabyya*) have exemplified the traditional passive cooling techniques.

Testing the integration of traditional passive cooling techniques within different designs is very crucial for more indoor thermal comfort without reliance on artificial means in hot arid climates. The better understanding of the technical aspects, traditional approaches and passive cooling techniques makes these techniques applicable and compatible among contemporary buildings. Finally, the chapter highlighted three contemporary designs that similarly tackled the issue of controlling the outside climatic conditions by employing traditional techniques in hot regions. The three designs provided indoor thermal comfort without much reliance on artificial tools and means.

The next chapter explains a number of traditional roofing forms, which have been employed in contemporary buildings in hot climates and desert communities to create energy efficient buildings and indoor thermal comfort environments. Curved roof geometry, form and construction materials are more emphasised in Chapter 4 in order to achieve better understanding of solar and thermal behaviours of their forms.

Reference List

1. Moor, F. Environmental Control Systems - *Heating Cooling Lighting*. (1993).
2. Boake, M.T. Passive Versus Active Solar Design: Opposing Strategies in Support of a New Sustainable Vernacular. *Architronic: In Support of a New Sustainable Vernacular* Vol. 4(NO. 3):p. 2.
3. Olgyay, V. *Design with climate: Bioclimatic Approach to architectural Regionalism*. New York: Some chapters based on cooperative research with Aladar Olgyay, Van Nostrand Reinhold; 1992.
4. Fathy, H. *Natural Energy and Vernacular Architecture, principles and examples with reference to hot -arid climates*, Chicago & London: Published for United Nations University by the university of Chicago press; 1986. (EDITED BY WALTER SHEARER; Abdel-Rahman; Ahmed Sultan.
5. Sophia and Stefan Behhling in Collaboration with Bruno Schindler Foreword by Norman Foster. *Solar Power The Evolution of Sustainable Architecture* 2000.
6. Elseragy, A. A. and Gadi M. B. Traditional Architecture, Energy Consciousness and Sustainability, *An approach to affordable and thermally comfortable buildings in hot-arid climates with special reference to Egypt* Proceedings of the Second World Conference on Technology Advances for Sustainable Development & Workshop on Renewable Energy & Development of Remote Areas 2002 Mar 11-2002 Mar 14; Cairo, Egypt.
7. Peter Stead, *Lessons in Traditional and Vernacular Architecture in Arid Zones. Housing in Arid Lands - Design and Planning*. London: The Architectural Press; 1984. (GOLANY, G.
8. Nahar, N. M., Sharam P. and Purohit M. M. Studies on solar passive cooling techniques for arid areas. *Energy Conversation and Management*, 1999; Vol. 40(No.3/4): pp. 89-95.
9. ArchNet Digital Architectural Library. [Web Page]; <http://www.archnet.org> . [Accessed Jul 2003].
10. Pearson, D. *Earth to Spirit - In Search of Natural Architecture*. Gaia books Ltd; 1994.
11. Fathy, H. *Architecture and Environment*. *Arid Land News Letter* 1994 Fall-1994 Winter; ALN No. 36.
12. Fathy H.. *Architecture for the poor An Experiment in Rural Egypt*. [Web Page] (1973).
13. Davidson, Cynthia C. *Tuwaiq Palace*. In *Legacies for the Future: Contemporary Architecture in Islamic Societies*. London: Thames and Hudson: 1998. (Cynthia C. Davidson (ed).
14. Davidson and Cynthia C. *Great Mosque of Riyadh and Old City Centre Redevelopment*, In *Architecture Beyond Architecture*. London: Academy Editions: 1995. (Cynthia C. Davidson, and I. S. e., editor).

15. Steel, J. *Sustainable Architecture - principles, paradigms, and case Studies.* (1997).
16. Aga Khan Award in Architecture. [Web Page]; <http://www.aka98.org/home.htm>.
17. Khan, H. U. National Commercial Bank. MIMAR 16: Architecture Development 1985.
18. Bansal, N. K. *Passive Building Design - A Hand of Natural Climatic Control.* Amsterdam, The Netherlands: Elsevier Science B.V.; (1994).

CHAPTER 4

ENERGY CONSCIOUS ROOF DESIGN IN HOT-ARID CLIMATES

4. ENERGY CONSCIOUS ROOF DESIGN IN HOT-ARID CLIMATES

In the previous chapter, a number of the traditional passive cooling techniques in hot arid regions has been discussed with their passive-cooling strategies. This chapter dwell on traditional roofing systems in general and their forms in particular in order to create more energy efficient buildings and indoor thermal comfort environments. In the beginning, humans were nomadic; people took shelter in caves and other naturally hollowed places above the ground. Over the years, skills have improved and simple shelters were built with mud and stone. Later, humans experimented wide variety of roofing techniques, designs, and materials according to the available construction technologies, spaces functions, and local people lifestyle.

All through the history, people were always trying to adapt their dwellings with the environment in order to create more suitable living conditions. Traditionally, dwellings and other buildings have been constructed with full respect to the characteristics of a particular geographical location in order to control its local climatic conditions. Consequently, different types of architecture have arisen to adapt different climatic and cultural conditions, which vary from region to region. Traditional and vernacular buildings showed real sustainability through employing native construction materials and techniques, which efficiently enabled them to minimize the environmental impacts and reduce the energy required to supply different climatic controllers [1].

Traditional buildings acquired the most possible use of renewable energy at this time by a number of passive techniques such as, wind-catchers to bring fresh-air in and employing the proper size and location for openings to create cross ventilation. In order to catch natural sunlight and avoid solar radiation, building orientation has been carefully chosen. Most traditional buildings in hot climates were opened towards inner-shaded-courtyards. Thus, traditional architecture avoided negative impacts on the environment and the eco-system. Modern architectural methods however generate a number of major environmental problems, which destructively influence the eco-system.

4.1 CLIMATE AND BUILDING DESIGN

The variation in the climatic conditions is the main motive behind the variety of buildings forms and orientations. It also creates the diversity in construction materials techniques. Consequently, building design, form, and the geometrical configurations may not suit various geographical locations or different climatic conditions. For example, roof shape, form, construction materials, and components should differ from location to another to appropriately suit particular climatic conditions.

Many traditional and vernacular buildings employed passive cooling techniques in order to provide indoor thermal comfort, particularly in hot-arid areas. Recently, due to modern life styles, economic growth, and advanced technologies, most of these passive techniques have been abandoned.

4.1.1 Roof Design in Hot-arid Climates

In the last two decades, serious consideration and worldwide research efforts have been noted on energy conservation in buildings, sustainable buildings, energy efficient buildings, and environmentally friendly buildings. Therefore, it is accepted that architects and designers should rely upon natural ventilation and day lighting much more in their designs to decrease non-renewable energy consumption in buildings. They also need to employ different passive techniques that keep the buildings elements properly shielded from solar radiation and heat gain.

The climate of hot-arid zones in general is characterised by high temperatures (40-50° C in summer), with sharp variations in both diurnal (*day/night*) and seasonal (*summer/winter*) temperatures. In such climatic conditions, the roof is the most fundamental part of the domestic building envelope in defining shelter and climate modification. Nearer to the equator, the roof receives and absorbs solar radiation significantly more than any other surface of the building. Roof design and the thermo-physical properties of roofing construction materials have considerable effects on indoor thermal comfort [2]. The variety of roofs designs, shapes, and construction materials has made roofs grow beyond being only a cover of the below-roof-spaces to become a symbol of wealth and position. Notably, temples and public places have had a factor of permanency rather than dwellings or homes for the people.

4.1.2 Thermal Performance of Roofs Form and Geometry

The roof is that part of the buildings which receives most of the solar radiation, and its shading is difficult. The roof is the only continuously exposed element of the building's envelope. Therefore, the design of a building envelope (*shape, form, and orientation*), especially the roof, plays a significant role in maintaining an acceptable level of thermal comfort in buildings.

Roofs are not only protecting the building from precipitation, but also the strongest thermal impacts (*heat loss and heat gain*) occur here. The roof receives the greatest amount of solar radiation, which is the main cause of heat and indoor thermal discomfort in hot-arid climates. As discussed previously in chapter three, the indoor thermal comfort depends on a number of climatic and physical factors. Significantly, it depends on the reduction of energy input that the intensity of solar irradiance above roofs causes in hot climates.

Traditional roof design has had a great influence on controlling the intercepted solar radiation. Both solar and thermal performance of a roof depends to a great extent on its form, the use of thermal insulation, thermal properties of construction material, and the reflectivity of the roofs skin [3]. Apart from roofs form and geometry, each of the other parameters has been appropriately investigated to determine and improve their thermal and solar capabilities. In addition to all the above parameters, traditional roofing systems have successfully provided a tangible indoor thermal comfort in the hot regions and desert harsh climatic conditions. This happened without understanding the relationship between the roof geometrical configurations (*roof form and orientation*) and insolation.

Traditionally, it has been realised that curved roofs are more effective than the flat ones in providing indoor thermal comfort in hot climates [4]. But it has not been clearly linked to roofs form or geometry. The research presented in this thesis aims to test curved roofs forms and geometrical capabilities in order to reduce the received solar radiation intensity on roofs surfaces. It therefore seeks better understanding of solar and thermal performances of such curved-roof forms, curvatures and orientations (*traditional domes and vaults*).

This chapter demonstrates different projects and trials of reintroducing such roofing systems (*vault and dome*) to the public, the designers, and the builders. It demonstrates different projects that have depended on curved roofs to control the outside climatic conditions. Therefore provide acceptable and desirable new settlements designs, which are adaptable with the desert harsh climatic conditions and able to reduce the cooling loads in buildings (*sustainable new settlements*).

Buildings envelope and roof have a great influence to keep indoor environments, which are greatly affected by outdoor climate, favourable and comfortable for occupants throughout the year. Preferably, this should be achieved without the need for, or use of artificial and mechanical devices. In order to control the intensity of the received solar radiation on roof surface, roofs geometric forms (*pitched, flat, curved, vaulted, etc.*) should not only follow the precipitation-flow-patterns but it should also follow the insolation parameters. This allows the roof surface to avoid or receive solar energy according to the climatic conditions and the geographical location requirements.

The use of vault, dome, and curved shapes as roofing systems can be traced back to most ancient architecture. As early as the 3rd millennium BC, they were very widely used in the Middle East countries and Egypt. Roman, Sassanid and Byzantine builders also used arches, vaults and cupolas fairly and widely before they were adopted in many regions of Europe [5].

The combined effect of solar radiation and ambient air conditions is expressed in the sol-air temperature concept. This includes three component temperatures: the outdoor air temperature, the fraction of solar radiation absorbed by the surface on which it is incident, and the long wave radiant heat exchange with the environment [6]. Sol-air temperature is the fictitious temperature of the outdoor air which, in the absence of radiant heat exchange would produce the same rate of heat transfer through building envelope (*roof and walls*) as the actual heat transfer mechanism between the sun, the surface of the roof, the outdoor air and the surroundings. Therefore, the received solar radiation intensity I (W/m^2) above roof outer-surface has a significant influence on the sol-air temperature (*see equation (4-1)*).

As it will be explained in details in Chapter 5, the intensity of the received solar radiation above surface is influenced by the receiving surface geometry and orientation. Traditional curved-roof forms (*dome and vaults*) will affect the sol-air temperature and consequently indoor temperature. O'Callaghan [7], identifies the sol-air temperature at a particular time by the following equation;

$$T_{sa} = T_o + R_o (aI - eI_1) \quad (4-1)$$

Where;

T_{sa} = sol-air temperature in °C

T_o = outside air temperature in °C.

R_o = the external surface resistance in $m^2 \text{ } ^\circ\text{C}/\text{W}$.

I = the intensity of direct plus diffuse solar radiation on the outer surface in W/m^2

I_1 = intensity of long-wave radiation from a black surface at the temperature of the environmental air which is equal to $100 \text{ W}/\text{m}^2$ for radiation from a horizontal roof to a cloudless sky and zero for a vertical wall because it is assumed that radiative gain from the ground balances radiative lost to the sky).

a = an absorption coefficient which varies from 0.5 for brick to 0.9 for a black surface.

e = the emissivity of the outer surface for long wave radiation (assumed = 0.9).

4.1.3 Roofing Construction Materials

Technical and material alternatives of traditional roofing techniques are available in most of developing-hot-arid countries, whereas sometimes they are restricted. Non-local or imported resources are often not affordable, and they are unable to provide the same climatic protection that can be achieved by using local and earth construction materials.

Due to their thermal properties, natural construction materials, mud bricks, and earth are suitable construction materials for roofs in dry climates, whereas a number of other conventional and traditional roofing construction material; such as cement bricks and reinforced concrete are not operatively effective in such climatic conditions.

New types of roofing construction materials such as burnt clay tiles, fibre concrete, asbestos sheet, monolithic concrete, organic materials, bituminous roofing, and roof gardens have been applied in several projects. Traditionally, vaulted and domed roofs and earth construction in general have simply provided durable roofing systems using renewable sources and materials that are locally available. Thus, they have performed as environmentally friendly techniques, on the one hand while on the other they avoided depleting those local materials and succeeded in creating thermally comfortable indoor environments [8].

4.2 TRADITIONAL CURVED ROOFS CONSTRUCTIONS (*Vaults and Domes*)

The 20th century in general, and developing countries in particular, has observed a serious need for depending upon sustainable buildings designs and technologies, which are mainly energy efficient and environmentally and socially friendly. There is a need for employing building techniques that are climatically conscious, economical, simple to erect, and affordable for both low-income and high-income housing [8].

The sought solutions have encouraged and renewed interest in low-energy designs, traditional passive cooling techniques, earth construction, and vault and dome roofing systems. Vaults, domes, and their construction techniques have their antiquity roots and a tradition in desert buildings (*hot-arid climate regions*), specially the Middle East, Egypt, and Iran. They have been developed to meet the local needs and climatic conditions. The results were often spectacular and durable [4].

4.2.1 Curved Roofs Geometrical Forms and Types

Geometrically, there are many forms of vaults and domes. Barrel vaults, Fig. (4-1) are the simplest forms, which in fact consist of a succession of identical arches. Barrel vaults can have steeper or flatter profiles to create semicircular, segmental, or catenary vaults. The catenary vault is very common as its form gives maximum stability with a minimum use of material. Combining barrel-vaults with the same profile generates a number of other types such as the groined vault or the domical vault [9], Fig. (4-1).

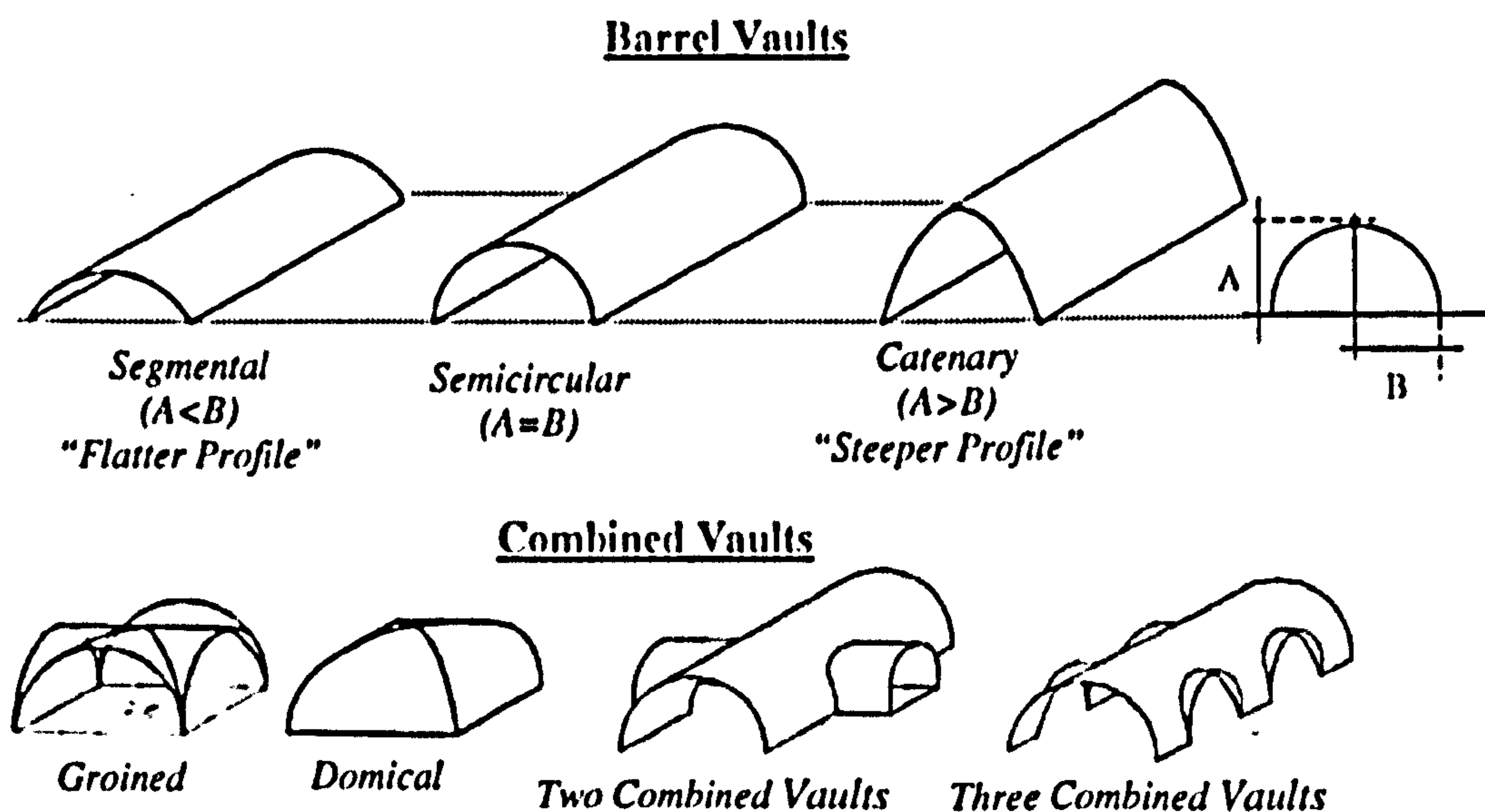


Figure 4-1 Geometric Forms of Different Vaults (After Stulz [9])

Domes are circular in plan; they are used to cover square or rectangular spaces by *pendentives* or *squiches*, Fig. (4-2). The rotation of an arch generates domes or cupolas. A cupola shape can be semicircular, segmental, conical, etc. As shown in Fig. (4-2) domes on *pendentives* can cover any kind of polygon shape. It is possible to combine either different domes or vaults with domes in one roofing system.

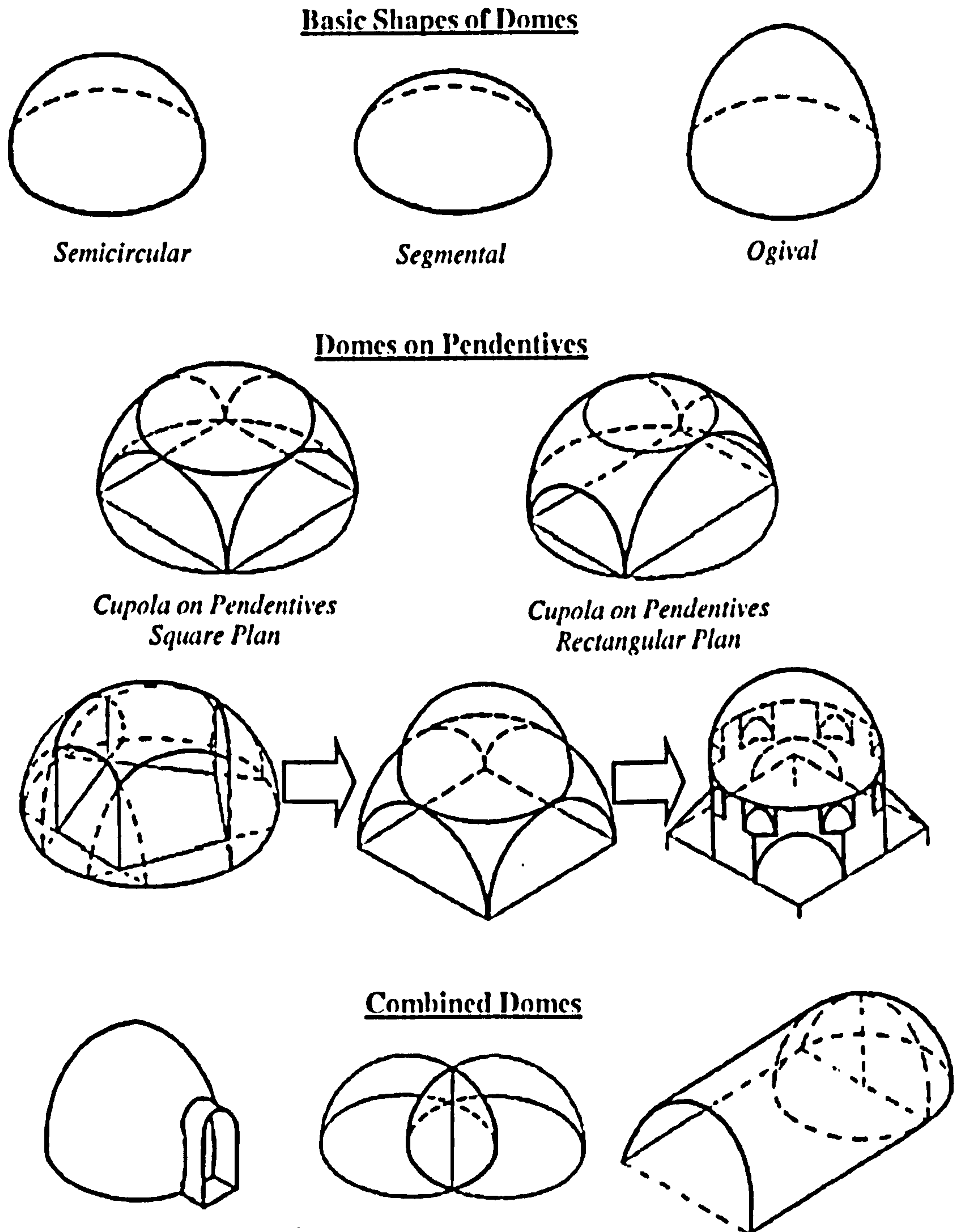


Figure 4-2 Forms and Types of Traditional Domes and Domes on Pendentives [10]

4.2.2 Curved Roofs Construction Technologies and Materials

The experience acquired over the last twenty years has allowed the designing and construction of traditional curved roofs and structures to be mastered once again. The technology in general is now used in several areas of the world but the local techniques are different. Initially launched in Niger, the “ Woodless Construction” program suggested simple technical solutions that are well suited to the local context, and follow particular strategies and policies of research and training to provide public knowledge amongst local people [9].

4.2.2.1 Curved Roofs, Vaults, and Domes Construction Materials

The materials used for curved roofs constructions can be the same as those used for walls and can be found locally. Construction is therefore less expensive, creates local job opportunities and avoids imported materials and consequently allows foreign currency savings in such developing communities. The mass thickness of such structure also provides a good heat storage capacity, which delays heat transmission in order to meet the comfort requirements in hot arid and desert regions. The mass thickness of those roofing systems gives good sound insulation as well.

Vaulted and domed roofs can be built with a variety of materials, including earth and dried mud blocks, cement or lime stabilised compressed blocks, and fired bricks and stones. Curved roofs can be constructed with or without formwork (*shuttering*), which is known as “Woodless Construction Technique”. The finishing materials vary according to the geographical location, climatic conditions, the building budget, and local resources around the site.

4.2.2.2 Woodless Construction Techniques (*Vaulted and Domed Mud Constructions*)

Woodless construction represents a very famous and traditionally well-known option for the erection of those roofing techniques. Regardless of the different names and technologies most of the traditional construction techniques for curved roofs can be classified as “Woodless Construction Technique” [10]. But while this may seem the most realistic and viable option, it may not be the optimum [10].

Woodless constructions are mainly originated from the development workshops experienced in Egypt and Iran, and lately in Tunisia and other regional countries [11]. Introducing woodless construction techniques using hand-made un-stabilised earth bricks aim to provide builders and the public with an affordable roofing technique using genuinely and locally available-earth-materials to achieve not only durable and good quality roofing systems but also energy efficient and sustainable roofing systems [12].

Traditional vaults and domes, which are erected by woodless construction techniques, depend widely on employing local resources and labour. Therefore, woodless construction techniques have greater potential in areas where labour is plentiful, and local construction materials are easily available like in most desert developing communities.

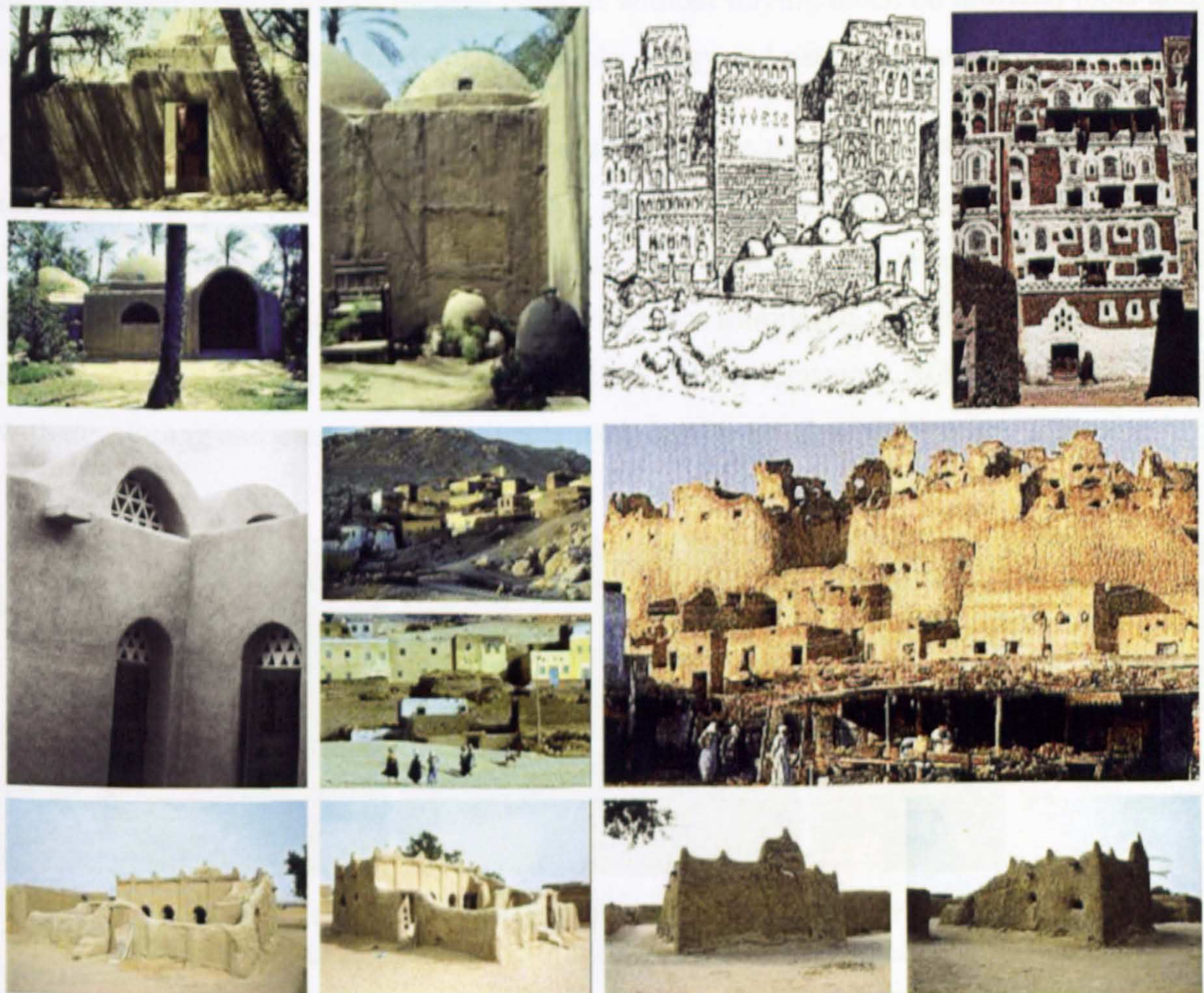


Figure 4-3 Traditional Buildings and Mud Constructions, Siwa and Upper Egypt
Source: ArchNet Digital Library [13]

Technically, these construction techniques suit both formal and informal building sectors. They are easy for local builders and the public to assemble, and thus are suited to build either simple shelters and houses or large public facilities with high standards of comfort to cope with modern lifestyles needs. Encouraging such construction techniques leads to the employment of local builders and materials, which exist in abundance. It also develops the local skills and stimulates the local and national economies. Hence, the need for imported building materials is reduced and local resources of energy are saved.

Due to their construction materials (*mud, adobe, and earth*) thermal properties, forms, and geometries, traditional roofs with woodless construction (*domed and vaulted roofs*) have succeeded in reducing the received solar radiation intensity on roofs surfaces. Moreover, they provided passive indoor thermal comfort without relying much on artificial tools and means, and therefore they saved non-renewable energy and natural resources.

Other advantages of woodless construction methods are that curved roofs built with this technique do not collapse unexpectedly, which is a common problem with other construction techniques and other roofs forms and geometries [9]. Woodless construction and vaulted and domed roofing using mud-bricks was introduced into the Shael in 1980 by Development Workshop, a small Canadian and French registered NGO [12], concerned with developing and promoting sustainable solutions for housing problems.



Figure 4-4 Different Types of Dried Mud and Earth Bricks;

Source: <http://www.johnnyrolfjanderooden.nl/firedmuho.htm>

4.2.2.3 Nubian Vaults and Domes

“Nubian” vault technique was developed in the hot-arid region of southern part of Egypt (*Nile-Valley-Kingdom*) 3000 years ago or even more. The Nubian Vault technique was employed over the centuries in Upper Egypt, to build vaults without any formwork. This technique is classified as one of the famous woodless construction technologies [14]. The basic vault form is very similar to that of an inverted catenary, the form taken by a chain suspended from its two ends, and thus, for the chain, a shape in pure tension, fig. (4-5). Ancient Egyptian Vaults were commonly constructed by the Nubian Vault technique and from adobes, such as the 3200 years old vaults, which stand within the temple precinct of *Ramses II* near Luxor [15].



Figure 4-5 The Nubian Way for Erecting Vaults, *Source: www.canellect.com* [14]

Nubian vault technique depends mainly on reclined arches that are made of adobe. As shown in Fig. (4-5) it needs vertical walls to support the inclined arches. Therefore, the cross section of the Nubian Vault, which is mainly loaded by its own weight, should have the form of an inverted catenary, so that it contains compressive stresses only [15].

Mud bricks are not capable of withstanding tensile forces, thus they are very strong in compression, the vault's shape allows self-standing in compression. The vault is built up in a series of courses, which incline towards the side of the supporting-wall. The shape of the vault, the inclination of the bricks courses, and the stickiness of the mud mortar, combine to keep the courses in place without shattering during construction.

In the Nubian Dome technique, mud bricks masons and builders determine the distance between the centre of the dome and the angle of each brick by using a wire or a radial arm that rotates around a central post [15]. Therefore, circumferential courses of adobes are laid using this movable guide, Fig. (4-6).

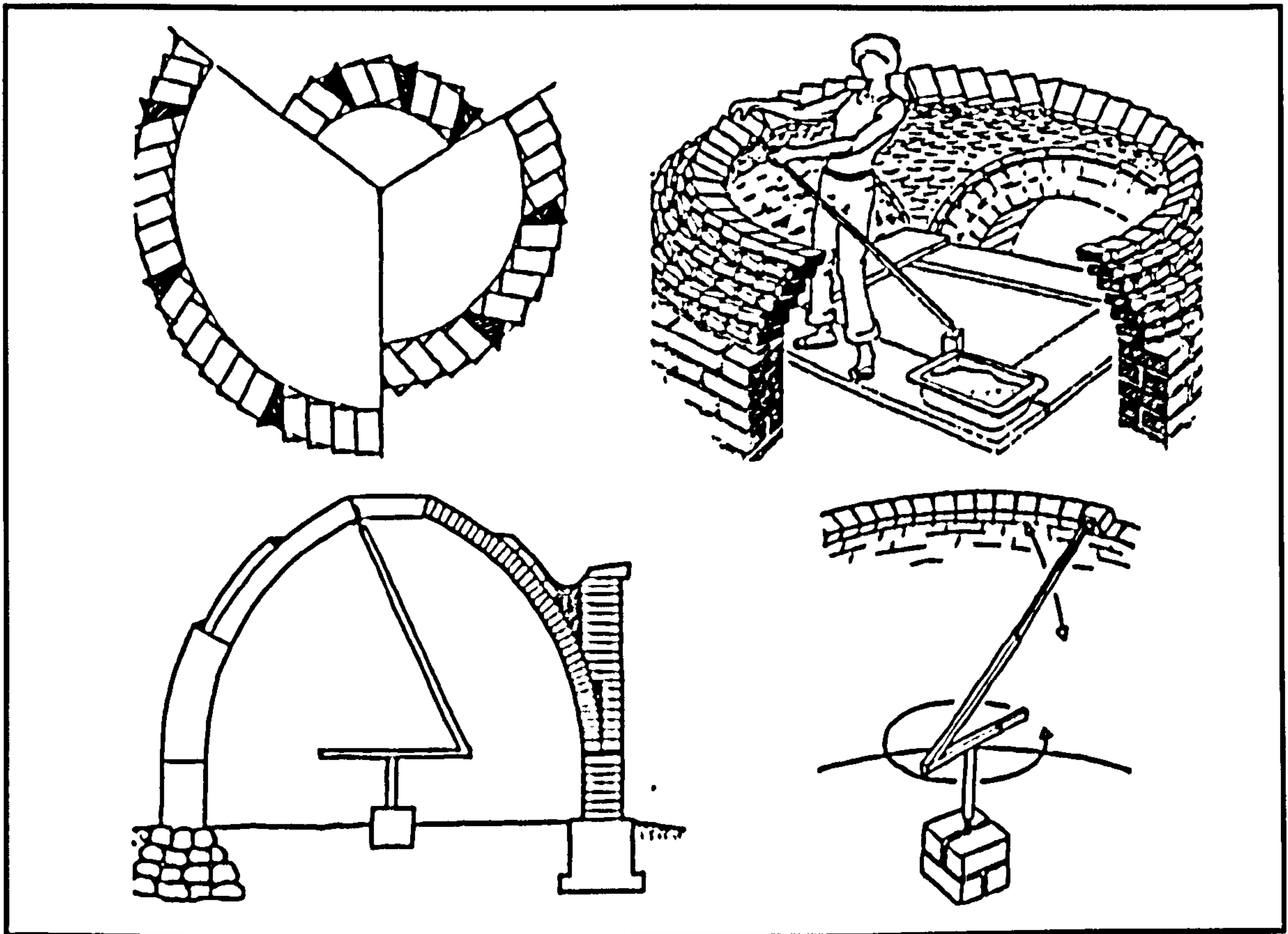


Figure 4-6 Modification of Nubian Dome with Eccentric Guide [15]

The main disadvantage of the Nubian Dome technique is that only spherical domes can be produced, as tensile ring forces occur at the bottom. Therefore, when covering larger spans, steel strips or reinforced concrete ring beams and other strengthening elements have to be added, otherwise domes might fail during the construction process. For these structural limitations, the hemispherical shape is the basic shape for traditional domes [15].

As numerously used for erecting domes in the Ancient Egypt, traditional woodless construction techniques were based only on un-stabilised mud bricks. Horizontal, concentric courses of un-stabilised mud-bricks are laid first at a shallow angle, then more sharp and acute towards the top[14]. So the concentric circles of the brick-courses get narrower towards the top of the dome.

Photos in Fig. (4-7) depict the traditional process of erecting a “Nubian Dome”. Bricks are placed side by side until each concentric course forms a complete ring or closed-circle. The shape of the dome produces external thrust at the lower part of the structure, which does not suit the use of un-stabilised earth bricks [14]. Like the vault, there is a considerable concern to send the forces of the dome down to the ground. Nowadays, Nubian techniques for erecting domes and vaults is one of the most famous woodless construction techniques, which is still utilised in many parts of the world after being established in the southern part of Egypt (*Upper Egypt*).



Figure 4-7 The traditional Process of Erecting Woodless Mud Bricks' Domes
Source: ArchNet Digital Library [13]

In order to avoid the disadvantages of Nubian dome and vault techniques, the “Woodless Construction Program” slightly modified this shape to allow the sides of the vault to take extra loading, which the trainee builders could easily build. The thickness of a supporting-wall depends on the design of the roof and the size of underneath spaces [10]. For small domestic construction with rooms no longer than three or four meters wide, the preferable thickness of the wall is about 40cm. The same walls' bricks can be used for foundations if they are away from the rainwater and damp. Other advanced foundation can be used, or even concrete, but these can make the building unaffordable for poorer clients.

On the other hand, strings and wires that are firmly fastened onto the end supporting-wall guide the vault shape. In erecting a vault it is vital to transfer the outward thrust of the supporting-wall to the ground through a thick-enough wall, or contain the thrust forces that conduce the collapse of the supporting-wall by an adjacent roof's counter-thrust, as shown in sketches in Fig. (4-8) (*After Stulz*) [9]). Understanding the effect of the vault's outward thrust enabled Iranian builders to build much flatter vaulted roofs than those that were common in Egypt [10].

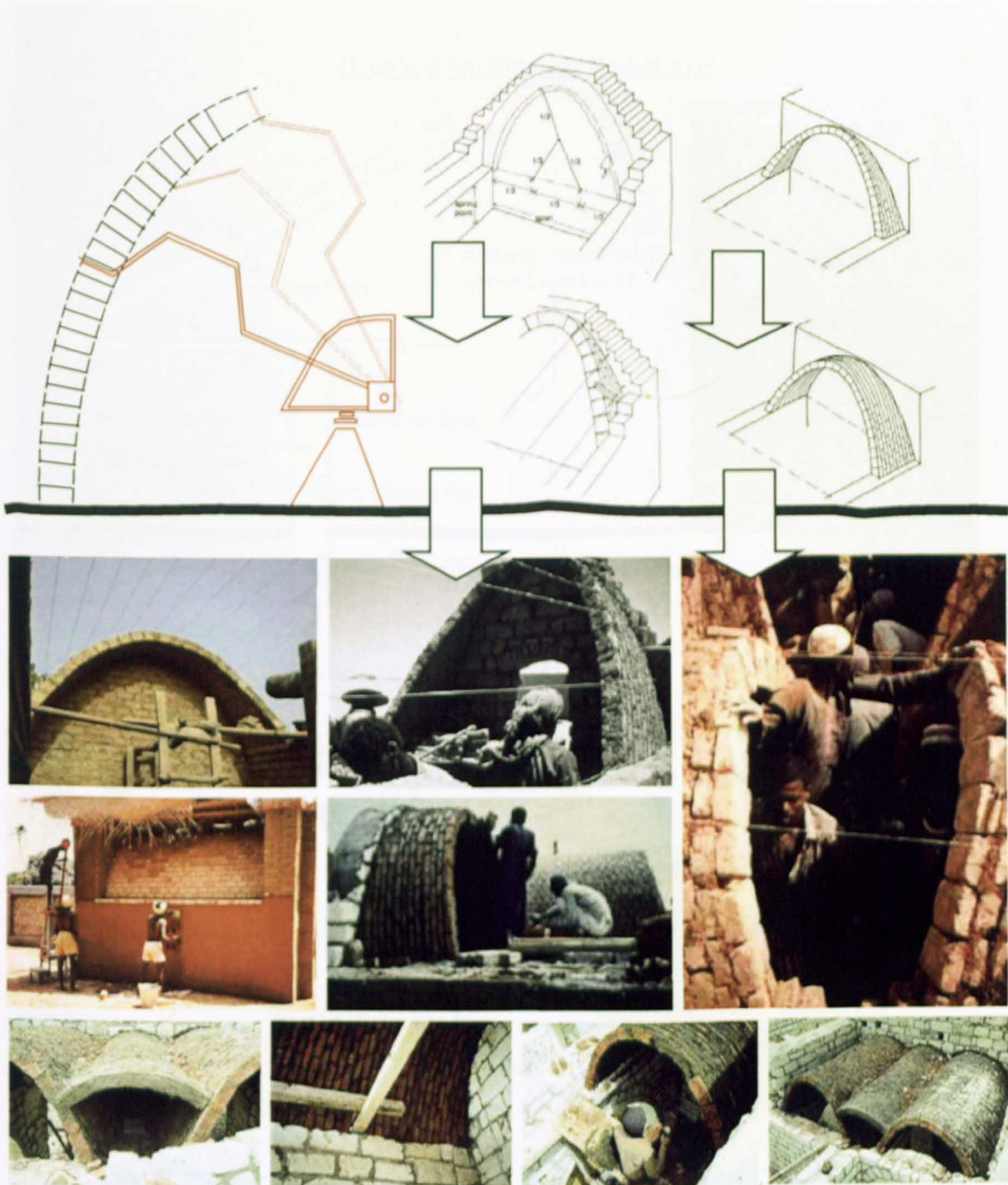


Figure 4-8 Vault Woodless Construction Methods, *Source: ArchNet Digital Library* [13]

It has been found repeatedly that lowering the spring point, Fig. (4-9) and making the dome sides with steeper angles helps to avoid this structural problem. In their development workshops, “Woodless Construction Program” [10] displaces the guiding arm away from the centre to lower the spring point without lowering the overall height of the roof. The mobile guide Fig. (4-9) is one-piece equipment, which trainee builders can use, although simple domes can still be built without it.

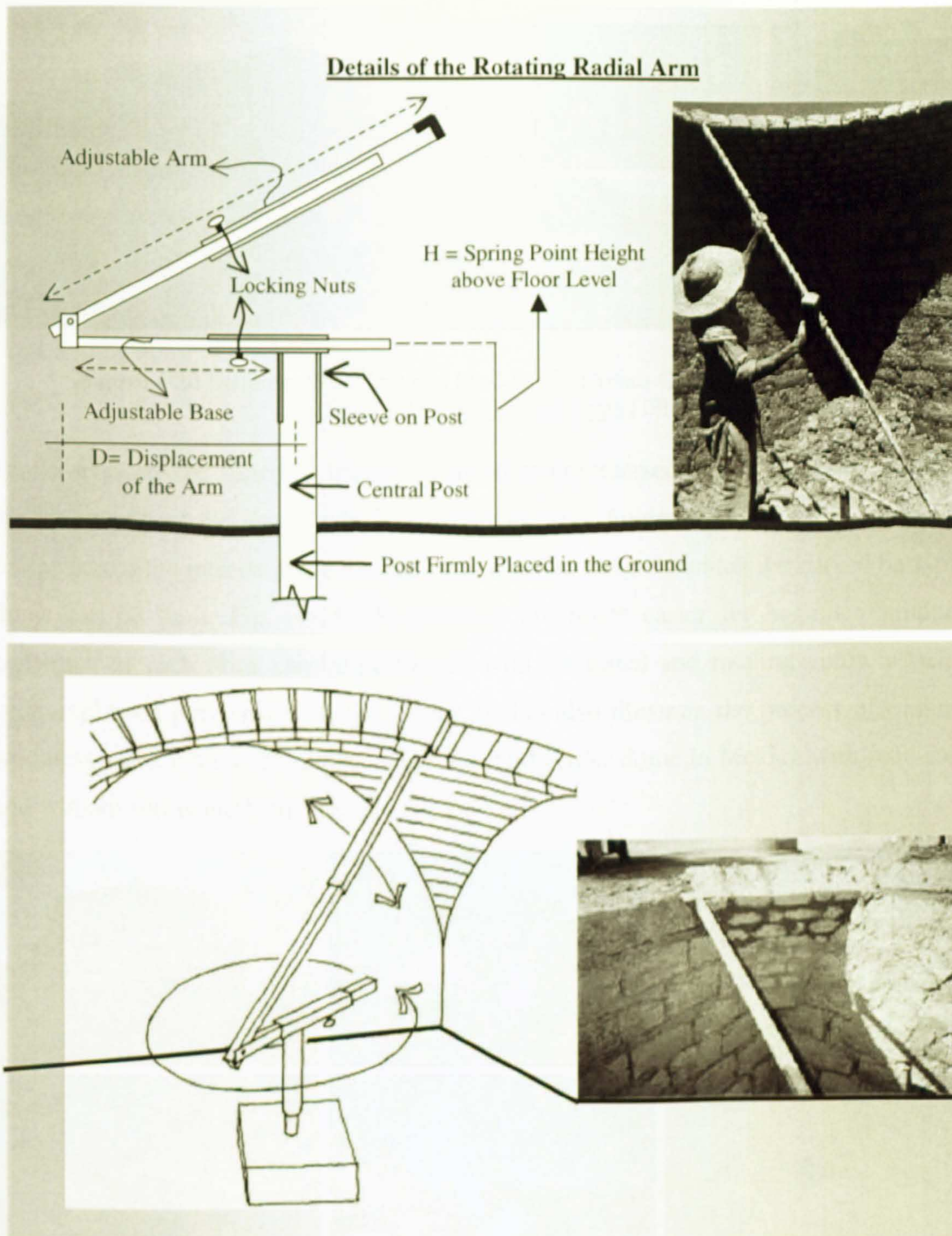


Figure 4-9 Mobile Guide for Erecting Woodless Mud Bricks' Domes (After Norton [10])

In general, single dome, domes, or combined domes and vaults can cover different plans or spaces (*square, rectangular, or round spaces*), Fig. (4-10). Therefore, nearly all domes construction techniques depended on either pendentives or squinch-arches to be built above square or rectangular spaces, Fig. (4-11). This process was geometrically illustrated in the beginning of this chapter (*refer to Fig. (4-2) page (81)*).



Figure 4-10 Different Woodless and Mud-Bricks Domes Covering Different Plans

Source: ArchNet Digital Library [13]

Pendentives are the spherical triangles formed at the intersection of the walls' corners on the lower part of the dome, which is called the rim. Squinch-arches are the arches that bridge across the interior angle formed by two walls, and over which the curved base of the dome can be built, Fig. (4-11). Pendentives are much easier for beginner builders to construct, as each brick can be positioned with the radial and rotating guide, which has been explained previously. Photos in Fig. (4-11) also illustrate the process of traditional woodless construction techniques to erect a mud-bricks dome in Mexico with mud-mortar and without formwork [16].



Figure 4-11 Woodless Stones and Mud Bricks Domes on Pendentives

Source: www.caeloproject.com [16]

Photos in Fig. (4-12) show a number of different woodless construction techniques for erecting traditional arches, vaults, and domes. As shown in Fig. (4-12), photos depict that large numbers of these techniques are still widely employed within some contemporary construction technologies in developing communities' desert regions. Their sustainable, energy efficient, and environmentally friendly potentialities and techniques must be explored. As will be discussed in more detail later in this chapter, different training workshops and programs have showed positive support towards reintroducing such traditional construction techniques to be reused in contemporary buildings, Fig. (4-13).



Figure 4-12 Woodless Bricks and Stones Constructions in Southern Part of Egypt
Source: ArchNet Digital Library [13]



Figure 4-13 Training Programs and Small Houses Provide Good Training For Local Beginner Masons [10]

4.2.2.4 Afghan and Persian Domes

Another technique to build domes and curved roofs without formwork has been used for centuries in Afghanistan [15]. This construction technique has been widely used to build traditional bell-shaped domes, which mainly depended on reclining arches at 30° with horizontal to be effectively erected, Fig. (4-14) [15].

The adobe blocks that form the arch should touch the ground at its lower edge. Therefore, the upper gap, which is generated at the top merge of the dome's two sides, has to be inserted with wedges, Fig. (4-14). A variety of architectural forms can be covered with this technique. Moreover, the Afghan and Persian bell-shaped domes can be appropriately combined with the Nubian dome technique.

The bell-shaped domes also can be erected by the normal Nubian dome techniques as in the domes of the Indian Institute of Technology in New Delhi, India, which will be discussed in more detail later in this chapter.

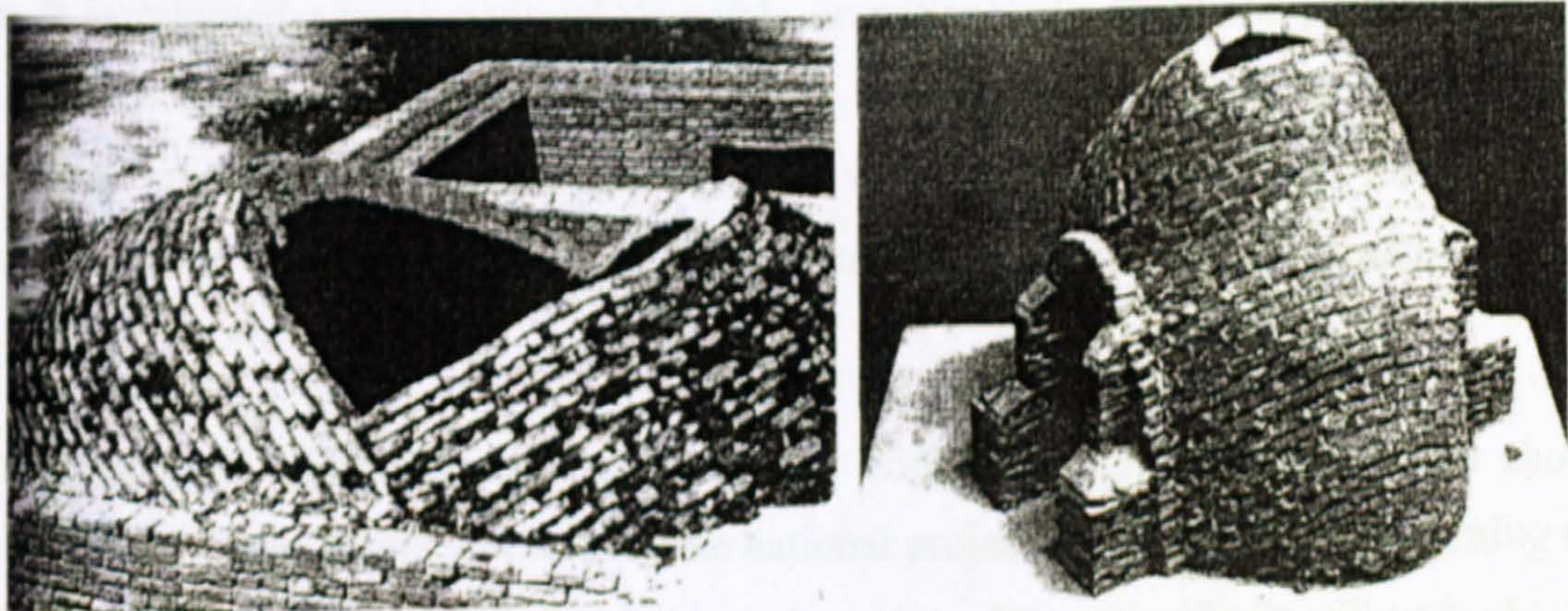


Figure 4-14 Bell-shaped Domes with Reclining Arches [15]

4.3 REINTRODUCING TRADITIONAL CURVED ROOFS

Despite many not-well-investigated aspects like their construction materials thermal properties, shape and form, and the proper orientation, vaults and domes succeeded traditionally to provide indoor thermal comfort in buildings. Nowadays, developing countries with extreme hot climates are desperately in need of reintroducing such roofing systems in new settlements.

As has been mentioned before in previous chapters, large numbers of developing countries new settlements are proposed in harsh desert and hot climatic conditions. Consequently, relying upon such roofing systems and other traditional passive cooling techniques improves sustainable environment perspectives, energy conservation means, and energy-efficient buildings.

4.3.1 Persuasive Introduction and Successive Publicity

The introduction of vaulted and domed roofing systems can be considered as successful when it is adopted among national demands or national development processes. Large demands on this traditional techniques grantee governmental training programs and a continuous construction market development with national or private funds. These programs ensure enough numbers of qualified masons to supply the construction market [9].

Introducing such traditional techniques through widely held public participation shows their ability to integrate the new large scale national projects successfully. Highlighting the successful features of curved roof techniques through traditional methods will undoubtedly illustrate the social and environmental benefits. Choosing a public participation methodology is very crucial towards making the public endorse a new approach that may solve public related issues. The public not only have to know their responsibilities throughout the development process but they also have to feel that their feedback is substantial even if the national outputs are very clear and positive.

Eventually the public themselves are the monitors of such techniques and their performances. Therefore, setting a proper context for such wide public participation needs specialists and experts in this particular field, but it is useful to review some curved roofs' social, technical, and functional aspects, which are almost public related [9];

- What are the problems that tend to be overcome by introducing curved roofs (*Vaults & Domes*).
- Show confidence that these techniques stand a real chance of suiting local conditions and matching the needs for the planned new settlements, their climatic conditions, and the people lifestyle as well.
- Explain the potential of these techniques towards solving the environmental problems of a particular local region.
- Illustrate that these techniques have a role to play where existing building systems have to rely heavily on artificial tools to control outdoor climatic conditions. Therefore, non-renewable energy resources are either no longer easy to obtain or severely consumed or rapidly degraded.
- According to their passive climatic control abilities that suit different climatic conditions, they not only suit poor housing, but middle and high income people are also targeted by this introduction, as they can use them as well.
- Vaults and domes are already well-known forms that are linked with a particular function or concept, sometimes not positive. Accordingly, convincing the public to adopt them may follow the fashionable, the environmental friendly, or cultural and architectural identity arguments.
- In general, traditional architectural vocabularies, and in particular vaults and domes appeared aesthetically as they have great cultural features that show off architectural identity, riches of the past, and regional heritage.

4.3.2 Training And Practical Skills Development Programs

Traditionally, builders learnt the skills of vault and dome building through a long process of training, which could last many years. At the beginning, long programs for introducing such roofing systems to the public of such new settlements. Whereas, a quick and firm base to develop the practical skills of masons and public is more needed.

After several years of providing training opportunities “Woodless Construction Training Program” concluded that programs, which equally introduce both learning by training and learning by doing are more effective. Therefore the local demand of masons and the public can be generated and satisfied directly on buildings sites. Formal training programs are properly possible where national, international, or private funds are available. In developing countries and Egypt in particular there are successful examples, which have been funded by the government, private, or jointly with either governmental or non-governmental international organisations.

Builders and public showing interest in the training techniques will be followed by a further period of raising skills standards to cover the technical problems and difficulties they faced. This creates technical and conceptual adjustments that allow the technique to be more suited for the local conditions. These processes are known as “onsite development workshop” that reviews the technical content for public, beginners, and well-trained builders. Also this is important to bring their skills up to date. They should learn the ability of passing on their learnt skills to other colleagues. Builders may be invited to train as team leaders and site managers in order to help later as trainers for smaller number groups.

The understanding of some crucial technical and structural aspects is very essential and important for the success of the construction process. On the other hand, the nature of the structure, its forces and the earth limits also require well understanding from all members who are handling every stage during designing, site preparations and other construction processes. The following parts of this chapter discuss in details those aspects.

4.3.3 Technical Future Update and Training for Architects and Building Designers

Training for local building engineers, designers, and architects develops the relationship between the builder and the designer in order to realise what the builders are capable to construct and to guarantee the final product quality through number of the onsite development workshops. The designers should have good knowledge of how these traditional constructions technologies work, and what are their main structural constrains and how the builders will exactly erect each span-height ratio [9,15]. Traditionally, this relationship was properly existed, whereas it is rarely developed nowadays.

Future training for designers must not only cover the concepts of traditional vaults and domes designs. But it is also important to investigate their thermal and solar performances in order to provide more desirable indoor thermal comfort without using non-renewable resources and artificial cooling systems. On the other hand, a number of new laboratory and computational tools has been developed to investigate and analyse the environmental performances of building envelope form, orientation, and construction material.

4.4 REVITALISATION OF TRADITIONAL CURVED ROOFS

With the advent of the industrial revolution, most of the inherited techniques and perfected knowledge of creating, using handmade tools, were lost and are now forgotten. Energy-intensive mechanised tools have damaged both indoor and outdoor environments. In the 20th century, and particularly from the beginning of the 1940s onwards, a number of pilot projects and contemporary successful initiatives that have followed the same framework of the traditional passive cooling techniques [8]. These recent initiatives are trying to provide reciprocal relations and integration between tradition and modernity. Moreover, they aim to understand the traditional passive cooling techniques to be properly employed in contemporary designs. Furthermore, these movements and trials strive to diminish the western hegemony and saving the vernacular heritage by restoration and conservation.

The previous chapter analysed and investigated different traditional techniques that have been implemented appropriately as passive climatic controllers in hot-arid regions. The following parts of this chapter demonstrate the work of a number of local and regional architects that have utilised curved roofs particularly as passive cooling techniques in various types of buildings in hot-arid regions. Throughout the last two decades, by employing traditional roofing techniques in their work, architects have not only showed their regions architectural character, but have demonstrated sustainable and energy efficient means that can provide indoor thermal comfort in hot climates without much reliance on artificial tools.

4.4.1 Hassan Fathy And Other Egyptian Architects

Across the Middle East and the tropics there are architects who have made number of successful attempts looking into traditional spirit and techniques. They are endeavouring to use them appropriately in their designs in term of creating more adaptable energy efficient architecture by the proper employing of traditional passive cooling techniques in hot-arid regions buildings.

Despite the tangible significant influence, experiences, and abilities that they have showed through their works, still only a few of local and regional architects are well known such as Hassan Fathy, Ramses Wisa Wasef, and Abdel Wahed Elwakil. Although there are structural and formal limitations of some natural and traditional building materials in such regions, they managed to show well integration with buildings new technologies and types, and users lifestyle.

As the following parts of this chapter show, Fathy's initiatives inspired many other architects and designers to integrate traditional techniques among their designs in order to suit both simple and luxury buildings.

4.4.1.1 Hassan Fathy Architectural Philosophies, Efforts, and Attempts

"Frankly, it has taken the architectural profession half a century to begin appreciating and understanding the importance of Fathy's ideas" [17].

The Egyptian architect Hassan Fathy (1900-1989) [18] is one of the most recognised architects who pioneered the revival of vaulted and domed roofing systems generally and the Nubian vaults and domes in particular. He reintroduced the use of vault and dome roofing techniques from 1941 onwards. Hassan Fathy was born on 23 March 1900, in Alexandria. He joined the faculty of Engineering to study architecture and graduated in 1926. Fathy's work and designs have succeeded to characterise Egyptian architecture and he successfully integrated number of traditional techniques within his designs. Fathy trained local inhabitants to make their own construction materials and build their own buildings [18].

Hassan Fathy is the first Egyptian architect in the 20th century who did not import architectural ideologies from the west [18]. He found the beauty of the Nubian architecture because of its own special character. Climatic conditions, public health considerations, and ancient craft skills also significantly affected his designs. Based on the structural massing of traditional buildings, Fathy incorporated dense mud brick walls and roofs, traditional courtyards, domed and vaulted roofs in most of his designs to provide passive cooling. He believed in their great effects of creating indoor thermal comfort without relying on artificial tools and means.

Hassan Fathy devoted himself not only for housing the poor in developing nations and providing indigenous environments at minimal cost, but also for improving their living standards by employing local skills and materials. Due to his knowledge of both Egyptians economic situation and traditional architecture Fathy achieved his goals. The following parts of this chapter exemplify different types of his work. The first two examples are development housing projects, whereas, the rest are three of his residential designs. For Fathy and his followers vaulted and domed mud brick structures represent both traditional architecture and technology and reflect their values and identities.

4.4.1.2 Hassan Fathy Development Housing Projects

Undoubtedly, using local materials, climatic conscious designs, and energy efficient techniques to control the outside harsh climatic conditions for developing communities is very crucial. On the other hand, sustainability, cost-efficiency must be seriously considered for a developing country such as Egypt, which suffers from not only high costs of energy but also expensive imported construction materials. Fathy successfully showed appropriate and practical approaches for designing in harsh hot climates. Such governmental projects mainly aim to develop new remote settlements in desert and uninhabited areas.

I. Sidi Krier Northern Shore Development Housing Project

The Planning Commission for the Development supported a development scheme for Sidi Krier costal area as a tourist resort facility on the Mediterranean shore of Egypt. Both the development theme and Fathy's designs and concepts mainly depended on employing traditional passive cooling techniques and curved roofs to offer the possibility of cost and energy efficient buildings and durable houses that were climatically appropriate [17].

The photos in Fig. (4-15) show the main architectural elements that Fathy appropriately employed through different buildings types of this project (residential, public, and services). Domes and vaults were widely utilised for roofing in order to provide thermal indoor comfort [17]. Top vents are in the direction of sea air. Patios (courtyards) face the water on the ground floor.



Figure 4-15 Photos of Sidi Kreer Housing Project, Egypt ;*Source: ArchNet Digital Library* [13]

II. The Village of New BARIS, Western Desert, Egypt, 1970

Dr. Salah Hhidayet, the head of the Egyptian Ministry of Scientific Research, asked Fathy to undertake design and supervision of a new settlement near the village of Baris, 60 km to the south of the town of *Kharga* (24.26°N and 30.33°E) [19], central Egypt. Baris, (*the Arabic pronunciation of Paris*), is an oasis in the western desert, which Fathy saw as an ideal chance to provide a climatic control prototype using traditional techniques and materials. Fathy began visiting towns in the same area, noting that houses were introverted and opened mainly onto inner courtyards. Thereby, inducing convective cooling and avoiding the outdoor high temperatures that frequently exceed 48°C during summer.

Fathy also noticed the effect of an opening between a paved and planted courtyard to create more passive cooling by convection. Initially, the proposed design emphasised the possibility of providing indoor thermal comfort by the natural control of; air temperature, air movement, relative humidity, and radiation [19]. Fig. (4-16) shows the importance of creating several pressure differential areas to generate air movement, and let heat transfers by convection from warm towards less warm spaces through these areas.

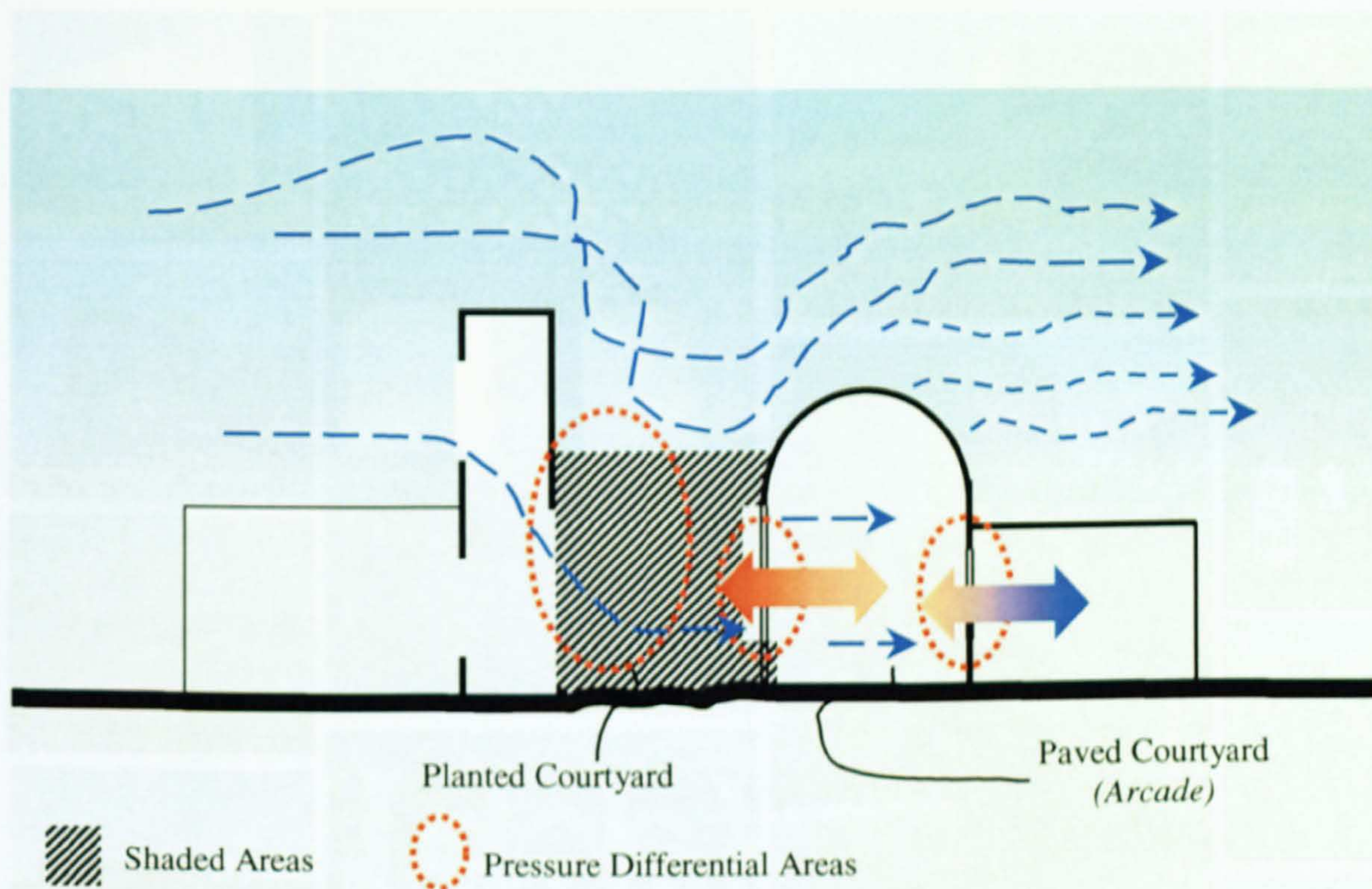


Figure 4-16 Analytical Sketch of Courtyard Typology (*New BARIS Village -Egypt*)

The projects photos in Fig. (4-17) show a number of the employed architectural vocabularies and techniques, which efficiently appeared as climatic controllers. Moreover, courtyards were effectively used in terms of catching the cooler breeze high above the desert surface, and bringing it into the courtyard and the house.

The designer decided to employ the system of internal courtyards to induce convective cooling along the shaded parts as the photos in Fig. (4-17) show. Furthermore, the design successfully directed air into the inner courtyards by wind catchers and towers that catch the higher cooler air above the desert and pass it to the inner courtyards, where hot air rises to be replaced by the cooler air that courtyards provide.



Figure 4-17 Photos of New BARIS Village (Houses & Market)

Source: ArchNet Digital Library [13]

4.4.1.3 Hassan Fathy Residential Designs

As has been noticed from the previously reviewed development projects, Hassan Fathy's works in general, and residential designs are significantly depended on employing traditional passive cooling techniques and curved roofs. His designs successfully offered the possibility of moderate-cost, durable, and climatically appropriate houses. Many of Fathy's residential projects, were built in local limestone because of a governmental ban on the use of mud-brick following the construction of the high dam.

I. Fouad Riad House, *Shabramant (29.56°N and 31.12°E), Egypt, (1967)*

The photos in Fig. (4-18) depict the traditional roofing techniques, which have been used as dominant element for providing passive cooling in all Fathy's designs in general and in this house particularly [20].



Figure 4-18 Fouad Riad House Roofing Systems, *Source: ArchNet Digital Library*[13]

II. Akil Sami House, *Dahshur (29.45°N and 31.14°E), Egypt (1978)*

The curved roofs (*domes and vaults*), wind-catchers (*Malqafs*), and courtyards are the main traditional passive techniques that the architect employed to protect the indoor thermal

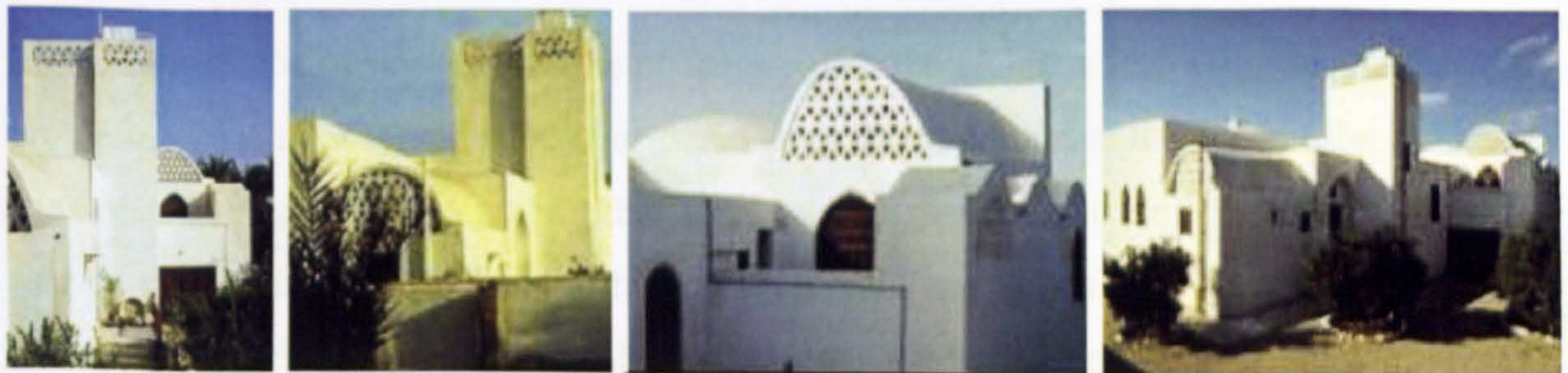


Figure 4-19 Akil Sami House, Egypt, *Source: ArchNet Digital Library*[13]

III. Casaroni House - Mit Rehan, Shabramant, Egypt (1980)

"The Casaroni residence, or "Mit Rehan" as it has been called by its owners, which means ['Pathway of the Basil'] in English [21]. It is one of the most elegant of Fathy's residential works yet to be built, Fig. (4-20). Construction was once again a significant reflector for traditional techniques and a strong link between tradition and modernity, which Fathy always relies on, to create an architectural identity for his region.

Notably, the traditional roofing system has been appropriately used to create indoor thermal comfort and protect indoor spaces from the outside hot climatic conditions. Domes and vaults have been employed to cover the house rooms, increase the interior volumes height and externally act as a solar radiation controller in order to reduce the intensity of the received solar radiation through their geometry and form configurations [21], Fig. (4-20).



Figure 4-20 Casaroni House (Exterior), *Source: ArchNet Digital Library*[13]

In the interim, the owner was able to cooperate with the architect in solving several special problems, which always must be considered as an important issue throughout the different construction stages. In this project, building users participation have figured out a natural way to protect the used limestone from the climatic conditions. The limestone has been coated with boiled oil from natural local plants to keep its soft yellow colour without changing.

Photos in Fig. (4-21) show different interior spaces, and how these spaces have been employed to strength the link between tradition and modernity in Fathy's design as well as the exterior elements. Therefore, the house's semi-enclosed and fully enclosed spaces are forming a well-integrated design. Despite their role for achieving the tradition-modernity link, inner traditional elements showed a great influence on the indoor thermal comfort as passive cooling techniques. Arched-windows, Mashrabiya, shaded-courtyard, and fountains are examples of traditional passive cooling techniques that have been successfully employed by Hassan Fathy for the *Casaroni House* interior.



Figure 4-21 Casaroni House (Interior & Courtyard), *Source: ArchNet Digital Library*[13]

4.4.1.4 Ramses Wissa Wassef (1911 – 1974)

Ramses Wissa Wassef was born in 1911, he graduated from the Ecole Des Beaux Arts in Paris in 1935 [22]. Wassef is another Egyptian pioneer architect and teacher who was interested in reviving traditional Egyptian buildings' crafts. It was in the course of one of his trips to Upper Egypt that Wassef discovered the beauty of the Nubian villages, where the houses are composed of mud brick vaults and domes. Wassef vaults and domes, which covered the complex of the El-Haraneya Arts Centre in Haraneya-Giza (30.01°N, 31.13°E), outskirts of Cairo, were constructed entirely of mud bricks [22]. El-Haraneya Arts Centre, Fig. (4-22), is Wassef's most famous project.

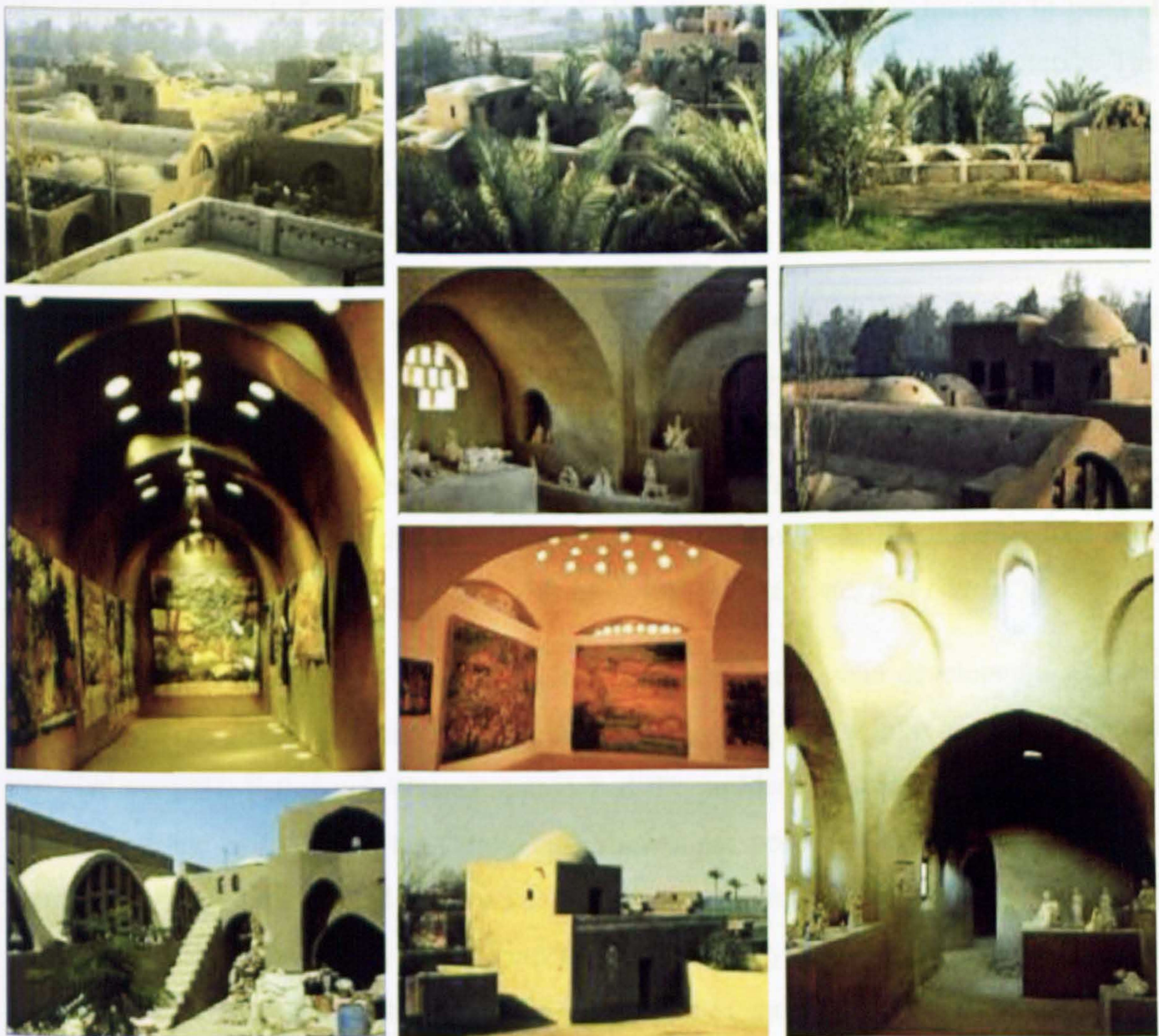


Figure 4-22 El-Haraneya Arts Centre, Egypt *Source: ArchNet Digital Library* [13]

The Ramses Wissa Wassef Art Centre, which was initiated as a weaving centre in 1952, comprising pottery, batik workshops, a tapestry showroom, a sculpture museum, middle-class residences, low-cost housing, and a farm. The art centre has been built on a flat, irregular site of approximately 50,000 square meters just outside the ancient village of Harraniya, which is situated a few kilometres southwest of Cairo and where the Pyramids of Giza are clearly visible [22].

As shown from the previous photos in Fig. (4-21), the courtyards of the workshops and the roofs shapes and forms exemplify Wissa Wassef's rejection of modern international architecture and his return to traditional forms with the use of mud bricks. Wassef's work also intends to search for new ways of developing those traditional techniques in general and mud-brick architecture in particular to serve a wide range of contemporary needs. The centre is also an unconventional teaching institute where the traditional crafts and building techniques of Egypt are kept alive and promoted. On the other hand, the centre encouraged and developed the creativity of the local human skills.

In general the centre demonstrates that traditional architecture with its curved roofing systems, local materials, and relatively unskilled labour showed better adaptation to the climate of hot-arid regions. Moreover, it is cheaper and more spacious than conventional flat modern buildings [22]. For Wissa Wassef and Hassan Fathy, domed and vaulted mud-brick structures represented the Egyptian architectural identity as these forms had been widely adopted by different Egyptian civilisations (*Ancient, Coptic, and Islamic*).

Wassef was once a partner of Egyptian architect Hassan Fathy, who developed a singular architectural language for his country and the region that would stop the foreign associations [23]. Fathy and Wassef approached the problem of reintroducing traditional architecture and culture from the Coptic and Muslim perspectives respectively. They both came up with a similar curved-roofing-language composed mainly of mud brick vaults and domes. They considered that this architectural language typifies the Egyptian historical traditions and evokes, but does not literally copy, the past and vernacular techniques.

4.4.1.5 Abdel Wahid El-Wakil

El-Wakil exemplifies the use of the traditional Egyptian vault and dome roofing systems in very prestigious projects and buildings. He was born in Cairo, on 7 Aug. 1943 [24]. Abdel Wahid El-Wakil graduated from Ain-Shams University in Cairo in 1965. Between 1965-1970 he lectured at the same university whilst studying and working with his mentor Hassan Fathy, the well-know proponent of traditional and vernacular architecture. El-Wakil was honoured with the Aga Khan Award for architecture in 1980 for his design of Halwa House in Agamey-Alexandria (31.08°N, 29.46°E), Egypt – 1975, Fig. (4-23) [25]. This prestigious prize was given not only to the project's architect, but also for the client *Mr. Esmat Ahmed Halwa*, and the master mason *Aladdin Moustafa*, who had also a close connection with Hassan Fathy through a number of projects.

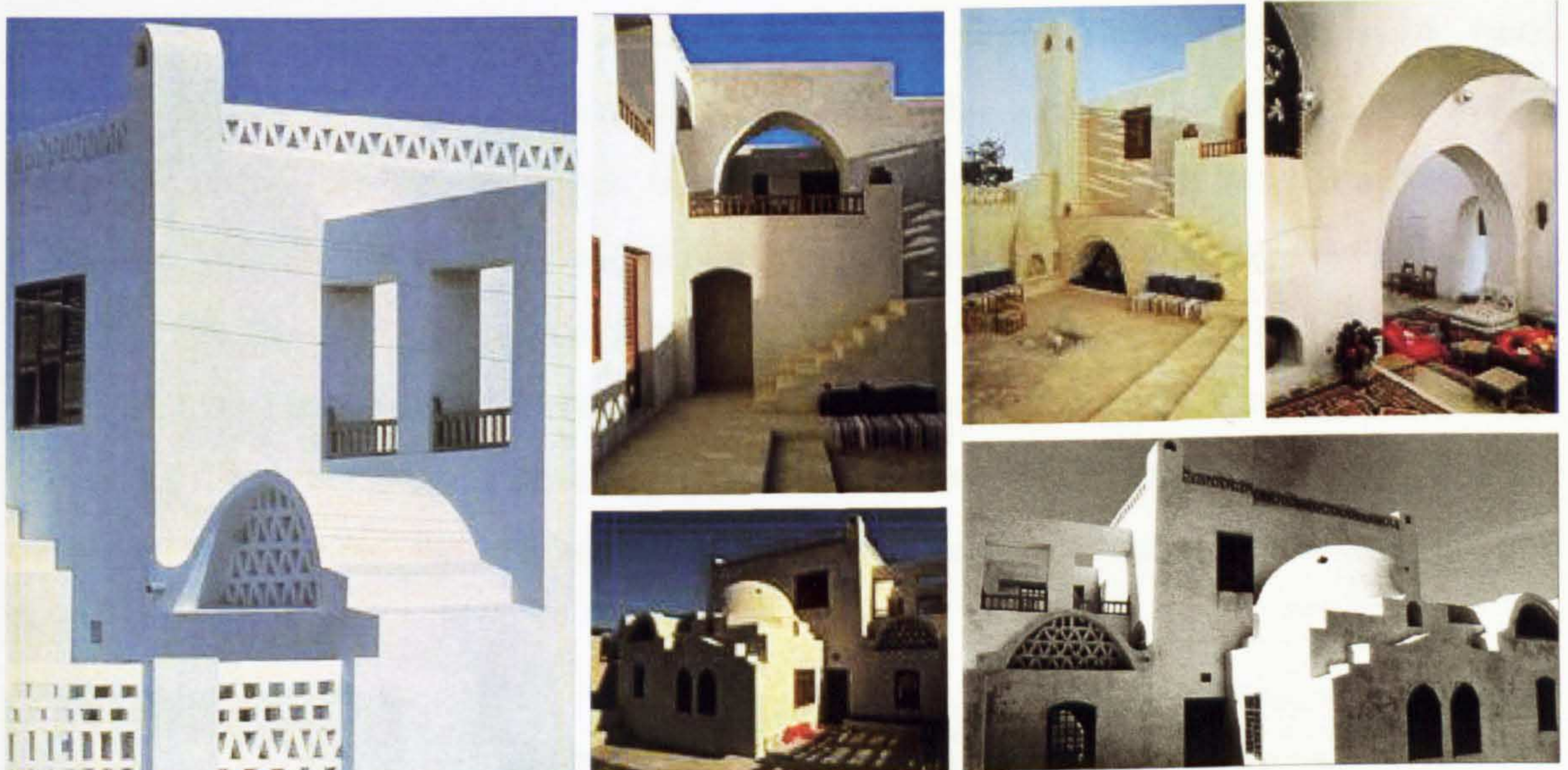


Figure 4-23 Halwa House, Agamy, Egypt *Source: ArchNet Digital Library* [13]

By employing his knowledge of Islamic architecture, El-Wakil reawakened an awareness of the value of traditional Islamic heritage. El-Wakil's view of vernacular, low-cost housing in the Middle East is very distinctive. He believes that vernacular and low-cost housing may be re-established only when people look intentionally at traditional architecture and its energy efficiency potentialities. El Wakil's work brings together many elements of traditional architecture, such as domes, vaults, arches and wooden structures that provide modern living standards.

The design of Halawa house works successfully with Egypt hot climate. Walls and roofs construction materials, shapes, and colours are designed to reduce heat gain during summer. Courtyards are shaded throughout the day to draw fresh air down through the wind-catchers. The Mashrabiyya (windscreen window) filters the sunlight. The house curved roofs, the main courtyard, the dome, the vaulted loggia, and arched openings are dominating the link with the region traditional architecture [25]. They have been successfully employed to reduce the needed energy for indoor thermal comfort in such hot-arid climates. Despite its architectural identity as a traditional element, the wind catcher is exemplifying a successful passive cooling technique to bring the desirable air in. Therefore, it has been located on the north side towards the direction of the prevailing wind in this seaside area.

Fig. (4-24) illustrates a number of black and white photos of building masonry work. Except the master mason, plasterer and carpenter, who were well-skilled craftsmen, all other labour done by local unskilled Bedouins. The vaults and arches were constructed by using the “inclined arch” or the Nubian Vaults systems and without shuttering [25]. Finally, with these projects of Fathy and other Egyptian architects one can see the work, which Hassan Fathy started, is being continued and expanded on by a new generation of architects. Their imaginative handling of traditional vocabulary was also enhanced by the consistent use of traditional methods of construction and the careful attention to details and skills.

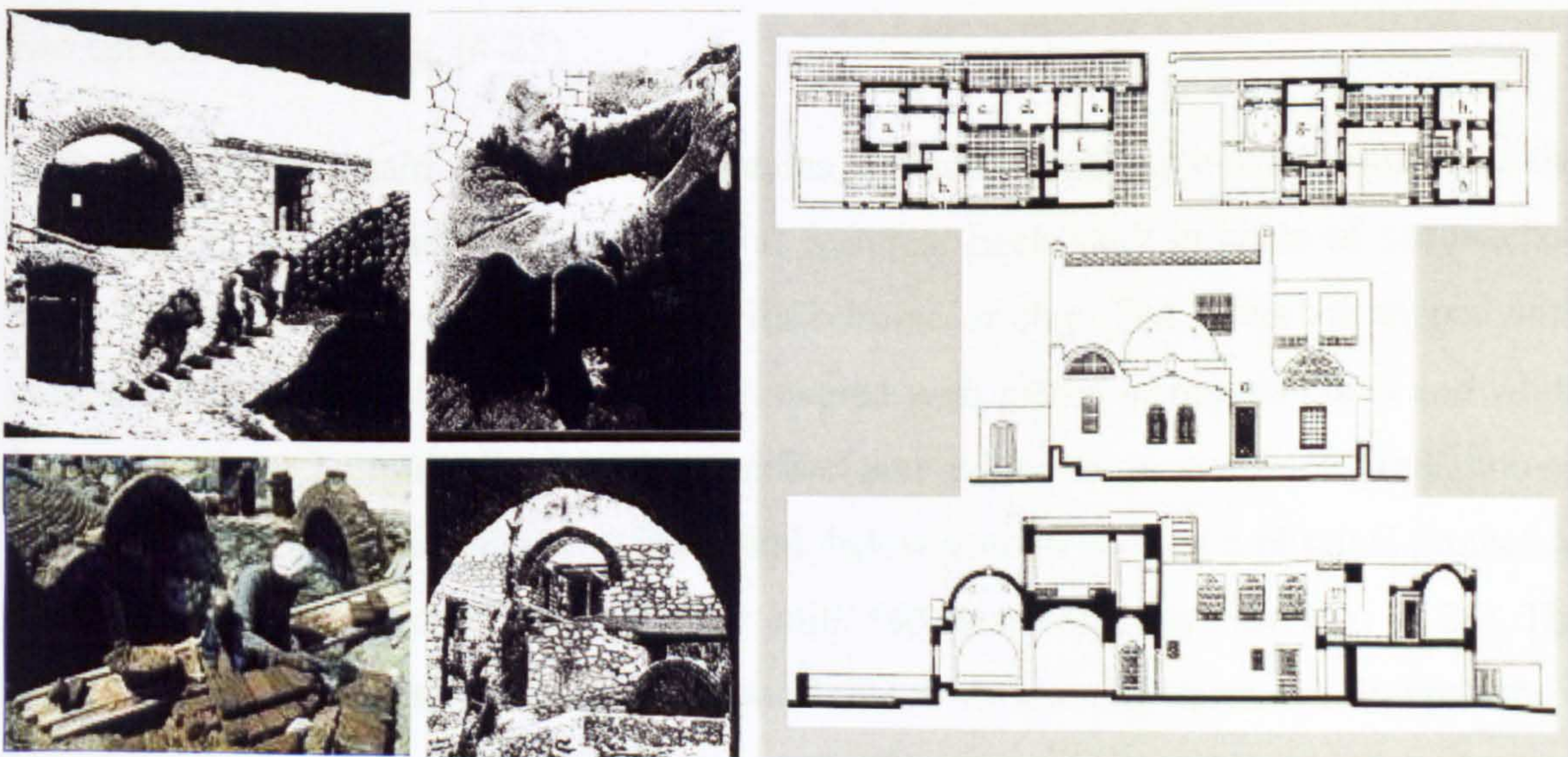


Figure 4-24 Architectural Drawings and Masonry Work of Halawa House

Source: ArchNet Digital Library [13]

4.4.2 Other Regional Architects Works

Balkrishna Doshi is an Indian architect. He was born in 1927 [13]. The fame that he obtains as a famous and well-known architect in India is not universal like Hassan Fathy and other architects in the region. But Doshi's design of Sanganth (*Doshi's Architectural Office*) in 1979-1981, in Ahmedabad-India (23.03°N , 72.40°E), is the most internationally well-known example of his work, Fig. (4-25). Doshi's foundation applies mainly traditional construction and arts. It conveys integrated designs that focus on local history and culture, climate, and environment [23].

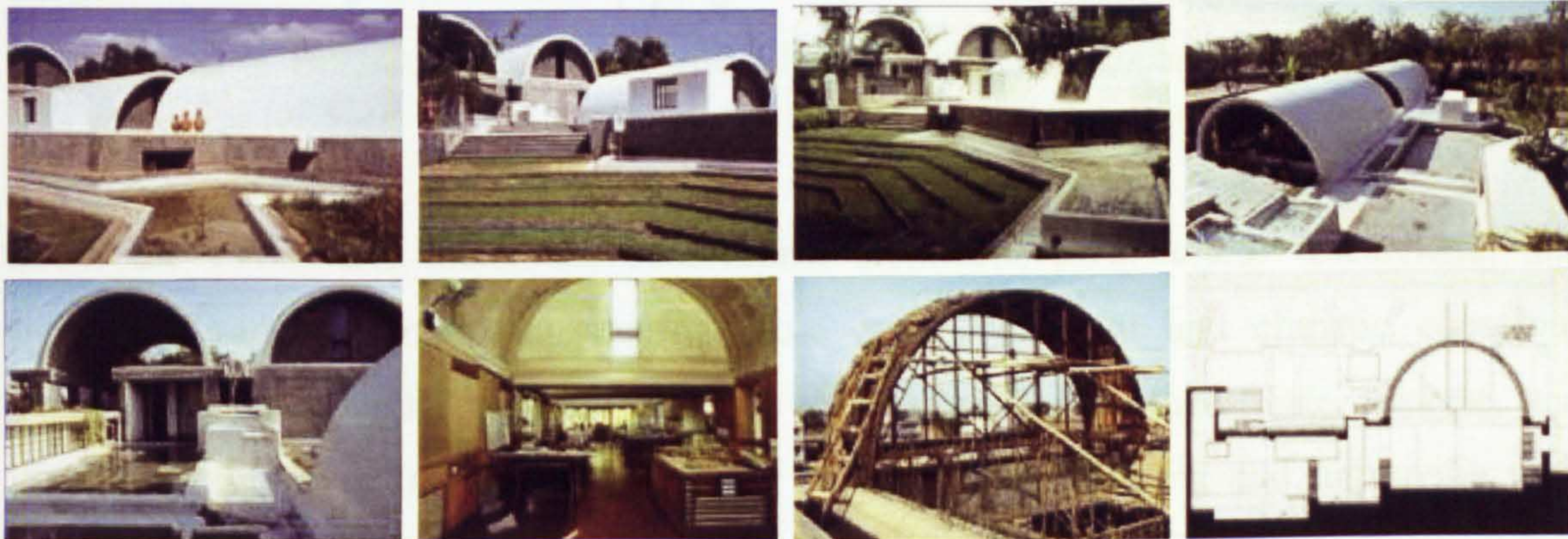


Figure 4-25 Sanganth, India *Source: ArchNet Digital Library* [13]

The building complex is a group of rectangular volumes, which are roofed by vaults and aligned along north-south axis in a green compound. It houses a number of design studios that are erected in a double height volume surmounted by two vaults. The design permits light to enter from the end-wall of the vaults by creating a flat roofed area in between the two curved surfaces, Fig. (4-25).

Both the complex main court, which contains a fountain with split-level pools, and the vaults reflect prime traditional architectural features. Each vault is made of sandwiched layers of pressed ferro cement together with ceramic or clay. The layers are topped with concrete shell. The surface of the shell is covered with pieces of broken china and white irregularly shaped mosaic tiles in order to reflect and reduce the received solar radiation on roofs surfaces. The west units have been sunk below ground level as a physical protection against the severe summer heat, while the units rise up towards the east, Fig. (4-25). The Sangath's vaults are inspired from the Wissa Wassef Museum in Harraniya, Egypt, which Doshi have noticed during his visit to the Aga Khan Award-winning projects in January 1978 [26].

4.4.3 Socio-cultural and Technical Development Workshops

Numbers of development workshops, which are mainly supported by either regional or international organisations, have adopted a number of traditional crafts' revival movements. Despite their social orientation, some of those organisations worked with Fathy in the early seventies towards establishing more developed approaches of introducing shelters and settlements for poorer people and new communities with inadequate resources (*developing countries*). Intended to revive and follow his ideas, numbers of development workshop programmes and organisations provide an increasing appreciation of Hassan Fathy's work and other traditional examples, through publications and exhibitions.

From the 1970s and thereafter, exhibitions, architects, architectural researchers, and building designers have been seeking more energy efficient and climatic conscious buildings. Consequently, they are showing more intentions to investigate, analyse, and discuss a number of traditional techniques in term of highlighting and improving their technicalities, functionalities and capabilities that proved moderate levels of passive indoor thermal comfort in extreme climates.

The French Association of Volunteers Progress (*AFVP*) also promoted numbers of individual projects that experimented the vaults and the domes constructions in the Sahel with the use of stabilised earth bricks. During the early 1980s, Fabricio Pedroza continued a work that started in Angola for constructing domes with fired bricks and later with special cement bricks in a school building in Senegal [10].

4.4.3.1 ADAUA Organisation and Two Successful Projects in Africa

ADAUA is the abbreviation of the Association for Development of Traditional African Urbanism and Architecture [27]. *ADAUA* is an organisation of people from different countries; its headquarters is located in Ouagadougou, Burkina Faso. It aims to revive and promote indigenous traditional architecture and to train local inhabitants in appropriate technologies. In addition to the well-known woodless development workshop program in Sahel, *ADAUA* began a series of projects using vaults and domes in Mauritania and Burkina Faso [27].

I. Satara Zone Housing, Rosso, Mauritania

Satara, where the project is situated, is a squatter area, which is approximately 30% of the town of Rosso (16.29° N, 15.53° W). The area was established by a number of families who sought refuge from floods during the 1950's. The population increased considerably in the 1970's. In 1975 the settlement was flooded and the government undertook emergency action to accommodate those whose dwellings were destroyed. In the same year ADAUA and SOCIGIM (the national government representative) began to find a permanent solution for Satara area problem. They aimed to build 1400 house units using self-build techniques, local materials and labour, and natural construction materials. From 1975 to 1977 a multi-disciplinary team from ADAUA studied the site's environmental conditions, local materials, traditional architectural vocabularies and construction techniques, and the population's socio-economic features [10].

Despite the frequent floods during the short winter season from July to September, this region is classified as a dry desert climate with a high temperature. ADAUA [27] constructed a pilot unit to demonstrate the advantages of using traditional roofing techniques (domes & vaults) and local construction materials. It built 12 house units for the public to approve the architectural configurations of units, Fig. (26-4). This has trained 25 masons, brick-makers and other labour. The construction of the initial units was a positive preparatory stage for the completion of the project outstanding units. Houses units vary in size, shape, and plan. Each unit is built on a particular area, which permits future extension according to the family needs.

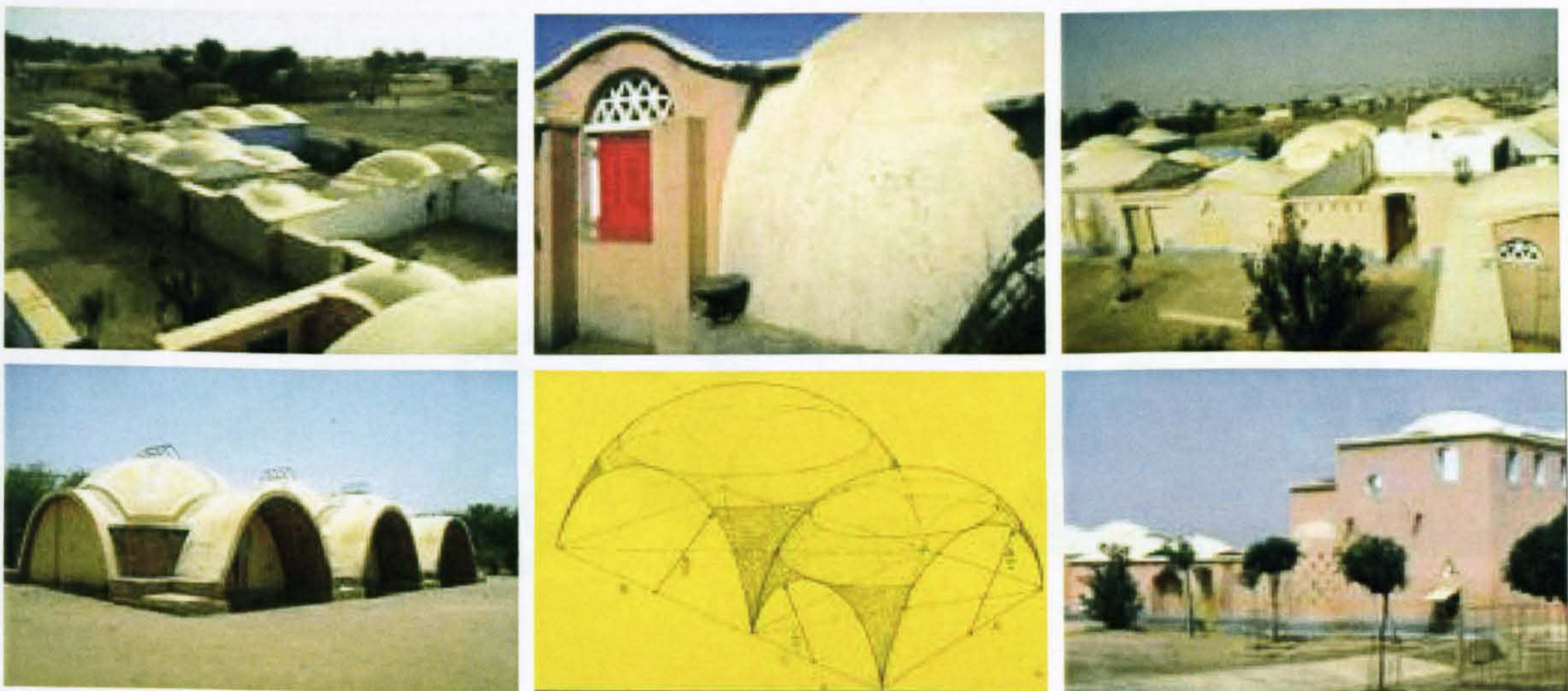


Figure 4-26 Satara Zone Housing, Mauritania *Source: ArchNet Digital Library* [13]

II. Regional Hospital, Kaedi, Mauritania

Fabrizio Carola who used fired bricks vaults and domes in several projects in Mauritania and Mali. This section reviews one of his designs, where he employed a special well-insulated double skin dome. Kaedi Regional Hospital [28], Fig. (4-27) is located in a remote sector of Mauritania, near the border of Senegal, (16.12° N & 13.32° W).



Figure 4-27 The Regional Hospital, Mauritania *Source: ArchNet Digital Library* [13]

Fabrizio Carola has built a low-cost extension to the local hospital in Kaedi, which uses a new locally-produced structural brick in an original design of domes, vaults, and arches. The complex, elegant structures of the extension, which includes wards, operating theatres, storerooms, consultation rooms, and corridors, are providing improved medical and primary health care for the rural population of this area. The use of brick has spared timber in a de-forested region; the doughnut and ovoid forms of the hospital diverse units represent an original contribution to the art of building with bricks [28], Fig. (4-28). The new hospital has become a source of pride to the people it serves. This project has proved that modern architecture, which is innovative, affordable, and appropriate, can be created with local skills and materials.

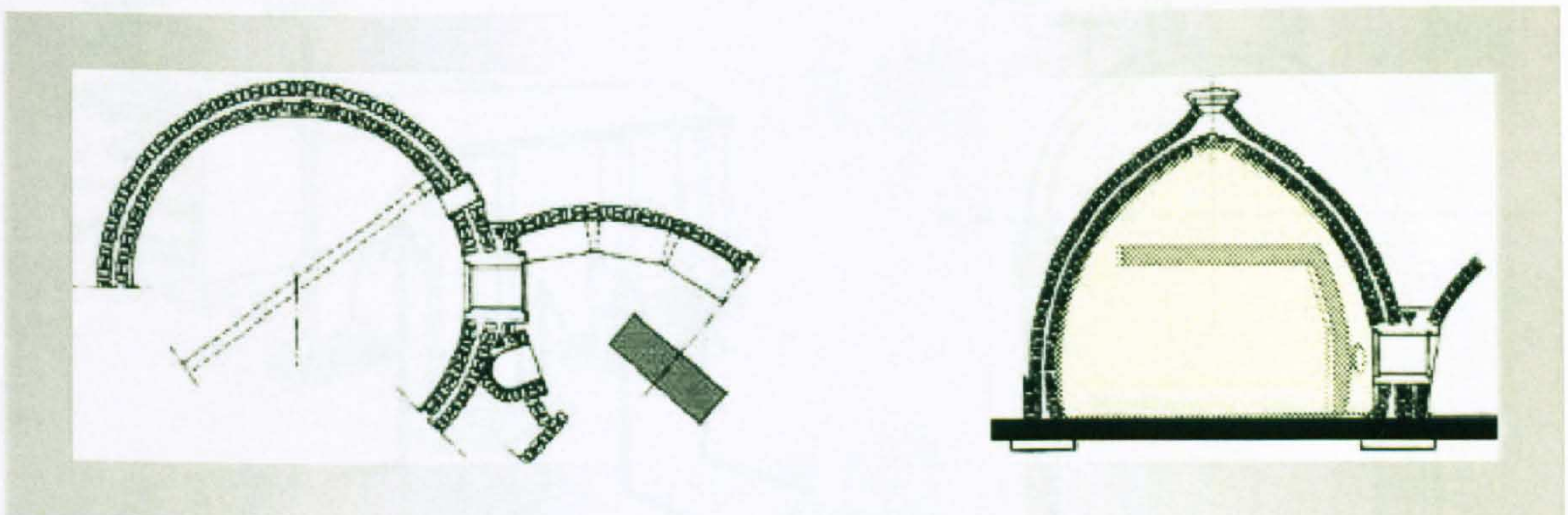


Figure 4-28 Plan and Cross Section of The Initial Space of The Regional Hospital, Mauritania
Source: ArchNet Digital Library [13]

4.4.3.2 The Agricultural Training Centre, Nianing, Senegal (14.20°N, 16.55°W)

In parallel, considerable research by **BREDA** (UNESCO's Regional Office for Education in Africa based in Dakar) was attributed to develop school roofing systems with vaults which were constructed by using plywood formwork, and shuttering with millet stalk [29], Fig. (4-29). The vaults thickness at the crown is only 4 cm. The vault has been erected by three layers of cement mortar stabilised with wire mesh at the top of the vault, the three layers lie above the shutter plywood, Fig. (4-29). Masonry buttresses have been built to counteract the vault's thrust.

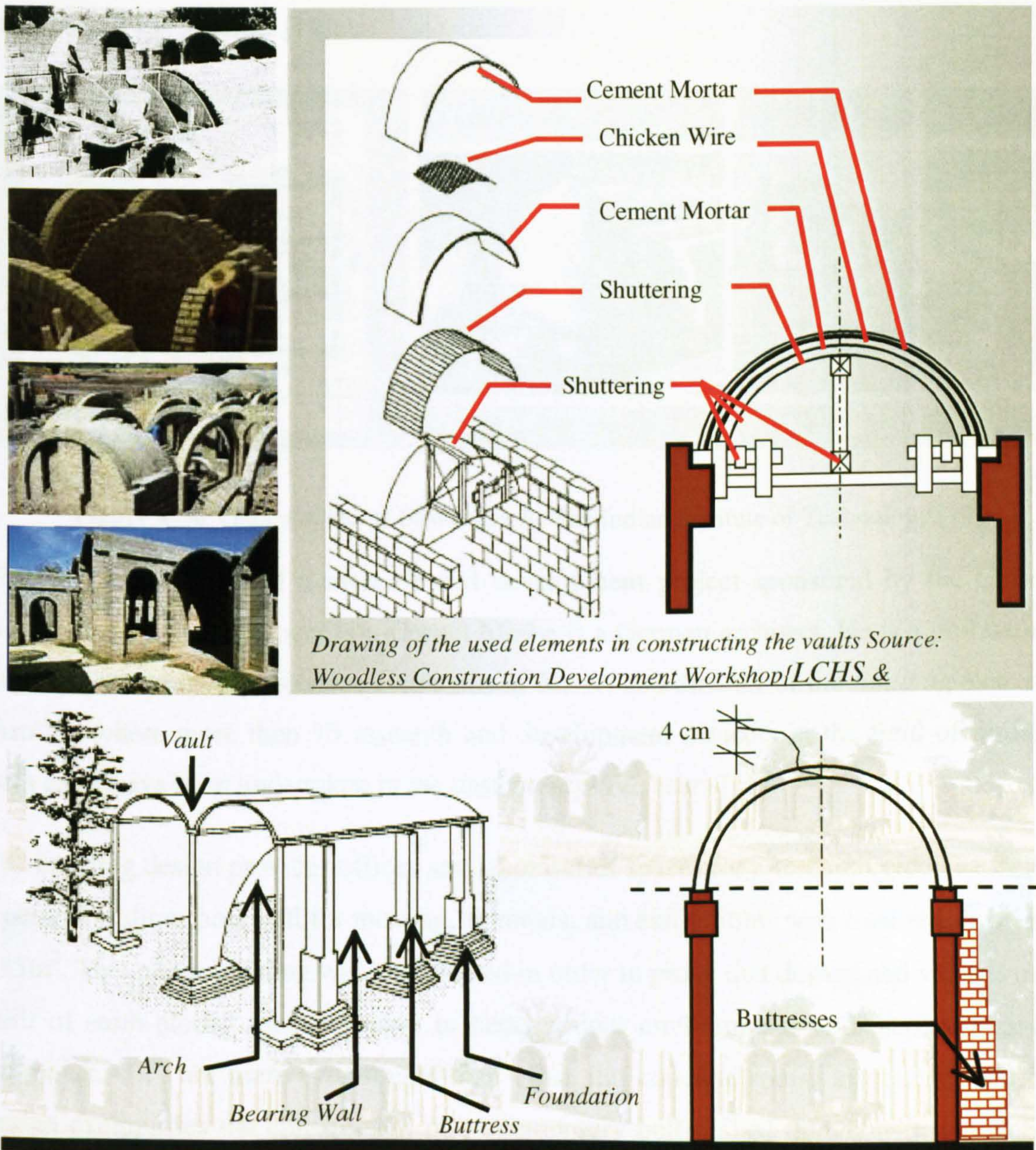


Figure 4-29 Drawings of The Structural System Developed by BREDA / Dakar
Source: (Sketches): Woodless Construction Development Workshop [10,29]

4.4.4 Research and Development Projects

(Vault and Dome Structures of The Indian Institute of Technology, New Delhi, India)

A number of research and development projects in developing communities, which initially represented part of a continuing research process has been undertaken by *International and Regional Academic Institutes* and sponsored by the governments. The office buildings of *Passive Solar Architecture Group of the Centre of Energy Studies at the Indian Institute of Technology* is one of these successful examples of such these research projects, Fig. (4-30). It verifies the possibility of saving 30% of building costs and 66% of energy costs by employing soil-blocks vaults and domes roofing systems in addition to earth tunnel fan systems [14].

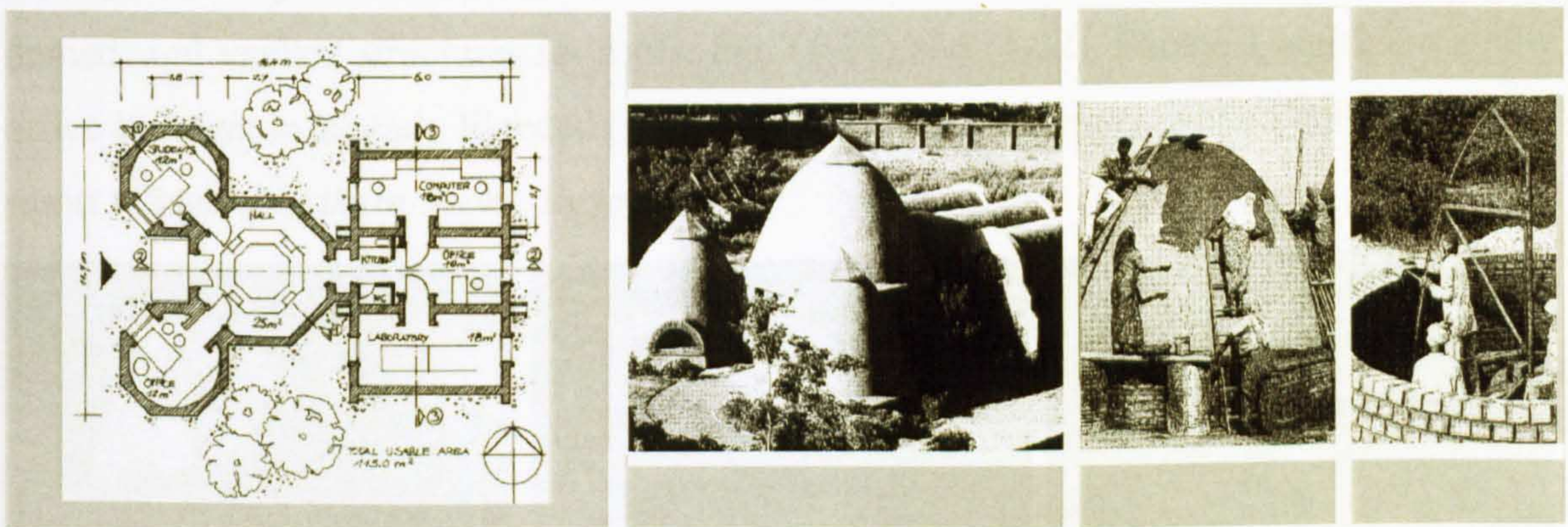


Figure 4-30 Vault and Dome Structures At The Indian Institute of Technology [14]

This project is a part of a research and development project sponsored by the German Agency for Technical Operation. Gernot Minke is a German architect. He is a professor in the *Department of Architecture, University of Kassel* and director of the *Building Research Institute* where more than 15 research and development projects in the field of building with earth have been undertaken in the past twenty-five years [15].

The building design provides offices and laboratories spaces for a research group as well as a central multipurpose hall for meeting, seminars, and exhibitions, with total usable area of 115m^2 . This office building was constructed in order to prove that domed and vaulted roofs built of earth-blocks are conducive to better indoor environments and thermal comfort. Moreover, they are more economical than other flat concrete roofs. In general, Minke's design exemplifies the construction of contemporary bell-shaped domes with the Nubian technique, which have been used thousands of years in Upper Egypt [14].

The general form of the building consists of three domes and three vaults. Vault and dome were erected of manually produced soil blocks, employing a rotational slip-form arm, Fig. (4-30). The vaults with a clear span of 2.9 meters and 3.6 meters height are built from adobes and without formwork following the traditional Nubian technique. A 100 m long stoneware pipe system was employed at a depth of 3.5 m to blow the ambient air by two fans. The blown air, which receives the constant earth temperature, cools the building in hot seasons and heats it in cold seasons. Approximately, the annual energy savings are 38000 kWh, which is about 2/3 of the total amounts. Furthermore, the building costs savings comparatively to a conventional flat ones is 22% [15].

Finally, the chapter reviews a number of new projects that have employed curved forms, domed, and vaulted structures for roofs, Fig. (4-31) and (4-32). Photos 1 and 2 are a new office building in Elwady Elgeded (*The New Valley-Upper Egypt*), while photo 3 is a new resort village (*Northern Shore, Egypt*).



Figure 4-31 New Projects, *Source: Egypt Architecture Online* [30]

In 1988 Ray Meekers designed the Agni-jata, Fig. (32-4). It represents a contemporary project, which is erected out of the region interests study and by using the well-known Nubian construction technique for erecting curved roofs. The Nubian vault construction technique was followed for all curved roofs of the project. The structure was built with mud blocks and mortar [31].



Figure 4-32 Agni Jata Building by Ray Meeker 1988
Source: <http://www.auroville.org/the-city/architecture/agnijata.htm> [31]

4.5 CONCLUSIONS

The chapter reviewed different contemporary projects that have employed curved forms, domed, and vaulted structures for roofs. It is concluded that traditional roofing systems have successfully provided indoor thermal comfort and deliberately erected to cope with the hot climate conditions. The chapter pointed out that the proper understanding of curved roofs forms allows better performance of roofs as energy efficient techniques. Therefore, looking deliberately to their forms and geometries potentialities in order to control the intensity of the received solar radiation on roofs surfaces. Despite of reflecting a traditional and architectural identity of the region, such roofing systems should provide indoor thermal comfort in contemporary buildings.

Due to its geometry, a flat roof receives solar radiation continuously throughout the day, at a rate that increases in the early morning and decreases in the late afternoon due to changes in both solar intensity and angle of the sun. The illustrated examples of this chapter verified that the roof form must be significantly considered in sunny and hot climates, especially during summer seasons. Ancient Egyptian vaults were commonly constructed by the Nubian techniques and from adobes, such as the 3200 years old vaults, which stand within the temple precinct of *Rameses II* near Luxor, south of Egypt. The chapter has discussed different geometrical forms of vaults and domes.

The chapter also described a number of traditional roofing techniques, which have been developed by number of local societies over many generations to achieve more appropriate roofing systems and provide the comfortable indoor environments using natural energy. Hassan Fathy's designs, which are mainly depended on both traditional passive cooling techniques and curved roofs offered the possibility of moderate-cost, durable, and climatically appropriate roofing techniques. The Nubian Vault technique as one of the famous woodless construction technologies that Hassan Fathy and others employed in their designs, has been numerously used for erecting the traditional vaults in the Ancient Egypt.

The numerous types of curved roofs allow a great variety of architectural models, and this technology was adapted to the most hot and arid climatic conditions. Although arches and vaults are traditionally used to cover limited spaces, they are perfectly well suited to spaces of up to tens of meters[3]. Thus they can meet the needs of any building program, public or private, low-cost or quality housing, public and religious buildings, shops, schools, etc.

The Nubian Dome technique was also known in Upper Egypt for thousands of years. In this technique, mud bricks masons and builders determine the distance between the centre of the dome and the angle of each brick by using a wire or a radial arm. Therefore, circumferential courses of adobes are laid using this movable guide. After discussing and exploring a number of pilot projects case studies, the chapter concluded that woodless construction techniques for erecting arches, vaults, and domes are the most practical and preferable construction techniques.

Due to their sustainability, energy and cost efficiency, and environmentally friendly potentialities, the chapter found out that the traditional curved roofs have to be widely employed in developing communities contemporary buildings and desert regions. Architecturally, vault and dome roofing techniques provide the potential to cover a variety of different spaces, both in size and shape. Moreover, due to their availability at site, earth, mud, clay, or stone construction materials eliminated transportation and many other costs. Furthermore, the needed local labour for such construction techniques is not expensive compared to other advanced techniques.

Finally, the survival of traditional roofing techniques over hundreds and thousands of years indicates that they surely possess knowledge that can still be of great value either in their original forms or for more passive cooling technologies in contemporary buildings. But much remains to be done to convince the populations of developing societies to look at tradition for more energy efficient solutions of their contemporary buildings and problems.

In the next chapter, the computational tool and methodology, which is applied for figuring out the solar performances of traditional curved roof forms and orientations will be discussed. Solar geometry and other related aspects are also reviewed among other research work, which has previously investigated the solar behaviour of different forms. Chapter 5 and the parametrical study chapters expand further to investigate the influence of roofs forms and geometries on the intensity of the received solar radiation on roofs surfaces.

Reference List

1. Khodabakhshi, Sh. Sustainable Construction and Vernacular Architecture of Iran, World Renewable Energy Congress VII (WREC 2002) 2002: Elsevier Science Ltd.
2. Zakaria, N. Z. Woods P. Roof Design and Thermal Performance of houses in Equatorial Climates, World Renewable Energy Congress VII (WREC 2002), Elsevier Science Ltd. 2002.
3. Elseragy, A. A. and Gadi M. B. Traditional Architecture, Energy Consciousness and Sustainability, *An approach to affordable and thermally comfortable buildings in hot-arid climates with special reference to Egypt* Proceedings of the Second World Conference on Technology Advances for Sustainable Development & Workshop on Renewable Energy & Development of Remote Areas 2002 Mar 11-2002 Mar 14; Cairo, Egypt.
4. Fathy, H. Architecture for the poor *An Experiment in Rural Egypt*. [Web Page] (1973).
5. Fathy, H. Natural Energy and Vernacular Architecture, *principles and examples with reference to hot -arid climates*,. Chicago & London: Published for United Nations University by the university of Chicago press; 1986. (EDITED BY WALTER SHEARER; Abdel-Rahman; Ahmed Sultan.
6. Givoni, B. Man, Climate And Architecture, 2nd Edition, Applied Science Publishers, London, 1976.
7. O'Callaghan, P. W. Building For Energy Conservation, Pergamon Press, London, 1978.
8. Fathy, H. Architecture and Environment. Arid Land News Letter 1994 Fall-1994 Winter; ALN No. 36.
9. Stulz and Roland Roofing Primer; A Catalogue of Potential Solutions, 1st ed. ed. Switzerland: SKAT; 2000. (Karl Wehrle; Daniel Schwitter, SKAT, editors.
10. Norton, J. Woodless Construction : Un-stabilised Earth Brick Vault Dome Roofing Without Formwork. Building Issues 1997; Vol.: 9 (No.2) pp:3-26.
11. Norton, J. Woodless Construction-1: An Overview. Building Advisory Service and Information Network 1995 Aug.
12. LCHS (Lund Centre for Habitat Studies), Norton J. Woodless Construction, 1997; Vol. 9 (No. 2).
13. ArchNet Digital Architectural Library. [Web Page]; <http://www.archnet.org> [Accessed July 2003].
14. India: Vault and Dome Structures At The Indian Institute of Technology, *New Delhi* . Mimar 2002 Jul;Vol. 41.
15. Minke, G. Earth Construction Handbook, *The Building Material Earth in Modern Architecture*. Southampton, Boston. WIT Press; 2000.
16. Nubian Vault Construction in Mexico using straw/ Clay blocks. [Web Page]; www.caeloproject.com. [Accessed Jul 2002].

17. **Steele, J.** *An Architecture for People: The Complete Works of Hassan Fathy*. London, United Kingdom: Thames and Hudson; 1997.
18. **Hassan Fathy main page, *Hassan Fathy Biography*** [Web Page]; www.geocities.com/egyptarchitect1/hasanfathi/hfmain.htm.
19. **Steele, J.** *The Hassan Fathy Collection. A Catalogue of Visual Documents at the Aga Khan Award for Architecture*, Bern, Switzerland: The Aga Khan Trust for Culture, 54; 1989.
20. **Rastorfer and Darl,** *The Late Houses of Hassan Fathy*. Singapore: Concept Media; 1985. (Hasan-Uddin Khan, ed, editor.
21. **Steele, J.** *The Hassan Fathy Collection. A Catalogue of Visual Documents at the Aga Khan Award for Architecture*, Bern, Switzerland: The Aga Khan Trust for Culture, 84; 1989.
22. **Taylor, B. B.** *Ramses Wissa Wassef Museum. MIMAR 35: Architecture in Development*. London, Concept Media Ltd 1990.
23. **Steele, J.** *The Complete Architecture of Balkrshna Doshi - Rethinking Modernism for The Development*, London: Thames and Hudson Ltd.; 1998.
24. **Profile: El-Wakil, MIMAR 1: Architecture in Development 1981**; Singapore: Concept Media Ltd.
25. **Holod, R. and Rastorfer, D.** *Halawa House. In Architecture and Community*. New York: Aperture. 1983. (Renata Holod ; Darl Rastorfer, eds, editors.
26. **Doshi, B.** *Toward an Appropriate Living Environment: Questions on Islamic Development, In Places of Public Gathering in Islam*. Philadelphia: Aga Khan Award for Architecture: 1980. (Linda Safran (ed), editor.
27. **ADAUA,** *Site Visit to Rosso, Mauritania. In Reading the Contemporary African City*. Singapore: Concept Media/The Aga Khan Award for Architecture; 1983. (Brian Brace Taylor (ed), editor.
28. **Davidson, C. C.** *Kaedi Regional Hospital. Architecture Beyond Architecture*, London: Academy Editions 1995; Cynthia C. Davidson, and Ismail Serageldin, eds.
29. **Eljack K.,** *An Agricultural training Centre: Case Study in Nianing, Senegal. Changing Rural Habitat, 1982, Vol. I: Case Studies*.
30. **Abdel-Mone'im, N. M.** *Egypt Architecture Online* [Web Page]; Accessed March 2002. Available at: <http://www.geocities.com/egyptarchitecture/>.
31. **Agni-Jata,** *Economic Earth Construction Designed by Ray Meeker*. [Web Page]; www.auroville.org/thecity/architecture/angijata.htm. [Accessed Jan 2001].

CHAPTER 5

SOLAR RADIATION ON DIFFERENT SURFACE GEOMETRIES

Principles, Tools, and Techniques

5. SOLAR RADIATION ON DIFFERENT SURFACE GEOMETRIES

Principles, Tools and Techniques

The first four chapters of this thesis describe a piece of research the aim of which was to provide a sound theoretical approach for traditional passive cooling techniques and curved roofs energy efficient potentialities. The previous chapters have reviewed a number of the regional pilot projects, which employed traditional passive cooling techniques in general and curved roofing systems in particular. Thus they draw attention towards the need to investigate the influence of curved roof forms and geometrical configurations on the thermal behaviours of buildings indoor spaces and environments.

This chapter discusses the relevant principles of solar radiation and solar geometry in order to provide better understanding of the main factors of overheating, which could be controlled in hot-arid zones. The Sun-Earth geometrical relation is also discussed in this chapter, in order to understand the geometrical parameters that influence the intensity of the received solar radiation on surfaces. This chapter reviews previous research applications, which have investigated the received solar radiation on sloped surfaces. The chapter also discusses a computational tool developed to calculate the received solar radiation on sloped surfaces with different orientation in the tropics. Finally, the methodology of employing this tool in testing the solar performance of curved roofs in hot-arid regions is described.

5.1 Solar and Architectural Design

Solar radiation is essential to life on earth. Solar radiation affects the earth's weather, which in turn shapes the natural environment [1]. Thus, it is vital to have a clear understanding of solar radiation for both architecture and building design, and in particular to determine the amount of energy intercepted by the buildings surfaces. The passive solar design for architecture has been defined as "a design technique that can increase human comfort and reduce the demands of energy production in buildings"[2]. There are two kinds of parameters affecting the thermal and solar performance of any building; the first is the outside climatic conditions that the building is subject to, such as solar radiation, air temperature, humidity and wind direction.

The second type is the architectural design variables that architect and building engineer should control to increase the environmental performance of the building and provide more indoor thermal comfort without much reliance on artificial tools. This type should look at the effective use of solar radiation and natural heating/cooling sources towards minimising the required energy for heating, cooling, lighting and occupants' thermal requirements in buildings. This may be achieved by different means; the following exemplify a number of architectural design parameters, which can be developed in order to provide passive solar design in architecture;

- General layout and building orientation.
- Envelope mass, geometric form and surface area.
- Roof geometry and form, roof mass and insulation layers.
- The thermal properties of the building envelope construction materials.
- Openings locations, sizes and outlet-inlet size ratio.
- Shading devices of openings and other envelope elements.
- Employing passive architectural elements and techniques (*Traditional*).

However, it is not always possible to give clear architectural recommendations for each climatic region, as thermal comfort norms in buildings are not only based on physical data and requirements. They are also based on other social and cultural factors such as religion, family structure, building traditions and financial needs, which always vary from case to case[3].

The solar radiation reaching the surface of the earth may be divided into two components: beam solar radiation coming directly from the sun's disk, and diffuse solar radiation coming from the whole of the sky except the sun's disk, Fig. (5-1) [4].

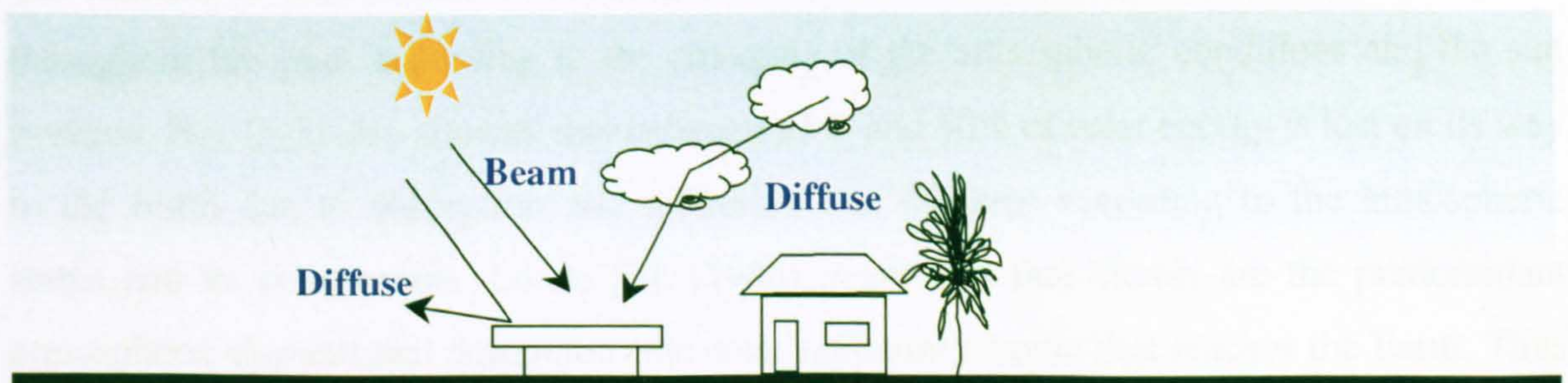


Figure 5-1 Beam and Diffuse Solar Radiation (After Exell [4])

5.1.1 Solar Radiation and Earth Thermal Balance

The sum of the beam and the diffuse solar irradiance falling on a horizontal surface facing upwards is called global solar irradiance. If I_b is the beam solar irradiance, $zeta$ is the angle of incidence of the solar beam on the horizontal surface, and I_d is the diffuse solar irradiance, then the global solar irradiance I_g is given by $I_g = I_b \cos zeta + I_d$ [5].

Fig. (5-2) and (5-3) illustrate the total amount of the heat absorbed by the earth [6]. It is balanced by a corresponding heat loss, heat releases from the ground and atmosphere by different ways (*radiation, evaporation and convection*).

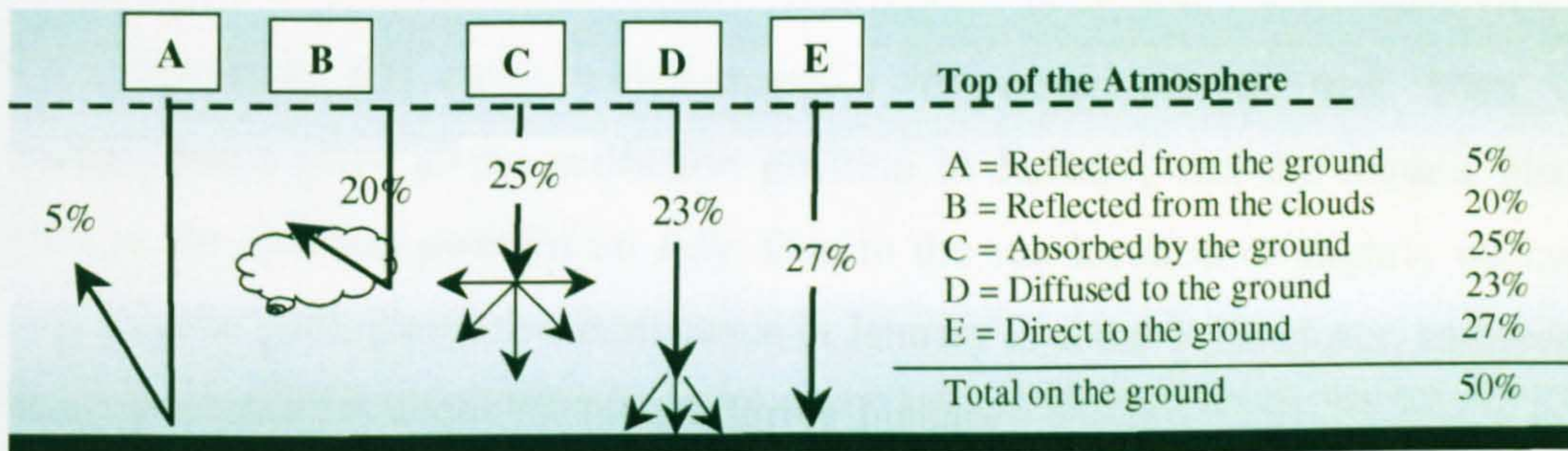


Figure 5-2 Solar Radiation Passage Through The Atmosphere[6]

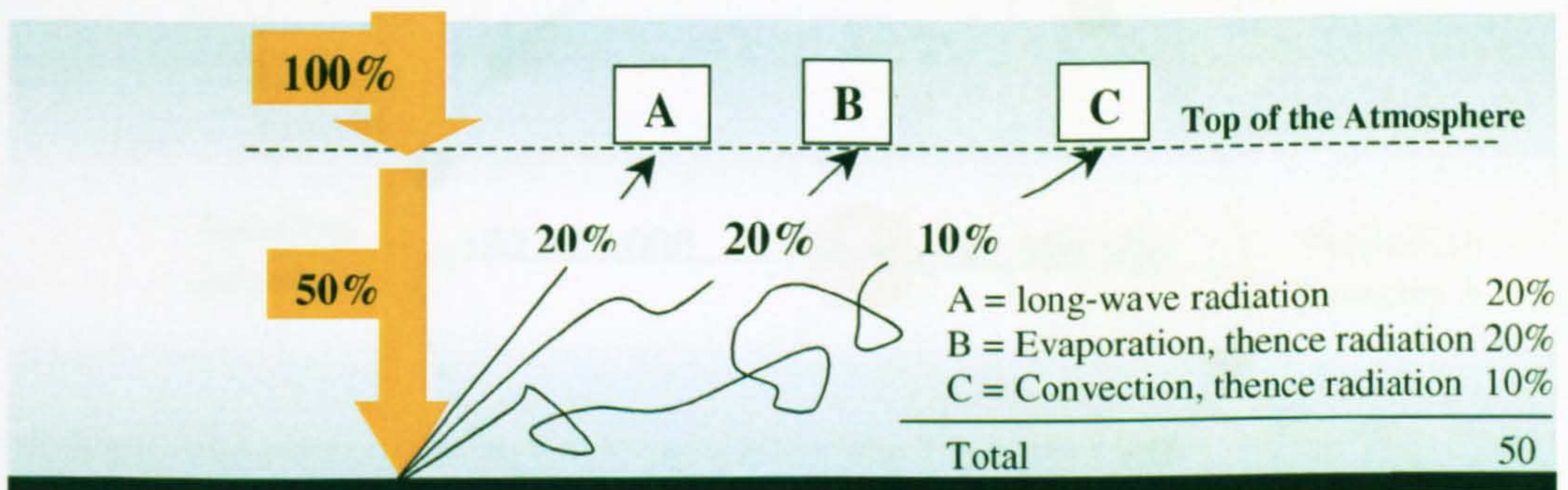


Figure 5-3 Heat Releases From The Ground & The Atmosphere[6]

The amount of solar radiation reaching the Earth surface varies greatly during the day and throughout the year, according to the changing of the atmospheric conditions and the sun position. Fig. (5-3) also showed that between 25% and 50% of solar energy is lost on its way to the Earth due to absorption and reflection that happens according to the atmospheric status and its components. Lunde [7], (1980) mentioned that clouds are the predominant atmospheric element that determines the solar radiation amount that reaches the Earth. Thus pollutants, moisture vapour and small airborne particles may influence this amount.

5.1.2 Solar Geometry

The sun is the center of the solar system that the rest of the planets revolve around. Earth is the third planet from the sun. This part is concerned about the geometry of the Earth-Sun relationship.

5.1.2.1 Earth-Sun Geometrical Relationships

The Earth shape is approximately a sphere. It completes one rotation around the sun every 365.25 days. The apparent part of the sun as seen from the earth is known as the ecliptic. The eccentricity of the earth orbit is very small ($e=0.01673$)[8].

Fig. (5-4) shows this move, which shapes a very nearly circular path. Thus, the shortest distance takes place at the perihelion position in January, and the longest distance takes place at the aphelion position on July. Due to the sun location of slightly off-centre to the earth circular path, the earth-sun distance in January is about 3.3% closer, and proportionally the solar intensity is about 7% higher during January.

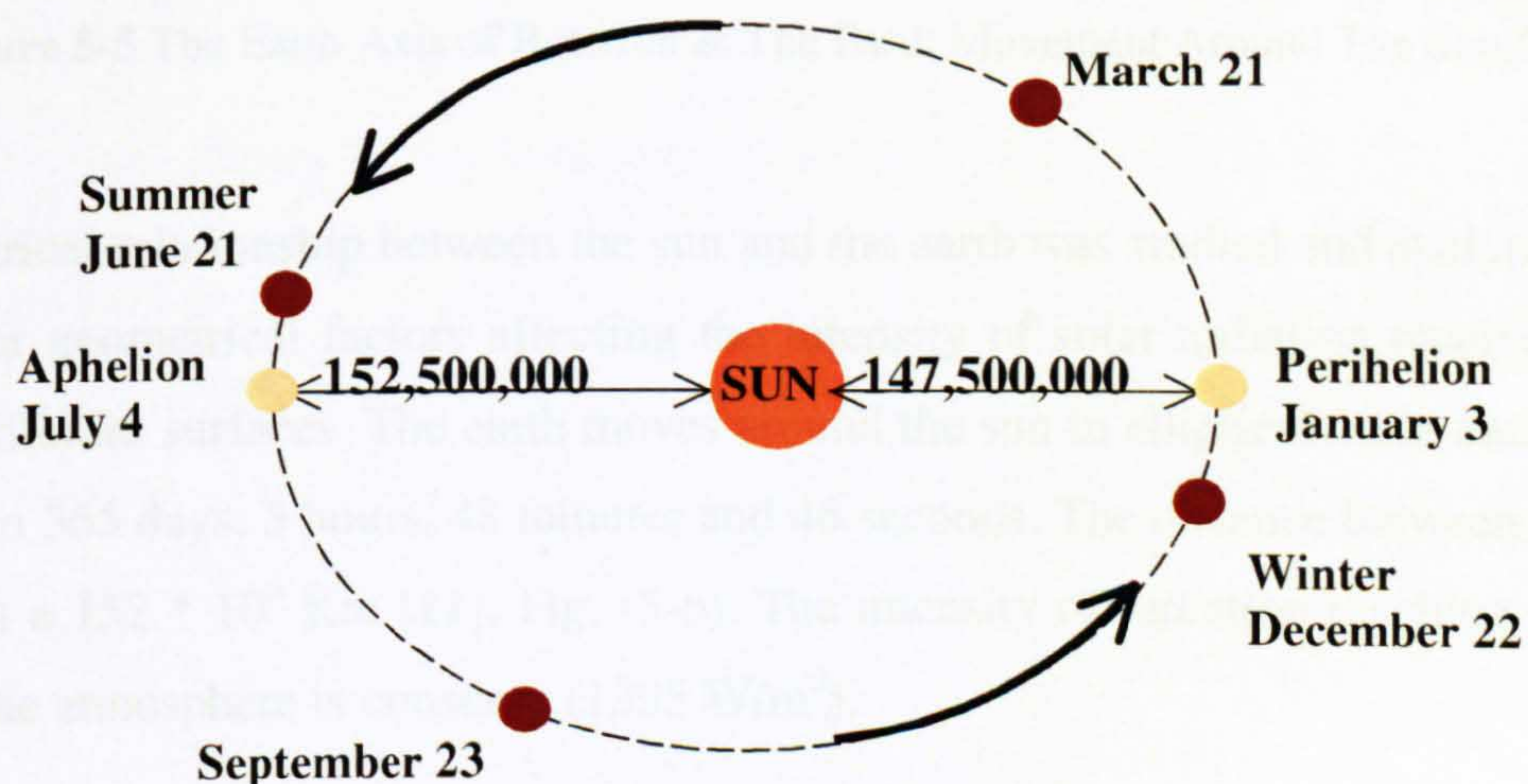


Figure 5-4 Earth -Sun Movement and Distance[9]

The earth revolves around its axis every 24 hours, each rotation makes one day[6]. This axis of rotation extends between the North and South poles, and it is tilted 23.45 degree from the perpendicular[10], Fig. (5-5). This tilt causes the different seasons, as it allows the sunrays to shine more directly and for longer periods of time at some locations during certain times of the year than others[9].

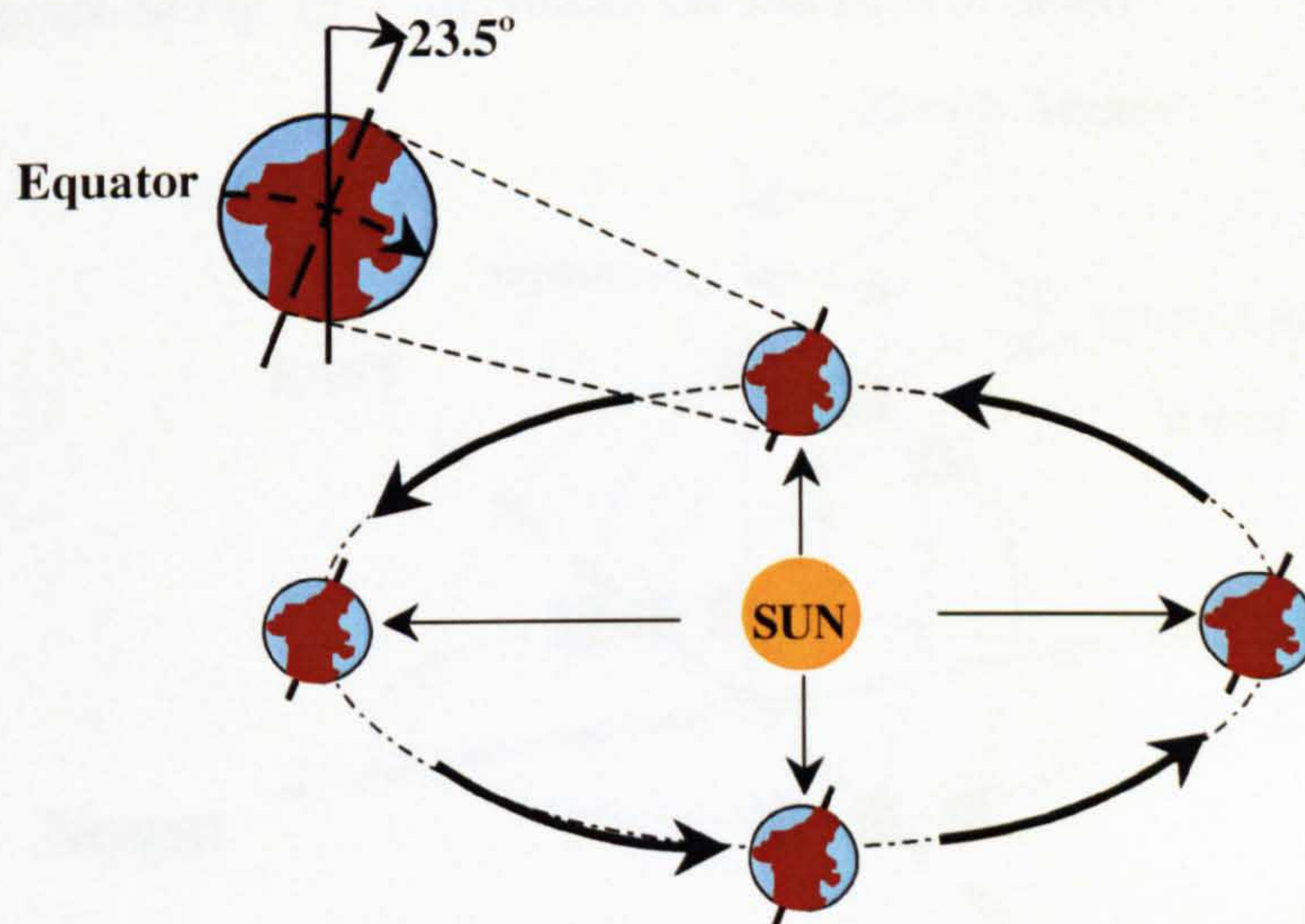


Figure 5-5 The Earth Axis of Rotation & The Earth Movement Around The Sun[9]

The geometrical relationship between the sun and the earth was studied and analysed to find out the solar geometrical factors affecting the intensity of solar radiation received on the earth and different surfaces. The earth moves around the sun in elliptical orbit, each cycle is completed in 365 days, 5 hours, 48 minutes and 46 seconds. The distance between earth and sun is about a $152 * 10^6$ Km [11], Fig. (5-6). The intensity of radiation reaching the upper surface of the atmosphere is constant, (1395 W/m^2).

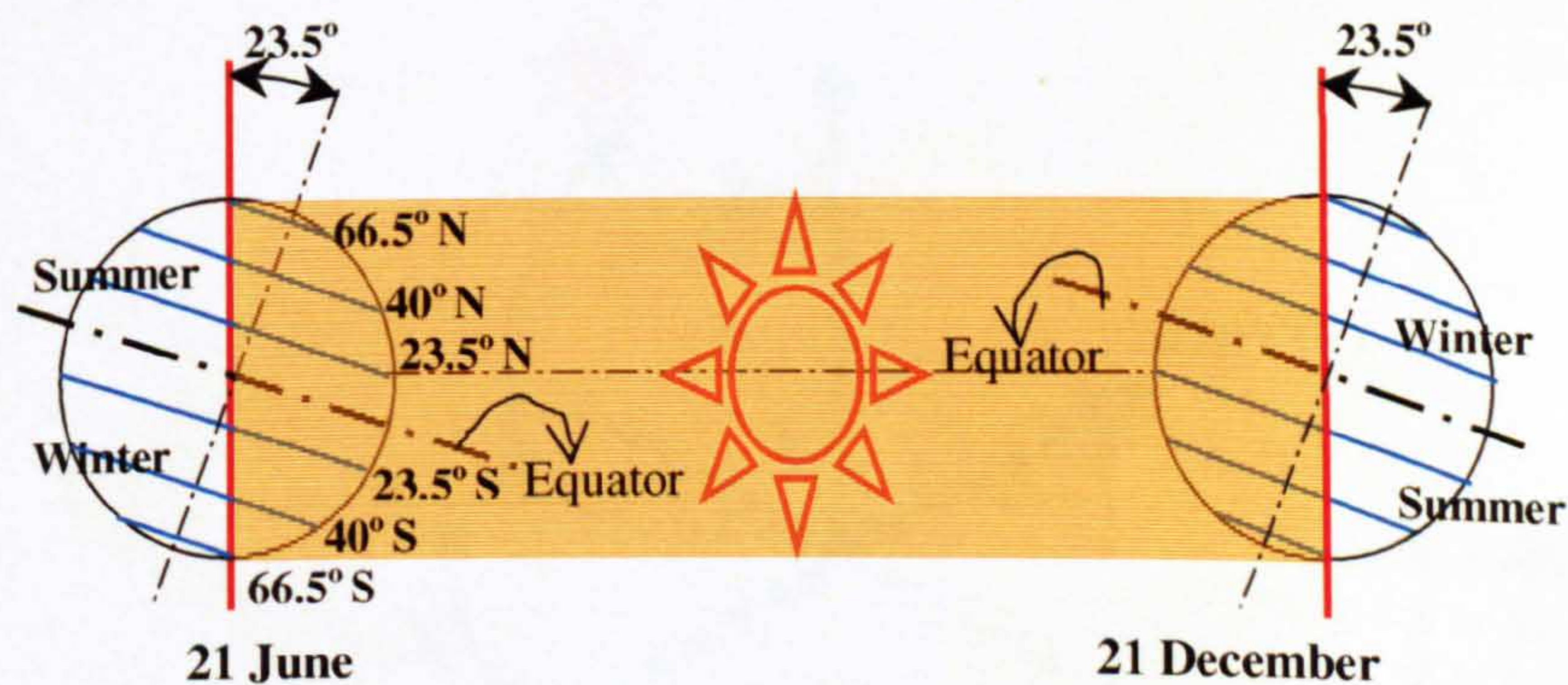


Figure 5-6 Earth -Sun Geometrical Relationship (After Muhaisen[9])

5.1.2.2 Sun Path and Position

As result of the directional and rotational process (earth with its tilt axis around the sun), yearly seasonal change causes are as follows: on 21 June, areas along latitude 23.5°N are normal to the sunrays with longest daylight period and maximum radiation. At the same time, latitude 23.5°S has the shortest daylight and minimum radiation. The three dimensional graph in Fig. (5-7) illustrates the sun path in detail.

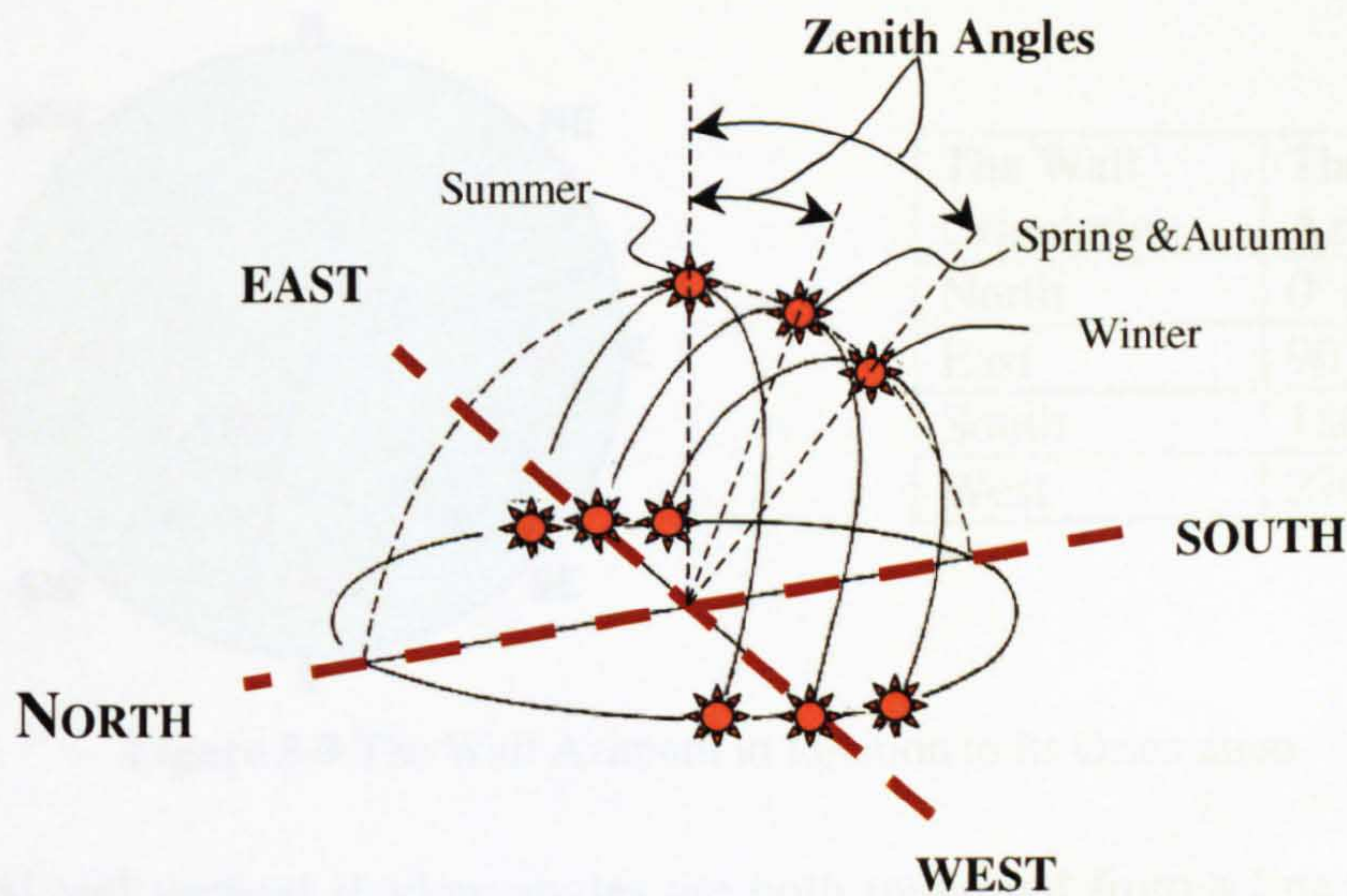


Figure 5-7 Sun Path Three Dimensional Diagram [11]

The sun position for selected latitudes at a particular time on the sky hemisphere is determined by two angles that resulted from the solar chart, Fig. (5-8):

1. *Solar altitude angle (X)*, which is the angle between the horizon plane and the sun-centre connecting line.
2. *Solar azimuth angle (Y)*, which the angle between the projections of the sun centre connecting line on the horizontal plane and the north-south direction.

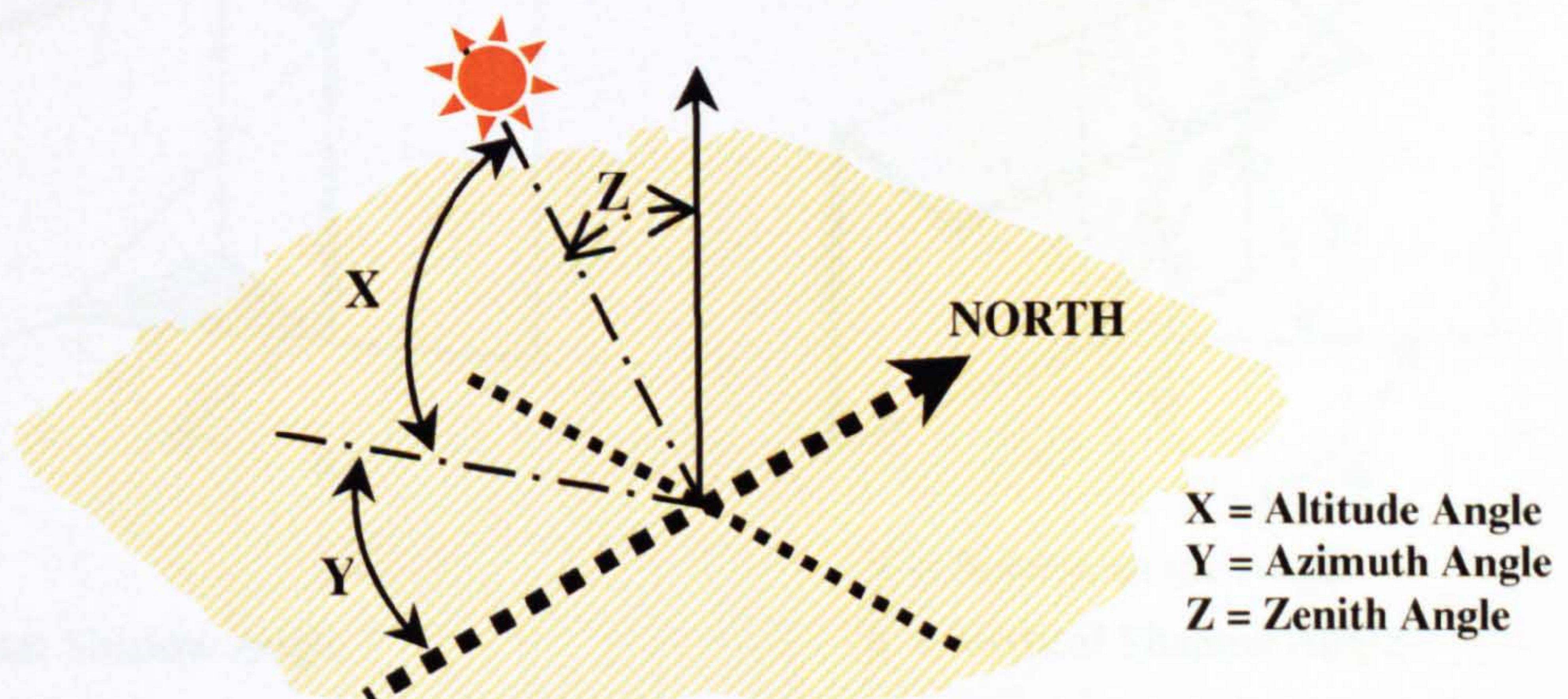
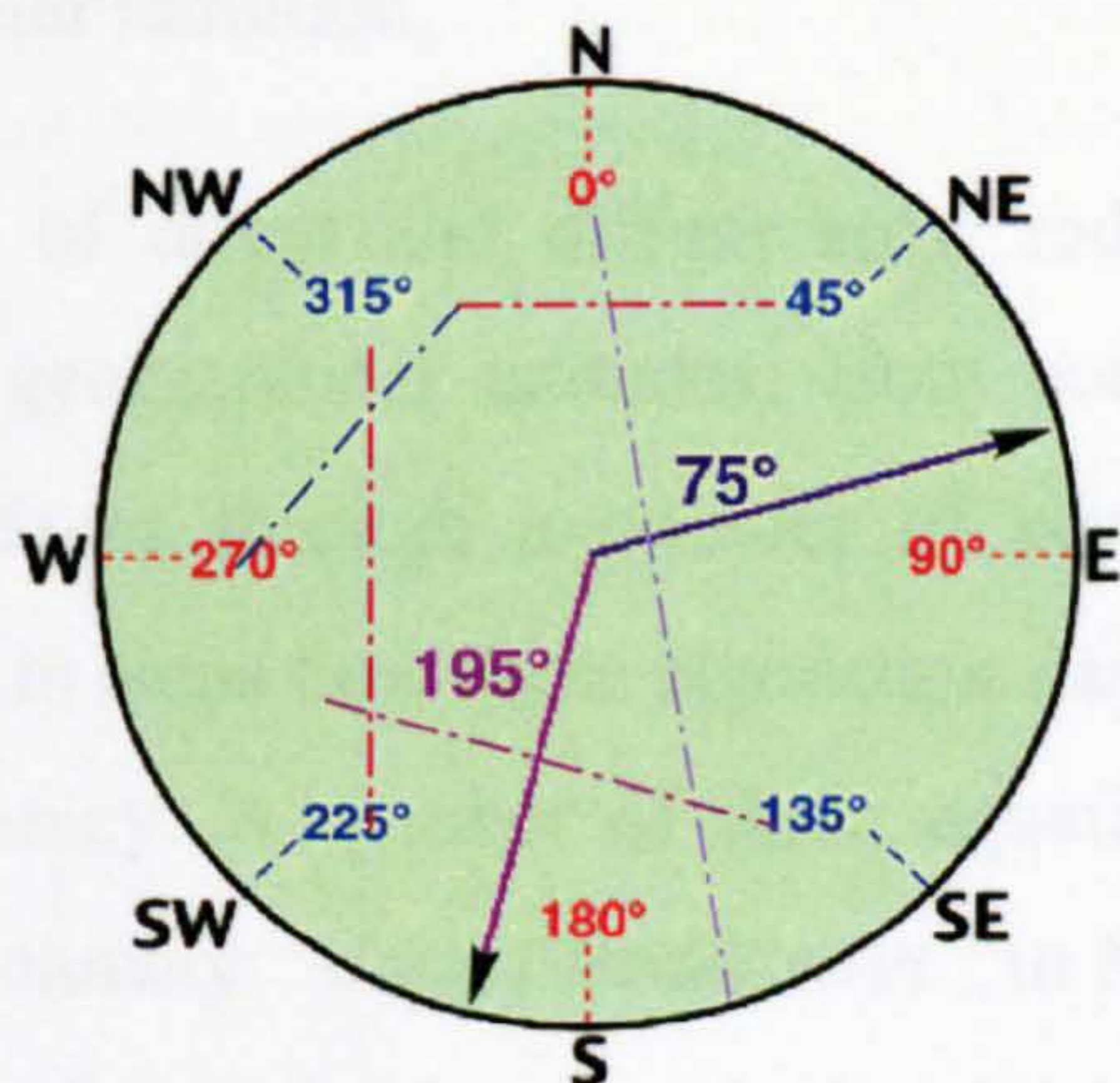


Figure 5-8 Solar Geometry (Altitude & Azimuth Angles) [11]

Altitude and azimuth angles for a particular latitude and time can be determined using the solar charts “*sun path diagrams*”, solar computer software or tabled references. Horizontal and vertical shadow angles can be defined as a function to these calculated angles (altitude and azimuth), Fig (5-9). The wall azimuth has to be defined first; Fig. (5-10) shows the different wall azimuths that are related to the wall's orientation (*the direction that a building's wall is facing*).



The Wall Orientation	The Wall Azimuth
North	0° or 360°
East	90°
South	180°
West	270°

Figure 5-9 The Wall Azimuth in Relation to Its Orientation

The horizontal and vertical shadow angles are both measured from a line perpendicular to the wall elevation. The horizontal shadow angle identifies the vertical shadow device and its design characteristics; it is calculated from the difference between the solar azimuth and wall azimuth. The vertical shadow angle identifies the horizontal device and its design characteristics, Fig. (5-10).

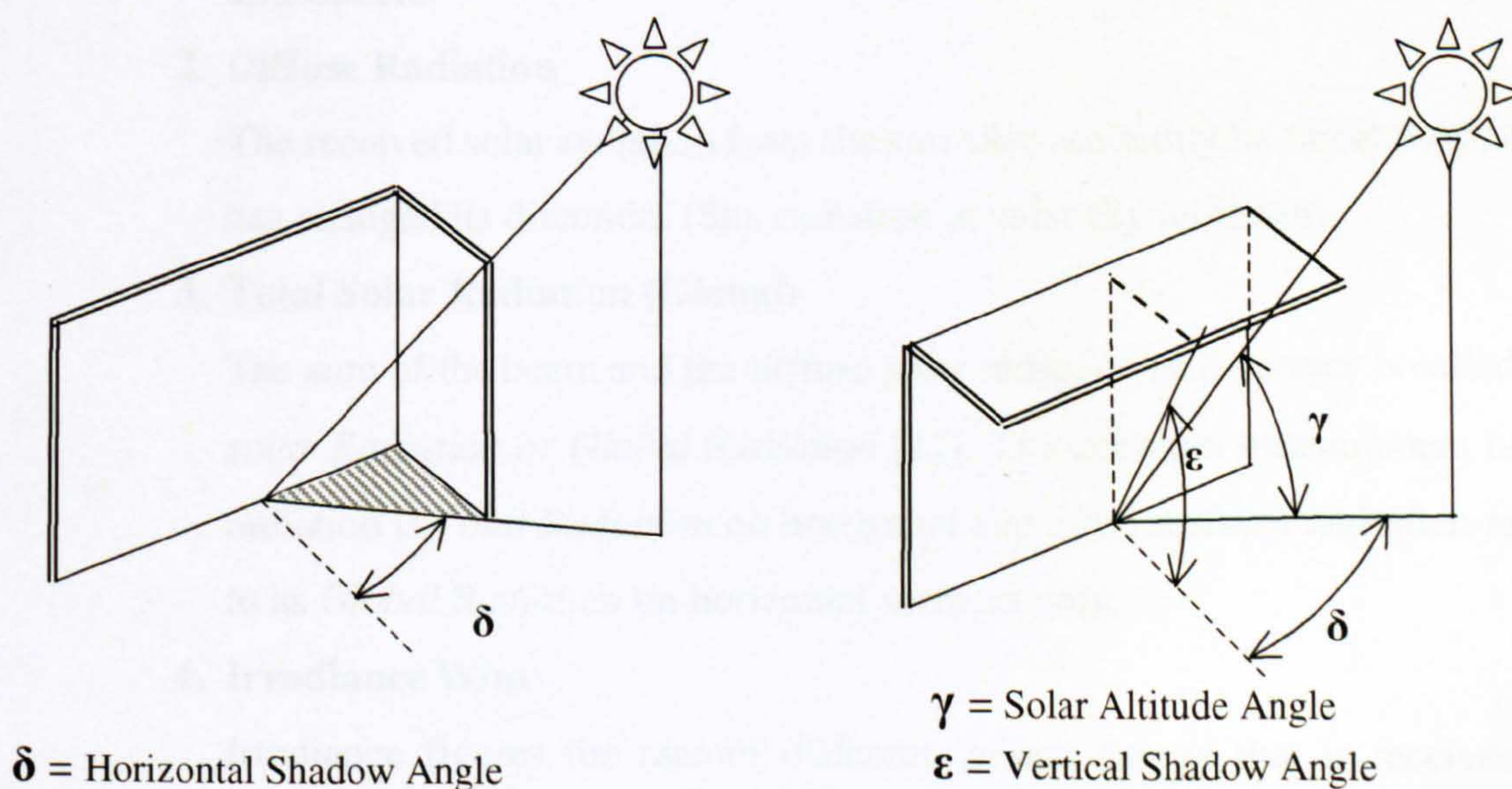


Figure 5-10 Vertical and Horizontal Shadow Angles[9]

5.2 ESTIMATION OF SOLAR RADIATION INTENSITY ON HORIZONTAL AND OBLIQUE SURFACES

Mainly, there are two components of solar radiation, which any solar design calculations are concerned with. The first is the direct solar radiation that comes directly from the sun. The second is the diffuse solar radiation, which is generated from the dispersing of the direct solar radiation through the atmosphere [12]. Global or total solar radiation means direct and diffuse solar radiation.

The data of direct and diffuse solar radiation on horizontal surfaces are available for different geographical latitudes. Both components can be mathematically calculated for tilted surfaces through a number of equations [1,13]. Muneer (1997) [1] in his book discusses in steps how these algorithms can be mathematically computed, with medium and high accuracy. A number of these equations, which deal with solar radiation on sloped surfaces, namely “*sloped Irradiation*” in Muneer’s book [1], has been applied for different architectural applications and for improving buildings environmental performances. Examples of these equations are explained later in this chapter (*refer to equations (5-3) - (5-6)*). Duffie and Beckman in their book [13], presented a number of definitions that explain the main parameters of the previous discussion.

1. Beam Radiation

The solar radiation received from the sun without having been scattered by the atmosphere.

2. Diffuse Radiation

The received solar radiation from the sun after scattering by the atmosphere has changed its direction. (Sky radiation or solar sky radiation)

3. Total Solar Radiation (Global)

The sum of the beam and the diffuse solar radiation on a surface is called *Total solar Radiation or Global Radiation* [12]. The common measurement of solar radiation is *Total Radiation* on horizontal and tilted surfaces and often referred to as *Global Radiation* on horizontal surfaces only.

4. Irradiance W/m^2

Irradiance figures the rate of different radiant energy that is received by a particular surface area. It is measured by watt per unit area W/m^2 .

5.2.1 Solar Radiation Intensity and Geographical Latitudes

The earth receives almost all of its energy from the sun in the form of radiation, so the sun is the dominating influence on the climate. The intensity of received solar radiation on a surface depends on many factors, such as the time (*seasonal variation*) and the location (*geographical latitude*), which are exemplified in the graphical comparison in Fig. (5-11). It shows different distributions of solar radiation intensities during a summer day (June) at three different latitudes 20°N , 25°N , & 30°N [14].

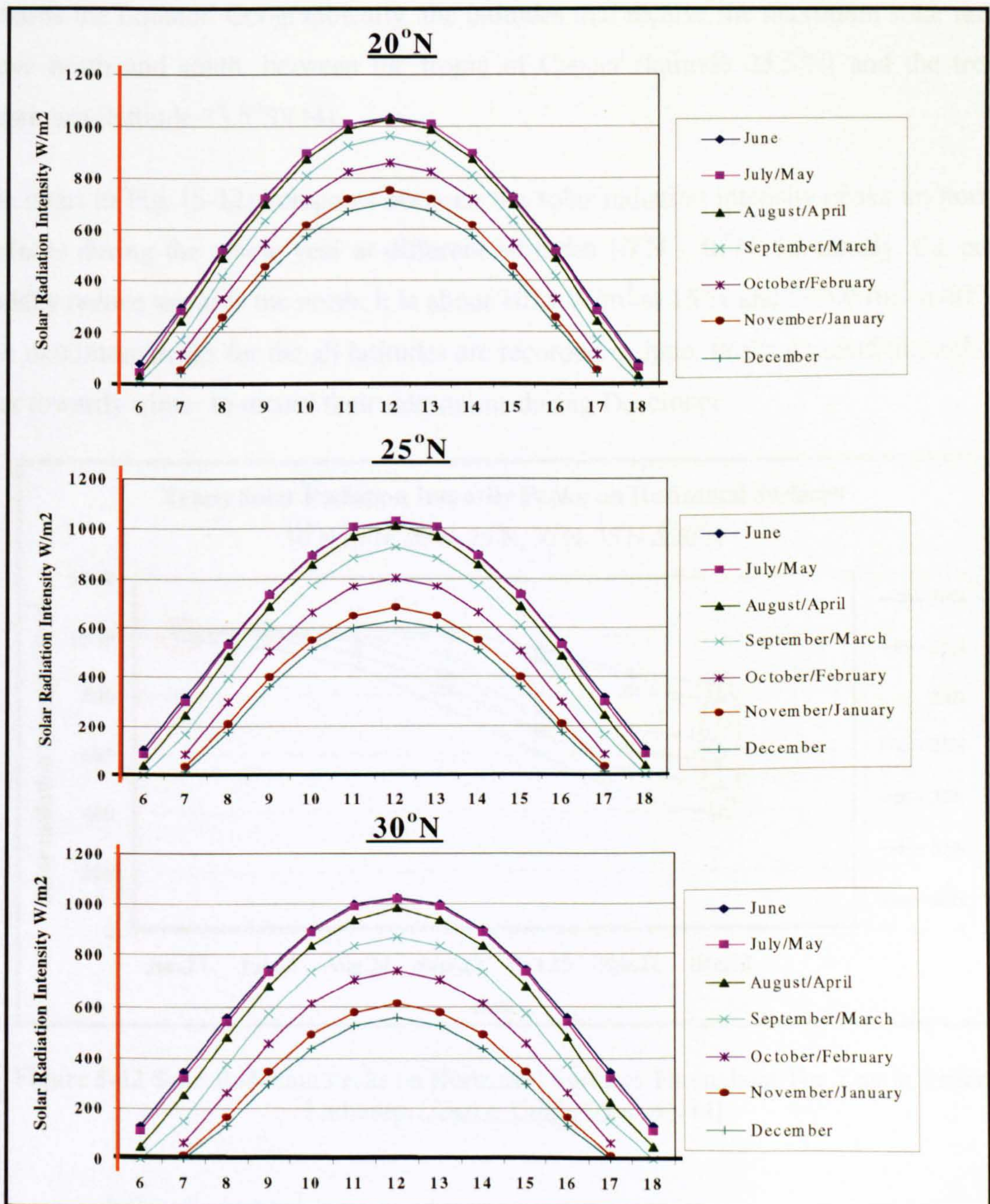


Figure 5-11 Direct Solar Radiation Intensity on Horizontal Surfaces At Different Latitudes; 20°N , 25°N and 30°N (Source: CIBSE Guide A) [14]

On the other hand, the receiving surface geometry, slope and orientation, have a significant impact on the solar radiation intensity. The charts in Fig. (5-11) show that the maximum intensities are recorded during June, and their peaks (*the maximum values during the day*) are recorded at midday. Generally, the form distribution of the received solar radiation intensity are very similar at the three latitudes; lowest values at morning hours before reaching the peaks at midday then starting to reduce again towards the end of the day. In the three locations the solar radiation intensity peak occurs at midday. The peak value increases towards the Equator. Geographically, the latitudes that receive the maximum solar radiation move north and south, between the tropic of Cancer (latitude 23.5°N) and the tropic of Capricorn (latitude 23.5°S)[14].

The chart in Fig. (5-12) compares between the solar radiation intensity peaks on horizontal surfaces during the whole year at different latitudes 10°N - 40°N . Obviously, the peaks at midday reduce towards the north; it is about 1025 W/m^2 at 15°N and 990 W/m^2 at 40°N [14]. The maximum peaks for the all latitudes are recorded in June. Peaks descend throughout the year towards winter to record their minimums during December.

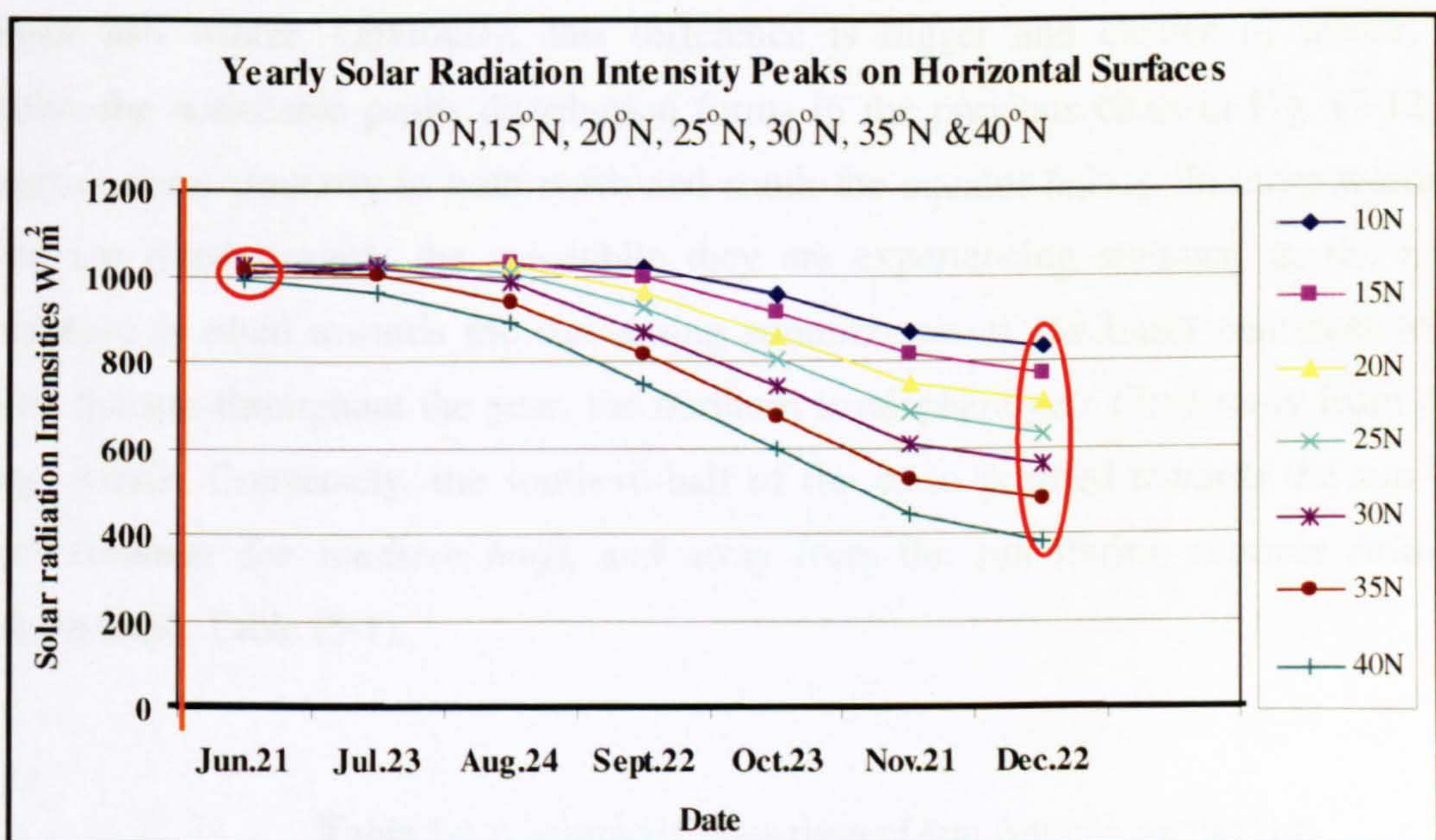


Figure 5-12 Solar Radiation Peaks on Horizontal Surfaces Throughout The Year at Different Latitudes, (*Source: CIBSE Guide A*) [14]

The previous graph also showed that peaks for the selected latitudes are almost around 1000 W/m^2 with no significant difference in summer. On the other hand, there is a clear difference between those peaks during winter in which they vary from 400 W/m^2 at 40°N to 800 W/m^2 at 10°N . This observable fact is apparently explained in Fig. (5-13).

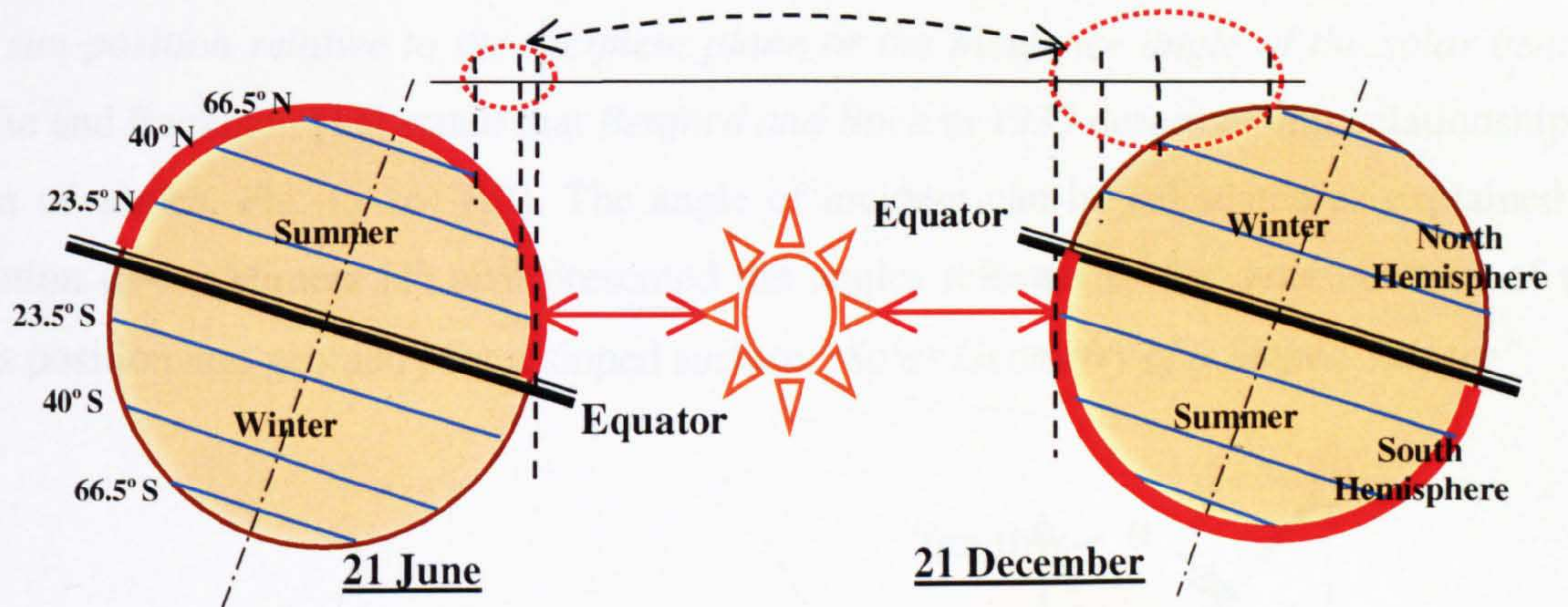


Figure 5-13 The Difference Between Peaks Due to Seasonal Variation[9]

Fig. (5-13) illustrates the difference in Earth to sun distances at different latitudes during summer and winter. Latitude 23.5°N appears more close to the sun than latitude 40°N during summer and winter. Obviously, this difference is bigger and clearer in winter, which explains the noticeable peaks distribution forms in the previous chart in Fig. (5-12). This scenario occurs similarly in both north and south the equator halves. In other words, both halves are tilted towards the sun while they are experiencing summer, as the northern hemisphere is tilted towards the sun during summer-season. As Earth continues to move around the sun throughout the year, the northern hemisphere gets tilted away from the sun during winter. Conversely, the southern-half of the earth is tilted towards the sun during winter (*summer for southern half*), and away from the sun during summer (*winter for southern half*), Table (5-1).

Table 5-1 A Seasonal Comparison of Sun Altitude Angles [14]

Latitude	Season	06:00	07:00	08:00	09:00	10:00	11:00	12:00	13:00	14:00	15:00	16:00	17:00	18:00
20°	Summer	8	21	35	48	62	76	86	76	62	48	35	21	8
	Winter		5	17	28	38	44	47	44	38	28	17	5	
30°	Summer	11	24	36	50	62	75	83	75	62	50	36	24	11
	Winter			11	21	29	35	37	35	29	21	11		

5.2.2 Solar Radiation Intensity and Recipient Surface Geometry (Solar Geometry of Sloped Surfaces)

As mentioned previously, the intensity of solar radiation received by a surface depends also on the geometrical relationships between the recipient plane and the incoming solar beam (the sun position relative to the recipient plane or the incidence angle of the solar beam). Duffie and Beckman [13] stated that *Benford and Bock* in 1939 described this relationship in terms of angles, Fig. (5-14) [13]. The angle of incidence can be calculated as explained in Equation (5-1). Muneer [1] also presented the angles relevant to the determination of the sun's position and geometry for a sloped surface "Solar Geometry of a Sloped Surface".

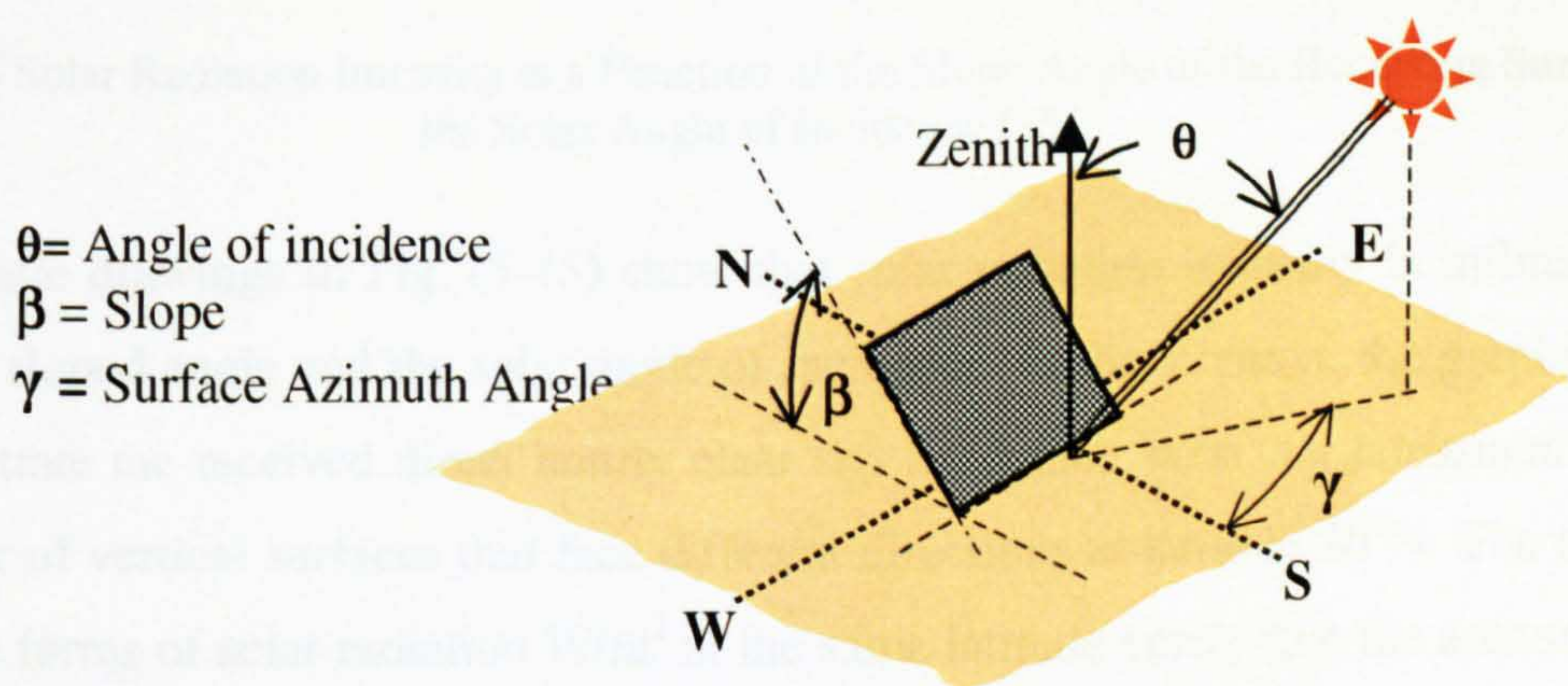


Figure 5-14 Solar Geometry [13]

$$\begin{aligned} \cos \theta = & \sin \delta \sin \phi \cos \beta - \sin \delta \cos \phi \sin \beta \cos \gamma \\ & + \cos \delta \cos \phi \cos \beta \cos \omega \\ & + \cos \delta \sin \phi \sin \beta \cos \gamma \cos \omega \\ & + \cos \delta \sin \beta \sin \gamma \sin \omega \end{aligned} \quad (5-1) [13]$$

Key to Equation 5-1 [13]

- ϕ Latitude, that is, the angular location north or south of the equator, north is positive. ($-90^\circ \leq \phi \leq 90^\circ$).
- δ Declination, that is, the angular position of the sun at solar noon with respect to the plane of the equator, north is positive. ($-23.45^\circ \leq \delta \leq 90^\circ$).
- β Slope, that is, the angle between the surface and the horizontal. $0 \leq \beta \leq 180^\circ$ ($\beta > 90^\circ$ (means that the surface has a downward facing component)).
- γ Surface azimuth angle, that is, deviation of the projection on a horizontal plane of the normal to the surface from the local meridian, with zero due to south, east is negative, west is positive. ($-180^\circ \leq \gamma \leq 180^\circ$)
- ω Hour angle, that is, the angular displacement of the sun east or west of the local meridian due to rotation of the earth on its axis 15° per hour, morning negative, afternoon positive.
- θ Angle of incidence, that is, the angle between the beam radiation on a surface and the normal to that surface.

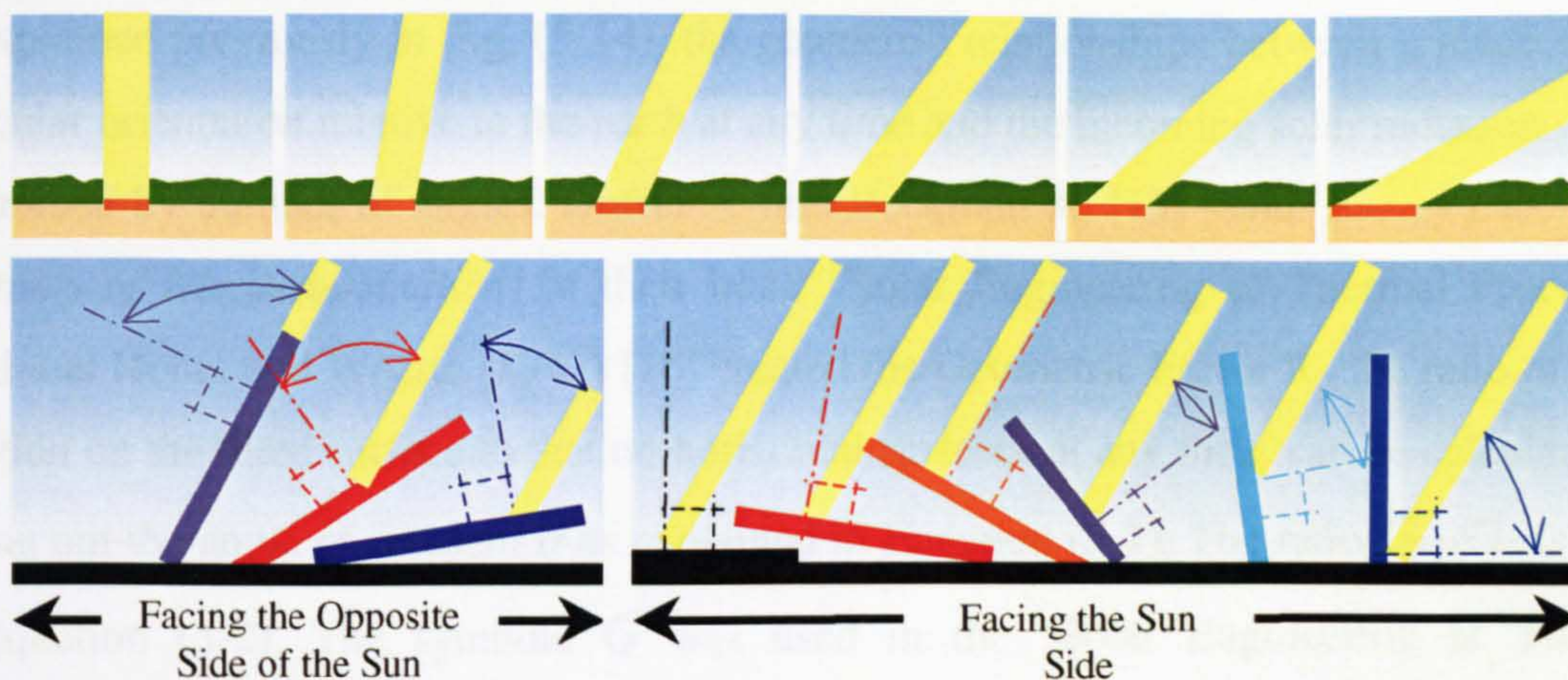


Figure 5-15 Solar Radiation Intensity is a Function of the Slope Angle of the Receiving Surface and the Solar Angle of Incidence [15]

The schematic drawings in Fig. (5-15) show that solar radiation intensity is influenced by the surface sloped angle and the solar angle of incidence. In this context, the graphs in Fig. (5-16) illustrate the received direct hourly clear sky irradiance W/m^2 on horizontal surface and number of vertical surfaces that face different directions at latitude $30^{\circ}N$. The different distribution forms of solar radiation W/m^2 at the same latitude verify that the amount of the incident solar radiation on surfaces varies significantly according to the receiver surface geometry and orientation [14].

The horizontal surface receives the greatest solar radiation intensity in summer and winter. East and West facing walls receive the second highest intensities. It is clearly recognised that the east the west walls receive direct hourly clear sky irradiance W/m^2 only during morning and afternoon respectively. They both receive zero W/m^2 at midday. The north only receive direct solar radiation during the early morning and the late afternoon. While, the south wall receives direct hourly clear sky irradiance during the hours from 10:00-15:00 only [14].

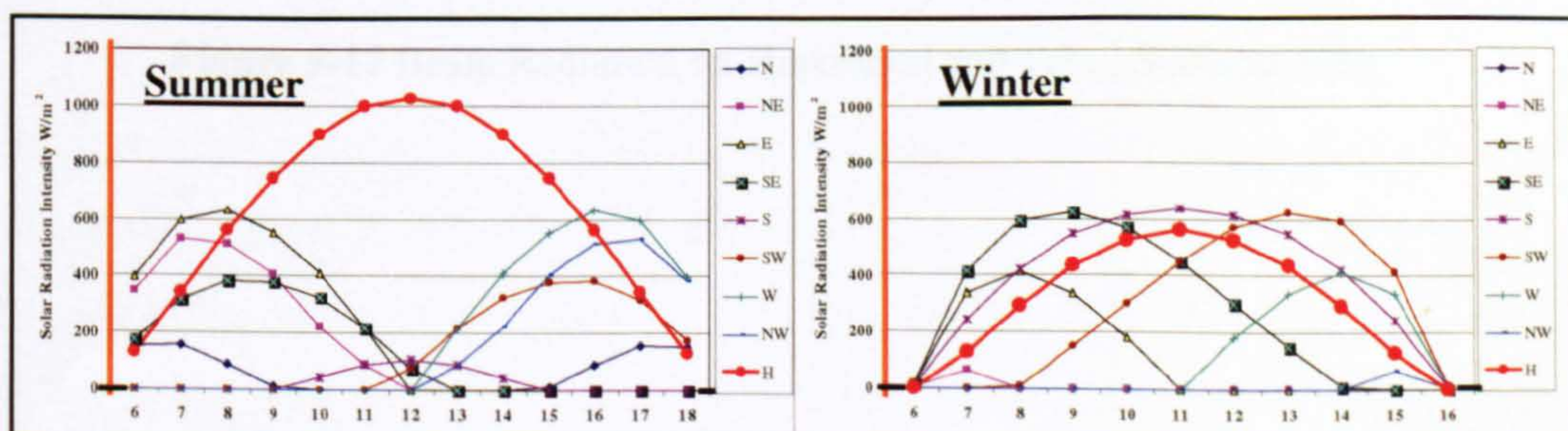


Figure 5-16 Direct Solar Radiation Received by Different Surfaces at $30^{\circ}N$ [14]

5.2.3 Ratio of Beam Radiation on Tilted Surface to that on Horizontal Surface

As explained previously in Fig. (5-14), the geometric relationships between a plane of any particular orientation relative to the earth at any time and the incoming solar radiation can be determined by number of angles. Duffie A. and Beckman A. [13] (*Solar Energy Laboratory, University of Wisconsin-Madison*) in their book “Solar Engineering of Thermal Processes” stated that Hottel and Woertz (1942) [16] created the Geometric Factor R_b ; the ratio of beam radiation on the tilted surface to that on horizontal surfaces at any time, can be calculated by finding out the angle of incident θ as explained in Equation (5-1). The ratio G_{bT}/G_b is given by Equation (5-2). The symbol G was used in the “Solar Engineering of Thermal Processes” book, whereas it was I in the original development by *Hottel and Woertz (1942)* [13].

$$R_b = \frac{G_{bT}}{G_b} = \frac{G_{bn} \cos \theta}{G_{bn} \cos \theta_z} = \frac{\cos \theta}{\cos \theta_z} \quad (5-2) [13]$$

Fig. (5-17) indicates the angle of incidence of beam radiation on the horizontal and the tilted surfaces. Duffie and Beckman stated that *Hottel and Woertz (1942)* pointed out that this equation provides a suitable method for calculating R_b for the most of common case [13]. They also showed a graphical method for finding out this ratio and solve these equations [13].

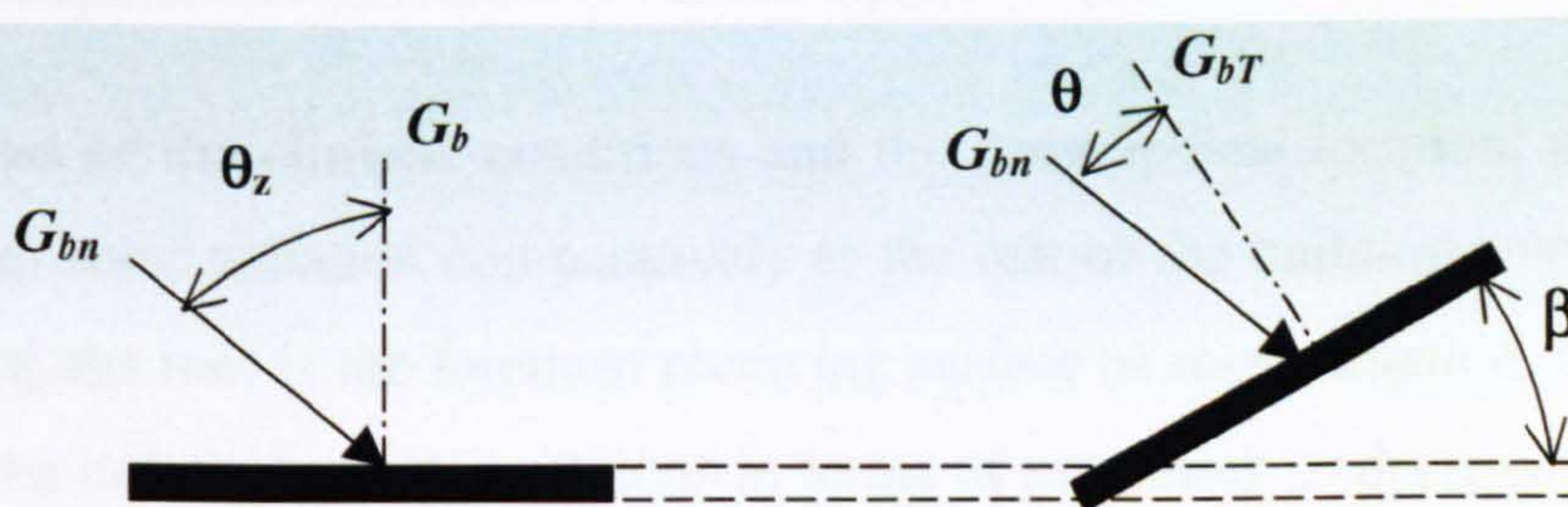


Figure 5-17 Beam Radiation on Horizontal and Tilted Surfaces [13]

5.2.4 Solar Radiation on Sloping Surfaces and on Curved Forms

Duffie and Beckman in their book (1991) presented equations, which are based on other related mathematical and empirical formulation for solar radiation on sloped surfaces of different orientations [13]. Muneer in his book (1997)[1] discussed these equations and others in order to develop the computation of monthly or daily sloped-irradiation at higher latitudes and especially on vertical surfaces facing orientation and any sloping surface facing south [1]. The magnitude of geographical location has been implied from Muneer's contribution. It was clear that the geographical location (latitude) must be taken into account when applying these algorithms.

The use of the mathematical and empirical equations of solar radiation on sloped surfaces facilitated the investigation of the solar and thermal behaviour of a number of traditional and new architectural developments. This may include courtyard forms, sloping and curved facades, large windows and roof forms; the latter has been addressed in this research.

Curved roofs in general and in particular domed and vaulted roofs have emerged as traditional elements in modern buildings and designs. Their potential in reducing heat gain and providing indoor thermal comfort are well recognised. Referring the advantages of curved roofs to the thermal properties of their construction materials or to their external colours is incomplete. Runsheng, et al stated that relating these advantages only to their reduction of the local radiant flux on a rounded surface and therefore resulting in lower surface temperatures also seem to be incomplete [17].

Regardless of the climatic conditions and the geographical location, the roof receives the maximum solar radiation comparatively to the rest of the building envelope elements [18]. Therefore, the roof is the foremost receiving surface of solar radiation, which can efficiently control the indoor thermal conditions in terms of increasing or decreasing the received solar radiation intensity on its surface.

Depending on the facts of solar radiation variations due to receiving surface slope and orientation, the present research aims to prove evidence of solar and thermal advantages of curved-roof form, curvature and orientation in hot-arid climates. Therefore, it is concluded that roof geometry and shape, among other factors, can significantly influence the intensity of the received solar radiation on buildings.

The optimum geometrical design of roofs can be accomplished by a careful understanding of the geographical latitude solar geometry and solar irradiance received by different geometries of roofs.

5.2.5 Previous Applications of Sloped Solar Irradiance On Curved Forms

An awareness of the requirement for the understanding of the solar behaviour of curved and tilted surfaces arose, thus, mathematical models for the calculation of the received solar radiation intensity on horizontal, vertical and tilted surfaces have been applied and developed [19], as a function of a number of factors such as local latitude, roof surface orientation (*azimuth of roof surface*), the slope angle of the receiving surface. Applying different irradiation formulas on sloped surfaces, a number of attempts has been carried out to investigate different solar and thermal behaviour of curved forms. The following sections (5.2.5.1) and (5.2.5.2) discuss two of these attempts.

5.2.5.1 Irradiation on an Inclined Planar Surface (Skylight Domes)

Laouadi, A., et al developed an optical model for predicting the transmittance, absorptance and reflectance of transparent domed skylights [19]. Solar data and properties are available only on planar surfaces either horizontal or vertical. (*Direct and diffuse solar intensities on vertical and horizontal surfaces*) (*CIBSE, IHVE Guides and else*) [14]. They can also be calculated for oblique surfaces as explained earlier in this chapter.

The incident solar irradiance on an inclined planar surface was given in this research work by:

$$\begin{aligned} I_{b,\beta} &= I_b \cos\theta_\beta, \quad \text{for beam radiation;} \\ \text{and } I_{d,\beta} &= I_{d,t}, \quad \text{for diffuse radiation} \end{aligned} \quad (5-3) [19]$$

Where:

$I_{b,\beta}$: beam irradiance incident on an inclined surface (W/m²);

$I_{d,\beta}$: diffuse irradiance incident on an inclined surface (W/m²);

I_b : beam solar radiation (W/m²);

I_d : sky diffuse solar radiation on a horizontal surface (W/m²);

$I_{d,t}$: total diffuse radiation on an inclined surface (W/m²);

θ_β : incidence angle on an inclined surface for beam radiation;

β : inclination angle of the surface with respect to the horizontal.

The incidence angle θ_β is given by (13):

$$\cos\theta_\beta = \cos\beta \cos\theta_z + \sin\beta \sin\theta_z \cos(\psi_s - \psi_f) \quad (5-4) [19]$$

With:

θ_z : sun zenith angle (or the incidence angle on a horizontal planar surface) ;

ψ_s : sun azimuth angle; and

ψ_f : surface azimuth angle (surface orientation with the respect to south direction)

The sun zenith angle θ_z is expressed in terms of the site latitude L , the sun declination angle δ and the hour angle ω as follows [13]:

$$\cos\theta_z = \cos L \cos \delta \cos \omega + \sin L \sin \delta \quad (5-5) [19]$$

Total diffuse radiation on an inclined surface $I_{d,t}$ is composed of the sky diffused radiation and the ground reflected radiation. The total diffuse radiation $I_{d,t}$ in general may be calculated as follows [13]:

$$I_{d,\beta} = I_d c_d + (I_b \cos\theta_z + I_d) c_r \quad (5-6) [19]$$

c_d and c_r are coefficients for diffuse and ground-reflected radiation respectively, which are a function of ground reflectance (albedo) ρ_g , circumsolar brightness coefficient (F_1), and horizon brightness coefficient (F_2). The value of F_1 is equal to zero in both isotropic diffuse skies and overcast skies, F_2 is also equal to zero only in isotropic skies, whereas both are not equal to zero at non-isotropic diffuse skies. Both c_d and c_r coefficients can be calculated using the model developed by Perez, et al [19].

5.2.5.2 Geometric Forms and Insolation Compared with Horizontal Surfaces

“Geometric forms and insolation” is the title of another research study done by Thanos N. Stasinopoulos (1998/1999) [20,21]. This study tested the solar energy R (global, direct, diffuse, ground reflected) incident upon the solid surface of area F exposed to solar radiation as the sum of the irradiation on the surface segments. As well as time and latitude, total (global) solar irradiance on different geometrical forms depends on various factors like the size, orientation and slope angle of each segment, atmospheric conditions and ground albedo. Stasinopoulos’s study [21] was based on finding out the ratio ϵ , in which $\epsilon = R/F$. This ratio is the mean solar radiation between the mean solar irradiance on the surface and is independent of the surface size. It indicates the potential of form to receive more or less solar radiation than others at the same time and place.

The study analysed the relationship between geometric shape and solar irradiation, it is based on the mean solar irradiance (ϵ) on several shapes that correspond to simple building types. Although it varies over time and place, mean solar irradiance (ϵ), is not a steady base for assessing forms in terms of insolation. It is more appropriate to correlate the mean irradiance (ϵ) on a form with the solar energy (ϵ_0), which indicates the ratio (R/F) for a horizontal surface at the same time and location [21].

The study introduced the notion of relative irradiance or ‘insolation Index’ (μ), which is defined as the ratio (ϵ/ϵ_0) of the mean solar irradiance on different geometrical surfaces (ϵ) to that on the horizontal plane (ϵ_0 , $\mu = \epsilon / \epsilon_0$). On the other hand, the ratio (ϵ/ ϵ_0) indicates the relative insolation on a given form, it is called the form insolation Index μ ; it refers to the capacity of the form to receive more or less solar irradiation comparatively to a horizontal surface under the same conditions due to its geometrical characteristics.

The relationship between the geometric properties of a curved roof and insolation level (solar radiation intensity) is explored in this study by comparing the μ -index of various curvatures. The μ -index is calculated in the following steps [20,21]:

- Partitioning of the exposed surface (F) in (n) segments of area (f_n), and calculation of the solar irradiance on each one.
- Calculation of the total energy (R) on the entire surface as the sum of the irradiance on each segment: ($R = \sum (i_n \cdot f_n)$).
- Calculation of the mean solar irradiance on the surface by dividing the total energy (R) on the total surface area (F): ($\epsilon = R/F$).
- The μ -index calculated by dividing the mean solar irradiance (ϵ) on the available horizontal one ϵ_0 : ($\mu = \epsilon / \epsilon_0$) [20].
- The irradiance calculation and all the subsequent computations in this study were performed on computer spreadsheets based on the algorithm developed by professor J. K. Page and other European scientists (*The European Solar Radiation Atlas ESRA*) [22]. The algorithm is applied for the calculation of direct, diffuse and ground reflected hourly irradiance on a plane at any orientation and slope, according to the following parameters:
 - Latitude and elevation of the location
 - Monthly average sunshine duration
 - Monthly link atmospheric turbidity factors
 - Annual a + b Angstrom coefficients [20,21].

Further processing of Stasinopoulos research study has led to various conclusions and findings, like the following [20,21]:

- **Insolation Index μ :** The μ -index varies from shape to shape, especially during summer. Monthly fluctuating of the global radiation indexes is generally narrow for low forms and wider for tall ones, while the diffuse radiation remains constant in all cases.
- **Irradiation Distribution:** The distribution of total solar irradiation on facets of a form depends not only on their size and orientation, but also on the time of the year.
- **Orientation Effects:** Changes of orientation affect monthly μ -index of a form, but the annual values remain practically constant.

- **μ -indexes and B/F ratio:** μ -indexes and “Base-to-Exposed-Surface” ratio B/F of a form have a direct linear relation. This is applied to all forms, locations, seasons and radiation types, notably the diffuse component. During winter and due to wider variations of direct components in tall form, some deviations from linearity occur, particularly at high latitudes (*51°N London*).

Most of the previous applications of the sloped solar mathematical models showed that solar radiation intensity on horizontal surfaces differ according to the receiving surface geometry and orientation (*surface azimuth angle*). Also, it has been demonstrated that R_b , which presents the ratio between the received direct beam radiation on the tilted surface I_{bt} to that on the horizontal surface I_b , is significantly influenced by the surface slope angle (β) [13].

As the aim of the research presented in this thesis is to create a comparative study between the solar performances of flat and curved roofs in hot-arid climates, a very limited number of similar attempts has been found. Some of these attempts employed solar computation models, which are based on either previous mathematical equations or on similar developed and alternated ones. However, the outputs of these attempts were sometime consistent and contradicted in others.

As a result, unclear architectural perception for the solar performance of different curved-roof, forms, curvatures and orientations existed before carrying out this research work. However, while preparing this thesis for submission a number of related attempts has been published in 2003. Consequently, the solar investigation of curved-roof forms, curvatures and orientations has been undertaken in this research. Different solar calculation tools have been searched in order to find an appropriate model for the architectural purpose of this research and at the same time enable large number of tests and investigations to cover a wide range of curved-roof forms and curvatures.

5.3 DESCRIPTION OF THE SOLAR RADIATION SIMULATION MODEL SRSM

Mathematical model codes appropriate for studying and calculating the intensity of the received solar radiation on different surfaces are included in different computer models. The mathematical basis of these models is similar, however their format may vary according to the specific use for which they are intended.

Keeping in mind what has been implied previously and from the work done by Muneer [1], that each set of equations for sloped surfaces solar radiation can be more appropriate for particular latitudes than others. This has been perceived as more accurate for solar calculations at particular geographical locations (*higher or lower latitudes*). For the purpose of the present architectural research carried out in the thesis and for the selected geographical location (Latitude 22-24N^o), a thorough research was done to find a computer model that calculates the solar radiation on sloped surfaces with any orientation and is especially designed for this geographical zone. However, other solar calculations models can be applied; for example J. K. Page and other European scientists model (*see page 138 in this chapter*). The European Solar Radiation Atlas ESRA also provides solar radiation data for horizontal and inclined surfaces [22].

Consequently, a computer program, which has been developed by Exell in 1986 and has been upgraded in 1999 [4], at King Mongkut's University of Technology Thonburi, was selected. This computer model can be correctly applied for the calculation of total hourly solar radiation intensity on horizontal and sloped surface with any orientation located between certain ranges of latitudes (*north and south of the equator*). A version of this model is based on Quick Basic (Solar Radiation Simulation Model for Quick Basic), the original version is based on BASIC*. Another version of this model has been built on JavaScript, which is available online [5]. Furthermore, personal contacts with the author of this model have been made to obtain more detailed information about the given model inputs and outputs. (*Appendix (A)*)

The author of this model mentioned that the formula which the model use to calculate the total daily solar radiation under a clear sky for any sloped surface is an empirical formula fitted to the values given for the tropics by Schuepp [23]. The formula uses a Fourier series; these Fourier series coefficients are polynomials as functions of latitude. The polynomials were fitted only in the latitude range 25N to 25S and they cannot be extrapolated beyond that range [4].

* Solar Radiation Simulation Model for Quick Basic is an upgraded version of the program described in: R. H. B. Exell, A program in BASIC for calculating solar radiation in tropical climates on small computers, *Renewable Energy Review Journal*, Vol. 8, No. 2, December 1986, Regional Energy Resources Information Centre, Asian Institute of Technology, Bangkok.

Solar Radiation Simulation Model (*SRSM*) [5] runs daily calculations throughout the year and at particular geographical latitudes north and south of the Equator. *SRSM* has been used in this research as a computer tool to calculate the Total Hourly Clear Sky Irradiance $I_{(HTCS)}$ W/m^2 on horizontal and different sloped tilt surfaces. It generates solar calculations for surface with any slope and azimuth angles in the tropics.

The geometrical configurations of any receiving surface have to be defined numerically in term of angles. These angles determine surface slope and azimuth angles (*orientation or the direction that the surface faces*). For this reason, and to make the model identify different curved-roof forms, curvatures and orientations, two geometrical resemblance techniques have been developed. This geometrical technique is based on the idea of resembling the curved-roof surfaces by a group of horizontal and oblique planar segments with different slope and azimuth angles. These geometrical techniques are fully explained in the following sections of this chapter.

SRSM also calculates the hourly position of the sun (*azimuth & zenith angles of the sun*). The computational model *SRSM* numerically identifies the planar segments and other input variables as discussed below.

Latitude (deg)

For more accurate calculations, the geographical latitude has to be in the tropics, (25°N-25°S of the Equator). However, calculation can be carried for other geographical latitudes.

Mean Daily Solar Irradiation on Horizontal Surface (MJ/m^2) For Each Month

In addition to the collected solar data for Aswan (23.58N°) [24], the mean solar irradiance on horizontal surfaces can be calculated using *SRSM*. The mean solar irradiance on horizontal surfaces for clear sky conditions in the selected region can be approximately estimated to about 75% of clouds sky conditions. Collected and calculated inputs for the selected geographical location are presented in *Appendix A*.

However, the accuracy of the employed data (collected or calculated) are not of great significance for a comparative evaluating of the solar performances of flat and curved roofs in hot-arid climates. **It was considered, that all outside conditions, geographical location and latitude, solar-time comparison and the geometrical resemblance techniques for all tested geometries are identical.**

Surface Slope Angle (Segment Tilt Angle)

The tilt angle (deg) is the angle between the surface and the horizontal plane, which is the same as the angle between the normal of that surface and the zenith. As shown in Fig (5-18), it is possible to calculate the slope angle for any tilted segment using different geometrical relations or equations (see Equations (5-7) & (5-8)).

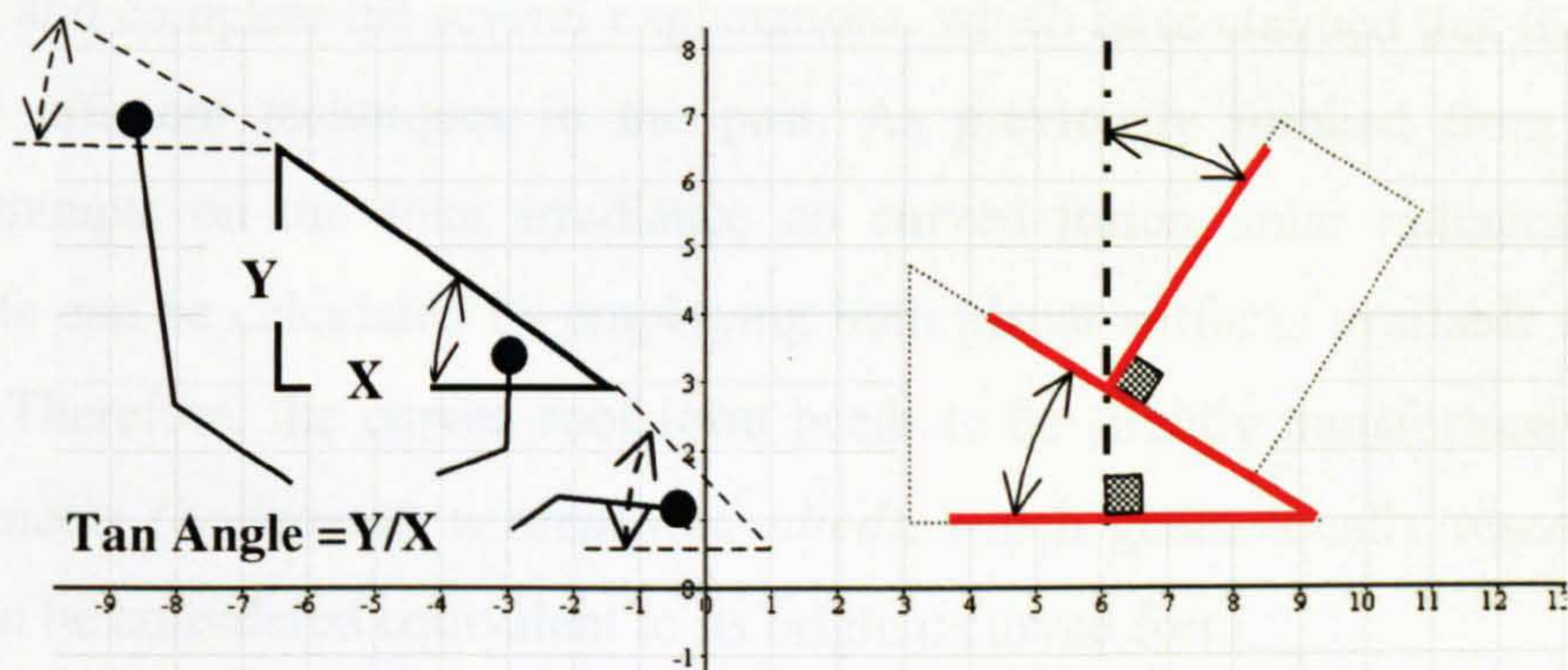


Figure 5-18 Geometrical Relations for Defining the Tilted Surface Geometry

The Orientation of Each Tilted Surface (*Planar Segment*)

Apart from flat roofs and fully symmetrical forms (cones, domes and hemispheres), the orientation of any three-dimensional roof form has to be considered as an effective and important parameter on the received solar radiation intensity on roofs surfaces. The orientation of any three-dimensional roof surface with a particular direction (main axis) also has to be numerically identified for the computational model in terms of angles (*surface azimuth angle*). The surface azimuth angle signifies the orientation of each tilted planer segment to be numerically defined into the *SRSM* formats [5]. The surface azimuth angle as an input for *SRSM* is the angle between South and the direction that the tilt surface (segment) is facing. It is measured towards south, where it is zero degree, and 180 degrees when the surface faces north. The azimuth angle is 90 degrees for surfaces facing west direction, and -90 degrees if facing east.

Days of the Year

The program computes data for the year 365 days, or for selected days at regular intervals. Day 1 is 1 January, day 2 is 2 January, and day 365 is 31 December. 30-daily steps create outputs data for each month [5].

5.4 CALCULATION OF SOLAR RADIATION INTENSITY ON CURVED AND FLAT ROOFS EXTERNAL SURFACES

The Solar Behaviours of Flat Roof and Number of Curved Roof Forms Using SRSM [5]

The prime objective of this research work is to test the influence of the traditional curved roof forms on the received $I_{(HTCS)}$ by the roof surface. Therefore, evaluate their solar behaviours and complete the several explanations, which have claimed that these roof forms are energy efficient techniques in the past. As previously implied from the reviewed research attempts on the solar irradiance on curved forms, solar radiation intensity on curved-roofs can be calculated by employing both planar surfaces available and calculated solar data. Therefore, the curved roof form needs to be slightly transformed to a group of planer segments (*horizontal, vertical and tilted*), which geometrically resemble a curved roof and can be considered equivalent to its original curved form.

Curved-roof form is considered as a group of inclined planer surfaces “segments”, which are generated along the curved roof according to the roof’s geometry. Therefore, calculating the sum of all solar radiation intensities above all segments that form a specific curved roof gives the total received intensity W/m^2 on this roof (*see equation (5-10)*). The geometrical resemblance techniques are explained in more details at the end of this chapter.

5.4.1 The Orientation of Curved Roof and Solar Radiation Intensity

For fully symmetrical forms (*form without main axis or direction*) such as domes and hemispheres, the impact of roof orientation on the intensity of the received solar radiation is insignificant. Whereas, the orientation impact on the solar behaviours of main-axis-forms or directed-forms, such vaults, is significant. This is because of at the time each half of the curved roof faces particular direction with different solar features. The following chapters explain the orientation influence on the received solar radiation by extended curved-roof surfaces (*Vaults*).

It is advisable to find out the most preferable curved roof orientation at the same climatic conditions and geographical latitude. Therefore, the calculations of the received solar radiation on different curved roof extended cross-section (*vaulted roofs*) have to be tested repeatedly at both principal and secondary directions.

For extended curved roof cross sections (vaulted roofs), *SRSM* enables running large number of calculations and at any direction. In Chapter 6 and 7, solar investigations have been carried out two times when each vaulted roof faces the two principal directions (*N-S* and *E-W*) and another two times when it faces the two secondary directions (*NW-SE* and *NE-SW*), Fig. (5-19). The figure illustrates different directions of vaulted-roof longitudinal axis in plan, and different curvature facing-directions as cross section (*For 3D illustrations see Fig. (5.21) and Fig. (5-22).*)

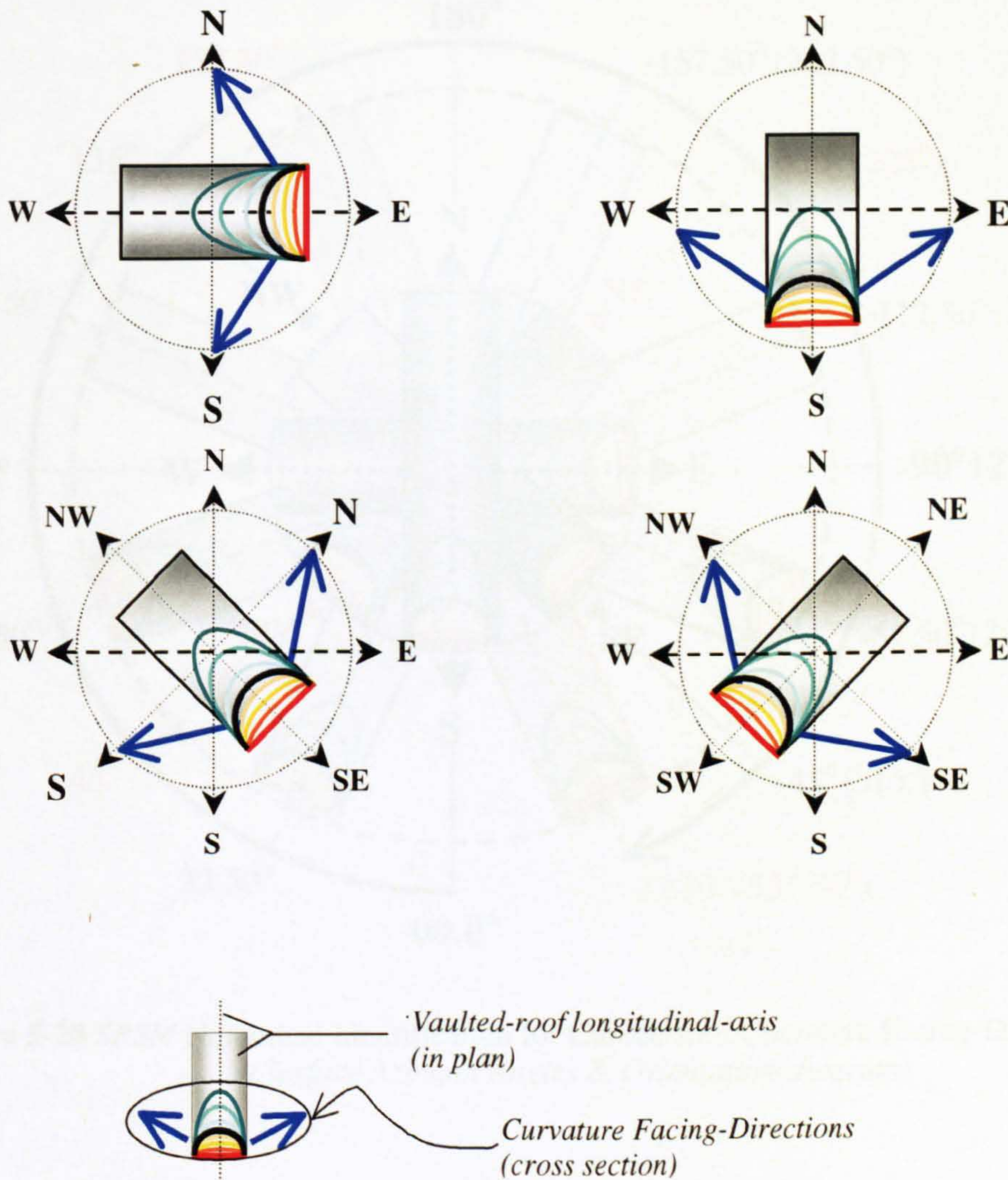


Figure 5-19 The Tested Principal Directions and Secondary Directions

For *SRSM* calculations, roof orientation is defined with respect to the south (*surface azimuth angle*). Thus, *SRMS* can run calculations for other directions, which are generated in between any two directions or at any other particular direction angle Fig. (5-20). Each planar segment orientation has to be identified by the surface azimuth angle. While, the inclination of each planar segment is defined with respect to the horizontal plane.

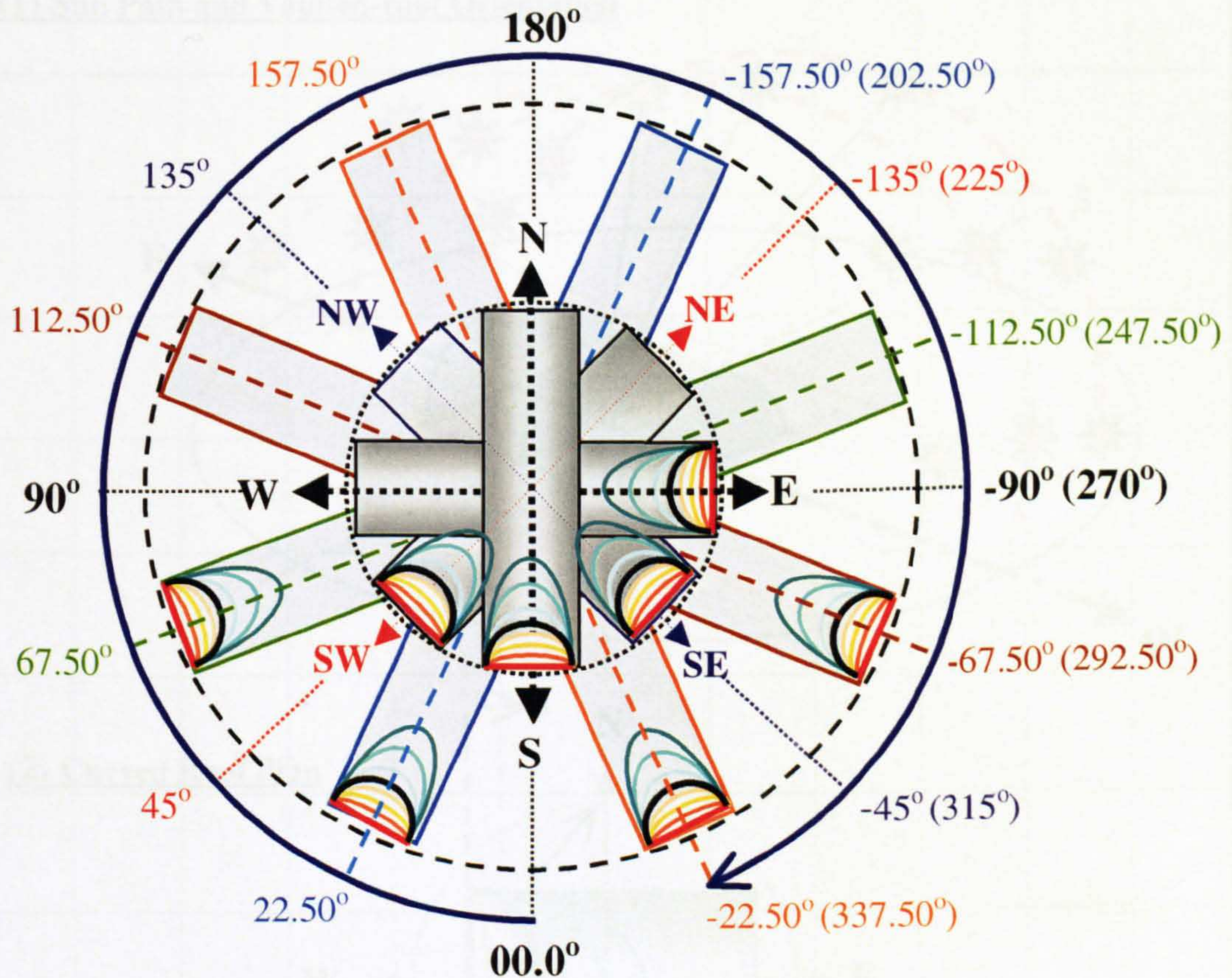


Figure 5-20 *SRSM* Numerical Identification for Curved-roof Curvature Facing-Direction (Surface Azimuth Angles & Orientation-diagram)

5.4.1.1 The Curved Roof Curvature Faces North and South Directions

(Extended CCS - Vaulted Roof)

Fig. (5-21) explains the curved roof curvature facing-direction; in this case, the longitudinal axis (*perpendicular on the CCS*) is the East-West axis. The curvature of the $CCS_{(std)}$ faces northward and southward. Any suggested curvature facing-direction for an extended CCS will be tested during summer and winter.

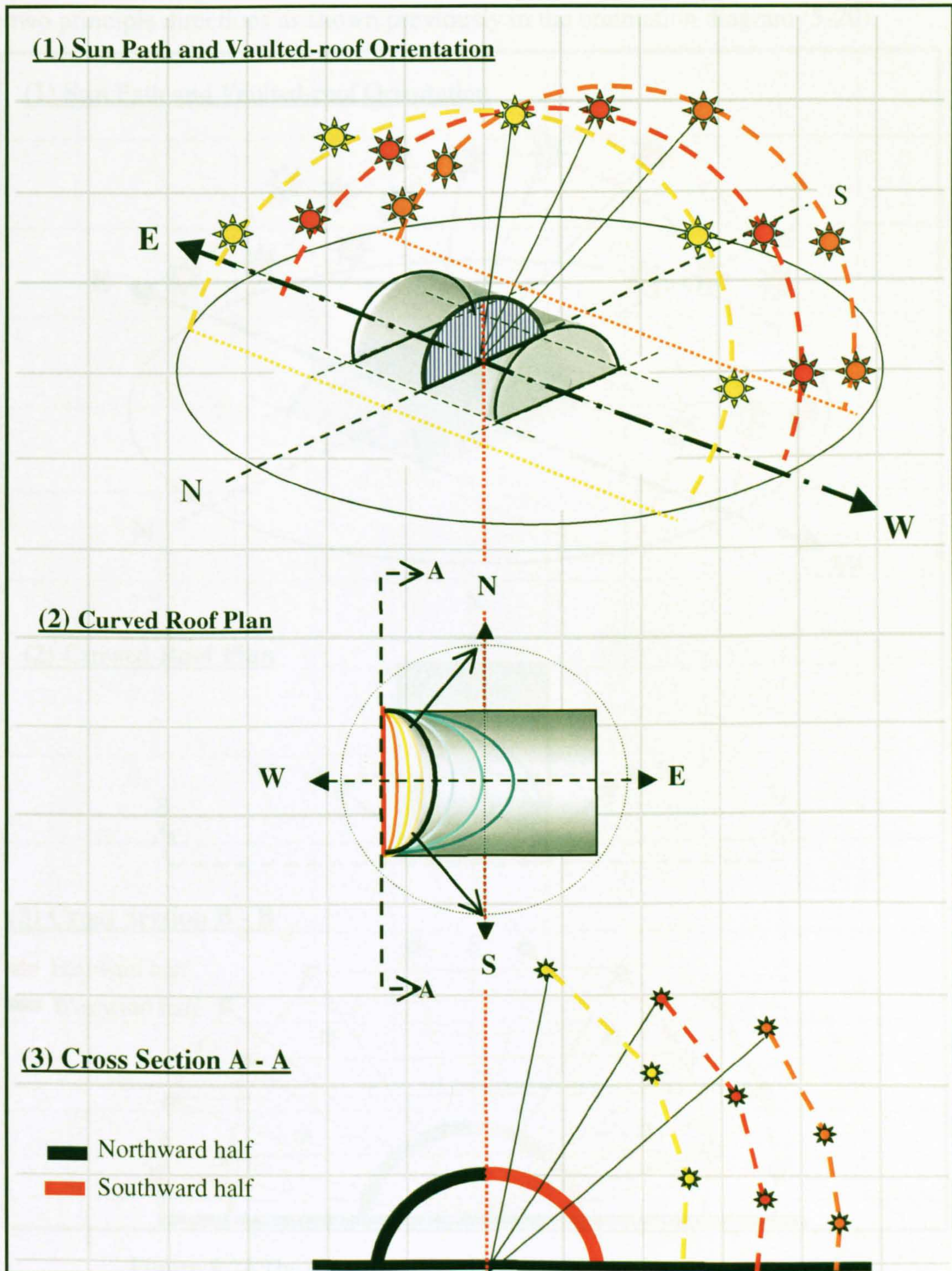


Figure 5-21 The CCS and Its Tilted Segments North and South Aspects

5.4.1.2 The Curved Roof Curvature Faces East and West Directions

(Extended CCS - Vaulted Roof)

Fig. (5-22) explains another curvature facing-direction, in this case, the longitudinal axis (perpendicular on the CCS) is the North-South axis. The curvature of the $CCS_{(std)}$ faces eastward and westward. As the cases of secondary directions, the longitudinal axis may rotate around the vertical axis any angle to allow the curvature face any direction in between the two principle directions as shown previously in the orientation diagram (5-20).

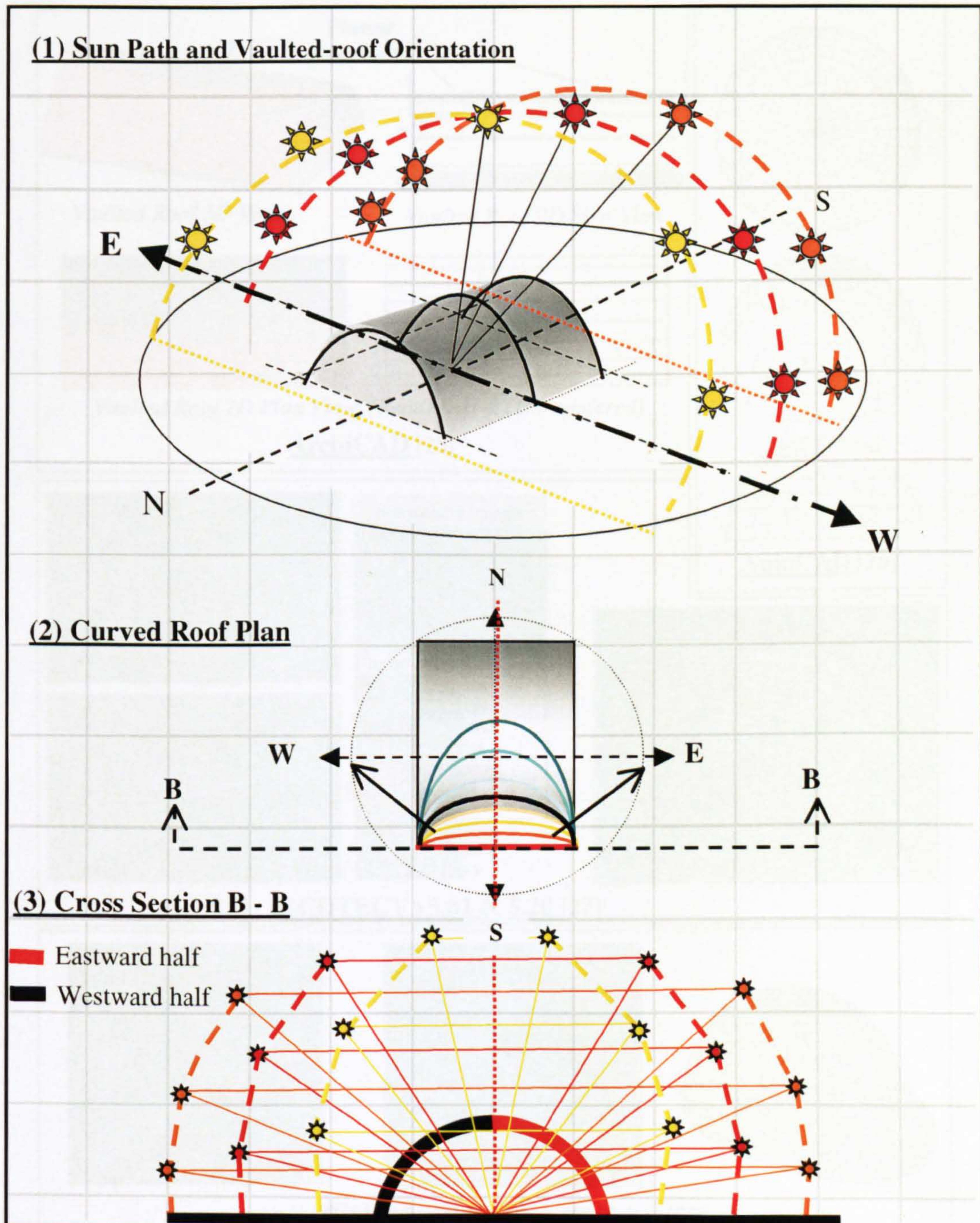


Figure 5-22 The CCS and Its Tilted Segments East and West Aspects

5.4.2 The Geometrical Resemblance of Curved Roofs (*Planar Segments and Facets*)

The geometrical resemblance used in this research is neither new nor only employed in this work. Customary, it has been used in many CAD tools to identify curved shapes, in which all curved three-dimensional forms have been geometrically considered as a group of planar segments, pixels, or stripes, Fig. (5-23). Sensibly, the more planar segment or pixel the more accurate results will be, this is viable regardless of the type of the curved forms tested-parameters or their performances that need to be evaluated.

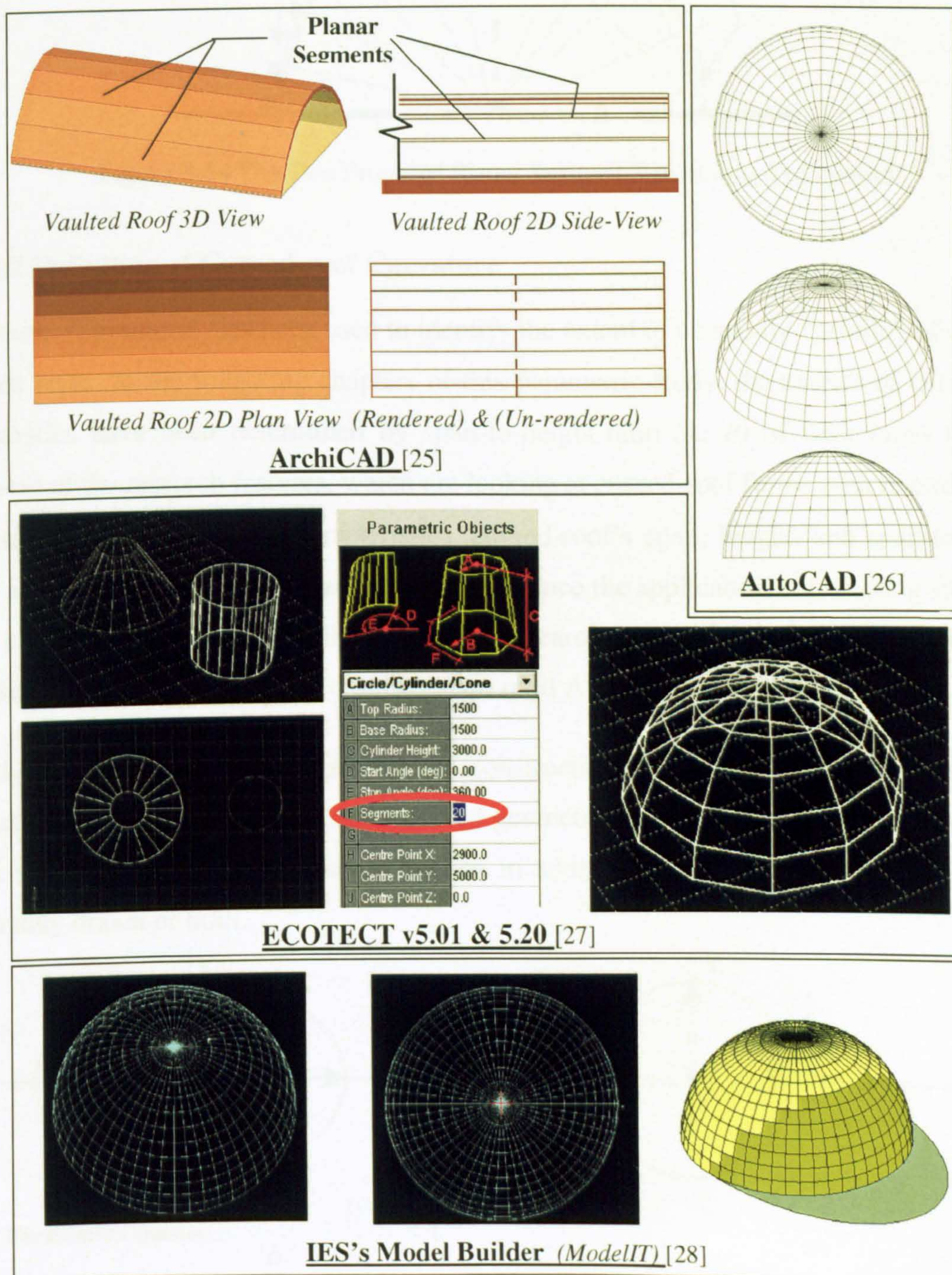


Figure 5-23 CAD Drawings and 2D and 3D Illustrations for Curved Forms

Fig. (5-24) shows the two proposed planar segments techniques for resembling the curved roof form and simplify the calculations of the received $I_{(HTCS)}$ on curved-roof cross section CCS.

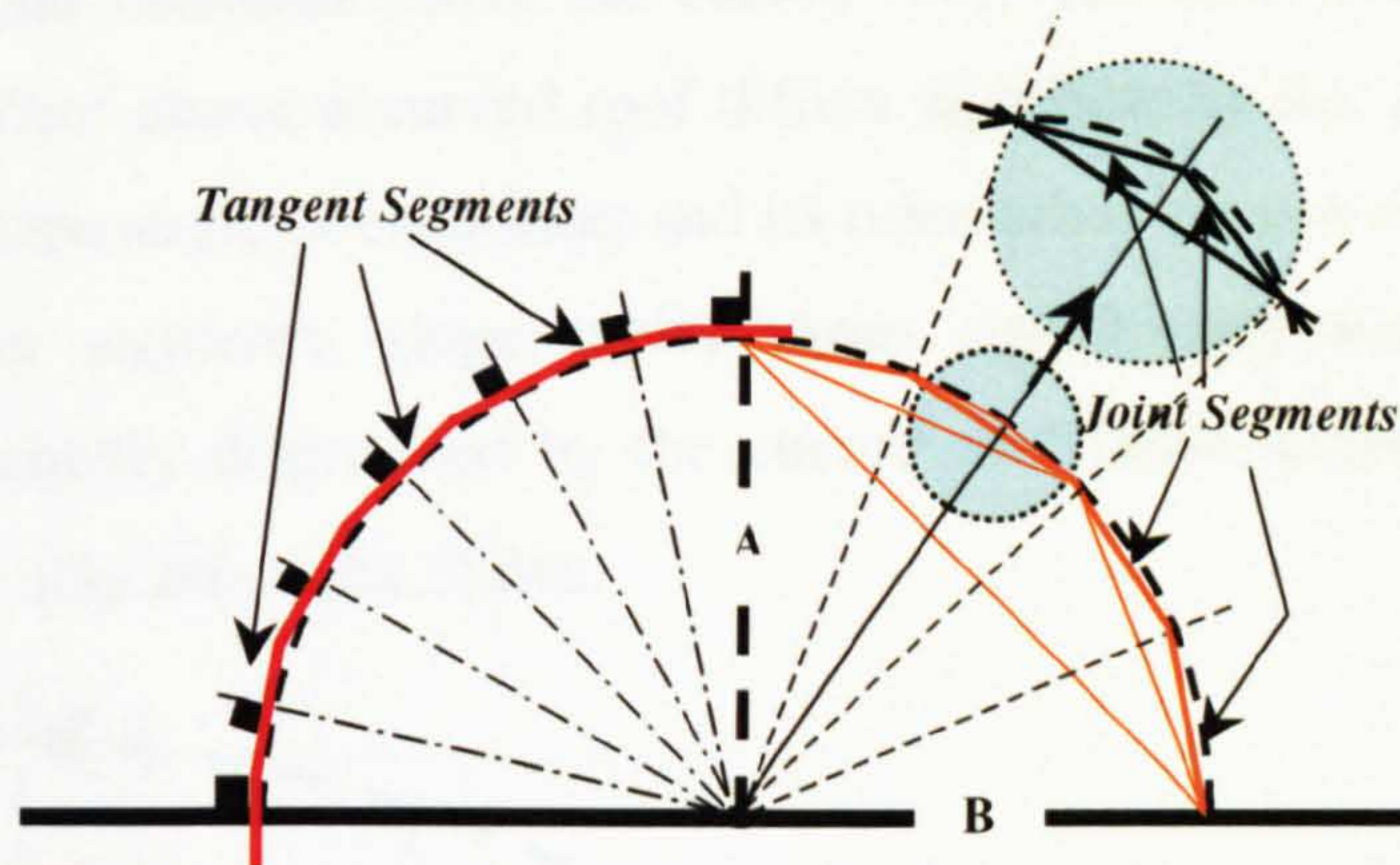
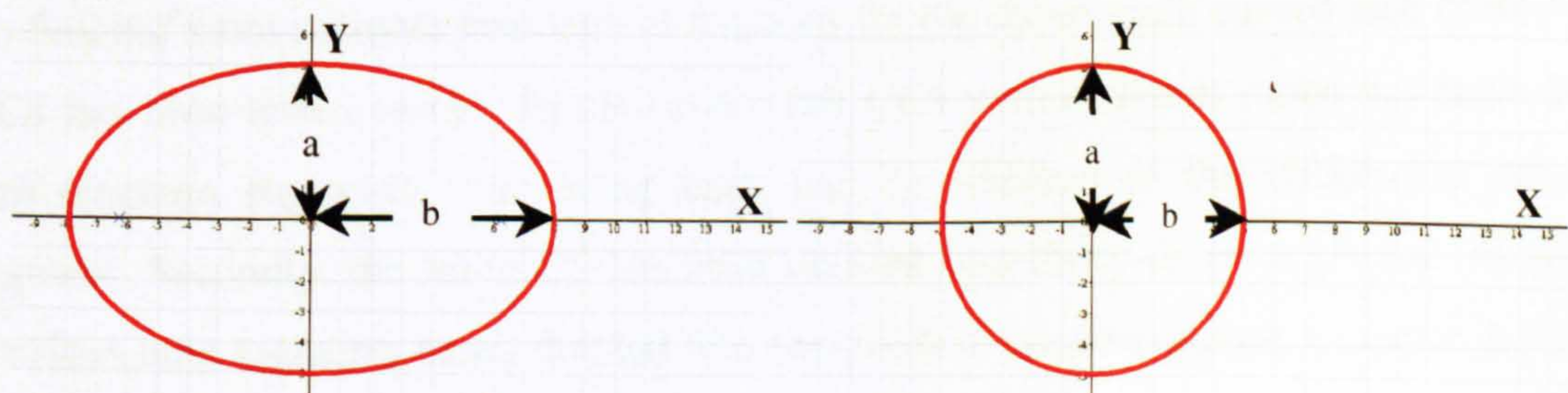


Figure 5-24 The Two Proposed Planar Segment Resembling Techniques

5.4.2.1 Definition of Curved-roof Curvature

The term “Curvature” has been used to identify the extent of concavity “profile” of different curved roofs. In the following chapters of this parametric study, the extents of curved-roof concavities have been determined by span-to-height-ratio ($A: B$) of their cross sections. Because of the research features, which are looking at curved-roof forms with regard to their structural and architectural characteristics, curved-roof’s span, height, and span-to-height-ratio are the most important parameters that influence the applicability of erecting stable and firm curved-roofs. Therefore, all CCS in this research are only generated from circles and ellipses, which can be determined only by two radii A and B as shown in Fig. (5-25).

In other words, due to their structural and construction applicability, curved-roofs that are generated from parabola or any other curved geometries are not considered in this research work as they need a defined curve-equation in addition to the main radii A and B to be accurately drawn or built.



The Ellipse Equation is: $\frac{(X)^2}{b^2} + \frac{(Y)^2}{a^2} = 1$

When $a = b$, the ellipse becomes a circle

Figure 5-25 Circles and Ellipses Algebraic-Equations-Form [29]

Similar to what is commonly used in many CAD programs, the tested curved roof in this parametrical study has been divided into number of planar facets to simplify the calculation of the received solar radiation above the curved roof. The received total clear sky solar irradiance $I_{(HRCs)}$ W/m^2 above a curved roof differs significantly from one facet to another according to the slope angle of each facet and its orientation (*which direction it faces*). The difference between segments' slope angles varies significantly according to the roof's curvature that is chiefly determined by the curved roof cross-section ratio **CCSR** (A: B ratio), Fig. (5-26). (*Also refer to Fig. (5-24)*).

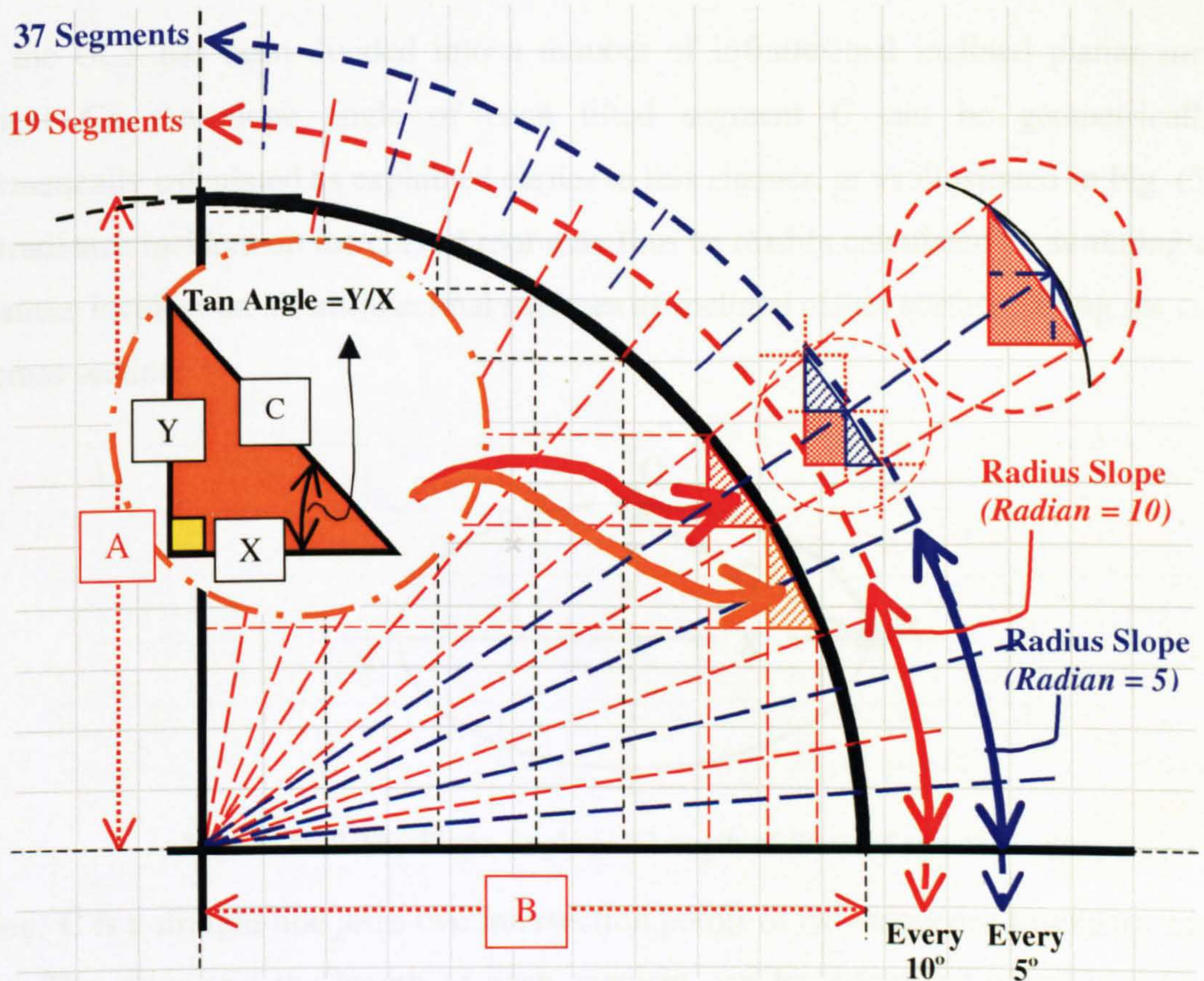


Figure 5-26 The Geometrical Resemblance of Curved Roof Cross Sections

To find out more accurate geometrical relations for the curve, each curved roof cross-section *CCS* has been tested twice. Firstly, every full *CCS* with different ratios has been divided into nineteen segments, nine along each half in addition to the middle-top horizontal segment. Secondly, the full *CCS* has been divided into thirty-seven segments, each of the previous nine segments being divided into two-folds to create eighteen segments along each half in addition to the middle-top horizontal segment.

For solar radiation calculations, the geometry of curved roofs, either domed or vaulted, is mainly defined by its cross-section-ratio CCSR which represents the ratio between the main two radiuses A and B (the vertical and the horizontal respectively). The research presented in this thesis tests the curved roofs that are originally generated from an ellipse or circle. The circle is a special case of an ellipse where $A = B$. All tested curved roofs have regular curvatures, which relate to certain ratios between the curved roof span and height. Each curved roof is geometrically defined by its cross section ratio (A: B), *CCSR (Curved-roof Cross-section Ratio)*.

After the CCS has been divided into a number of infinitesimal inclined planar surfaces (segment *C*), the slope angle of each tilted segment *C* can be geometrically or mathematically calculated as explained earlier in this chapter, or as illustrated in Fig. (5-27). The irradiance incident on the curved roof may thus be readily calculated by summing up all irradiances incident on all infinitesimal surfaces as inclined planer surfaces along the curved roof cross section.

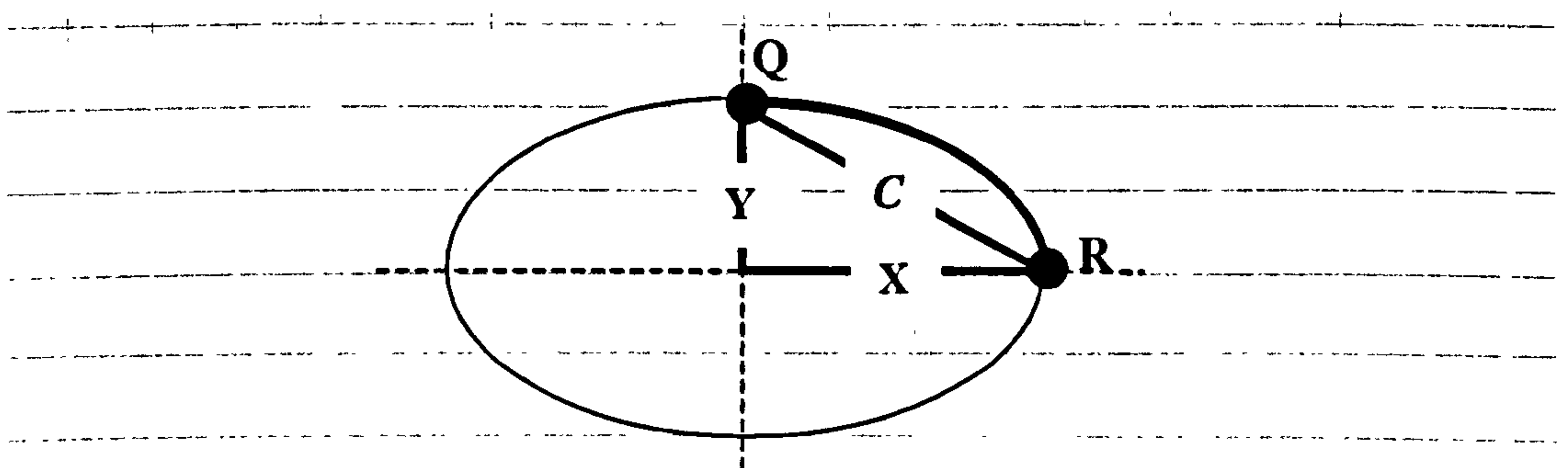


Figure 5-27 The Slope Angle and Length of Planar Segments

Segment *C* is a straight line joins two intersection points of two-sequenced-radiuses with the curve. The slope and the length of each segment can be calculated geometrically or in algebraic-equation-form, as the gradient β of line *C*, and the distance between Q and R can be calculated by equations (5-7) & (5-8):

$$C = \sqrt{Y^2 + X^2} \quad (5-7) [29]$$

$$\text{Tan } \beta = \frac{Y}{X} \quad (5-8) [29]$$

The exact length of the curved sector **QR** in Fig. (5-28) or any other sector along the roof curvature can be calculated using equation (5-9):

$$\text{Circle Perimeter} = 2\pi b$$

$$\text{Ellipse Perimeter} = 2\pi \sqrt{\frac{(a^2 + b^2)}{2}} \quad (5-9) [29]$$

Solar design and hourly clear sky irradiance calculations above curved roofs can be carried out by resembling the original form of the curved-roof to a number of tilted planar surfaces (segments). Hourly clear sky irradiance calculations on tilted-planar-segments are more accurate. Planar segments are basically generated either from a number of tangent planar segments or from joint-planar-segments, as shown in Fig. (5-28).

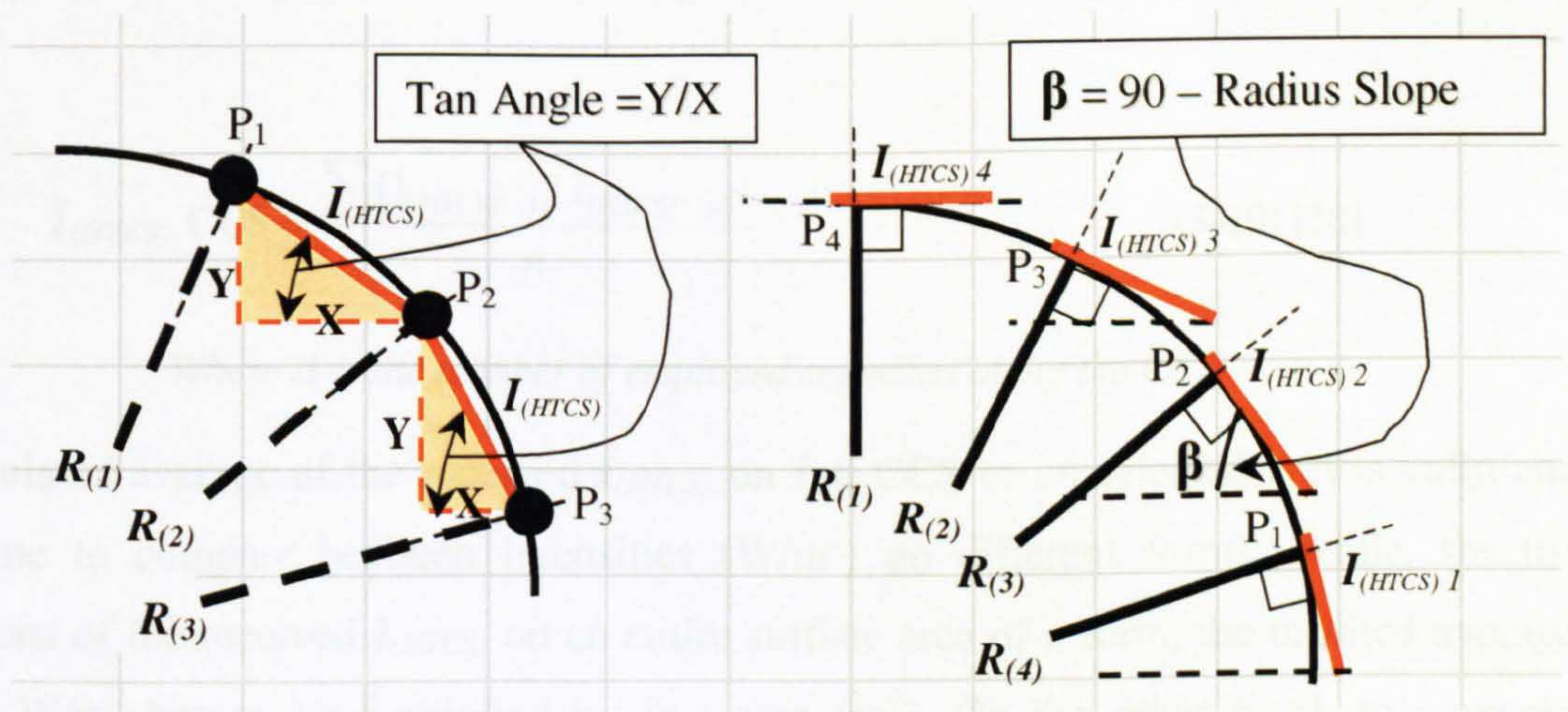


Figure 5-28 The Resemblance Techniques of Curved Roofs and Segments Slopes

The tangent-planar-segments are used only to define a single case, which is named the standard curved roof $CCS_{(std)}$, where its CCSR is $A=B$. On the other hand, the different CCSR of the other curved roofs (CCS_1 , CCS_2 , CCS_3 , CCS_4 , CCS_5 , CCS_6 and CCS_7) are geometrically defined by joint-planar-segments [30]. Fig. (5-28) also shows that each radius R intersects the curved roof at point P , each segment joints two sequential intersection-points along the curve, P_1 and P_2 , P_2 and P_3 or P_3 and P_4 and so on. The gradients of both types of the generated segments can be geometrically and mathematically defined. According to each planar segment slope, SRSM can find out the $I_{(HTCS)}$ on each segment. The intensity of the received irradiance is function of the receiver surface tilt angle and orientation.

5.4.3 Calculating The Total Received Solar Radiation Intensity (W/m^2) on a CCS

The hourly clear sky irradiance $I_{(HTCS)}$ on the full CCS can be determined by calculating the average of the received $I_{(HTCS)}$ on number of planar segments along the CCS. In other words, it is the sum of the received $I_{(HTCS)}$ on all planar segments along the CCS divided by their number, Equation (5-10). In general, the calculations methodology depends on computing the received $I_{(HTCS)}$ on each tilted planar segment by the SRSM, then calculating the average of the received $I_{(HTCS)}$ on group of planar segments, which resemble either full CCS or a particular sector of a curved roof. Along side with using the model results for sloped surfaces, the author had to develop a large number of Microsoft Excel Spreadsheets in order to supplement the evaluation of the solar behaviour of different curved-roof, forms, curvatures and orientations. Due to the oversize of these spreadsheets, Appendix (A) shows only samples of these spreadsheets.

$$I_{(HTCS)} \text{ CCS} = \frac{\sum (I_{(HTCS) (1)}; I_{(HTCS) (n)})}{n} \quad (5-10) [30]$$

Where n is the number of employed segments along the CCS

The calculated average of the received $I_{(HTCS)}$ on full CCS or on selected part is valid and appropriate to compare between intensities (W/m^2) on different forms. While, for the calculations of the received $I_{(HTCS)}$ on an entire surface area of a form, the resulted average intensity W/m^2 has to be multiplied by this area (m^2). On the other hand, to compare between the total solar radiation intensities fall on two surface areas of two different forms, the surface areas have to be equal. In the case of different surface areas, the intensity W/m^2 has to be multiplied by a factor that represents the surface areas ratio. Therefore, having equal surface areas of different shapes does not mean that they must cover the same plan dimensions.

SMSR and *Microsoft Excel* enabled to investigate large number of *CCSR* in order to evaluate the solar behaviour of curved-roof form, curvature and orientation. For hot-arid climates, receiving less solar radiation and controlling the indoor thermal environments without artificial tools are crucial objectives of roof design and architecture. This procedure worked effectively to test the influence of curved-roof curvature and orientation to reduce the received solar radiation intensity.

5.5 CONCLUSIONS

Chapter 5 searched the theory that stands behind different solar calculations on horizontal and sloped surfaces. These equations and their continuous developments are believed to be fundamental for any computing model that handles the topic of solar radiation on tilted surfaces. Muneer [1] stated that there are equations that enables the computation of monthly or daily sloped irradiation on vertical surfaces with eastern, western and northern aspects and any sloping surface facing south, based on the previous work done in this field. The work done by Muneer [1] drew the attention of the author of this thesis that these equations were designed to test sloped surfaces solar radiation for particular latitudes. Thus, a thorough research was done to find a computer model that is especially designed for calculating the solar radiation on sloped surfaces in the tropics.

The existing literature relating to the subject of finding out the intensity of the received solar radiation above differently tilted and oriented surfaces has been reviewed in this chapter. A number of previous researchers has investigated different types of solar behaviours of oblique surfaces and others have tested the relationship between the form and insolation. Others have tested the solar performances of transparent domed skylights.

Most of these researches were based on a number of the mathematical models and equations, which has been developed gradually to simplify the calculations of solar radiation on tilted surfaces and different forms. Therefore, evaluate the energy efficient abilities and insolation potentials of the surface geometry in general and the curved roof forms in particular to reduce the received solar irradiation on building envelopes. This may lessen the required cooling loads in such harsh hot climatic conditions and provide indoor thermal comfort without artificial means.

However, during the last 10 years, computer software calculations and physical experimental tests have become the most successful research tools that approached the area of exploring the environmental performances of buildings envelopes and testing their design variables independently.

The chapter described the computational tool, which the research uses to calculate the solar performance of a number of traditional roofing forms. The chapter also concludes the architectural need of carrying out research work aims at comparing between the solar performances of flat and curved roofs in hot-arid climates. Evaluating the solar performance of curved roof form explores their passive cooling means in order to prove that the produced indoor thermal comfort is attributed to curved-roof forms and geometry among other factors.

This chapter suggested the geometrical technique for resembling the curved roof forms in order to simplify the calculations of solar radiation intensity on the roof external surfaces. Regardless of the nature of the tested parameters, increasing the number of planar segments will produce more accurate simulation of the curved forms.

The curved roof curvature has been identified in this chapter by its cross section ratio, span-to-height-ratio, A: B, which has three possibilities; $A=B$, $A>B$, or $A<B$. The two proposed techniques of resembling planar-segments have been described in this chapter. The first geometrical resemblance of the standard curved roof cross section $CCS_{(std)}$ is explained in the next chapter.

The first four chapters have referred most of the indoor thermal comfort explanations of curved roof to the high thermal mass of roof construction material (*mud and adobe*) and the larger inner-volumes of their ceilings. Consequently, most of the regional architects and the preceding research works have attributed the produced indoor thermal comfort in such indoor spaces to the same factors. This chapter draw attention that curved-roof form, curvature and orientation must be taken into account for testing their solar and thermal performances.

Roof geometry (*form, curvature and orientation*) appears to have a significant influence towards minimising the cooling or heating loads and consequently reduce the need for artificial thermal comfort providers in buildings. Therefore, due to what has been concluded in this chapter (*the angular nature of their forms and orientation*), the diversity of the received $I_{(HTCS)}$ along the curved roof outer surfaces at the same latitude and time is expected.

The solar investigations framework of the thesis following chapters examines the solar performance of two curved roof forms (vaults and domes) with different curvatures and orientations. Each form's solar performance has been measured in summer and winter. Therefore, a large number of solar characteristics on different curved roof forms has been implied.

In the next chapter, the calculations of the Hourly Total Clear Sky Irradiance $I_{(HTCS)}$ W/m^2 on a semicircular vaulted-roof cross section and a flat roof will be carried out in order to investigate the solar performances of semicircular vaulted-roof outer surface. The thesis following chapters, which represent the research empirical study aims to prove that roof form and geometry have a significant impact on the received solar irradiation above roof surfaces. Therefore, verify that traditional curved roof forms have performed among other elements as energy efficient and sustainable techniques in buildings in hot-arid climates.

Reference List

1. Muneer, T. Solar Radiation & Daylight Models for the Energy Efficient Design of Buildings. Oxford, UK: Butterworth-Heinemann, 1997.
2. Boake, M. T. Passive Versus Active Solar Design: Opposing Strategies in Support of a New Sustainable Vernacular, *Architronic: In Support of a New Sustainable Vernacular* Vol. 4(NO. 3):p. 2.
3. Edited by M. S, D. A., *Passive Cooling of Buildings*, European Commission (Directorate General xvii for Energy), (1996).
4. Exell, R. H. B. A program in BASIC for calculating solar radiation in tropical climates on small computers. *Renewable Energy Review Journal*, 1986 Dec; Vol. 8(No. 2).
5. "SRSM" Solar Radiation Simulation Model for Quick Basic, Regional Energy Resources Information Centre, Asian Institute of Technology, Bangkok.
<http://www.jgsee.kmutt.ac.th/exell/Solar/SolradJS.htm>
6. Koenigsberger, O. H., et al. *Manual of Tropical housing and Building - Part one: Climatic Design*. (1973).
7. Lunde, J. and Peter, *Solar Thermal Engineering*. Canada: John Wiley and Sons, Inc., 1980.
8. Sayigh, A. A. M., *Solar Energy Application in Buildings*. Academic Press, Inc 1979.
9. Muhaisen, A. S., *Influence of Building Form on its Solar Energy Potential in Different Climates and Latitudes* [Nottingham: University of Nottingham, 2001. Msc Dissertation.
10. Hamdy, I. F. *Architectural Approach to The Energy Performance of Buildings in a hot-dry climate, with special reference to Egypt* [Bath: University of Bath, (1986). Ph.D. Thesis.
11. Southern AER, *Earth Sun Geometry, A Quarterly Activity Bulletin of The South Carolina Department of Natural Resources-Southeast Regional Climate Center* 2001 Spring; *Vol. 7(No. 1)*.
12. Radosavljevic, J. and Dordevic, A. Defining of the Intensity of Solar Radiation on Horizontal and Oblique Surfaces on Earth, *FACTA UNIVERSITATIS, Series: Working and Living Environmental Protection* Vol. 2(No. 1):pp. 77-86.
13. Duffie, J. and Beckman W. *Solar Energy Laboratory University of Wisconsin-Madison, Solar Engineering of Thermal Processes*, 2nd ed., New York: John Wiley & Sons, 1991.
14. CIBSE Guide A, *Design Data*, London, UK: The Chartered Institute of Building Service Engineers, (1999).
15. *Earth Sun Geometry Applet* [Web Page]. Available at <http://cwx.prenhall.com/bookbind/pubbooks/lutgens3/medialib/earthsun/earthsun.html>. (Accessed 2002 Jan 11).
16. Hottel, H. C. and Woertz B. B. Performance of Flat Plate Solar Heat Collectors. *Transactions of the American Society of Mechanical Engineers* 1942;Vol. 64,(91).
17. Runsheng, T., Meir, I. A. and Etzion, Y. An Analysis of Absorbed Radiation by Domed and Vaulted Roofs as Compared with Flat Roofs. *Energy and Buildings* 2003;Vol. 35:pp: 539-48.

18. Mukhtar, Y. A. Roofs in Hot Dry Climates, *with special reference to northern Sudan*, Overseas Building Notes-Information on Housing and Construction in Tropical and Sub-Tropical Countries 1978 Oct;(No.182).
19. Laouadi, A. and Atif, M. R. Transparent Domed Skylights: *Optical Model for Predicting Transmittance, Absorptance and Reflectance*. International Journal of Lighting Research and Technology 1998;Vol. 30(No. 3): pp. 111-8.
20. Stasinopoulos, T. N. Form Insolation Form Index; *notes on the relation of geometric shape and solar irradiation*, Environmentally Friendly Cities - *Proceedings of PLEA 98 Passive and Low Energy Architecture*. Lisbon, Portugal. 1998.
21. Stasinopoulos, T. N. Geometric Forms & Insolation; *An analytical Study of the Influence of Shape on Solar Irradiation* [Dept. of Architecture: National Technical University of Athens, Athens, 1999. Doctoral Dissertation.
22. Bourges, B. and Scharmer, K. The New European Solar Radiation Atlas: A Tool for Designers, Engineers and Architects. Information System for Renewable Energy (WIRE), International Solar energy Society ISES Publication <http://wire0.ises.org>
23. Schuepp, W. Solar Radiation. N. Robinson (ed), Amsterdam: Elsevier, 1966.
24. The International American Agency for Development. Solar Radiation Atlas for Egypt, Renewable Energy Authorisation - Ministry of Electricity and Energy, Cairo, 1990.
25. ARCHICAD 7.0 [A Comprehensive tool for Architecture, enables users to harness the power of integrated 3D modelling.
26. AutoCAD [Licensed Software University Package].
27. ECOTECH V5 [The complete building design & environmental analysis tool. Square One's flagship software. It features a designer-friendly 3D modelling interface fully integrated with acoustic, thermal, lighting, solar and cost functions.].
28. IES (Ve Version 4.1) [Licensed Software University Package]. Integrated Environmental Solutions Ltd. 2001.
29. Ellipse and Circle Java Applets, <http://mathinsite.bmth.ac.uk/html/applets.html> (Accessed 2001 Feb 20).
30. Elseragy, A. A and Gadi, M. B. Roof Geometric Forms and Solar Irradiation Intensity In Hot-Arid Climates. Proceeding of the ISES Solar World Congress 2003, ISES 2003, Solar Energy for a Sustainable Future, 2003 Jun 14-2003 Jun 19; Svenska Mässan Congress Centre, Göteborg, Sweden.

CHAPTER 6

SOLAR BEHAVIOUR OF FLAT AND SEMICIRCULAR VAULTED ROOFS WITH DIFFERENT ORIENTATIONS

Semicircular Curved Roof Cross Section $CCS_{(std)}$ (37 Planar Tangent-Segments)

6. SOLAR BEHAVIOUR OF FLAT AND SEMICIRCULAR VAULTED ROOFS WITH DIFFERENT ORIENTATIONS

In the previous a chapter, number of the preceding research work investigated the solar behaviour of different roof forms and compared between the received solar radiation on flat and oblique surfaces. The employed computational tool, which calculates the received solar radiation on different forms external surfaces have been also explained in the previous chapter (*Solar Radiation Simulation Model - SRSM*) [1].

This chapter presents calculations for the Hourly Total Clear Sky Irradiance $I_{(HTCS)}$ W/m^2 on a semicircular curved roof cross section and a flat roof. It discusses the received solar radiation on the outer surfaces of the standard curved roof cross section $CCS_{(std)}$. The two proposed planar segments (*Joint and Tangent*) for curved roof geometrical resemblance have been explained previously in chapter 5. The full curve of $CCS_{(std)}$ is geometrically resembled by 37 planar segments [2]. In addition to the middle top horizontal segment, each half of $CCS_{(std)}$ has been resembled by eighteen tangent segments.

The hourly clear sky irradiance $I_{(HTCS)}$ on a full $CCS_{(std)}$ can be determined by calculating the average of all $I_{(HTCS)}$ received by every planar segment along the $CCS_{(std)}$ as explained before in Chapter 5 (Refer to equation (5-10)). In other words, by dividing the sum of all segments $I_{(HTCS)}$ along the $CCS_{(std)}$ by the segments number as in Equation (6-1).

$$I_{(HTCS)} = \frac{\sum (I_{(HTCS)_1} : I_{(HTCS)_n})}{n} \text{ W/m}^2 \quad \text{Equation 6-1}$$

Where n is the segments number

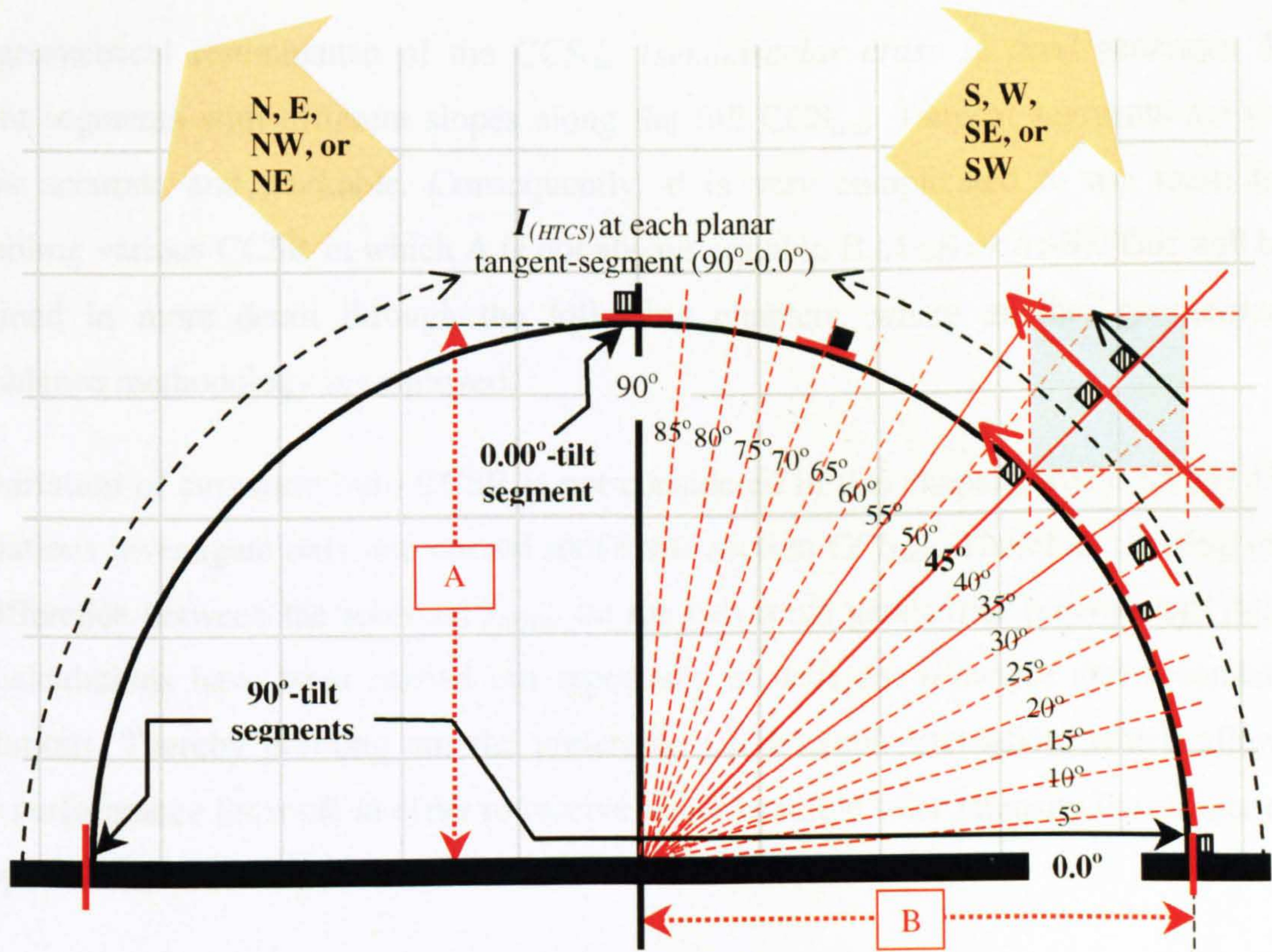
6.1 DATA INPUT AND $CCS_{(std)}$ GEOMETRY RESEMBLANCE

Semicircular Curved-roof Cross Section $CCS_{(std)}$

The geographical latitude of Aswan ($23.58^\circ N$ of the equator) has been chosen to represent the hot-arid regions of the southern part of Egypt or Upper Egypt as it is usually called (*due to the flow of Nile south to north*). Refer to Egypt maps in Chapter 2. As explained earlier, CCS is the curved-roof cross-section and $CCSR$ represents its height-to-span ratio (A: B). For $CCSR_{(std)}$ A always equals B (*i.e. semicircular curved-roof cross section*). $CCS_{(std)}$ and CCS_l with either 19 or 37 segments having exactly the same $CCSR$, but they having different geometrical resemblance.

Due to its workability, the tangent segments technique has been only applied for the case of $CCS_{(std)}$ geometrical resemblance. For both geometrical resemblance techniques, each segment should have an independent slope angle, which differs from the previous and the subsequent slopes. Moreover, all CCSR radiuses slope angles must be the same for all CCSR. This makes the tangent segment, which only moves perpendicularly along the radius technique very difficult to resemble various CCSR as the case of the following chapters.

As shown in Fig. (6-1), the $CCS_{(std)}$ geometrical resemblance begins with two tangent planar segments at the bottom, which are tilted 90° from the horizontal perpendicular to the 0.0° -radiuses at the lowest ends of the $CCS_{(std)}$. The thirty-seven tangent segments begin at the lowest two ends of the curve then at each side they incline upwards until the horizontal segment at the middle-top of the curve.



Roof	CCSR	Radius Slopes (Radian = 5°) & Slope Angles of Resembling Planar Tangent Segments									
		5°	10°	15°	20°	25°	30°	35°	40°	45°	
		85	80	75	70	65	60	55	50	45	
$CCS_{(std)}$	A=B	50°	55°	60°	65°	70°	75°	80°	85°	90°	
		40	35	30	25	20	15	10	5	0.0	

Figure 6-1 $CCS_{(std)}$ Geometrical Resemblance (Tangent Segment Technique) (37 segments)

Fig. (6-1) also illustrates that each 90° segment and the rest of each half $CCS_{(std)}$ segments are facing either, principal directions, (*north-south or east-west*), or secondary directions, (*northwest-southeast or northeast-southwest*). The rest of the segments along the curved roof cross section (*the two halves of the $CCS_{(std)}$*) are tangents, the same as the two 90° -segments.

All tangent segments along the two halves of the $CCS_{(std)}$ touch the curve at tangent points. Each segment deviates at a right angle with one radius (*perpendicular to the radiuses*). Therefore, each half curve includes 17 radiuses with a 5° radian (*radian is the angle between two radiuses*). This means that the full $CCS_{(std)}$ includes 34 radiuses plus the 3 principle radiuses (*one-side- 0.0° -radius, other-side- 0.0° -radius, and the 90° -radius*). The three principle radiuses respectively form the two 90° -segments and the horizontal middle-top segment, Fig. (6-1).

The geometrical resemblance of the $CCS_{(std)}$ (*semicircular cross section*) generates 37 tangent segments with different slopes along the full $CCS_{(std)}$. Tangent segments are not always accurate and workable. Consequently, it is very complicated to use them for resembling various CCSR in which A is not always equal to B ($A < B$ or $A > B$). This will be explained in more detail through the following chapters, where another geometrical resemblance methodology is employed.

The variation of curvature ratio CCSR is not considered in this chapter, where *SRSM* [3] calculations investigate only one curved roof cross section $CCS_{(std)}$. Therefore, finding out the difference between the received $I_{(HTCS)}$ on the two roofs geometries (*curved and flat*). The calculations have been carried out repeatedly at different principle and secondary orientations. Thereby pointing out the preferable curved roof orientation, which allows better performance for roofs in order to receive either bearable solar intensity in summer or appropriate solar intensity in winter.

6.2 SOLAR PERFORMANCE OF SEMICIRCULAR CURVED ROOF

(The $CCS_{(std)}$ Curvature Faces Principal Directions) (N-S) & (E-W)

This section examines the solar performance of a semicircular curved roof, and calculates $I_{(HTCS)}$ on two roofs geometries; flat roofs and $CCS_{(std)}$. Fig. (6-2) explains the unlimited facing orientations of a curved roof (*vault*). Each orientation and direction is numerically described for *SRSM* calculations. Appendix (A) displays examples of the hourly solar radiation calculations at each segment along the extended CCS. (See Appendix (A) pages (4-6))

The calculations have been carried out to test the solar performance of $CCS_{(std)}$ at two principal directions. Firstly, when the two halves of $CCS_{(std)}$ face northward and southward (N-S). Secondly, when they are oriented eastwards and westwards (E-W). At each principal orientation, results have been repeatedly generated during summer and winter. Thus, in order to find out the $I_{(HTCS)}$ behaviours on the same roof geometry $CCS_{(std)}$ at different orientations in summer and winter. Principle directions are emphasised in Fig. (6-2).

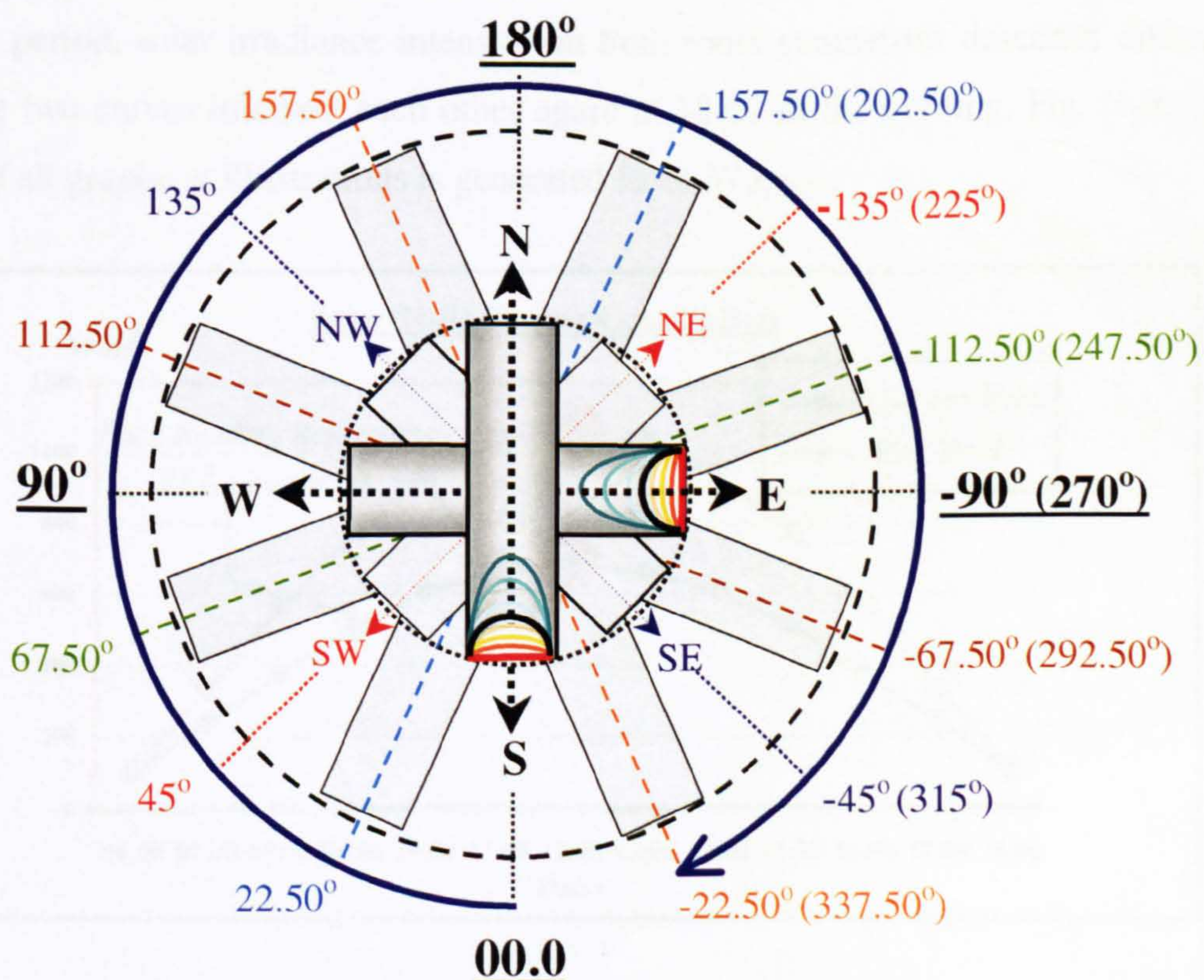
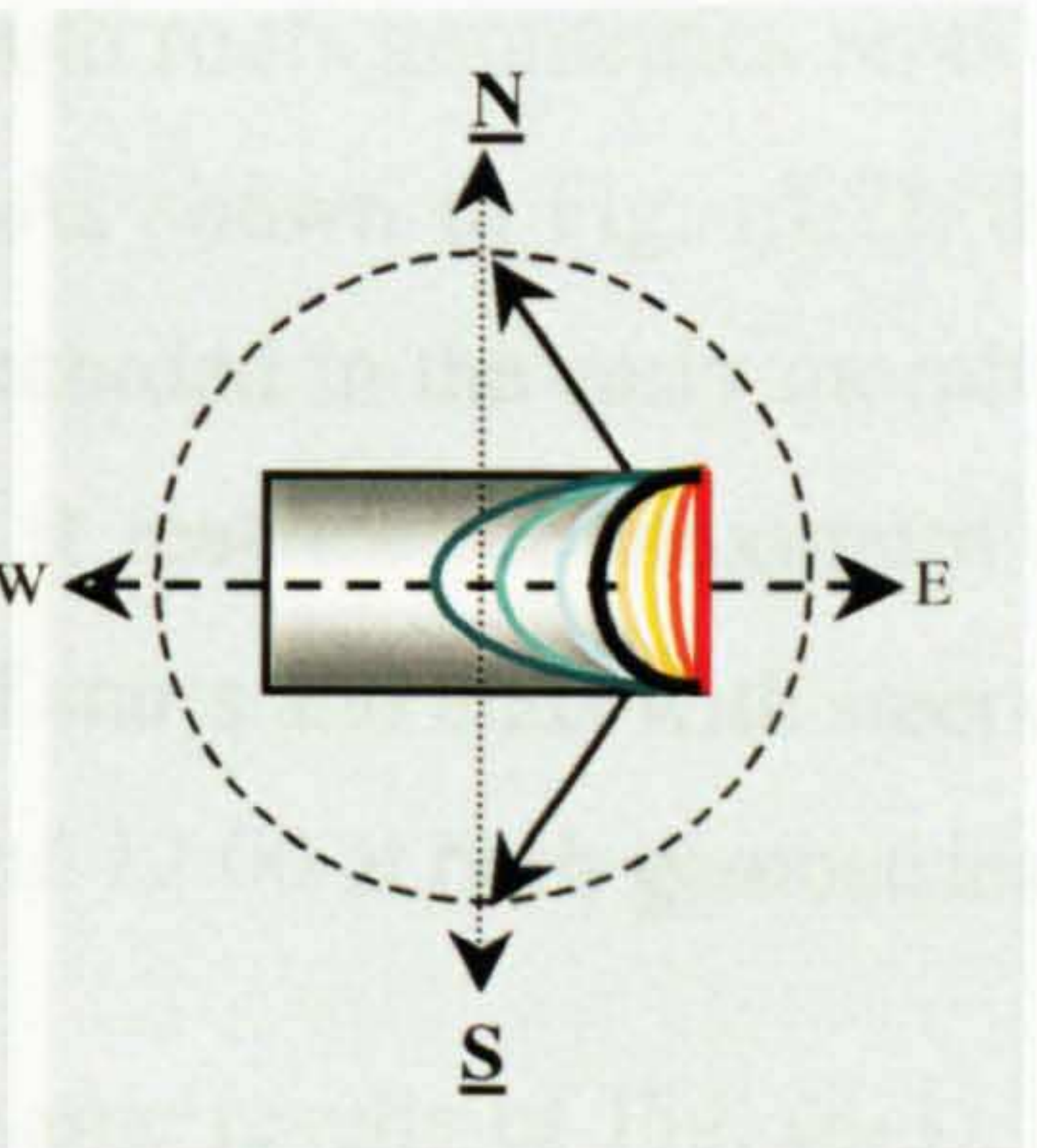


Figure 6-2 Numerical Definition For The Principal Facing-Direction (N-S) & (E-W)

6.2.1 $CCS_{(std)}$ Curvature Faces NORTH and SOUTH

This is the first principal-orientation that the study will employ. In this case, the longitudinal axis (*perpendicular on the CCS*) is the East-West axis. The curvature of the $CCS_{(std)}$ faces northward and southward. This case will be tested repeatedly during summer and winter in order to point out in which season can the curved roof geometry significantly reduce the received $I_{(HTCS)}$ on the flat roof.



6.2.1.1 $CCS_{(std)}$ Faces (N-S) During June

Fig. (6-3) shows two distribution forms of $I_{(HTCS)}$ -values on the two tested roofs, (flat and $CCS_{(std)}$) during summer. The maximum received solar irradiance on both roofs takes place at midday. In summer, both roofs geometries have similar characteristics of $I_{(HTCS)}$ -curves ($I_{(HTCS)}$ -values distribution forms). Each roof $I_{(HTCS)}$ -curve ascends differently after 06:00 in the morning, where both are intersected. They reach their maximum at midday. During the afternoon period, solar irradiance intensity on both roofs geometries descends differently before the two curves intersect each other again at 18:00 in the evening, Fig. (6-3). Each reading of all graphical illustrations is generated from 37 $I_{(HTCS)}$.

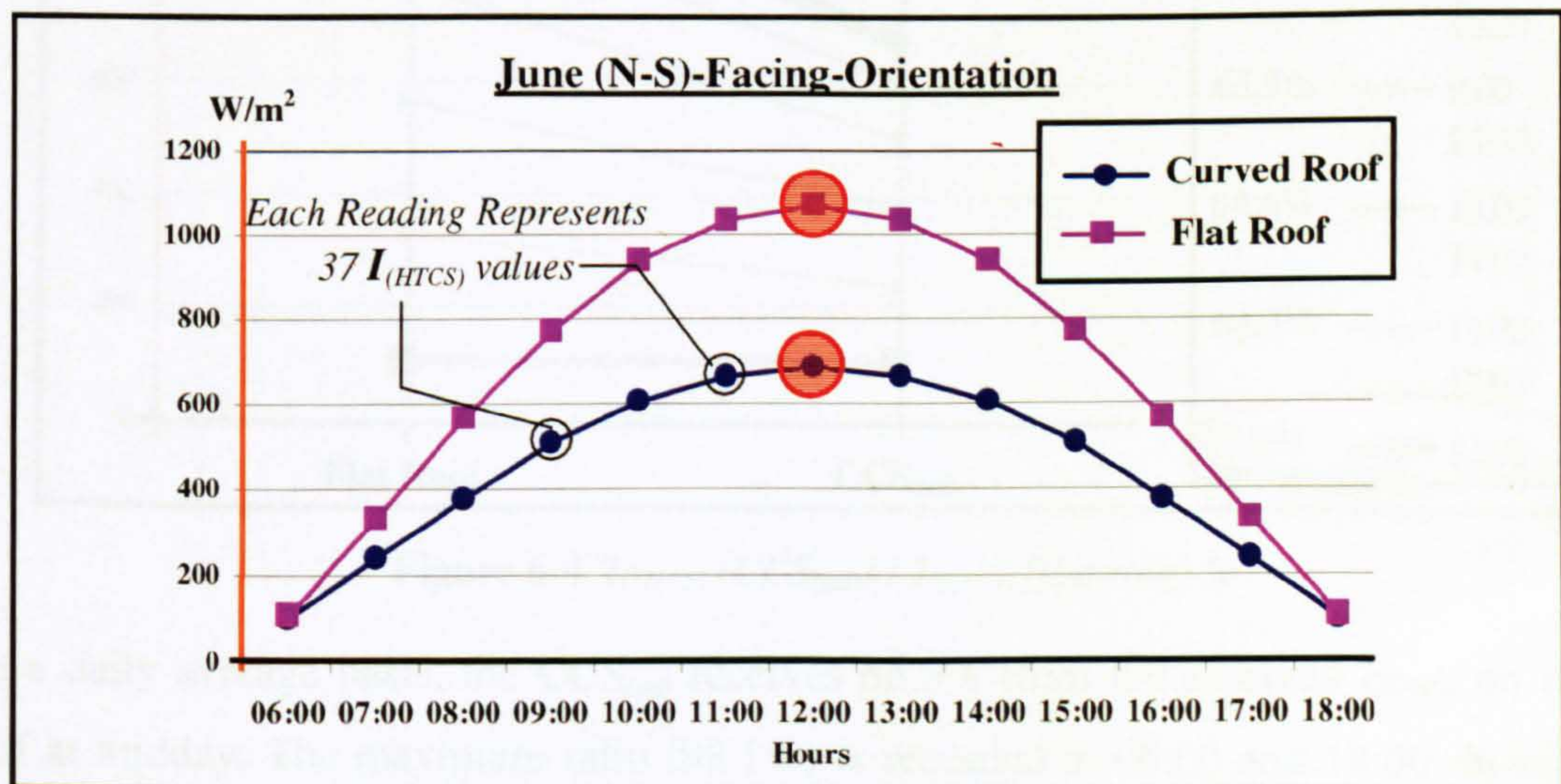


Figure 6-3 $I_{(HTCS)}$ (W/m²) on Flat Roof and $CCS_{(std)}$

In both roofs geometries, the $I_{(HTCS)}$ -curve has symmetrical increase and decrease gradients around the midday axis. At 06:00 and 18:00, approximately both roofs geometries receive equal $I_{(HTCS)}$ -values, (104 W/m² and 106 W/m² respectively). As shown in Fig. (3-7), the minimum difference between the two $I_{(HTCS)}$ -curves has been recorded in the early morning and the late afternoon. This difference slightly increases till it reaches the maximum at midday (1070 – 683 = 387 W/m²). The $I_{(HTCS)}$ -curve for flat roof starts and ends with steeper gradients compared to $CCS_{(std)}$ ones, then it gets smoother around 12:00 at both geometries.

Fig. (6-4) illustrates another graphical way of discussing the same results of Fig. (6-3). It presents an hourly proportional comparison between the $I_{(HTCS)}$ -values on the $CCS_{(std)}$ and the flat roof. At principal directions, both roofs $I_{(HTCS)}$ -mirrored-values are equal around the midday axis. Therefore, the graph discusses only seven readings throughout the day instead of the thirteen daytime readings.

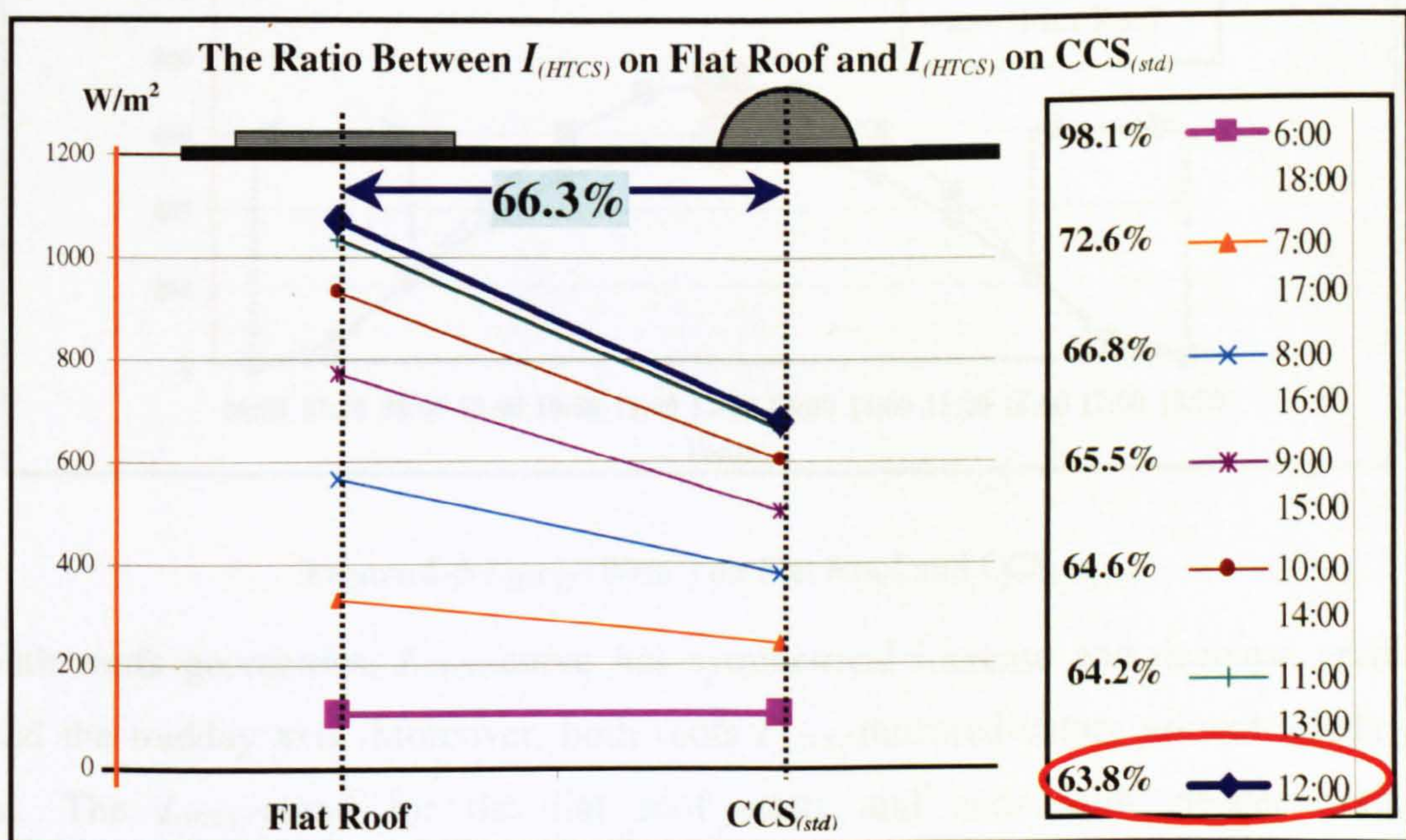


Figure 6-4 $I_{(HTCS)} (CCS_{(std)}) / I_{(HTCS)} (flat\ roof) \%$

On a daily-average basis, the $CCS_{(std)}$ receives 66.3% from the received $I_{(HTCS)}$ on the flat roof at midday. The maximum ratio (98.1%) is recorded at 06:00 and 18:00. In summer, minimum ratios mean maximum solar efficiency for curved roofs in terms of receiving the least $I_{(HTCS)}$.

6.2.1.2 $CCS_{(std)}$ Faces (N-S) During December

Fig. (6-5) shows the received $I_{(HTCS)}$ on a flat roof and $CCS_{(std)}$ in winter. Identical to the previous scenario in summer, the maximum received solar radiation on each roof takes place at midday. Moreover, in winter both roofs have similar characteristics of $I_{(HTCS)}$ -curves. The two $I_{(HTCS)}$ -curves remain very close until 08:00. After 08:00 they ascend differently before reaching their maximum at midday. During the afternoon the $I_{(HTCS)}$ -curve for each roof geometry descends differently until 16:00, where the two curves intersect each other again and remain very close until the sunset. Thus, at 08:00 and 16:00, the $CCS_{(std)}$ and the flat roof $I_{(HTCS)}$ -values are nearly equal, (221 W/m^2 and 224 W/m^2 respectively)) Fig. (6-5).

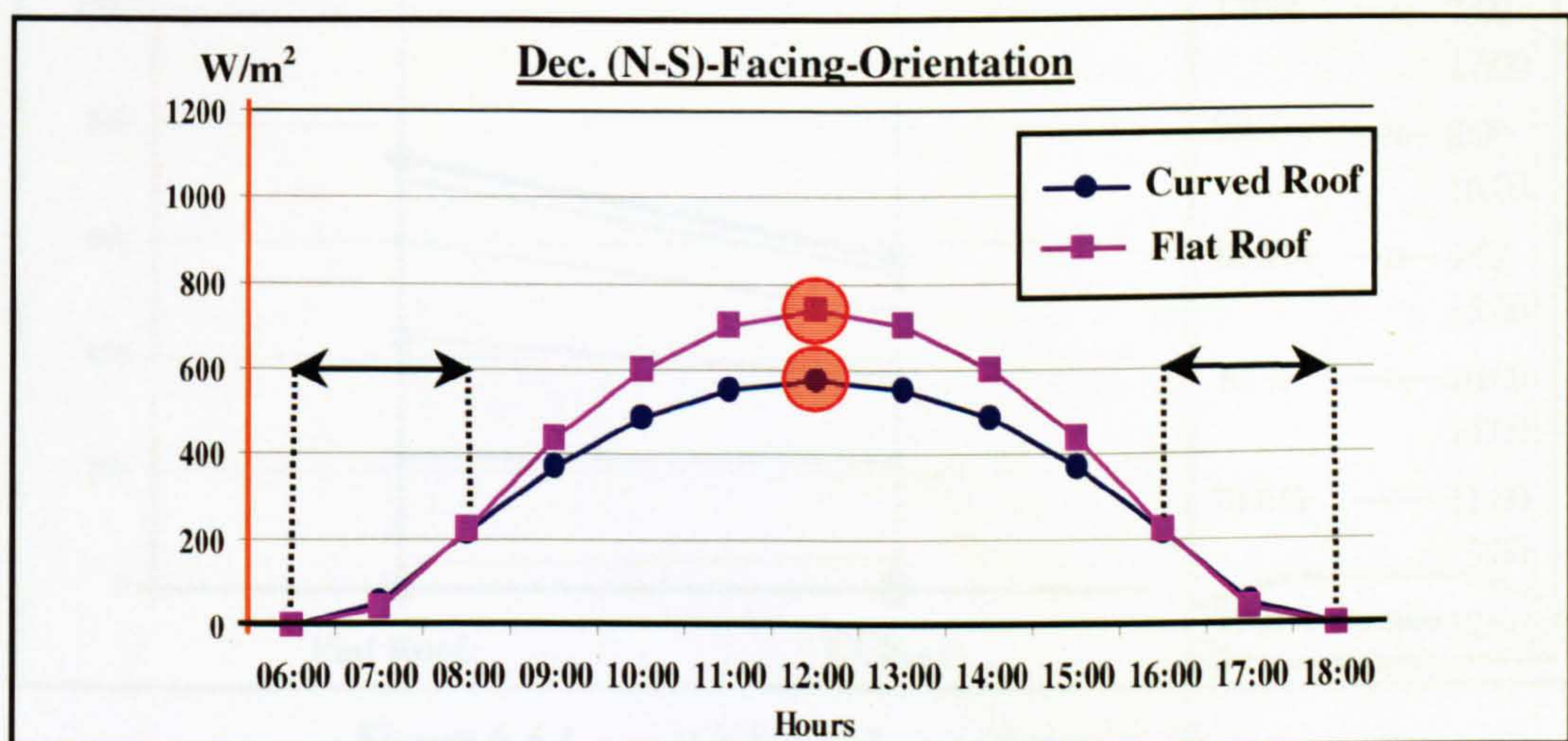


Figure 6-5 $I_{(HTCS)}$ (W/m^2) on Flat Roof and $CCS_{(std)}$

In both roofs geometries, $I_{(HTCS)}$ -curve has symmetrical increase and decrease gradients around the midday axis. Moreover, both roofs $I_{(HTCS)}$ -mirrored-values around midday are equal. The $I_{(HTCS)}$ -curve for the flat roof starts and ends with steeper gradients comparatively to the $CCS_{(std)}$ ones. The gap between the two roofs $I_{(HTCS)}$ -curves reaches its maximum at midday, ($740 - 576 = 164 \text{ W/m}^2$).

Compared to the summer scenario, the period time of the noticeable difference has shorted 4 hours in winter (from 06:00 & 18:00 to 08:00 & 16:00). This means that the $CCS_{(std)}$ enables to receive $I_{(HTCS)}$ similar to the flat roof ones during the early morning and the late afternoon hours, which is desirable in winter. Moreover, the $CCS_{(std)}$ receives slightly more solar radiation than the flat roof at 07:00 and 17:00, (55.5 W/m^2 and 40 W/m^2 respectively).

Fig. (6-6) presents another graphical way to display the previously derived results. It describes a proportional comparison between $I_{(HTCS)}$ -values on both roofs at each hour during daytime in winter. Relevant to the same scenario of principal directions, where $I_{(HTCS)}$ -mirrored-values around midday are equal, Fig. (6-6) presents six pairs of the hourly daytime readings in addition to the midday reading. Both roofs geometries do not receive solar radiation at 06:00 and 18:00 (*i.e. in winter before 07:00 and after 17:00 there are no measurable solar radiation intensities*).

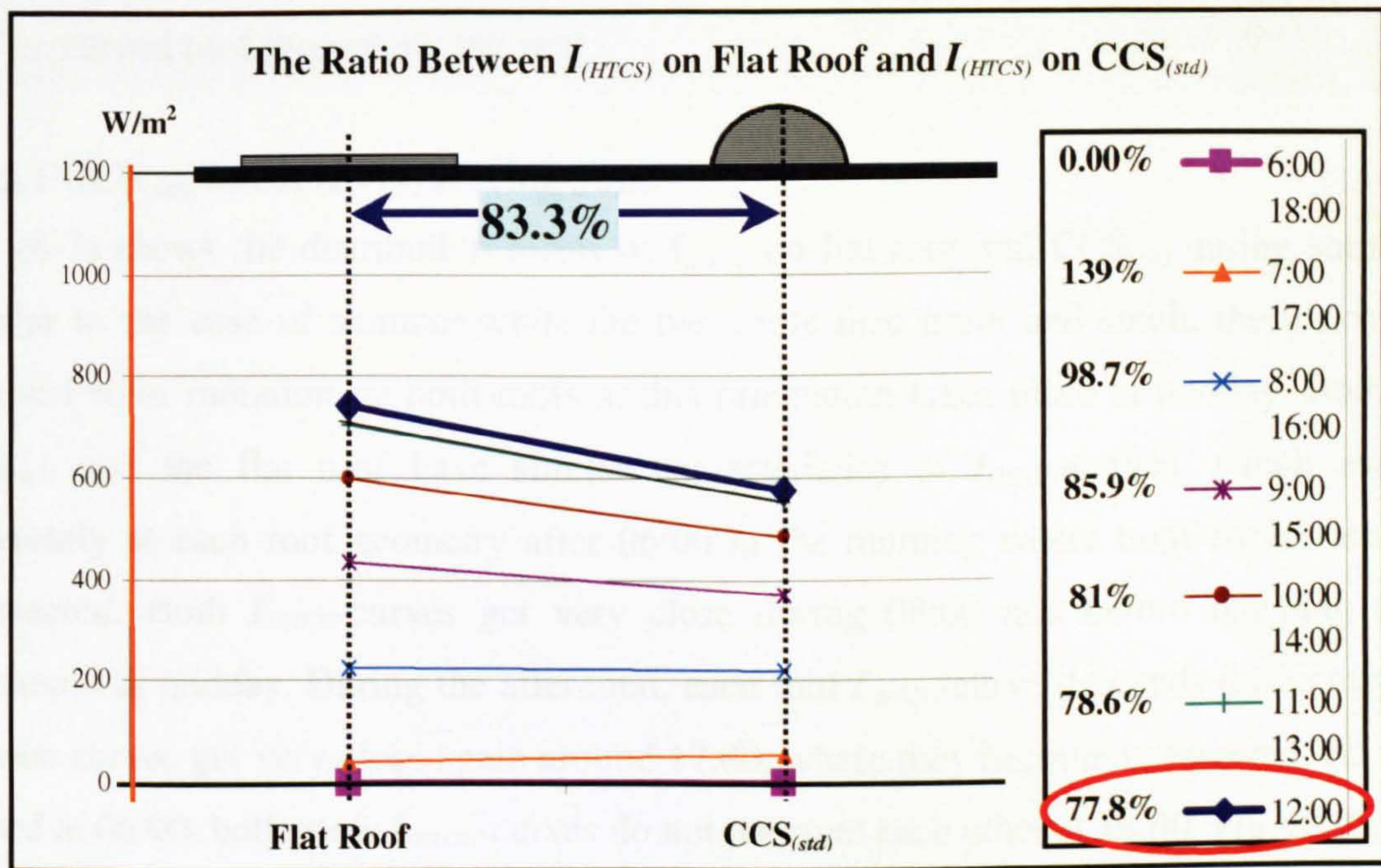
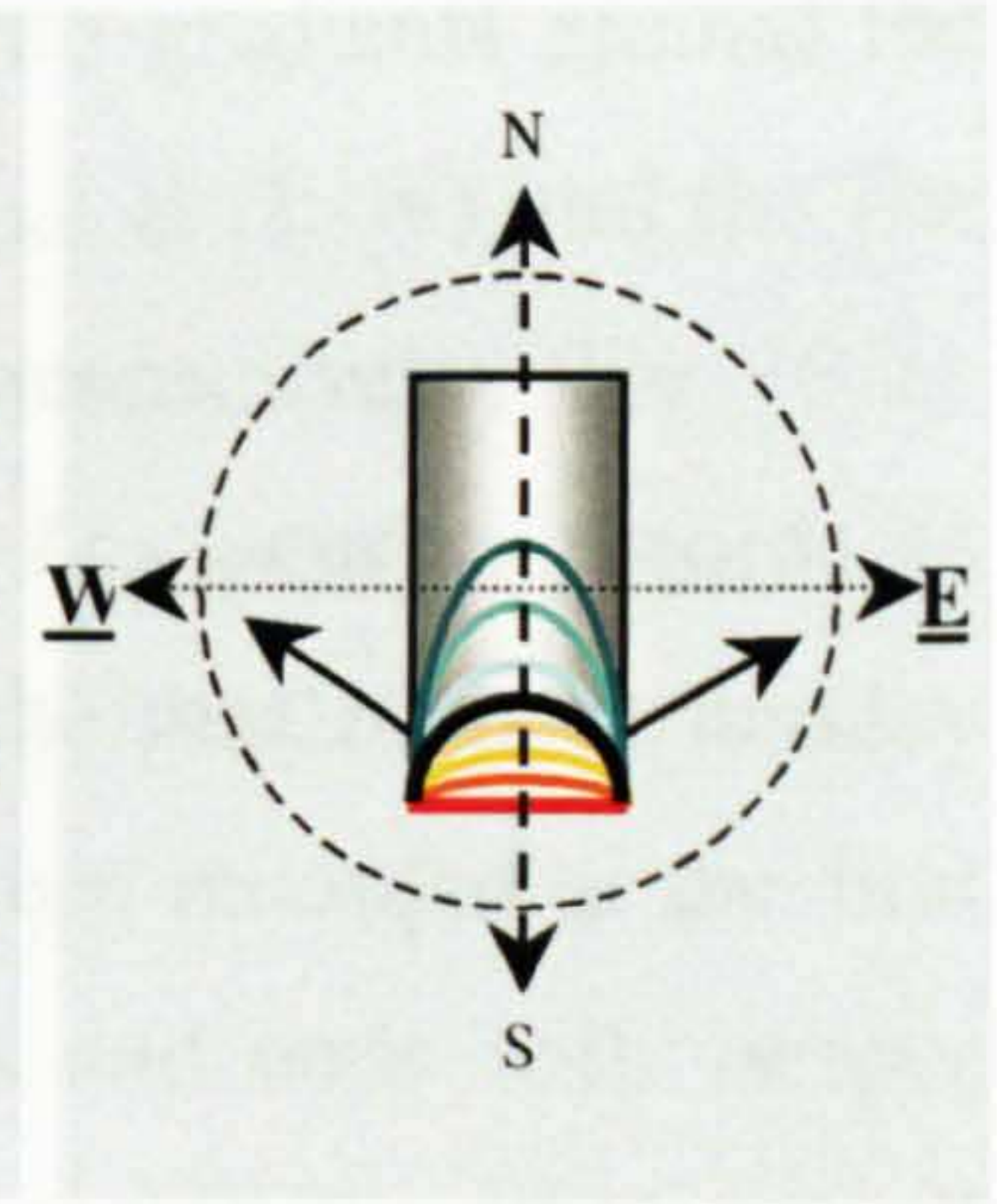


Figure 6-6 $I_{(HTCS)} (CCS_{(std)}) / I_{(HTCS)} (flat\ roof) \%$

Fig. (6-6) shows that the proportional ratio of the received $I_{(HTCS)}$ on the flat roof to that on the $CCS_{(std)}$ varies from its maximum at 07:00 and 17:00 (139%) to (77.8%) at midday. On the daily average basis, that $CCS_{(std)}$ receives 83.3% of the received on the flat roof. This means that in winter, the curved roof receives an extra 17% of $I_{(HTCS)} (flat-roof) / I_{(HTCS)} (CCS_{(std)})$ ratio compared to summer. This may be preferable during winter, where reducing the received solar radiation on roofs surfaces is not needed as it is in summer.

6.2.2 $CCS_{(std)}$ Curvature Faces EAST and WEST

This is the second principal orientation that the study will employ. In this case, the longitudinal axis (*perpendicular on the CCS*) is the (N-S) axis. The two halves of the $CCS_{(std)}$ face eastward and westward. As same as the previous principle orientation, this case will be also tested independently during summer and winter, in order to determine the solar performance of the curved roof throughout the year.



6.2.2.1 $CCS_{(std)}$ Faces (E-W) During June

Fig. (6-7) shows the distribution forms of $I_{(HTCS)}$ on flat roof and $CCS_{(std)}$ during summer. Similar to the case of summer while the two roofs face north and south, the maximum received solar radiation on both roofs at this orientation takes place at midday. Both the $CCS_{(std)}$ and the flat roof have similar characteristics of $I_{(HTCS)}$ -curves, which ascend differently at each roof geometry after 06:00 in the morning where both curves are not intersected. Both $I_{(HTCS)}$ -curves get very close during 08:00 and before reaching their maximum at midday. During the afternoon, each roof $I_{(HTCS)}$ -curve descends differently till the two curves get very close again around 17:00, where they become intersected. As they started at 06:00, both roofs $I_{(HTCS)}$ -curves do not intersect each other at 18:00, Fig. (6-7).

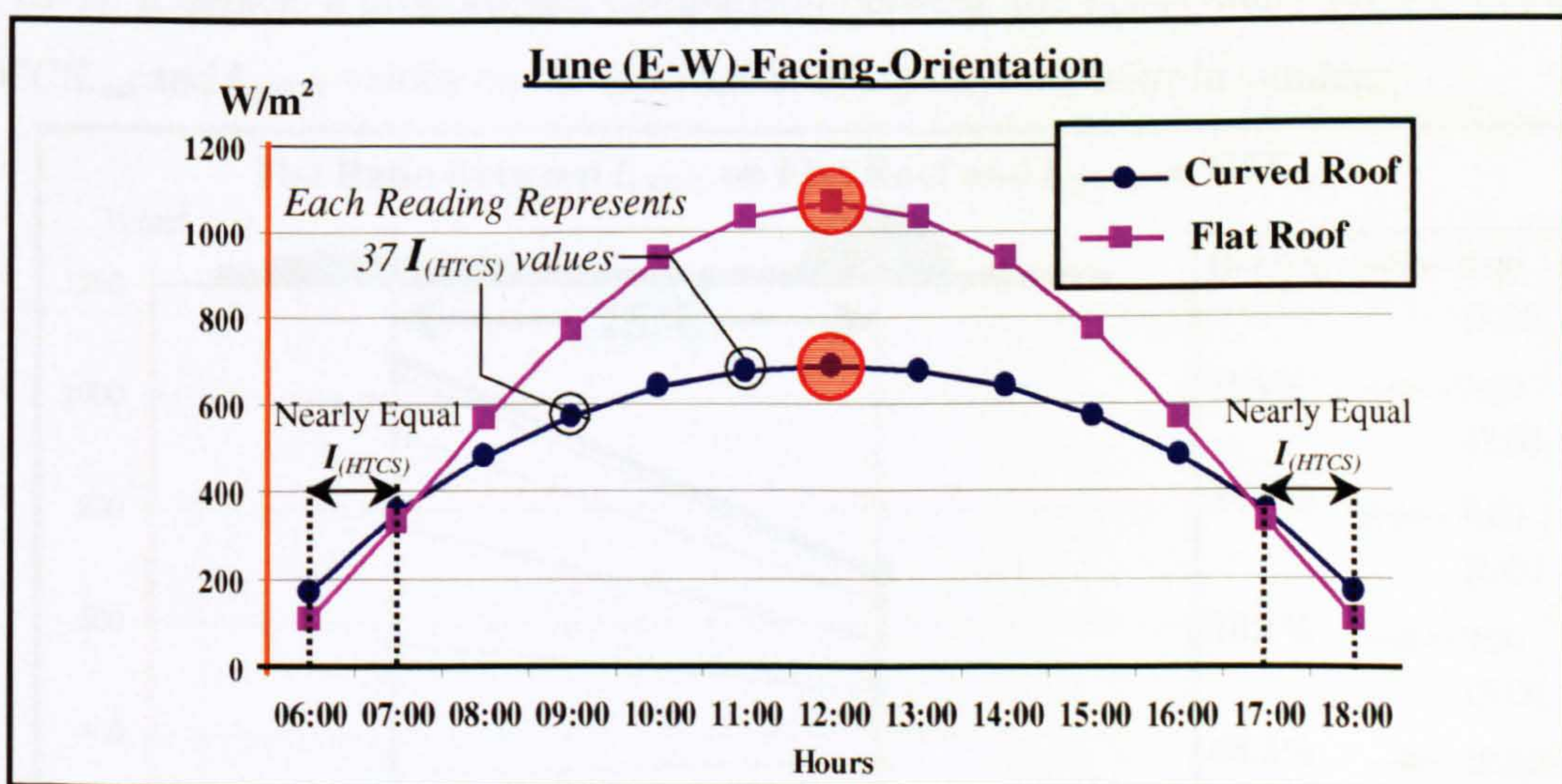


Figure 6-7 $I_{(HTCS)}$ (W/m²) on Flat Roof and $CCS_{(std)}$

Similarly to what has been recorded during summer at the first principal-orientation, (N-S), $I_{(HTCS)}$ -curves in both roofs have symmetrical increase and decrease gradients around the midday axis. Dissimilarly to (N-S), at 06:00 and 18:00 the $CCS_{(std)}$ at (E-W) and the flat roof do not receive equal $I_{(HTCS)}$ -values, (170 W/m^2 and 106 W/m^2 respectively), Fig. (6-7). As shown in Fig. (6-7), the desirable difference between the two $I_{(HTCS)}$ -curves records its minimum at 08:00 and 16:00. It slightly increases till it reaches the maximum at midday ($1070 - 684 = 386 \text{ W/m}^2$). This is nearly identical to what has been recorded at the first principal-direction (N-S) in summer. Flat roof $I_{(HTCS)}$ -curve starts and ends with steeper gradients compared to the $CCS_{(std)}$. $I_{(HTCS)}$ -curves of both geometries get smoother around the noon period.

Due to sun altitude angle and curved-roof orientation, $CCS_{(std)}$ receives more solar radiation intensity than the flat roof only during two time periods ($06:00-7:00$ and $17:00-18:00$). These time periods are significantly influenced by season and orientation (*These time periods did not exist when the $CCS_{(std)}$ faced (N-S) in summer*). With the comparison to (N-S), the desirable time in which the $CCS_{(std)}$ receives less solar radiation compared to the flat roof is 2 hours shorter when the $CCS_{(std)}$ faces (E-W). It starts one hour later and it ends one hour earlier with the comparison to the (N-S) case.

Fig. (6-8) shows another graphical way to illustrate the same previously derived results in Fig. (6-7). It depicts a proportional comparison between the $I_{(HTCS)}$ -values on the facing-(E-W) $CCS_{(std)}$ and $I_{(HTCS)}$ -values on the flat roof at every daytime hour in summer.

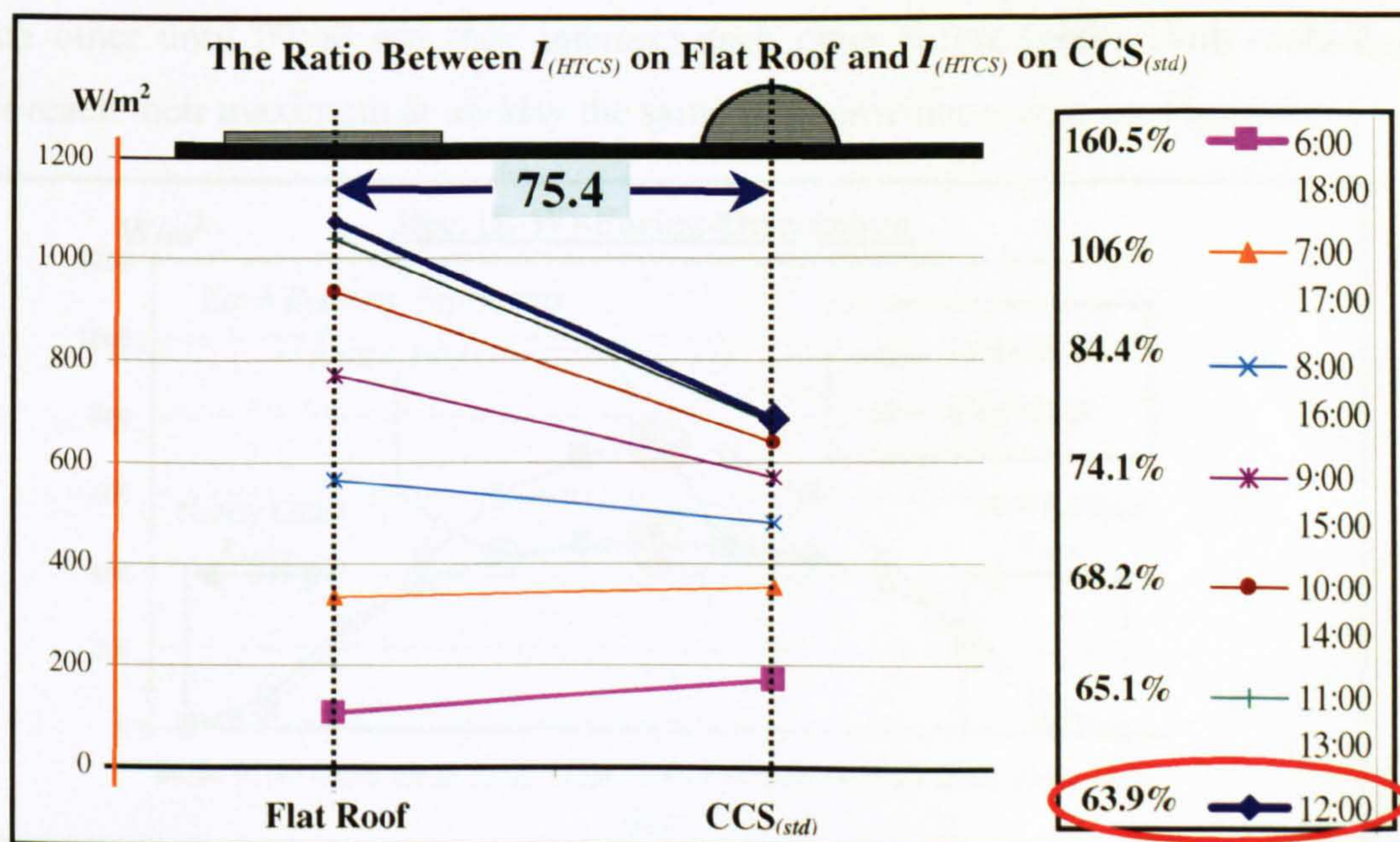


Figure 6-8 $I_{(HTCS)}(CCS_{(std)}) / I_{(HTCS)}(\text{flat roof}) \%$

As a result of the equalled $I_{(HTCS)}$ -mirrored-values around the midday axis, especially when principal directions are employed, Fig. (6-8) analyses only seven hourly readings instead of thirteen. The ratio between the received $I_{(HTCS)}$ on the $CCS_{(std)}$ to that on the flat roof records its maximum at 06:00 and 18:00 (160.51%). This means that the $CCS_{(std)}$ significantly receives more solar radiation than the flat roof during this period, which is not preferable during summer. But during these times solar radiation intensity is still bearable (*less than 400 W/m²*), which cannot effect the indoor conditions to any great extent.

The minimum proportional ratio (63.9%) is recorded at midday. Minimum ratio means maximum solar efficiency for the curved roof during summer in terms of receiving the least $I_{(HTCS)}$. On the daily average bases, $CCS_{(std)}$ receives about 75.4% from the $I_{(HTCS)}$ that the flat roof received. This is higher than the (N-S) ratio by approximately 9%. Therefore, (E-W)-orientation seems not preferable for curved roofs in summer the same as the (N-S).

6.2.2.2 $CCS_{(std)}$ Faces (E-W) During December

Fig. (6-9) shows $I_{(HTCS)}$ on a flat roof and curved roof $CCS_{(std)}$ during winter. Similar to all previous cases and particularly to the (N-S)-facing-orientation in winter, the maximum received solar radiation on both roofs takes place at midday. Moreover, both roofs geometries $I_{(HTCS)}$ -curves have similar characteristics.

Independently, each roof $I_{(HTCS)}$ -curve ascends after 06:00 in the morning where both $I_{(HTCS)}$ -curves are intersected. They behave differently after 06:00. The two curves get very close to each other until 09:00 and they intersect each other before 09:00. Both roofs $I_{(HTCS)}$ -curves reach their maximum at midday the same as in previous scenarios, Fig.(6-9).

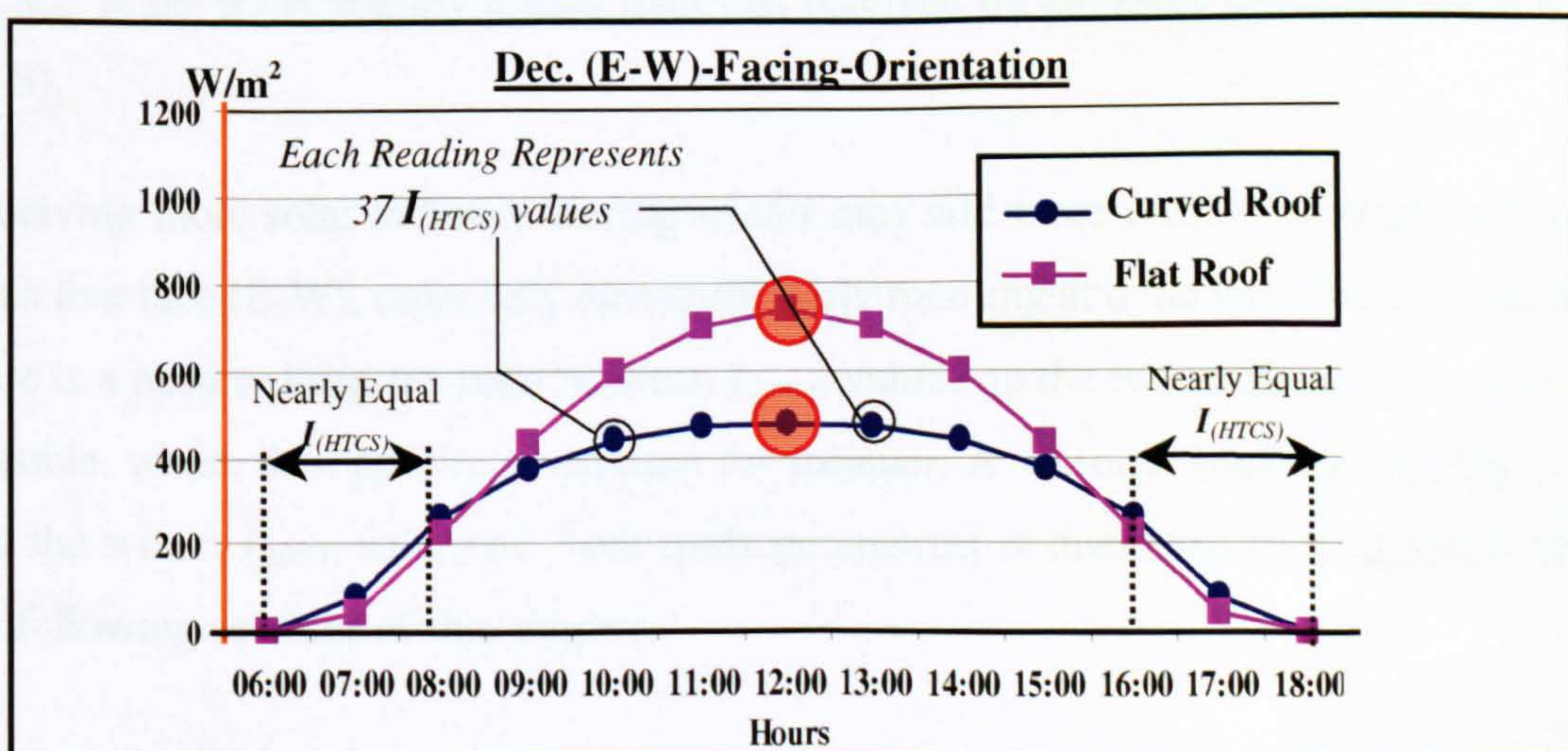


Figure 6-9 $I_{(HTCS)}$ (W/m²) on Flat Roof and $CCS_{(std)}$

During the afternoon the $I_{(HTCS)}$ -curve for each roof behaves symmetrically to its behaviour prior to midday. Each $I_{(HTCS)}$ -curve descends differently till the two curves get very close after 15:00. They intersect each other again before 16:00 and they remain very close until the sunset, Fig. (6-9). In both geometries the $I_{(HTCS)}$ -curve has symmetrical increase and decrease gradients around the midday axis. Both roofs geometries do not receive solar radiation at 06:00 and 18:00, (*in the early morning and the late afternoon*). At 07:00 and 17:00 the $CCS_{(std)}$ receives slightly more $I_{(HTCS)}$ than the flat roof, ($55.5W/m^2$ and $40W/m^2$ respectively). Both roofs geometries receive approximately equal $I_{(HTCS)}$ -values in the early morning and the late afternoon, Fig. (6-9).

Compared to the summer scenario at the same orientation, the noticeable difference between the two roofs $I_{(HTCS)}$ -curves has shorted 2 hours. It has delayed one hour before midday (*09:00 in winter instead of 08:00 in summer*), and it took place one hour earlier during the afternoon (*15:00 in winter instead of 16:00 in summer*), Fig. (6-9).

As shown in Fig. (6-9), the difference between the two $I_{(HTCS)}$ -curves records its minimum in the early morning and the late afternoon hours. The difference increases and reaches the maximum at 12:00 ($740 - 576 = 164 W/m^2$). Flat roof $I_{(HTCS)}$ -curve starts and ends with steeper gradients comparatively to $CCS_{(std)}$ ones. Both roofs $I_{(HTCS)}$ -curves get smoother around noon period.

Similar to what has been noticed previously during winter in (N-S), Fig. (10-6) also shows that the $CCS_{(std)}$ receives more solar radiation than the flat roof during the early morning and the late afternoon hours. Even more, the received solar radiation intensity by the $CCS_{(std)}$ at (E-W) is slightly higher than that received on the same geometry when it faced (N-S).

Receiving more solar radiation during winter may add more credits for employing curved roofs that face (E-W), especially during the early morning and the late afternoon. In winter, there is a need to keep the ratio between $I_{(HTCS)}$ -values on the two roofs surfaces as small as possible, while, the opposite is required for summer. A seasonal ratio between the summer and the winter $I_{(HTCS)}$ -values of both roofs geometries is discussed in more detail through the following sections of this chapter.

A proportional comparison between $I_{(HTCS)}$ -values on a flat and curved roofs at (E-W) is discussed in Fig. (6-10) at each hour during the daytime in winter. On daily average basis, the (E-W)-facing $CCS_{(std)}$ receives about 78.6% of the received $I_{(HTCS)}$ on the flat roof.

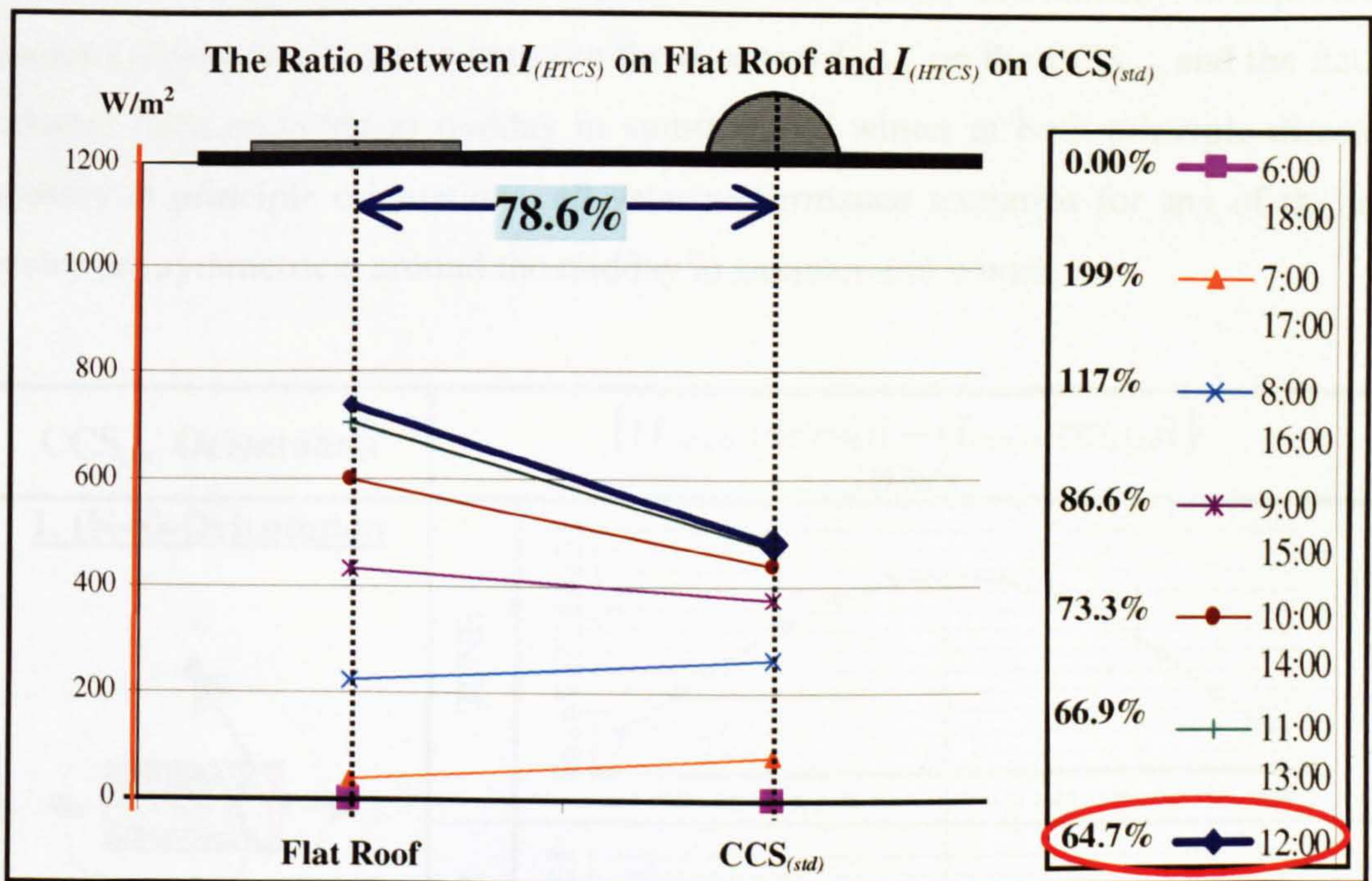


Figure 6-10 $I_{(HTCS)}(CCS_{(std)}) / I_{(HTCS)}(flat\ roof) \%$

Because of the equalled $I_{(HTCS)}$ -mirrored-values around the midday axis, Fig. (10-6) discusses only seven readings instead of thirteen. At 06:00 and 18:00 both roofs do not receive solar radiation (*i.e. in winter before 07:00 and after 17:00 there is no measurable solar radiation intensities*). The $I_{(HTCS)}(flat\ roof) / I_{(HTCS)}(CCS_{(std)})$ ratio records its maximum at 07:00 and 17:00 (199%). However, this may result insignificant differences between the receipted energy on the two simulated roof-geometries.

The minimum percentage (64.7%) has been recorded at midday. This means that the $CCS_{(std)}$ nearly receives double the flat roof $I_{(HTCS)}$ -values during the early morning and the late afternoon, Fig. (6-10). Therefore, (E-W) is not preferable for curved roof in winter, the same as (N-S), which provided a higher ratio (83.3%).

The curved roof $I_{(HTCS)}$ -midday-values at the two principle orientations (N-S) & (E-W) are not equal in winter, but they are equal in summer. Consequently, $I_{(HTCS)}(flat\ roof) / I_{(HTCS)}(CCS_{(std)})$ proportional ratios are not equal at both principal directions in winter, but are equal in summer.

6.2.3 The Calculated Difference Between $I_{(HTCS)}$ on Flat Roof and $I_{(HTCS)}$ on $CCS_{(std)}$ Faces Principal Directions (N-S) & (E-W)

Fig. (6-11) compares the calculated difference between the received $I_{(HTCS)}$ on a $CCS_{(std)}$ and a flat roof according to the seasonal variation and the $CCS_{(std)}$ orientation. As expected the maximum calculated difference between the received $I_{(HTCS)}$ on the $CCS_{(std)}$ and the flat roof has always been recorded at midday in summer and winter at both principle directions. Customary at principle orientations, all solar performance scenarios for any of the tested geometry are symmetrical around the midday in summer and winter.

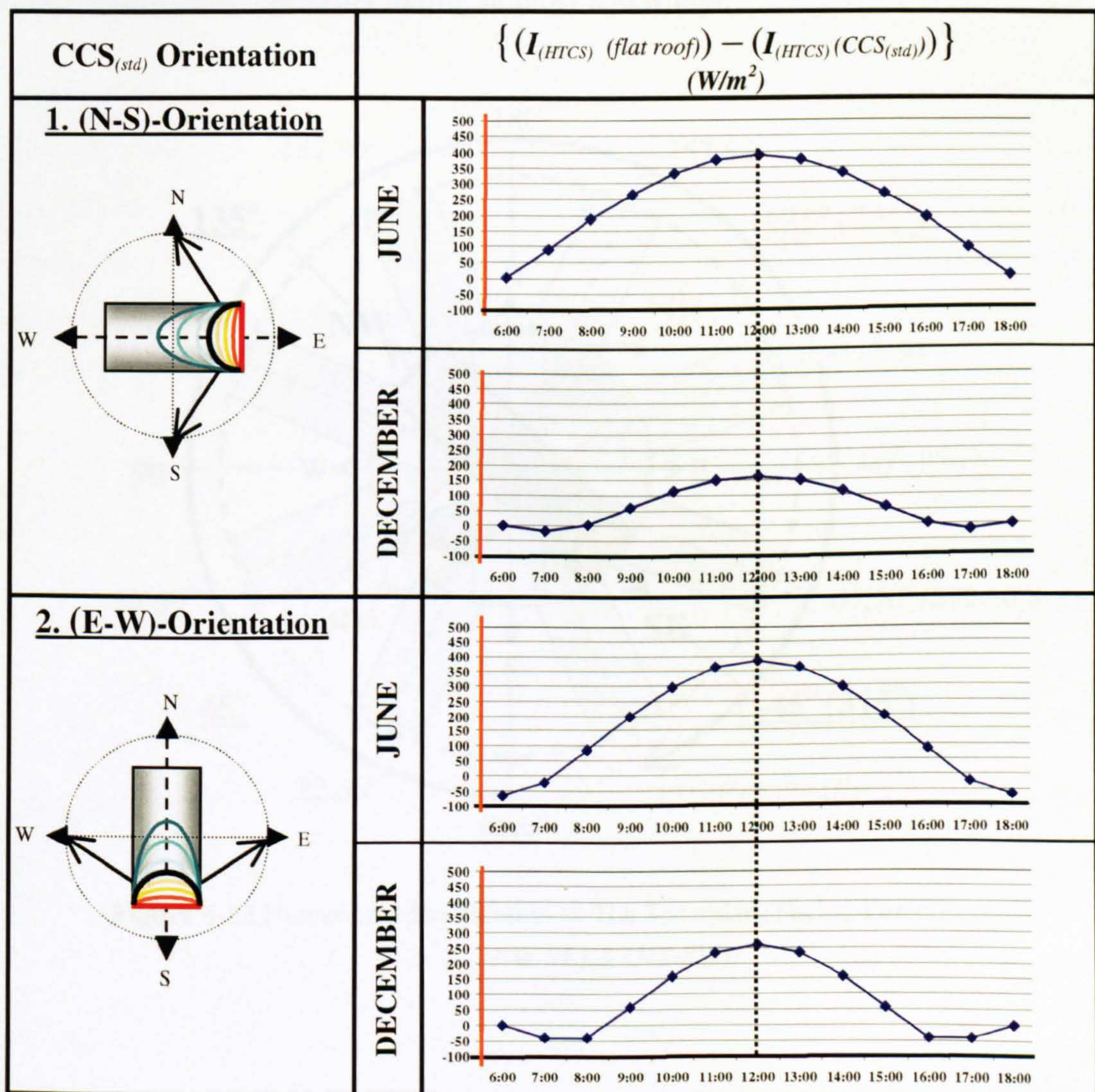


Figure 6-11 The Difference Between $I_{(HTCS)}$ on Flat Roof and $CCS_{(std)}$

6.3 THE SOLAR PERFORMANCE OF SEMICIRCULAR CURVED ROOF

(CCS_(std) Curvature Faces Secondary Directions) (NW-SE) & (NE-SW)

After investigating its solar performance at principal directions, this part examines the solar performance of a semicircular curved roof facing secondary directions. Calculations have been carried out to test the solar performance of a CCS_(std) facing two secondary directions similar to the procedures of the principle directions. Firstly, when the CCS_(std) curvature faces (NW-SE), and secondly, when it is oriented towards (NE-SW), Fig.(6-12). At each secondary orientation, the performance of $I_{(HRCs)}$ on the same roof geometry CCS_(std) has been investigated repeatedly during summer and winter.

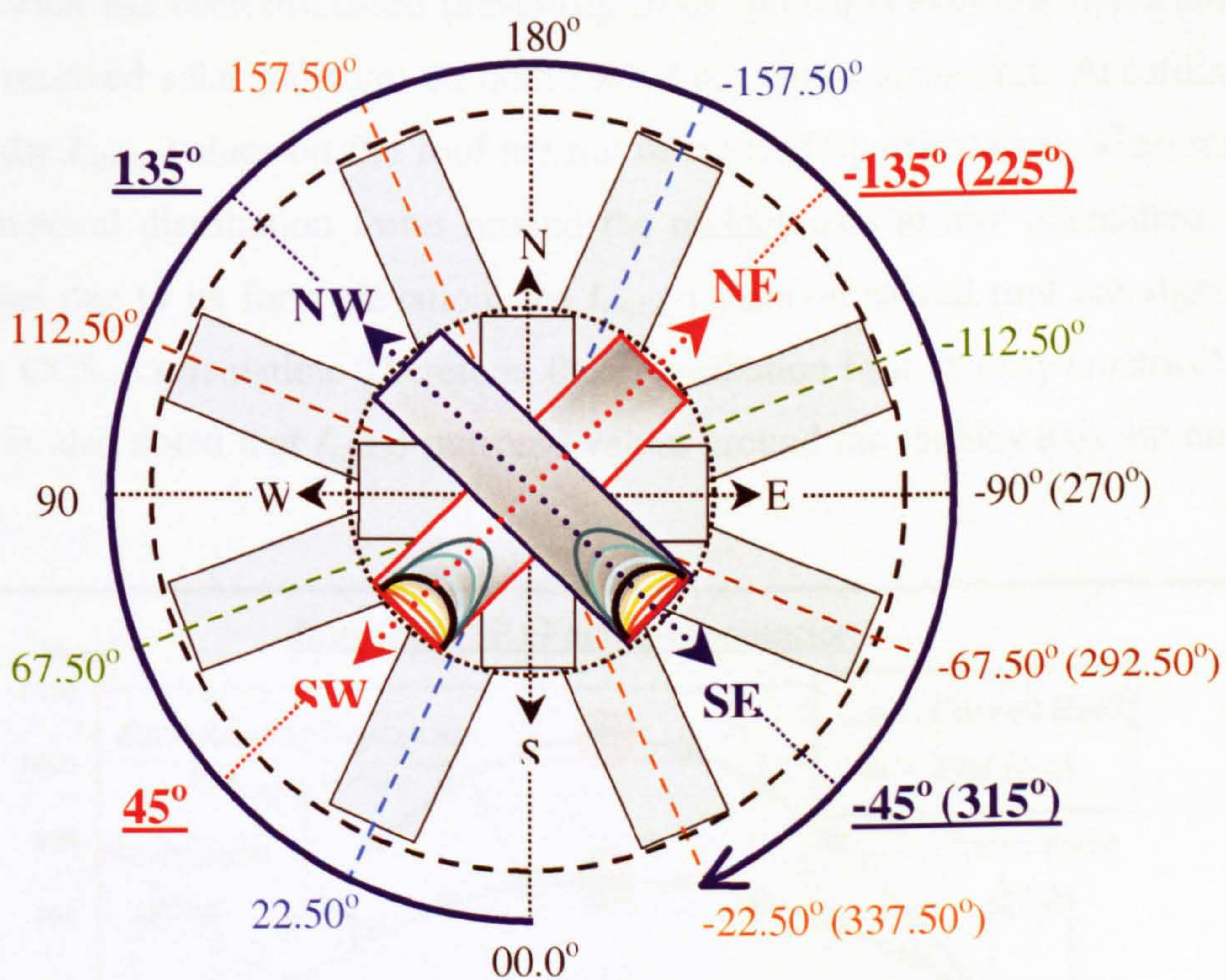
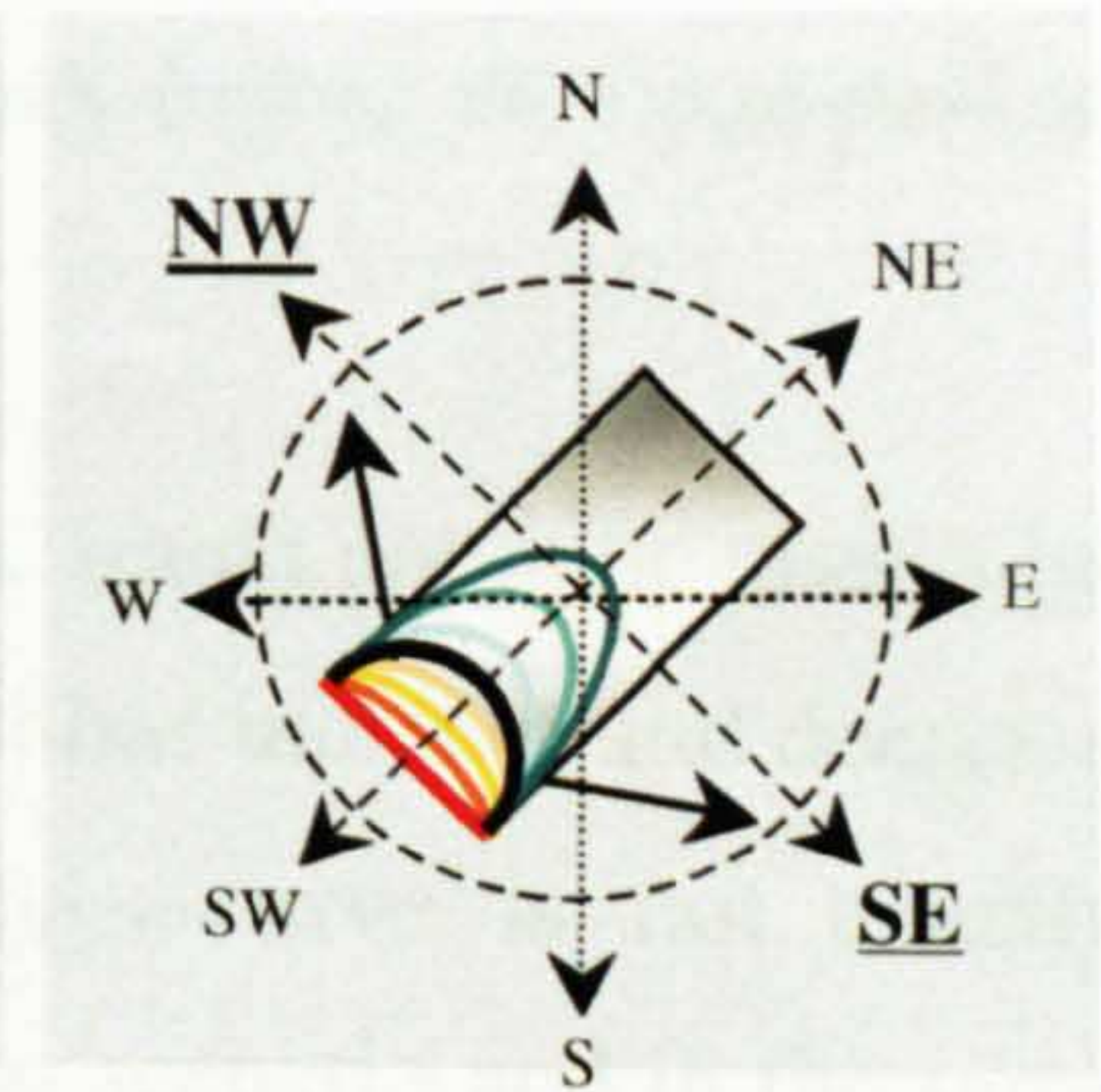


Figure 6-12 Numerical Identification of The Secondary Facing-Directions (NW-SE) & (NE-SW)

6.3.1 $CCS_{(std)}$ Curvature Faces NORTHWEST and SOUTHEAST

This is the first secondary orientation that the study will employ. In this case, the longitudinal axis (perpendicular on the CCS) is the NE-SW axis. The two halves of the $CCS_{(std)}$ face NW and SE. This case is tested during summer and winter in order to compare between the received $I_{(HTCS)}$ on the curved roof and the flat roof during different seasons.



6.3.1.1 $CCS_{(std)}$ Faces (NW-SE) During June

Fig. (6-13) shows the $I_{(HTCS)}$ on flat and curved roofs facing (NW-SE) during summer. Similar to what has been discussed previously in the principal direction applications, the maximum received solar radiation on both roofs takes place at midday. According to its geometry, the $I_{(HTCS)}$ -values on flat roof are not influenced by orientation. Therefore, they have symmetrical distribution forms around the midday axis at any orientation. On the contrary, and due to its form elevation, the $I_{(HTCS)}$ -values on curved roof are significantly effected by $CCS_{(std)}$ orientation. Therefore, their distribution form is unsymmetrical around midday. It is also noted that $I_{(HTCS)}$ -mirrored-values around the midday axis are not equal, Fig. (6-13).

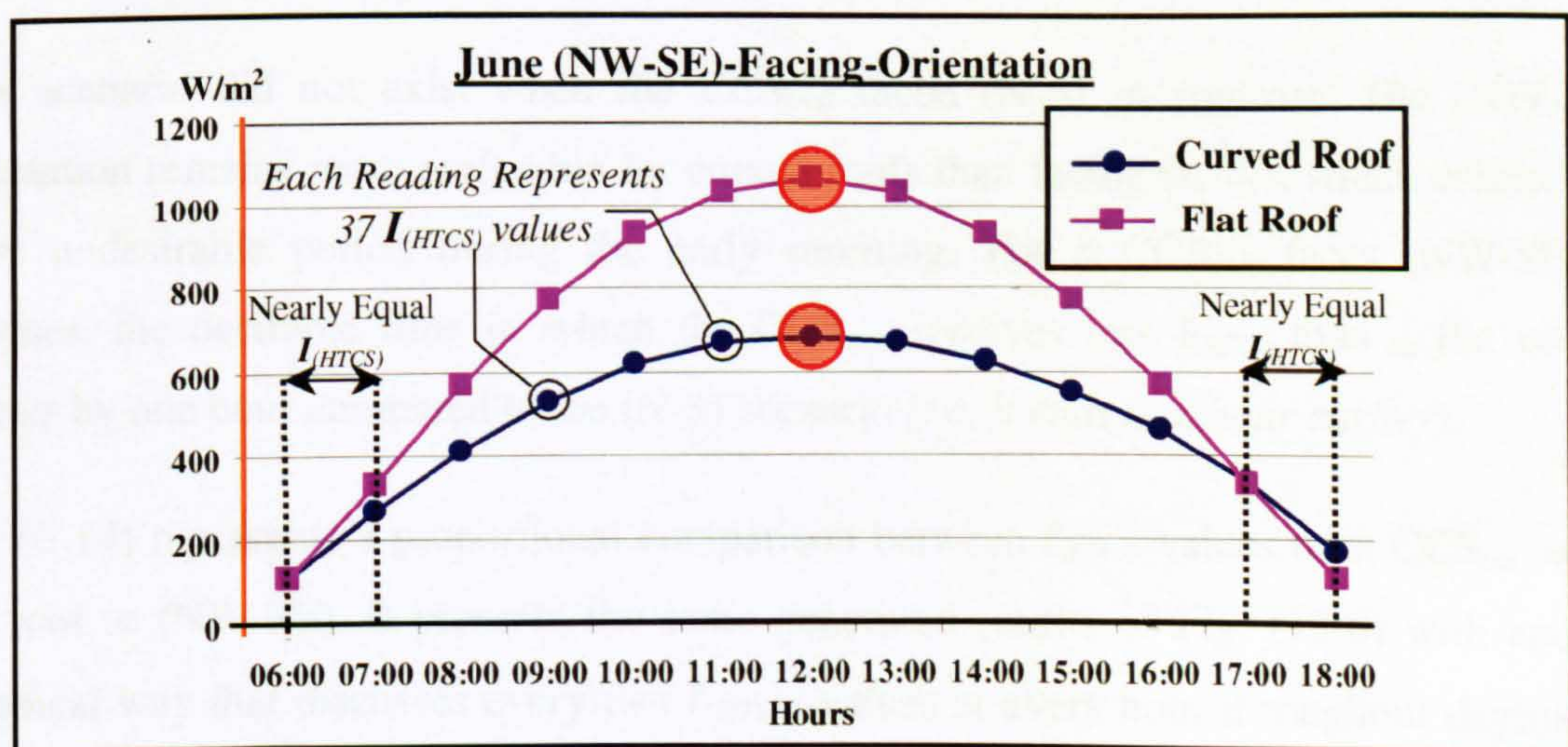


Figure 6-13 $I_{(HTCS)}$ (W/m²) on Flat Roof and $CCS_{(std)}$

$I_{(HTCS)}$ -curves in both roofs geometries ascend independently after 06:00 in the morning where both are intersected. They reach their maximum at midday. During the late afternoon each roof $I_{(HTCS)}$ -curve descends differently till the two curves intersect each other again around 17:00. At 18:00 the two curves become not intersected, Fig. (6-13).

Apart from the late afternoon hours, both roofs $I_{(HTCS)}$ -curves in this secondary orientation (NW-SE) seem to be identical to the (N-S) ones in summer, (*only before the noon period, whereas in the afternoon they are similar to the (E-W) ones*).

The $I_{(HTCS)}$ -curve for the flat roof has exactly symmetrical values, which are quite dissimilar to what has been recorded during summer at (N-S). Moreover, it has increase and decrease gradients around the midday axis, whereas, the $CCS_{(std)}$ $I_{(HTCS)}$ -curve is not exactly symmetrical. Instead of 06:00 and 18:00 at the (N-S)-orientation scenario and in the same season, both roofs geometries receive approximately equal $I_{(HTCS)}$ -values only at 06:00 in the morning, (108 W/m^2 and 106 W/m^2 respectively), whereas they record 168 W/m^2 and 106 W/m^2 at 18:00. So, the desirable difference between the two $I_{(HTCS)}$ -curves form an unsymmetrical shape.

The minimum difference between the two $I_{(HTCS)}$ -curves is recorded at 06:00 and 17:00 instead of 06:00 and 18:00 as in the (N-S) orientation. Then it slightly increases until they reach the maximum at midday ($1070 - 684 = 386 \text{ W/m}^2$). This is exactly identical to what has been recorded at the two principal directions in summer. Fig. (13-6) also shows that throughout the day there is only one period (17:00-18:00) in which the $CCS_{(std)}$ receives more $I_{(HTCS)}$ than the flat roof.

This scenario did not exist when the $CCS_{(std)}$ faced (N-S) in summer. The (NW-SE)-orientation remains more preferable for curved roofs than facing (E-W), which created one more undesirable period during the early morning. For a $CCS_{(std)}$ faces (NW-SE) in summer, the desirable time in which the $CCS_{(std)}$ receives less $I_{(HTCS)}$ than the flat roof is shorter by one hour compared to the (N-S) scenario (*i.e. it ends one hour earlier*).

Fig. (6-14) represents a proportional comparison between $I_{(HTCS)}$ -values on a $CCS_{(std)}$ and a flat roof at (NW-SE). It presents the same generated results of Fig. (13-6) with another graphical way that discusses every two $I_{(HTCS)}$ -values at every hour throughout daytime in summer. For a $CCS_{(std)}$ facing secondary directions the $I_{(HTCS)}$ -mirrored-values are not equal around the midday axis.

Therefore, Fig. (6-14) discusses the daytime thirteen hourly-readings. There were only seven readings when the curvature faced principal directions, in which the $I_{(HTCS)}$ -mirrored-values around the midday axis are exactly equal.

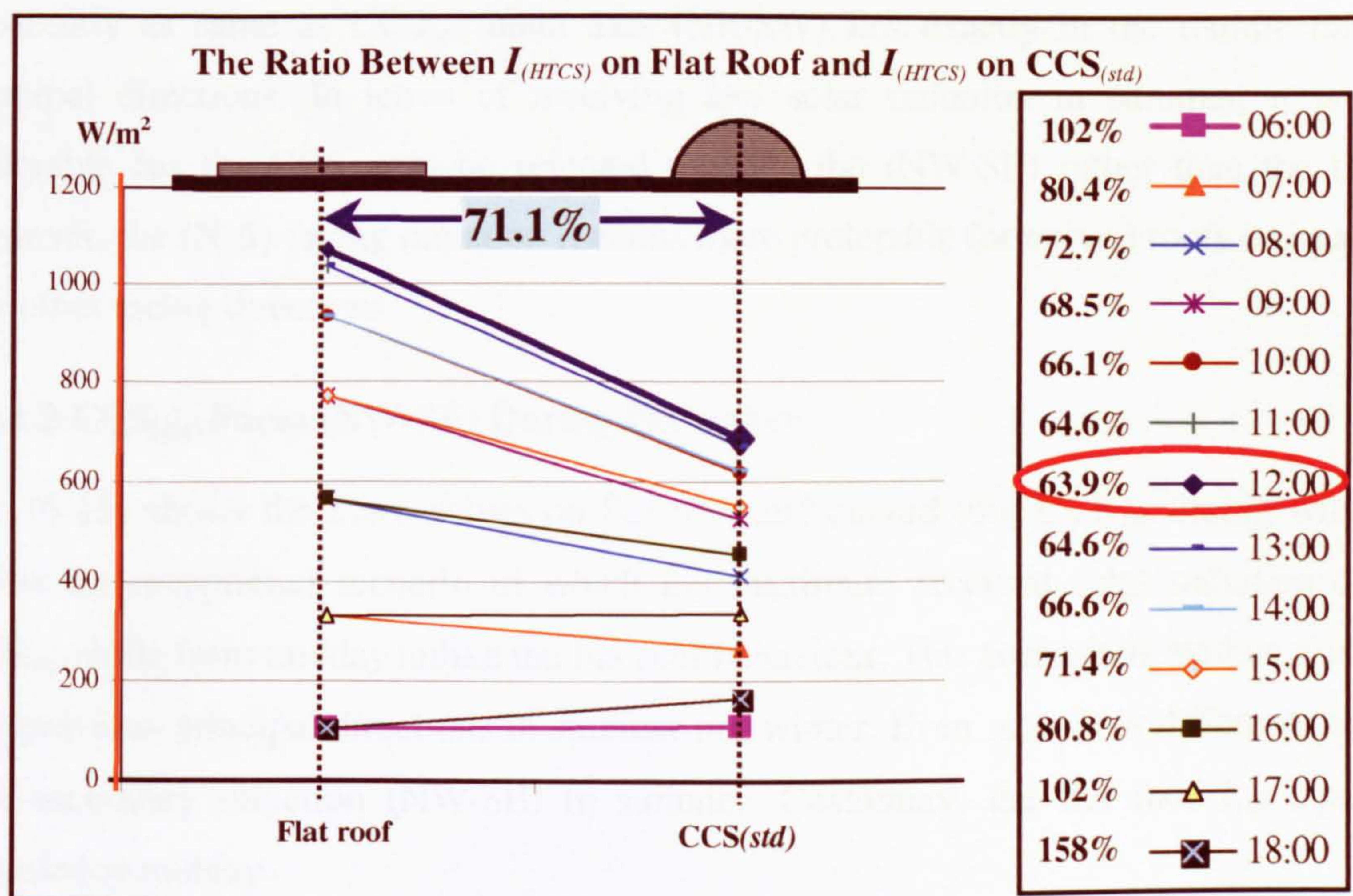


Figure 6-14 $I_{(HTCS)} (CCS_{(std)}) / I_{(HTCS)} (flat\ roof) \%$

Fig. (6-14) shows that the $I_{(HTCS)}$ -mirrored-values on flat roof are identical. But in the $CCS_{(std)}$, there are significant differences between the early morning and the late afternoon $I_{(HTCS)}$ -mirrored-values. This is not the case around the noon period on the same geometry $CCS_{(std)}$, where differences are insignificant. For example, the $I_{(HTCS)}$ -mirrored-values of (10:00 & 14:00) and (11:00 & 13:00) are almost similar values.

As shown above in Fig. (6-14), the percentage of the received $I_{(HTCS)}$ on the $CCS_{(std)}$ to that on the flat roof records its maximum at 18:00 (158%). This means that the $CCS_{(std)}$ receives more $I_{(HTCS)}$ than the flat roof by one and half fold during the late afternoon, which is undesirable for summer. The minimum percentage (63.9%), which means maximum solar efficiency for the $CCS_{(std)}$ in summer has been recorded at midday. On the daily average bases, the $CCS_{(std)}$ receives about 71.1% of the received $I_{(HTCS)}$ on the flat roof.

The calculated ratio between $I_{(HTCS)}$ on the $CCS_{(std)}$ and $I_{(HTCS)}$ on the flat roof (71.7%) fits between the previous two ratios of the two principal directions (N-S & E-W) (66.3% & 75.4%), in summer. Moreover, it fits nearly in the middle between the two percentages, apparently as same as $CCS_{(std)}$ main axis (NE-SW) lies exactly in the middle between principal directions. In terms of receiving less solar radiation in summer, it is more preferable for the $CCS_{(std)}$ to be oriented towards the (NW-SE) rather than the (E-W). However, the (N-S)-facing direction remains more preferable for curved roofs compared to any other facing directions.

6.3.1.2 $CCS_{(std)}$ Faces (NW-SE) During December

Fig. (6-15) shows the $I_{(HTCS)}$ -values on flat roof and curved roof $CCS_{(std)}$ during winter. It shows an exceptional scenario in which the maximum received solar radiation on the $CCS_{(std)}$ shifts from midday unlike the flat roof behaviour. This scenario is neither similar to any previous principal directions in summer nor winter. Even more it is different than the first secondary direction (NW-SE) in summer. Customary, the flat roof $I_{(HTCS)}$ -peak is recorded at midday.

Each $I_{(HTCS)}$ -curve in both geometries ascends after 06:00 in the morning. They intersect each other around 09:00, in which $I_{(HTCS)}$ -values are nearly equal, (430W/m² and 434 W/m²). The $CCS_{(std)}$ and the flat roof $I_{(HTCS)}$ -curves are very close during the early morning period. After 09:00, they keep ascending differently until reach their peaks. The $CCS_{(std)}$ and the flat roof $I_{(HTCS)}$ -curves descend after their peaks time (11:00 and 12:00 respectively), they intersect each other again around 17:00 in the evening, Fig.(6-15).

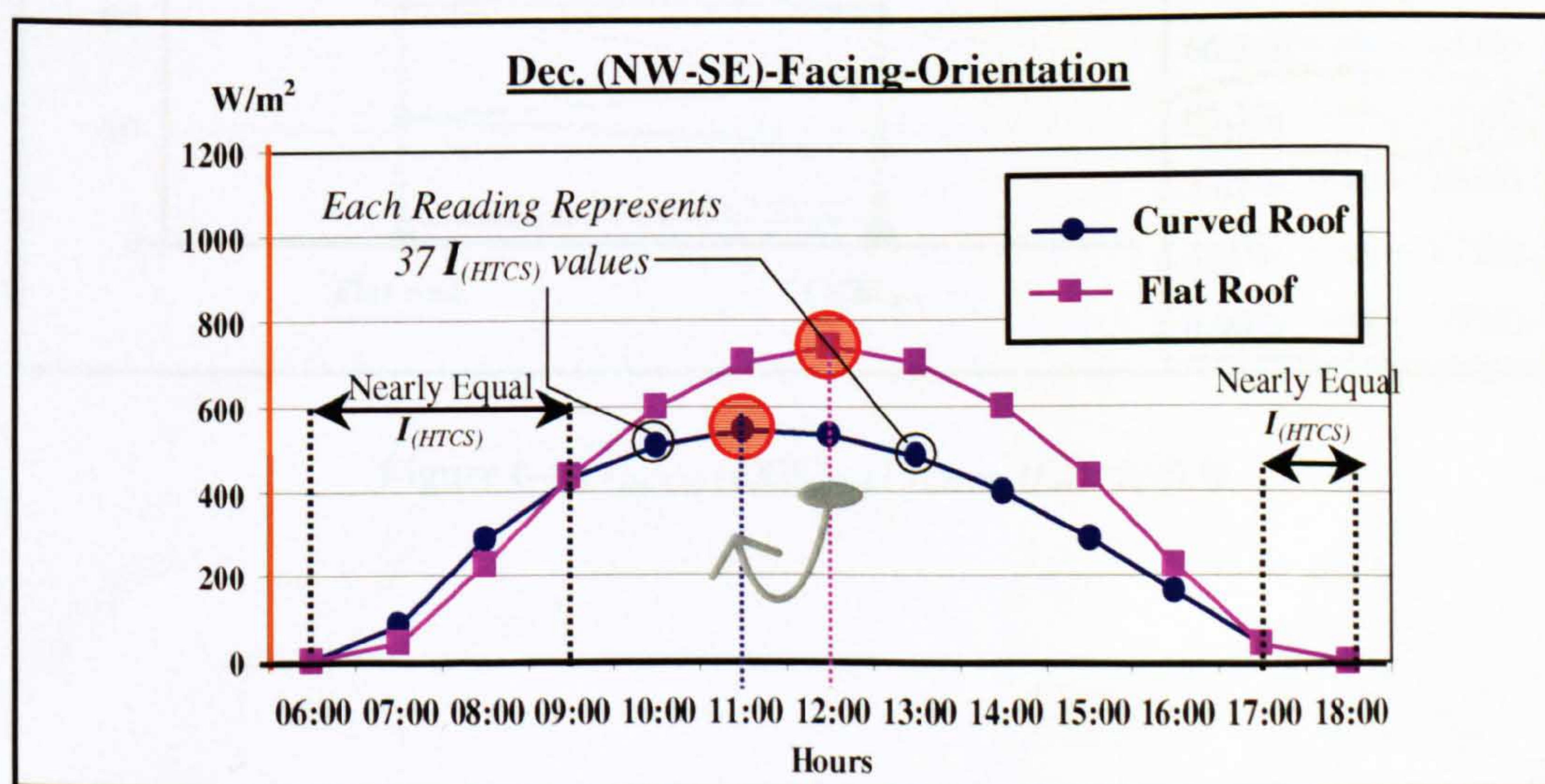


Figure 6-15 $I_{(HTCS)}$ (W/m²) on Flat Roof and $CCS_{(std)}$

Apparently, the $CCS_{(std)}$ $I_{(HTCS)}$ -curve descends smoother compared to its ascending. Only the flat roof $I_{(HTCS)}$ -curve has exactly symmetrical increase and decrease gradients around the peak axis. At 06:00 and 18:00 both roofs do not receive solar radiation (*i.e. in winter before 07:00 and after 17:00 there is no measurable solar radiation intensities*).

Notably, after 06:00 and during the early morning period, the $CCS_{(std)}$ receives $I_{(HTCS)}$ more than the flat roof. Unlike what has been observed in summer, the noticeable difference between the two roofs $I_{(HTCS)}$ -values in winter has delayed 3 hours (06:00 in summer instead of 09:00 in winter). As shown in Fig. (6-15), the difference between the two roofs $I_{(HTCS)}$ -curves records its minimum around 09:00 and in the late afternoon hours (17:00 & 18:00). Unlike to all previous cases, the maximum difference is not recorded at the peak (11:00 in this exceptional case). But rather it has shifted to 13:00 (704– 483 = 221 W/m²).

Fig. (6-16) applies another graphical way for displaying the same results of Fig. (6-15). It represents a proportional comparison between $I_{(HTCS)}$ -values on the two roofs geometries at (NW-SE).

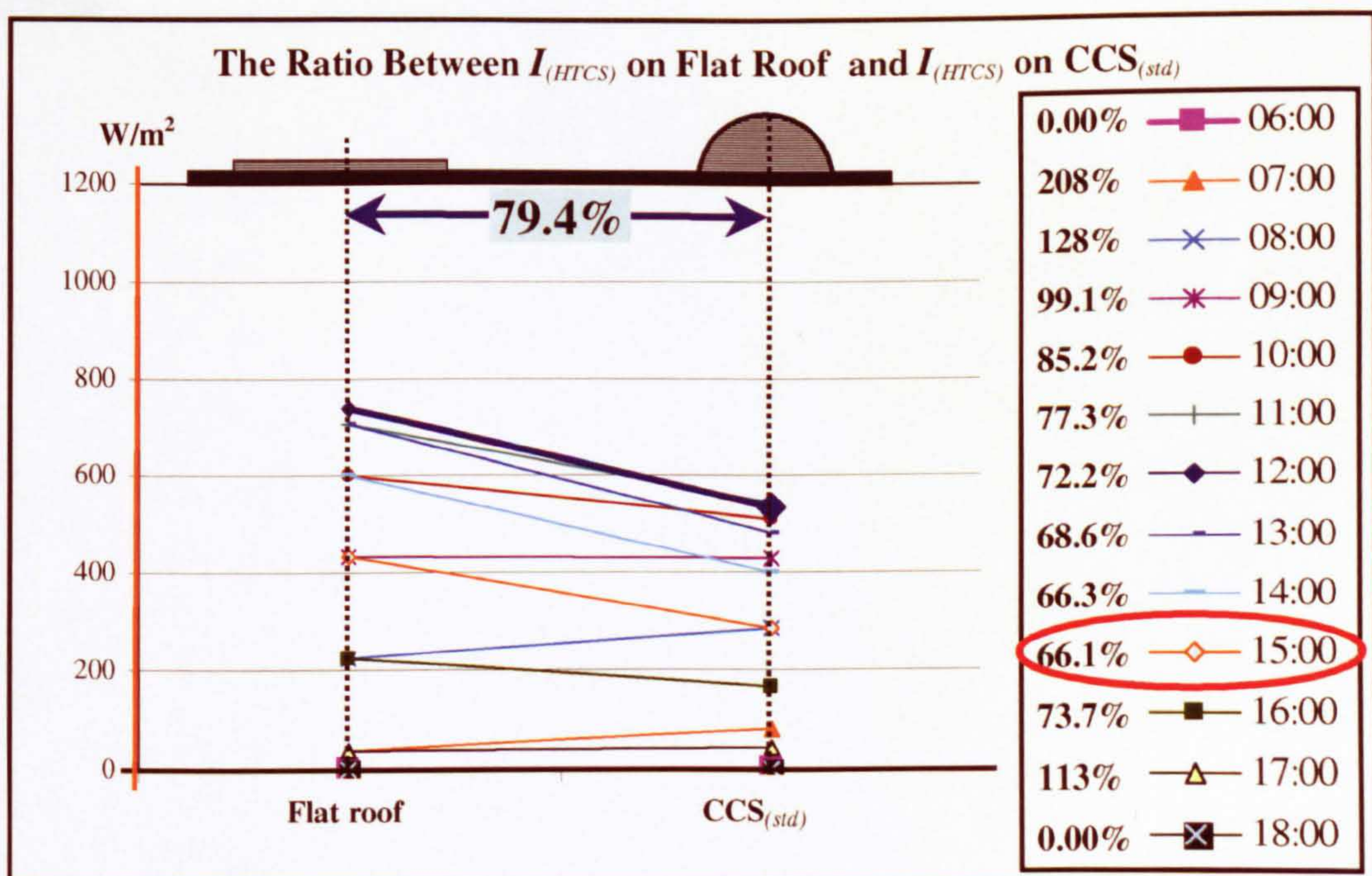


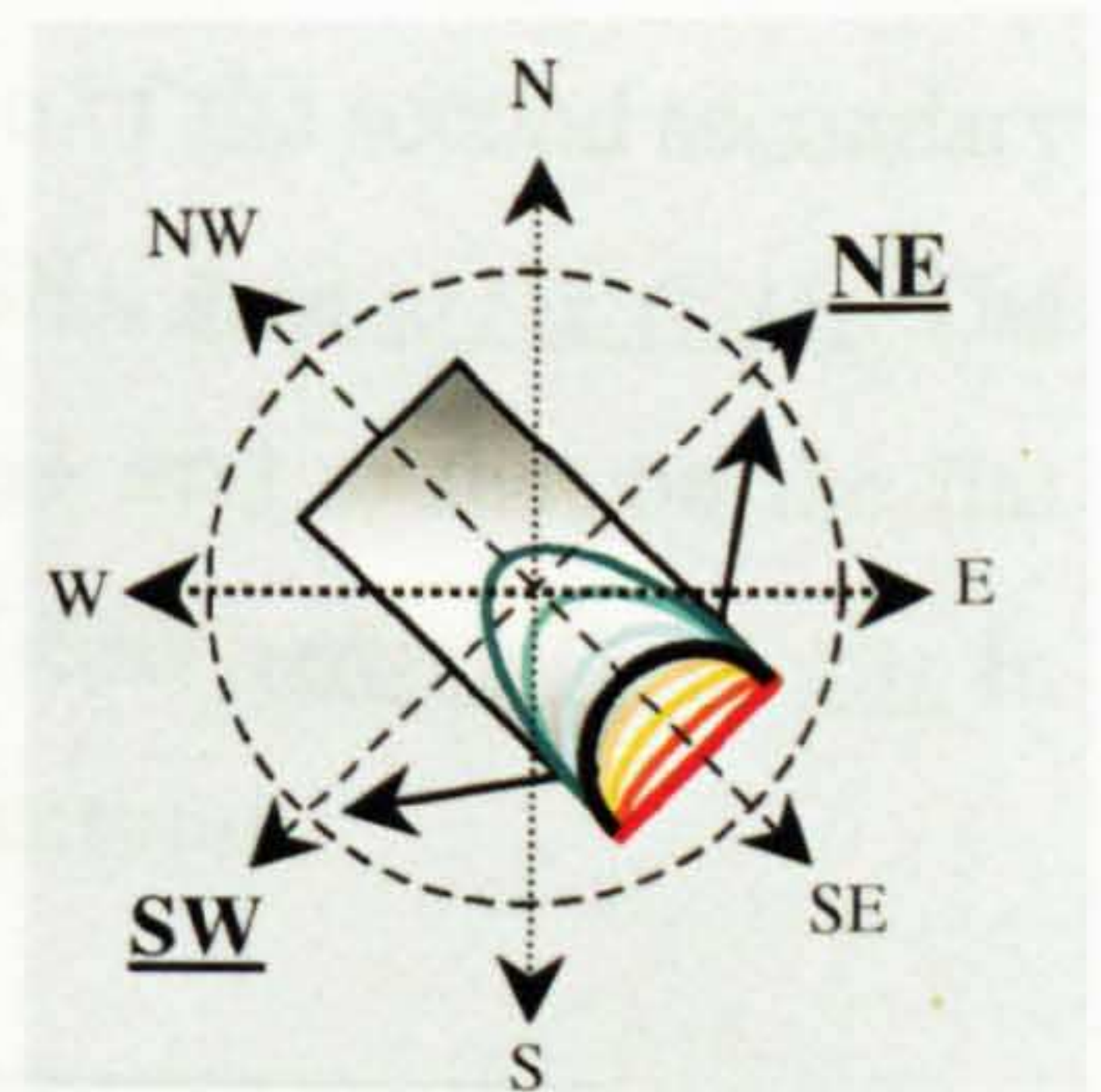
Figure 6-16 $I_{(HTCS)} (CCS_{(std)}) / I_{(HTCS)} (flat\ roof) \%$

Fig. (6-16) depicts that there is clear difference between the $I_{(HTCS)}$ -mirrored-values in the early morning and in the late afternoon. This difference becomes difficult to notice around the noon period. The percentage of the received $I_{(HTCS)}$ on the $CCS_{(std)}$ to that on the flat roof records its maximum at 07:00 (208%). This means that during the early morning, the $CCS_{(std)}$ receives more than double of the received $I_{(HTCS)}$ on the flat roof. This is may be preferable in winter, where the minimum percentage of the received $I_{(HTCS)}$ on the $CCS_{(std)}$ to that on the flat roof (66.1%) is recorded at 15:00 instead of the midday as in summer.

On the daily average bases, the $CCS_{(std)}$ receives about 79.4% of the received $I_{(HTCS)}$ -values on the flat roof. On the other hand, this ratio fits approximately in the middle between the ratios of the two principal facing directions (N-S) and (E-W) in winter, (83.3% & 78.6% respectively), the same as the $CCS_{(std)}$ main axis (NE-SW) lies in the middle between the two principal directions. In terms of receiving more $I_{(HTCS)}$ in winter, it is preferable for the $CCS_{(std)}$ curvature to face (NW-SE) rather than facing (E-W). While, the (N-S)-facing direction is more preferable for the $CCS_{(std)}$ in winter compared with any other facing directions.

6.3.2 $CCS_{(std)}$ Curvature Faces **NORTHEAST** and **SOUTHWEST**

This is the second secondary orientation that the study employs. In this case, the longitudinal axis (*perpendicular on the CCS*) is the (NW-SE) axis. The two halves of the $CCS_{(std)}$ face NE and SW. This case is tested during summer and winter in order to clarify the curved roof solar performance throughout the year compared to the flat roof.



6.3.2.1 $CCS_{(std)}$ Faces (NE-SW) During June

Fig. (6-17) shows $I_{(HTCS)}$ -values and distribution forms on a flat roof and a $CCS_{(std)}$ facing (NE-SW) in summer. This is an identically inverted scenario of the previous secondary direction (NW-SE), in which all features and analyses are inversed around the midday axis, (*refer to Fig. (6-13)*). Therefore, the maximum received solar radiation on both roofs takes place at midday. The flat roof has a symmetrical $I_{(HTCS)}$ -curve around the midday axis, whereas the $CCS_{(std)}$ has unsymmetrical $I_{(HTCS)}$ -curve. The same as the first secondary orientation, the $CCS_{(std)}$ $I_{(HTCS)}$ -mirrored-values around the midday axis are not equal.

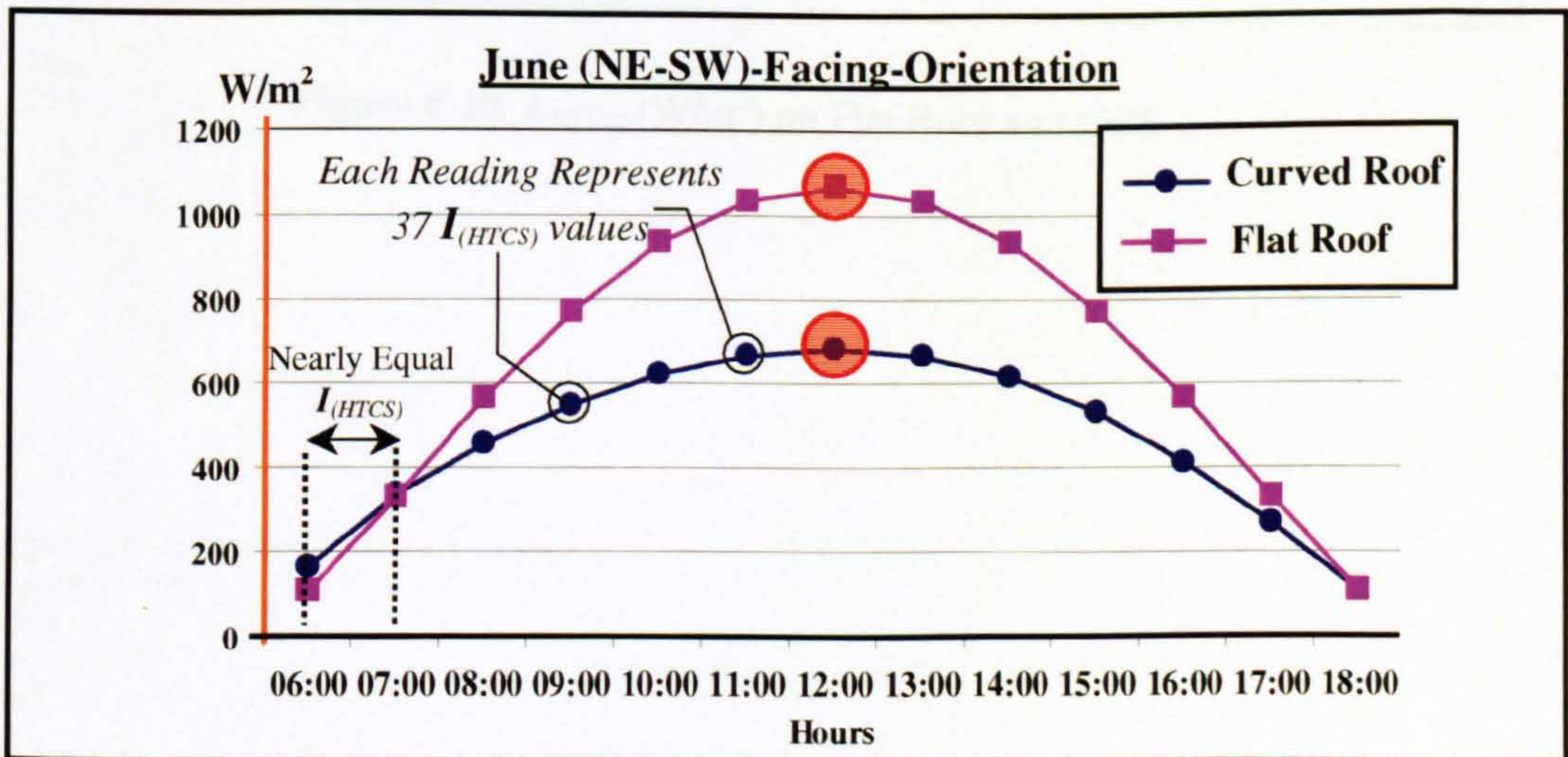


Figure 6-17 $I_{(HTCS)}$ (W/m²) on Flat Roof and $CCS_{(std)}$

In summer, the proportional comparison between the $I_{(HTCS)}$ -values on the $CCS_{(std)}$ and the flat roof at (NE-SW) is an inverted scenario of (NW-SE) (*refer to Fig.(6-14)*). Therefore, the daily average ratios are the same at the both secondary directions.

6.3.2.2 $CCS_{(std)}$ Faces (NE-SW) During December

The same as in summer, Fig. (6-18) shows that the winter scenario of the second secondary direction (NE-SW) is identically inversed of the first one, (NW-SE), *Refer to Fig. (6-15)*. The proportional comparison between the $I_{(HTCS)}$ -values on the $CCS_{(std)}$ and to that on the flat roof is the inverted scenario of the first secondary direction (NW-SE) (*refer to Fig.(6-16)*). In winter, the daily average ratios are the same at both secondary directions.

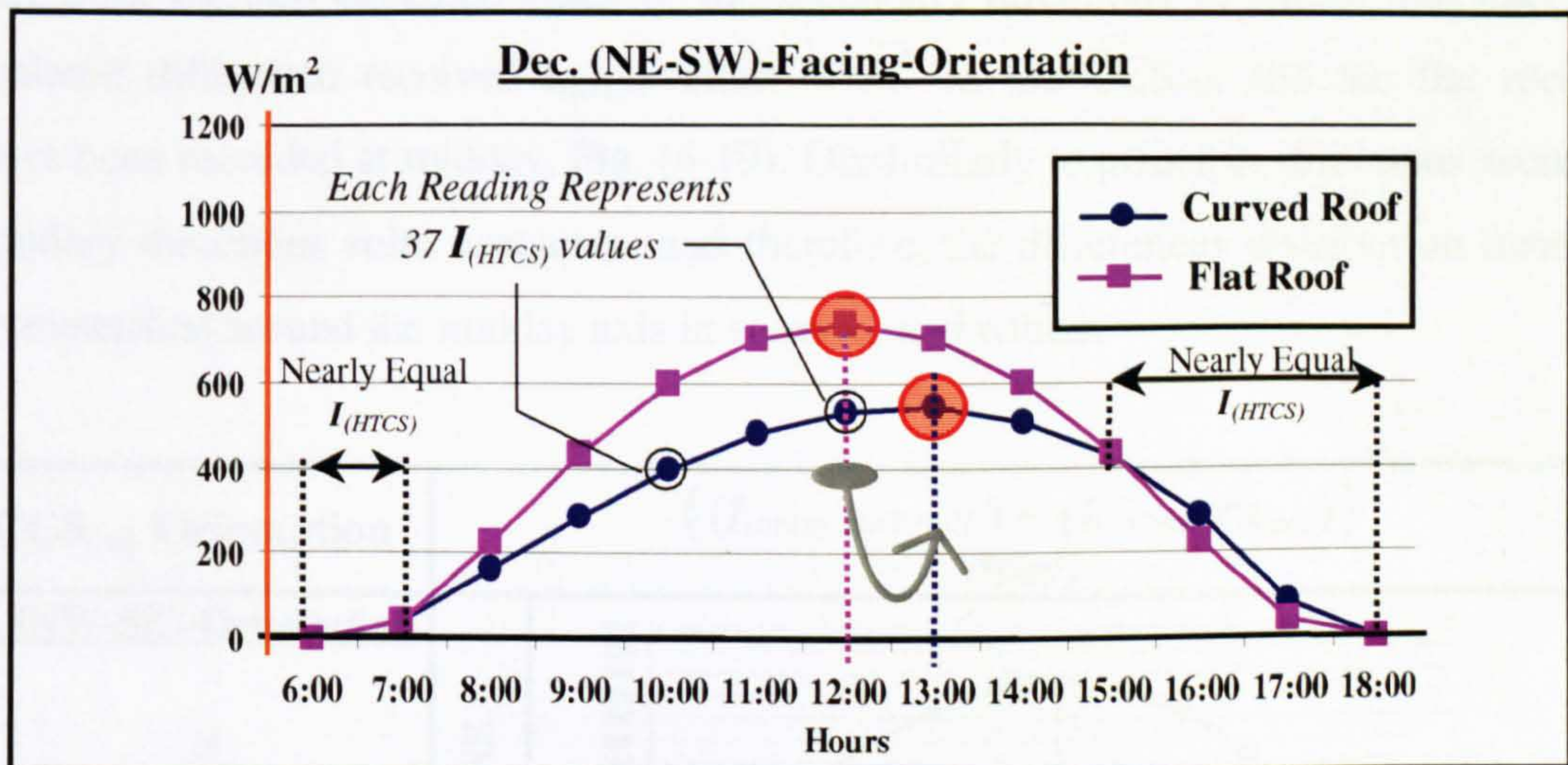


Figure 6-18 $I_{(HTCS)}$ (W/m²) on Flat Roof and $CCS_{(std)}$

6.3.3 The Calculated Difference Between $I_{(HTCS)}$ on Flat Roof and $I_{(HTCS)}$ on $CCS_{(std)}$ Faces Secondary-Directions (NW-SE) & (NE-SW)

Fig. (6-19) compares the calculated difference between the received $I_{(HTCS)}$ -values on the $CCS_{(std)}$ and the flat roof throughout summer day and winter day. Seasonal variation and roof orientation are the comparison factors. The previous proportional comparisons and in particular the generated percentage accurately figures the solar efficiency of the $CCS_{(std)}$. Apart from the two excepted cases of the secondary directions in winter, the maximum calculated difference received $I_{(HTCS)}$ -values W/m^2 on the $CCS_{(std)}$ and the flat roof has always been recorded at midday, Fig. (6-19). Dissimilarly to principle directions scenarios, secondary directions solar scenarios, and therefore, the differences distribution forms are unsymmetrical around the midday axis in summer and winter.

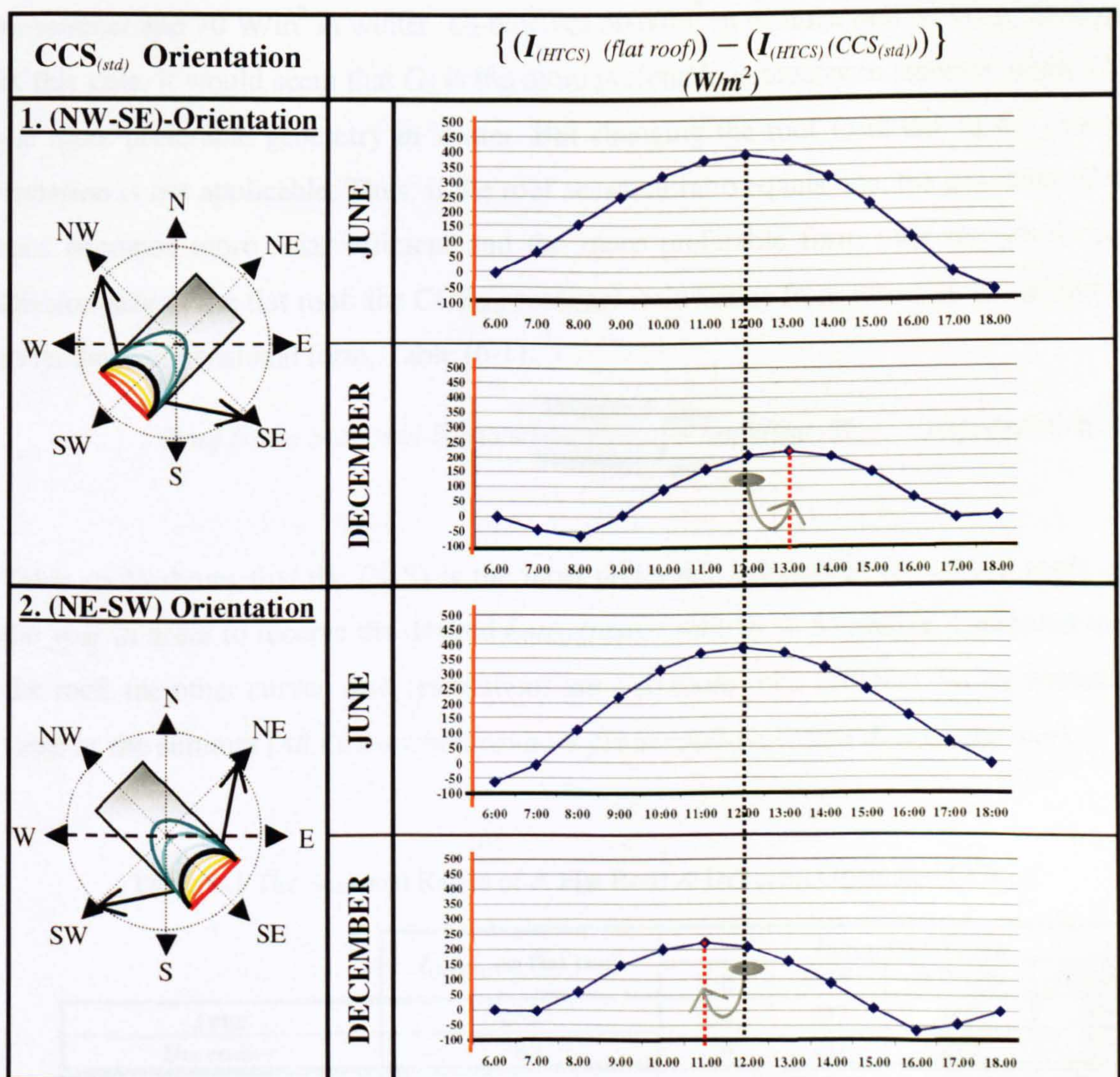


Figure 6-19 The Difference Between $I_{(HTCS)}$ on Flat Roof and $CCS_{(std)}$

6.4 FORM SEASONAL RATIO

(Ratio Between The Received Day-Average $I_{(HTCS)}$ on Roof in Summer to that Received in Winter)

It is expected that any roof geometry receives less $I_{(HTCS)}$ in winter compared to summer, whereas it is preferable to receive as much solar radiation as possible during winter. This part of the empirical study points out the difference between the flat and curved roofs seasonal behaviours, which are articulated by the roof geometry seasonal ratio. Roof form-seasonal-ratio means the ratio between the $I_{(HTCS)}$ -day average on this roof in winter to that in summer. This form seasonal ratio will be examined at every principal and secondary orientation. This ratio figures out the roof geometry that can significantly minimise the received $I_{(HTCS)}$ on roof surface only during summer and do not act similarly in winter.

For example, G_1 & G_2 , are two different surface geometries, where G_1 receives 100W/m^2 in summer and 70 W/m^2 in winter. G_2 receives 50W/m^2 in summer and 40 W/m^2 in winter. In this case, it would seem that G_2 is the more preferable geometry in summer, while G_1 is the more preferable geometry in winter. But changing the roof form due to the seasonal variation is not applicable. Thus, if the roof seasonal ratio equals one, the geometry of this roof becomes more solar efficient and the more preferable form over the whole year. Dissimilarly to the flat roof, the $\text{CCS}_{(std)}$ seasonal-ratio varies from direction to another due to its three-dimensional form, Table (6-1).

$$\text{Roof Form Seasonal-Ratio} = \frac{\text{Winter } I_{(HTCS)}}{\text{Summer } I_{(HTCS)}} \text{ W/m}^2 \% \quad \text{Equation 6-2[2]}$$

Table (6-1) shows that the (N-S) is the most preferable orientation for curved roofs over the year in order to receive the desired $I_{(HTCS)}$ (nearer ratio to 1). Moreover, compared to the flat roof, the other curved roof orientations are also more solar efficient during winter, the same as the summer (All CCS orientations have greater seasonal ratios than the flat roof).

Table 6-1 The Seasonal Ratios of A Flat Roof & Different Orientated $\text{CCS}_{(std)}$

	$I_{(HTCS)}$ on flat roof	$I_{(HTCS)}$ on $\text{CCS}_{(std)}$			
		N-S	E-W	NW-SE	NE-SW
June	659	437	497	469	469
December	365	304	287	290	290
Form Seasonal Ratio%	55.4%	69.6%	57.7%	61.8%	61.8%

In this context, Fig. (6-20) illustrates the day average of the received $I_{(HTCS)}$ on the $CCS_{(std)}$ and that received on the flat roof at different principle and secondary orientations. Each graph compares between the summer differences and the winter differences of the received $I_{(HTCS)}$ on both roof geometries at each orientation. The winter differences are always less than the summer ones, which indicates that the influence of the curved form on the received $I_{(HTCS)}$ is significant in summer only. The graphs in Fig. (6-20) also verify that curved roof form is more solar efficient in winter compared to the flat roof due to the curved roof form-seasonal-ratio, which is nearer to 1. Moreover, the form-seasonal-ratio of the $CCS_{(std)}$ faces secondary direction (*NW-SE or NE-SW*) is near to 1 compared to the same geometry when it faces the second principle direction (*E-W*).

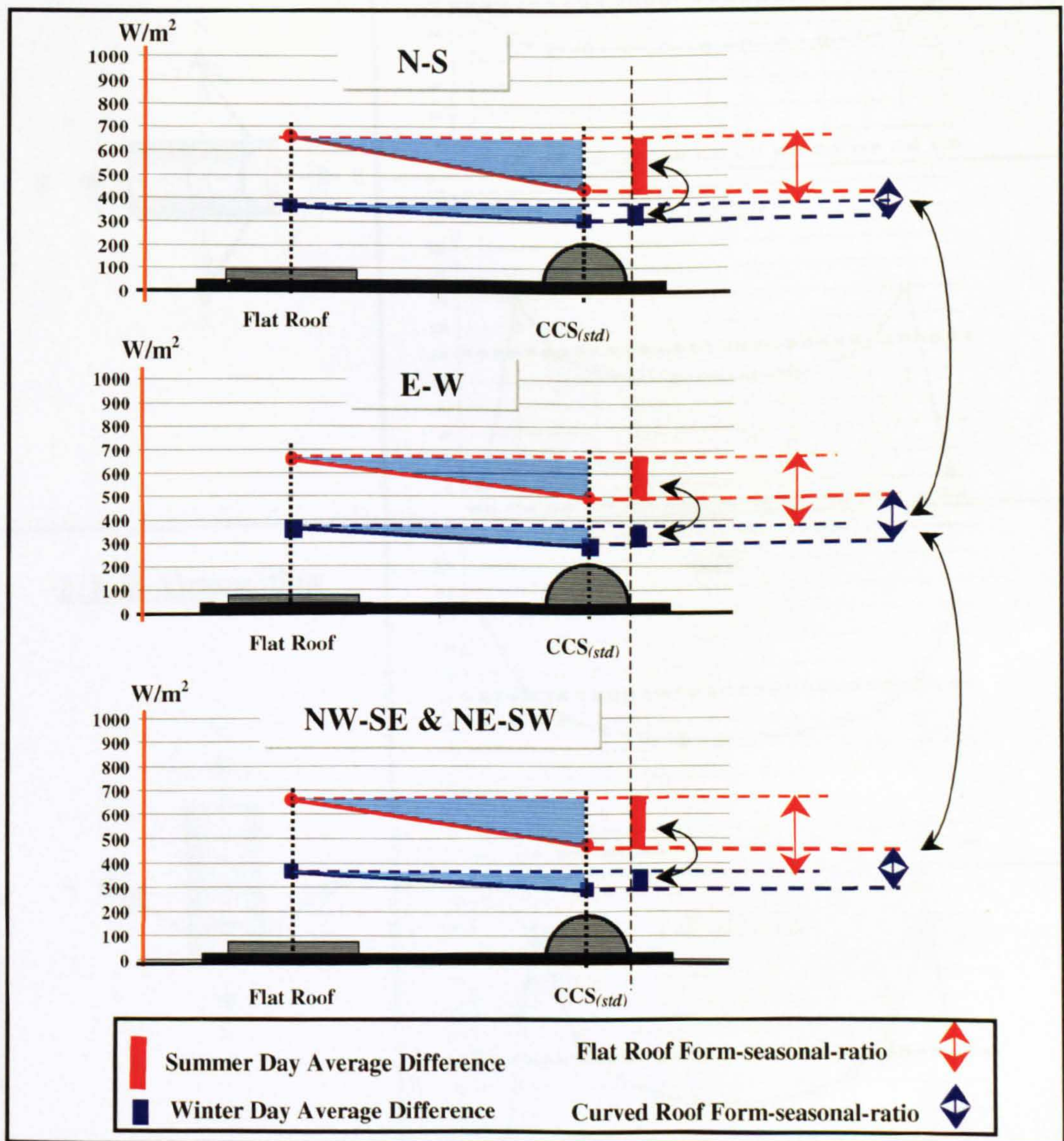


Figure 6-20 The received $I_{(HTCS)}$ Day Average on the $CCS_{(std)}$ and The Flat Roof at Different Orientations.

6.5 THE HOURLY RATIO BETWEEN $I_{(HTCS)}$ ON $CCS_{(std)}$ AND $I_{(HTCS)}$ ON FLAT ROOF

Fig. (6-21) and (6-22) illustrate the ratio percentage (%) between the received $I_{(HTCS)}$ on $CCS_{(std)}$ and that on flat roof at each hour throughout the day. Fig. (6-21) compares between the summer and winter ratios at both principle orientations (*N-S*) and (*E-W*). As expected, the ratios distribution forms are symmetrical around the midday axis for both principle directions in summer and winter.

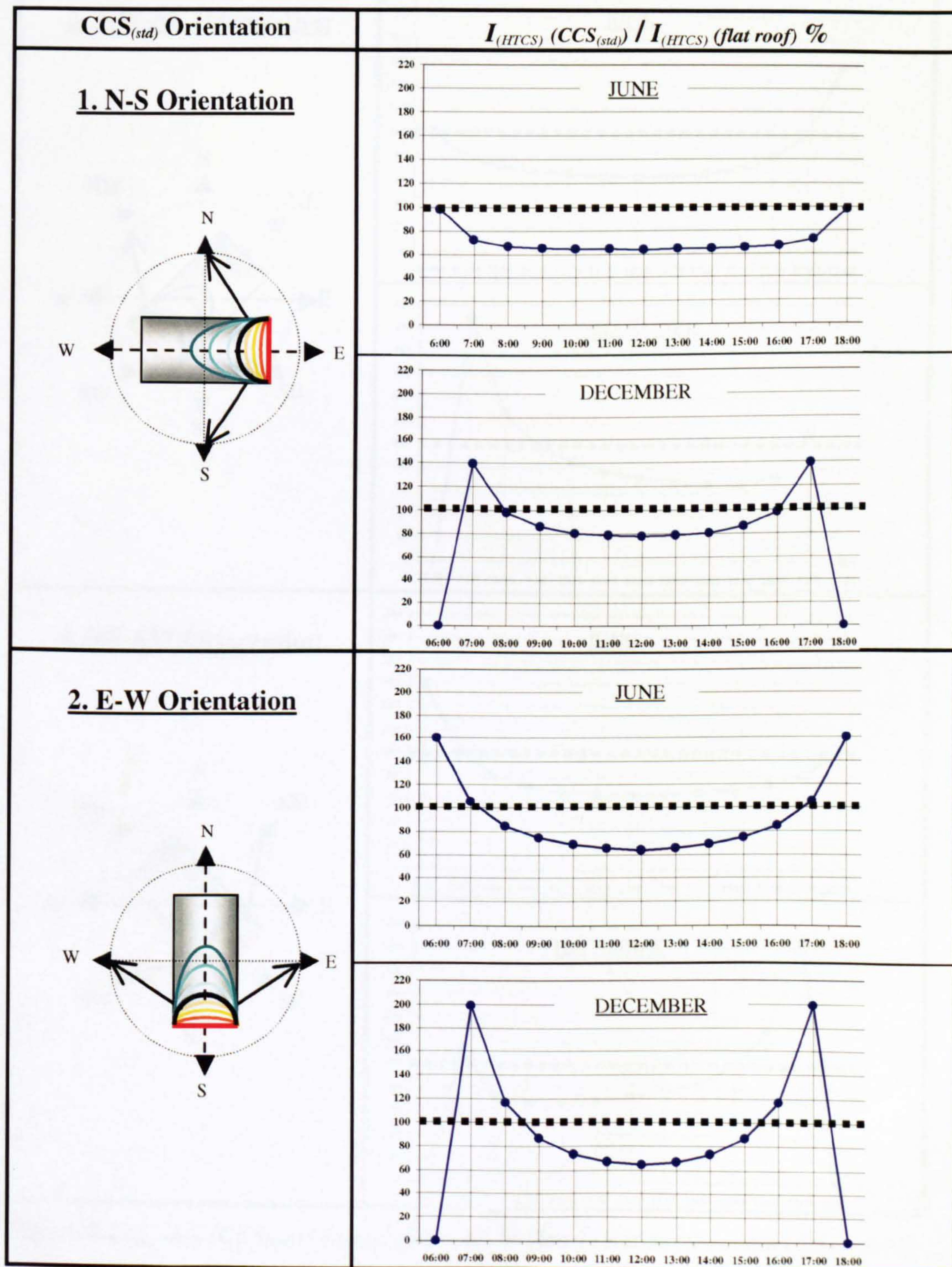


Figure 6-21 $I_{(HTCS)} (CCS_{(std)}) / I_{(HTCS)} (flat\ roof) \%$ Hourly Ratios (Principle Directions)

Fig. (6-22) compares between the summer and winter ratios when curved roof curvatures face secondary directions (N-S) and (E-W). Similar to all solar findings and results of secondary direction, the ratios distribution forms in Fig. (6-22) are unsymmetrical around the midday axis for both secondary directions in summer and winter. Each season scenario is inverted symmetrically in comparison to the other secondary direction.

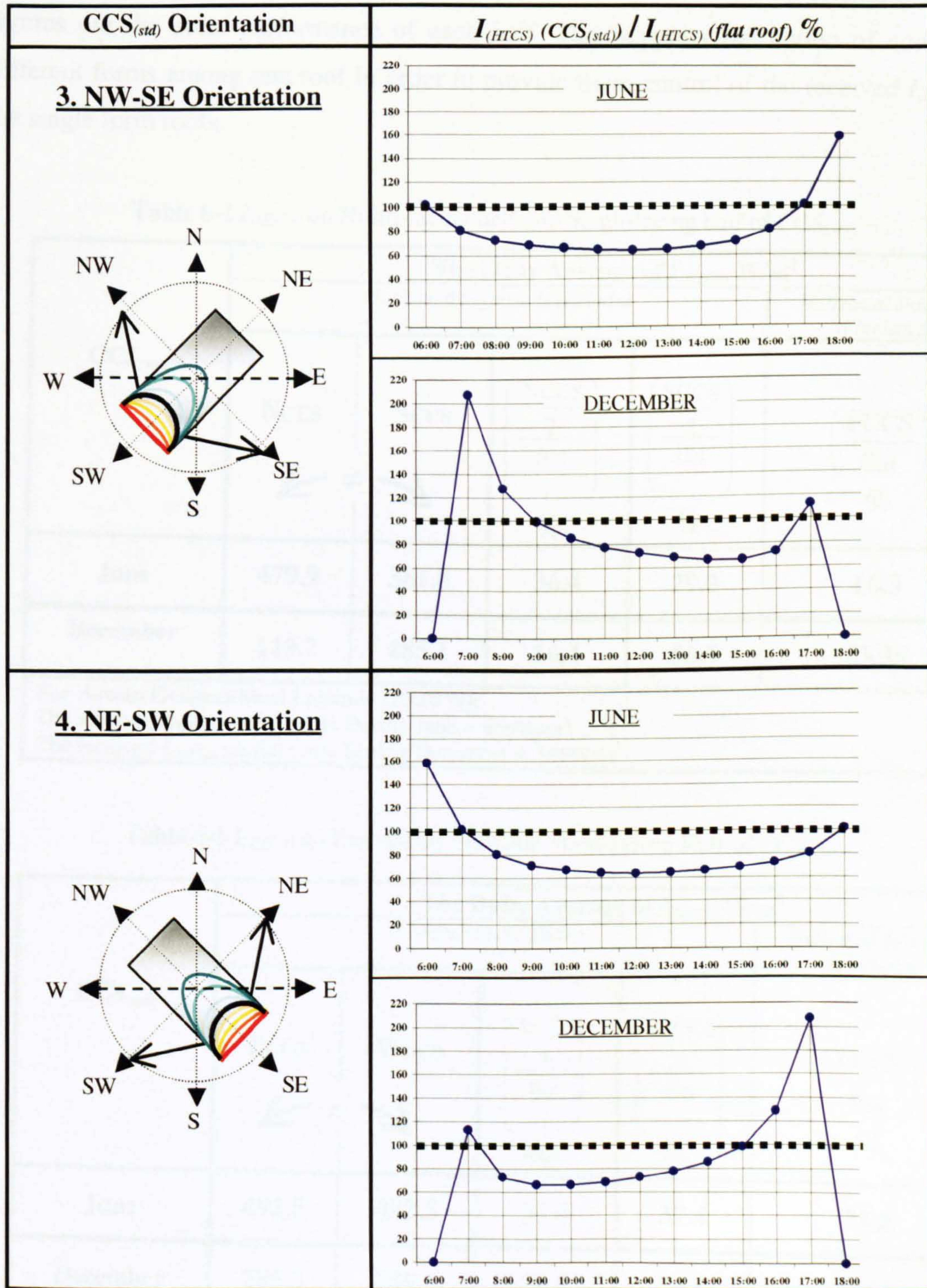


Figure 6-22 $I_{(HTCS)}(CCS_{(std)}) / I_{(HTCS)}(flat\ roof) \%$ Hourly Ratios (Secondary Directions)

6.6 THE SOLAR PERFORMANCE OF A HALF CURVED ROOF (*Half-CCS_(std)*)

It has been found out that curved roofs receive significantly less solar radiation than flat roofs due to their geometrical configurations (*from and orientation*). At every principle and secondary direction, Tables (6-2), (6-3), (6-4), & (6-5) calculate the received $I_{(HTCS)}$ on each half of the full $CCS_{(std)}$. The $I_{(HTCS)}$ on each half is a function of its facing orientation, and it figures out the solar performance of each half. This supports the notion of combining different forms among one roof in order to provide more control of the received $I_{(HTCS)}$ on the single form roofs.

Table 6-2 $I_{(HTCS)}$ on North-facing half and South-facing half of $CCS_{(std)}$

$CCS_{(std)}$	The Daily Average of $I_{(HTCS)}$ W/m^2				
	Horizontal Segment is Excluded				Horizontal Segment is Included
	NCCS	SCCS	$\left(\frac{NCCS}{2}\right)$ flat %	$\left(\frac{SCCS}{2}\right)$ flat %	$\left(\frac{FCCS}{flat}\right)$ %
	← ≠ →				
June	479.9	381.8	36.4	29.0	66.3
December	119.7	485.1	16.4	66.5	83.38
For Aswan Geographical Latitude (23.58°N): The received $I_{(HTCS)}$ on flat roofs During June = 659W/m ² The received $I_{(HTCS)}$ on flat roofs During December = 365W/m ²					

Table 6-3 $I_{(HTCS)}$ on East-facing Half and West-facing Half of $CCS_{(std)}$

$CCS_{(std)}$	The Daily Average of $I_{(HTCS)}$ W/m^2				
	H Segment is Excluded				Horizontal Segment is Included
	ECCS	WCCS	$\left(\frac{ECCS}{2}\right)$ flat %	$\left(\frac{WCCS}{2}\right)$ flat %	$\left(\frac{FCCS}{flat}\right)$ %
	← = →				
June	492.5	492.5	37.4	37.4	75.4
December	285.3	285.3	39.1	39.1	78.6
For Aswan Geographical Latitude (23.58°N): The received $I_{(HTCS)}$ on flat roofs During June = 659W/m ² The received $I_{(HTCS)}$ on flat roofs During December = 365W/m ²					

Table 6-4 $I_{(HTCS)}$ on Northwest-facing Half and Southeast-facing Half of $CCS_{(std)}$

$CCS_{(std)}$	The Daily Average of $I_{(HTCS)}$ W/m ²				
	<i>H Segment is Excluded</i>				<i>Horizontal Segment is Included</i>
	NWCCS ← ≠ →	SECCS	$\left(\frac{NWCCS}{2}\right)$ flat %	$\left(\frac{SECCS}{2}\right)$ flat %	$\left(\frac{CCS}{flat}\right)$ %
June	489.9	437.4	37.2	33.2	71.2
December	159.1	416.3	22.0	57.0	79.5

For Aswan Geographical Latitude (23.58°N):
 The received $I_{(HTCS)}$ on flat roofs During June = 659W/m²
 The received $I_{(HTCS)}$ on flat roofs During December = 365W/m²

Table 6-5 $I_{(HTCS)}$ on Northeast-facing Half and Southwest-facing Half of $CCS_{(std)}$

$CCSR_{(std)}$	The Daily Average of $I_{(HTCS)}$ W/m ²				
	<i>H Segment is Excluded</i>				<i>Horizontal Segment is Included</i>
	NECCS ← ≠ →	SWCCS	$\left(\frac{NECCS}{2}\right)$ flat %	$\left(\frac{SWCCS}{2}\right)$ flat %	$\left(\frac{CCS}{flat}\right)$ %
June	489.9	437.4	37.2	33.2	71.16
December	159.1	416.3	22.0	57.0	79.45

For Aswan Geographical Latitude (23.58°N):
 The received $I_{(HTCS)}$ on flat roofs During June = 659W/m²
 The received $I_{(HTCS)}$ on flat roofs During December = 365W/m²

6.7 CONCLUSIONS

SRSM [3] produced valuable predictions with accurate procedures calculating the total clear sky intensity of solar radiation on the semicircular curved roof (initial case $CCS_{(std)}$), in which $CCSR$ always equals 1 ($A = B$). At the same geographical latitude, *SRSM* results showed that the ratio between the received solar radiation amount (W/m^2) by flat roof differs significantly from that received by sloped surfaces which resemble the form of a curved roof.

By testing the same $CCSR$ at different orientations, the parametrical study and *SRSM* have highlighted the magnitude of CCS orientation to control the received solar radiation intensity. It has been noticed that the calculated solar radiation amount on one planar segment varies significantly if either its slope angle or orientation has been slightly changed. At all principal-directions, solar radiation readings, $I_{(HTCS)}$ -values, and consequently the resulted difference due to the geometrical configurations are exactly identical around the midday-axis. $I_{(HTCS)}$ -curves for any geometry are exactly symmetrical around the midday axis. In both summer and winter, regardless to the roof geometry, $I_{(HTCS)}$ -peaks are recorded at midday.

Despite testing only one curvature (*invariable CCSR in this chapter*), it can be concluded that the generated reductions in the $I_{(HTCS)}$ -values and their distribution forms on the two tested roofs keep varying from one case to another due to $CCS_{(std)}$ orientation and seasonal variation. It is also clearly noticed that $I_{(HTCS)}$ -curves and their shapes are always symmetrical around the midday axis. Moreover, regardless of roof forms and relevant to the sun position at midday in summer, which is almost perpendicular to geographical latitudes near the equator ($23.58^\circ N$), both roofs $I_{(HTCS)}$ -values at the two principal orientations are identical during midday.

The low position of the sun in winter increase the orientation influences on the received $I_{(HTCS)}$ as long as the tested geometry has three-dimensional form or height. On the daily average basis, the (N-S)-facing-orientation seems to be the more energy-efficient in terms of making the $CCS_{(std)}$ receives 66.3% of the received $I_{(HTCS)}$ on the flat roof. Whereas, the (E-W)-facing $CCS_{(std)}$ receives 75.4% of that received on the flat roof .

Excluding the flat roof, $I_{(HTCS)}$ -values and other generated results are not identical around midday in secondary-directions. The $I_{(HTCS)}$ -curve for any geometry except the flat roof is not exactly symmetrical around the midday axis. Secondary directions showed that both roofs $I_{(HTCS)}$ -peaks are recorded at midday only during summer. In winter, only the flat roof $I_{(HTCS)}$ -peak is recorded at midday, whereas the $CCS_{(std)}$ $I_{(HTCS)}$ -peaks are recorded variably at different hours either before or after midday. Table (6-6) illustrates the percentages of the received day average $I_{(HTCS)}$ on different oriented $CCS_{(std)}$ to the flat roof during summer and winter. The table may help figuring out the more preferable form and orientation for curved roofs according to the geographical latitude and the desired solar intensity.

Table 6-6 The Ratio Between The Received $I_{(HTCS)}$ on $CCS_{(std)}$ and Flat Roof

Roof Geometry		Day Average $I_{(HTCS)}$ W/m ²		$\frac{I_{(HTCS)} CCS_{(std)}}{I_{(HTCS)} \text{ Flat Roof}}$ %	
		June	Dec.	June	Dec.
Flat Roof		659	365		
CCS _(std)	N-S	437	304	66.3	83.3
	E-W	497	287	75.4	78.6
	NW-SE	469	290	71.1	79.4
	NE-SW	469	290	71.1	79.4

In the next chapter, the received $I_{(HTCS)}$ on seven different curved-roof curvatures ($CCSR$) in order to find out the influence of curved-roof curvature on the received $I_{(HTCS)}$. To create more accurate geometrical resemblance and solar findings, solar investigations along the seven $CCSR$ will be applied on 19 and 37-joint-segments instead of the $CCS_{(std)}$ 37 tangent-segments. The following measurements exemplify the framework done in this chapter and the following chapters:

1. Each curved roof curvature solar behaviour, (*Eight extended curved roof cross-section ratios CCSR, vaulted roofs*) and three rotating $CCSR$ (*domed roofs*).
2. Hourly and day-average solar performances of each curved roof form curvature and orientation.
3. Solar comparisons between the received $I_{(HTCS)}$ on flat and different curved roof forms curvatures and orientations.

Reference List

1. "SRSM" Solar Radiation Simulation Model for Quick Basic, Exell, R. H. B., Regional Energy Resources Information Centre, Asian Institute of Technology, Bangkok. <http://www.jgsee.kmutt.ac.th/exell/Solar/SolradJS.htm>
2. Elseragy, A. A. and Gadi, M. B. Roof Geometric Forms and Solar Irradiation Intensity In Hot-Arid Climates Proceeding of the ISES Solar World Congress 2003, ISES 2003, Solar Energy for a Sustainable Future 2003. Jun 19-14-2003; Svenska Mässan Congress Centre, Göteborg, Sweden.
3. Exell, R. H. B. A program in BASIC for calculating solar radiation in tropical climates on small computers. Renewable Energy Review Journal, Dec., 1986; Vol. 8 (No. 2).

CHAPTER 7

SOLAR BEHAVIOUR OF FLAT AND VAULTED ROOFS WITH DIFFERENT CURVATURES AND ORIENTATIONS

(19 & 37 Planar Joint-Segments)

7. SOLAR BEHAVIOUR OF FLAT AND VAULTED ROOFS WITH DIFFERENT CURVATURES AND ORIENTATIONS

In the previous chapter, the solar performance of the semicircular curved roof cross section $CCS_{(std)}$ has been discussed in order to measure the solar performance of curved roof form and orientation. A comparison between the received solar radiation on the external surfaces of the $CCS_{(std)}$ to that received on flat roof was discussed in Chapter 6. In the same context, this chapter investigates the received $I_{(HTCS)}$ on different seven curved roof curvatures (CCSR). It compares the received $I_{(HTCS)}$ on seven CCSR and the $CCS_{(std)}$ to that received on the flat roof. Instead of the $CCS_{(std)}$ thirty seven tangent segments, each CCS in this chapter has been resembled by 19 joint-segments.

Solar investigations along the same seven curvatures CCSR are applied in this chapter using 37-joint-segments in order to generate more accurate resemblance and solar findings[2]. At the end of this chapter, a graphical comparison between the generated results from the both tests (*19 and 37 resembling joint segments*) is presented in order to validate the generated results from the nineteen joint segments.

For circles or semicircles, any tangent is always perpendicular to a radius that intersects the circle at a tangent point. Therefore, the same radius may generate tangent segment at each CCSR. This creates tangents with the same slope angle along the radius. Moreover, the same tilted radius cannot generate accurate tangents for all CCSR. Furthermore, if the tested curve is not a part of a full circle, only perpendiculars on the main radiuses (*A & B*) can form tangent segments as in the ellipse cases, Fig. (7-1). In this context, tangent segments cannot be applied with varying curvatures CCS as the case discussed in this chapter. This chapter tested CCSR, where *A* is not always equal *B* (*i.e. A=B, A>B, & A<B*), are geometrically resembled by joint-planar-segments instead of tangent ones.

As it has been explained previously in Chapter 5, the term “curvature” has been used to identify curved-roof’s extent of concavity “profile”. This means that different curved-roof cross sections are determined by span-to-height-ratio (*A: B*). Therefore, this chapter CCS with different *A-to-B-ratios* are only generated from circles and ellipses, which can be determined only by two radii *A* and *B* as shown in Fig. (5-25).

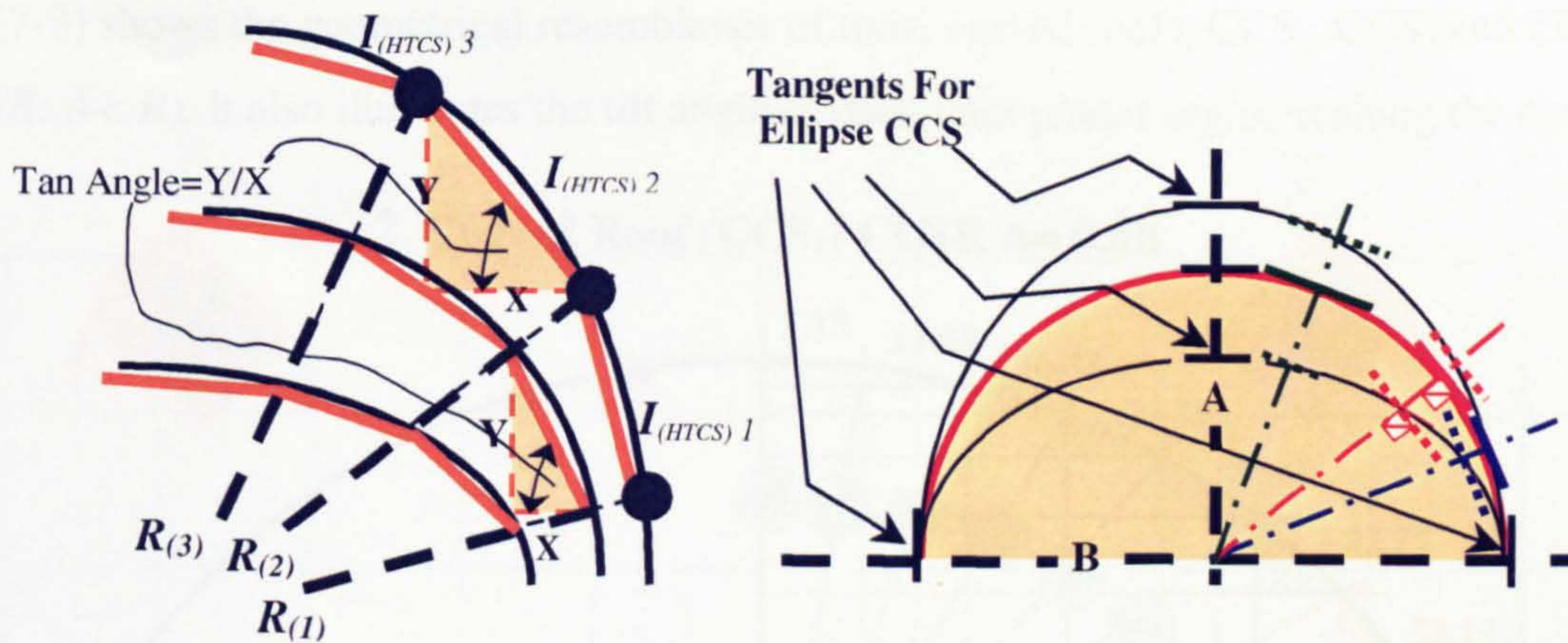


Figure 7-1 Tangent Segment is not Applicable For The Ellipse CCSR (where $A \neq B$)

Regardless of the CCSR, the seven CCS must be resembled similarly and invariably. This means that the number of the employed radial-lines and their slope angles must be stabilised in all tested CCSR as shown in Fig. (7-1).

7.1 DATA INPUT AND CURVED ROOFS GEOMETRICAL RESEMBLANCE

Different Curved Roof Curvatures (Varying CCSR; $CCSR_1 - CCSR_7$) (19 Joint Segments)

The following figures show the geometrical resemblance of seven CCSR using the joint segments technique. Each half-CCS has been resembled by nine joint segments in addition to the horizontal one at the middle-top of the curve. Fig. (7-2) shows the geometrical resemblance of the first curved roof CCS_1 , which is a semicircular CCS ($CCSR: A=B$).

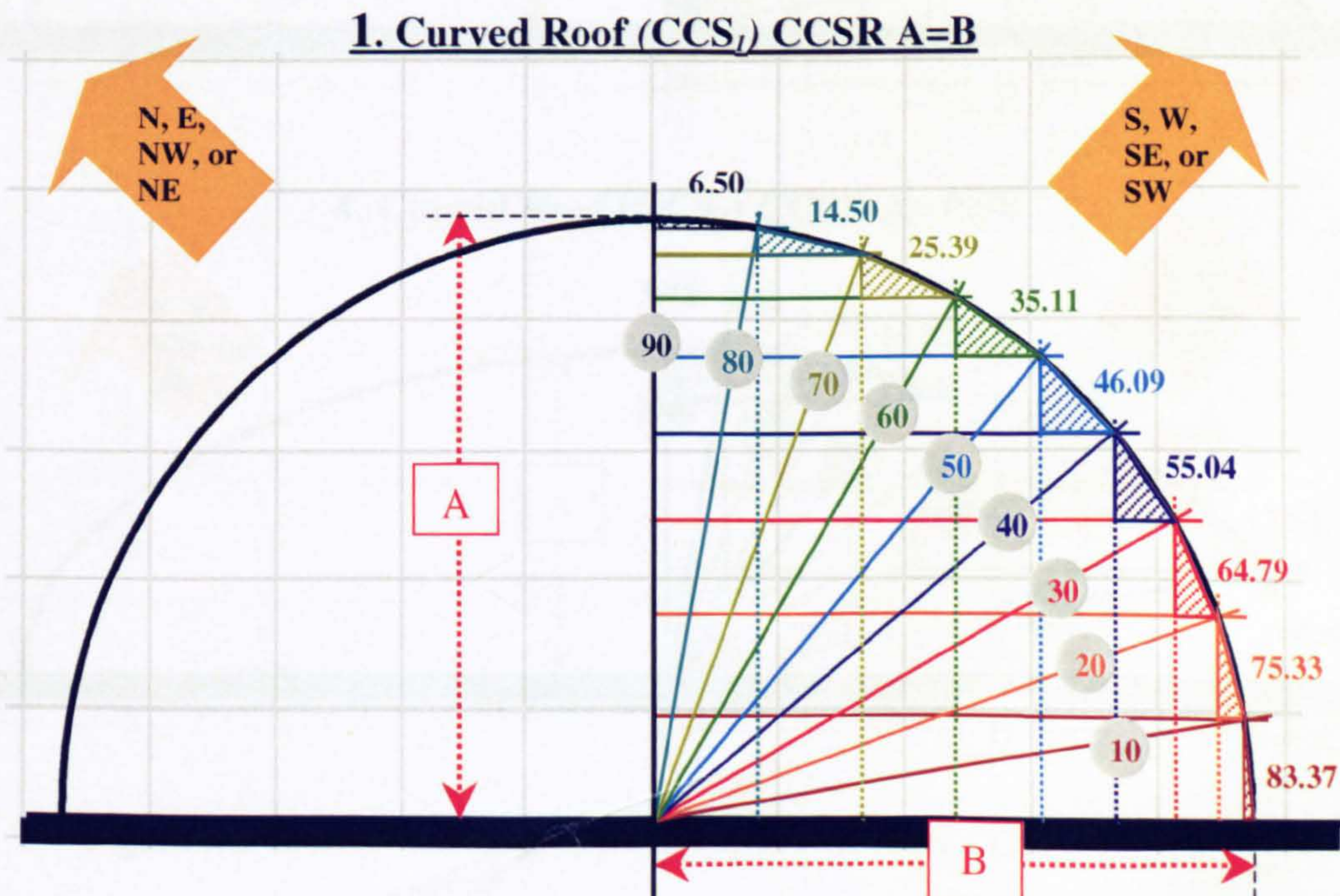


Figure 7-2 Geometrical Resemblance of CCS_1 ($CCSR: A = B$)

Fig. (7-3) shows the geometrical resemblance of three curved roofs, CCS_2 , CCS_3 and CCS_4 . ($CCSR: A < B$). It also illustrates the tilt angle of each joint planar segment along the curve.

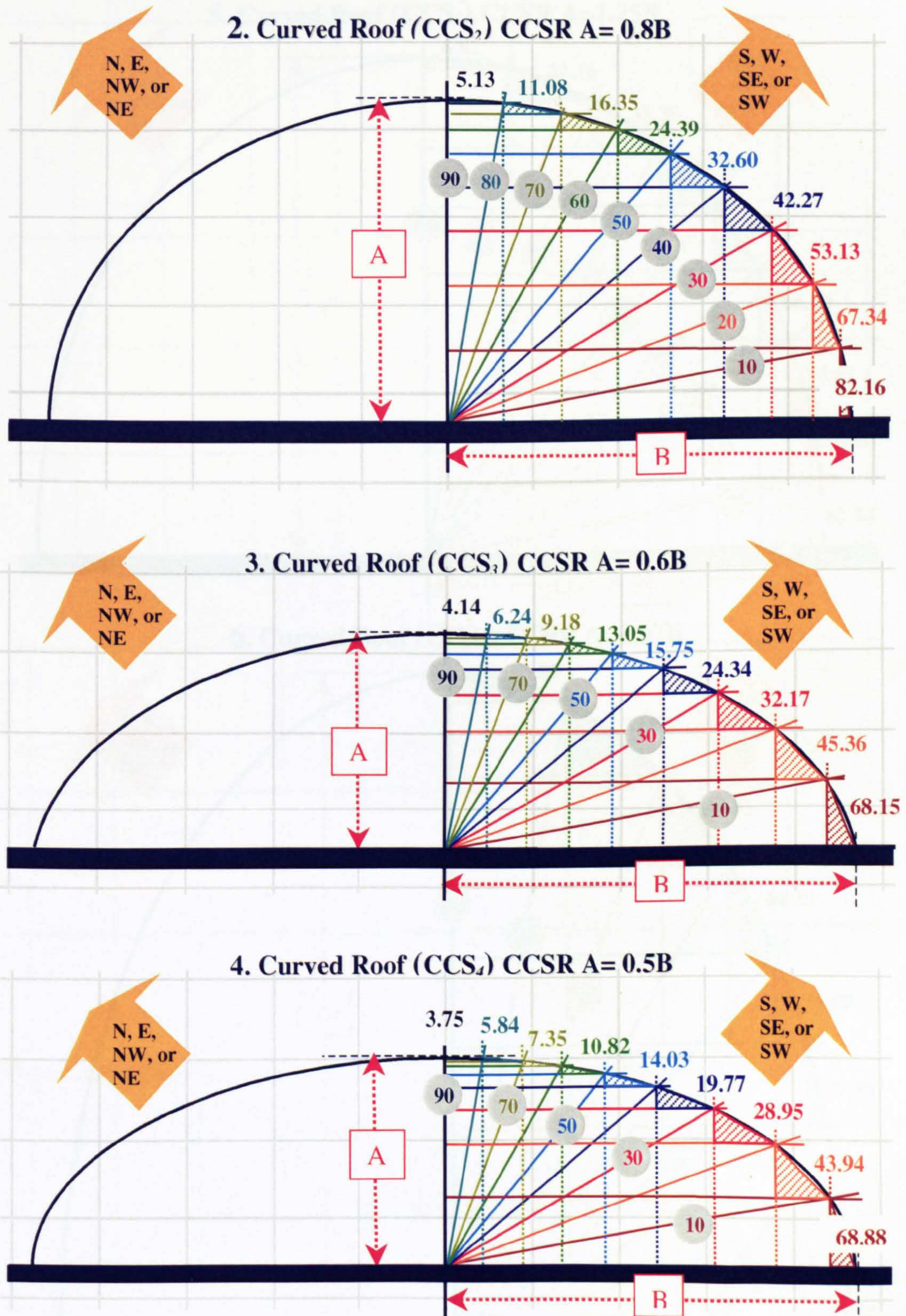


Figure 7-3 Geometrical Resemblance of CCS_2 , CCS_3 , & CCS_4 ($CCSR: A < B$)

Fig. (7-4) and (7-5) show the geometrical resemblance of CCS_5 , CCS_6 and CCS_7 ($CCSR: A > B$) and each joint planar segment tilt angle along the curve.

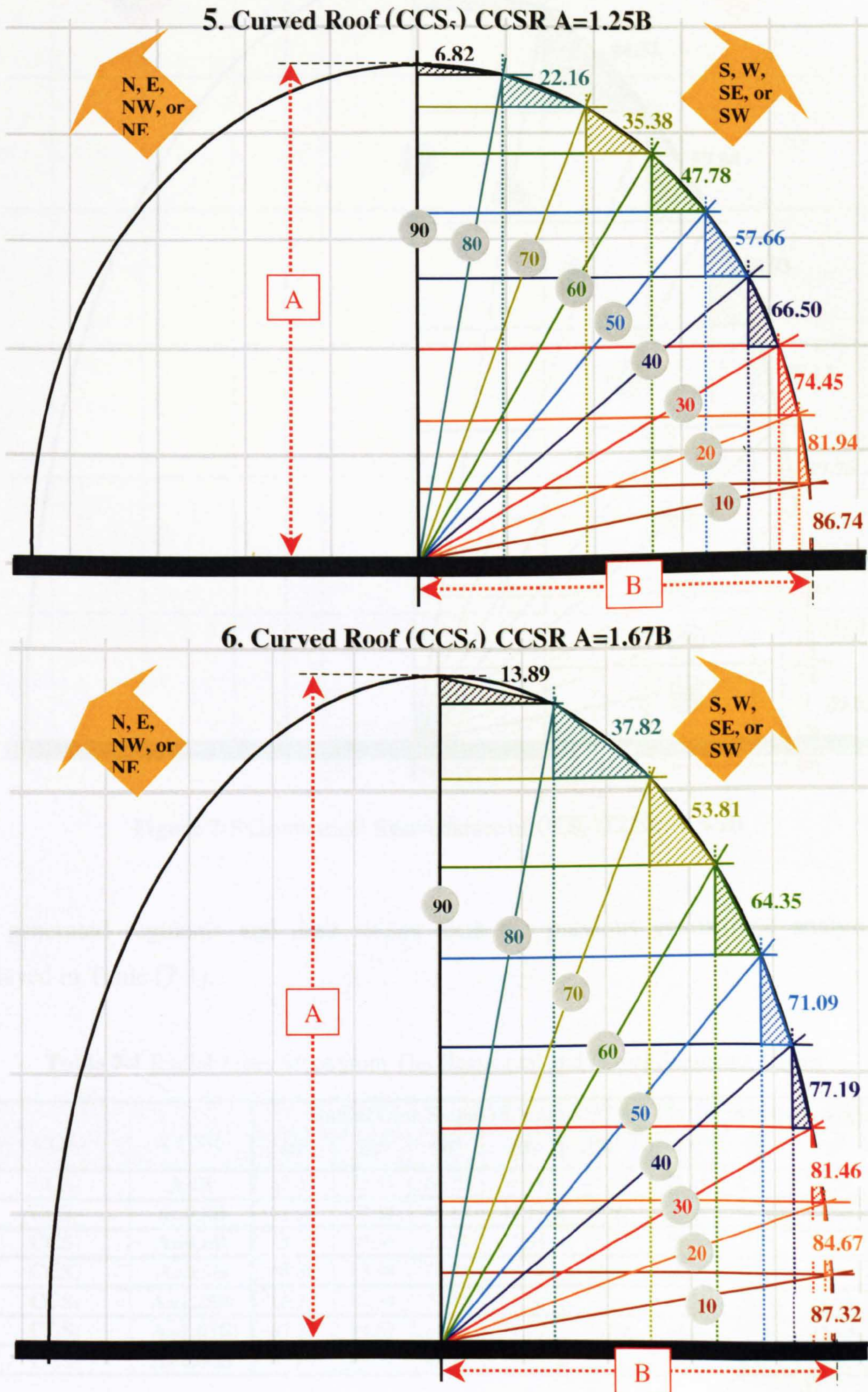


Figure 7-4 Geometrical Resemblance of CCS_5 & CCS_6 ($CCSR: A > B$)

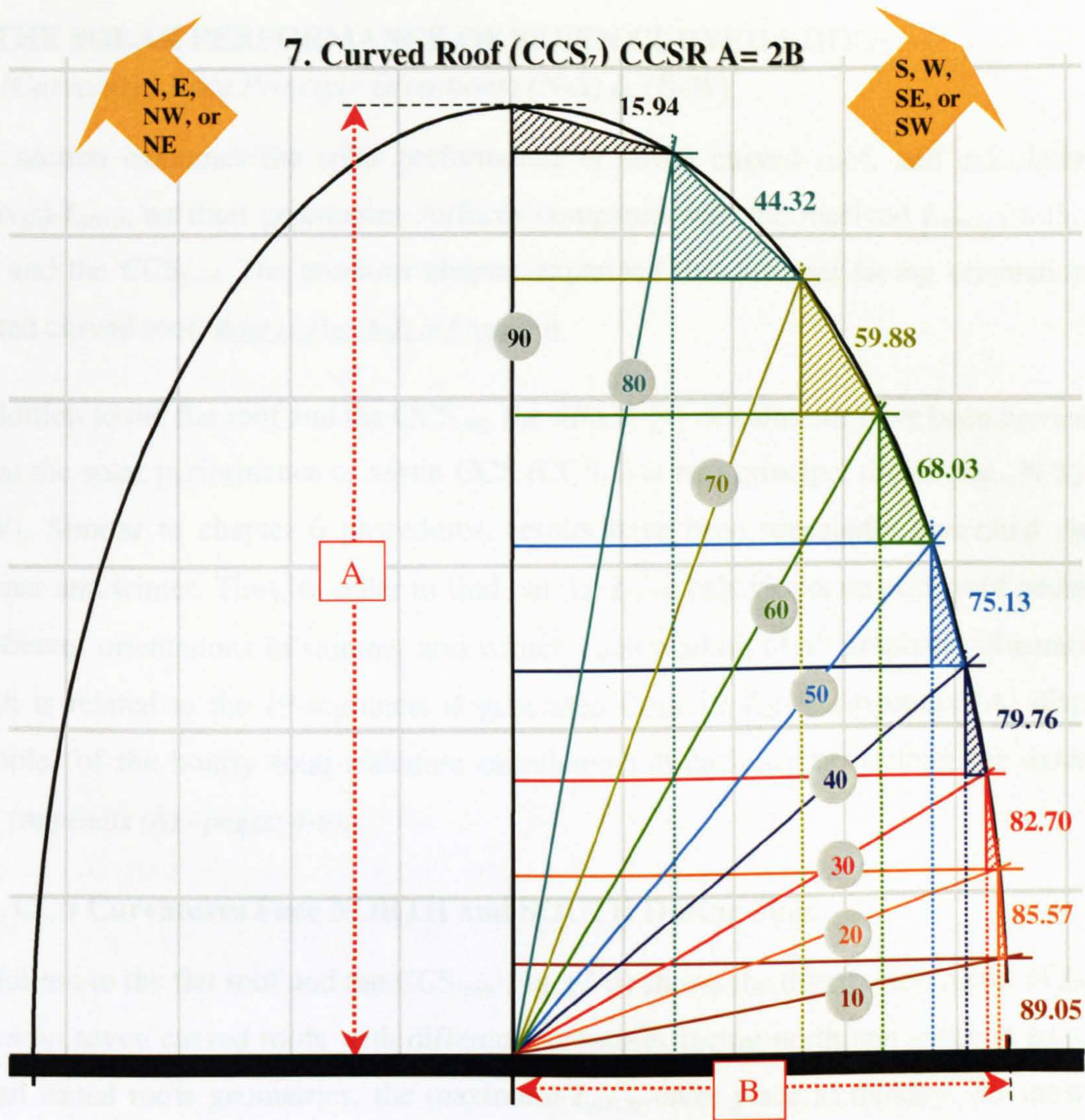


Figure 7-5 Geometrical Resemblance of CCS₇ (CCSR: A > B)

The generated segments and their slopes from the previous geometrical analysis are displayed in Table (7-1).

Table 7-1 Radial Lines Slops from The Horizontal and Planar Segments Slopes

CCS	CCSR	Radial Line Slopes (<i>Radian = 10°</i>) & Planar Segments Slopes								
		10°	20°	30°	40°	50°	60°	70°	80°	90°
* CCS ₁	A=B	83.37	75.33	64.79	55.04	46.09	35.11	25.39	14.50	6.50
CCS ₂	A=0.8B	82.16	67.34	53.13	42.27	32.60	24.39	16.35	11.08	5.13
CCS ₃	A=0.6B	68.15	45.36	32.17	24.34	15.75	13.05	9.18	6.24	4.14
* CCS ₄	A=0.5B	68.88	43.94	28.95	19.77	14.03	10.82	7.35	5.84	3.75
CCS ₅	A=1.25B	86.74	81.94	74.45	66.50	57.66	47.78	35.38	22.16	6.82
CCS ₆	A=1.67B	87.32	84.67	81.46	77.19	71.09	64.35	53.81	37.82	13.89
* CCS ₇	A=2.00B	89.05	85.57	82.70	79.76	75.13	68.03	59.88	44.32	15.94

7.2 THE SOLAR PERFORMANCE OF SEVEN CURVED ROOFS

(Curvatures Face Principle Directions) (N-S) & (E-W)

This section examines the solar performance of seven curved roof, and calculates the received $I_{(HTCS)}$ on their geometries surfaces compared with the received $I_{(HTCS)}$ on the flat roof and the $CCS_{(std)}$. The previous chapter explained the different facing orientations of vaulted curved roof. *Refer to Fig. (6-2) in Chapter 6.*

In addition to the flat roof and the $CCS_{(std)}$, the *SRSM* [4] calculations have been carried out to test the solar performance of seven CCS (CCS_{1-7}) at two principal directions, (N-S) and (E-W). Similar to chapter 6 procedures, results have been repeatedly generated during summer and winter. Thus, in order to find out the $I_{(HTCS)}$ behaviours on each roof geometry at different orientations in summer and winter, each reading of all graphical illustrations, which is related to the 19-segmnets is generated from 19 $I_{(HTCS)}$. Appendix (A) displays examples of the hourly solar radiation calculations at each segment along the extended CCS (*Appendix (A) - pages: 4-6*).

7.2.1 CCS Curvatures Face NORTH and SOUTH During June

In addition to the flat roof and the $CCS_{(std)}$, Fig. (7-6) shows the distribution forms of $I_{(HTCS)}$ -values on seven curved roofs with different curvatures facing north and south in summer. For all tested roofs geometries, the maximum $I_{(HTCS)}$ takes place at midday. As shown in Fig. (7-6), all roofs geometries $I_{(HTCS)}$ -curves ($I_{(HTCS)}$ -values distribution forms) have similar characteristics. Each roof $I_{(HTCS)}$ -curve ascends differently after 06:00 in the morning until they reach their maximum at midday.

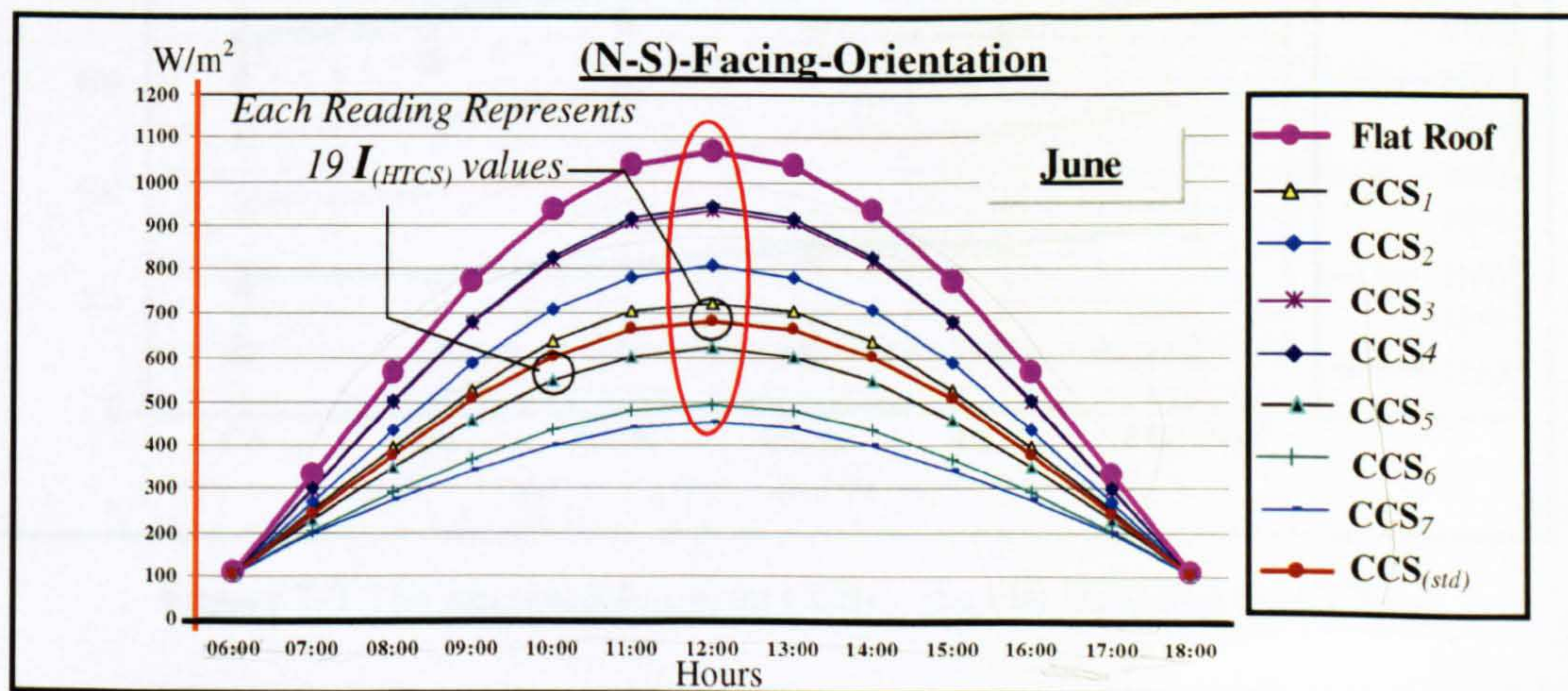


Figure 7-6 $I_{(HTCS)}$ (W/m^2) on the CCS_{1-7} , the $CCS_{(std)}$ and the Flat Roof

During the afternoon period, all roofs $I_{(HTCS)}$ -curves descend differently before they intersect each other again at 18:00 in the evening, Fig. (7-6). At 06:00 and 18:00, approximately the CCS_{1-7} , the $CCS_{(std)}$ and flat roof receive equal $I_{(HTCS)}$ -values. As shown in Fig. (7-6), the minimum difference between the flat roof $I_{(HTCS)}$ -curve and each CCS $I_{(HTCS)}$ -curve has always been recorded in the early morning and the late afternoon hours. These differences slightly increase till they reach the maximum at midday. The flat roof $I_{(HTCS)}$ -curve starts and ends with steeper gradients compared CCS_5 , CCS_6 and CCS_7 where $CCSR$ is $A > B$. While, the $I_{(HTCS)}$ -curves of other curved roofs, which their $CCSR$ is $A < B$ start and end with steep gradients as the flat roof ones.

Fig. (7-7) and (7-8) illustrate another graphical way of discussing the same results of Fig. (7-6). They present hourly comparison between the $I_{(HTCS)}$ -values on the seven CCS from one side and the $CCS_{(std)}$ and the flat roof from the other. At principal directions, the $I_{(HTCS)}$ -mirrored-values of all roofs geometries are equal around the midday axis. Therefore, each graph discusses only seven readings throughout the day instead of the thirteen daytime readings (six pairs of the hourly daytime readings in addition to the midday reading). Fig. (7-7) shows that the received $I_{(HTCS)}$ increases with the decrease of the $CCSR$ ("A" decreases). The maximum $I_{(HTCS)}$ is recorded on the flat roof, where A equals zero.

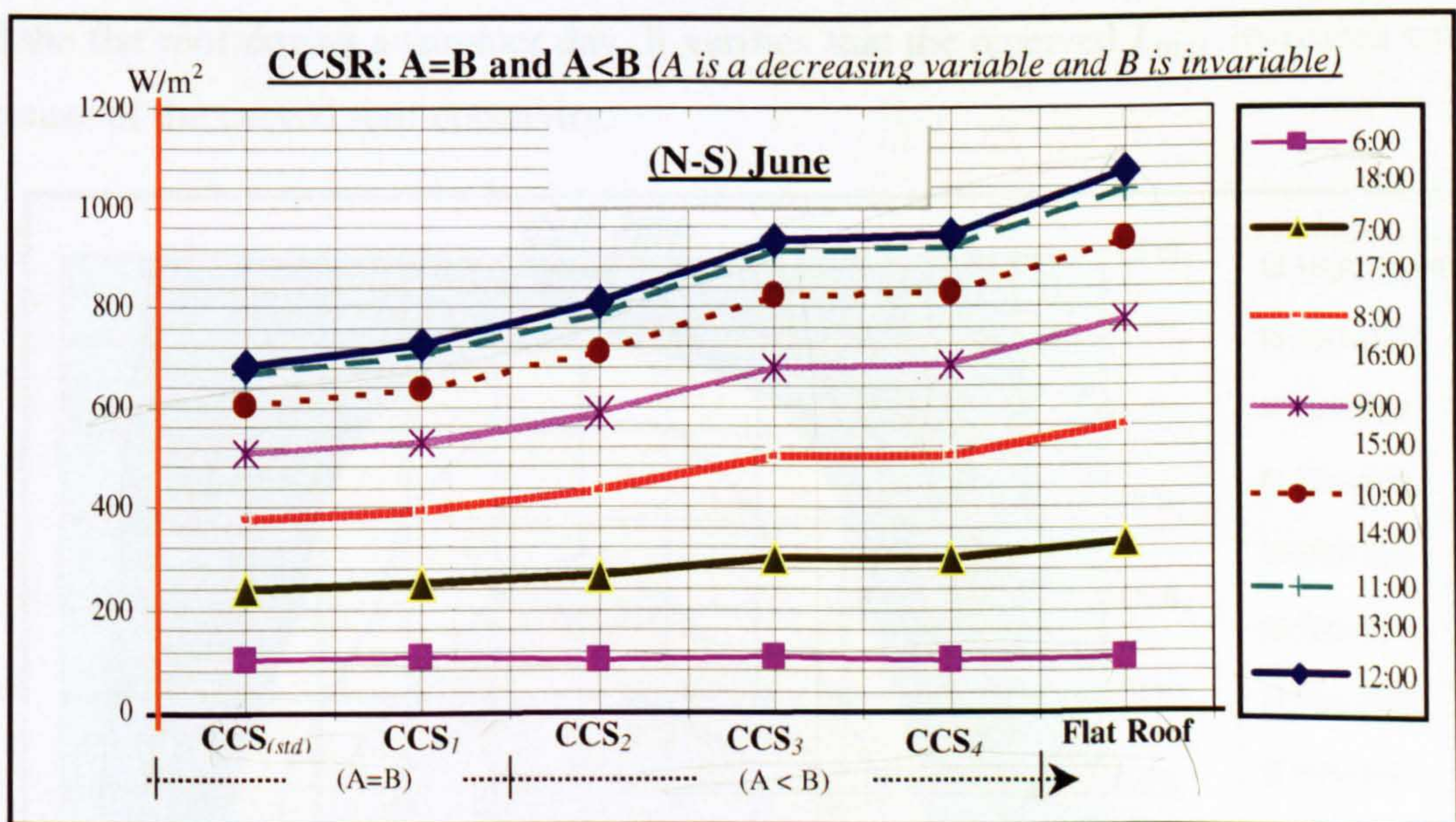


Figure 7-7 The Received $I_{(HTCS)}$ on CCS_{1-4} , the Flat Roof and the $CCS_{(std)}$

Fig. (7-8) shows that the received $I_{(HTCS)}$ on different roofs geometries decreases with the increase of the CCSR ("A" increases). The minimum received $I_{(HTCS)}$ is recorded on the CCS_7 , where A equals 2B. This means that the CCS_7 is the most preferable curvature in order to receive the least solar irradiance in summer.

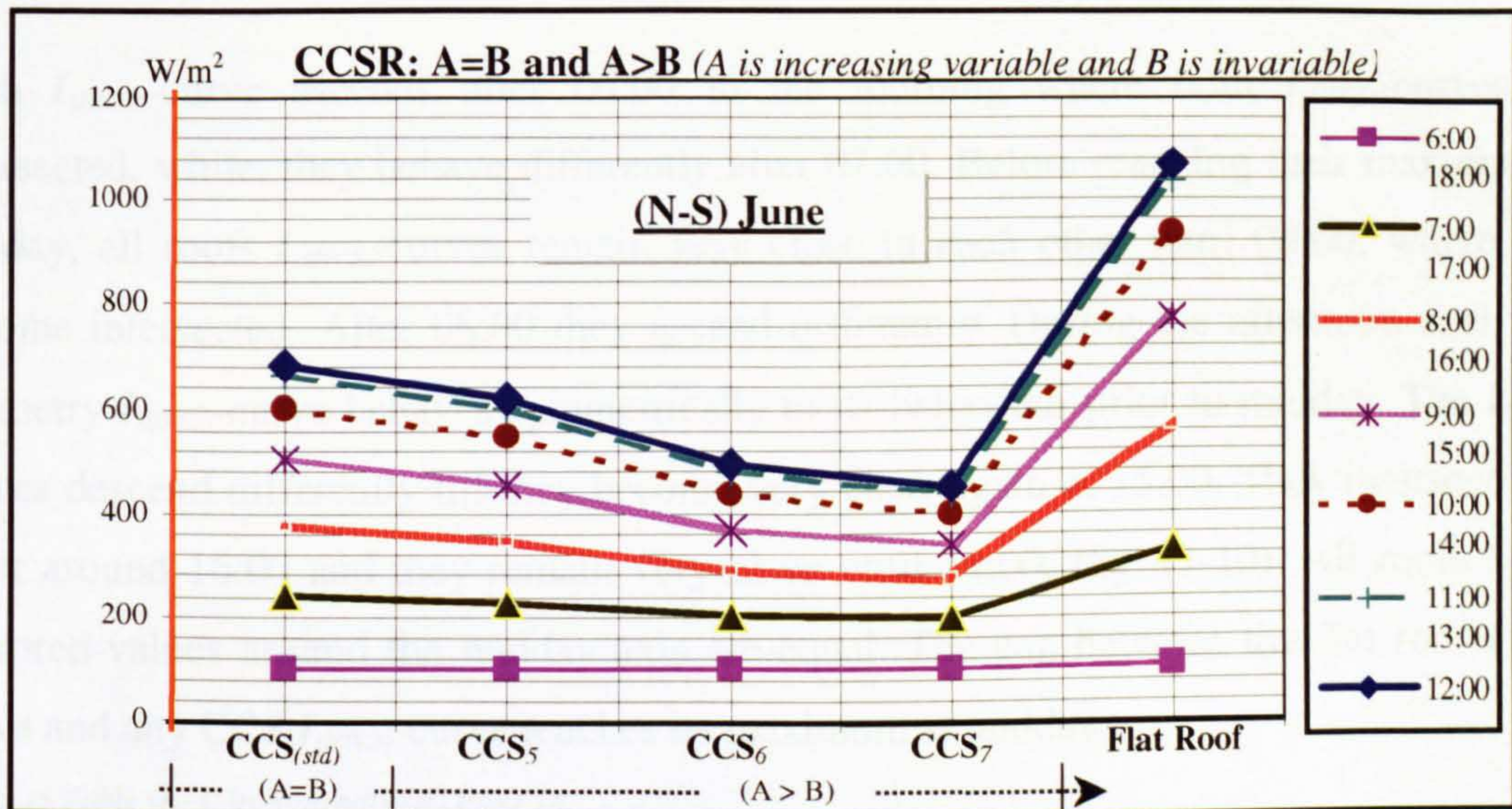


Figure 7-8 The Received $I_{(HTCS)}$ on CCS_{5-7} , the Flat Roof and the $CCS_{(std)}$

Fig. (7-9) displays the calculated $I_{(HTCS)}$ that received on each CCS in addition to the $CCS_{(std)}$ and the flat roof during a summer day. It verifies that the received $I_{(HTCS)}$ increases with the decrease of the curved roof concavity.

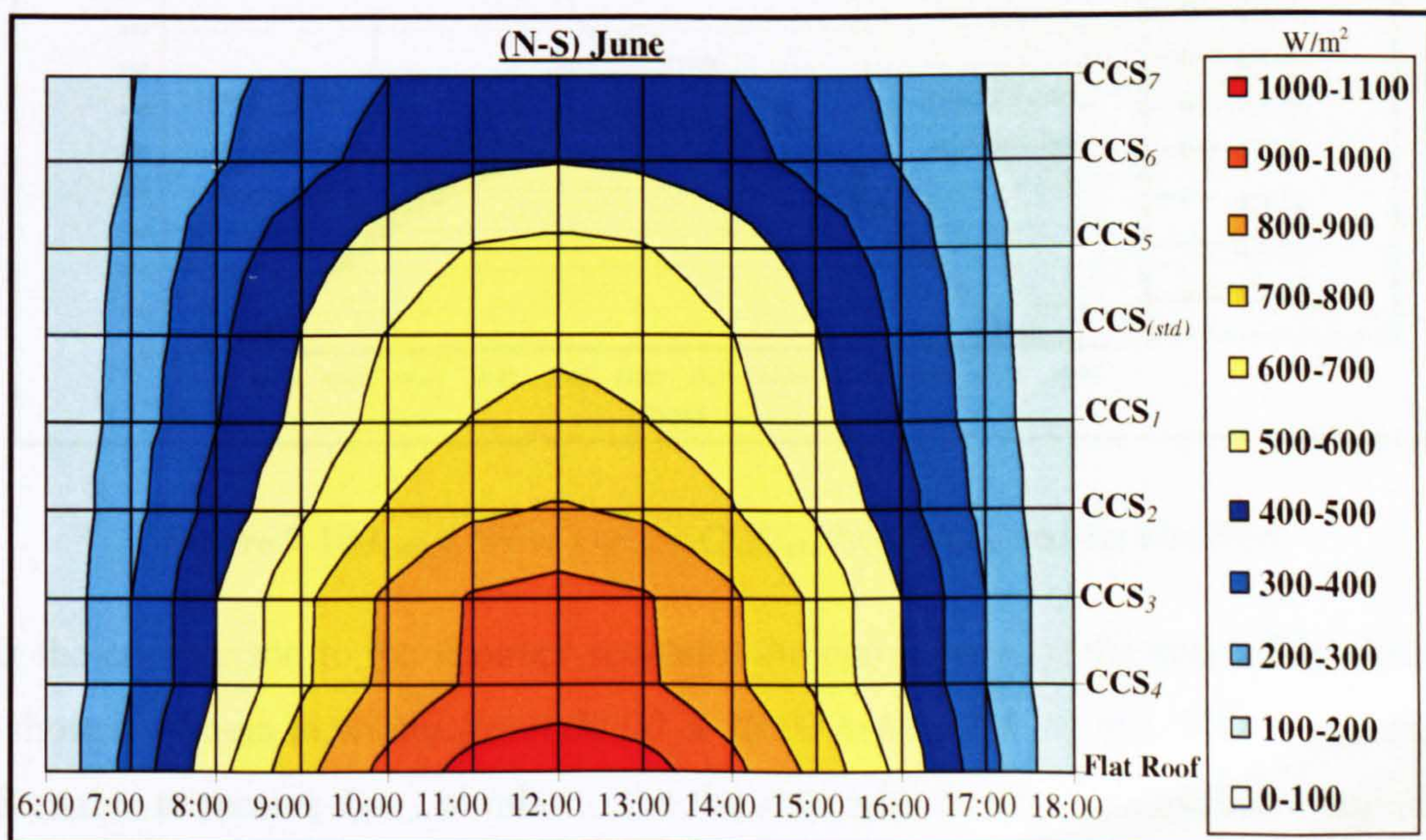


Figure 7-9 Alternated Arrangements of the Received $I_{(HTCS)}$ on the Tested Roofs

7.2.2 CCS Curvatures Face NORTH and SOUTH During December

Comparing with the flat roof and the $CCS_{(std)}$, Fig. (7-10) shows the received $I_{(HTCS)}$ on the seven CCS with their different curvatures facing north and south in winter. All roofs $I_{(HTCS)}$ -curves have similar characteristics around the midday axis. The maximum received solar radiation on each roof takes place at midday.

Each $I_{(HTCS)}$ -curve ascends after 06:00 in the morning where both $I_{(HTCS)}$ -curves are intersected, while, they behave differently after 07:00. Before reaching their maximum at midday, all roofs $I_{(HTCS)}$ -curves remain very close to each other until 08:00, where they become intersected. After 08:00 they ascend differently. During the afternoon each roof geometry $I_{(HTCS)}$ -curve behaves symmetrically to its behaviour prior to midday. The $I_{(HTCS)}$ -curves descend differently till they become very close again at 15:00. They intersect each other around 16:00 and they remain very close until 18:00, Fig. (7-10). All roofs $I_{(HTCS)}$ -mirrored-values around the midday axis are equal. The gap between the flat roof $I_{(HTCS)}$ -curve and any CCS $I_{(HTCS)}$ -curve reaches its maximum at midday.

Refer to Table (A-3) in Appendix (A) Page 14.

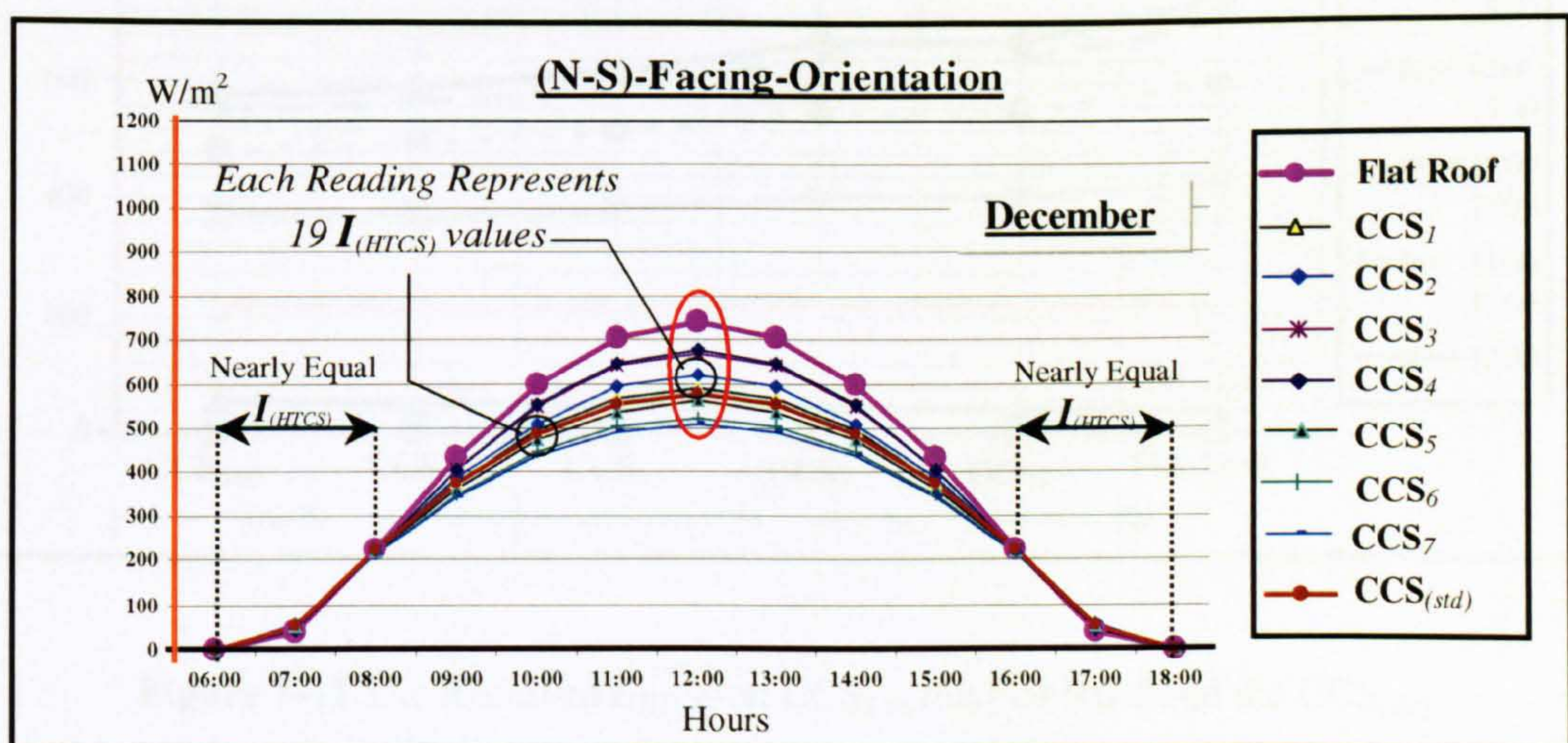


Figure 7-10 $I_{(HTCS)}$ (W/m^2) on the CCS_{1-7} , the $CCS_{(std)}$ and the Flat Roof

With the comparison to the summer scenario, the period time of the noticeable difference has shorted 4 hours in winter (*from 06:00 & 18:00 to 08:00 & 16:00*). This means that the CCS enable to receive $I_{(HTCS)}$ similar to the flat roof ones during the early morning and the late afternoon hours, which is desirable in winter. Moreover, the curved roofs receive slightly more $I_{(HTCS)}$ than the flat roof during these periods.

Fig. (7-11) and (7-12) illustrate another graphical way of displaying the same results of Fig. (6-7). They present hourly comparison between the $I_{(HTCS)}$ -values on the seven CCS, the $CCS_{(std)}$ and the flat roof. At principal directions, the $I_{(HTCS)}$ -mirrored-values of all roofs geometries are equal around the midday axis. Therefore, each graph discusses only seven readings throughout the day instead of the thirteen daytime readings (*six pairs of the hourly daytime readings in addition to the midday reading*).

Similar to the summer scenario, Fig. (7-11) shows that the received $I_{(HTCS)}$ on roofs surfaces increases with the decrease of CCSR ("A" decreases). The maximum $I_{(HTCS)}$ is recorded on the flat roof, where A equals zero. In winter, the differences between the received $I_{(HTCS)}$ on one geometry and another is insignificant with the comparison to the summer ones (*in winter the increases are not acute like in summer*).

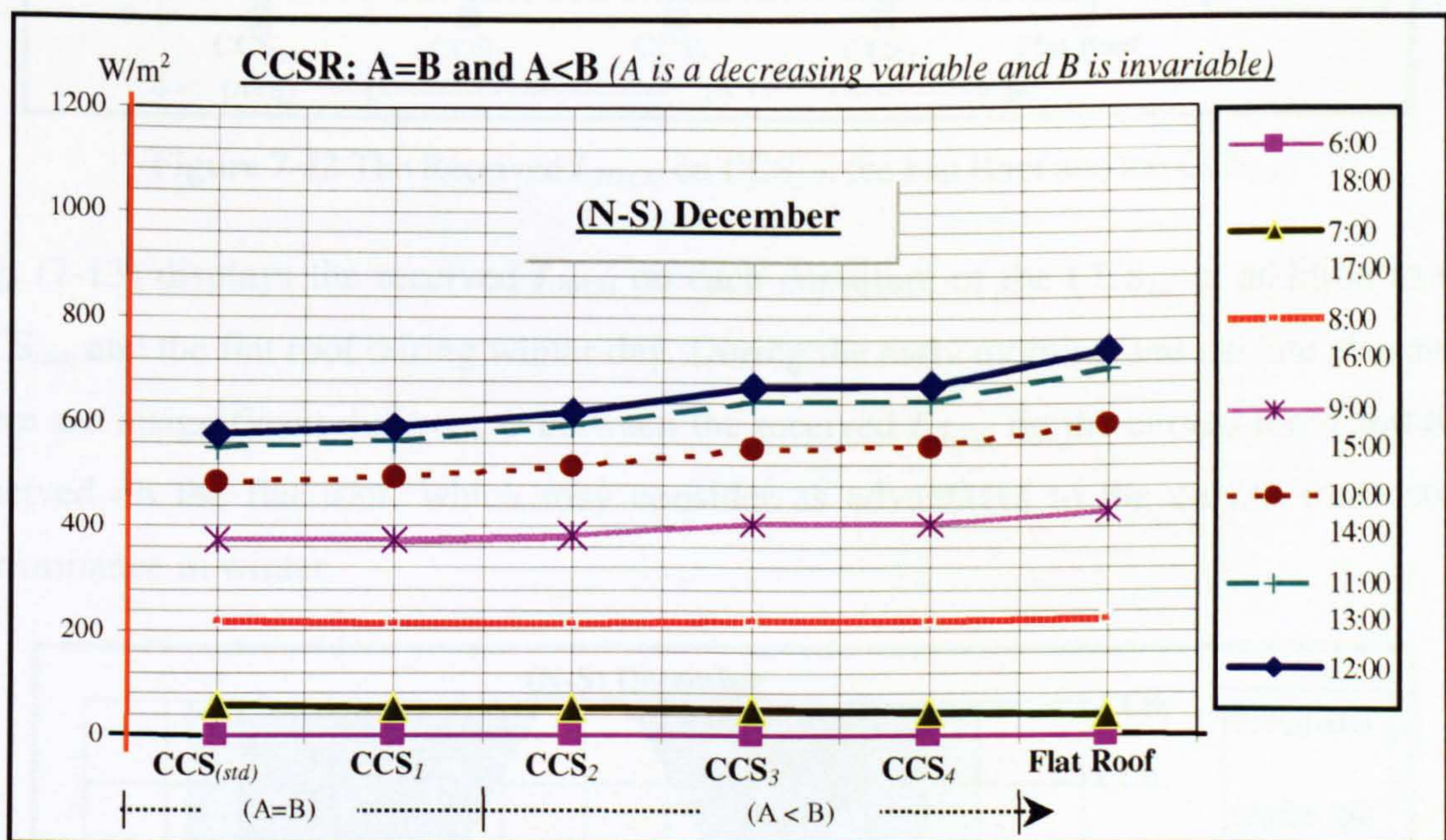


Figure 7-11 The Received $I_{(HTCS)}$ on CCS_{1-4} , the Flat Roof and the $CCS_{(std)}$

The same as the summer, Fig. (7-12) shows that the received $I_{(HTCS)}$ on different roofs geometries decreases with the increase of the CCSR ("A" increases). The maximum $I_{(HTCS)}$ is recorded on the flat roof, where A equals zero.

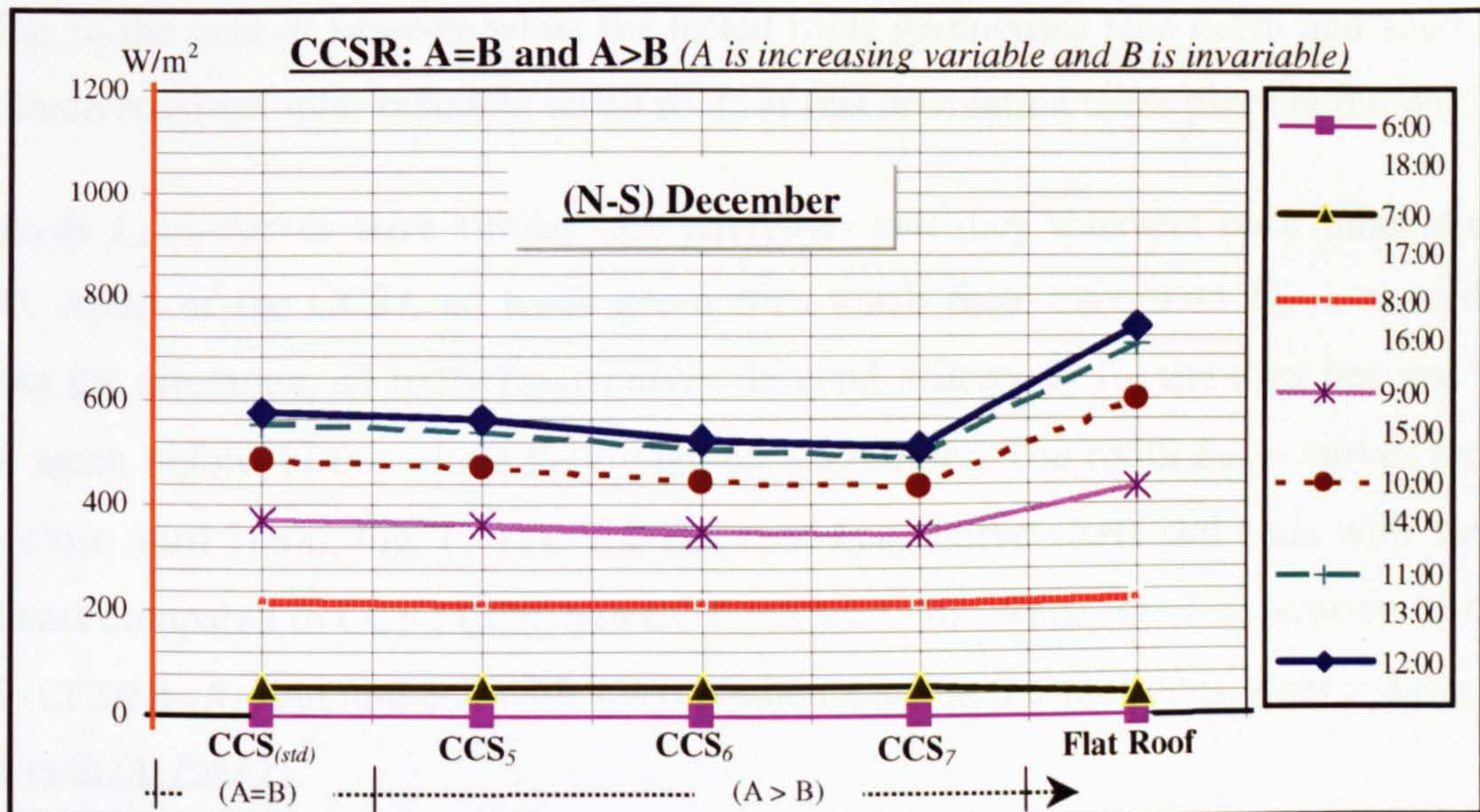


Figure 7-12 The Received $I_{(HTCS)}$ on CCS_{5-7} , the Flat Roof and the $CCS_{(std)}$

Fig. (7-13) displays the received $I_{(HTCS)}$ on each curvature of the CCS_{1-7} in addition to the $CCS_{(std)}$ and the flat roof during winter day. During the early morning and the late afternoon there are insignificant differences between the received $I_{(HTCS)}$ on the curved roofs and that received on the flat roof, which may consider as advantages to the curved roofs solar performance in winter.

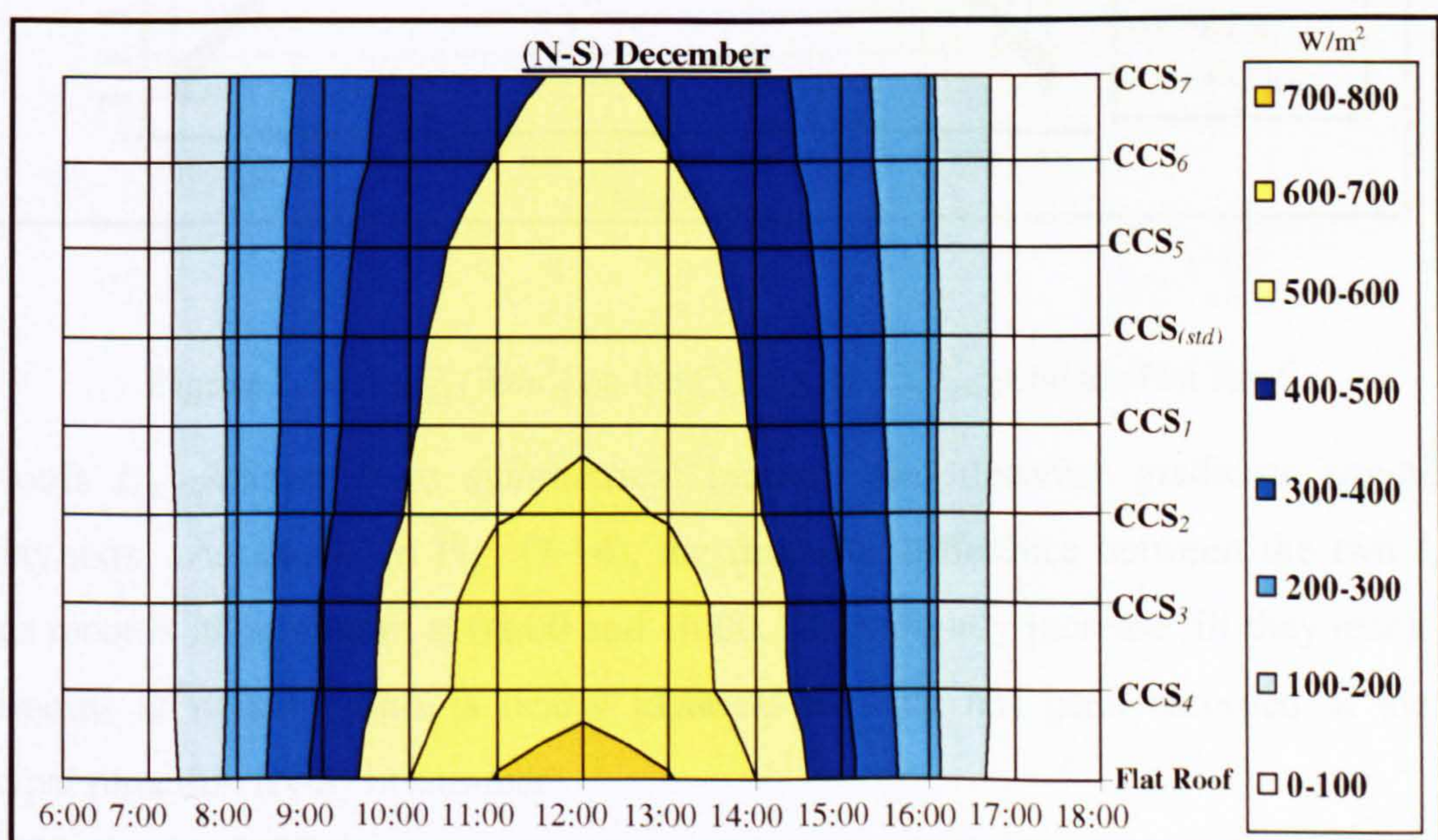


Figure 7-13 Alternated Arrangements of the Received $I_{(HTCS)}$ on the Tested Roofs

7.2.3 CCS Curvatures Face EAST and WEST During June

In addition to the $CCS_{(std)}$ and the flat roof, Fig. (7-14) shows the distribution forms of the received $I_{(HTCS)}$ on seven CCS with different curvatures facing east and west in summer. Similar to the case of summer while the tested roofs geometries face north and south, the maximum received solar radiation on all roofs at this orientation takes place at midday.

All roofs $I_{(HTCS)}$ -curves have similar characteristics and they intersect each other around 08:00. Apart of the CCS_7 , all roofs geometries reach their maximum $I_{(HTCS)}$ at midday. During the afternoon, all roofs $I_{(HTCS)}$ -curves descend differently till the they become very close again before 17:00, where they intersect each other. The roofs $I_{(HTCS)}$ -curves remain very close until 18:00, Fig. (7-14). The flat roof $I_{(HTCS)}$ -curve starts and ends with steeper gradients compared to CCS_5 , CCS_6 and CCS_7 ($CCSR A > B$). While, the $I_{(HTCS)}$ -curves of other CCS ($CCSR A < B$) start and end with steep gradients as the flat roof ones. Refer to Table (A-4) in Appendix (A) Page 15.

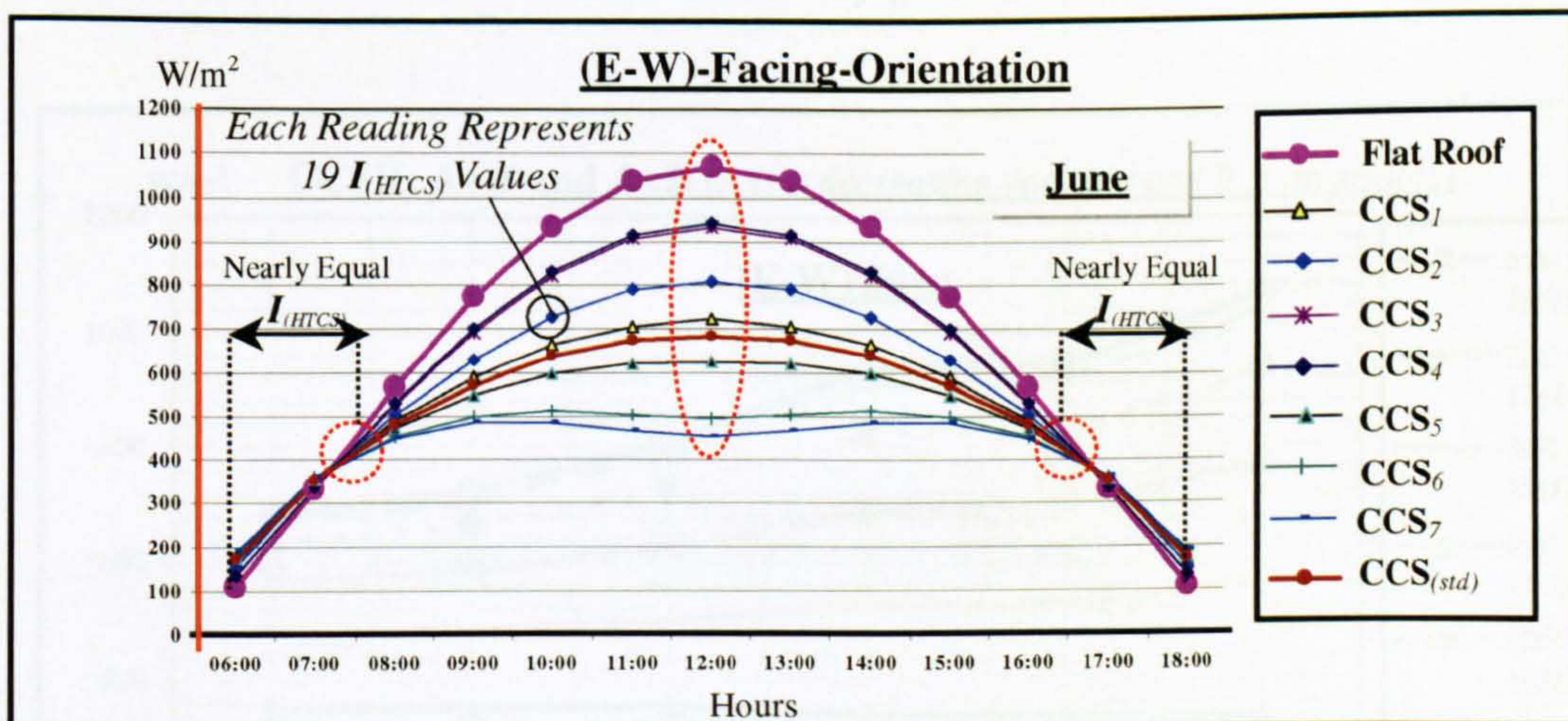


Figure 7-14 $I_{(HTCS)}$ (W/m^2) on the CCS_{1-7} , the $CCS_{(std)}$ and the Flat Roof

All roofs $I_{(HTCS)}$ -curves have symmetrical increase and decrease gradients around the midday axis. As shown in Fig. (7-14), the desirable difference between the two $I_{(HTCS)}$ -curves records its minimum at 08:00 and 16:00. They slightly increase till they reach their maximums at midday. This is nearly identical to what has been recorded at the first principal direction (N-S) in summer.

Fig. (7-15) and (7-16) show another graphical way to illustrate the same previously derived results in Fig. (7-14). They depict proportional comparison between the $I_{(HTCS)}$ -values on the seven CCS at (E-W) and $I_{(HTCS)}$ -values on the flat roof at every daytime hour in summer at the same orientation. As a result of the equalled $I_{(HTCS)}$ -mirrored-values around the midday axis at the principal directions, Fig. (7-15) analyses only seven hourly readings instead of the thirteen daytime readings.

In the early morning and the late afternoon hours there are insignificant differences between the received $I_{(HTCS)}$ on the curved roofs compared to the noon period differences. Apart of (06:00, 07:00, 17:00, & 18:00), the figure shows that the received $I_{(HTCS)}$ on the CCS increases with the decreasing of the CCSR ("A" decreases), until it reaches its maximum on the flat roof, where A equals zero. This means that all curved roofs CCS receive more solar radiation than the flat roof during these hours, which is not preferable during summer. These time periods did not exist when the tested roofs faced the (N-S). Although during these times solar radiation intensity is still bearable (*less than 400 W/m²*), which cannot effect the indoor conditions to any great extent.

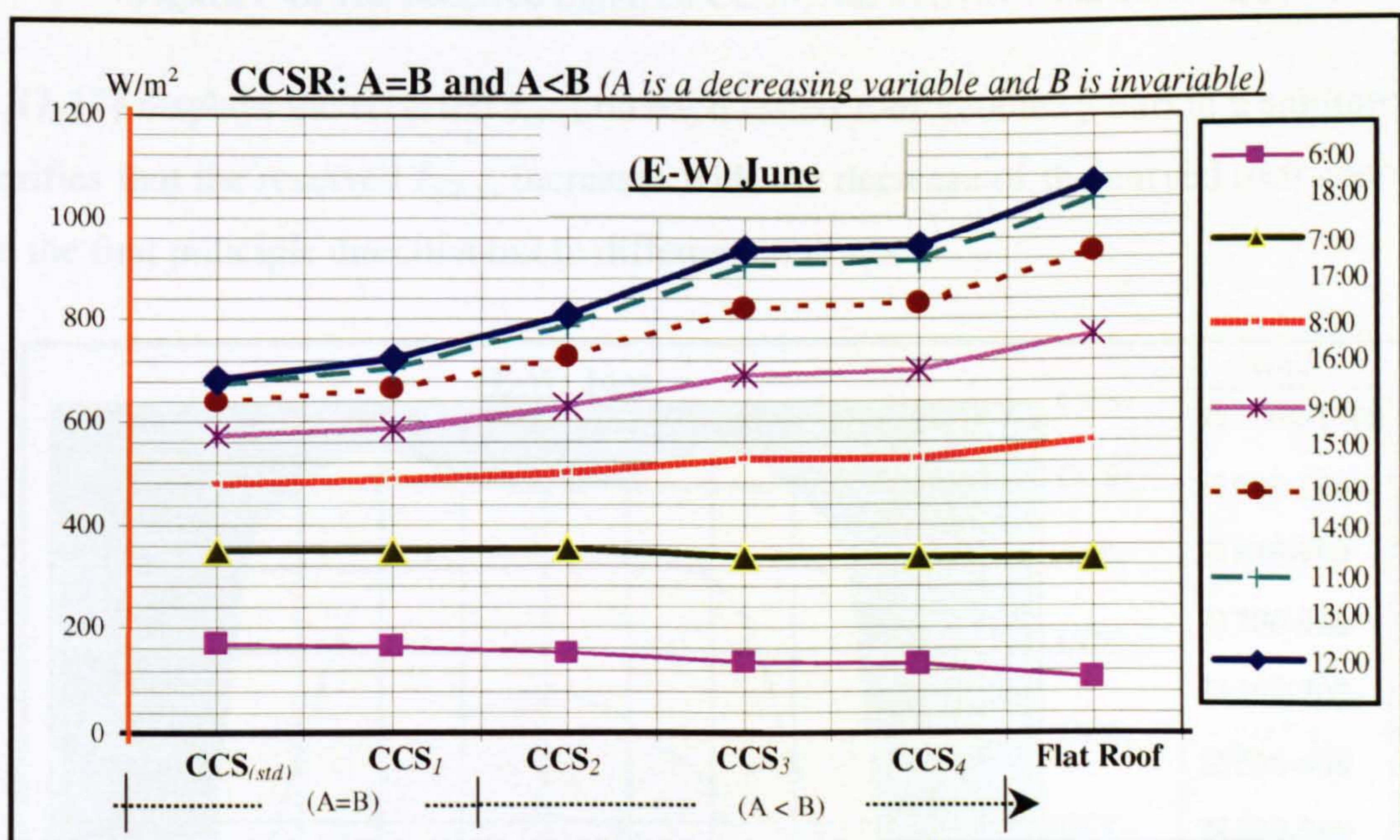


Figure 7-15 The Received $I_{(HTCS)}$ on CCS₁₋₄, the Flat Roof and the CCS_(std)

Fig. (7-16) shows that the received $I_{(HTCS)}$ on different roofs face (E-W) decreases with the increase of the CCSR ("A" increases). The minimum received $I_{(HTCS)}$ is recorded on the CCS_7 , where A equals 2B. This means that the CCS_7 is the most preferable curvature in comparison to other CCS curvatures in summer. At midday time, CCS_7 , where A equals 2B, receives less $I_{(HTCS)}$ than the rest of roof geometries.

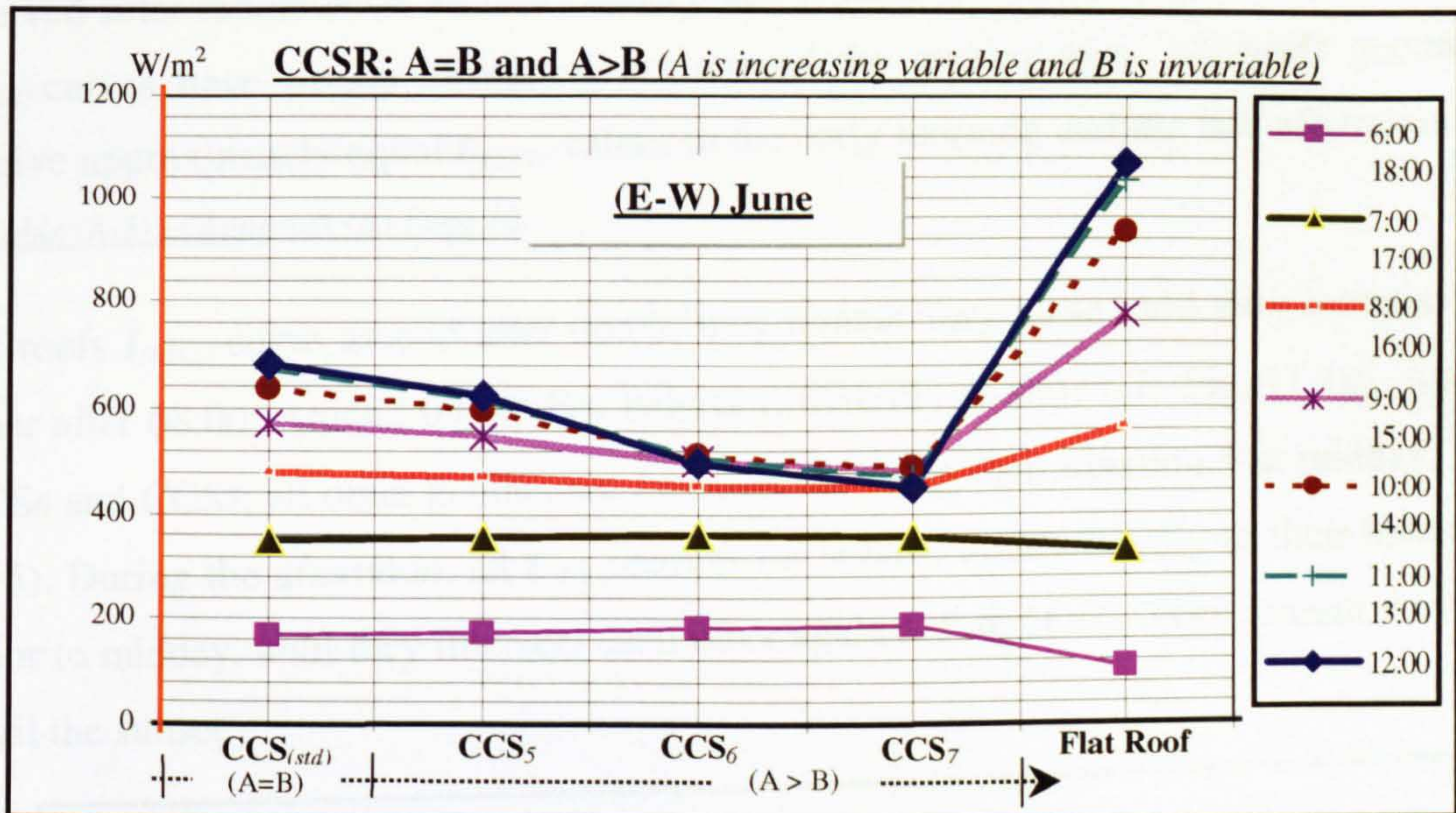


Figure 7-16 The Received $I_{(HTCS)}$ on CCS_{5-7} , the Flat Roof and the $CCS_{(std)}$

Fig. (7-17) displays the received $I_{(HTCS)}$ on each tested roof geometry during a summer day. It verifies that the received $I_{(HTCS)}$ increases with the decrease of the curved roof concavity as in the first principle direction but in different contours.

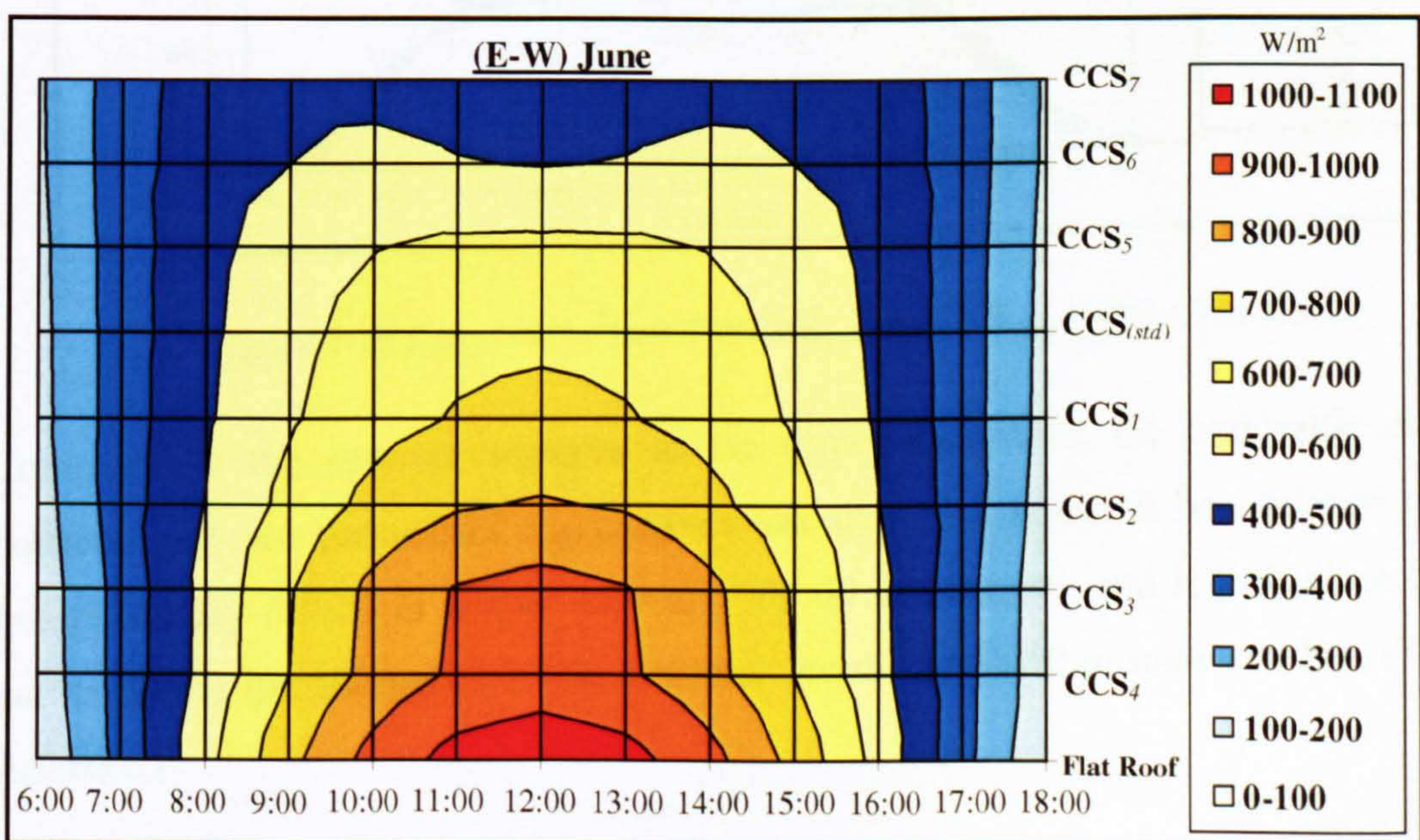


Figure 7-17 Alternated Arrangements of the Received $I_{(HTCS)}$ on the Tested Roofs

7.2.4 CCS Curvatures Face EAST and WEST During December

Compared with flat roof and the $CCS_{(std)}$, Fig. (7-18) shows the received $I_{(HTCS)}$ on the seven CCS with their different curvatures facing east and west during winter. Similar to all previous cases and particularly to the (N-S)-facing-orientation in winter, the maximum received solar radiation on all roofs takes place at midday. Moreover, all roofs geometries $I_{(HTCS)}$ -curves have similar characteristics around the midday axis. All roofs geometries receive approximately equal $I_{(HTCS)}$ -values in the early morning and the late afternoon. *Refer to Table (A-5) in Appendix (A) Page 16.*

All roofs $I_{(HTCS)}$ -curve ascend after 06:00, they remain very close until they intersect each other after 08:00. Around 09:00 they behave differently as shown in Fig. (7-18). Apart of CCS_6 and CCS_7 , all other geometries $I_{(HTCS)}$ -curves reach their maximum at midday, Table (7-5). During the afternoon, all $I_{(HTCS)}$ -curves for behave symmetrically to their behaviours prior to midday, until they intersect each other again before 16:00. They remain very close until the sunset.

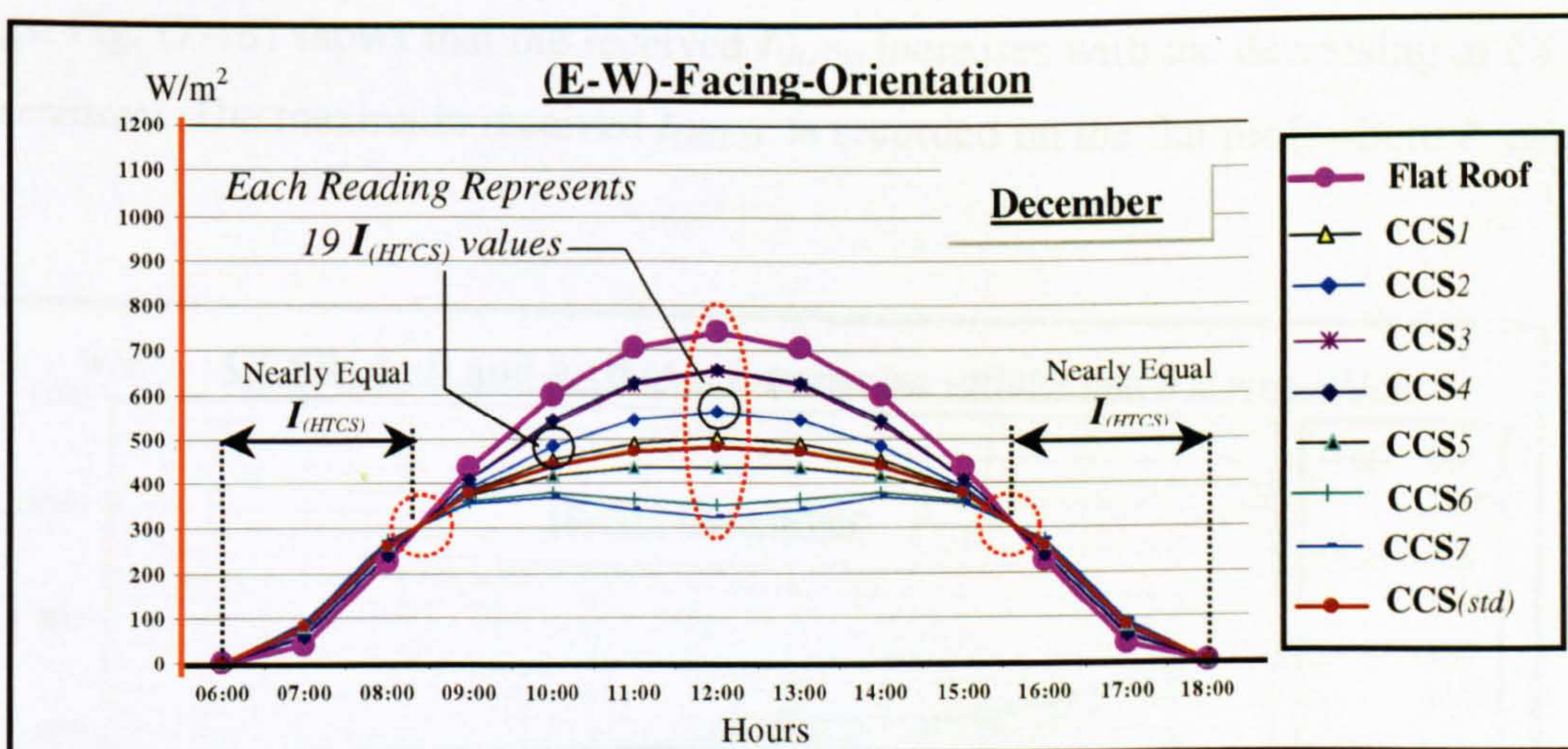


Figure 7-18 $I_{(HTCS)}$ (W/m^2) on The CCS_{1-7} , the $CCS_{(std)}$ and the Flat Roof

Compared to the summer scenario at the same orientation, the noticeable difference between any two geometries $I_{(HTCS)}$ -curves has shorted 2 hours. It has delayed one hour before midday (09:00 in winter instead of 08:00 in summer), and it took place one hour earlier during the afternoon (15:00 in winter instead of 16:00 in summer), Fig. (7-18). *(See Appendix:)*

Similar to what has been noticed previously during winter in (N-S), Fig. (7-18) also shows that the different CCS receive more solar radiation than the flat roof during the early morning and the late afternoon hours. Even more, the received solar radiation intensity by the curved roofs at (E-W) is slightly higher than that received on the same geometries when they faced (N-S). Refer to Fig. (7-10).

Receiving more solar radiation during winter may add more credits for employing curved roofs that face (E-W), especially during the early morning and the late afternoon. In winter, there is a need to keep the ratio between $I_{(HTCS)}$ -values on curved roofs to that on flat roofs as small as possible, while, the opposite is required for summer. A seasonal ratio between the received summer and winter $I_{(HTCS)}$ -values of curved and flat roofs has been discussed in Chapter 6.

Fig. (7-19) illustrates another graphical way of discussing the same results of Fig. (7-18). Because of the equalled $I_{(HTCS)}$ -mirrored-values around the midday axis, the figures discuss only six pairs of readings in addition to the midday reading instead of the thirteen daytime readings. Fig. (7-18) shows that the received $I_{(HTCS)}$ increases with the decreasing of CCSR ("A" decreases). The maximum received $I_{(HTCS)}$ is recorded on the flat roof, where A equals zero.

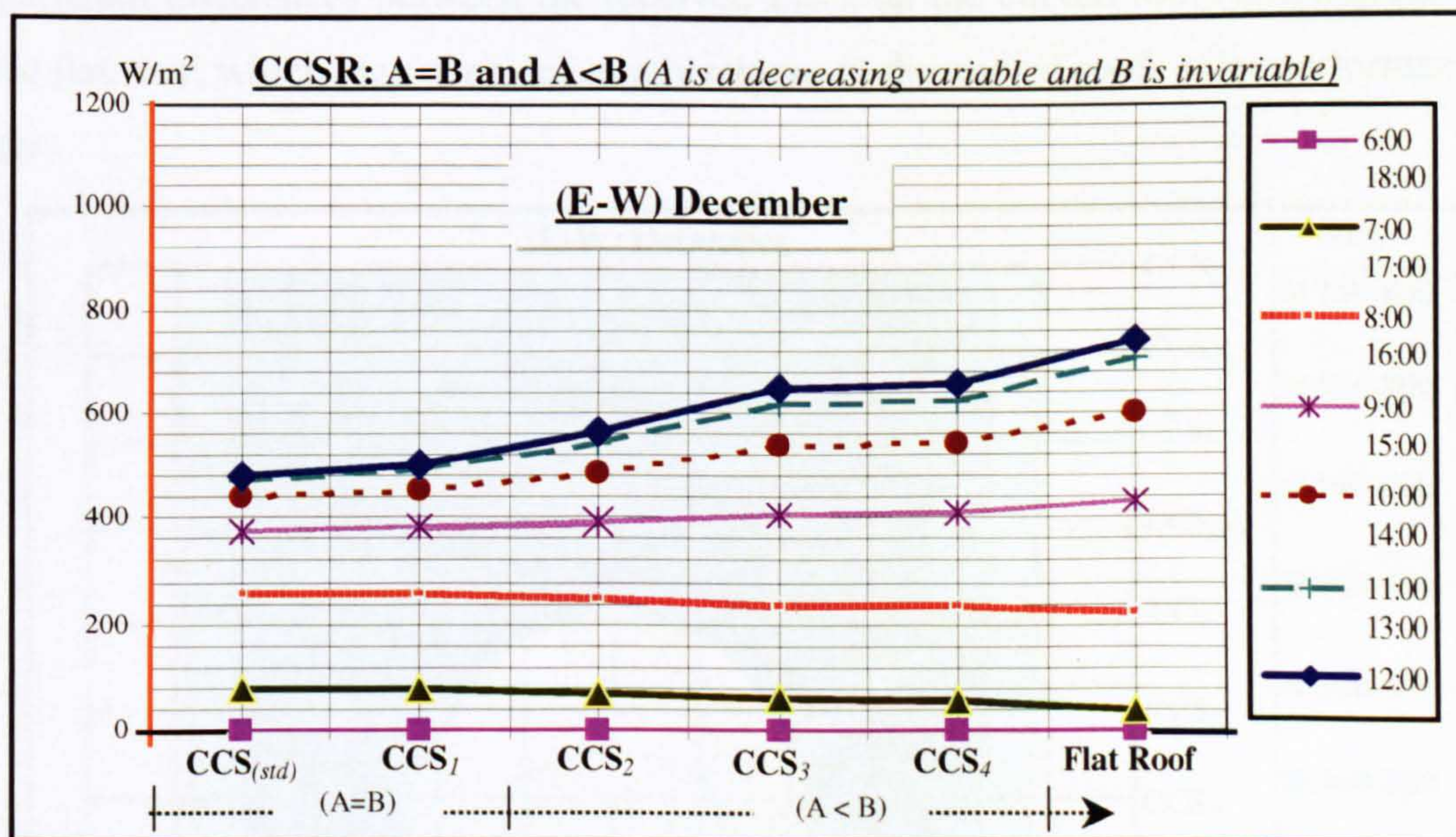


Figure 7-19 The Received $I_{(HTCS)}$ on CCS_{1-4} , the Flat Roof and the $CCS_{(std)}$

Fig. (7-20) shows that the received $I_{(HTCS)}$ on different roofs geometries decreases with the increasing of the CCSR ("A" increases). In winter, during the early morning and the late afternoon there are insignificant differences between the received $I_{(HTCS)}$ on each CCS (CCS_5 , CCS_6 , CCS_7).

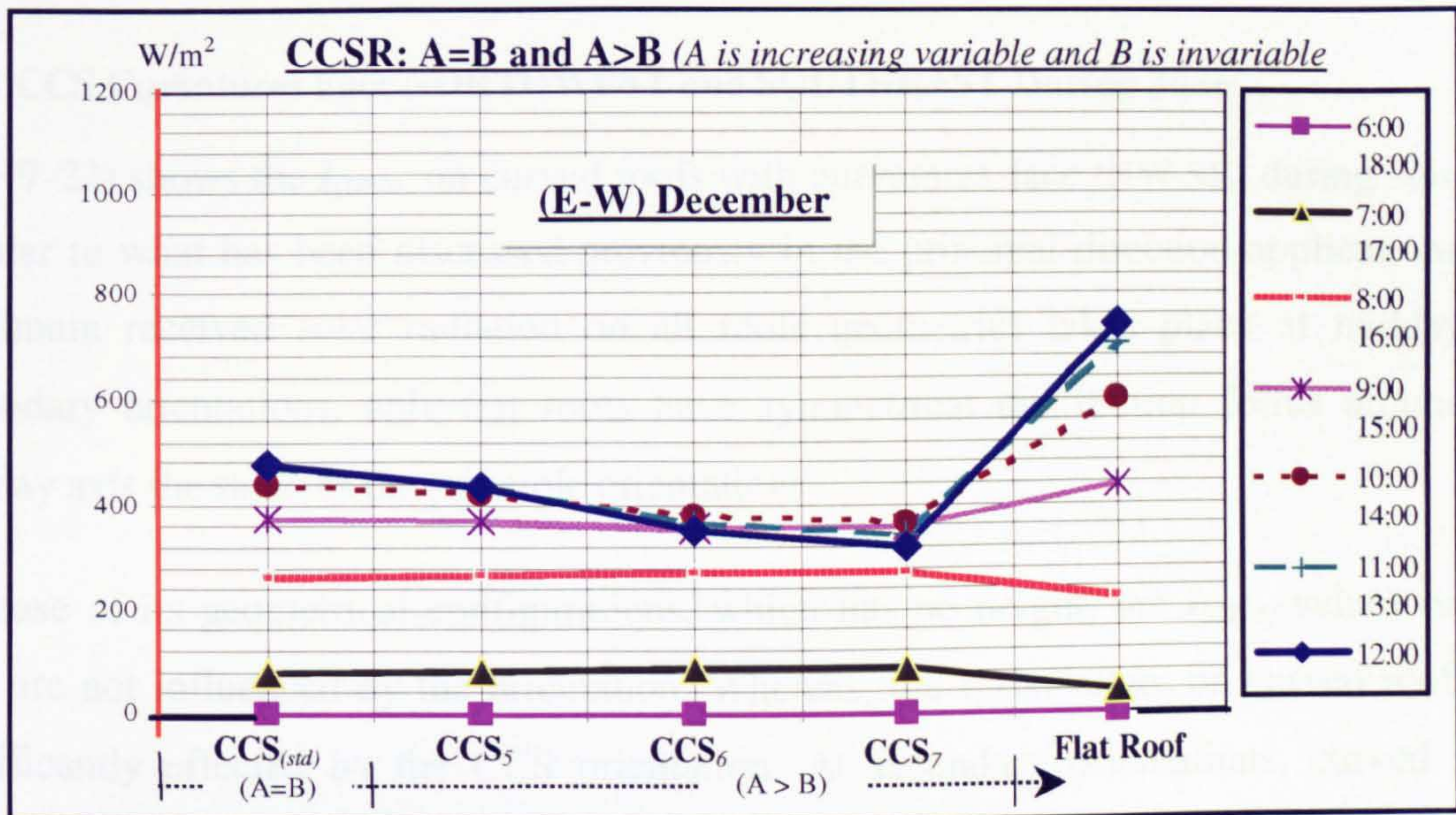


Figure 7-20 The Received $I_{(HTCS)}$ on CCS_{5-7} , the Flat Roof and the $CCS_{(std)}$

Fig. (7-21) presents the received $I_{(HTCS)}$ on all tested roofs geometries at the (E-W) orientation during a winter day. During the early morning and the late afternoon there are insignificant differences between the received $I_{(HTCS)}$ on the curved roofs and that received on the flat roof, which may consider as advantages to the curved roofs solar performance in winter.

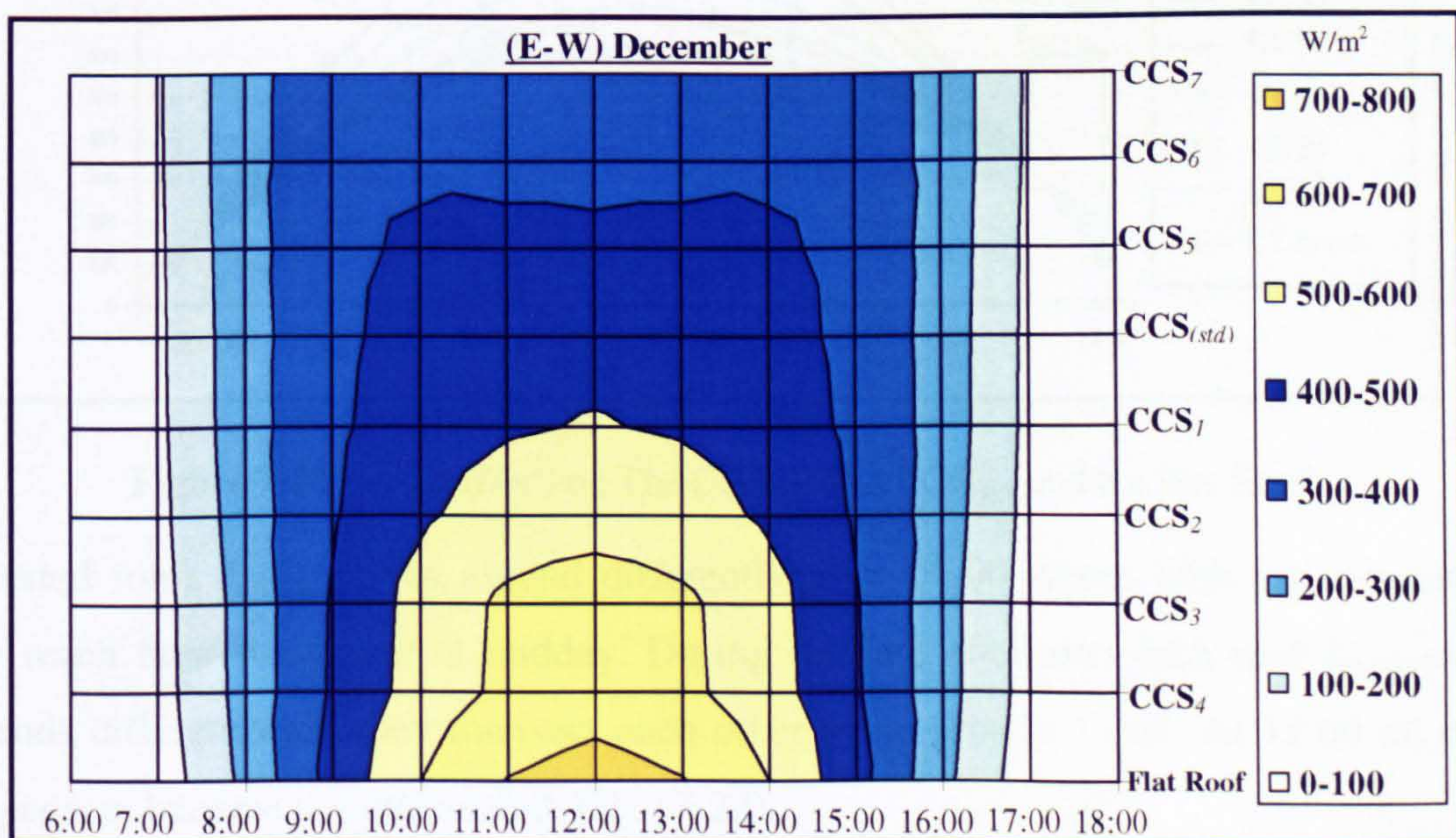


Figure 7-21 Alternated Arrangements of the Received $I_{(HTCS)}$ on the Tested Roofs

7.3 THE SOLAR PERFORMANCE OF SEVEN CURVED ROOFS

(Curvatures Face Secondary Directions) (NW-SE) & (NE-SW)

This part discusses the solar performance of seven curved roofs (CCS_{1-7}), in which the curvatures face secondary directions (NW-SE) & (NE-SW)

7.3.1 CCS Curvatures Face NORTHWEST and SOUTHEAST During June

Fig. (7-22) shows the $I_{(HTCS)}$ on curved roofs with curvatures face (NW-SE) during summer. Similar to what has been discussed previously in the principal direction applications, the maximum received solar radiation on all roofs geometries takes place at midday. At secondary orientations, only flat roofs have symmetrical distribution forms around the midday axis the same as the principle orientations.

Because of its geometrical configurations, which has no height, the $I_{(HTCS)}$ -values on flat roof are not influenced by the orientation. Whereas, the $I_{(HTCS)}$ -values on curved roofs are significantly effected by the CCS orientation. At secondary orientations, curved roofs three-dimensional form creates unsymmetrical $I_{(HTCS)}$ -curves and unequal $I_{(HTCS)}$ -mirrored-values around the midday axis, Fig. (7-22). Refer to Table (A-6) in Appendix (A) Page 17.

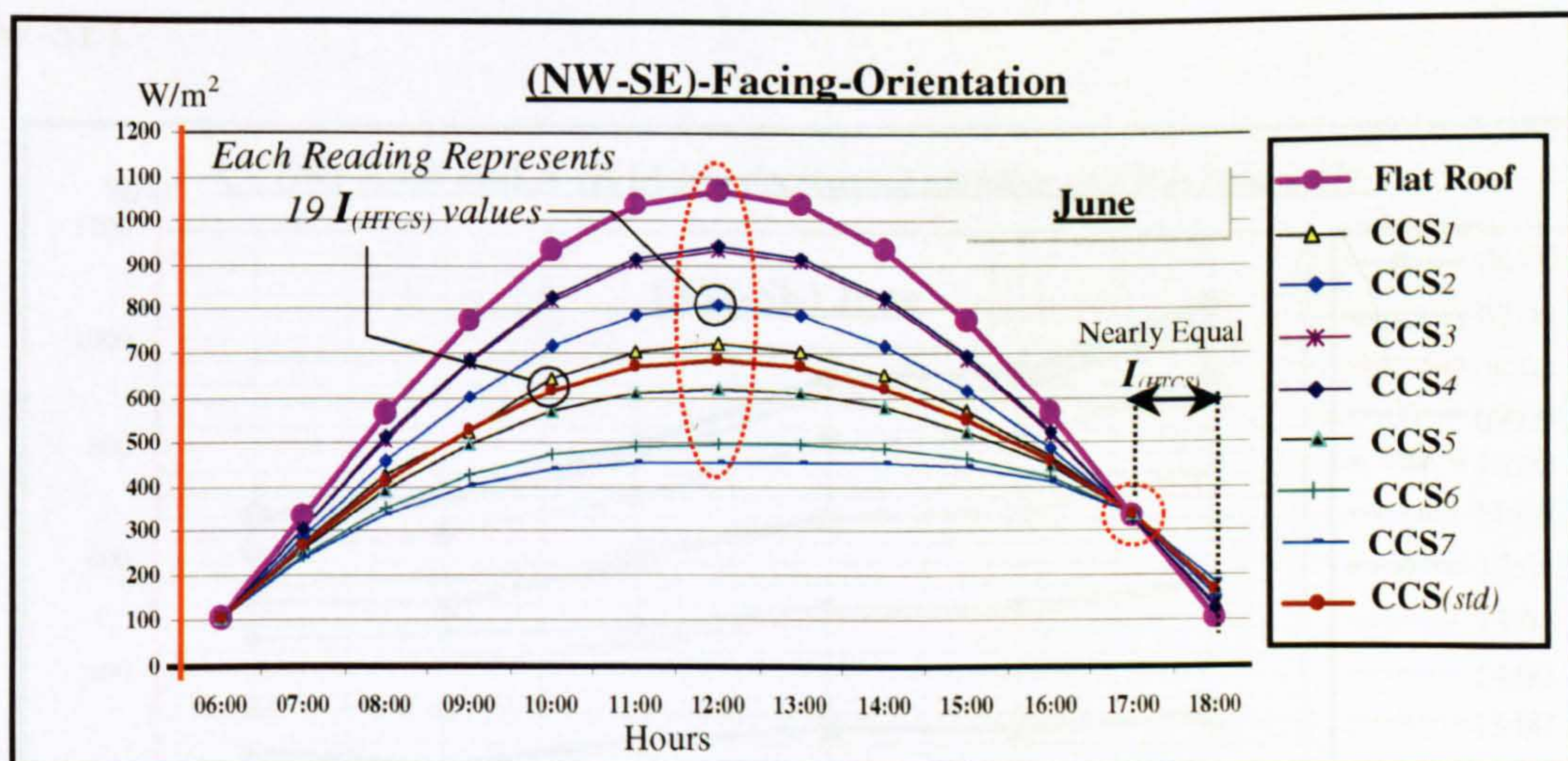


Figure 7-22 $I_{(HTCS)}$ (W/m^2) on The CCS_{1-7} , The $CCS_{(std)}$ and the Flat Roof

All tested roofs $I_{(HTCS)}$ -curves ascend differently after 06:00 where both are intersected. They reach their maximum at midday. During the late afternoon each roof $I_{(HTCS)}$ -curve descends differently till they intersect each other again around 17:00. At 18:00 all roofs $I_{(HTCS)}$ -curves become not intersected, Fig. (7-22).

Apart from the late afternoon hours, all roofs $I_{(HTCS)}$ -curves in this secondary orientation (NW-SE) seem to be identical to the (N-S) ones in summer, (only before the noon period, whereas in the afternoon they are similar to the (E-W) ones). Only the flat roof $I_{(HTCS)}$ -curve has symmetrical increase and decrease gradients around the midday axis, whereas, the curved roofs CCS_{1-7} $I_{(HTCS)}$ -curves are not symmetrical. Only at 06:00 in the morning, all roofs receive approximately equal $I_{(HTCS)}$ -values (this scenario took place the (N-S)-orientation in 06:00 and 18:00).

Fig. (7-22) also shows that throughout the day there is only one period (17:00-18:00) in which the curved roofs receive more $I_{(HTCS)}$ than the flat roof. This scenario did not exist when the CCS curvatures faced (N-S) in summer. The (NW-SE)-orientation remains more preferable for curved roofs than facing (E-W), where one more undesirable period during the early morning (06:00-07:00) has been created. For CCS curvatures face (NW-SE) in summer, the desirable time in which the curved roof receives less $I_{(HTCS)}$ than the flat roof has shorted by one hour compared to the (N-S) scenario (i.e. it ends one hour earlier).

Fig. (7-23) and (7-24) represent a proportional comparison between $I_{(HTCS)}$ -values on the seven curved roofs CCS_{1-7} compared to the $I_{(HTCS)}$ -values on the $CCS_{(std)}$ and the flat roof at (NW-SE).

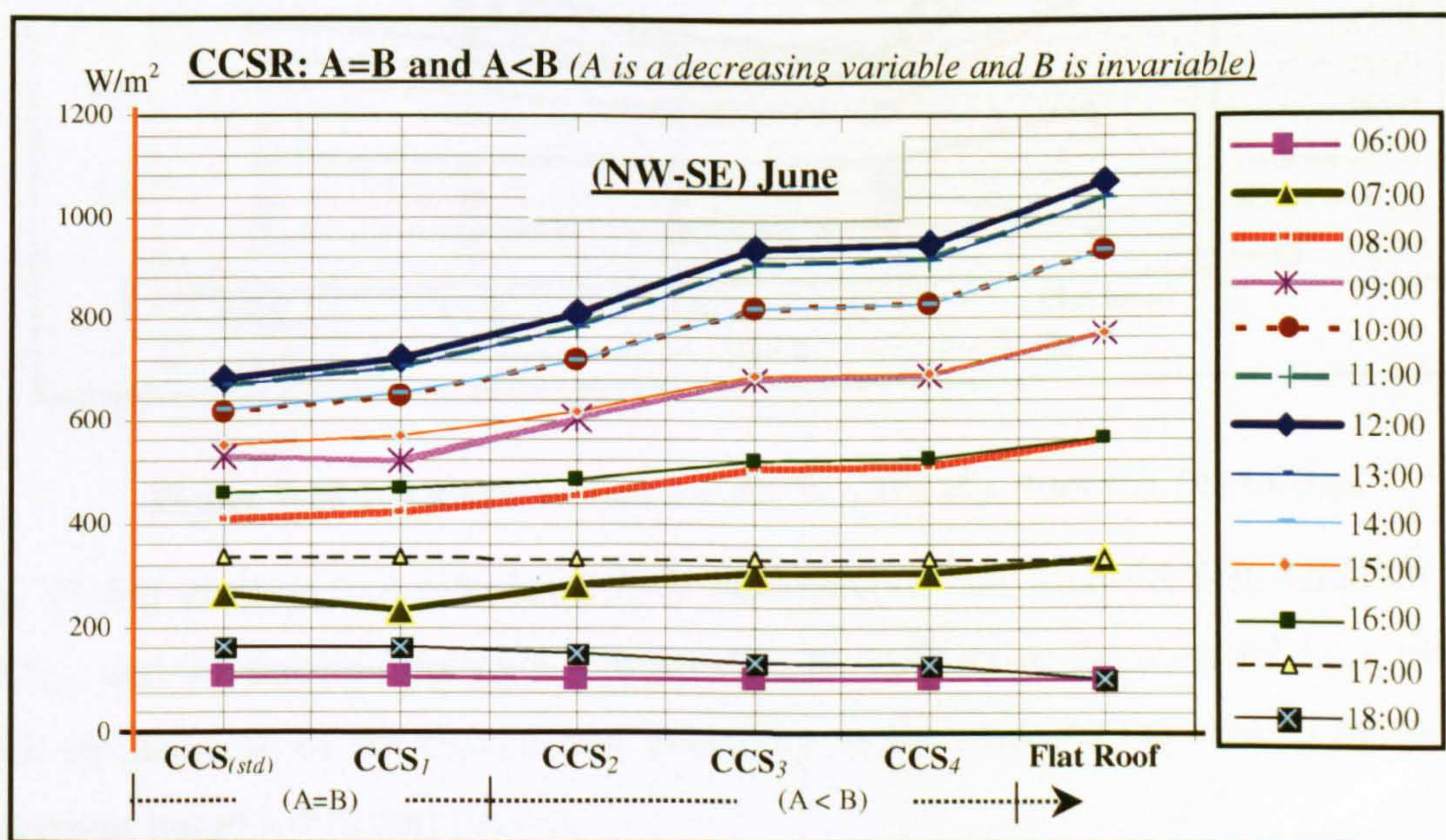


Figure 7-23 the Received $I_{(HTCS)}$ on CCS_{1-4} , the Flat Roof and the $CCS_{(std)}$

The two graphs present the same generated results of Fig. (7-22) with another graphical way that discusses each roof geometry $I_{(HTCS)}$ -values at every hour throughout daytime in summer. At secondary directions, the CCS $I_{(HTCS)}$ -mirrored-values are not equal around the midday axis. Fig. (7-24) discusses the thirteen daytime readings on CCS_1 , CCS_2 , CCS_3 and CCS_4 ($A=B$ and $A<B$). Fig. (7-23) shows that the received $I_{(HTCS)}$ increases with the decreasing of CCSR (" A " decreases), until it reaches the maximum on the flat roof, where A equals zero. In addition to the $CCS_{(std)}$ and the flat roof,

Fig. (7-24) discusses the daytime thirteen hourly-readings for CCS_5 , CCS_6 and CCS_7 (CCSR: $A>B$). Fig. (7-24) shows that the received $I_{(HTCS)}$ decreases with the increase of CCSR (" A " increases). At midday time, CCS_7 , where A equals $2B$, receives less $I_{(HTCS)}$ than the rest of roof geometries.

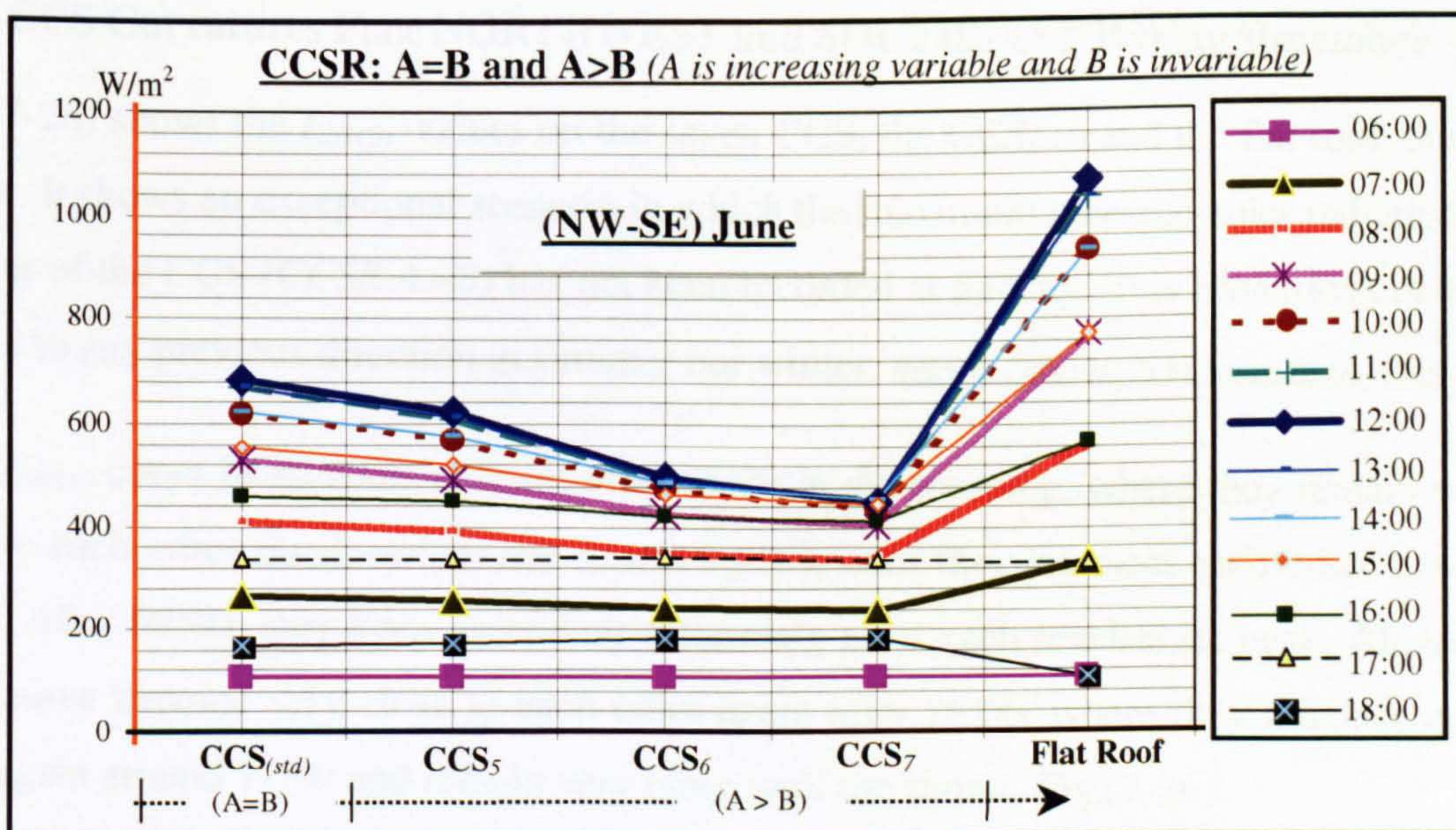


Figure 7-24 The Received $I_{(HTCS)}$ on CCS_{5-7} , The Flat Roof and The $CCS_{(std)}$

Fig. (7-25) displays the calculated $I_{(HTCS)}$ that received on each CCS in addition to the $CCS_{(std)}$ and the flat roof during a summer day. It verifies that the received $I_{(HTCS)}$ increases with the decrease of the curved roof concavity as the same as the case in the principle directions but in a different pattern.

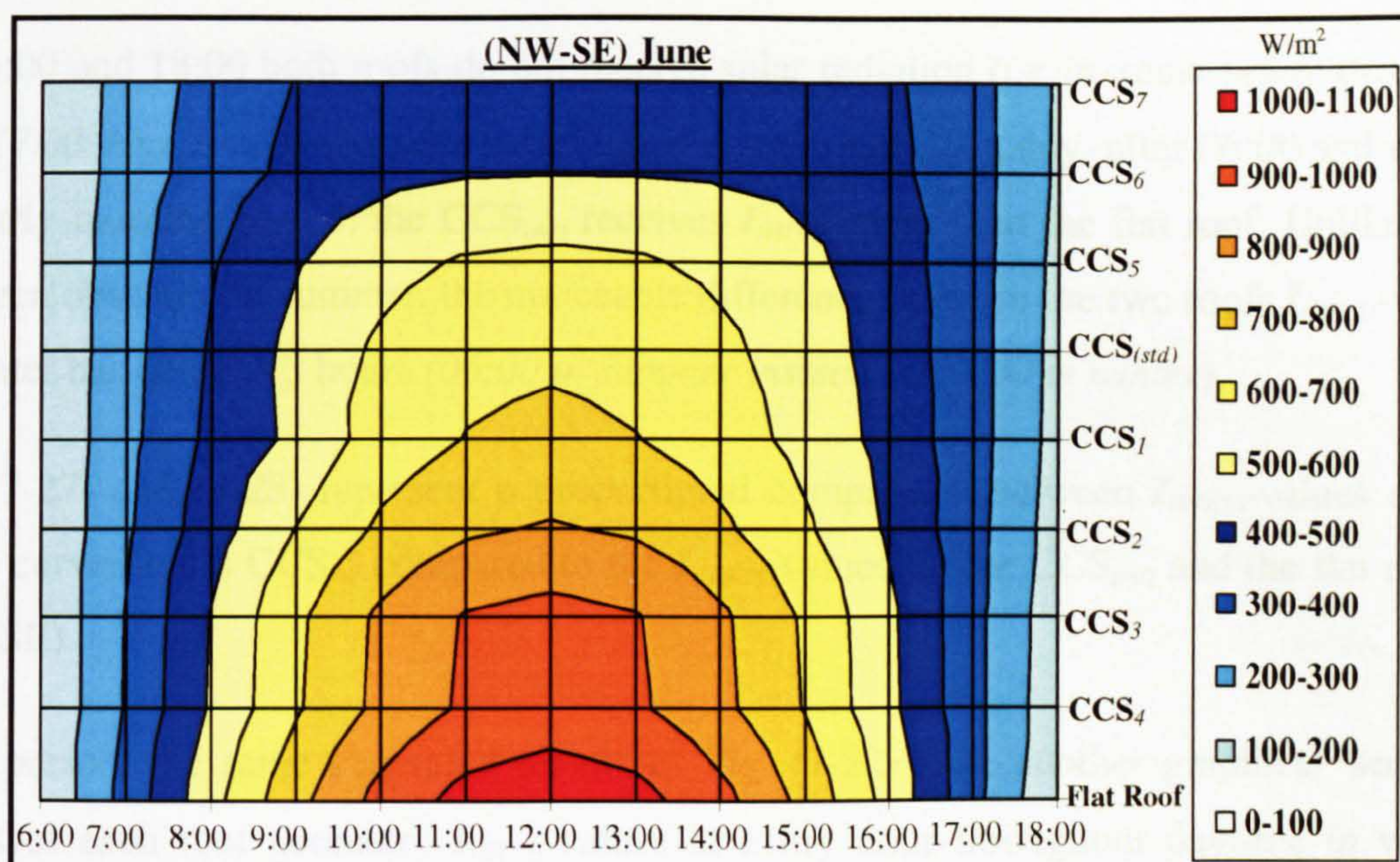


Figure 7-25 Alternated Arrangements of the Received $I_{(HTCS)}$ on the Tested Roofs

7.3.2 CCS Curvatures Face NORTHWEST and SOUTHEAST During December

Fig. (7-26) shows the $I_{(HTCS)}$ -values on the seven CCS, the $CCS_{(std)}$ and the flat roof during winter. It shows an exceptional scenario in which the maximum received solar radiation on number of the CCS ($CCSR A > B$) has not been recorded at midday. This scenario is neither similar to any previous direction in summer nor winter. Refer to Table (A-7) in Appendix (A) Page 18.

Each $I_{(HTCS)}$ -curve in all roofs ascends after 06:00 in the morning, where they remain very close to each other ($I_{(HTCS)}$ -values are nearly equal), until they intersect each other around 09:00. After 09:00, they keep ascending differently until each reaches its peak. All roofs $I_{(HTCS)}$ -curve become very close to each other again after 16:00, where they intersect each other again around 17:00 and remain very close until the sunset, Fig.(7-26).

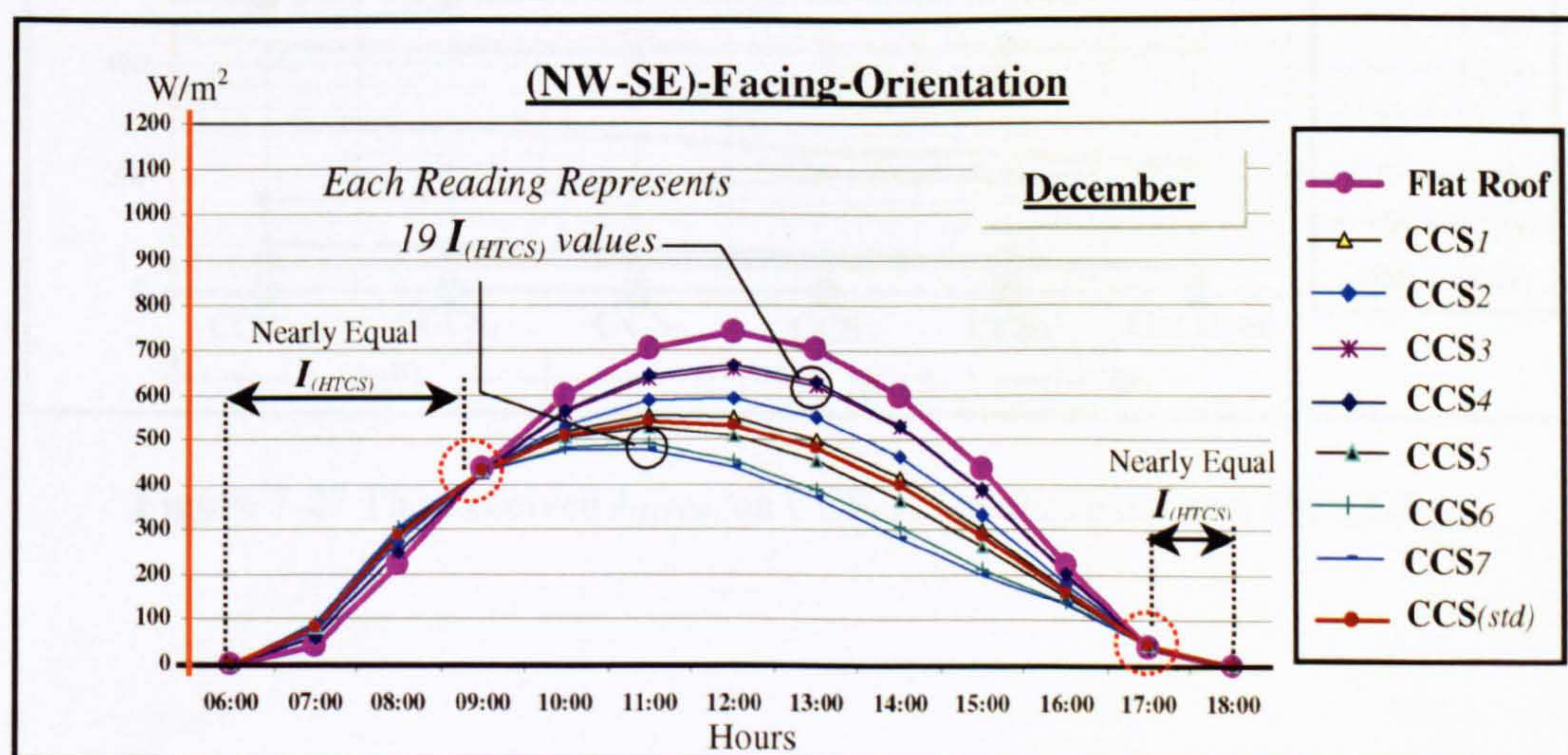


Figure 7-26 $I_{(HTCS)}$ (W/m^2) on The CCS_{1-7} , The $CCS_{(std)}$ and The Flat Roof

At 06:00 and 18:00 both roofs do not receive solar radiation (*i.e.* in winter before 07:00 and after 17:00 there is no measurable solar radiation intensities). Notably, after 06:00 and during the early morning period, the $CCS_{(std)}$ receives $I_{(HTCS)}$ more than the flat roof. Unlike what has been observed in summer, the noticeable difference between the two roofs $I_{(HTCS)}$ -values in winter has delayed 3 hours (06:00 in summer instead of 09:00 in winter).

Fig. (7-27) and (7-28) represent a proportional comparison between $I_{(HTCS)}$ -values on the seven curved roofs CCS_{1-7} compared to the $I_{(HTCS)}$ -values on the $CCS_{(std)}$ and the flat roof at (NW-SE).

They present the same generated results of Fig. (7-22) with another graphical way that discusses each roof geometry $I_{(HTCS)}$ -values at every hour throughout daytime in winter. Similar to summer scenarios at secondary directions, the CCS $I_{(HTCS)}$ -mirrored-values are not equal around the midday axis. Therefore, Fig. (7-27) discusses the thirteen daytime readings on CCS_1 , CCS_2 , CCS_3 and CCS_4 ($A=B$ and $A<B$). Apart from the early morning and the late afternoon, Fig. (7-27) shows that the received $I_{(HTCS)}$ increases with the decreasing of CCSR (" A " decreases), until it reaches the maximum on the flat roof, where A equals zero.

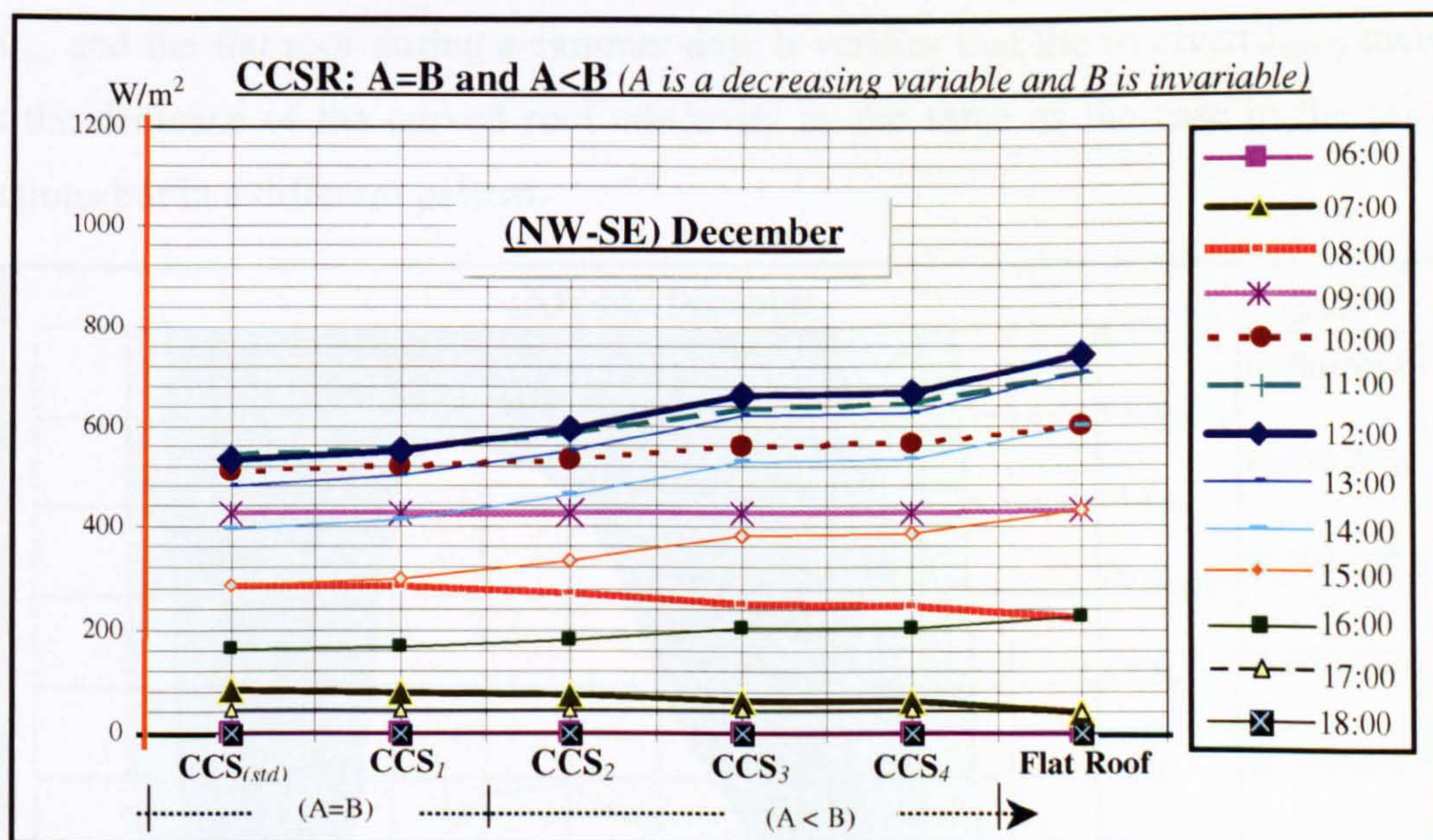


Figure 7-27 The Received $I_{(HTCS)}$ on CCS_{1-4} , The Flat Roof and The $CCS_{(std)}$

In addition to the $CCS_{(std)}$ and the flat roof, Fig. (7-28) discusses the daytime thirteen hourly-readings for CCS_5 , CCS_6 and CCS_7 (CCSR: $A > B$). Apart from the early morning and the late afternoon, Fig. (7-28) shows that the received $I_{(HTCS)}$ decreases with the increase of CCSR ("A" increases).

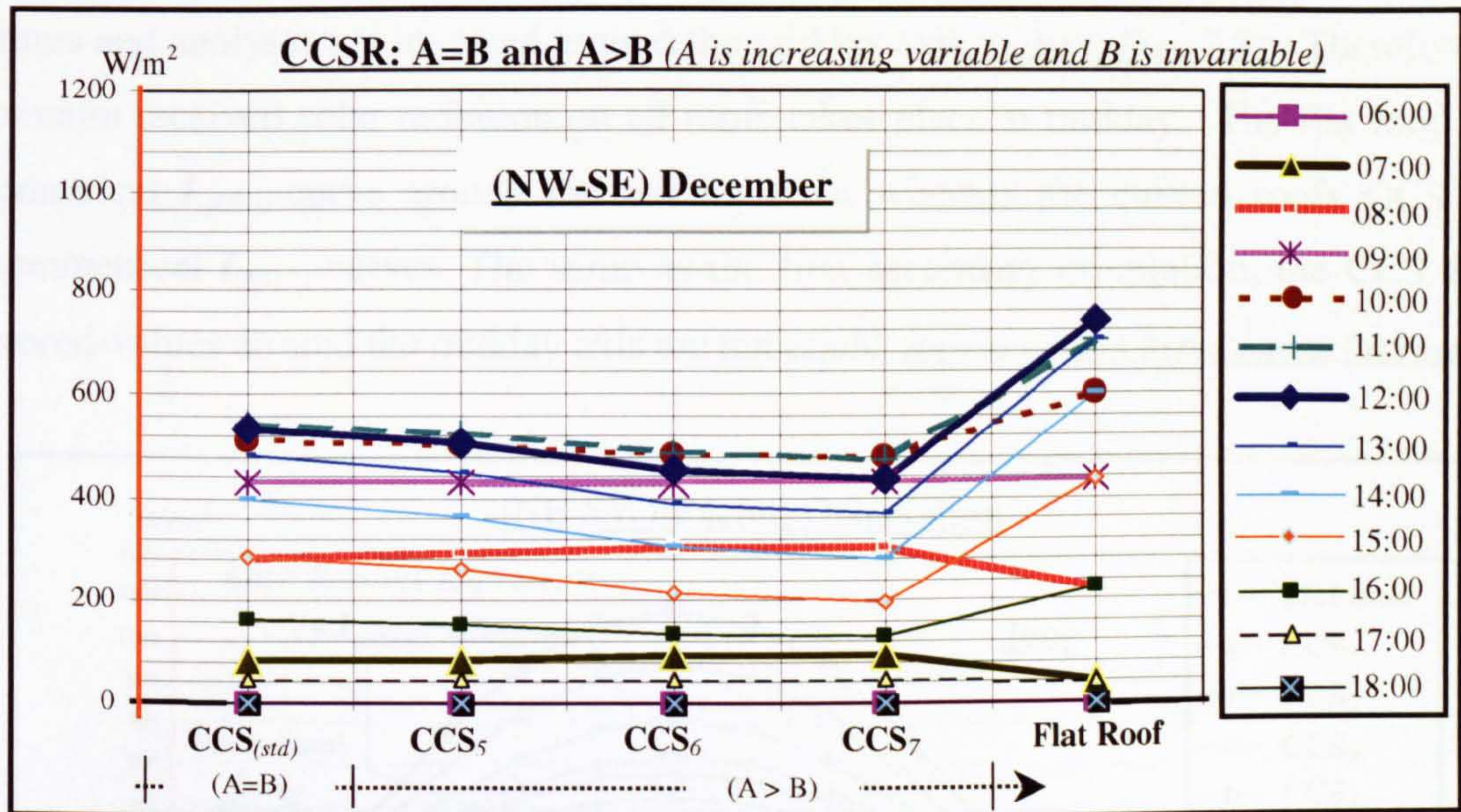


Figure 7-28 The Received $I_{(HTCS)}$ on CCS_{5-7} , The Flat Roof and The $CCS_{(std)}$

Fig. (7-29) displays the calculated $I_{(HTCS)}$ that received on each CCS in addition to the $CCS_{(std)}$ and the flat roof during a summer day. It verifies that the received $I_{(HTCS)}$ increases with the decrease of the curved roof concavity as the same as the case in the principle directions but in a different pattern.

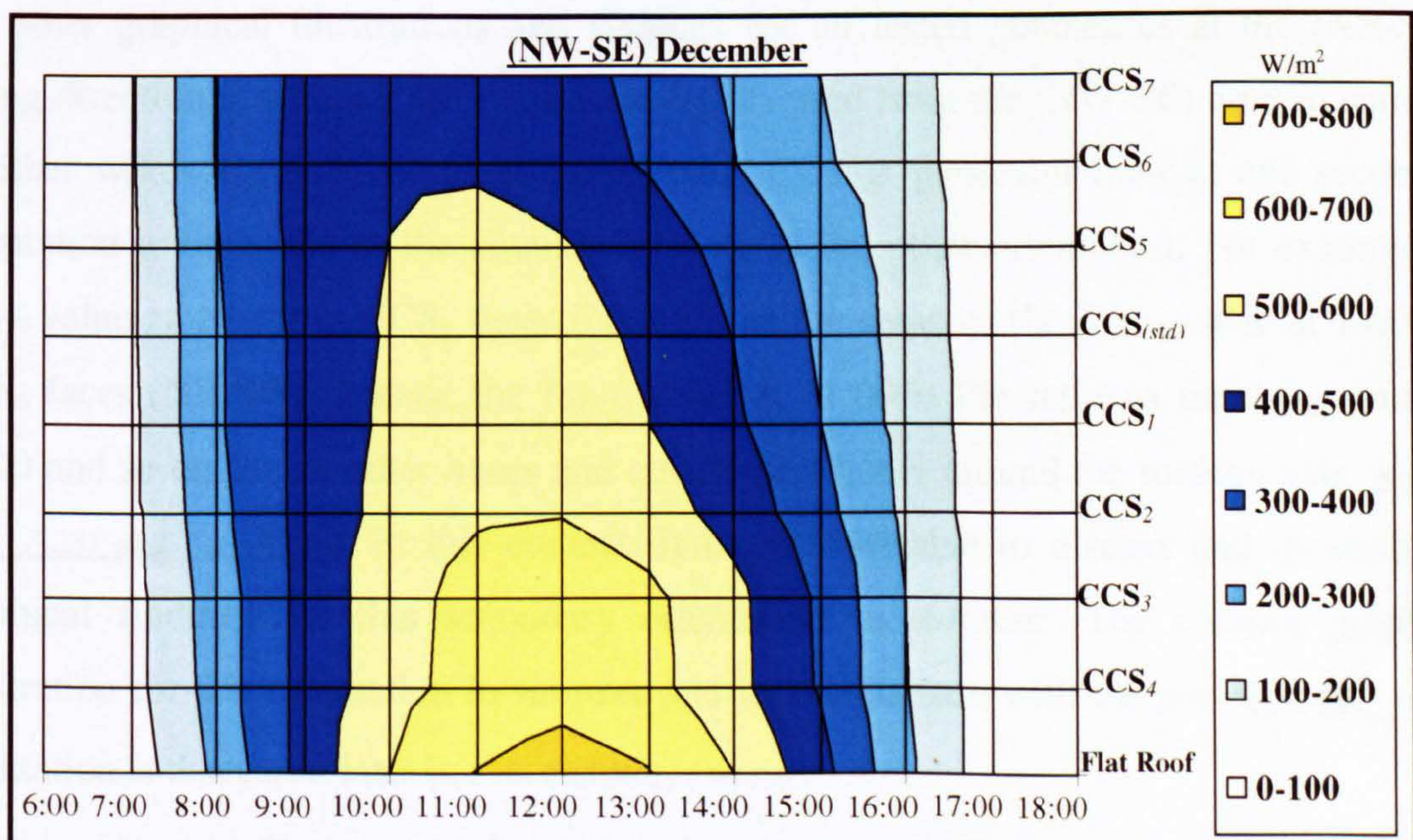


Figure 7-29 Alternated Arrangements of The Received $I_{(HTCS)}$ on The Tested Roofs

7.3.3 CCS Curvatures Face NORTHEAST and SOUTHWEST During June

Fig. (7-30) shows $I_{(HTCS)}$ -values and distribution forms on seven CCS face (NE-SW) in comparison to the received $I_{(HTCS)}$ on the flat roof and the $CCS_{(std)}$ in summer. This is an identically inverted scenario of the previous secondary direction (NW-SE), in which all features and analyses are inverted around the midday axis, (refer to Fig. (7-22)). Therefore, the maximum received solar radiation on all roofs takes place at midday. The flat roof has a symmetrical $I_{(HTCS)}$ -curve around the midday axis, whereas the curved roofs CCS have unsymmetrical $I_{(HTCS)}$ -curves. The same as the first secondary orientation, the CCS $I_{(HTCS)}$ -mirrored-values around the midday axis are not equal. Refer to Table (A-8) in Appendix (A) Page 19.

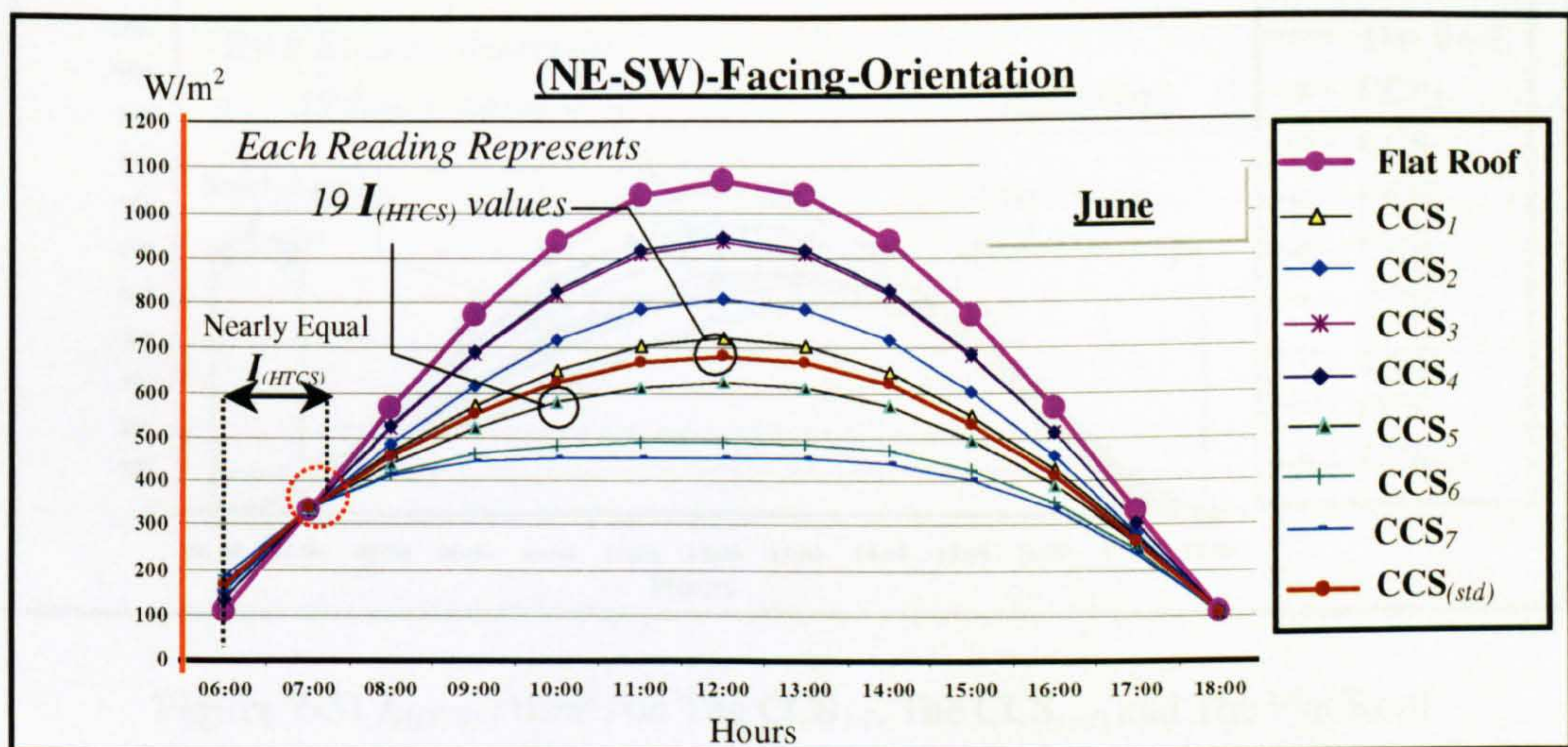


Figure 7-30 $I_{(HTCS)}$ (W/m^2) on The CCS_{1-7} , The $CCS_{(std)}$ and The Flat Roof

All other graphical illustrations and findings for all tested geometries at the (NE-SW)-facing direction in summer are symmetrically inverted from the (NW-SE) ones in summer. In other words the solar performance of each CCS at particular hour at one secondary orientation is the same as the counterpart hour at the other orientation. For example the $I_{(THCS)}$ value at 10:00 on CCS_6 faces (NW-SE) is the same as the $I_{(THCS)}$ value at 14:00 on CCS_6 faces (NE-SW). Likely, the $I_{(THCS)}$ value at 11:00 is the same as the $I_{(THCS)}$ value at 13:00 and so on for all other hours and counterpart hours around the midday axis. Refer to Fig. (7-23) and Fig. (7-24). In this context, it is not advisable to discuss and illustrate the graphical findings for this secondary orientation in summer. The contour graphical illustration for this orientation in summer and its comparison with the previous secondary orientation is discussed later in this chapter, (section 7.6).

7.3.4 CCS Curvatures Face NORTHEAST and SOUTHWEST During December

The same as in summer, Fig. (7-31) shows that the winter scenario of the second secondary direction (NE-SW) is identically inverted of the first one, (NW-SE), *refer to Fig. (7-26)*. The proportional comparison between the $I_{(HTCS)}$ -values on the $CCS_{(std)}$ and to that on the flat roof is the inverted scenario of the first secondary direction (NW-SE) (*Refer to Fig.(7-27) and Fig. (7-28)*). In winter, the daily average ratios are the same at the both secondary directions. *Refer to Table (A-9) in Appendix (A) Page 20.*

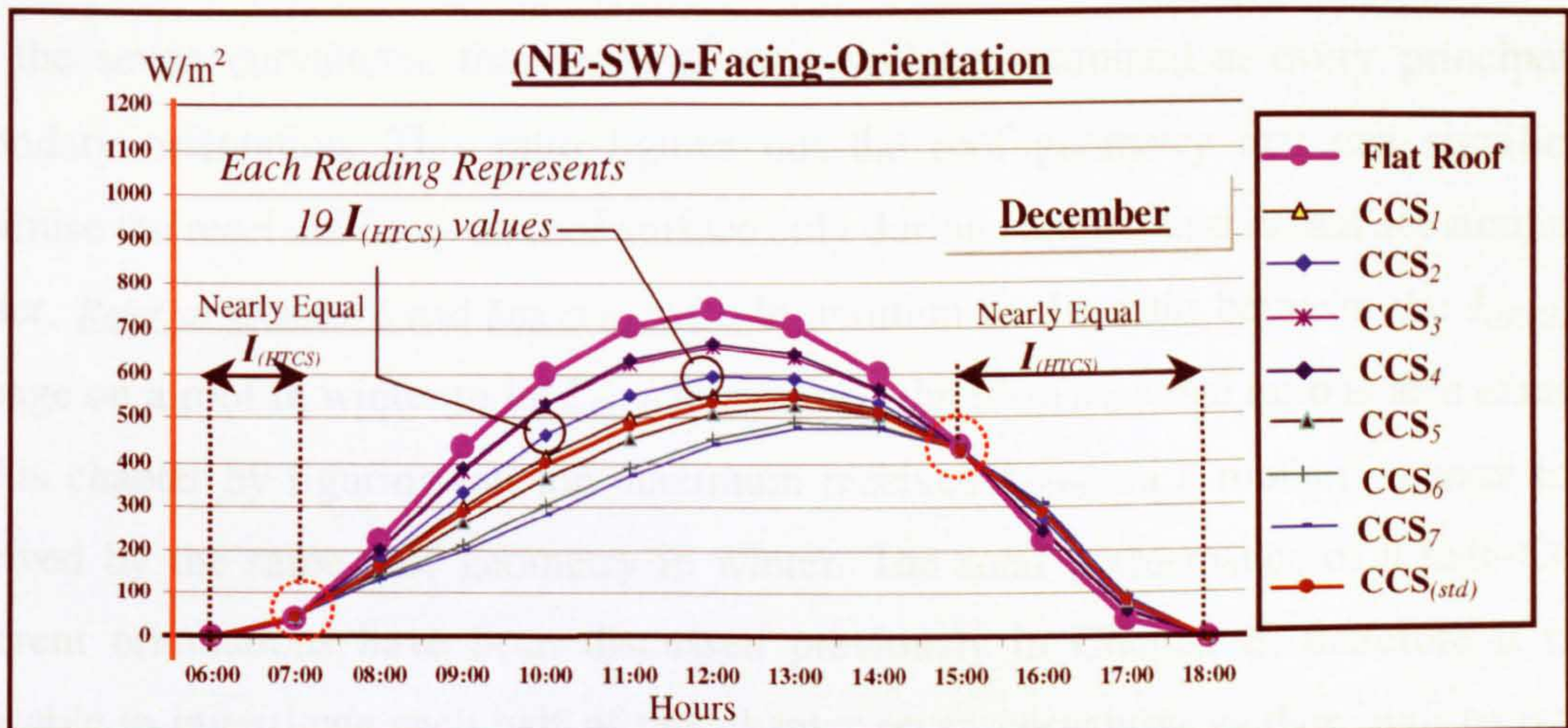


Figure 7-31 $I_{(HTCS)}$ (W/m^2) on The CCS_{1-7} , The $CCS_{(std)}$ and The Flat Roof

Similar to the same concept for summer scenarios, all other graphical illustrations and findings for all tested geometries at the (NE-SW)-facing direction in winter are symmetrically inverted from the (NW-SE) ones in winter. In other words the solar performance of each CCS at particular hour at one secondary orientation is the same as the counterpart hour at the other orientation. For example the $I_{(THCS)}$ value at 10:00 on CCS_6 faces (NW-SE) is the same as the $I_{(THCS)}$ value at 14:00 on CCS_6 faces (NE-SW). Likely, the $I_{(THCS)}$ value at 11:00 is the same as the $I_{(THCS)}$ value at 13:00 and so on for all other hours and counterpart hours around the midday axis. (*Refer to Fig.(7-27) and Fig. (7-28)*).

In this context, it is not advisable to discuss and illustrate the graphical findings for this secondary orientation in summer. The contour graphical illustration for this orientation in winter and its comparison with the other secondary orientation is discussed later in this chapter, (*section 7.6*).

7.4 FORM SEASONAL RATIOS

As has been pointed out through the previous chapter and this chapter, any roof geometry receives less $I_{(HTCS)}$ in winter compared to summer, whereas it is preferable to receive as much solar radiation as possible during winter. A form seasonal ratio for seven curvatures (CCS_1 - CCS_7) is carried out in this part following the same concept of the previous chapter, which figured out the difference between the flat roof and $CCS_{(std)}$ seasonal behaviours. As explained previously in Chapter 6, form-seasonal-ratio means the ratio between the $I_{(HTCS)}$ -day average on this roof in winter to that in summer.

For the seven curvatures, this seasonal ratio will be examined at every principal and secondary orientation. This ratio figures out the roof geometry that can significantly minimise the received $I_{(HTCS)}$ on roof surface only during summer and do not act similarly in winter. Refer to Chapter 6 and Equation (6-2). In addition to the ratio between the $I_{(HTCS)}$ -day average on a roof in winter to its $I_{(HTCS)}$ in summer, the form seasonal ratio is also examined in this chapter by figuring out the maximum received $I_{(HTCS)}$ on a roof in summer to that received by the same roof geometry in winter. The solar performance of a half-CCS at different orientations have been discussed previously in Chapter 6, therefore it is not advisable to investigate each half of this chapter seven curvatures as there will be no new implications. Refer to Tables (6-2), (6-3), (6-4), & (6-5)

The following graphical predictions may add advantages to all curved roof curvatures and orientations during winter, the same as in summer. They illustrate that roof curvature CCSR and orientation have great influences on the form- seasonal-ratio. As implied from $CCS_{(std)}$ in Chapter 6, and according to the following findings, the CCS_7 appears as the most preferable form over the year with the comparison to the rest of the other curved roof curvatures. It receives the desired $I_{(HTCS)}$ in both seasons (*the nearest form-seasonal-ratio to 1*).

Fig. (7-32) illustrates the differences between the summer maximum received $I_{(HTCS)}$ and the winter maximum received $I_{(HTCS)}$ on the tested geometries (CCS_{1-7} , $CCS_{(std)}$ and flat) at the (N-S)-facing direction. The graph shows that form seasonal ratios (the difference between summer and winter) vary from one geometry to another. As explained previously, the more solar efficient roof geometry is that geometry which has seasonal ratio equal or near to 1.

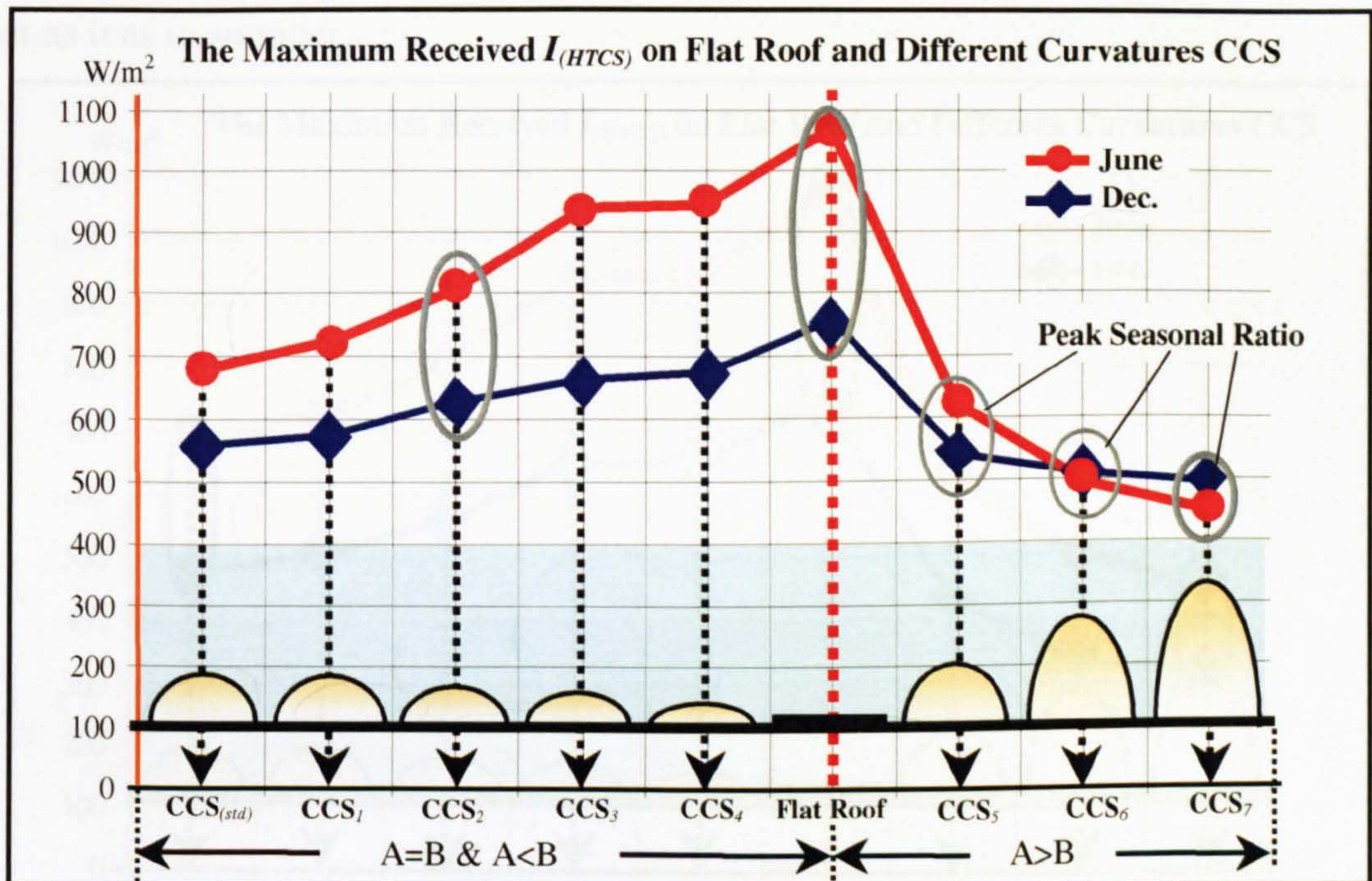


Figure 7-32 The Maximum Received $I_{(HTCS)}$ on Different Forms of Roofs (The Principle Direction (N-S)) (Peak Seasonal Ratio)

Fig. (7-33) illustrates the day average of the received $I_{(HTCS)}$ on the same tested roof geometries in summer and winter. CCS_5 , CCS_6 and CCS_7 has nearly equal summer and winter day-average $I_{(HTCS)}$, which means more solar efficient form.

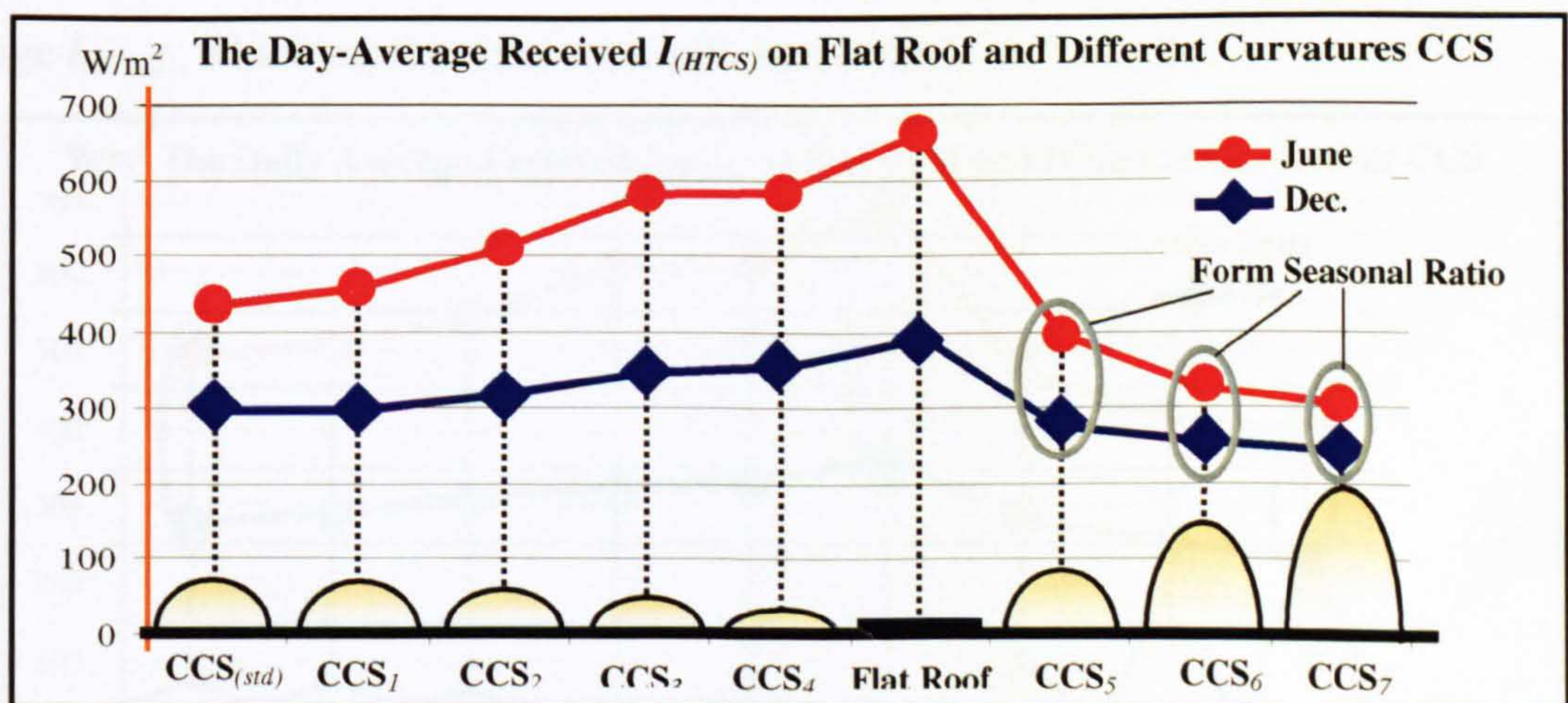


Figure 7-33 The Day Average Received $I_{(HTCS)}$ on Different Forms of Roofs (The Principle Direction (N-S)) (Form Seasonal Ratio)

Fig. (7-34) illustrates the differences between the summer maximum received $I_{(HTCS)}$ and the winter maximum received $I_{(HTCS)}$ on the tested geometries (CCS_{1-7} , $CCS_{(std)}$ and flat) at the (E-W)-facing direction. The graph shows that the differences between the two season behaviours of the seven CCS when curvatures face (E-W) are dissimilar to those in the previous principle direction (N-S). It verifies that (N-S) is more preferable than (E-W) in winter as it is in summer.

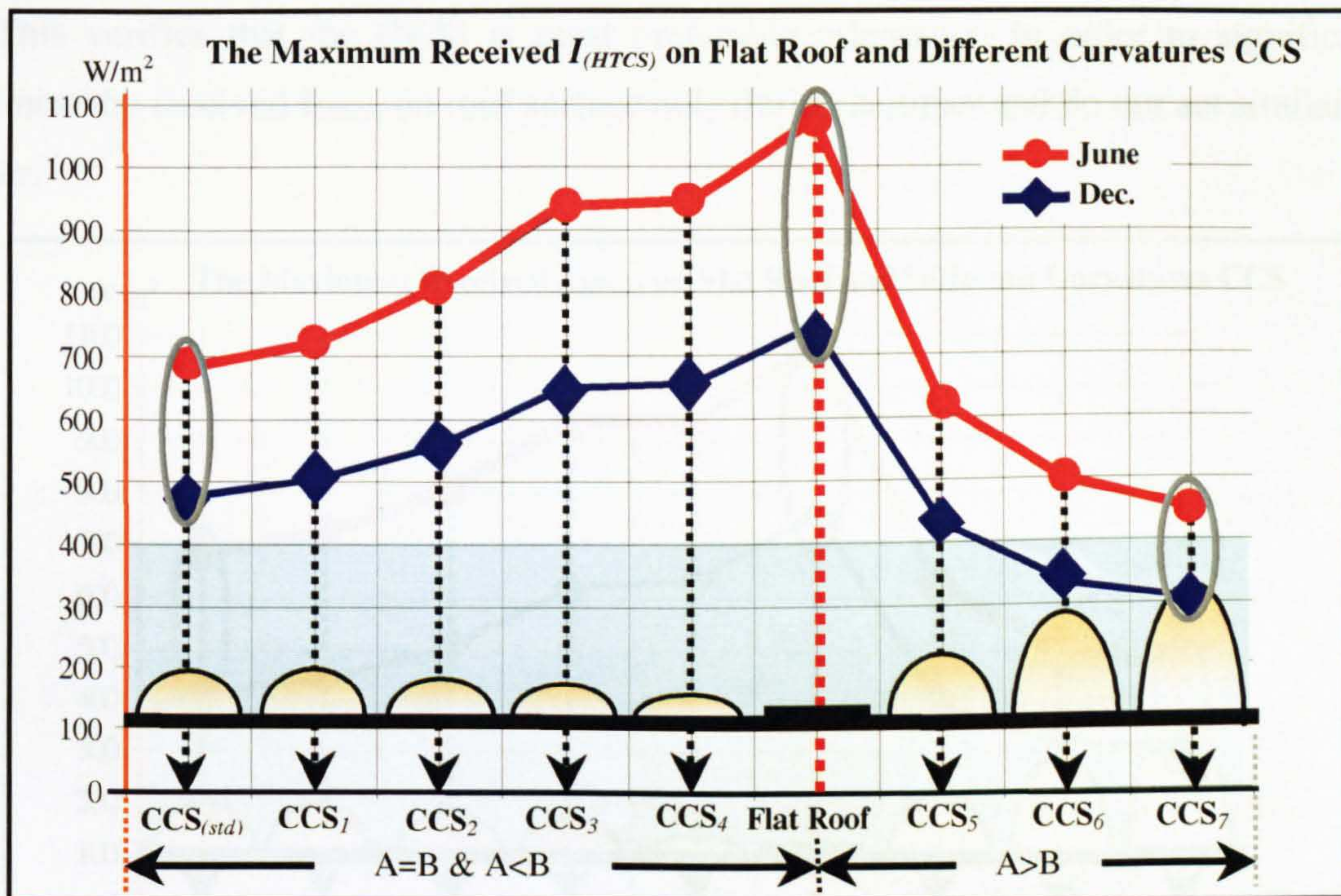


Figure 7-34 The Maximum Received $I_{(HTCS)}$ on Different Forms of Roofs (The Principle Direction (E-W)) (Peak Seasonal Ratio)

Fig. (7-35) illustrates the day average of the received $I_{(HTCS)}$ at the same orientation (E-W) in summer and winter. CCS_5 , CCS_6 and CCS_7 has nearly equal summer and winter day-average $I_{(HTCS)}$, which means more solar efficient form.

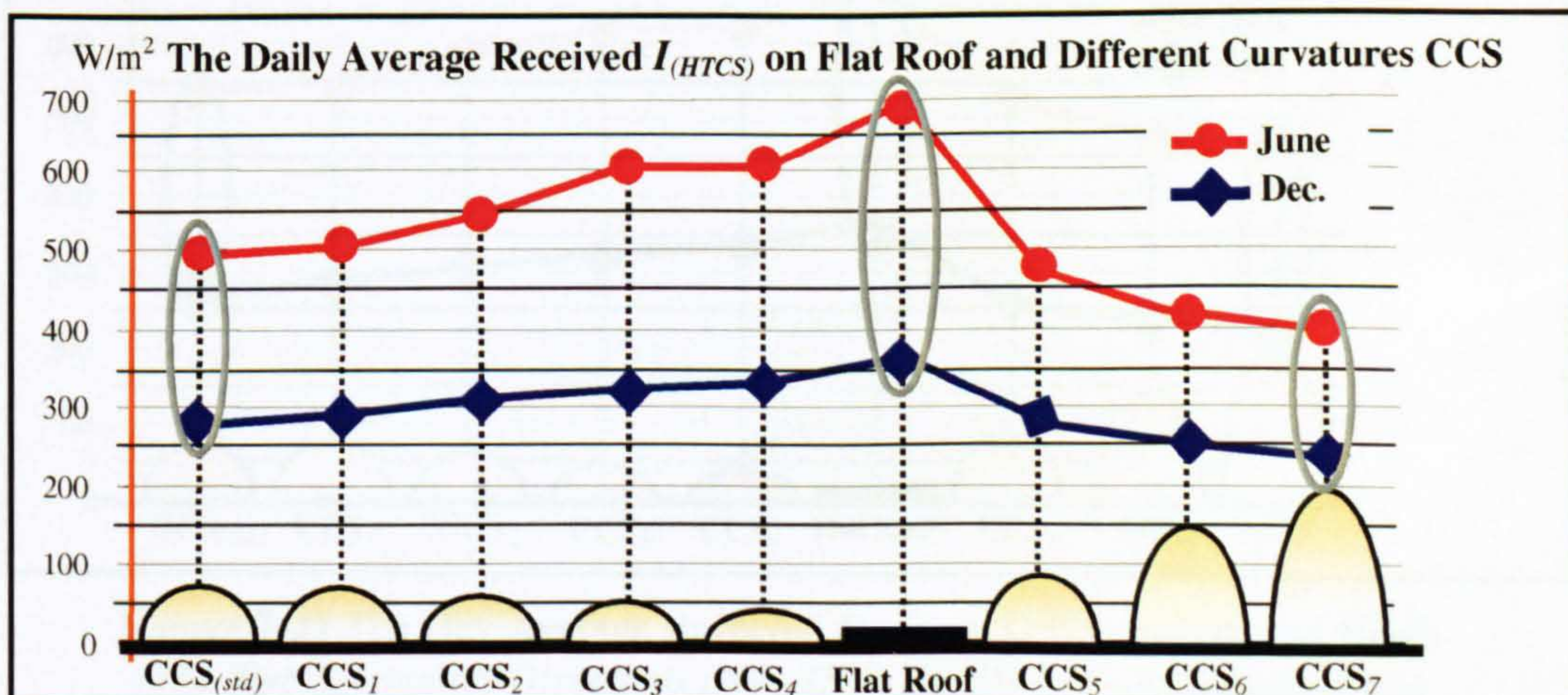


Figure 7-35 The Day Average Received $I_{(HTCS)}$ on Different Forms of Roofs (The Principle Direction (E-W)) (Form Seasonal Ratio)

Fig. (7-36) and Fig. (7-37) illustrate the same previously discussed solar performances on the same tested geometries, but when the curvatures face secondary directions. The graphs show that the differences between the two season behaviours of the seven CCS when curvatures face either (NW-SE) or (NE-SW) are dissimilar to those in the previous principle directions (N-S) or (E-W). The graphical findings show that the secondary directions are more solar efficient than the E-W) but it is not the case comparatively to (N-S). This verifies that the (N-S) is most preferable orientation in order to significantly minimise the received $I_{(HTCS)}$ on roof surface only during summer and do not act similarly in winter.

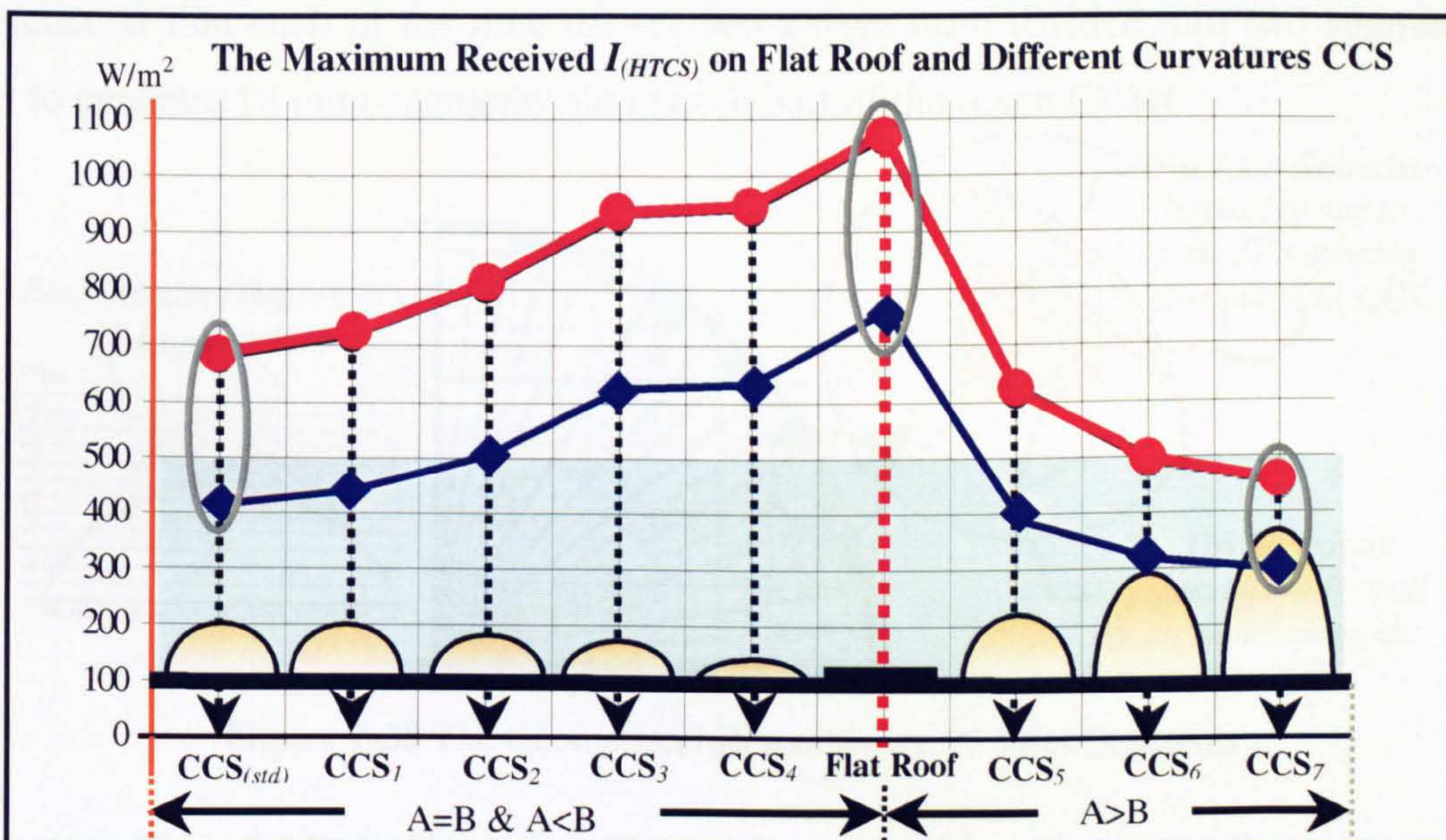


Figure 7-36 The Maximum Received $I_{(HTCS)}$ on Different Forms of Roofs (The Two Secondary Directions (NW-SE & NE-SW)) (Peak Seasonal Ratio)

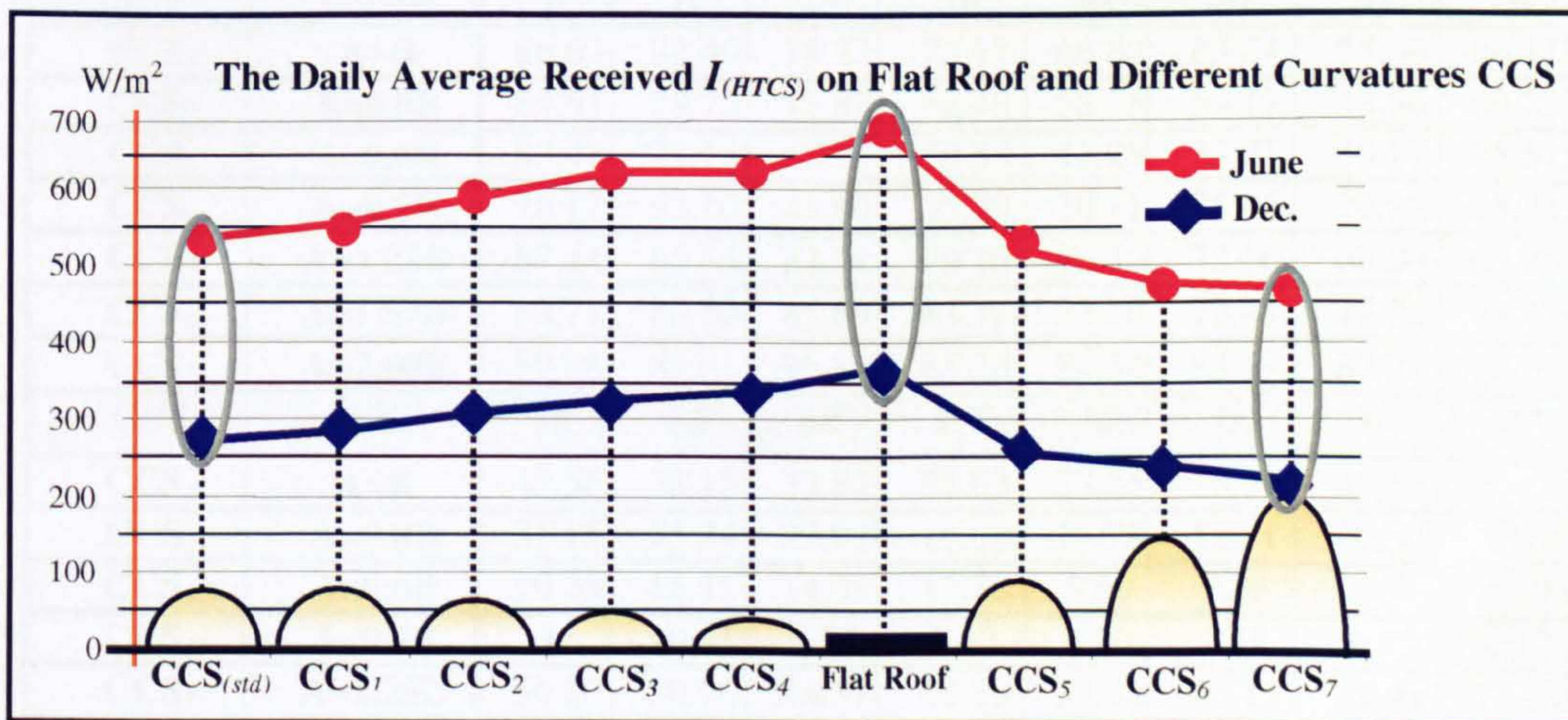


Figure 7-37 The Day Average Received $I_{(HTCS)}$ on Different Forms of Roofs (The Two Secondary Directions (NW-SE & NE-SW)) (Form Seasonal Ratio)

7.5 DATA INPUT AND CURVED ROOFS GEOMETRICAL RESEMBLANCE

Different Curved Roof Curvatures (Varying CCSR; $CCSR_1 - CCSR_7$) (37 Joint Segments)

This section discusses the geometrical resemblance of the same seven CCSR using the same joint segments technique, but every 5° radian instead of 10° radian (the angle between every two subsequent radial lines), Fig. (7-38). Each half-CCS has been resembled by eighteen joint segments in addition to the horizontal one at the middle-top of the curve. The slope angles of the 37-joint-segments along each curved roof cross section are displayed in Table (7-10). The geometrical resemblance for the 37-joint-segments has been carried out similar to the 19-joint-segments one. Refer to Fig. (7-2), (7-3) and (7-4). The only difference is that each of the nine tilt segments have been divided into two segments in order to generate 18 joint-segments along each half of the seven CCSR.

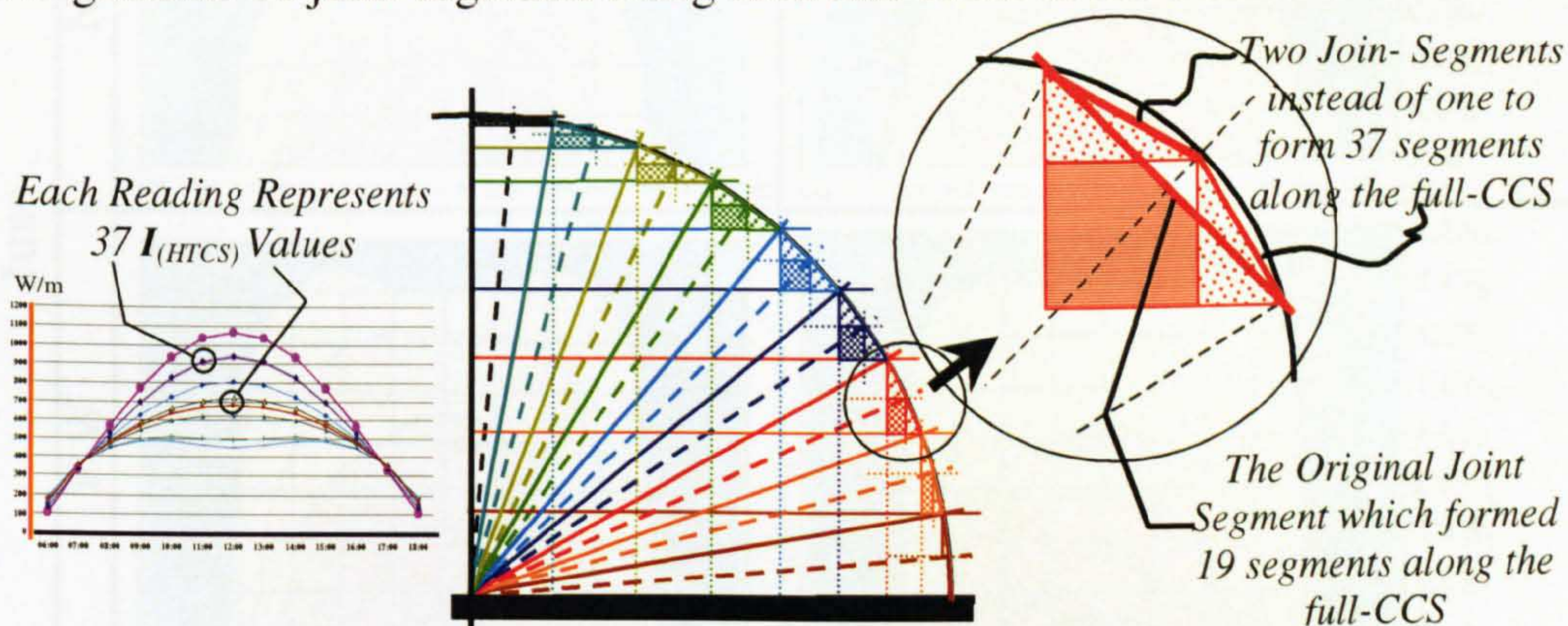


Figure 7-38 The Geometrical Resemblance 37 Joint Segments

Table 7-2 Radial Slopes from The Horizontal and Planar Segments Slopes

CCS	CCSR	Radial Lines Slopes (Radian = 5°) & Planar Segments Slopes								
		5°	10°	15°	20°	25°	30°	35°	40°	45°
CCS_1	A=B	86.63	82.40	78.27	73.77	66.80	63.34	57.44	54.11	47.12
CCS_2	A=0.8B	84.61	78.70	71.87	62.48	55.75	50.19	43.56	40.23	34.28
CCS_3	A=0.6B	82.47	73.11	57.68	50.57	41.28	35.27	30.17	25.51	21.12
CCS_4	A=0.5B	76.17	62.10	47.60	35.78	30.11	25.46	20.98	15.25	14.38
CCS_5	A=1.25B	87.41	85.84	82.97	79.26	76.46	73.66	68.00	63.85	59.67
CCS_6	A=1.67B	88.71	86.20	85.69	83.11	82.40	79.44	78.24	75.17	72.83
CCS_7	A=2.00B	89.88	87.61	86.11	85.23	84.54	83.49	82.77	80.56	77.55
CCS	CCSR	50°	55°	60°	65°	70°	75°	80°	85°	90°
CCS_1	A=B	43.56	38.15	32.85	27.03	23.45	16.07	12.63	8.13	5.00
CCS_2	A=0.8B	31.15	25.34	22.93	18.08	15.78	12.71	10.32	7.89	3.54
CCS_3	A=0.6B	19.35	16.11	14.03	12.38	8.69	7.26	5.87	4.98	2.79
CCS_4	A=0.5B	11	10.71	8.25	8.13	6.80	6.18	4.73	4.12	2.10
CCS_5	A=1.25B	56.30	50.90	44.37	40.39	33.43	25.15	20.46	11.14	4.83
CCS_6	A=1.67B	70.20	65.36	61.22	57.33	49.61	43.03	32.03	19.40	7.26
CCS_7	A=2.00B	76.45	71.96	69.91	65.11	60.56	52.24	42.30	27.49	9.25

7.6 COMPARISON BETWEEN THE RECEIVED $I_{(HTCS)}$ on different CCSR

This section represents a graphical comparison between the findings of the received $I_{(HTCS)}$ on the resembled geometries by using both the 19-joint-segments and the 37-joint-segments techniques. The generated results from both techniques are very similar. Fig. (7-39) displays the both 19 and 37 joint-segments $I_{(HTCS)}$ values when the curvatures face principle orientations (N-S & E-W) in summer and winter. It shows that the 37-joint-segments results are more accurate and precise.

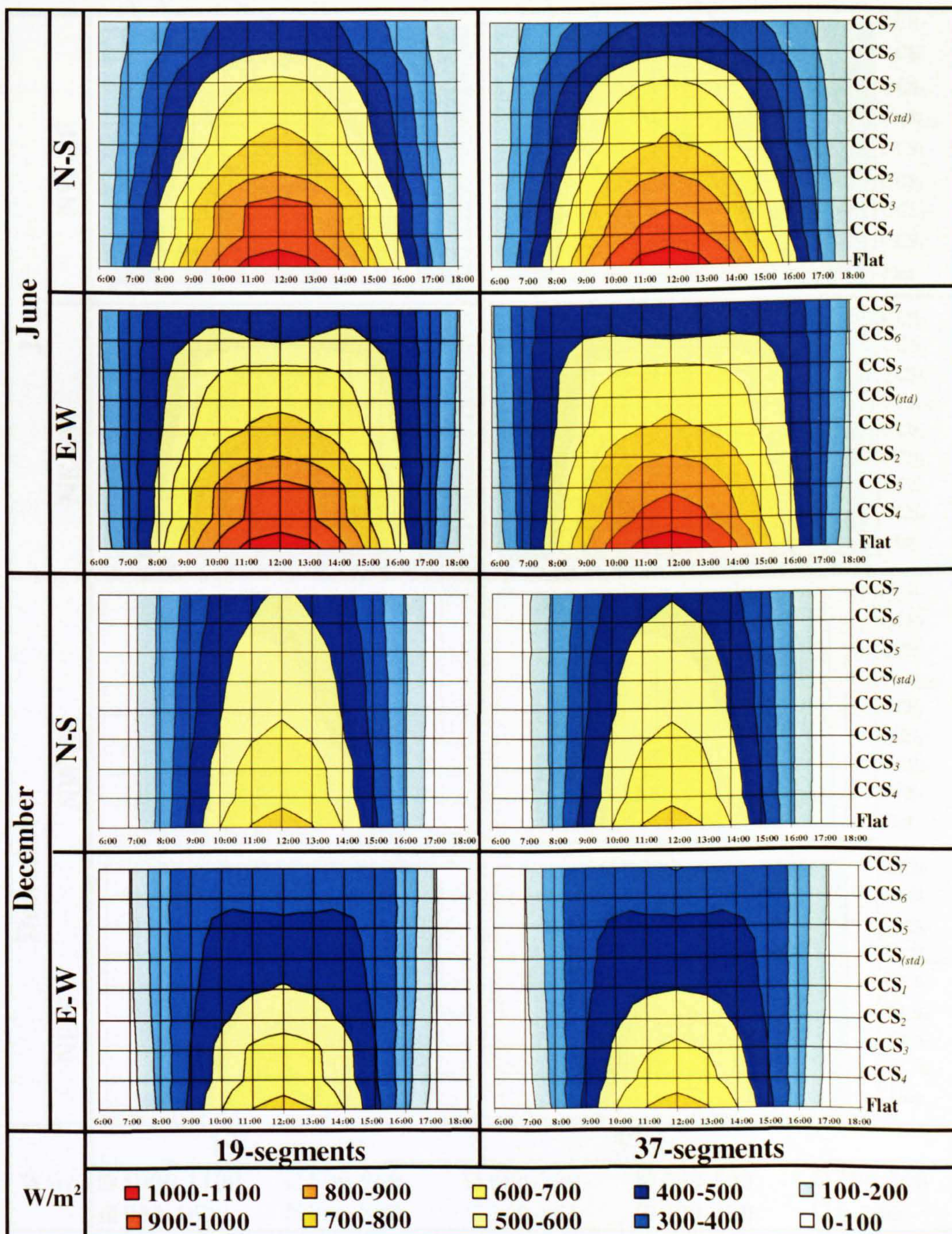


Figure 7-39 Comparison Between The Received $I_{(HTCS)}$ on 19 and 37 Joint Segment Curved Roofs (Principle Directions)

As has been explained previously in this chapter, each resulted reading for the 19-segments findings have been generated from 19 $I_{(HTCS)}$ values. In this context, each displayed reading in the 37-segment graphical illustrations is generated from 37 $I_{(HTCS)}$ values, Fig.(7-39) and Fig.(7-40). The $I_{(HTCS)}$ values for both cases (19 & 37 joint-segments) when their curvatures face secondary orientations (NW-SE & NE-SW) in summer and winter are displayed in Fig.(7-40).

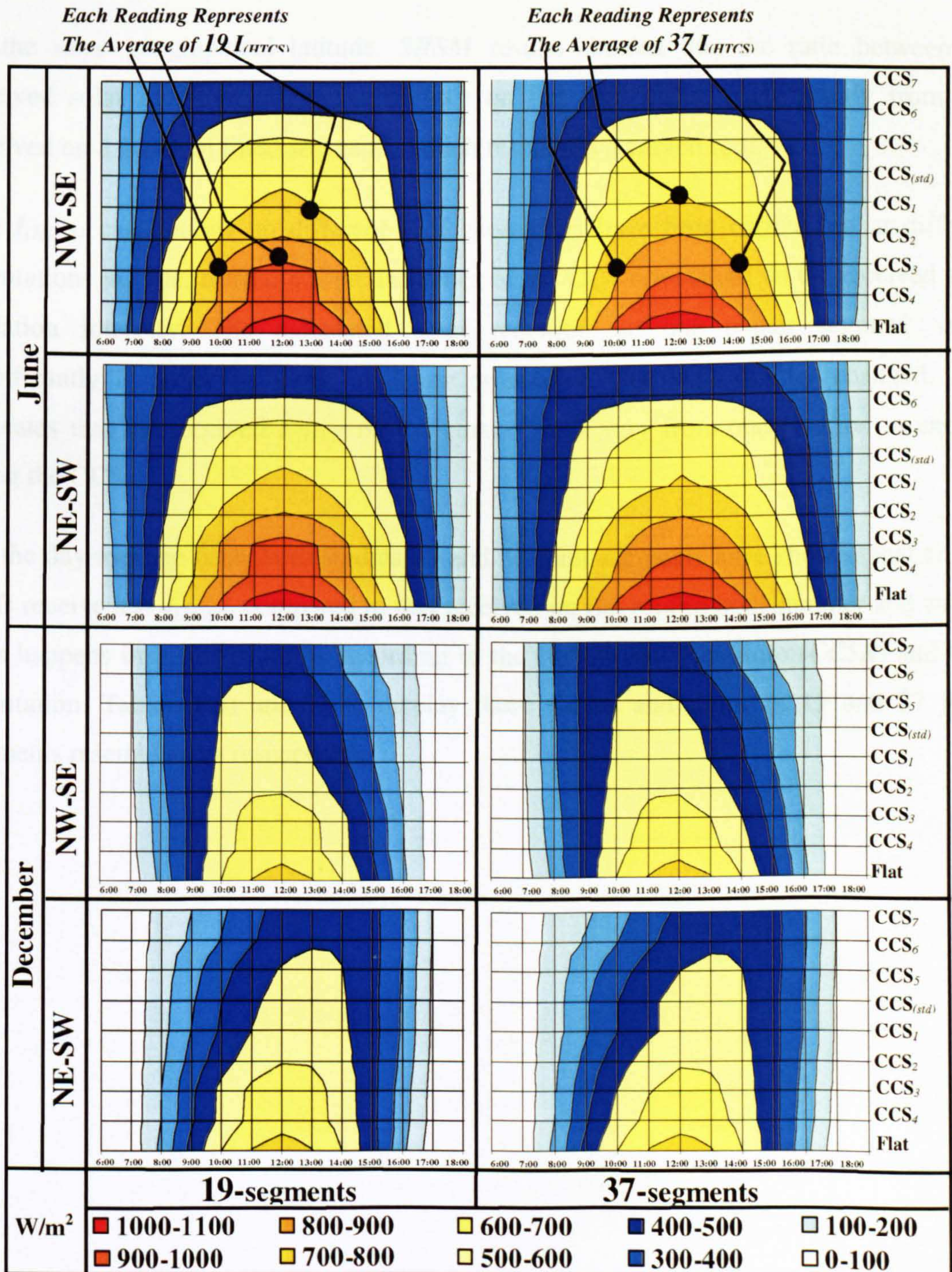


Figure 7-40 Comparison Between the Received $I_{(HTCS)}$ on 19 & 37 Joint segment
(Secondary Directions)

7.7 CONCLUSIONS

A number of computational simulation tools for analysing buildings environmental performance has been reviewed in order to test their abilities to calculate the received $I_{(HTCS)}$ on different surfaces geometries. *SRSM* [3] produced valuable predictions with accurate procedures calculating the total clear sky intensity of solar radiation on curved roofs with different curvatures.

At the same geographical latitude, *SRSM* results showed that the ratio between the received solar radiation intensities (W/m^2) on flat roof differs significantly from that received on a group of tilted segments, which resembles a curved roof.

The $I_{(HTCS)}$ calculations on different roof geometries have been carried out at different orientations in order to find out the influence of the CCS orientation on the received solar radiation intensity. The calculated solar radiation on one planar segment varies significantly if either its slope angle or orientation has been slightly changed. This indicates that the received $I_{(HTCS)}$ on the curved roofs vary from one position to another along the CCS.

On the day-average base, both studies 19 and 37 joint segments have showed that curved roofs receive less $I_{(HTCS)}$ compared to that received on flat roof in both summer and winter. This happens in different ratios according to the curved roof curvature (*CCSR*) and CCS orientation. Table (7-3) and (7-4) display these values and ratios in 19 and 37 joint-segments resemblances respectively.

Table 7-3 The Ratio Between the Received $I_{(HTCS)}$ on Different CCS ($CCSR: A=B, A<B, \& A>B$) to that on the Flat Roof (19 Segments)





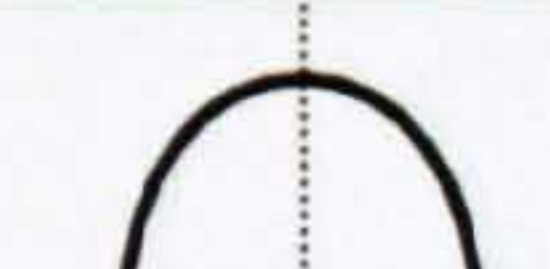



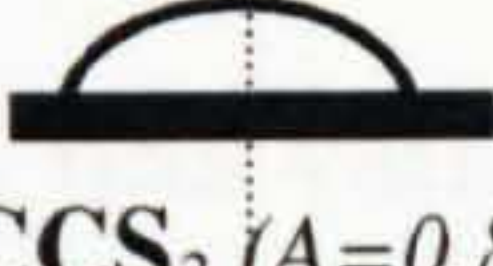
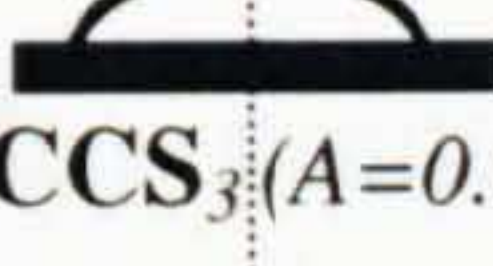
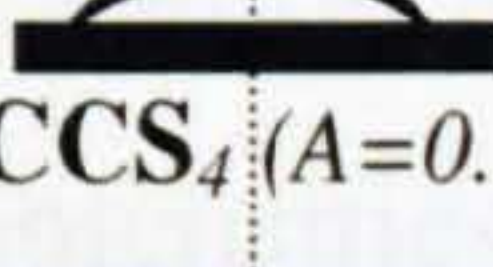



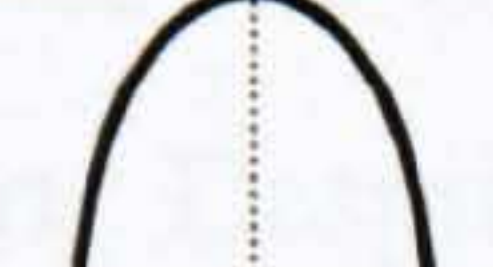
Roof Geometry & Orientation			Day Average $I_{(HTCS)}$ W/m ²		$\frac{I_{(HTCS)} \text{ CCS}}{I_{(HTCS)} \text{ flat roof}} \%$	
			June	Dec.	June	Dec.
A = B	 CCS ₁ (A=B)	N-S	459	308	69.6	84.3
		E-W	512	295	77.7	80.9
		NW-SE	484	297	73.3	81.3
		NE-SW	486	297	73.4	81.3
A < B	 CCS ₂ (A=0.8B)	N-S	507	318	76.9	87.1
		E-W	584	312	89	85.4
		NW-SE	528	313	80.1	85.7
		NE-SW	528	313	80.1	85.7
	 CCS ₃ (A=0.6B)	N-S	581	338	88.1	92.6
		E-W	599	337	90.8	92.3
		NW-SE	590	337	89.5	92.3
		NE-SW	590	336	89.5	92.1
	 CCS ₄ (A=0.5B)	N-S	586	340	88.9	93.1
		E-W	603	339	91.1	92.8
		NW-SE	595	339	90.2	92.8
		NE-SW	595	339	90.2	92.8
Flat Roof (A=B=0)			659	365		
A > B	 CCS ₅ (A=1.25B)	N-S	400	296	60.6	81.1
		E-W	473	276	66.3	75.6
		NW-SE	441	279	66.9	76.4
		NE-SW	440	279	66.7	76.4
	 CCS ₆ (A=1.67B)	N-S	328	281	49.7	76.9
		E-W	425	252	64.5	69
		NW-SE	383	258	58.1	70.1
		NE-SW	381	257	57.8	70
	 CCS ₇ (A=2B)	N-S	304	276	46.1	75.6
		E-W	409	244	62.1	66.8
		NW-SE	364	250	55.2	68.5
		NE-SW	364	250	55.2	68.5

Table 7-4 The Ratio Between the Received $I_{(HTCS)}$ on Different CCS ($CCSR: A=B, A<B, \& A>B$) to that on the Flat Roof (37 Segments)

Roof Geometry & Orientation			Day Average		$\frac{I_{(HTCS)} \text{ CCS}}{I_{(HTCS)} \text{ flat roof}} \%$	
			$I_{(HTCS)}$ W/m ²		June	Dec.
			June	Dec.	June	Dec.
A = B	 CCS ₁ (A=B)	N-S	449	306	69.6	83.8
		E-W	512	292	76.9	80.1
		NW-SE	480	294	72.9	80.6
		NE-SW	480	294	72.9	80.6
A < B	 CCS ₂ (A=0.8B)	N-S	503	318	76.4	87.1
		E-W	544	310	82.6	85
		NW-SE	525	311	79.7	85.2
		NE-SW	525	311	79.7	85.2
	 CCS ₃ (A=0.6B)	N-S	553	331	83.9	90.7
		E-W	580	327	88	89.7
		NW-SE	567	328	86	89.9
		NE-SW	567	328	86	89.9
	 CCS ₄ (A=0.5B)	N-S	587	341	89.1	93.4
		E-W	604	339	91.7	93
		NW-SE	596	339	90.4	92.9
		NE-SW	596	339	90.4	92.2
 Flat Roof (A=B=0)			659	365		
A > B	 CCS ₅ (A=1.25B)	N-S	391	293	59.4	80.3
		E-W	467	273	70.9	74.8
		NW-SE	433	278	65.7	76.2
		NE-SW	434	277	65.8	75.9
	 CCS ₆ (A=1.67B)	N-S	321	279	48.8	76.5
		E-W	419	250	63.6	68.5
		NW-SE	377	255	57.2	69.9
		NE-SW	377	255	57.2	69.9
	 CCS ₇ (A=2B)	N-S	280	270	42.5	74
		E-W	392	236	59.5	64.7
		NW-SE	345	242	52.3	66.4
		NE-SW	344	243	52.2	66.5

At principal directions, both studies results have showed that the $I_{(HTCS)}$ -mirrored-values of all roofs geometries are equal around the midday axis in both summer and winter. All roofs $I_{(HTCS)}$ -curves are exactly symmetrical around the midday axis. The maximum received $I_{(HTCS)}$ on all roofs are recorded at midday. At secondary orientations, curved roofs three-dimensional form causes unsymmetrical $I_{(HTCS)}$ -curves and unequal $I_{(HTCS)}$ -mirrored-values around the midday axis in both summer and winter. As expected, the $I_{(HTCS)}$ -values on flat roof are not influenced by the orientation.

Apart from the (N-S) orientation in summer, the curved roofs often receive more $I_{(ITCS)}$ than the flat roof in the early morning and the late afternoon in both summer and winter. This scenario may appear as an advantage for employing curved roofs in winter where reducing the received $I_{(ITCS)}$ on roof surface is not required. For CCSR where $A > B$, it is concluded that the ratios between the received $I_{(ITCS)}$ on the same CCS vary significantly from one orientation to another in both summer and winter. This scenario happens only in summer for CCSR where $A < B$. At the same orientation, the received $I_{(ITCS)}$ on different CCSR vary significantly in both summer and winter at the expanded-concavity curved roofs. Whereas, this variation diminishes at the compressed-concavity curved roofs, Tables (7-3) and (7-4).

The chapter also pointed out that the (N-S)-facing direction is the most preferable curvature orientation in both summer and winter. Regardless to the CCS curvature, the north-south orientation allowed the tested CCS to receive the minimum and the maximum solar radiation intensities in summer and winter respectively. Also the findings showed that for the (N-S)-facing-direction, the CCS₇ recorded the minimum received $I_{(ITCS)}$ in summer, whereas the CCS₄, which is the most compressed-concavity curvature, received the maximum $I_{(ITCS)}$ in winter, Table (7-3) and (7-4).

Generally, it is concluded that the curved roof form, geometry and orientation have great influences on controlling the intensity of the received solar radiation on roofs surfaces. Thus, they reduce the required energy for cooling in hot climates and it provides indoor thermal comfort. Despite their construction materials thermal properties and thickness, traditional roofs forms contributed towards passive indoor thermal comfort environments.

The next chapter investigates the received $I_{(ITCS)}$ characteristics on three domed roofs, which each has different curvature CCSR.

Reference List

1. **Elseragy, A. A. and Gadi, M. B.** Roof Geometric Forms and Solar Irradiation Intensity In Hot-Arid Climates Proceeding of the ISES Solar World Congress 2003, ISES 2003, Solar Energy for a Sustainable Future 2003 Jun 14-2003 Jun 19; Svenska Mässan Congress Centre, Göteborg, Sweden.
2. **"SRSM" Solar Radiation Simulation Model for Quick Basic, Exell, R. H. B.** Regional Energy Resources Information Centre, Asian Institute of Technology, Bangkok. <http://www.jgsee.kmutt.ac.th/exell/Solar/SolradJS.htm>
3. **Elseragy, A. A. and Gadi, M. B.** Computer Simulation of Solar Radiation Received by Curved Roof in Hot-Arid Regions, Proceedings of the Building Simulation 2003 Aug 11-2003 Aug 14; EINDHOVEN, Netherlands.
4. **Exell, R. H. B.** A Program in BASIC for Calculating Solar Radiation in Tropical Climates on Small Computers. Renewable Energy Review Journal, 1986 Dec; Vol. 8 (No. 2).

CHAPTER 8

SOLAR BEHAVIOUR OF FLAT AND DOMED ROOFS WITH DIFFERENT CURVATURES

(18 Resembling Horizontal-Rings)

(Each Ring Comprises 24 Different Oriented Planar Segments)

8. SOLAR BEHAVIOUR OF FLAT AND DOMED ROOFS WITH DIFFERENT CURVATURES

The previous chapter discussed the solar performance of a number of extended cross-section curvatures CCSR (*vaulted roofs*). The two geometrical resemblance techniques (*19 and 37 joint-segments*) have been applied in order to test the solar behaviour of each CCS external surfaces. This chapter investigates the received $I_{(HTCS)}$ characteristics on another curved roof forms (*domed roofs*) with different curvatures of a rotated CCS. It compares the received $I_{(HTCS)}$ on three domed roofs to that received on the flat roof. In addition to the horizontal top ring, each dome in this chapter is composed of 18 rings with different slope angles.

Fig. (8-1) shows the geometrical resemblance of three domed roofs employing the same generated slope angles from the thirty-seven joint segments of the vaulted roofs in the previous chapter. The dome surface has been geometrically resembled by groups of planar segments. Each group of planar segments has the same tilt angles and constitutes one ring by full rotation around the vertical axis, Fig. (8-1).

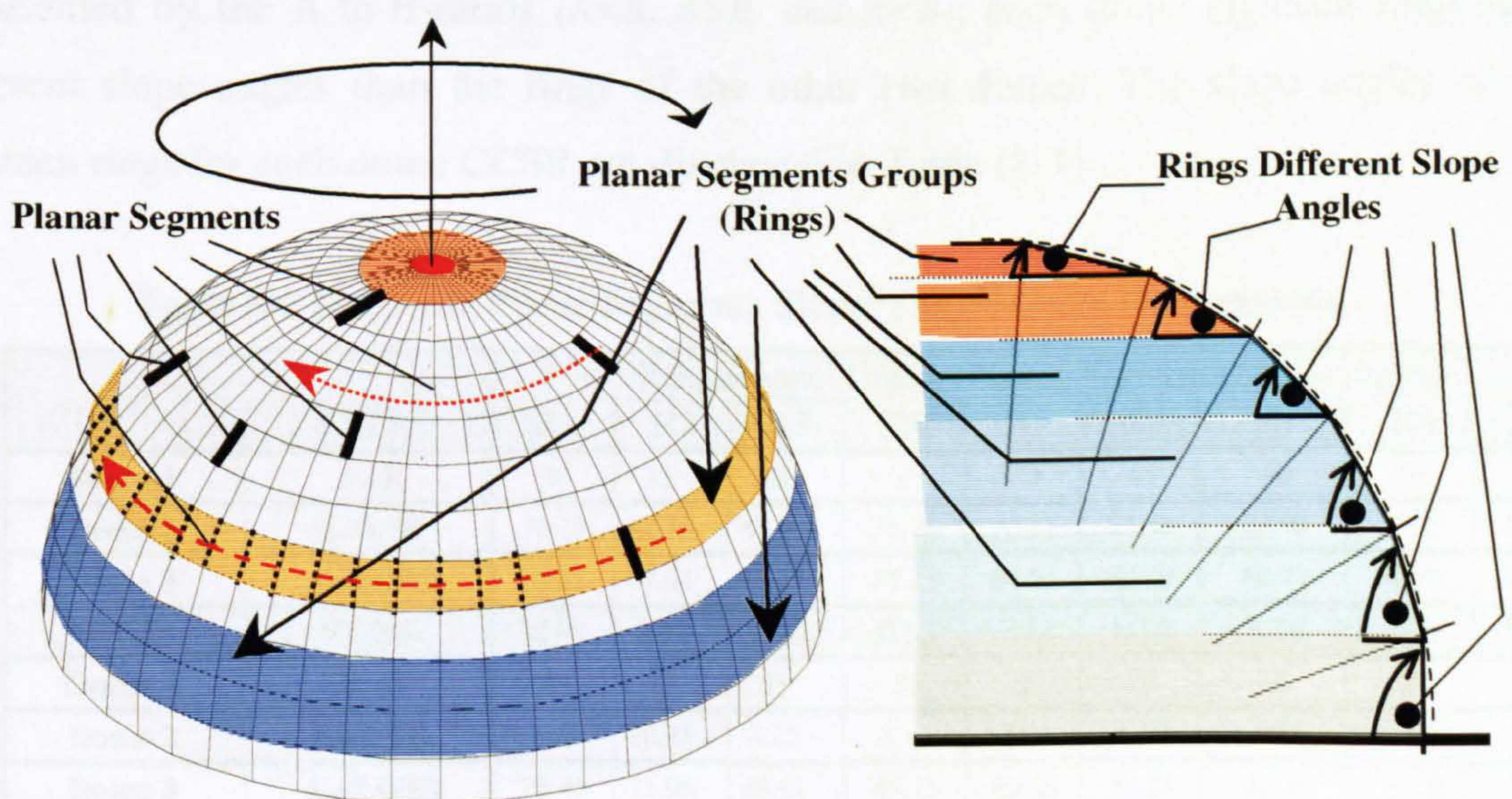


Figure 8-1 Dome Geometrical Resemblance (*Each ring has different slope angle*)

8.1 DATA INPUT AND DOMED FORMS GEOMETRICAL RESEMBLANCE

The *SRSM* [1] calculations have been carried out for three domes with different CCSR, Fig. (8-2). The solar performance of each dome CCSR has been investigated throughout the day in summer and winter.

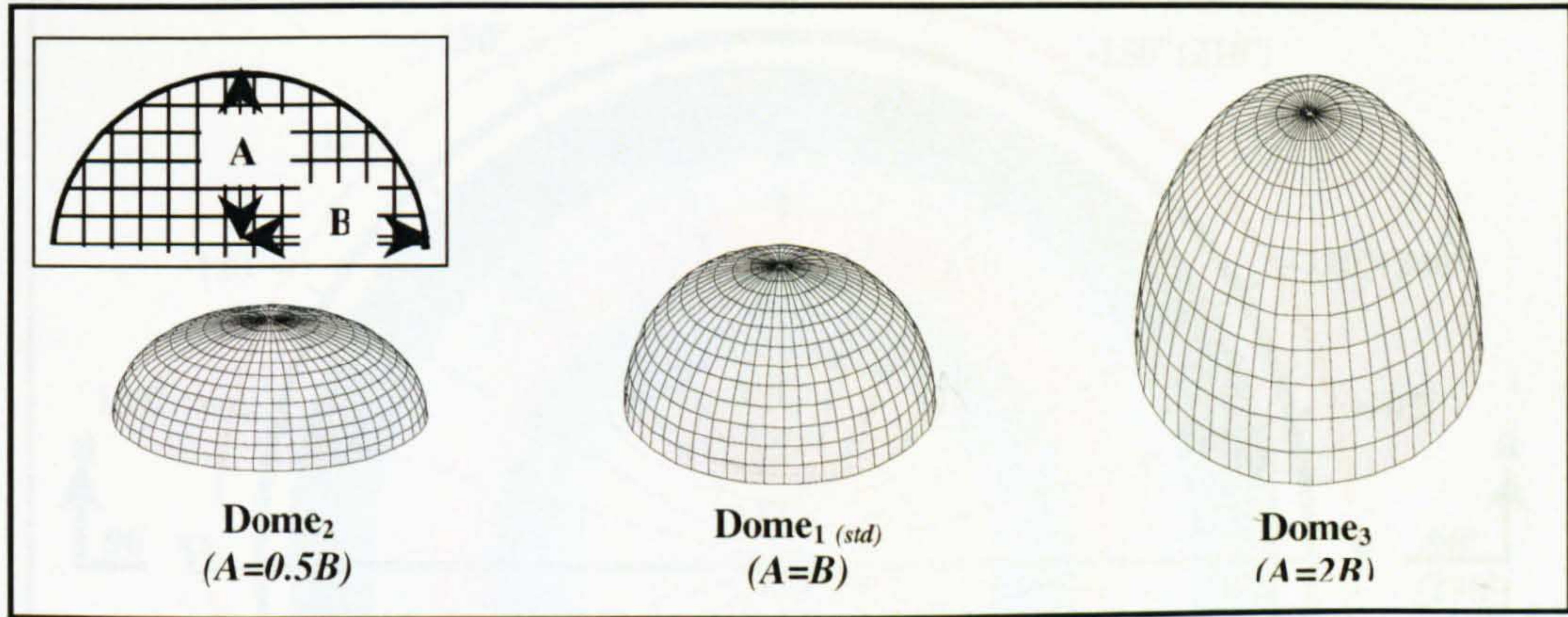


Figure 8-2 The Three CCSR of the Tested Domed Roofs

The slope angles of the planar segments, which form the dome surface and rings, are exactly the same as the previously generated angles for vaults roofs with particular CCSR ($A=B$, $A=0.5B$, or $A=2B$). As expected, according to the dome curvature, which is represented by the A-to-B-ratios ($A=B$, $A>B$, and $A<B$), each dome eighteen rings have different slope angles than the rings of the other two domes. The slope angles of the eighteen rings for each dome CCSR are displayed in Table (8-1).

Table 8-1 Rings and Planar Segments Slopes (*Angles from the horizontal*)

CCS	CCSR	Rings Slope Angles (<i>Planar Segments Slope Angles</i>)								
		R1	R2	R3	R4	R5	R6	R7	R8	R9
Dome 1	A=B	90	85	80	75	70	65	60	55	50
Dome 2	A=0.5B	76.17	62.10	47.60	35.78	30.11	25.46	20.98	15.25	14.38
Dome 3	A=2.00B	89.88	87.61	86.11	85.23	84.54	83.49	82.77	80.56	77.55
CCS	CCSR	R10	R11	R12	R13	R14	R15	R16	R17	R18
Dome 1	A=B	45	40	35	30	25	20	15	10	5
Dome 2	A=0.5B	11	10.71	8.25	8.13	6.80	6.18	4.73	4.12	2.10
Dome 3	A=2.00B	76.45	71.96	69.91	65.11	60.56	52.24	42.30	27.49	9.25

As has been explained earlier in this chapter, each ring is formed as a group of planar segments which has the same slope angle. Each ring has a tilt angle, which is the segment tilt angle. In other words, each ring is formed by a full rotation (360°) of one planar segment to face as many different orientations as possible, Fig. (8-3).

The rotation around the north-south axis starts and ends at the south-facing orientation in a clock-wise direction, Fig. (8-3) also illustrates the geometrical resemblance of the first dome ($Dome_1$ (std) where $A=B$).

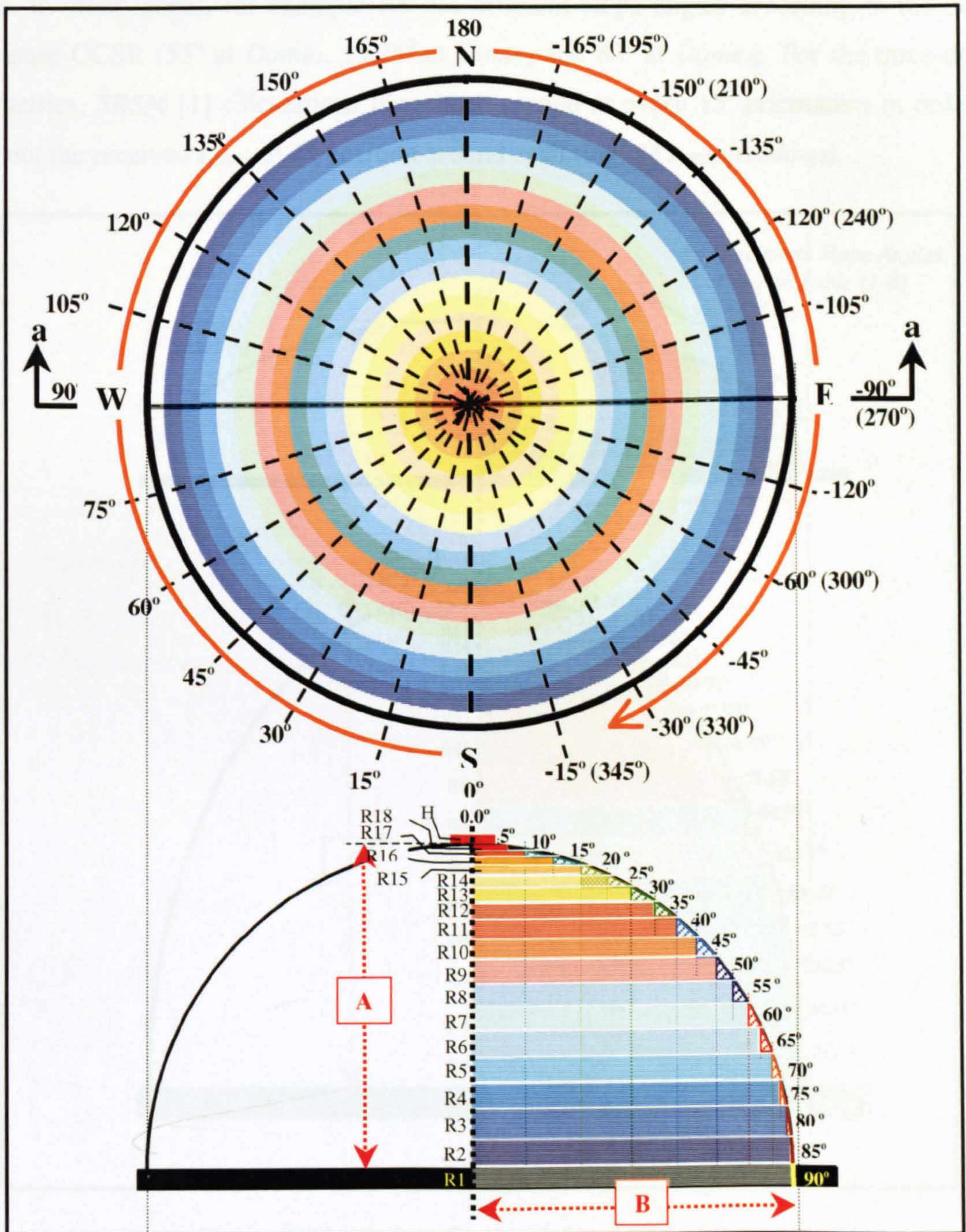


Figure 8-3 Rings and Planar Segment Orientations & Section a-a for $Dome_1$ ($A=B$)

Fig. (8-4) illustrates the geometrical resemblance of the rest of the tested dome geometries, (*Dome₂* and *Dome₃* where $A=0.5B$ and $A=2B$ respectively). As has been mentioned previously in this chapter, each dome curvature will create different 18 tilted resembling rings. In other words, for example R8 has different slope angles according to the dome curvature CCSR (55° at *Dome₁*, 15.25° at *Dome₂* and 80° at *Dome₃*). For the three dome geometries, *SRSM* [1] calculations have been carried at every 15° -orientation in order to find out the received $I_{(HTCS)}$ at 24 position around each ring ($24 I_{(HTCS)}$ readings).

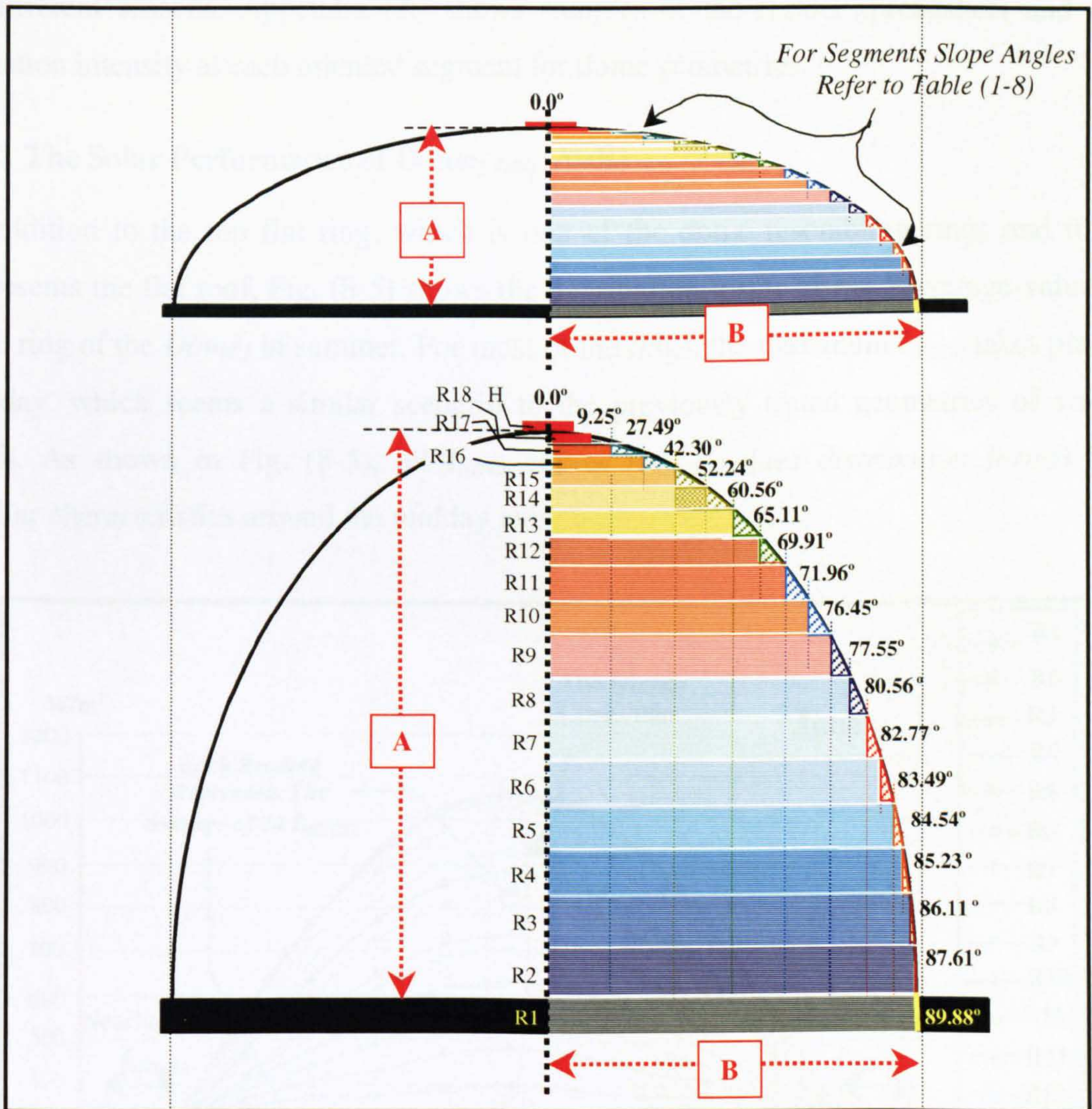


Figure 8-4 Section a-a for *Dome₂* ($A=0.5B$) and *Dome₃* ($A=2B$) ($A < B$ & $A > B$ respectively)

8.2 THE SOLAR PERFORMANCE OF DIFFERENT DOMED ROOF CURVATURES

This section examines the solar performance of three domed roofs, and calculates the received $I_{(HTCS)}$ on their geometries surfaces compared with the received $I_{(HTCS)}$ on the flat roof. According to its geometry, dome has not a particular orientation as the case of vaulted roof. Dome shape faces all directions at the same time. Similar to the previous chapter procedures in chapters 6 and 7, results have been repeatedly generated during summer and winter. Thus, in order to find out the $I_{(HTCS)}$ behaviours on each roof geometry at different seasons. Appendix (A) shows samples of the results spreadsheet and solar radiation intensity at each oriented segment for dome geometries.

8.2.1 The Solar Performance of Dome₁ (std) (A=B)

In addition to the top flat ring, which is one of the dome resembling rings and it also represents the flat roof, Fig. (8-5) shows the distribution forms of $I_{(HTCS)}$ -average-values on each ring of the Dome₁ in summer. For most of the rings, the maximum $I_{(HTCS)}$ takes place at midday, which seems a similar scenario to the previously tested geometries of vaulted roofs. As shown in Fig. (8-5), all $I_{(HTCS)}$ -curves ($I_{(HTCS)}$ -values distribution forms) have similar characteristics around the midday axis.

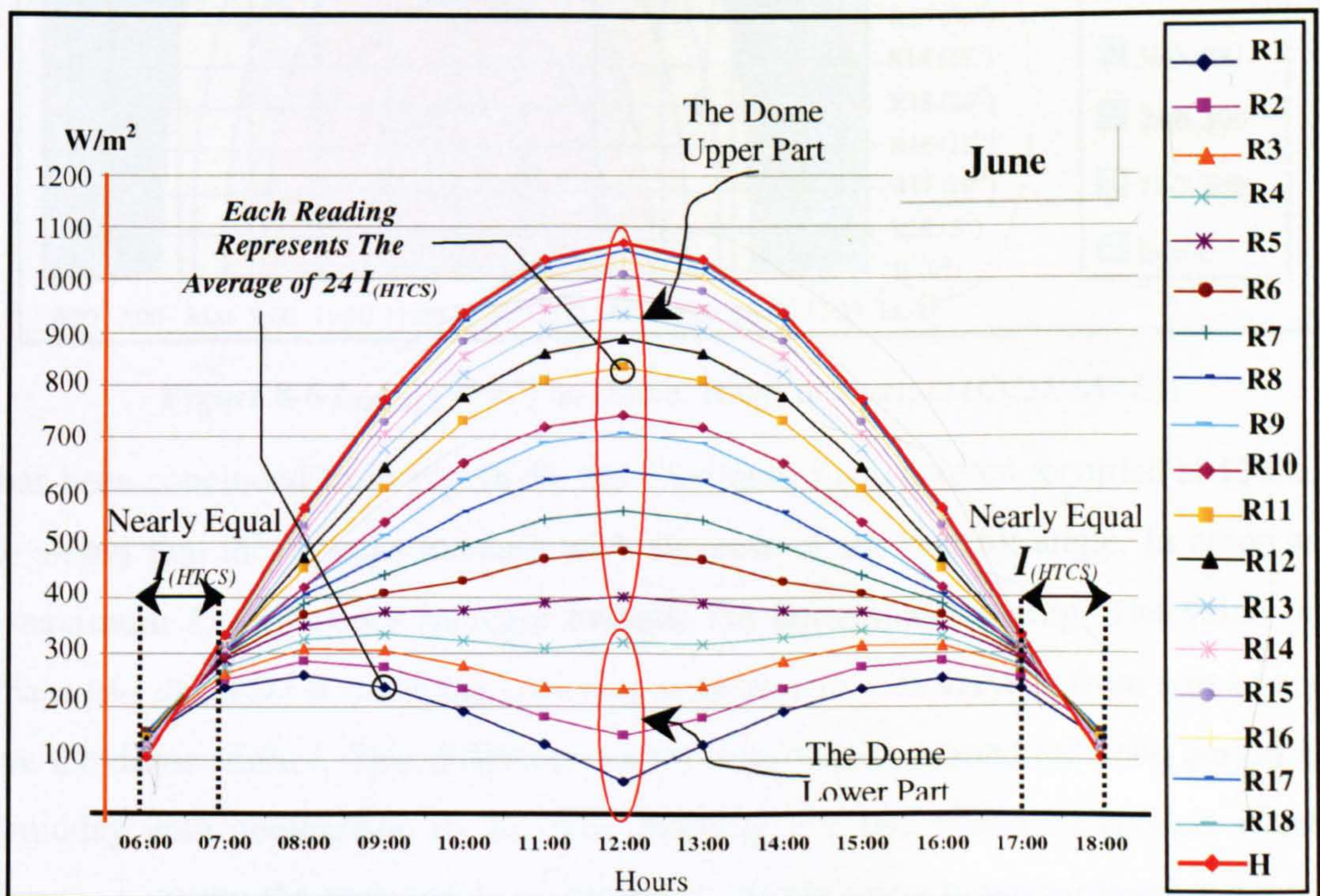


Figure 8-5 $I_{(HTCS)}$ (W/m^2) on Dome₁ Rings in Summer (CCSR (A=B))

As shown from the previous graph, the first four rings (R1, R2, R3, & R4) showed different behaviours than the rest of the rings, the maximum $I_{(HTCS)}$ -values have been not recorded at 12:00. In the early morning and the late afternoon, number of the resembling rings receive more $I_{(HTCS)}$ than the flat roof (flat roof is represented by the H ring in this study). Fig. (8-6) illustrates another graphical way that presents the received $I_{(HTCS)}$ above each ring of $Dome_1$ in summer. It also shows that the $I_{(HTCS)}$ -values in general increase towards the top ring (increase upwards on the dome surface). As has been explained in the previous graph, each reading of all graphical illustrations in this chapter is generated from 24 $I_{(HTCS)}$.

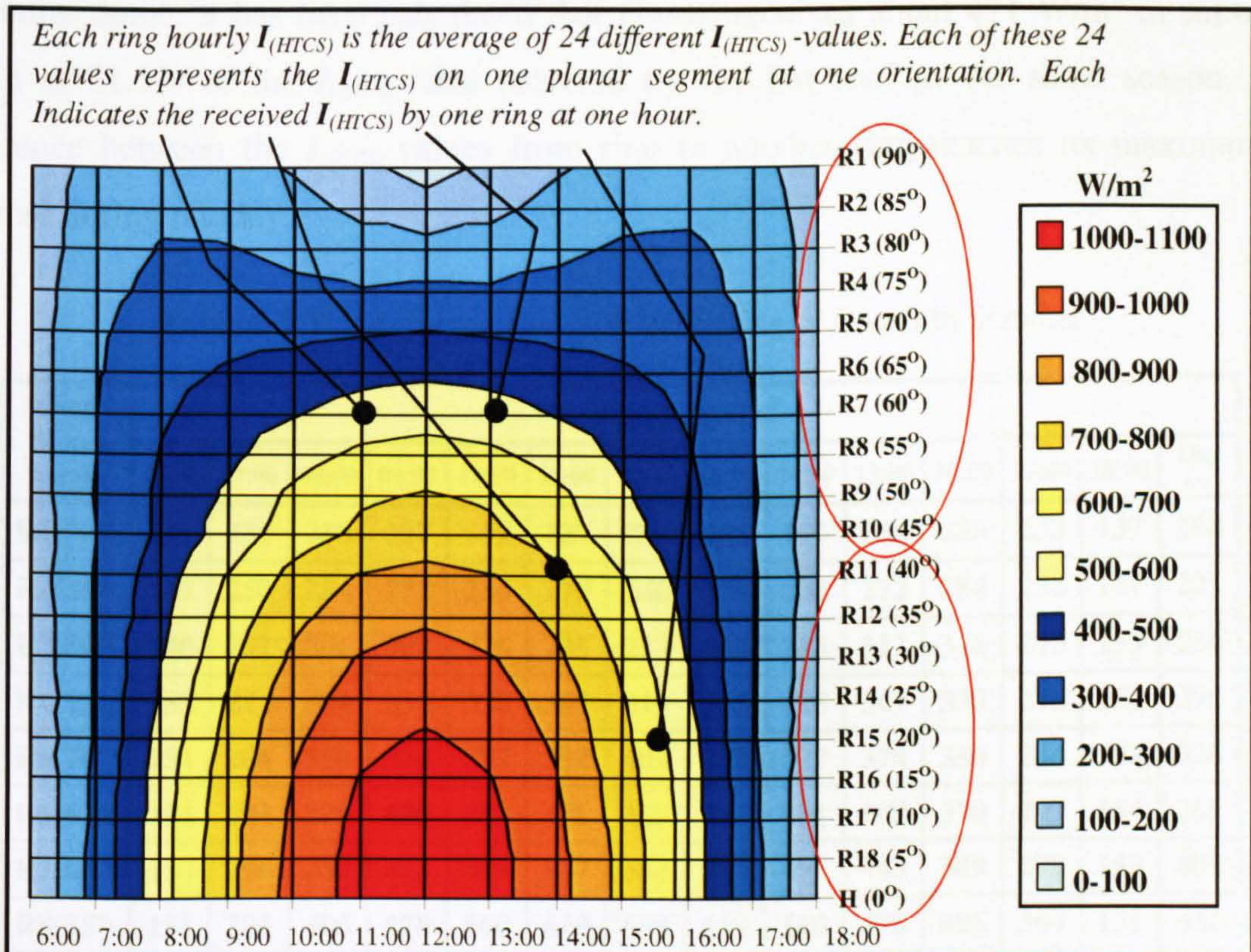


Figure 8-6 $I_{(HTCS)}$ (W/m²) on $Dome_1$ Rings in Summer (CCSR (A=B))

As has been concluded from Fig. (8-5), the maximum $I_{(HTCS)}$ is often recorded at 12:00. Fig. (8-6) shows that these peaks increase with decrease of the ring tilt angle. In other words, the maximum $I_{(HTCS)}$ -values increase towards the horizontal top ring. The value of this increase (the difference between $I_{(HTCS)}$ on ring to another ring) is varying from part to another above the dome surface. This difference varies significantly around the noon period and at the midday with comparison to the early morning and late afternoon periods where the difference between the received $I_{(HTCS)}$ on ring to another ring is insignificant. Refer to Table (8-2).

Moreover, the lower part of the dome surface (90° - 45°) shows different performance than the upper part (45° - 0.0°). In summer, during the early morning and the late afternoon the $I_{(HTCS)}$ increases only until the middle ring (R10 45°) then it starts decreasing towards the horizontal top ring. During midday, it keeps increasing through all the rings and not only until (R10 45°). Thus it is not possible to find out an angle coefficient that represents the value of solar radiation increase or decrease due to the change in the ring or the segment slope angle. Table (8-2) displays the hourly $I_{(HTCS)}$ -values that received by each ring of *Dome₁* during summer. It also shows the daily average $I_{(HTCS)}$ that received by each ring and the entire dome. It has been calculated that *Dome₁* receives about 471 W/m^2 in summer, which is 71.5% of the $I_{(HTCS)}$ that received by the flat roof in the same season. The difference between the $I_{(HTCS)}$ values from ring to another ring reaches its maximum in summer during midday.

Table 8-2 The Received $I_{(HTCS)}$ on Each Ring of *Dome₁* in Summer

Ring Slope Angle	$I_{(HTCS)}$ W/m ²													Day Av.
	06:00	07:00	08:00	09:00	10:00	11:00	12:00	13:00	14:00	15:00	16:00	17:00	18:00	
R1(90°)	141	236	258	237	191	127	59.1	128	190	234	253	233	137	186
R2(85°)	145	250	284	272	234	179	146	179	234	272	284	252	147	221
R3(80°)	148	262	306	304	276	235	233	239	283	312	314	270	153	256
R4(75°)	152	273	324	334	320	307	319	315	328	341	330	276	152	290
R5(70°)	154	286	350	374	377	392	404	392	377	374	350	286	154	328
R6(65°)	154	293	370	409	431	471	485	471	431	409	370	293	154	365
R7(60°)	153	299	389	443	495	547	564	547	495	443	389	299	153	401
R8(55°)	151	304	406	478	560	619	638	619	560	478	406	304	151	436
R9(50°)	149	308	422	516	621	687	708	687	621	516	422	308	149	470
R10(45°)	140	298	421	540	651	720	743	720	651	540	421	298	140	483
R11(40°)	142	310	454	604	730	808	833	808	730	604	454	310	142	533
R12(35°)	137	310	474	642	776	860	887	860	776	642	474	310	137	560
R13(30°)	131	308	498	676	818	905	934	905	818	676	498	308	131	585
R14(25°)	125	309	519	705	853	945	975	945	853	705	519	309	125	606
R15(20°)	118	315	536	729	882	978	1009	978	882	729	536	315	118	625
R16(15°)	111	322	550	748	905	1003	1035	1003	905	748	550	322	111	640
R17(10°)	105	328	560	761	922	1022	1054	1022	922	761	560	328	105	650
R18(5°)	105	331	565	769	931	1033	1066	1033	933	770	567	332	106	657
H(0°)	106	332	567	772	935	1037	1070	1037	935	772	567	332	106	659
Dome₁ (A=B)	135	299	434	543	627	678	693	678	628	543	435	299	135	471

Fig. (8-7) shows the distribution forms of $I_{(HTCS)}$ -values on $Dome_1$ eighteen rings in winter. For all rings, the maximum $I_{(HTCS)}$ takes place at midday. All rings $I_{(HTCS)}$ -curves ($I_{(HTCS)}$ -values distribution forms) have similar characteristics around the midday axis. The graph in Fig. (8-7) illustrates that during winter most of the $Dome_1$ rings receive $I_{(HTCS)}$ more than that received by the flat roof during two time-periods (06:00-08:00 in the morning and 16:00-18:00 in the afternoon). This scenario is longer than the summer, which appears as an advantage for employing domed roofs in winter as it as in summer.

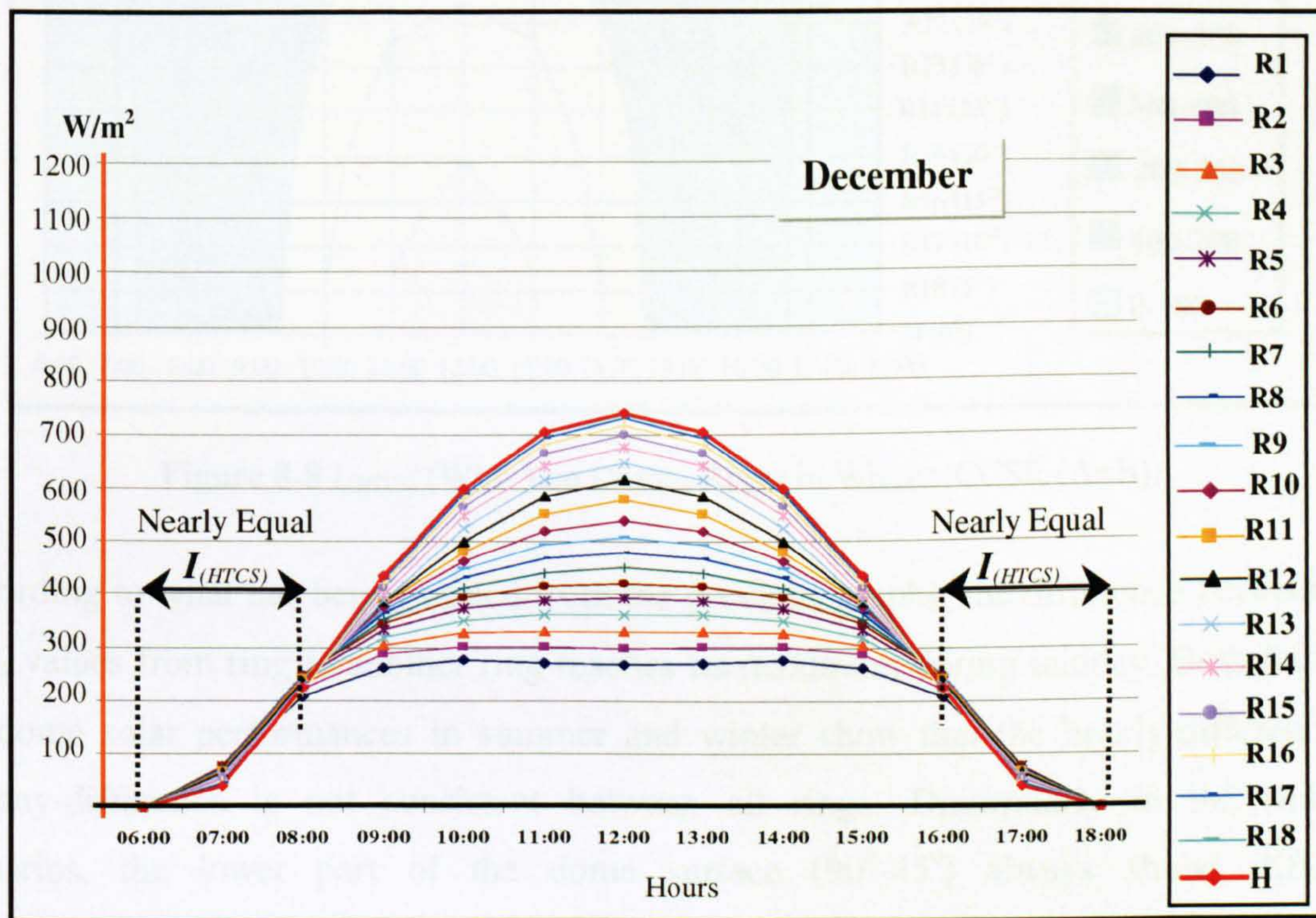


Figure 8-7 $I_{(HTCS)}$ (W/m^2) on $Dome_1$ Rings in Winter (CCSR ($A=B$))

Fig. (8-8) illustrates another graphical way that presents the received $I_{(HTCS)}$ above each ring of $Dome_1$ in winter. It also shows that the $I_{(HTCS)}$ -values in general increase towards the top horizontal-ring (increase upwards on the dome surface). As has explained in the previous graph, each reading of the contour graph in Fig. (8-8) and all other graphical illustrations in this chapter is generated from 24 $I_{(HTCS)}$.

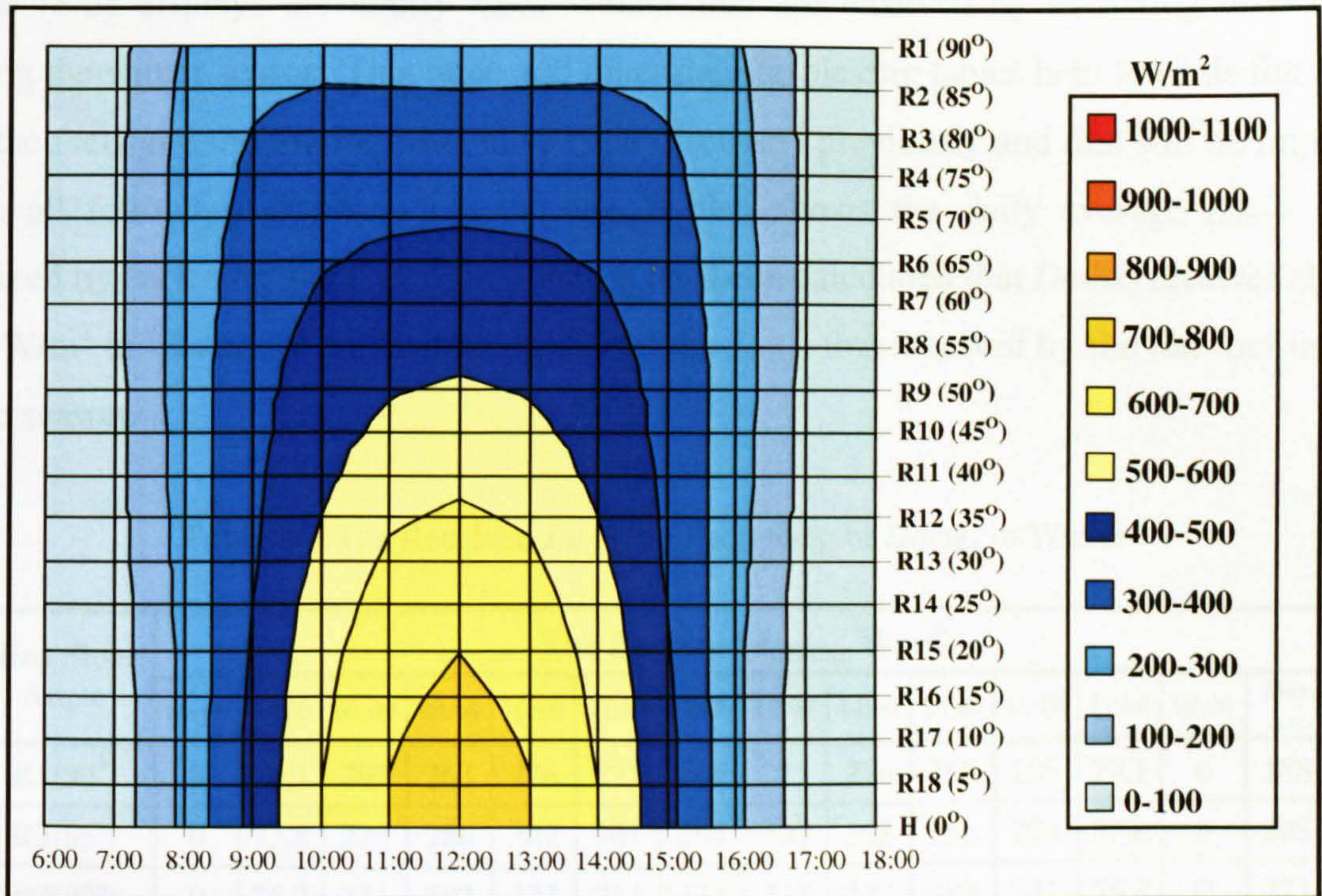


Figure 8-8 $I_{(HTCS)}$ (W/m²) on Dome₁ Rings in Winter (CCSR (A=B))

According to what has been implied from the previous graphs, the difference between the $I_{(HTCS)}$ values from ring to another ring reaches its maximum during midday. Both findings for dome solar performances in summer and winter show that the hourly-difference or midday-difference is not consistent between all rings. Dissimilarly to the summer scenarios, the lower part of the dome surface (90°-45°) always shows different performance than the upper part (45°-0.0°) only during the early morning and the late afternoon. Moreover, during the early morning and the late afternoon the $I_{(HTCS)}$ increases only until the middle ring (R10 45°) and then it starts decreasing till horizontal top ring. During midday and the rest of the day, it keeps increasing through all the rings and not only until (R10 45°). Thus it is not possible to find out an angle coefficient that represents the value of solar radiation increase or decrease due to the change in the ring or the segment slope angle. *Refer to Table (8-3)*

Table (8-3) displays the hourly $I_{(HTCS)}$ -values that are received by each ring of $Dome_1$ during the winter season. This table and other data-displaying tables help towards figuring out the facts and the findings that have been discussed previously and that will be implied from all following graphical illustrations. It also shows the daily average $I_{(HTCS)}$ that received by each ring and the entire dome. It has been calculated that $Dome_1$ receives about 294 W/m^2 in winter, which is about 80.5% of the $I_{(HTCS)}$ that received by the flat roof in the same season.

Table 8-3 The Received $I_{(HTCS)}$ on Each Ring of $Dome_1$ in Winter

Ring Slope Angle	The Received $I_{(HTCS)}$ W/m^2													Day Av.
	06:00	07:00	08:00	09:00	10:00	11:00	12:00	13:00	14:00	15:00	16:00	17:00	18:00	
R1(90°)	0	70.1	209	263	276	271	266	271	276	263	209	70.1	0	188
R2(85°)	0	73.8	223	286	302	301	299	301	302	286	223	73.8	0	205
R3(80°)	0	75.3	231	303	327	331	331	331	327	303	231	75.3	0	221
R4(75°)	0	75.8	237	319	350	360	360	360	350	319	237	75.8	0	234
R5(70°)	0	75.9	242	332	373	388	393	388	373	332	242	75.9	0	247
R6(65°)	0	75.4	246	344	393	416	422	416	393	344	246	75.4	0	259
R7(60°)	0	74.5	248	354	413	442	452	442	413	354	248	74.5	0	270
R8(55°)	0	73.3	248	364	431	468	481	468	431	364	248	73.3	0	281
R9(50°)	0	71.5	248	371	448	494	510	494	448	371	248	71.5	0	290
R10(45°)	0	69.5	245	375	464	520	541	520	464	375	245	69.5	0	299
R11(40°)	0	67	242	381	481	552	580	552	481	381	242	67	0	310
R12(35°)	0	64.3	237	384	501	587	616	587	501	384	237	64.3	0	320
R13(30°)	0	60.6	231	388	526	617	648	617	526	388	231	60.6	0	330
R14(25°)	0	57.2	225	398	549	643	676	643	549	398	225	57.2	0	340
R15(20°)	0	53.4	219	411	567	665	699	665	567	411	219	53.4	0	348
R16(15°)	0	49	217	421	581	682	717	682	581	421	217	49	0	355
R17(10°)	0	44.6	221	429	591	694	730	694	591	429	221	44.6	0	361
R18(5°)	0	40.4	223	433	598	702	737	702	598	433	223	40.4	0	364
H(0°)	0	40	224	434	600	704	740	704	600	434	224	40	0	365
Dome₁ (A=B)	0	63.8	232	368	462	518	537	518	462	368	232	63.8	0	294

8.2.2 The Solar Performance of Dome₂ A= 0.5B

The curvature of this domed roof has a flatter profile (*less concavity*) in comparison to the previous one (*Dome₁ A=B (std)*). The CCSR of this dome is $A=0.5B$. Fig. (8-9) shows the distribution forms of $I_{(HTCS)}$ -values on *Dome₂* eighteen rings in summer. Apart from R1 (76.16°), the maximum $I_{(HTCS)}$ on all rings takes place at midday. As shown in Fig. (8-9), all $I_{(HTCS)}$ -curves ($I_{(HTCS)}$ -values distribution forms) have similar characteristics around the midday axis. In this same season, the dome $I_{(HTCS)}$ scenarios are very similar to the vault roof ones at principle directions.

The graph in Fig. (8-9) illustrates that during summer most of the *Dome₂* rings receive $I_{(HTCS)}$ less than that received by the flat roof except few number of the dome lower part rings during both early morning and late afternoon. This scenario is very similar to the *Dome₁* where CCSR is A equals B. This dome geometry appears as the preferable profile (concavity) for domes in order to receive less solar radiation intensity in summer.

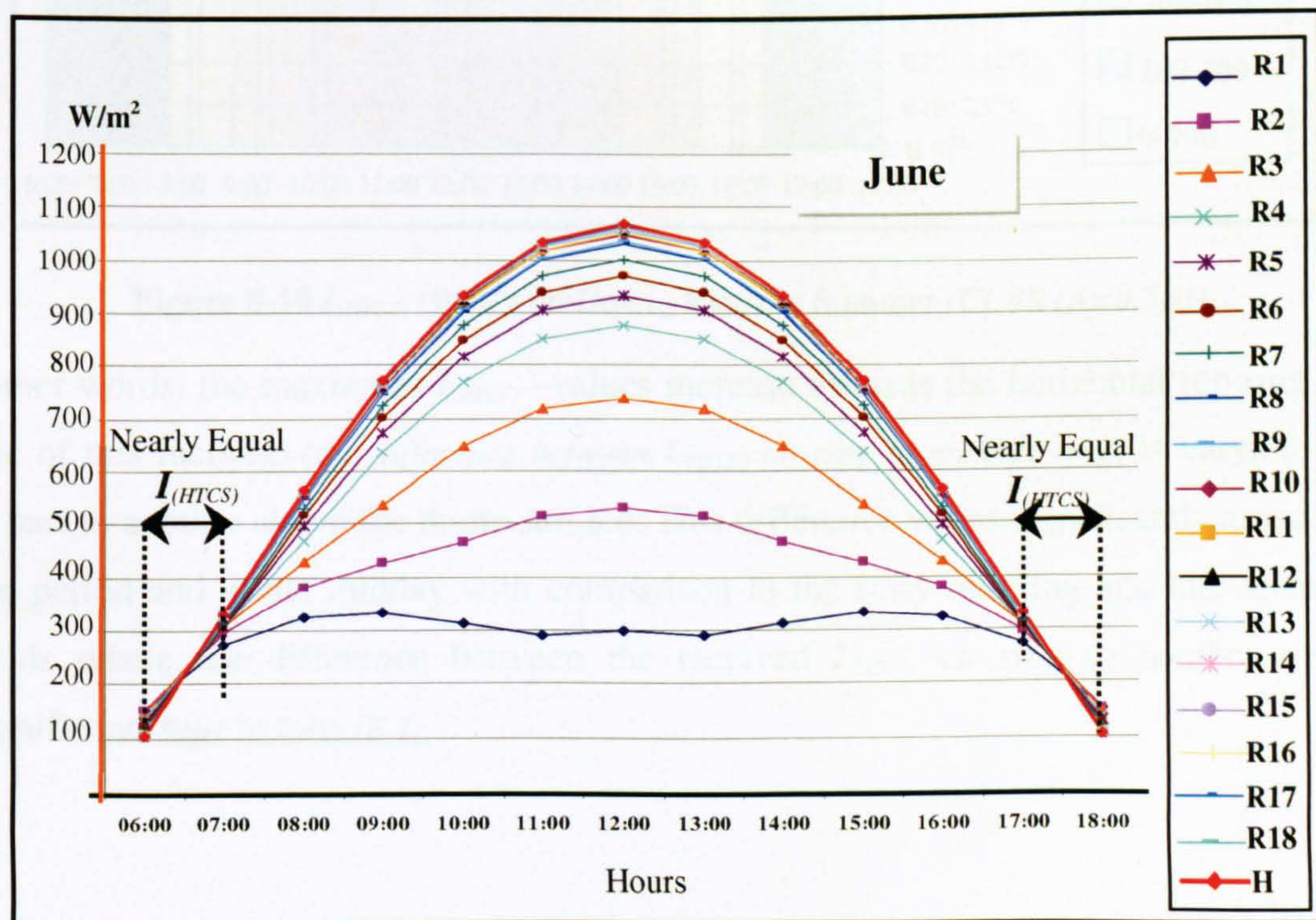


Figure 8-9 $I_{(HTCS)}$ (W/m^2) on *Dome₂* Rings in Summer (CCSR ($A=0.5B$))

Fig. (8-10) illustrates another graphical way that presents the received $I_{(HTCS)}$ above each ring of $Dome_2$ in summer. This dome geometry has similar scenarios during summer to that discussed in the previous dome ($A=B$), in which the $I_{(HTCS)}$ -values in general increase towards the top ring (*increase upwards on the dome surface*).

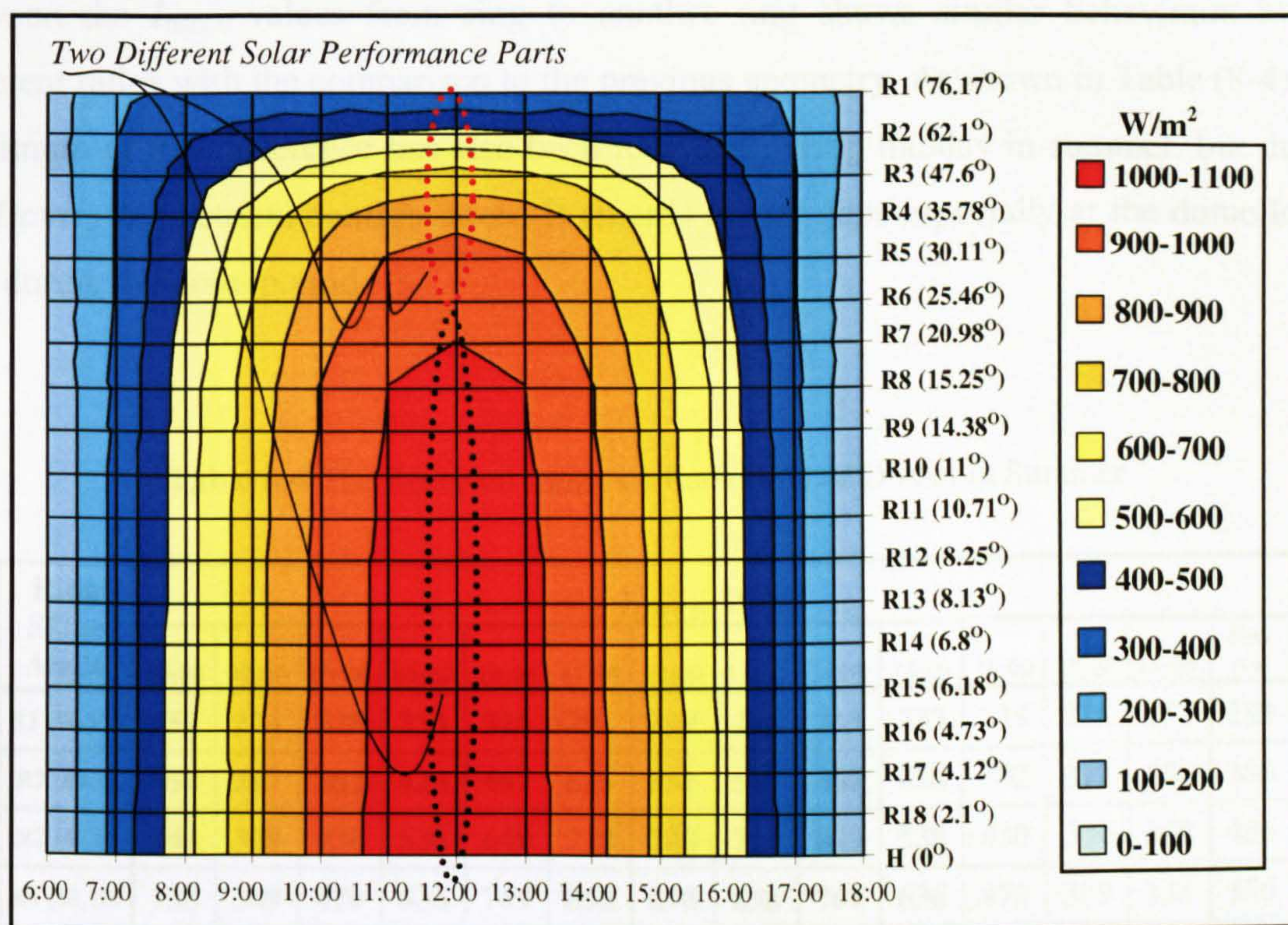


Figure 8-10 $I_{(HTCS)}$ (W/m^2) on $Dome_2$ Rings in Summer ($CCSR (A=0.5B)$)

In other words, the maximum $I_{(HTCS)}$ –values increase towards the horizontal top ring. The value of this increase (*the difference between $I_{(HTCS)}$ on ring to another ring*) is varying from one part to another above the dome surface. This difference varies significantly around the noon period and at the midday with comparison to the early morning and late afternoon periods where the difference between the received $I_{(HTCS)}$ on ring to another ring is insignificant. Refer to Table (8-4).

Table (8-4) displays the summer hourly $I_{(HTCS)}$ values that received by each ring of $Dome_2$, where $A=0.5B$. It also shows the daily average $I_{(HTCS)}$ that received by each ring and the entire dome. It has been calculated that $Dome_2$ receives about 597 W/m^2 in summer, which is 90.6% of the $I_{(HTCS)}$ that received by the flat roof in the same season. The difference between the $I_{(HTCS)}$ values from ring to another ring shows similar behaviours but in different ratios with the comparison to the previous geometry. As shown in Table (8-4), the maximum of this difference has also been recorded during midday in summer, but due to the $Dome_2$ geometrical configurations it records bigger gaps especially at the dome lower part during the noon period.

Table 8-4 The Received $I_{(HTCS)}$ on Each Ring of $Dome_2$ in Summer

Ring Slope Angle	$I_{(HTCS)}$ W/m^2													
	06:00	07:00	08:00	09:00	10:00	11:00	12:00	13:00	14:00	15:00	16:00	17:00	18:00	Day Av.
R1 (76.17)	152	274	325	333	315	291	299	291	315	333	325	274	152	283
R2 (62.1)	154	297	382	428	467	515	531	515	467	428	382	297	154	386
R3 (47.6)	148	309	430	538	649	718	740	718	649	538	430	309	148	486
R4 (35.78)	138	309	470	636	769	852	878	852	769	636	470	309	138	556
R5 (30.11)	131	309	498	675	817	905	933	905	817	675	498	309	131	585
R6 (25.46)	125	308	517	702	850	941	971	941	850	702	517	308	125	604
R7 (20.98)	119	313	533	725	877	972	1002	972	877	725	533	313	119	621
R8 (15.25)	111	322	549	747	904	1002	1034	1002	904	747	549	322	111	639
R9 (14.38)	110	323	551	750	908	1006	1038	1006	908	750	551	323	110	641
R10 (11)	106	327	558	759	919	1019	1051	1019	919	759	558	327	106	648
R11 (10.71)	106	327	559	760	920	1020	1052	1020	920	760	559	327	106	649
R12 (8.25)	105	329	562	765	926	1027	1059	1027	926	765	562	329	105	653
R13 (8.13)	105	329	562	765	927	1027	1059	1027	927	765	562	329	105	653
R14 (6.8)	105	330	564	767	929	1030	1063	1030	929	767	564	330	105	655
R15 (6.18)	105	330	564	768	930	1031	1064	1031	930	768	564	331	105	656
R16 (4.73)	106	331	566	770	932	1033	1066	1033	932	770	566	331	106	657
R17 (4.12)	104	330	565	769	932	1034	1067	1035	933	771	566	331	105	657
R18 (2.1)	106	332	567	772	935	1036	1069	1036	935	772	567	332	106	659
H(0)	106	332	567	772	935	1037	1070	1037	935	772	567	332	106	659
Dome₂ (A=0.5B)	118	319	520	695	834	921	950	921	834	695	521	319	118	597

Fig. (8-11) shows the distribution forms of $I_{(HTCS)}$ -values on $Dome_2$ eighteen rings in winter. For all rings, the maximum $I_{(HTCS)}$ takes place at midday. As shown in Fig. (8-11), all $I_{(HTCS)}$ -curves ($I_{(HTCS)}$ -values distribution forms) have similar characteristics around the midday axis. The graph in Fig. (8-11) illustrates that during winter most of the $Dome_2$ rings receive $I_{(HTCS)}$ more than that received by the flat roof during two time-periods (06:00-08:00 in the morning and 16:00-18:00 in the afternoon). This scenario is very similar to the previous geometry ($A=B$) in the same season. Also it is longer than summer scenario for the same dome geometry ($A=0.5B$), which appears as an advantage for employing domed roofs in winter.

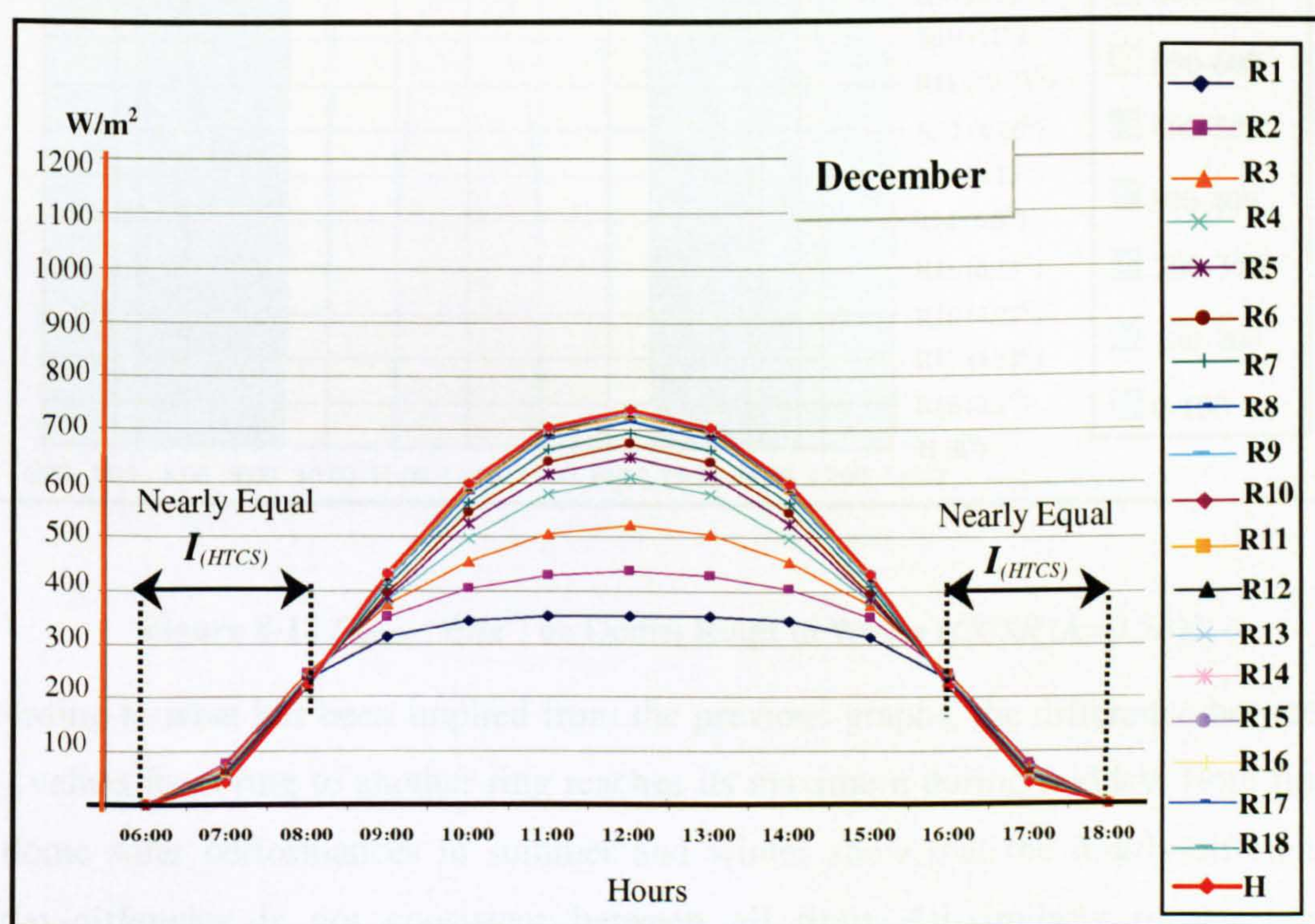


Figure 8-11 $I_{(HTCS)}$ (W/m^2) on $Dome_2$ Rings in Winter ($CCSR (A=0.5B)$)

Fig. (8-12) illustrates another graphical way that presents the received $I_{(HTCS)}$ above each ring of $Dome_2$ in winter. It also shows that the $I_{(HTCS)}$ -values in general increase towards the top ring (increase upwards on the dome surface).

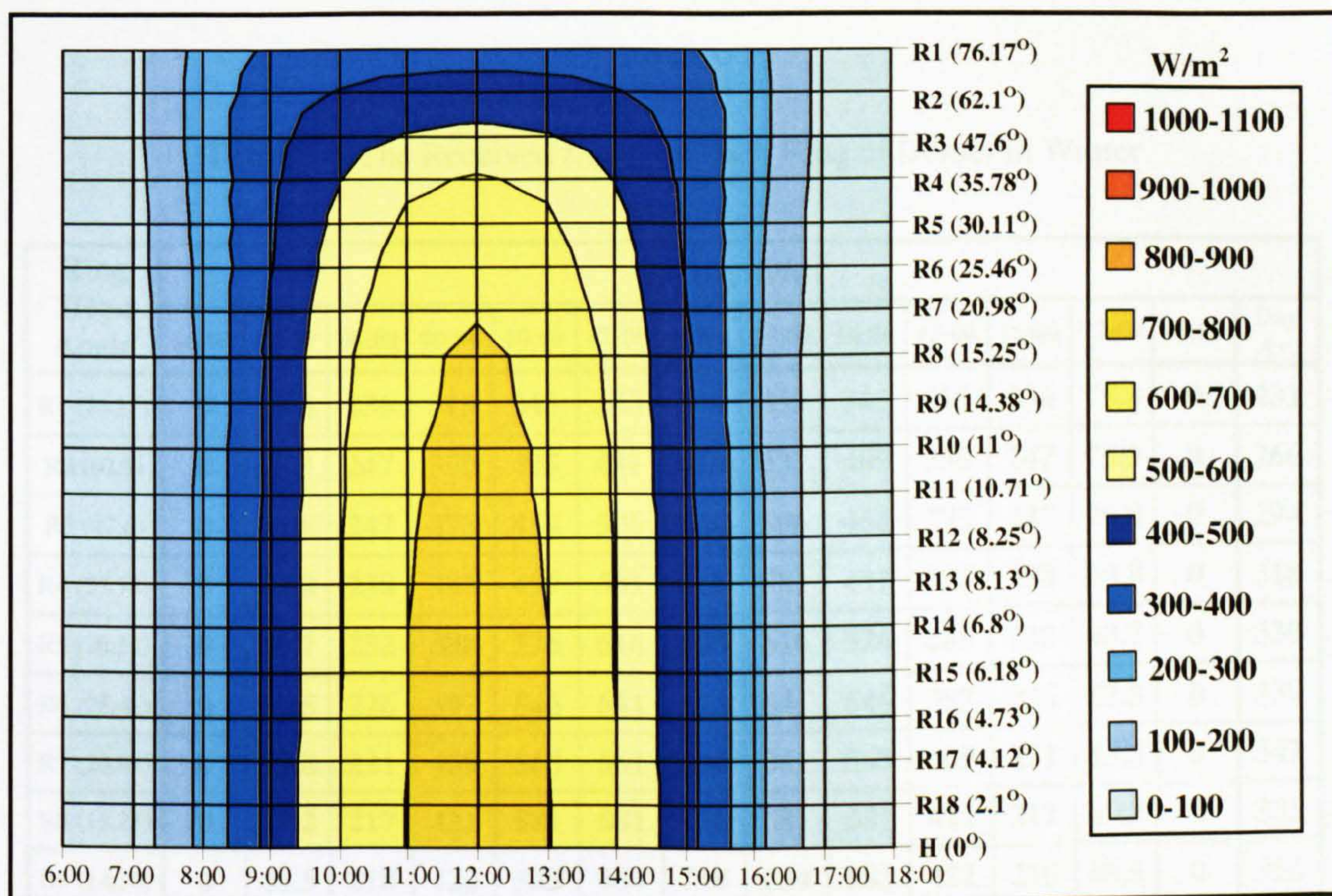


Figure 8-12 $I_{(HTCS)}$ (W/m^2) on $Dome_2$ Rings in Winter ($CCSR (A=0.5B)$)

According to what has been implied from the previous graphs, the difference between the $I_{(HTCS)}$ values from ring to another ring reaches its maximum during midday. Both findings for dome solar performances in summer and winter show that the hourly-difference or midday-difference is not consistent between all rings. Dissimilarly to the previous geometry scenarios, $Dome_2$ solar performance in winter has classified the dome surface into two parts; below and above the third ring (R3 47.6°). During the early morning and the late afternoon the $I_{(HTCS)}$ increases only until the third ring (R3 47.6°) and then it starts decreasing till horizontal top ring. During midday and the rest of the day, it keeps increasing through all the rings and not only until (R3 47.6°). Refer to Table (8-5).

Table (8-5) displays the winter hourly $I_{(HTCS)}$ -values that received by each ring of $Dome_2$, where $A = 0.5B$. It also shows the daily average $I_{(HTCS)}$ that received by each ring and the entire dome. It has been calculated that $Dome_2$ receives about 340 W/m^2 in winter, which is about 93.23% of the $I_{(HTCS)}$ that received by the flat roof in the same season.

Table 8-5 The Received $I_{(HTCS)}$ on Each Ring of $Dome_2$ in Winter

Ring Slope Angle	$I_{(HTCS)} \text{ W/m}^2$													Day Av.
	06:00	07:00	08:00	09:00	10:00	11:00	12:00	13:00	14:00	15:00	16:00	17:00	18:00	
R1 (76.17)	0	75.8	236	315	345	353	354	353	345	315	236	75.8	0	231
R2 (62.1)	0	75.3	247	350	405	431	439	431	405	350	247	75.3	0	266
R3 (47.6)	0	70.8	247	373	456	506	524	506	456	373	247	70.8	0	294
R4 (35.78)	0	64.8	238	383	497	581	611	581	497	383	238	64.8	0	318
R5 (30.11)	0	60.7	232	388	526	616	648	616	526	388	232	60.7	0	330
R6 (25.46)	0	57.5	226	397	546	641	673	641	546	397	226	57.5	0	339
R7 (20.98)	0	53.8	221	409	563	661	694	661	563	409	221	53.8	0	347
R8 (15.25)	0	49.2	217	421	581	681	716	681	581	421	217	49.2	0	355
R9 (14.38)	0	48.5	218	422	583	684	718	684	583	422	218	48.5	0	356
R10 (11)	0	45.5	220	427	590	692	727	692	590	427	220	45.5	0	360
R11 (10.71)	0	45.2	221	428	590	693	728	693	590	428	221	45.2	0	360
R12 (8.25)	0	43	222	430	594	697	733	697	594	430	222	43	0	362
R13 (8.13)	0	42.9	222	431	594	698	733	698	594	431	222	42.9	0	362
R14 (6.8)	0	41.8	223	432	596	700	735	700	596	432	223	41.8	0	363
R15 (6.18)	0	41.3	223	432	597	700	736	700	597	432	223	41.3	0	363
R16 (4.73)	0	40.3	223	433	598	702	738	702	598	433	223	40.3	0	364
R17 (4.12)	0	40.1	224	434	599	702	738	702	598	433	223	39.9	0	364
R18 (2.1)	0	39.7	224	434	600	704	739	704	600	434	224	39.7	0	365
H(0)	0	40	224	434	600	704	740	704	600	434	224	40	0	365
Dome₂ ($A=0.5B$)	0	51.4	227	409	551	639	670	639	550	409	227	51.4	0	340

8.2.3 The Solar Performance of Dome₃ A= 2B

The curvature of this domed roof has a steeper profile (*more concavity*) in comparison to the previous geometries *Dome₁* ($A=B$ (*std*)) and *Dome₂* ($A=0.5B$). The CCSR of this dome is $A=2B$. Fig. (8-13) shows the distribution forms of $I_{(HTCS)}$ -values on *Dome₃* eighteen rings in summer. For all rings, the maximum $I_{(HTCS)}$ takes place at midday. As shown in Fig. (8-13), all $I_{(HTCS)}$ -curves ($I_{(HTCS)}$ -values distribution forms) have similar characteristics around the midday axis.

The graph in Fig. (8-13) illustrates that during summer most of the *Dome₃* rings receive $I_{(HTCS)}$ less than that received by the flat roof except number of the dome lower part rings during both early morning and late afternoon. This scenario is very similar to the *Dome₁* where CCSR is A equals B. This dome geometry appears as the preferable profile (concavity) for domes in order to receive less solar radiation intensity in summer.

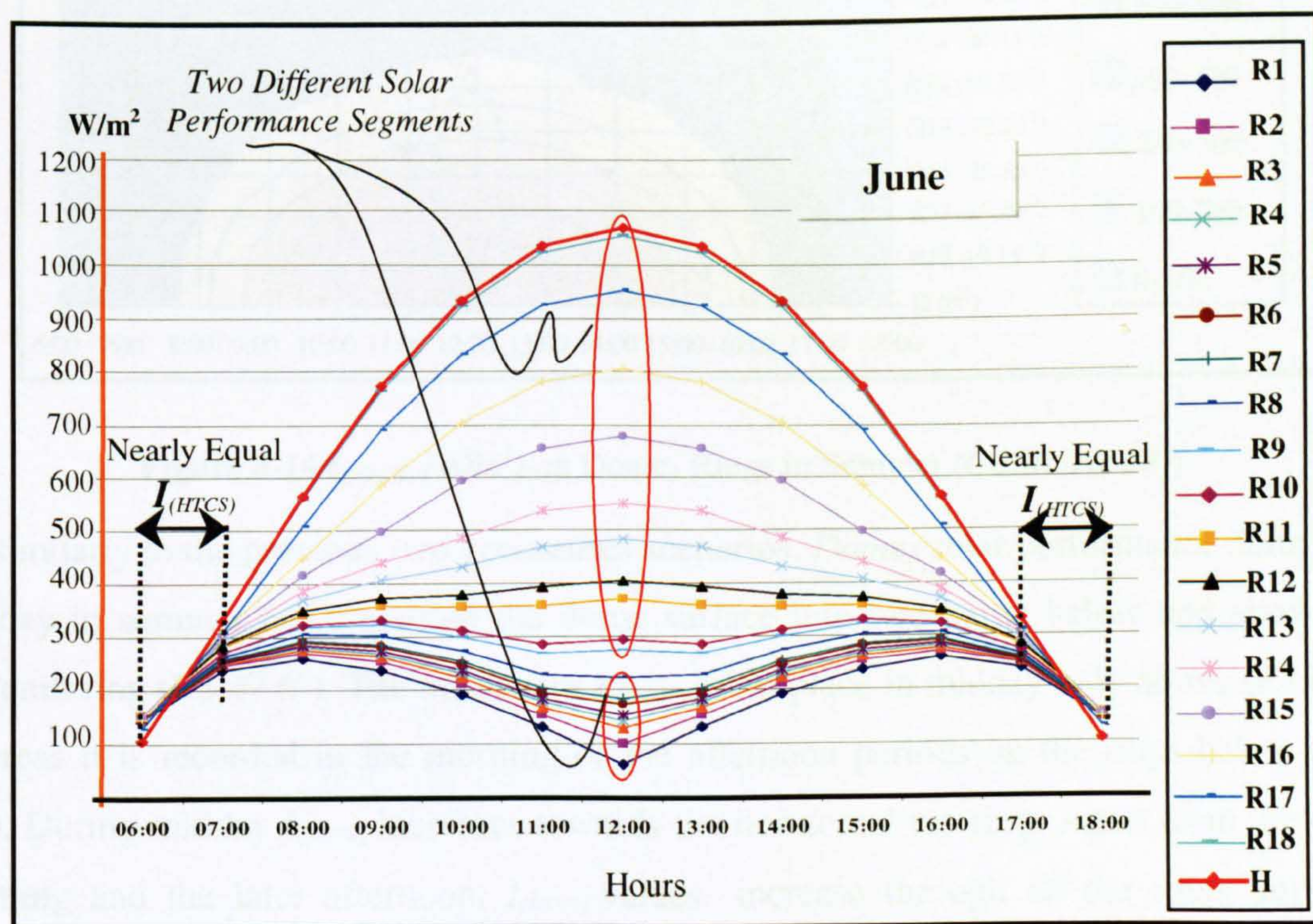


Figure 8-13 $I_{(HTCS)}$ (W/m^2) on Dome₃ Rings in Summer (CCSR ($A=2B$))

Fig. (8-14) illustrates another graphical way that presents the received $I_{(HTCS)}$ above each ring of $Dome_3$ in summer. This dome geometry has similar scenarios during summer to that discussed in the previous geometries ($A=B$ & $A=0.5B$), in which the $I_{(HTCS)}$ -values in general increase towards the top ring (*increase upwards on the dome surface*).

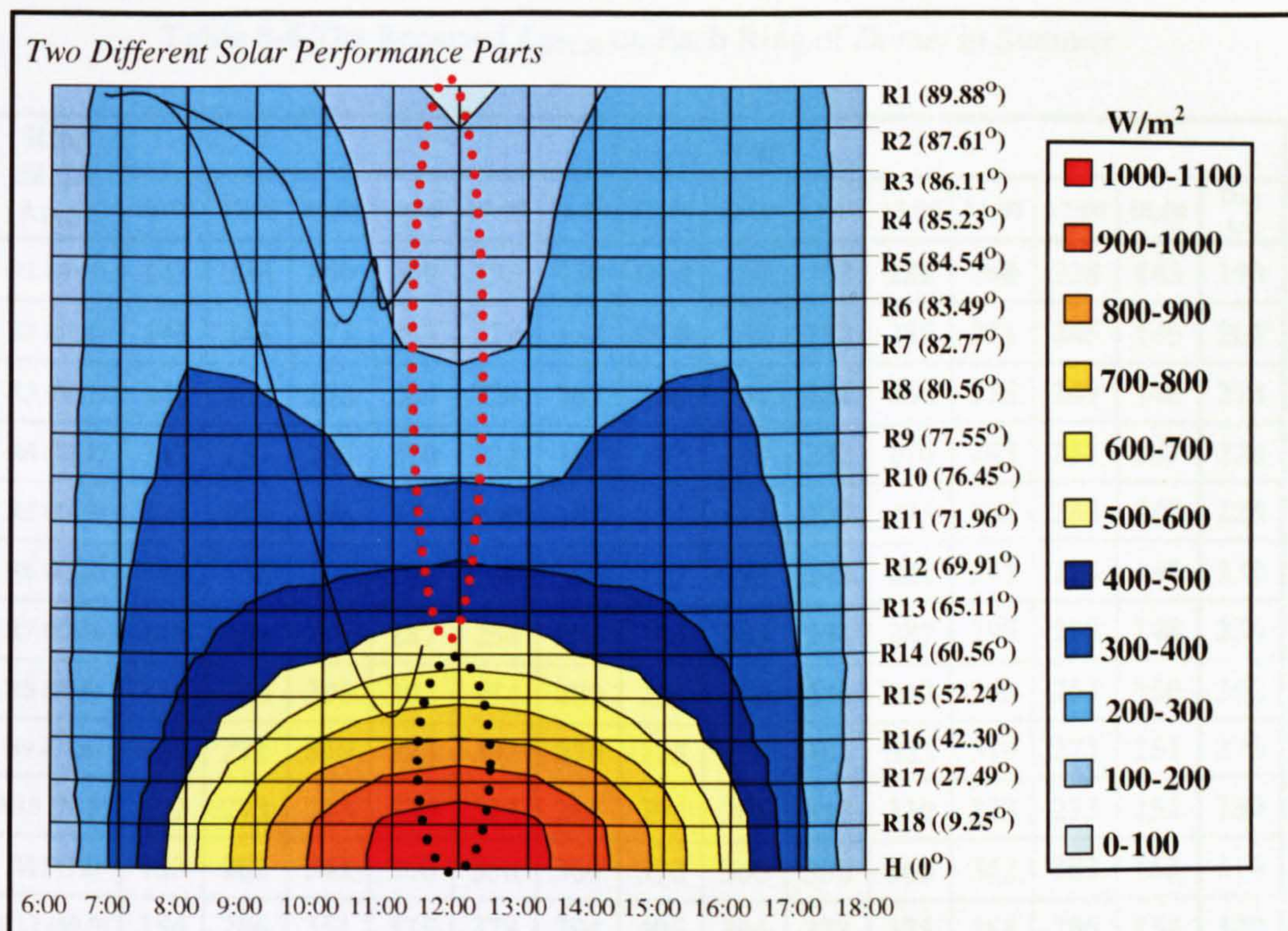


Figure 8-14 $I_{(HTCS)}$ (W/m^2) on $Dome_3$ Rings in Summer ($CCSR (A=2B)$)

Dissimilarly to the previous two geometries scenarios, $Dome_3$ solar performance during the midday in summer has classified the dome surface into two parts; below and above the eleventh ring (R11 71.96 $^{\circ}$). The maximum $I_{(HTCS)}$ takes place in midday only above (R11 71.96 $^{\circ}$), whereas it is recorded in the morning or the afternoon periods on the rings below (R11 71.96 $^{\circ}$). During midday $I_{(HTCS)}$ increases towards the horizontal top ring. Apart from the early morning and the later afternoon, $I_{(HTCS)}$ -values increase through all the rings until the horizontal top ring. During the early morning and the late afternoon, they keep increasing until two or three rings before the horizontal (*according to the time*). Refer to Table (8-6).

Table (8-6) displays the summer hourly $I_{(HTCS)}$ -values that received by each ring of $Dome_3$, where $A=2B$. It also shows the daily average $I_{(HTCS)}$ that received by each ring and the entire dome. It has been calculated that $Dome_3$ receives about 348 W/m^2 in summer, which is 52.8% of the $I_{(HTCS)}$ that received by the flat roof in the same season.

Table 8-6 The Received $I_{(HTCS)}$ on Each Ring of $Dome_3$ in Summer

Ring Slope Angle	$I_{(HTCS)}$ W/m ²													Day Av.
	06:00	07:00	08:00	09:00	10:00	11:00	12:00	13:00	14:00	15:00	16:00	17:00	18:00	
R1 (89.9)	143	238	260	239	193	130	60.4	130	193	239	260	238	143	190
R2 (87.6)	145	245	271	255	212	152	99.8	152	212	255	271	245	145	205
R3 (86.1)	146	249	278	264	224	167	126	167	224	264	278	249	146	214
R4 (85.2)	147	251	283	270	232	177	142	177	232	270	283	251	147	220
R5 (84.5)	147	253	286	275	239	184	154	184	239	275	286	253	147	225
R6 (83.5)	148	256	291	282	248	195	172	195	248	282	291	256	148	232
R7 (82.8)	148	258	295	287	254	203	184	203	254	287	295	258	148	236
R8 (80.6)	150	263	305	302	274	230	223	230	274	302	305	263	150	252
R9 (77.6)	151	271	319	323	301	270	275	270	301	323	319	271	151	273
R10 (76.5)	152	273	323	330	312	286	294	286	312	330	323	273	152	280
R11 (72)	153	282	342	360	356	360	370	360	356	360	342	282	153	314
R12 (69.9)	154	286	351	375	378	394	405	394	378	375	351	286	154	329
R13 (65.1)	154	293	370	408	430	470	484	470	430	408	370	293	154	364
R14 (60.7)	153	299	387	438	486	537	553	537	486	438	387	299	153	396
R15 (52.2)	150	306	415	499	595	657	678	657	595	499	415	306	150	456
R16 (42.3)	144	310	447	585	706	782	806	782	706	585	447	310	144	520
R17 (27.5)	128	309	509	691	836	926	955	926	836	691	509	309	128	596
R18 (9.25)	105	329	561	763	924	1024	1057	1024	924	763	561	329	105	651
H(0)	106	332	567	772	935	1037	1070	1037	935	772	567	332	106	659
Dome₃ (A=2B)	143	279	361	406	428	431	427	431	428	406	361	279	143	348

Fig. (8-15) shows the distribution forms of $I_{(HTCS)}$ -values on $Dome_2$ eighteen rings in winter. For most of the rings, the maximum $I_{(HTCS)}$ takes place at midday. As shown in Fig. (8-15), all $I_{(HTCS)}$ -curves ($I_{(HTCS)}$ -values distribution forms) have similar characteristics around the midday axis. The graph in Fig. (8-15) illustrates that during winter most of the $Dome_3$ rings receive $I_{(HTCS)}$ more than that received by the flat roof during two time-periods (06:00-08:00 in the morning and 16:00-18:00 in the afternoon). This scenario is very similar to the previous dome geometries ($A=B$ & $A=0.5B$) in the same season. Also it is longer than summer scenario for the same dome geometry ($A=2B$), which is desired for winter conditions.

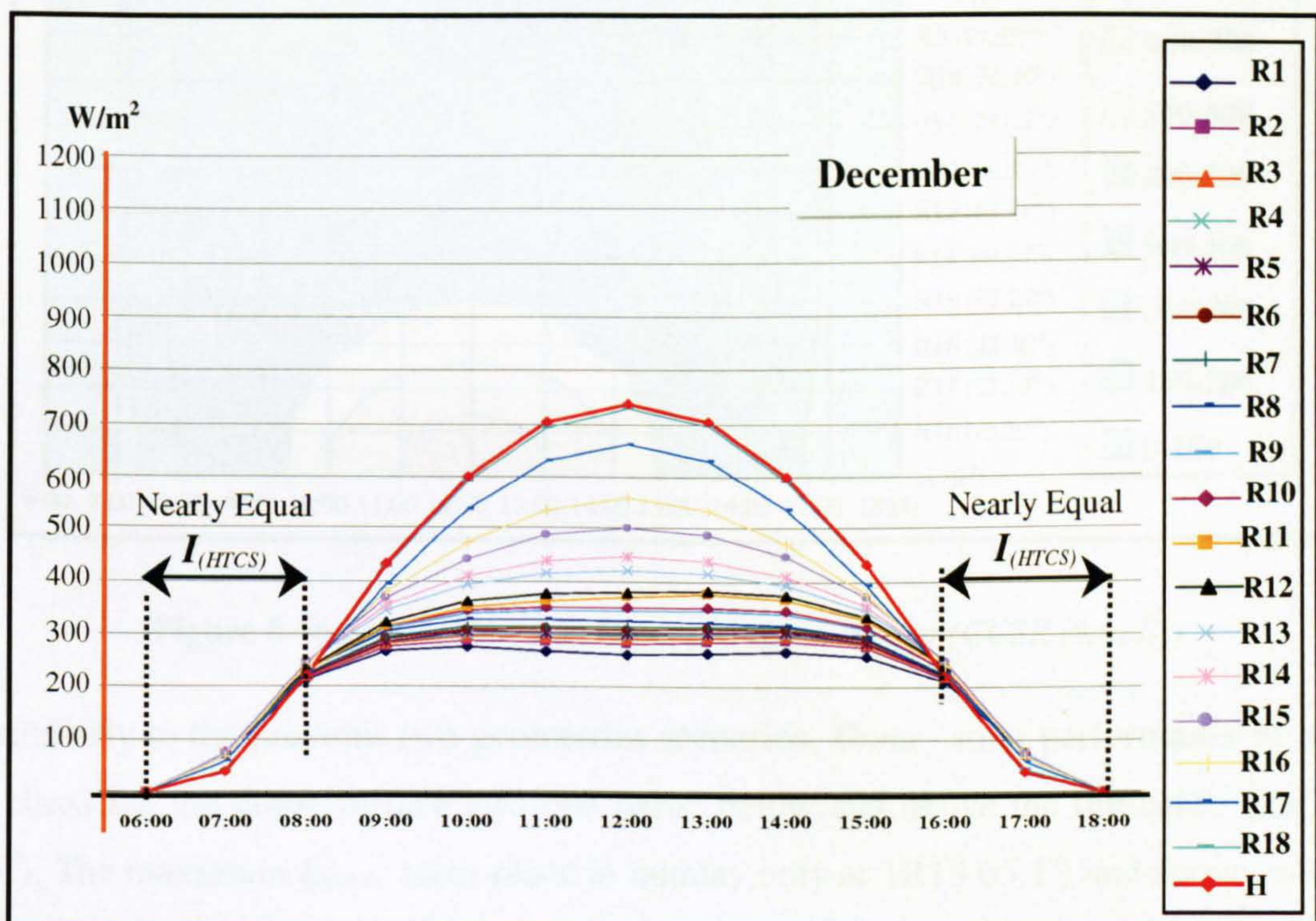


Figure 8-15 $I_{(HTCS)}$ (W/m^2) on $Dome_3$ Rings in Winter ($CCSR (A=2B)$)

Fig. (8-16) illustrates another graphical way that presents the received $I_{(HTCS)}$ above each ring of $Dome_3$ in winter. It also shows that the $I_{(HTCS)}$ -values in general increase towards the top ring (increase upwards on the dome surface).

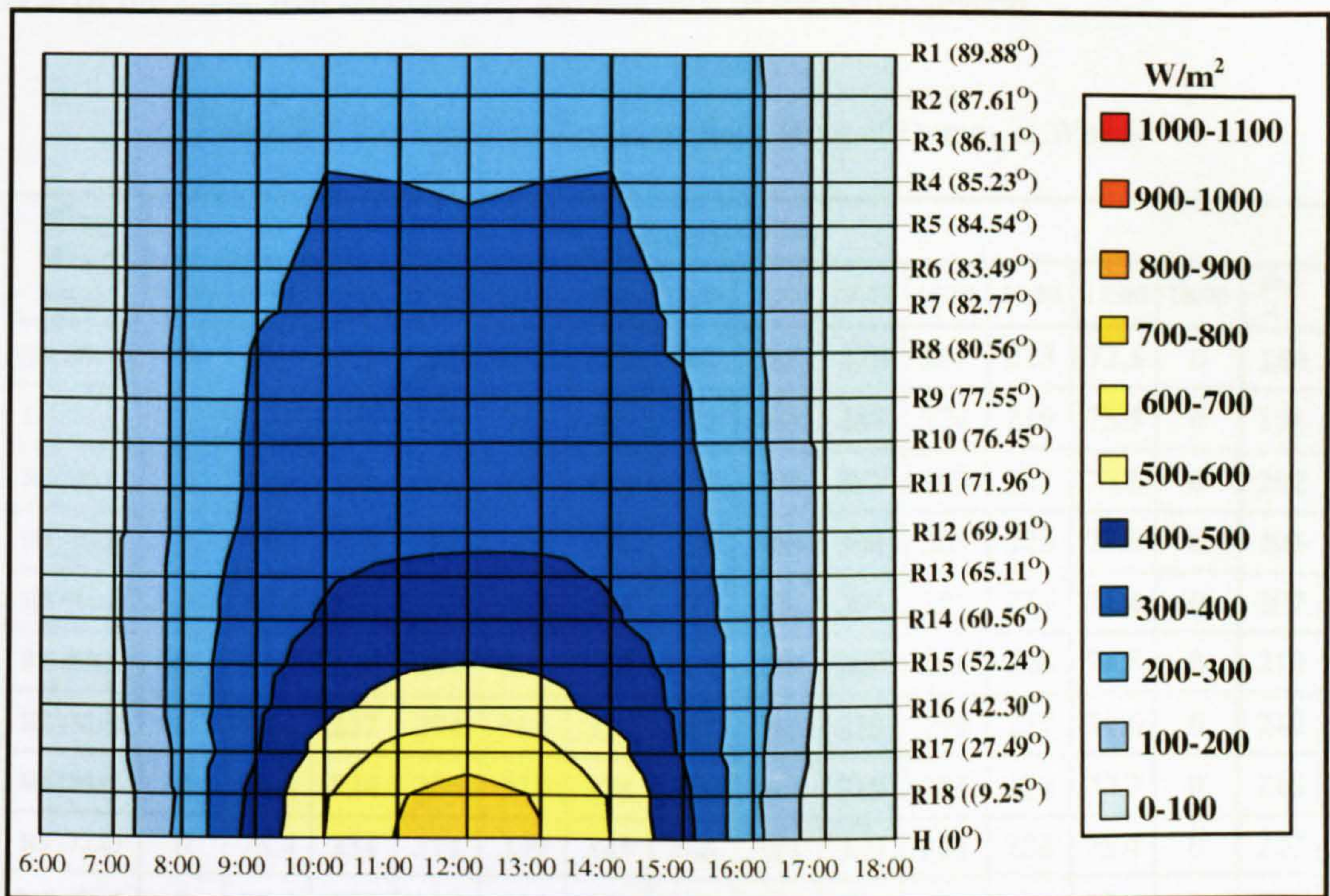


Figure 8-16 $I_{(HTCS)}$ (W/m^2) on $Dome_3$ Rings in Winter ($CCSR (A=2B)$)

Dissimilarly to the previous two geometries scenarios, $Dome_3$ solar performance in winter has classified the dome surface into two parts; below and above the thirteenth ring (R13 65.1°). The maximum $I_{(HTCS)}$ takes place in midday only at (R13 65.1°) and above, whereas it is recorded in the morning or the afternoon periods on the rings below (R13 65.1°). During midday $I_{(HTCS)}$ increases towards the horizontal top ring. Apart from the early morning and the later afternoon, $I_{(HTCS)}$ -values increase with the decrease of the rings tilt angle till reach the maximum on the horizontal top ring. During the early morning and the late afternoon, they keep fluctuating. Refer to Table (8-7).

Table (8-7) displays the winter hourly $I_{(HTCS)}$ -values that received by each ring of $Dome_3$, where $A=2B$. It also shows the daily average $I_{(HTCS)}$ that received by each ring and the entire dome. It has been calculated that $Dome_3$ receives about 250 W/m^2 in winter, which is about 68.64% of the $I_{(HTCS)}$ that received by the flat roof in the same season.

Table 8-7 The Received $I_{(HTCS)}$ on Each Ring of $Dome_3$ in Winter

Ring Slope Angle	$I_{(HTCS)} \text{ W/m}^2$													Day Av.
	06:00	07:00	08:00	09:00	10:00	11:00	12:00	13:00	14:00	15:00	16:00	17:00	18:00	
R1 (89.9)	0	73.4	216	269	277	269	262	265	270	261	213	72.5	0	188
R2 (87.6)	0	73.5	219	276	289	285	282	285	289	276	219	73.5	0	198
R3 (86.1)	0	73.8	221	282	297	294	292	294	297	282	221	73.8	0	202
R4 (85.2)	0	73.8	223	285	301	300	298	300	301	285	223	73.8	0	205
R5 (84.5)	0	74.4	224	287	305	304	302	304	305	287	224	74.4	0	207
R6 (83.5)	0	74.5	226	291	309	310	309	310	309	291	226	74.5	0	210
R7 (82.8)	0	74.6	227	294	313	314	314	314	313	294	227	74.6	0	212
R8 (80.6)	0	76.8	234	306	327	328	326	323	318	295	224	73.3	0	218
R9 (77.6)	0	75.4	234	311	339	345	346	345	339	311	234	75.4	0	227
R10 (76.5)	0	75.4	235	314	344	351	352	351	344	314	235	75.4	0	230
R11 (72)	0	73.5	231	315	351	363	372	377	364	327	240	76	0	238
R12 (69.9)	0	74.1	236	323	362	376	380	382	374	333	243	75.8	0	243
R13 (65.1)	0	75.5	246	344	393	416	422	416	393	344	246	75.5	0	259
R14 (60.7)	0	74.8	247	353	410	439	447	439	410	353	247	74.8	0	269
R15 (52.2)	0	72.7	248	368	441	487	502	488	446	372	251	73.5	0	288
R16 (42.3)	0	68.5	244	378	473	535	560	534	471	377	242	68.1	0	304
R17 (27.5)	0	59.1	228	392	538	631	663	631	538	392	228	59.1	0	335
R18 (9.25)	0	43.7	221	428	592	694	730	695	592	429	221	43.9	0	361
H(0)	0	40	224	434	600	704	740	704	600	434	224	40	0	365
Dome₃ (A=2B)	0	69.9	231	329	382	408	416	408	383	329	231	69.9	0	250

8.2. The Solar Performance of The Three Dome Geometries and Flat Roof

This part compares between the received $I_{(HTCS)}$ by each dome geometry throughout the day and that received by the flat roof in summer and winter. Fig. (8-17) depicts that *Dome₃* receives the minimum $I_{(HTCS)}$ in both seasons. Another graphical way of presenting $I_{(HTCS)}$ -values and distribution curves for each dome with comparison to the flat roof and other two domes will be presented in Chapter 9 (see Fig. (9-15)). This will be discussed through a comparison, which will be held to validate the solar results above semicircular domed-roof using another simulation tool.

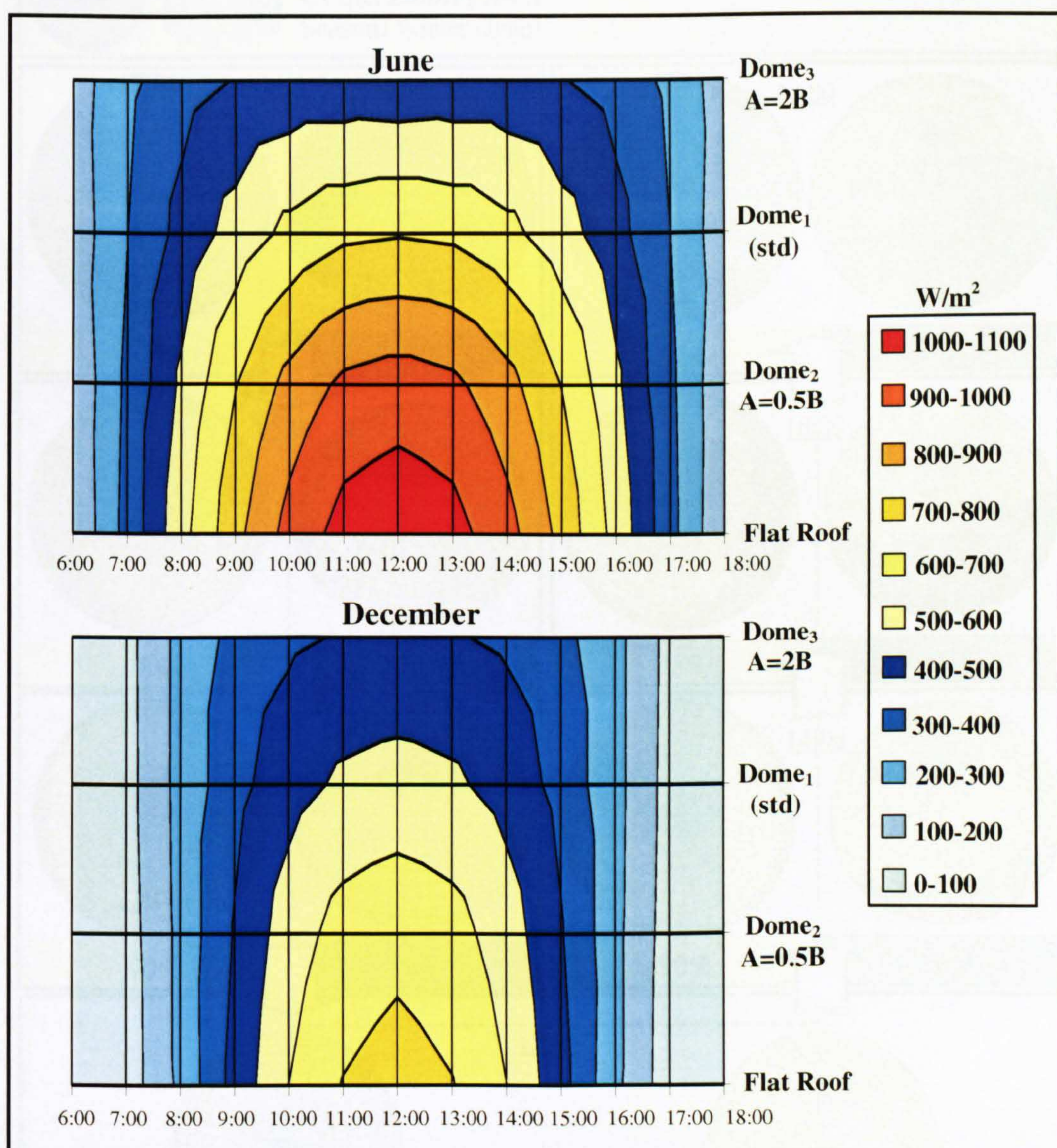


Figure 8-17 $I_{(HTCS)}$ (W/m^2) Day Average on The Three Domes and The Flat Roof in Summer & Winter

8.3 DOMED ROOFS SHADE-ANALYSIS

A shade-analysis study has been carried out for the three dome geometries where A equals B and also for *Dome₂* and *Dome₃* where A is not equal B ($A < B$ & $A > B$ respectively). The IES's *SUNCAST* and *APACHE* [2] applications have been employed to find out the exposed and the self-shaded areas patterns and their ratios above the three dome geometries every 2 hours in summer and winter. Fig. (8-18) shows *Dome₁* shade-analysis in summer. (Pattern ratios have been calculated by *APACHE*) (Refer to Appendix (B) (Page 21-23))

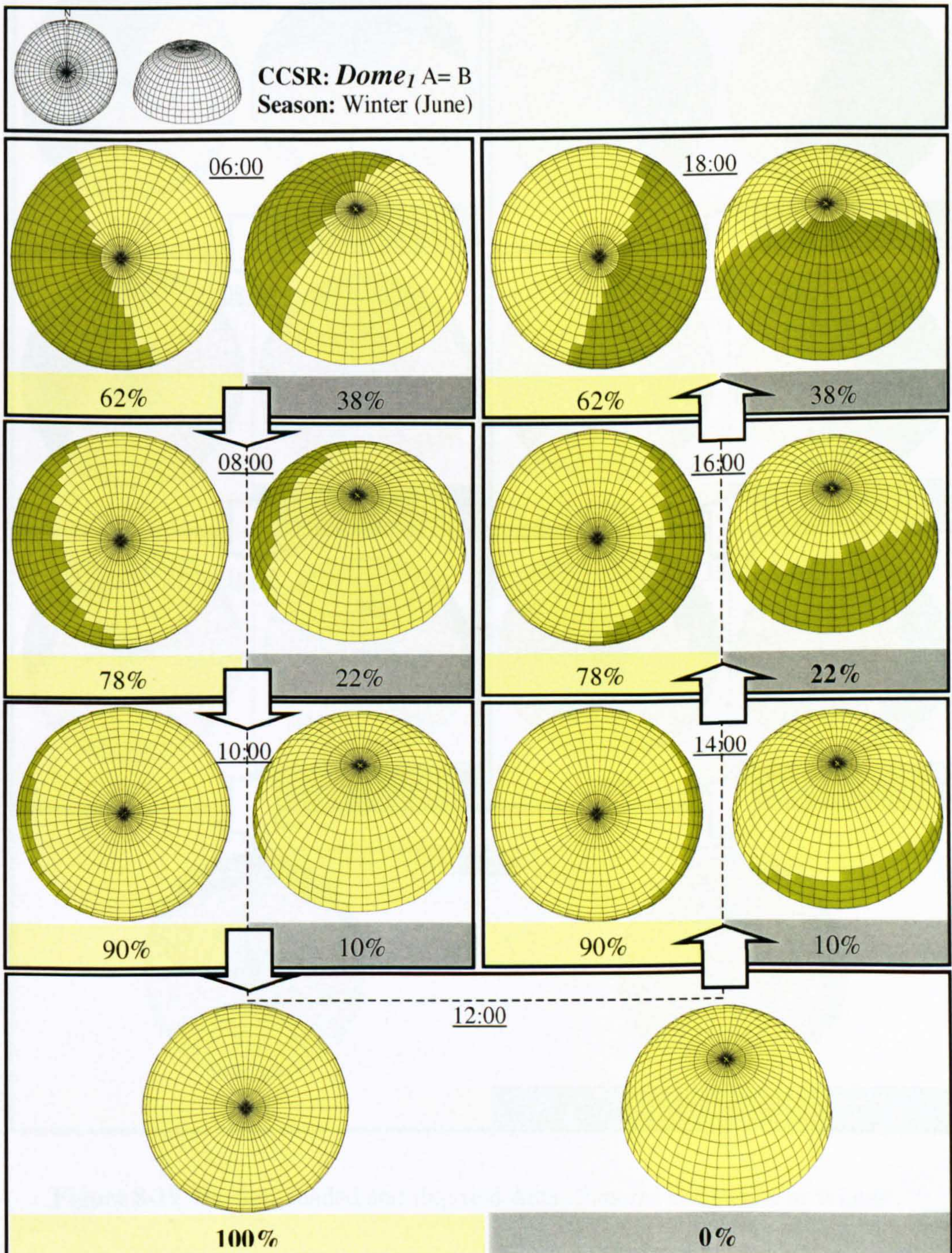


Figure 8-18 The Self-shaded and Exposed Areas Patterns and Ratios in Summer

Fig. (8-19) shows the shade-analysis for the same dome geometry in winter. The shade-analysis in Fig. (8-19) illustrates the exposed and the self-shaded areas and their ratios above *Dome₁* in winter. Refer to Table (8-8)

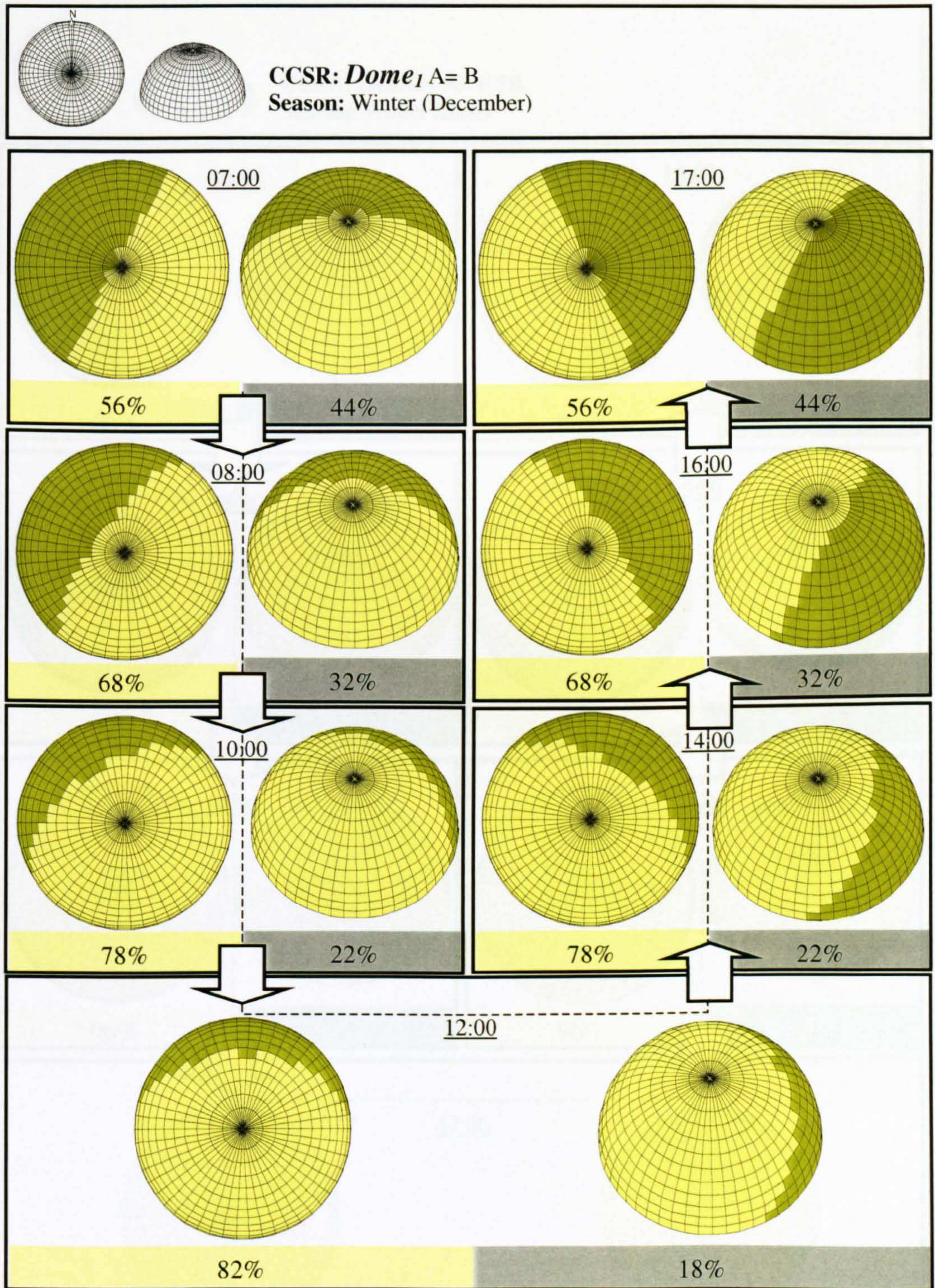


Figure 8-19 The Self-shaded and Exposed Areas Patterns and Ratios in Winter

Fig. (8-20) shows the shade-analysis for another dome geometry ($A=0.5B$) in summer. The shade-analysis in Fig. (8-20) illustrates the exposed and the self-shaded patterns and their ratios above *Dome₂* in summer. Refer to Table (8-9)

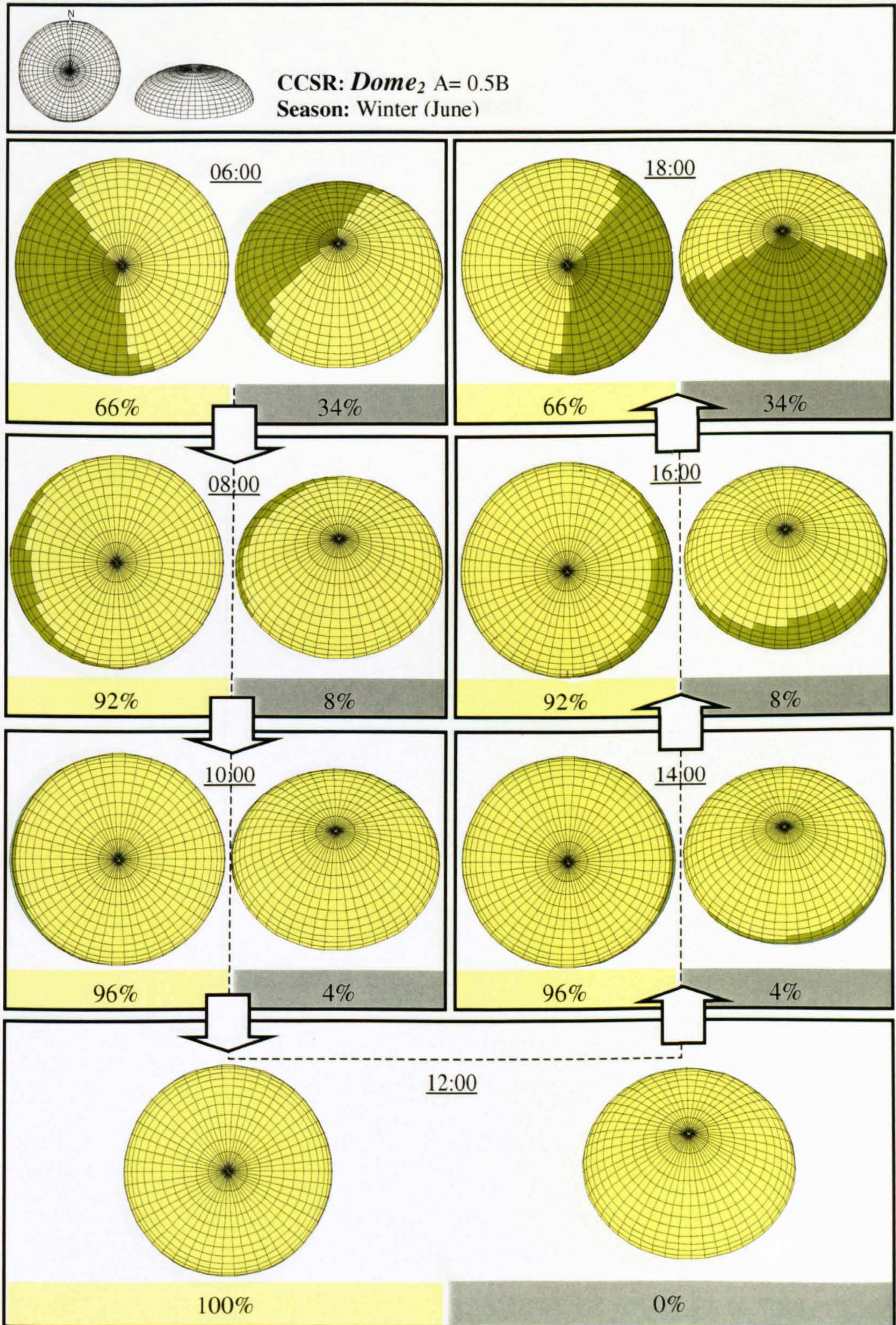


Figure 8-20 The Self-shaded and Exposed Areas Patterns and Ratios in Summer

Fig. (8-21) shows the shade-analysis for the same dome geometry in winter. The shade-analysis images in Fig. (8-21) illustrate the exposed and the self-shaded areas, ratios and patterns above *Dome₂* in winter. *Refer to Table (8-9)*

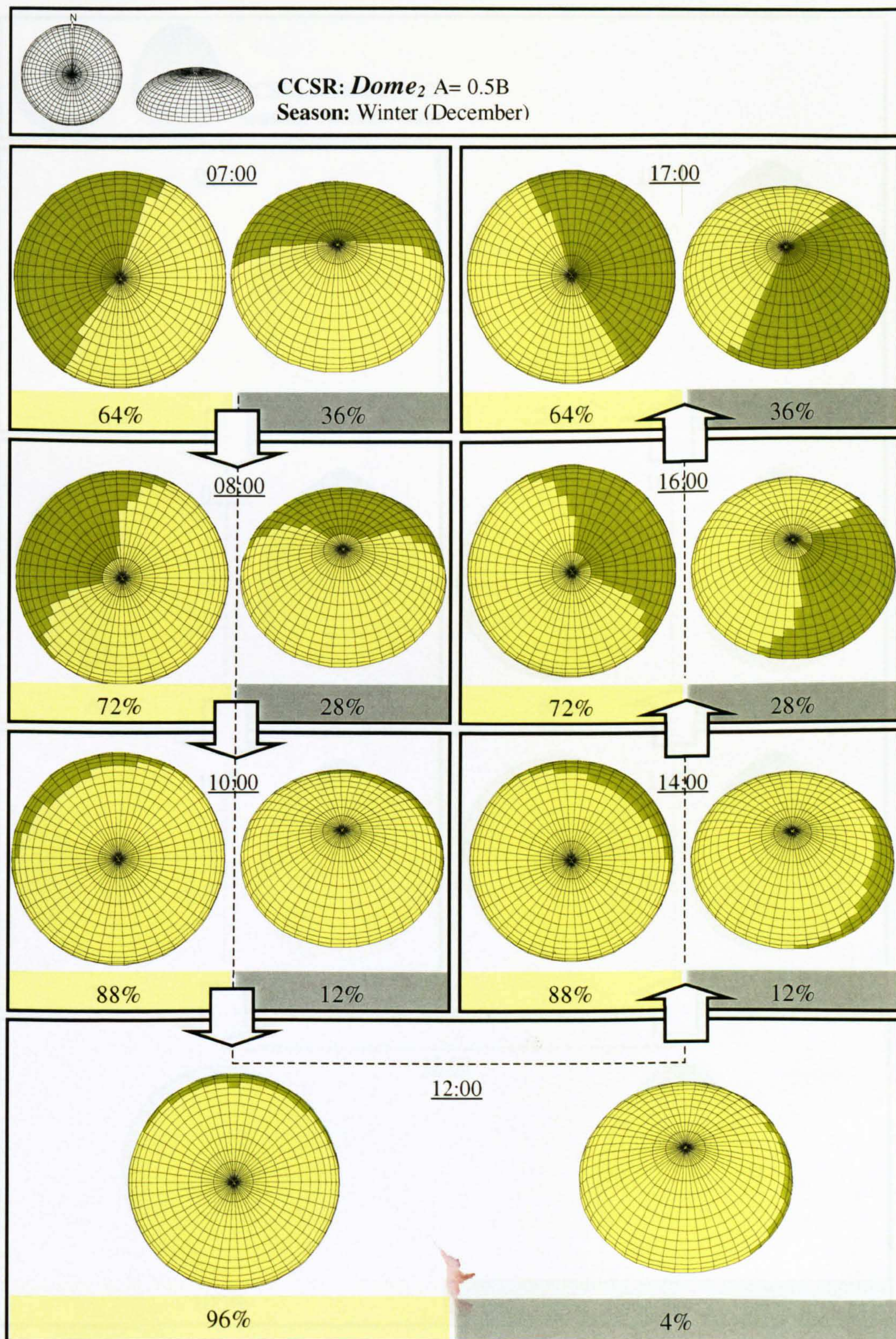


Figure 8-21 The Self-shaded and Exposed Areas Patterns and Ratios in Winter

Fig. (8-22) shows the shade-analysis for the same dome geometry in summer. The shade-analysis images in Fig. (8-22) illustrate the exposed and the self-shaded areas, ratios and patterns above *Dome₃* in summer. *Refer to Table (8-9)*

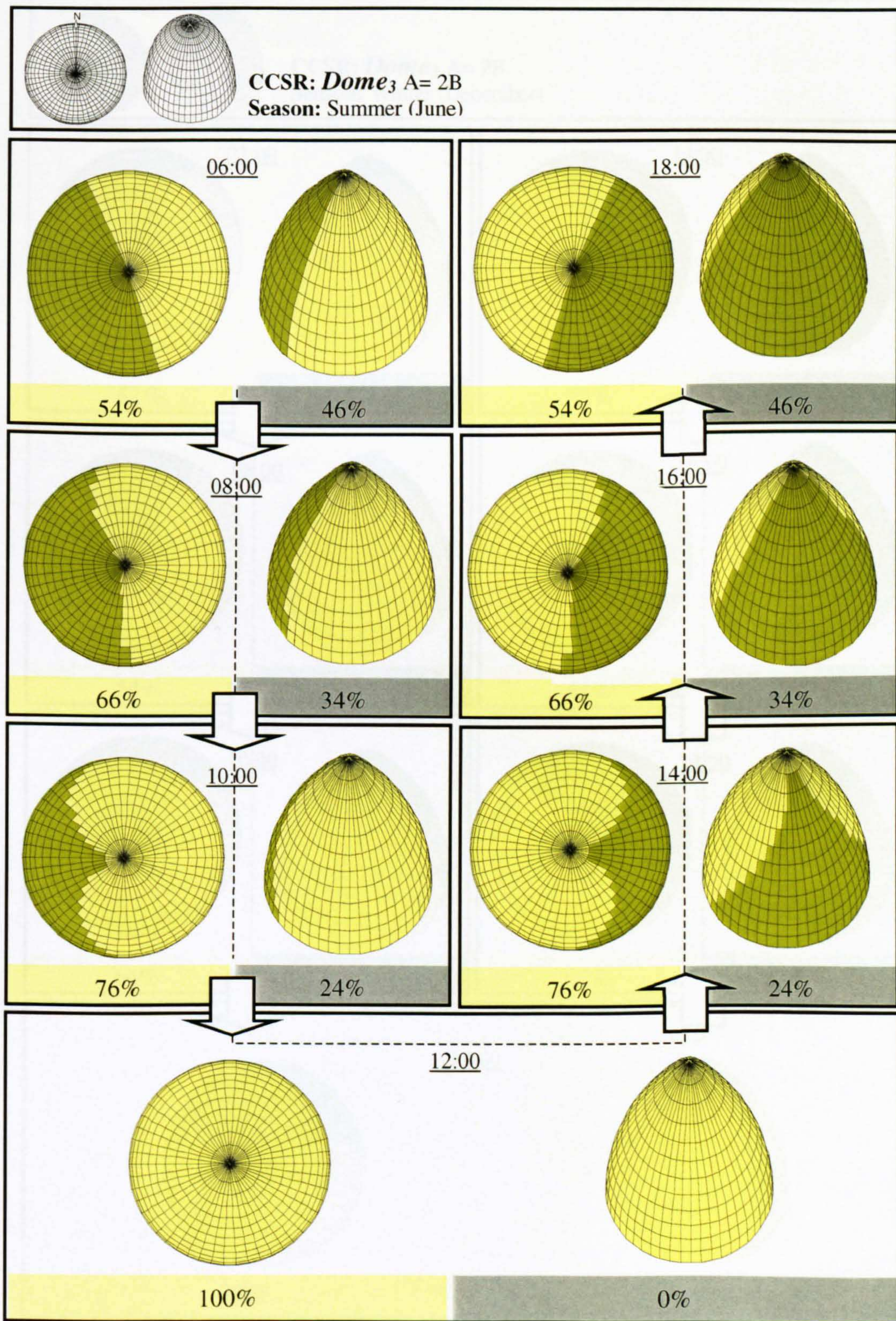


Figure 8-22 The Self-shaded and Exposed Areas Patterns and Ratios in Summer

Fig. (8-23) shows the shade-analysis for the same dome geometry in winter. The shade-analysis images in Fig. (8-23) illustrate the exposed and the self-shaded areas, ratios and patterns above *Dome₃* in winter. Refer to Table (8-9)

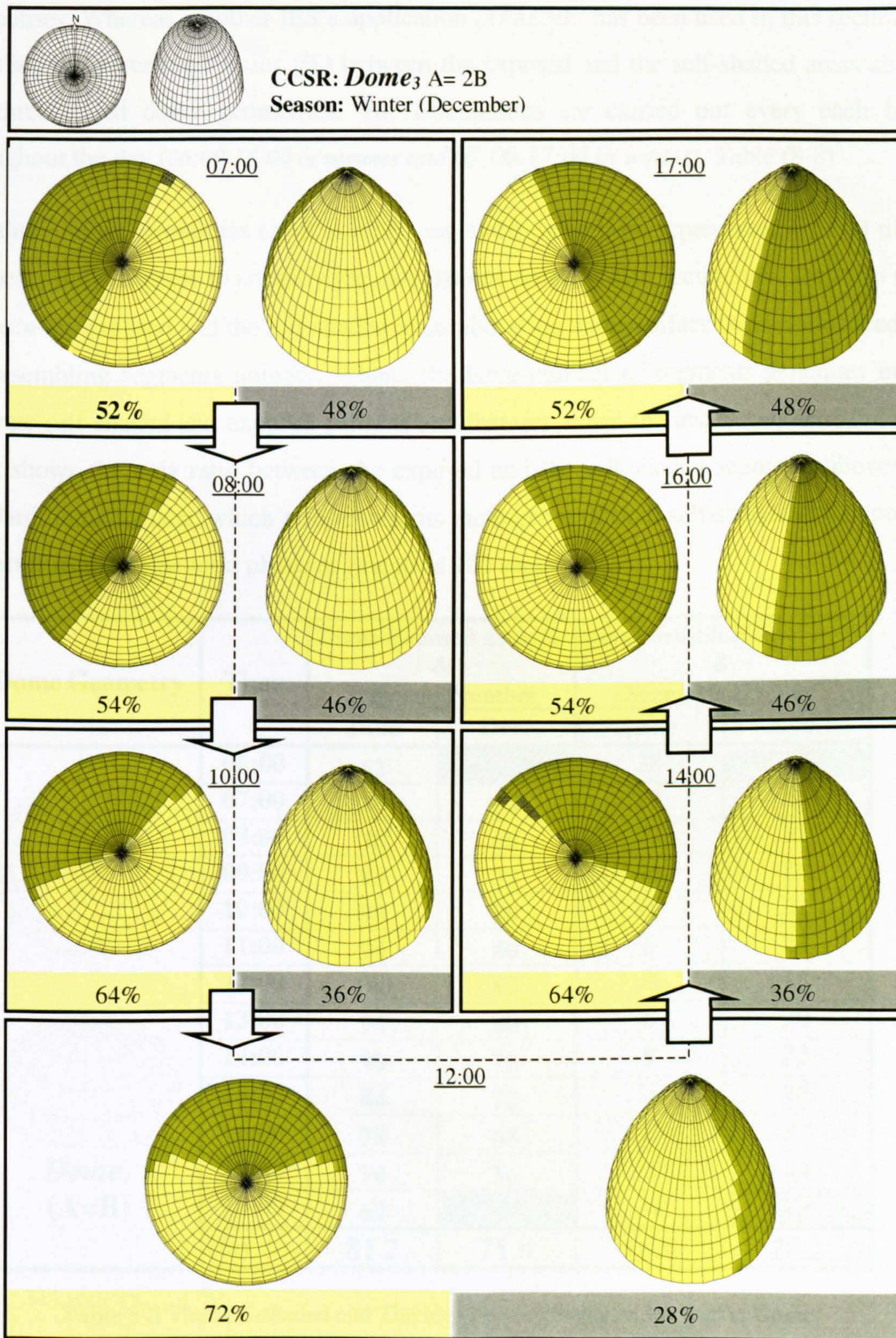


Figure 8-23 The Self-shaded and Exposed Areas Patterns and Ratios in Winter

8.3.1 The Ratios of Self-Shaded and Exposed Areas Above Domed Roofs

As has what explained in the previous section, IES's [2] *SUNCAST* solar application has been employed to find out the exposed and the shaded patterns only above different dome geometries. Whereas, another IES's application (*APACHE*) has been used in this section to calculate the percentage ratios (%) between the exposed and the self-shaded areas above the three tested dome geometries. The calculations are carried out every each hour throughout the day (06:00-18:00 in summer and 07:00-17:00 in winter), Table (8-8).

The three dome geometries ($A=B$, $A=0.5B$, and $A=2B$) have been represented by 100 tilted segments only in order to simplify the calculations process. The accuracy of the ratio (%) between the exposed and the self-shaded areas above the dome surface is not influenced by the resembling segments number. Where, the large number of segments generates more accurate self-shaded and exposed patterns and features above the tested geometry. Table (8-8) shows the area ratio between the exposed and the self-shaded segments above the standard dome surface, which also represents the number of both self-shaded and exposed segments as the dome total planar segments is 100 segments.

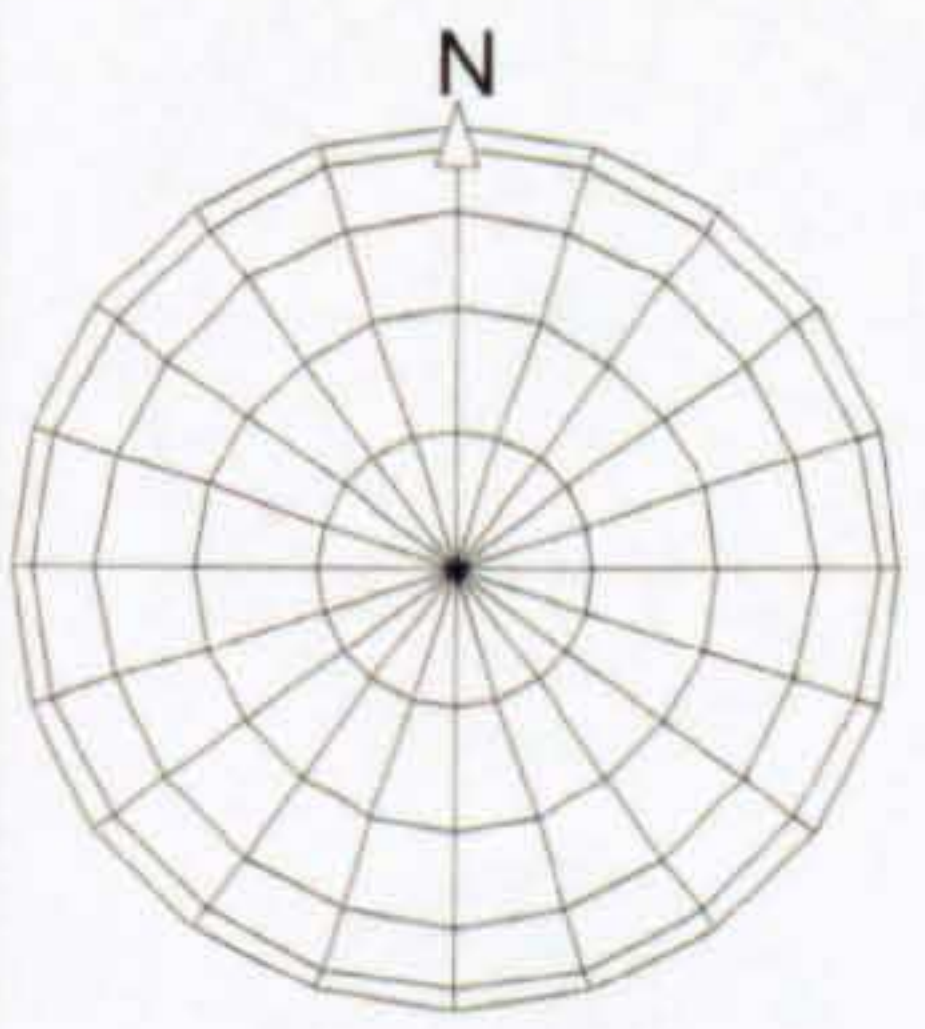

Dome Geometry	Time	Dome Exposed Area % & Segments Number		Dome Self-Shaded Area % & Segments Number	
		June	Dec.	June	Dec.
		  Dome₁ (A=B)	06:00	62	/ / / / / / / / / /
07:00	70		56	30	44
08:00	78		68	22	32
09:00	84		72	16	28
10:00	90		78	10	22
11:00	94		80	6	20
12:00	100		82	0	18
13:00	94		80	6	20
14:00	90		78	9	22
15:00	84		72	16	28
16:00	78		68	12	32
17:00	70		56	30	44
18:00	62		/ / / / / / / / / /	38	/ / / / / / / / / /
Day Av.	81.2	71.8	18.8	28.2	

Table 8-8 The Self-shaded and The Exposed Segments and Areas on Dome₁

Table (8-9) shows the area ratio between the exposed and the self-shaded segments above $Dome_2$ and $Dome_3$ surfaces, which also represents the number of both self-shaded and exposed segments, as the total number of each dome planar segments is 100 segments.

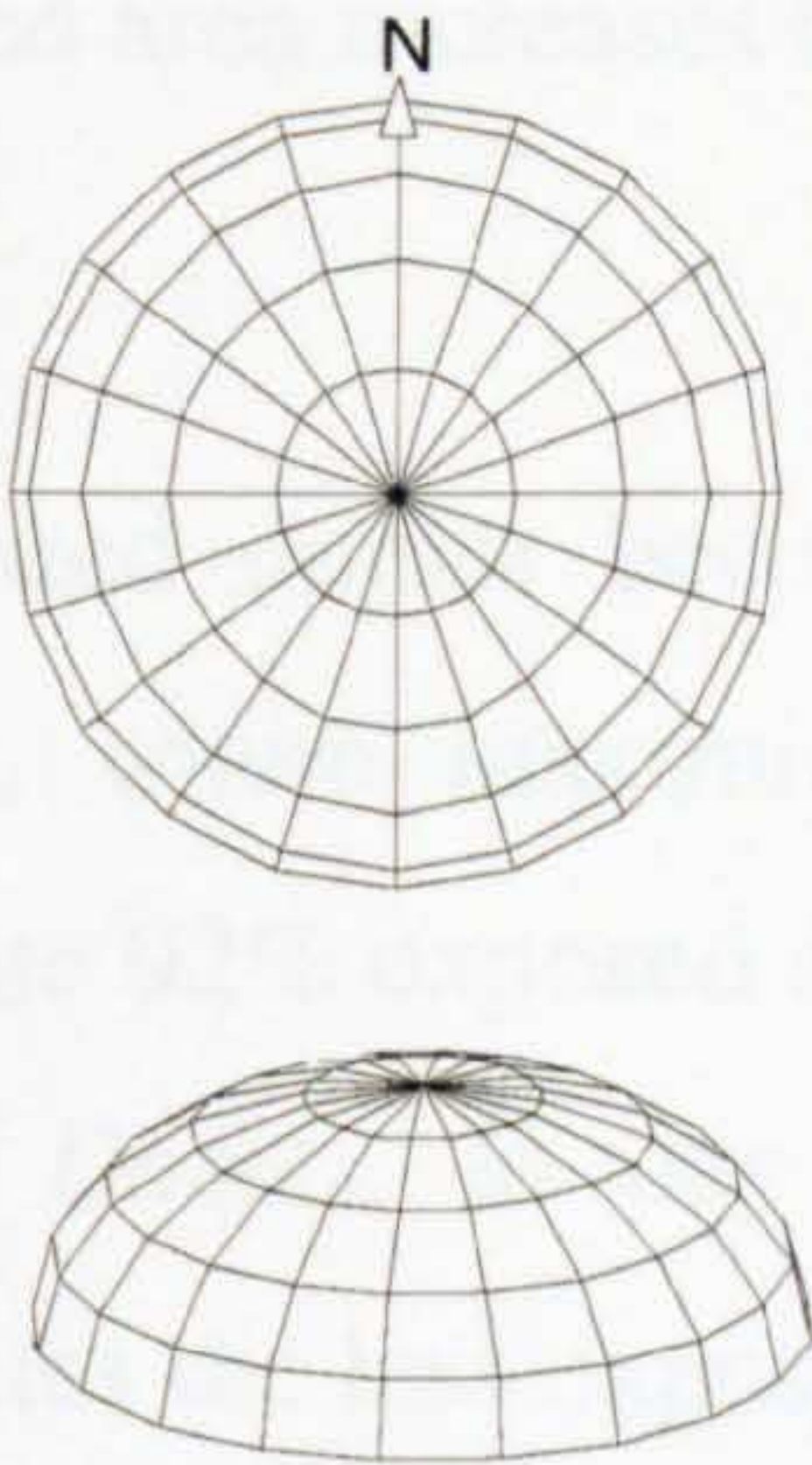
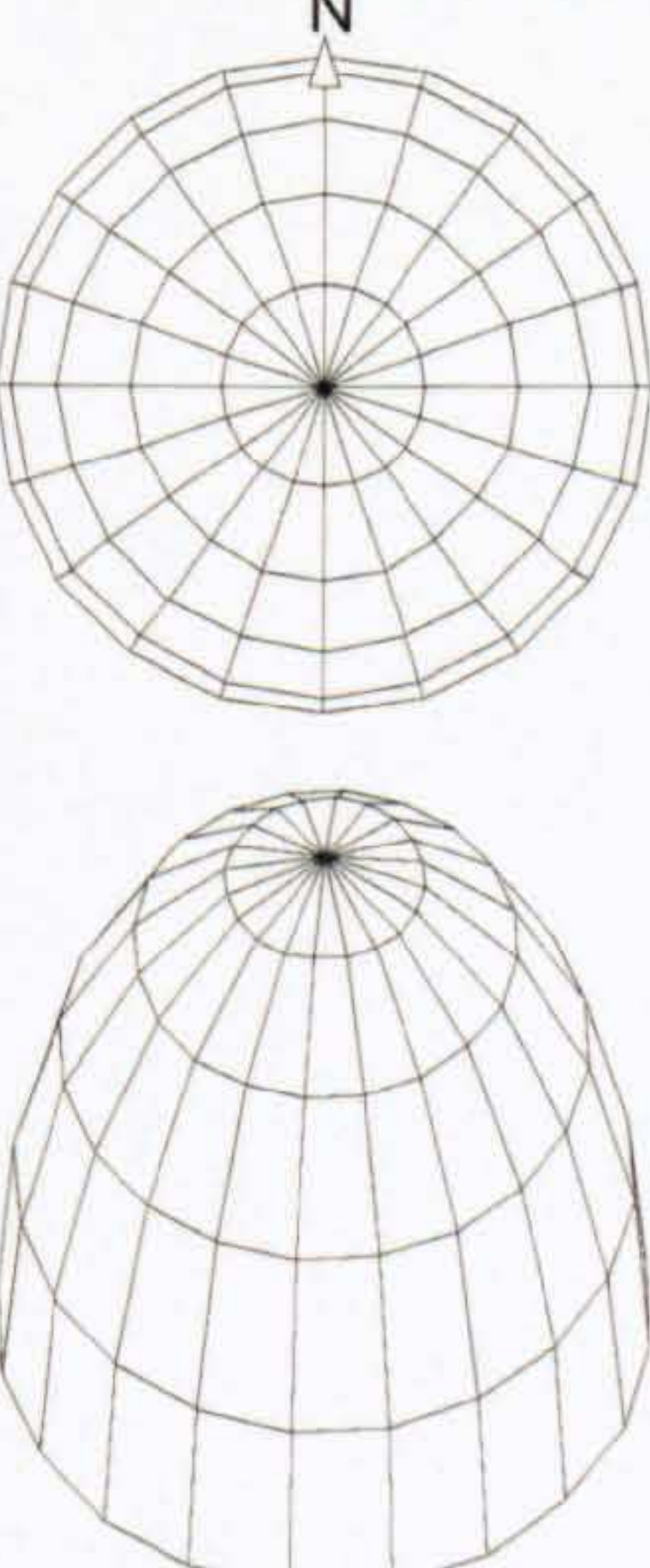
Dome Geometry	Time	Dome Exposed Area % & Segments Number		Dome Self-Shaded Area % & Segments Number	
		June	Dec.	June	Dec.
 <p>$Dome_2$ ($A=0.5B$)</p>	06:00	66		34	
	07:00	78	64	22	36
	08:00	92	72	18	28
	09:00	94	80	16	20
	10:00	96	88	14	12
	11:00	98	92	12	8
	12:00	100	96	0	4
	13:00	98	92	12	8
	14:00	96	88	14	12
	15:00	94	80	16	20
	16:00	92	72	18	28
	17:00	78	64	22	36
	18:00	62		36	
Day Av.	88	80.7	12	19.3	
 <p>$Dome_3$ ($A=2B$)</p>	06:00	54		46	
	07:00	60	52	40	48
	08:00	66	54	34	46
	09:00	70	60	30	40
	10:00	76	64	24	36
	11:00	82	68	18	32
	12:00	100	72	0	28
	13:00	82	68	18	32
	14:00	76	64	24	36
	15:00	70	60	30	40
	16:00	66	54	34	46
	17:00	60	52	40	48
	18:00	54		46	
Day Av.	70.5	60.7	29.5	39.3	

Table 8-9 The Self-shaded and The Exposed Segments and Areas on $Dome_2$ & 3

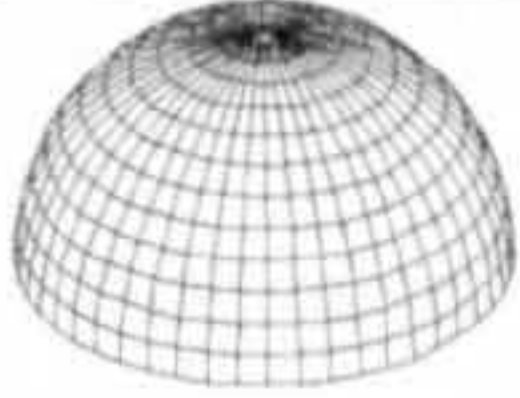
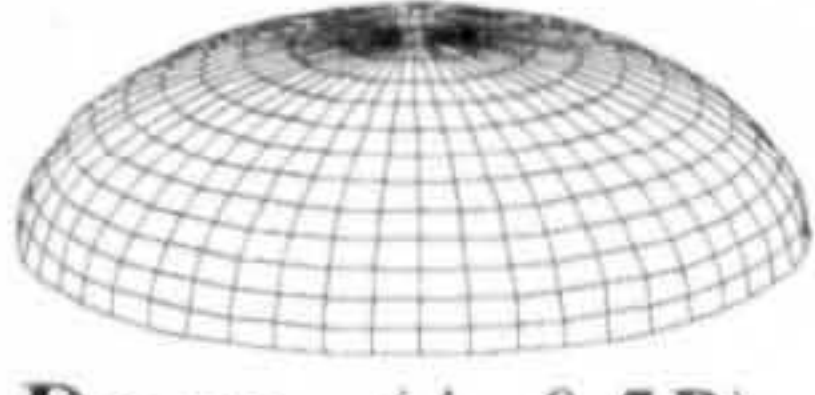
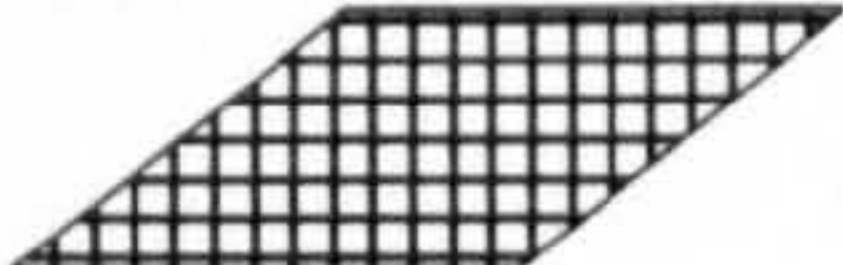
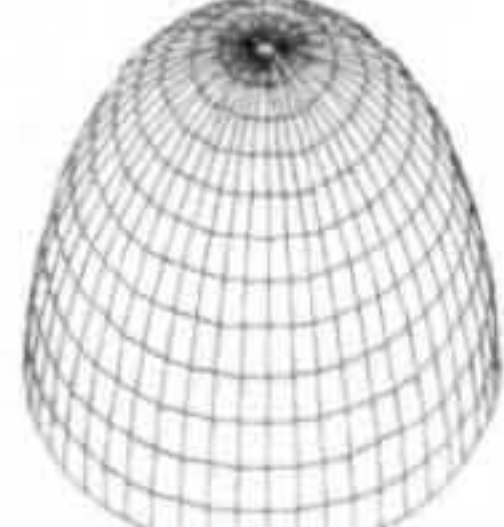
This shade-analysis study verifies that the generated self-shaded and exposed areas and patterns above the tested domed roof geometries slightly differ from one curvature to another curvature according to CCSR. In both seasons, the *SUNCAST* generated images showed that the larger self-shade area throughout the day above the three tested dome forms is recorded in the early morning and the late afternoon periods. In winter, where maximizing the exposed area is desired, *Dome₂* geometry enables to generate 92% exposed area at midday, whereas this ratio is 82% above *Dome₁*, and is 72% above *Dome₃*. The exposed area increases towards midday where it records the maximum ratio in summer and winter.

All tested domes become approximately fully exposed during midday in summer. In winter, where maximizing the exposed area is desired, *Dome₂* geometry enables to generate 92% exposed area at midday, whereas this ratio is 82% above *Dome₁*, and is 72% above *Dome₃*. In day average, the shade-analysis study showed that *Dome₃* ($A=2B$) generates the less exposed area (70.5%) compared to the other dome geometries in summer, which means that *Dome₃* is preferable in summer. Whereas, *Dome₂* records the maximum exposed area in winter (80.7%), which is desired for winter climatic conditions.

8.4 CONCLUSIONS

Using SRSM and IES's *SUNCAST* and *APACHE* applications, this chapter has investigated the solar performance and shade analysis of different dome geometries with comparison to the flat roof. On the day average base, number of tests have showed that domed roofs receive less $I_{(HTCS)}$ compared to that received on flat roof in both summer and winter. This happens in different ratios according to the dome curvature (*CCSR*). Table (8-10) displays the $I_{(HTCS)}$ - values on three domed roofs and their ratios in comparison to the flat ones.

Table 8-10 The Day Average of The Received $I_{(HTCS)}$ on Different Dome Curvatures and Their Ratios To That on The Flat Roof

Domed Roof Geometry		Day Average $I_{(HTCS)}$ W/m ²		$\frac{I_{(HTCS)}_{CCS}}{I_{(HTCS)}_{flat\ roof}}$ %	
		June	Dec.	June	Dec.
A=B	 <i>Dome₁ (A=B)</i>	471	294	71.47	80.54
A<B	 <i>Dome₂ (A=0.5B)</i>	597	340	90.59	93.15
 <i>Flat Roof (A=B=0)</i>		659	365		
A>B	 <i>Dome₃ (A=2B)</i>	348	250	52.80	68.49

All domes and rings $I_{(HTCS)}$ -curves are exactly symmetrical around the midday axis. The maximum received $I_{(HTCS)}$ on the three tested dome geometries are recorded at midday. Apart from a number of rings with tilt angles, the maximum received $I_{(HTCS)}$ at each ring is recorded at midday as well. As expected, the $I_{(HTCS)}$ -values on flat roof are not influenced by the orientation.

The domed roofs often receive more $I_{(HTCS)}$ than the flat roof in the early morning and the late afternoon in both summer and winter. This scenario may appear as an advantage for employing domes in winter where reducing the received $I_{(HTCS)}$ on roof surface is not required. The chapter also pointed out that the dome steeper-profile ($A=2B$) is the most preferable curvature concavity in both summer and winter. Generally, it is concluded that the domed roof form and geometry have great influences on controlling the intensity of the received solar radiation on roof surfaces.

Unlike the vaulted roofs, the orientation has not allowed the tested domes to receive different solar radiation intensities in both seasons. In the previous chapter, the received solar radiation intensity by the same vaulted roof geometry has varied significantly due to the orientation as the same as the curvature CCSR. Whereas, dome curvature and its composed segments face all directions at the same time, which means that the dome geometry has no particular orientation. Thus, the intensity of the received solar radiation by a dome roof has one value at any direction. However, the orientation still has an influence on the total intensity received by the entire domed surface due to its influence on each planar segment $I_{(HTCS)}$.

The shade-analysis study in this chapter verifies that the generated self-shaded and exposed areas and patterns above the tested domed roof geometries slightly differ from one curvature to another curvature according CCSR. In both seasons, the IES generated images showed that the larger self-shade area throughout the day above the three tested dome forms is recorded in the early morning and the late afternoon periods. In winter, where maximizing the exposed area is desired, *Dome₂* geometry enables to generate 92% exposed area at midday, whereas this ratio is 82% above *Dome₁*, and is 72% above *Dome₃*. The exposed area increases towards midday where it records the maximum ratio in summer and winter.

All tested domes become approximately fully exposed during midday in summer. In winter, where maximizing the exposed area is desired, *Dome₂* geometry enables to generate 92% exposed area at midday, whereas this ratio is 82% above *Dome₁*, and is 72% above *Dome₃*. In day average, the shade-analysis study showed that *Dome₃* ($A=2B$) generates the less exposed area (70.5%) compared to the other dome geometries in summer, which means that *Dome₃* is preferable in summer. Whereas, *Dome₂* records the maximum exposed area in winter (80.7%), which is desired for winter climatic conditions.

Finally, both curved-roof forms; vault and dome with their varying curvatures have enabled to reduce the received solar radiation intensity and generate self-shaded areas on their surface with the comparison to the flat roof. Therefore, they can decrease the required energy for cooling in hot climates in order to provide indoor thermal comfort without much reliance on artificial and non-renewable energy resources. Despite their construction materials thermal properties and thickness, traditional curved-roof forms have contributed towards passive indoor thermal comfort environments in hot-arid regions.

In the next chapter, the overall conclusions of this research presented in this thesis are briefly summarised. Chapter 9 validates the different simulation results and the research work general findings. Full-scale investigations are also discussed as proposed further research work and development.

Reference List

1. "SRSM" Solar Radiation Simulation Model for Quick Basic, Exell, R. H. B. Regional Energy Resources Information Centre, Asian Institute of Technology, Bangkok. <http://www.jgsee.kmutt.ac.th/exell/Solar/SolradJS.htm>
2. IES (VE Version 4.1) [Licensed Software University Package]. Integrated Environmental Solutions Ltd. 2001.

CHAPTER 9

CONCLUSIONS, VALIDATION, AND FURTHER DEVELOPMENTS

9. CONCLUSIONS, VALIDATION AND FURTHER DEVELOPMENTS

The research described in this thesis aims to provide sound architectural and scientific bases from which investigations into solar behaviours of traditional curved roof forms and geometries might be undertaken with confidence. The work in this research can be classified into two parts.

Part one (the first 4 chapters) is considered as an approach to this research in which the research problem, objectives and necessity have been described. This part dwelled on energy crisis and the non-renewable energy limited resources and environmental problems in order to form an alert to rethink traditionally for more energy efficient buildings and passive cooling technologies in developing communities with desert and hot climatic conditions.

Part two (the empirical study chapters) represents the main core of this research. It carried out a large number of solar investigations and calculations for the solar radiation intensity received by different roof forms and orientations. Therefore, they have generated different graphical results in order to illustrate the solar behaviour of roofs outer surfaces due to variation in their geometries. This part of the thesis have pointed out that both curved-roof forms (*vault and dome*) facilitate a significant decrease in the received solar radiation intensity above roof outer-surface.

In this chapter the findings of the theoretical and empirical analyses are brought together so that they could be compared in a constructive approach for further related research and development. The main conclusions of the research are briefly summarised in this chapter. It also presents the research validation and novelty aspects.

9.1 TRADITIONAL PASSIVE COOLING TECHNIQUES AND THE NEED FOR ENERGY EFFICIENT CONTEMPORARY ARCHITECTURE

The need of energy efficient buildings due to over population and the demand of energy and resources high demands are discussed in Chapter 2. The research study-geographical latitudes are 20°-30°N the equator. Passive cooling strategies are essential in order to avoid overheating in hot regions. In this context, Chapter 3 has reviewed a number of passive cooling principles, which have been applied through different traditional techniques.

The review of a number of existing architectural examples that have successfully employed passive cooling techniques in different parts of the developing world with hot climatic conditions is presented in Chapter 4. These techniques showed a successful performance for providing indoor thermal comfort in buildings in hot-arid regions. However, some designers in a number of such regions still consider employing traditional passive cooling techniques to provide indoor thermal comfort is not of significance.

9.1.1 Architectural Proposals of The Tested Curved Roofs Different Building Types

In the last few years, it has become increasingly evident that traditional techniques for passive cooling and heating are widely used around different parts of the world in order to provide indoor thermal comfort. Moreover, as a result of being demanded for a diverse range of new applications, traditional techniques are being applied in the developed world for both passive cooling and heating and have become compatible with advanced technologies and new construction materials.

Curved roofs (*vaults and domes*) are architectural identity elements, which were cited to have sound and strong link with the cultural, climatic and environmental features of the desert communities in general and southern parts of Egypt in particular. On the other hand, solar radiation is believed to be the main cause of overheating in such climatic regions. Roofs are the most exposed building element to sun's heat. In this context, the research has selected the roof form and geometry to find out their influences on the received solar radiation intensity above roofs outer surfaces.

These simulated curved-roof forms, curvatures and orientations have proved effective solar performance in term of controlling the received solar radiation intensities above roofs in summer and winter. However, the architectural applications of these curved-roof forms, curvatures and orientations must suit the building type and its inner-space functions. These forms may also have solar disadvantages, which can be overcome by architectural solution. This section discusses the architectural potential of different curved-roofs applications for both architectural masses and building types in hot arid regions.

9.1.1.1 Different Architectural Masses and Compositions

Traditional curved forms (Vaulted and domed) can be used for roofing any simple, complex, regular, or irregular architectural masses and compositions. Vault and dome can be employed above roofs as single elements or combined. The roofing system of an architectural mass could be constructed from a number of vaults, domes, or a composition of vaults and domes together.

1. Simple Architectural Masses (Single rooms - *Single inner-spaces*)

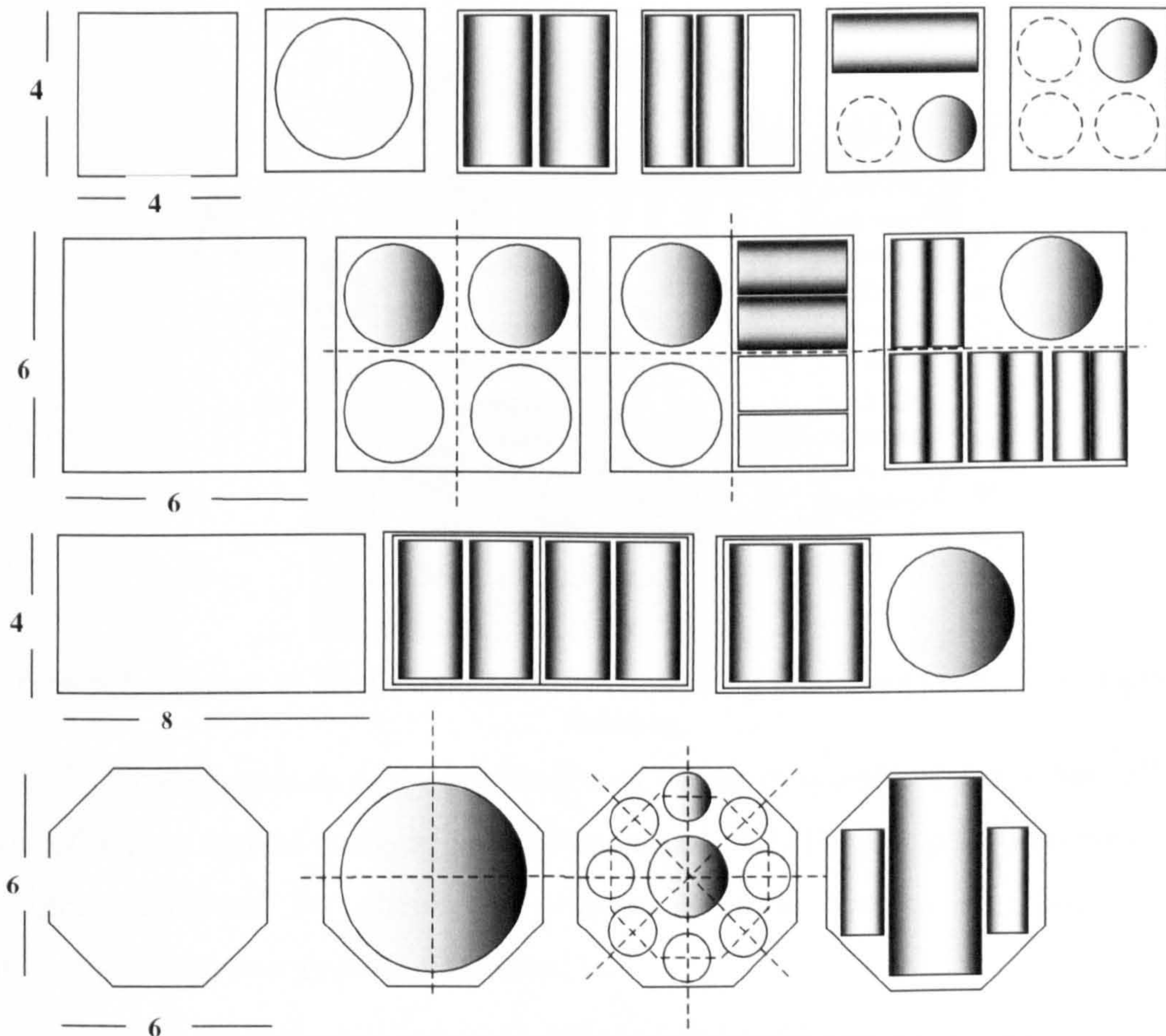


Figure 9-1 Diagram Illustrating Different Ways of Combing Vaults and Domes on Principle Single Spaces

2. Composite Architectural Masses (Combined Simple inner-spaces)

The mixing between different vault orientations may be due to the change in the inner space function and purposes and due to the preferred curvature or orientation for achieving a higher comfort level for the occupants. Fig. (9-2) shows a regular composition of vaults and domes that can be used in the design of single storey houses, nurseries or multicultural centres, with a central courtyard, that can be used for higher levels of sun shading, orientation, privacy and natural ventilation.

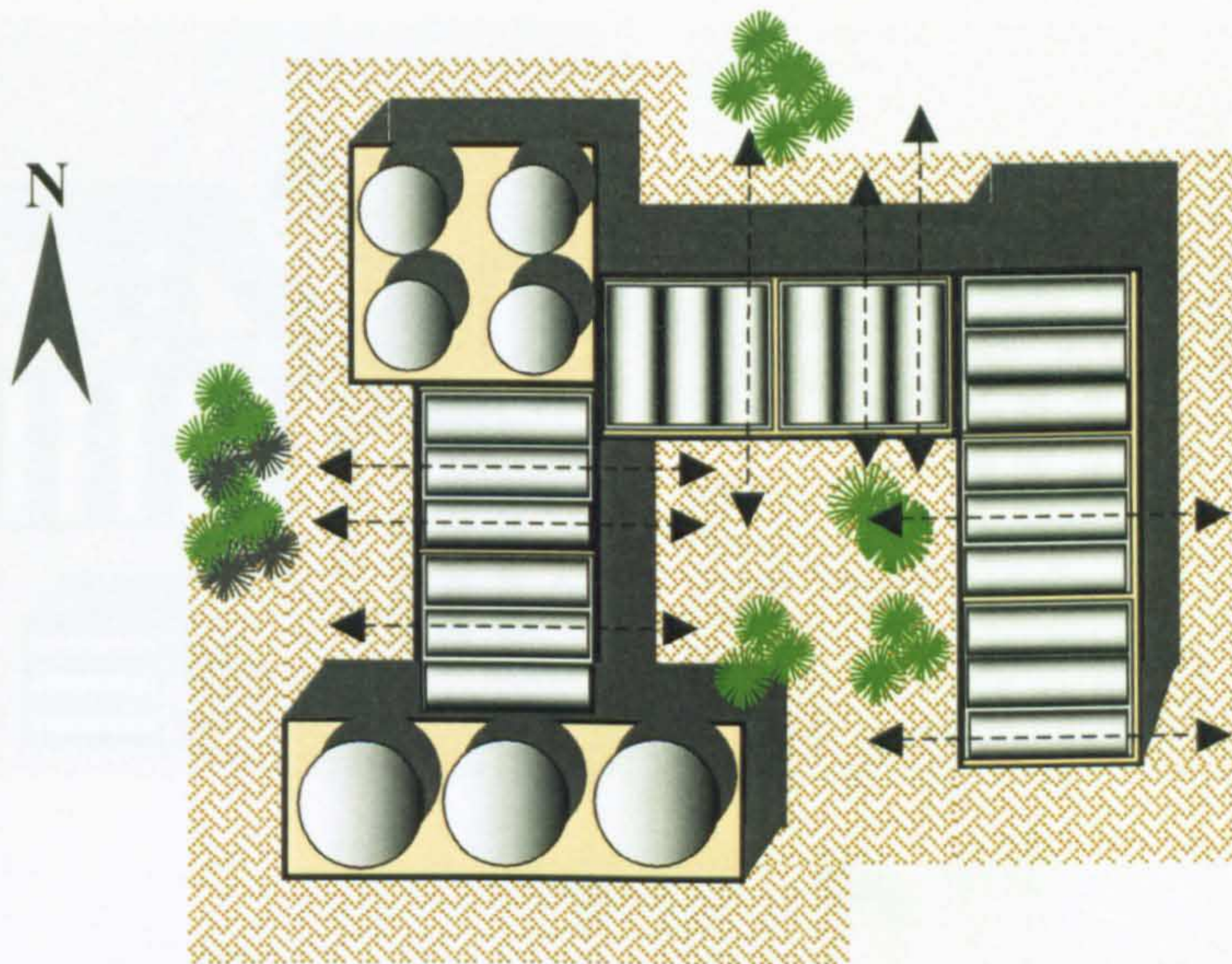


Figure 9-2 A Layout of The Possible Use of Composite of Vaults and Domes in a Single Storey Building

Fig. (9-3) shows proposals of the application of domes in social housing, where all different rooms of houses may be designed as a whole curved roof. These applications have proven to be highly attractive for clients in different projects because of their architectural characteristics and energy saving abilities [1].

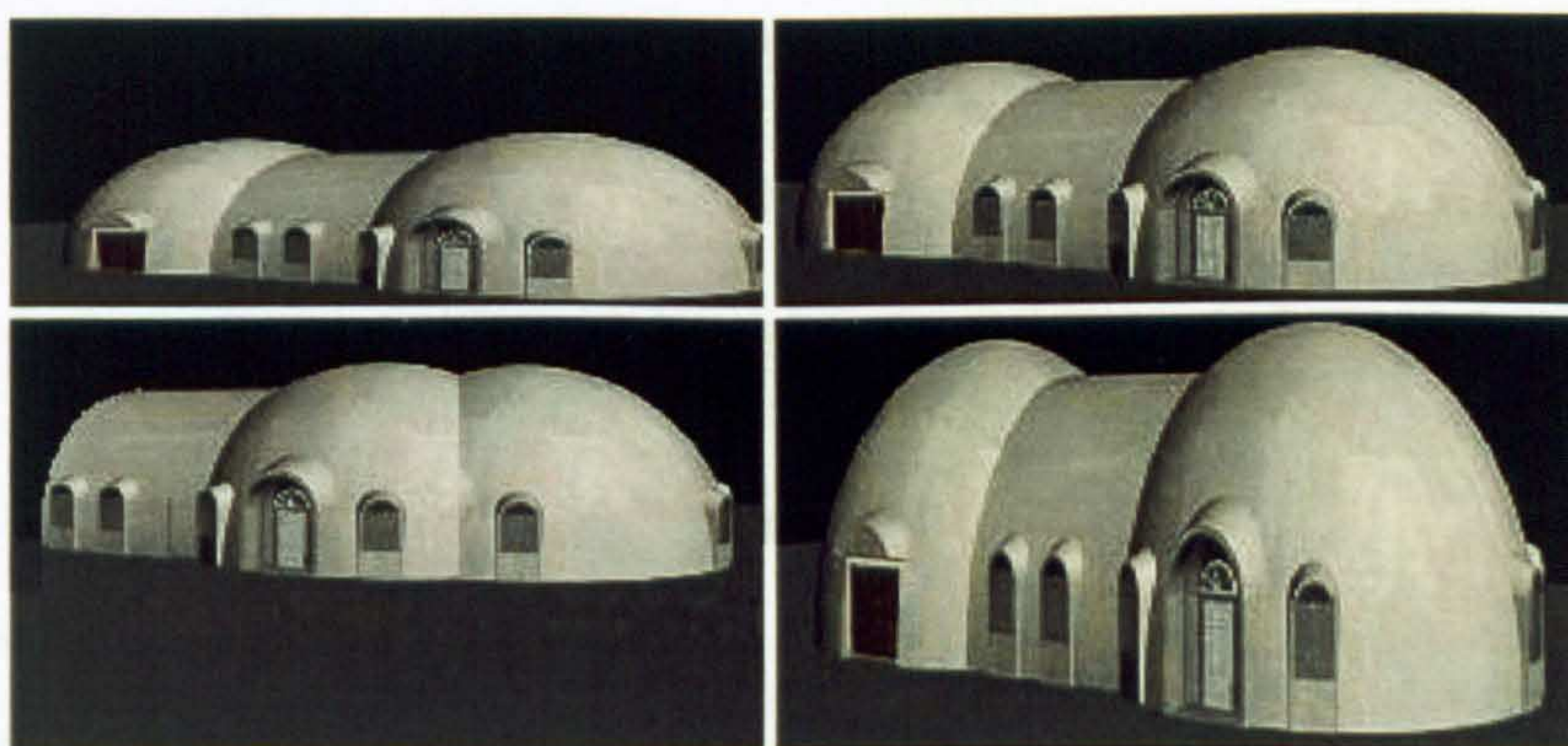


Figure 9-3 Different Proposals of a Domed House

3. Irregular Architectural Masses (*Large and Complex inner-spaces*)

An irregular architectural mass covered with different curved-roof forms (vaults and domes) is shown in Fig. (9-4); the vaults can have the same or different orientation. These and other ideas can all be applied in different architectural projects, after undergoing a climatic study of the site and its orientation. Proper curvatures design of domes and vaults (height-to-span-ratio) should be chosen according to their solar and thermal behaviours as the previous parametric studies in this thesis proved. However looking at their aesthetic values and function suitability are very important.

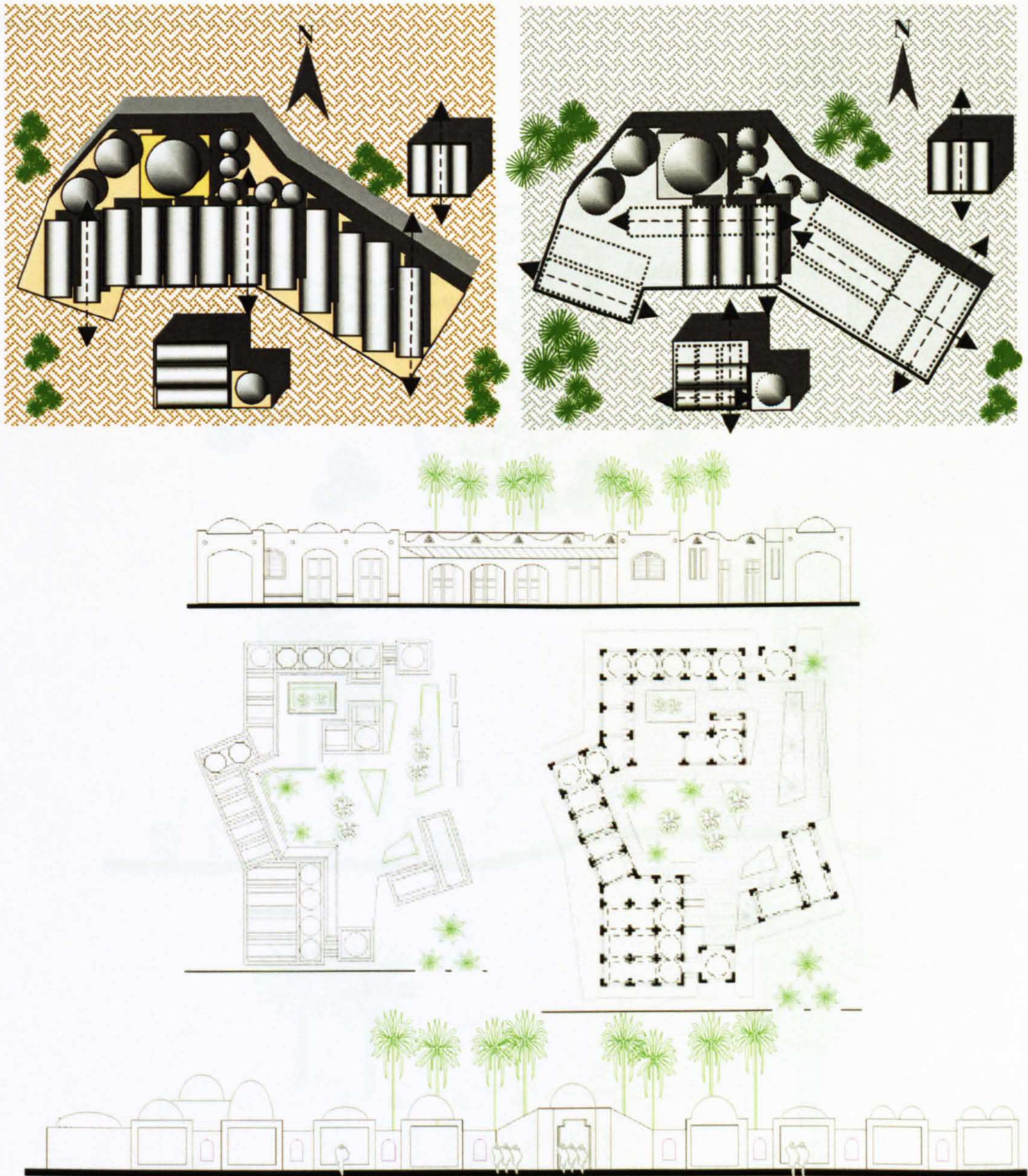


Figure 9-4 Composition, Orientation and Curvatures of Curved Roofs in Architectural Applications (*Layout, Plans And Elevations*)

4. Organic and Curvilinear Forms

The choice of organic forms and design in architecture is sometimes needed for projects with special needs, construction materials and climatic conditions. Such designs end up with very attractive forms and exciting internal spaces for both clients and occupants. Domes and vaults are highly successful for roofing such spaces in many aspects.

Community's nurseries, preschools, primary schools and multipurpose halls, or environmental and nature exhibitions can be designed employing such organic forms and construction material construction.

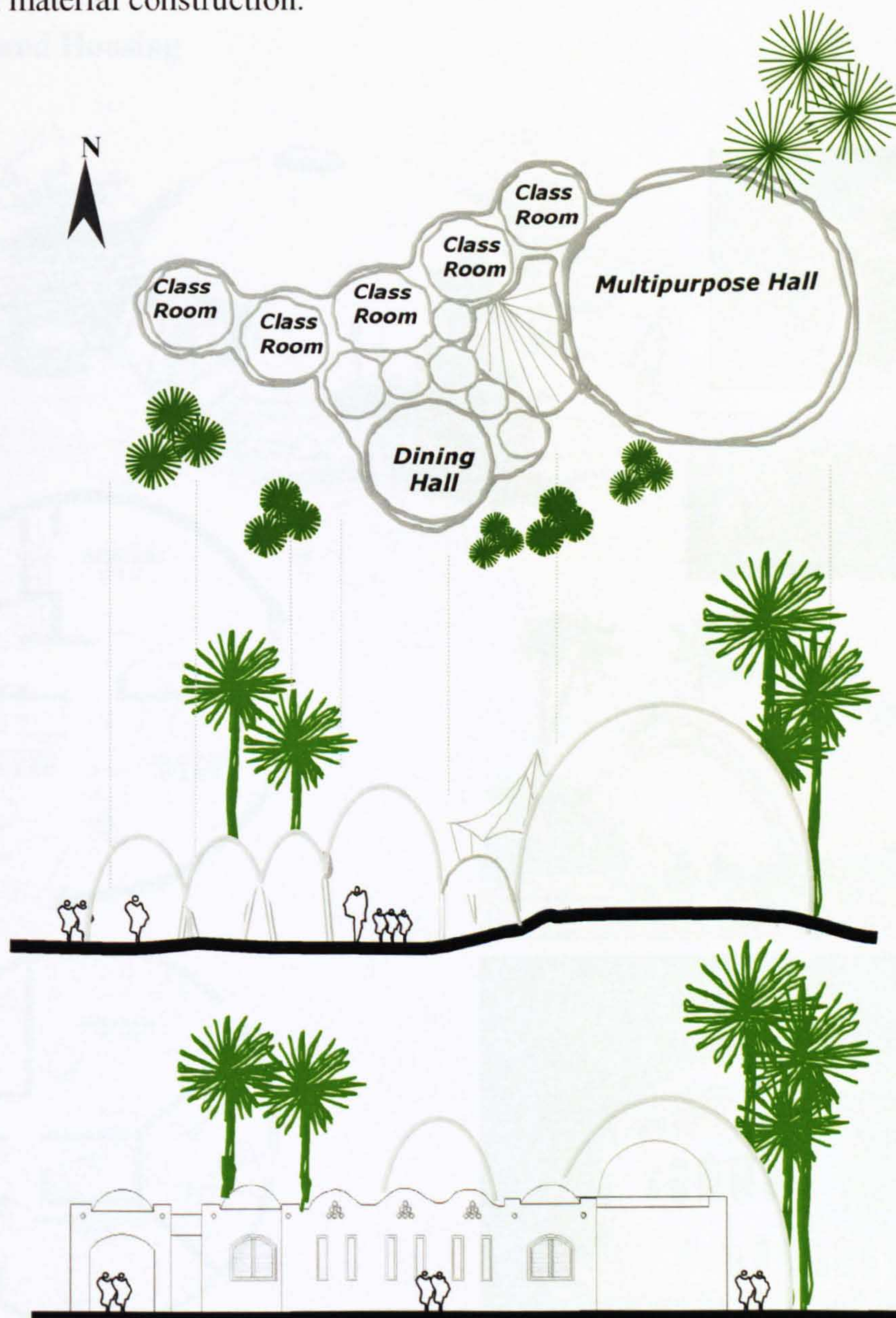


Figure 9-5 Plan, Section and Elevation of an Architectural Proposal for a Nursery, Primary School, or Multicultural Community Centre

9.1.1.2 Different Building Types (*Inner-Spaces Functional Suitability*)

The research has investigated the solar performance of several curved-roof forms and curvatures (height-to-span-ratio), some of these curvatures can suit particular building types and functions, according to the orientation of the site and the inclination angle of the curved surface according to the quantitative study performed earlier in this research. This section discusses the relationship between the curved-roof geometry (Curvature and orientation) and the function of a particular architectural space. The following parts discuss some of the building types, which can be covered and designed using domes and curved roofs.

i. Domestic and Housing

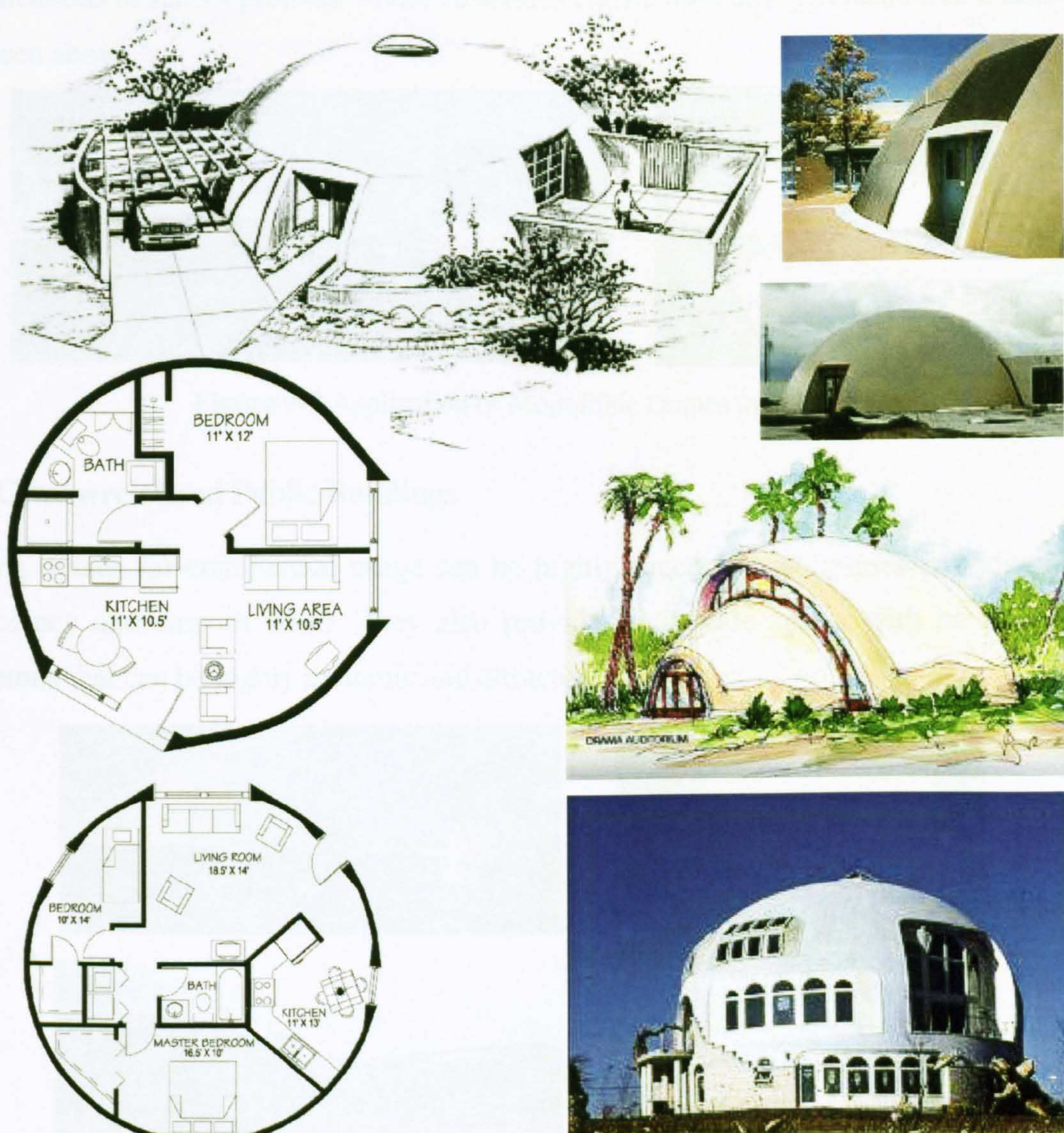


Figure 9-6 Modern Applications of Domed Domestic Housing

Fig. (9-7) shows different applications of monolithic domes [2], which have been designed by David B. South, the president of the Monolithic Dome Institute, and his brothers. They developed an efficient method for building a strong dome using a continuous spray-in-place process. In 1976, after years of planning and development they built the first Monolithic Dome in Shelley, Idaho. In 1979, the first patent was awarded for the Monolithic Dome construction process. Such ideas will allow concrete domes to be built from 100 to 300 meters in diameter. These huge structures are ideal for indoor sports facilities and stadiums.

ii. Schools

Fig. (9-7) shows another application of curved-roofs and domes for different architectural applications in school projects. These structures can be used as a gymnasium or a school pod as seen above.



Figure 9-7 Application of Monolithic Domes in Schools [2]

iii. Commercial and Public Buildings

Using domes for commercial usage can be highly successful as besides providing energy efficiency and ease of build. They also provide clear wide spans, with no intermediate columns that can be highly aesthetic and attractive.

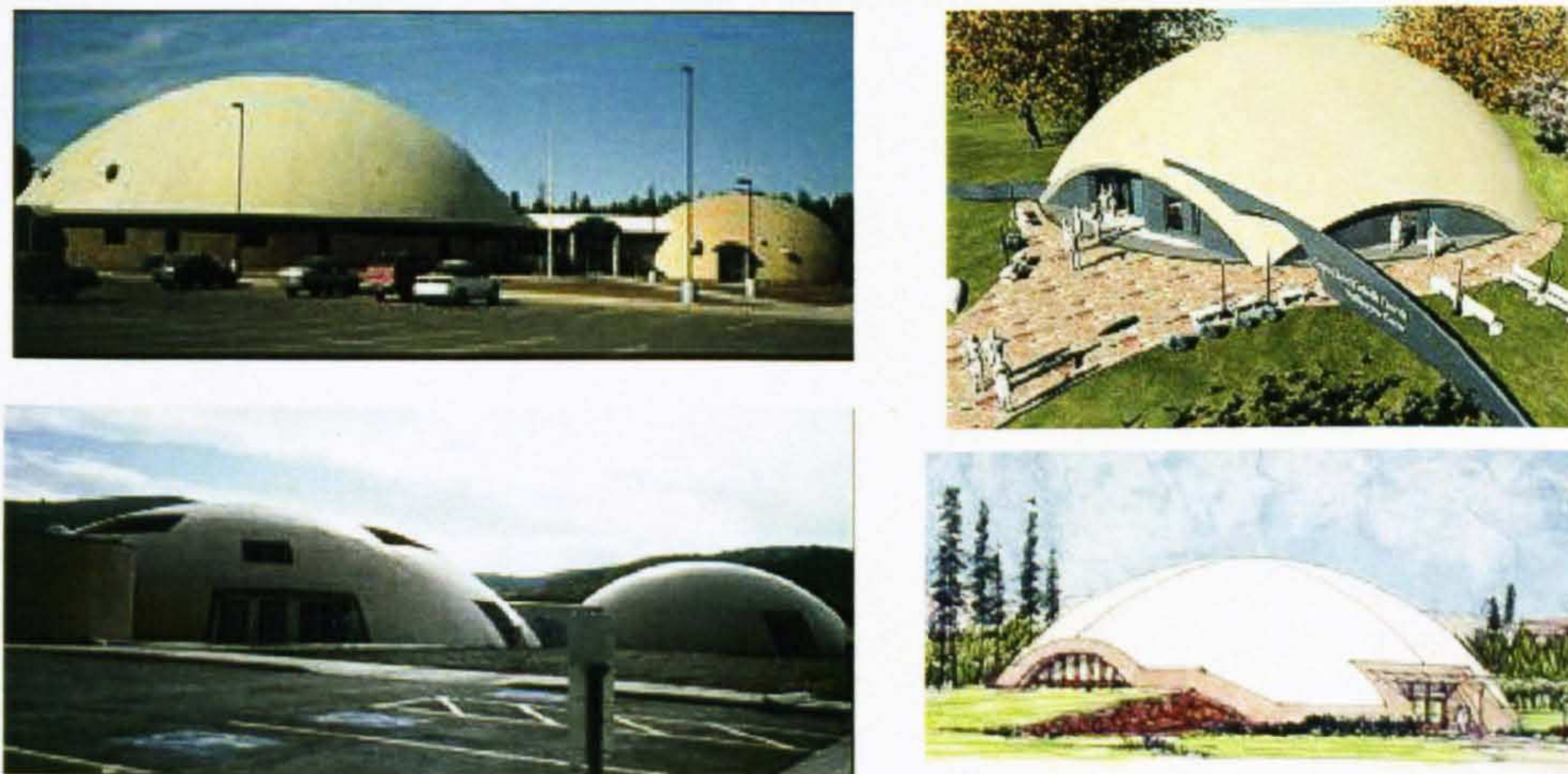


Figure 9-8: Curved-roofs in Commercial and Public Buildings [2]

iv. Churches and Mosques

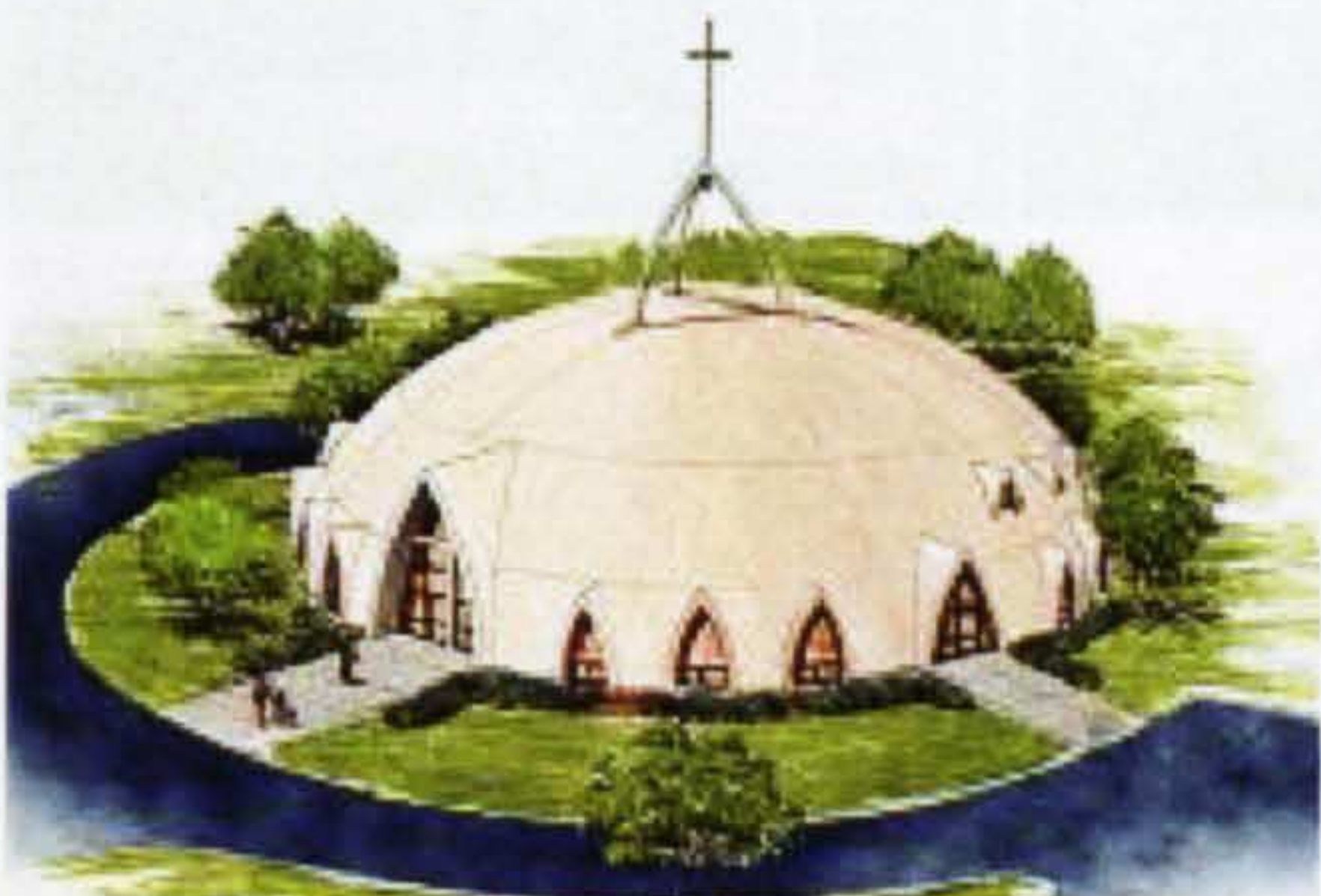
The use of vault, domes and curved surfaces in religious buildings has been in the architectural practice for centuries now. Besides its aesthetic properties, it has always achieved better comfort levels for their occupants. Most of ancient churches and mosques we find that the thing that all of them has in common is the dome. Successful examples are the Mohamed Ali Mosque in Cairo, Pantheon in Rome, St. Paul's Cathedral in London, the Hagia Sofia in Istanbul and many others. Spacious and spectacular domes provide near-absolute free span, without internal columns for support, attractive interiors with the feeling of the sky top as well as energy efficiency.



Qabba Mosque, Saudi Arabia



Tengku Tengah Zaharah Mosque, Malaysia



Church, USA



Qornish Mosque, Saudi Arabia

Figure 9-9 Domes and Vaults in Mosques and Churches

v. Multipurpose and Sport Halls

The application of domes in sport halls and multipurpose applications is one of the most common applications since roman amphitheatre. It provides a structural efficient space where people can meet and practice different sports without any intermediate obstacles, in wide span and free-standing enclosures.

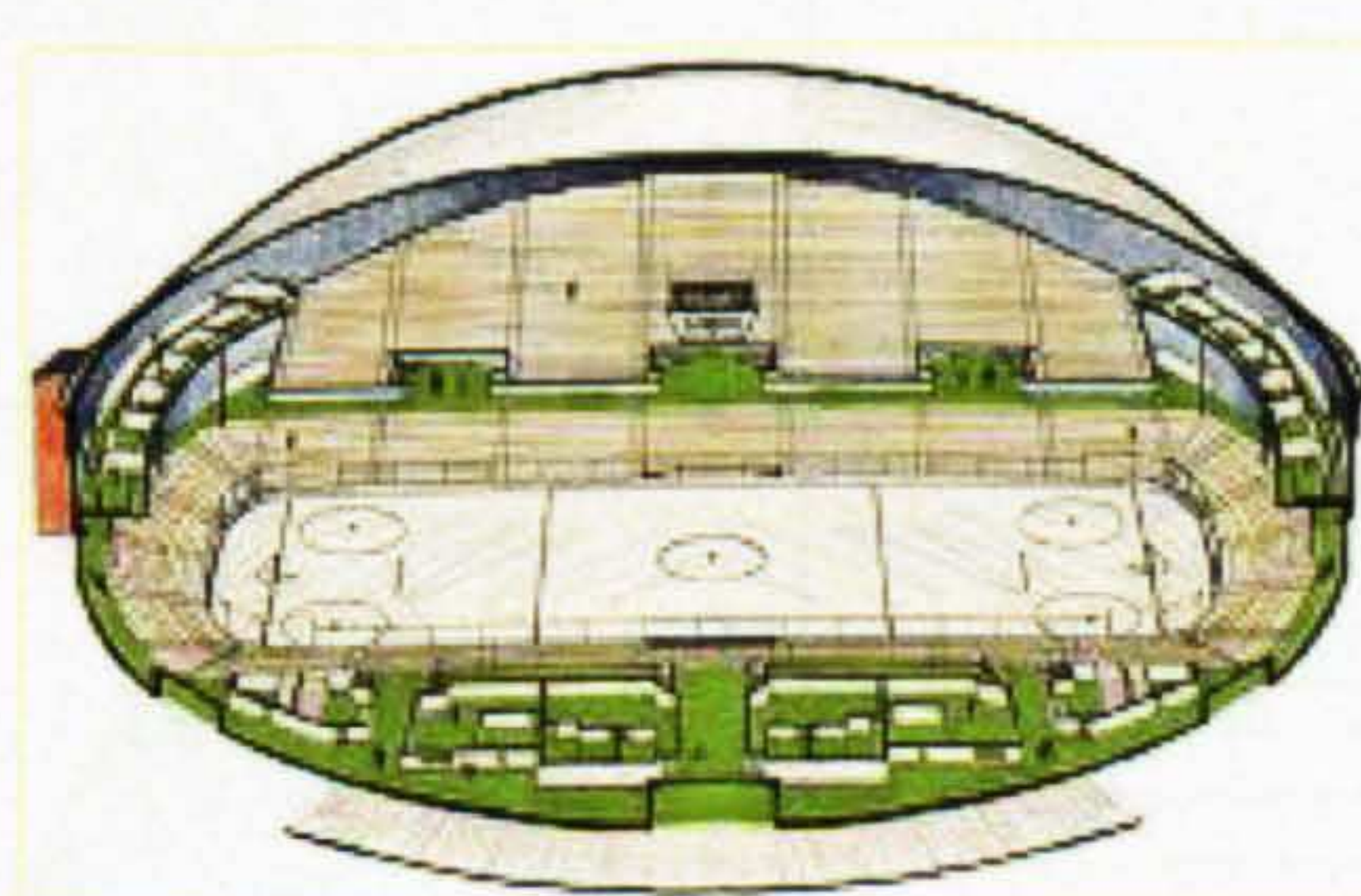
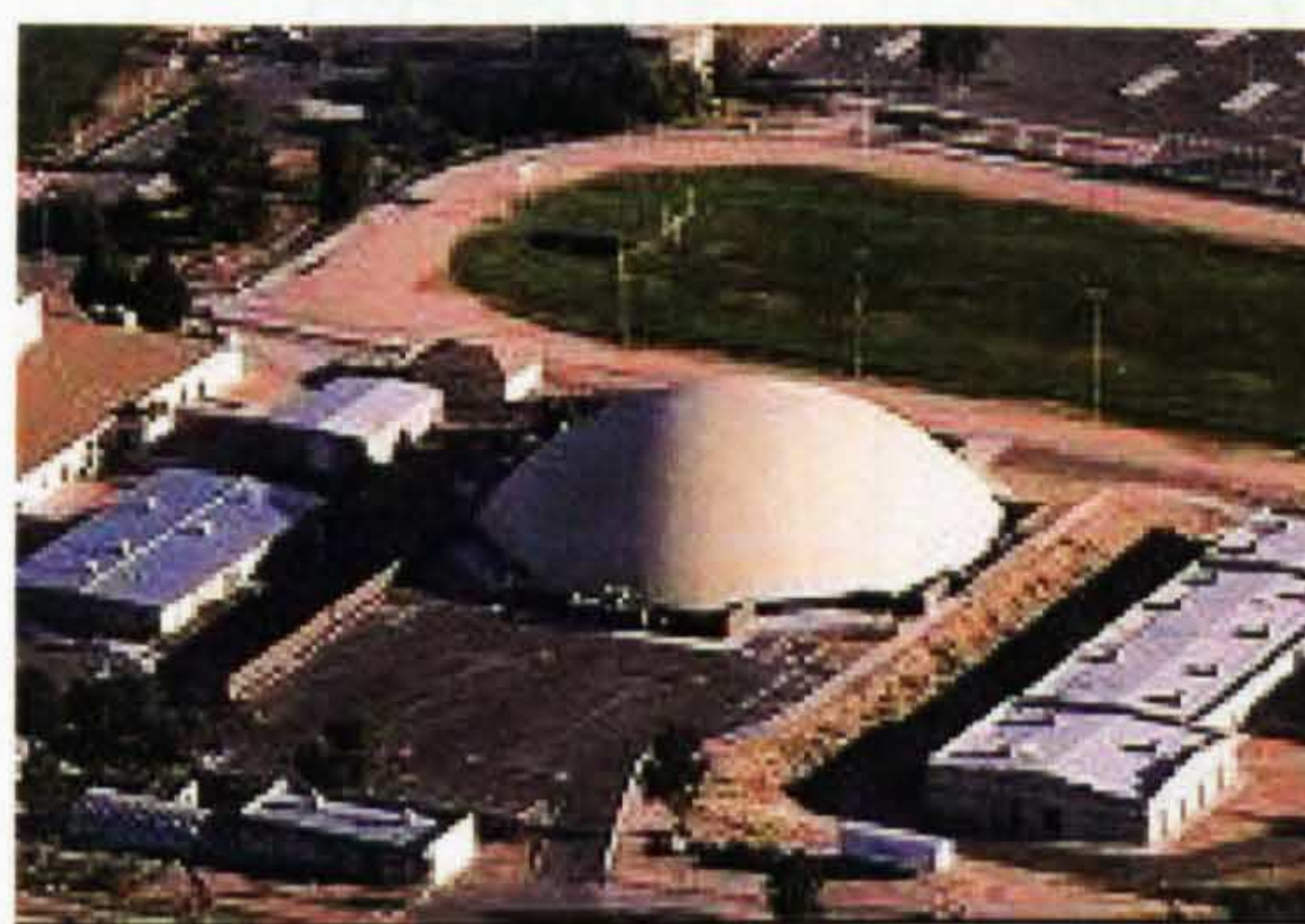
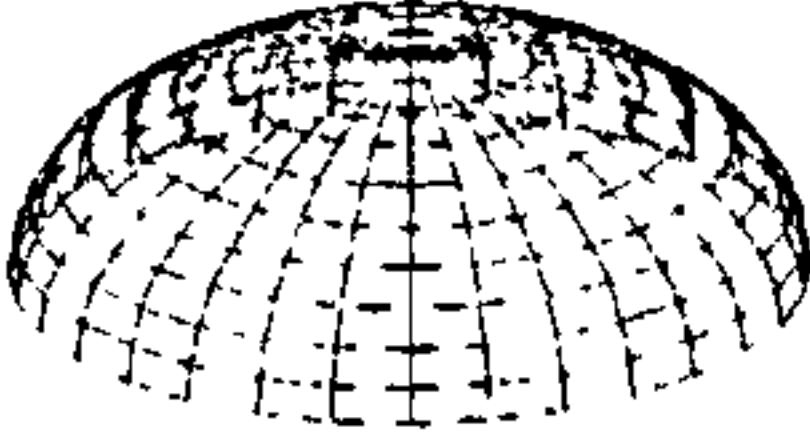
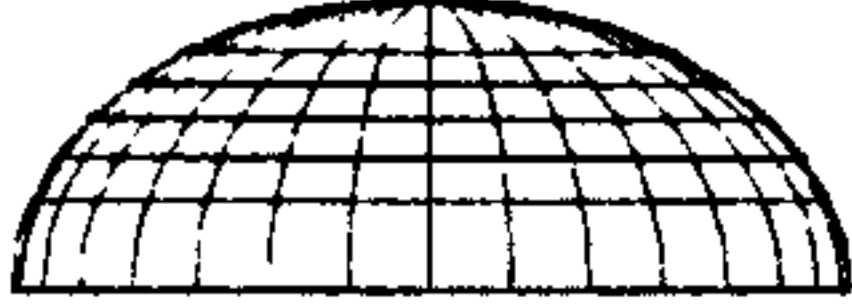
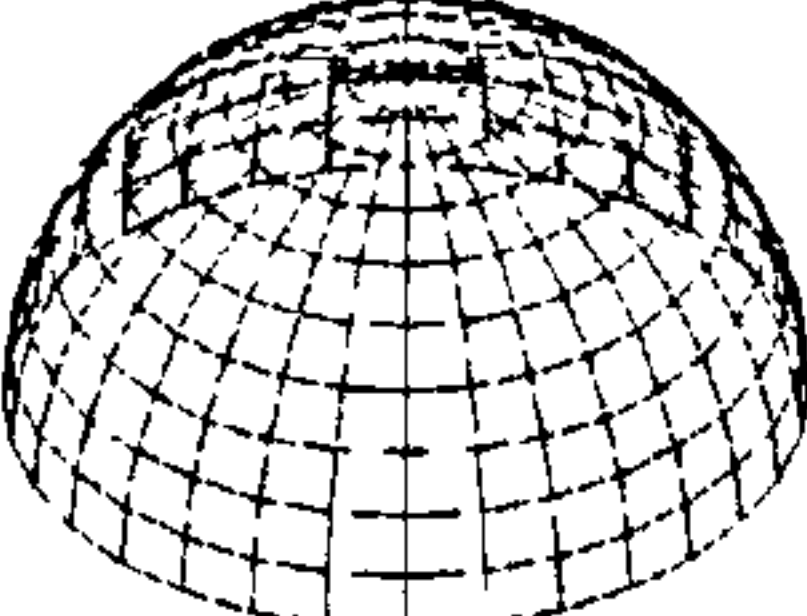
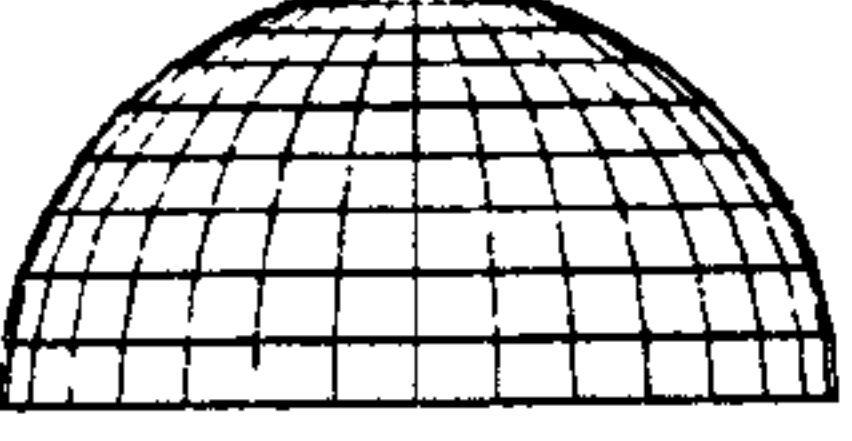
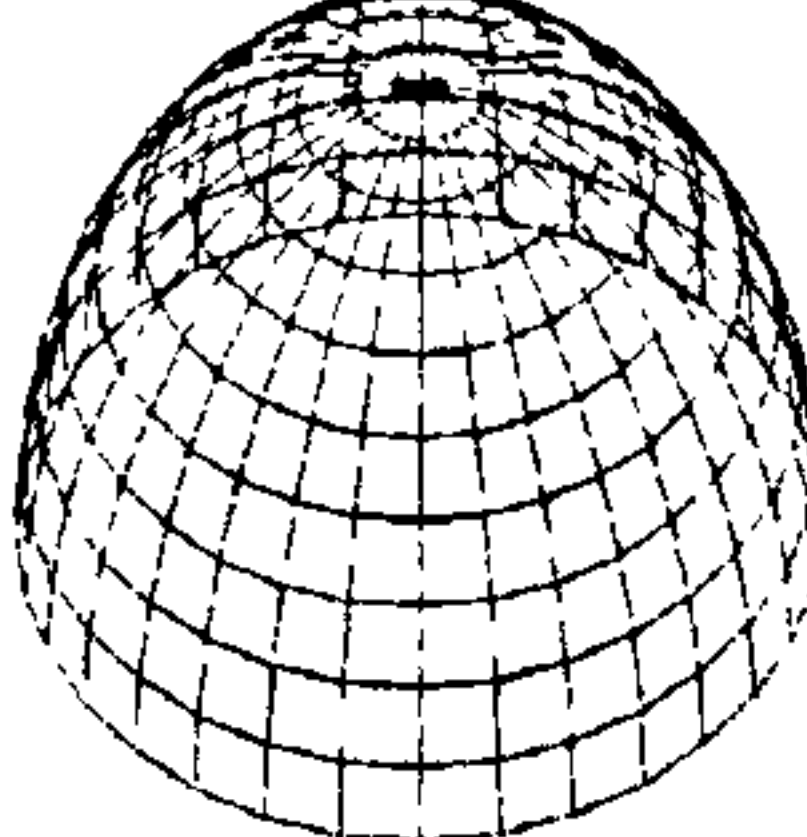
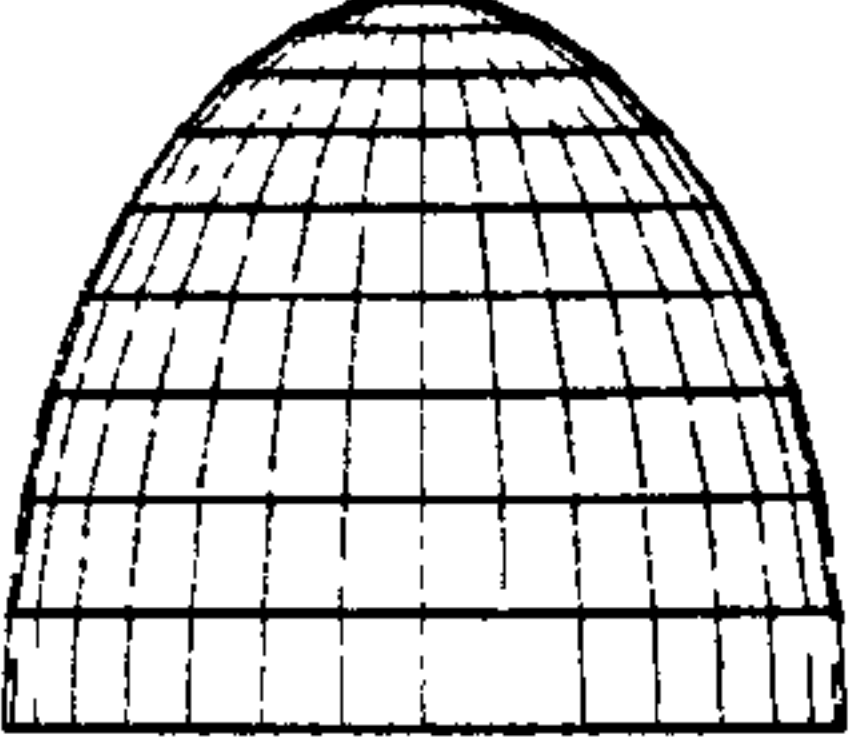


Figure 9-10 Domes for Multipurpose and Sports Halls[2]

Table (9-1) shows the main geometric profiles (Curvatures) of curved roofs, which may be employed into architectural design to build domes and vaults. These forms shapes are shown individually. They can be intersected with each other to provide many additional combinations as explained previously in this chapter.

Table 9-1 Curved- roofs Main Geometric Profiles (Curvatures) and Their Architectural Proposals

Inner Space Functions Suitability	Perspective	Side-View
<p>Low profile Curved Roofs: This is the most efficient shape to cover the greatest amount of floor space. It is useful for both large and small domes. Also it can be used for indoor swimming pools, shelters, military and air force planes shelters.</p>		
<p>Hemispherical and Semicircular Vaulted Roofs: Surface area is double the floor area. Useful for high volume buildings, like, sport halls and circus halls. Also for lecturer rooms and theatres. This curved-form can be suitable for smaller buildings like homes.</p>		
<p>High profile Curved Roofs: The most volume for the least floor area. Water tanks, storage buildings, multipurpose and sport halls, unique looking homes and ideal for theatres and large public buildings. Also useful for bulk storage. It is very tall versus its floor area.</p>		

9.2 SOLAR RADIATION INTENSITY AND THE RECEIVER SURFACE GEOMETRY

Chapter 5 searched the theory that stands behind different solar calculations on horizontal and sloped surfaces. These equations and their continuous developments are believed to be fundamental for any computing models that handle the topic of solar radiation on tilted surfaces. Muneer [3] stated that there are equations that enables the computation of monthly or daily sloped irradiation on vertical surfaces with eastern, western and northern aspects and any sloping surface facing south, based on the previous work done in this field [3]. The work done by Muneer [3] drew the attention of the author of this thesis that these equations were designed to test sloped surfaces solar radiation for particular latitudes. Thus, a thorough research was done to find a computer model that is especially designed for calculating the solar radiation on sloped surfaces in the tropics.

In addition to these fundamental reference books, Chapter 5 has also reviewed other published work, which has differently applied the idea of slope irradiation. These researches have calculated the received solar radiation intensity above tilted and different oriented surfaces using the same equations.

Stasinopoulos (1998 & 1999) [4] investigated different types of solar behaviours of oblique surfaces and have also tested the relationship between the form and insolation. Laouadi and Atif (1998 & 2001) [5-7] research has tested the solar performances of transparent domed skylights. The research presented in this thesis concerns only about the intensity of the received solar radiation above the outer-surface of curved roofs with the comparison to that received on flat roof outer-surface.

The research undertaken in this thesis has specifically developed geometrical resemblance implementations along different curved-roof forms. The proposed geometrical resemblance methodology in this thesis is inspired from the CAD drawing tools and software. Customary in CAD tools, most curved forms have been geometrically resembled by group of planar segments, pixels, or stripes. This technique is often employed in two and three-dimensional CAD drawings.

The different curved-roof forms and curvatures have been identified by their cross section ratio, span-to-height-ratio, $A: B$, which has three possible cases, $A=B$, $A>B$, or $A<B$. The solar performance of seven-curved roof cross sections (CCS_{1-7}) have been tested in Chapter 7. Dome as one of the curved-roof traditional forms has also been geometrically resembled by the same concept using different implementation to suit the dome form. The dome surface has been geometrically resembled by groups of planar segments, which constitute the dome rings. As explained previously in Chapter 8, each ring is formed by 24 planar segments, which have different orientations and the same slope angles.

9.3 VALIDATION OF RESEARCH TOOLS

This part discusses other solar and thermal investigations carried out using the ECOTECH and IES (*APACHE*) respectively. However, a self-shaded investigation on different domed-roof curvatures has been undertaken in Chapter 8 using the computer simulation tools (IES). The investigations carried out by other computer simulation tools aim to validate further the SRSM results. They also show different ways and techniques for testing solar and indoor thermal performances of curved-roof geometries.

9.3.1 Self-Shaded Areas on Domed Roof Surfaces

This study analysed the self-shaded and the exposed patterns and ratios above three dome geometries ($A=B$, $A<B$, and $A>B$ respectively). The study verifies that curved-roof curvature has great effect on curved-roofs self-shading quality. The findings of this study have completed the explanation of curved-roof geometrical abilities to reduce the received solar radiation intensity above roofs in hot-rid climates. Briefly, the generated self-shaded and exposed areas and patterns above the tested domed roof geometries slightly differ from one curvature to another according CCSR

The study has been carried out using the IES software package (*Integrated Environmental Solutions*) (EV 4.1). The IES's *SUNCAST* [8] application has been employed to find out the patterns of the exposed and the self-shaded areas and segments above the three dome geometries every 2 hours in summer and winter. The patterns ratios have been generated by *APACHE* [8].

In both seasons, the IES generated images showed that the larger self-shaded area throughout the day above the three tested dome forms was recorded in the early morning and the late afternoon periods. In winter, where maximizing the exposed area is desired, *Dome₂* geometry enables to generate 92% exposed area at midday, whereas this ratio is 82% above *Dome₁*, and is 72% above *Dome₃*. The exposed area increases towards midday where it records the maximum ratio in summer and winter.

In day average, the shade-analysis study showed that *Dome₃* ($A=2B$) generates the less exposed area (70.5%) compared to the other dome geometries in summer, which means that *Dome₃* is preferable in summer. Whereas, *Dome₂* records the maximum exposed area in winter (80.7%), which is desired for cooler climatic conditions.

Both curved-roof forms; vault and dome with their varying curvatures have enabled to reduce the received solar radiation intensity and generate self-shaded areas on their surface with the comparison to the flat roof. Therefore, they can decrease the required energy for cooling in hot climates in order to provide indoor thermal comfort without much reliance on artificial and non-renewable energy resources.

Moreover to the advantages achieved by their use of local construction materials (*mud and adobe*) thermal properties and thickness, traditional curved-roof forms have contributed towards passive indoor thermal comfort environments in hot-arid regions. It also became apparent that the angular nature of the curved roof planar segments could significantly affect the thermal conditions within the spaces they cover.

9.3.2 ECOTECH Solar Radiation Intensity Modelling

ECOTECH [9] is a 3D modelling interface fully integrated with acoustic, thermal, lighting and solar calculations software. ECOTECH v5.01 and v5.20 have been used to calculate solar radiation intensities on semicircular dome and flat roof has been carried out using the ECOTECH “Solar Exposure Application” [3].

ECOTEECT results validate the previous research results, which have been generated by the SRSM in Chapters 6,7,and 8. The ECOTEECT “Solar Exposure Application” proved that the received solar radiation intensities differ significantly according to the receiver surface form (*Flat, Curved, Dome, etc...*). According to the available climatic data profiles of ECOTEECT, “Al-Riyadh 24.60°N” climatic data was used, being similar to the conditions of Aswan 23.58°N. This section reviews some information about the ECOTEECT v5.01 & v5.20 [4].

ECOTEECT enables to calculate the incident solar radiation on any surface and its percentage shading. This section illustrates number of the solar tests for Flat and dome roof forms. “Solar-exposure” study is one of the ECOTEECT thermal analysis applications. In order to eliminate the effect of construction material thermal properties and U values, both geometries have been tested employing the same construction material and roof layer components (Standard).

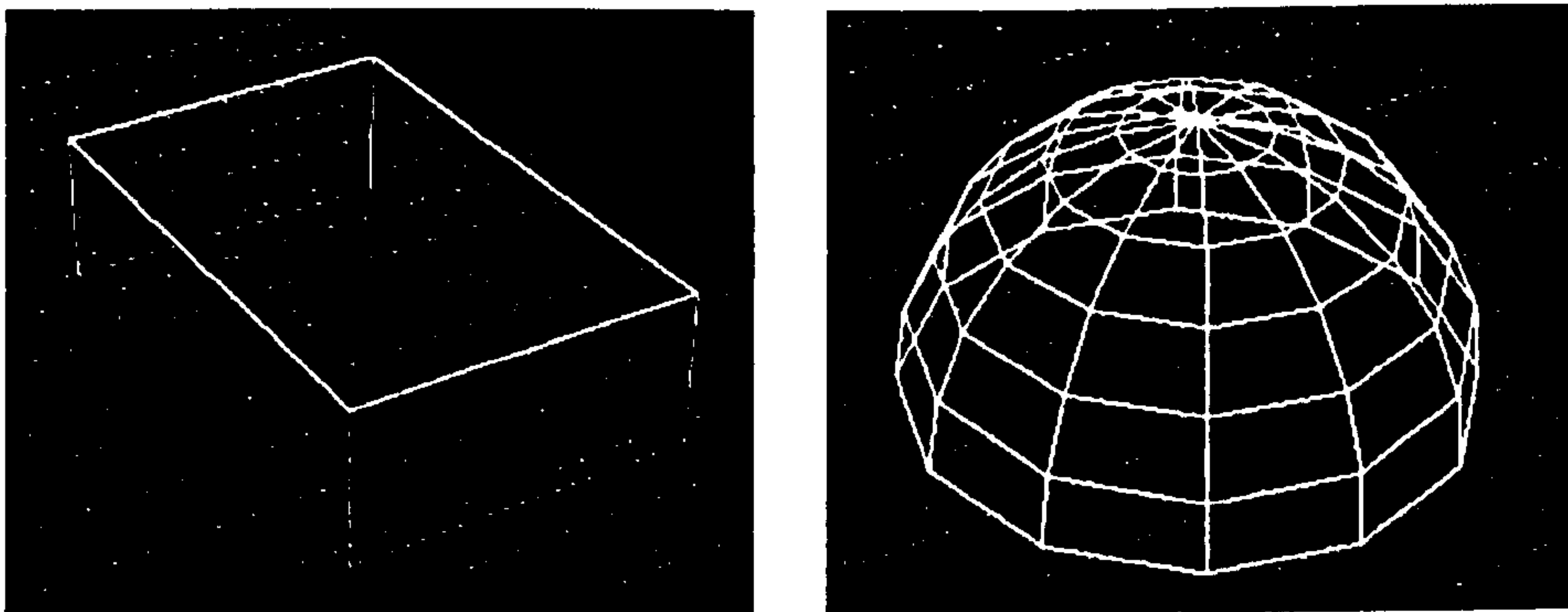


Figure 9-11 Geometrical Models For ECOTEECT Solar Tests

9.3.2.1 Solar Radiation Intensity on Flat Roof

The solar exposure study has to be carried out for each segment along the domed roof form separately and object by object, where each object has different orientation and slope angle (*Azi. and Alt. As sown the outputs data file*). Therefore, computing the average of all segments calculations for finding out the received solar radiation above the entire surface of the dome roof. The *ECOTECT v5.01* slides in Fig. (9-12) show Object no.5 (Flat Roof) calculations and monthly (*day-average*) solar intensities distributions.

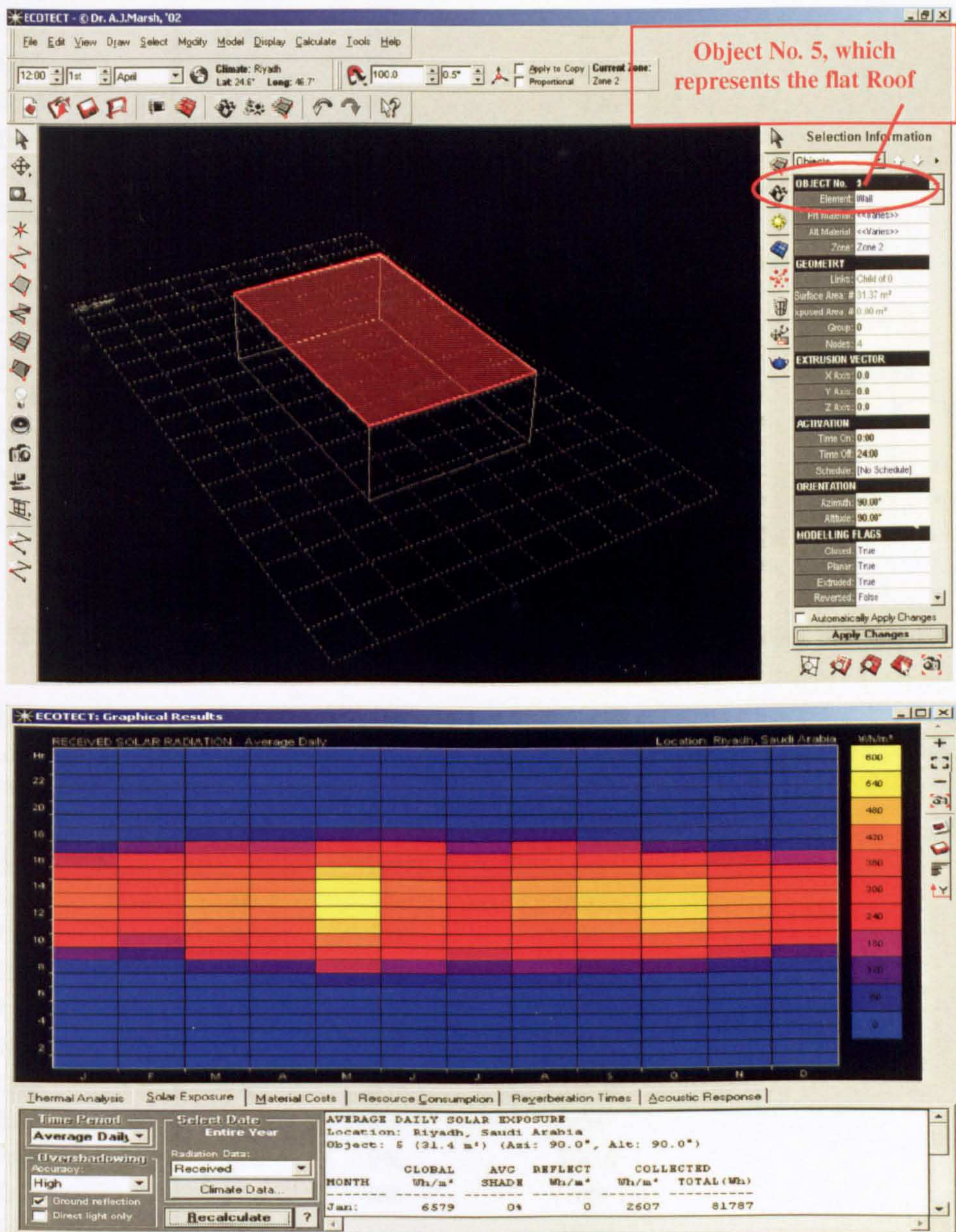


Figure 9-12 ECOECT Solar Intensity Distribution

The following tables display the calculated results of solar radiation intensity (W/m^2) received on flat roof in summer and winter respectively.

Table 9-2 Solar Radiation Intensity (W/m^2) Received on Flat Roof in *Summer*

HOURLY SOLAR CALCULATIONS (FLAT ROOF)

Location: Riyadh, Saudi Arabia

Date: 15th June

HOURLY	*SUN ANGLE	SOLAR SHADE	Received (W/m^2)
06:00	79.2	0%	90
07:00	66.2	0%	295
08:00	53.0	0%	578
09:00	39.5	0%	798
10:00	25.9	0%	980
11:00	12.3	0%	1056
12:00	2.0	0%	1100
13:00	15.3	0%	1056
14:00	28.9	0%	980
15:00	42.4	0%	798
16:00	55.9	0%	578
17:00	69.1	0%	295
18:00	81.9	0%	90
TOTALS			8694
AVERAGE			668.78

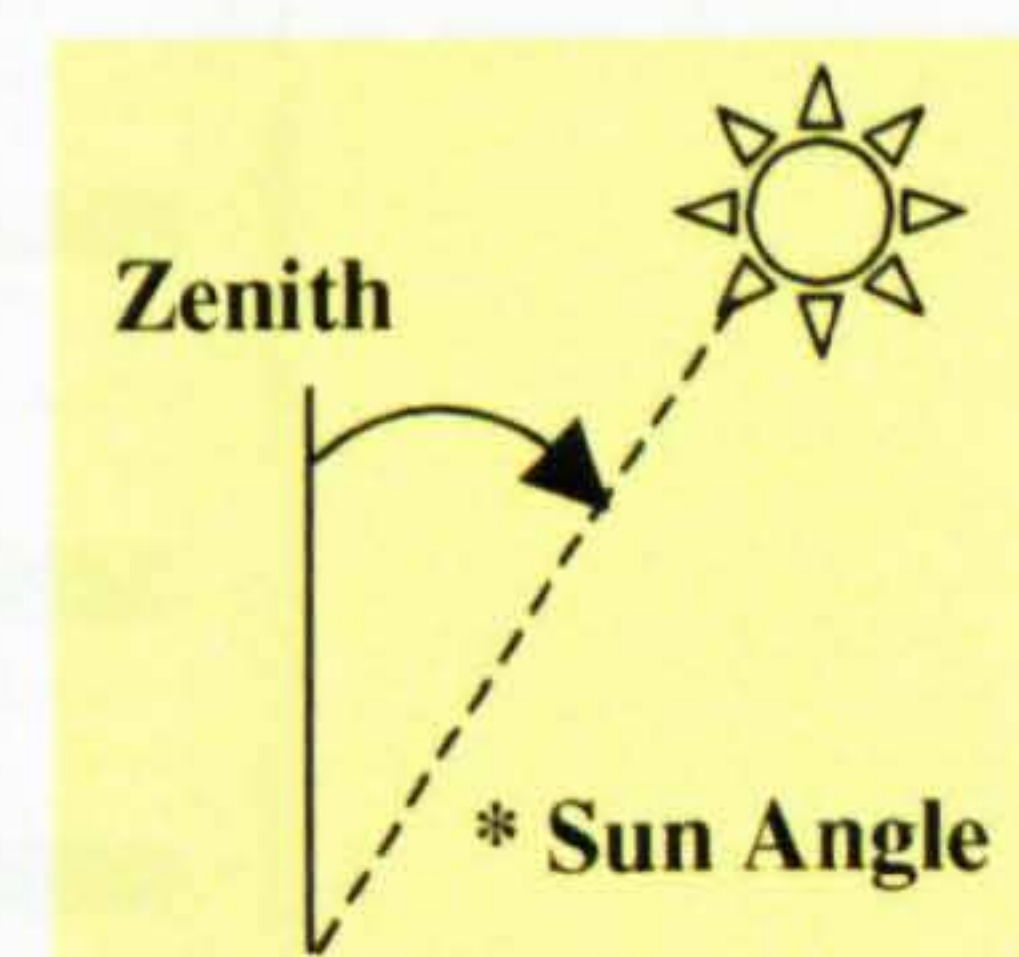


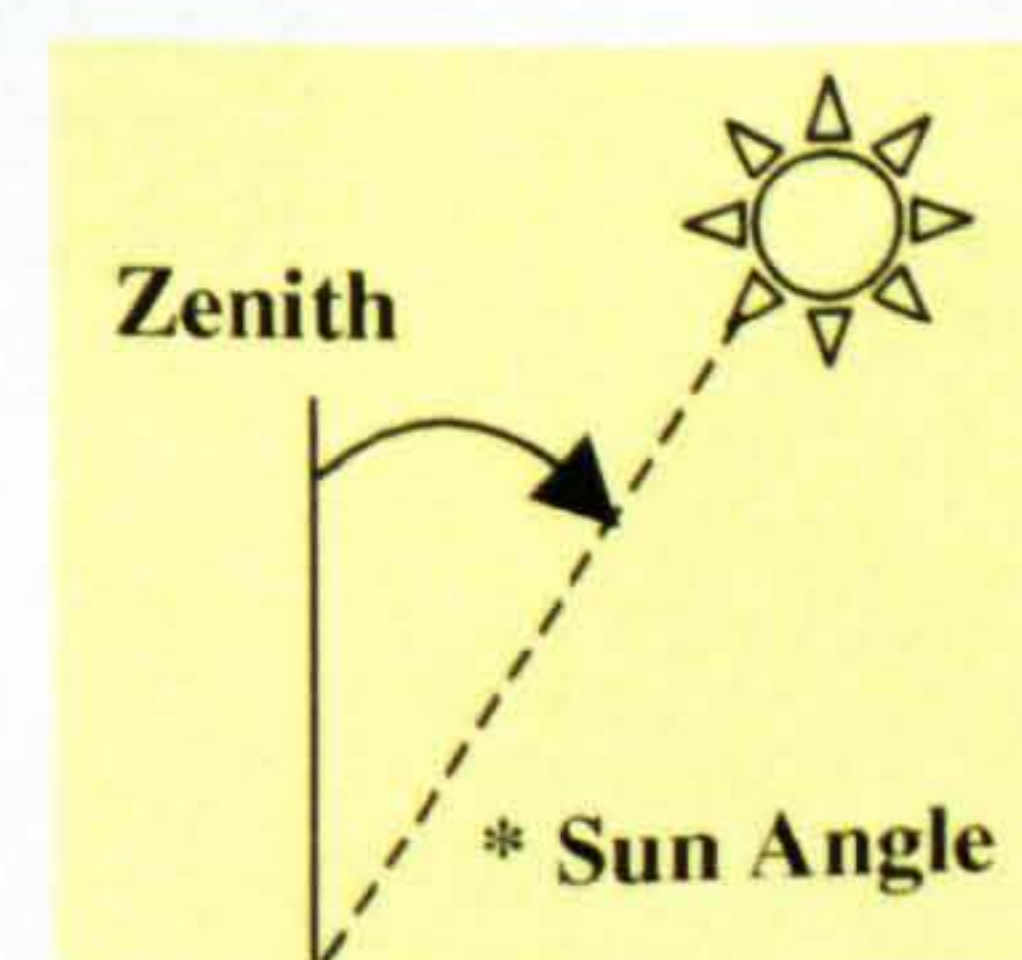
Table 9-3 Solar Radiation Intensity (W/m^2) Received on Flat Roof in *Winter*

HOURLY SOLAR CALCULATIONS (FLAT ROOF)

Location: Riyadh, Saudi Arabia

Date: 15th December

HOURLY	*SUN ANGLE	SOLAR SHADE	Received (W/m^2)
06:00	86	4%	0
07:00	84.7	3%	46
08:00	73.1	2%	257.6
09:00	62.9	0%	499.1
10:00	54.6	0%	690
11:00	49.3	0%	809.6
12:00	47.9	0%	851
13:00	50.9	0%	809.6
14:00	57.6	0%	690
15:00	66.7	0%	499.1
16:00	77.6	2.5%	257.6
17:00	83.5	3.5%	46
18:00	86.3	3%	0
TOTALS			5455.6
AVERAGE			419.7



9.3.2.2 ECOTEECT Solar Intensity Simulation on Semicircular Domed-roof

ECOTEECT “solar-exposure” application has been employed to carry solar radiation intensity calculations for domed geometry “Hemisphere” Fig. (9-13). ECOTEECT v5.2 (2003) is a developed version of ECOTEECT v5.01 (2002). ECOTEECT v5.01 calculates the solar radiation intensity (W/m^2) on each segment along the domed roof surface as separate object, where each segment “object” has different orientation and slope angle (*Azi. and Alt. As shown the outputs data file*). Therefore, computing the average of all segments calculations for finding out the received solar radiation above the entire surface of the dome roof. Fig. (9-13) (a) & (b) show this difference.

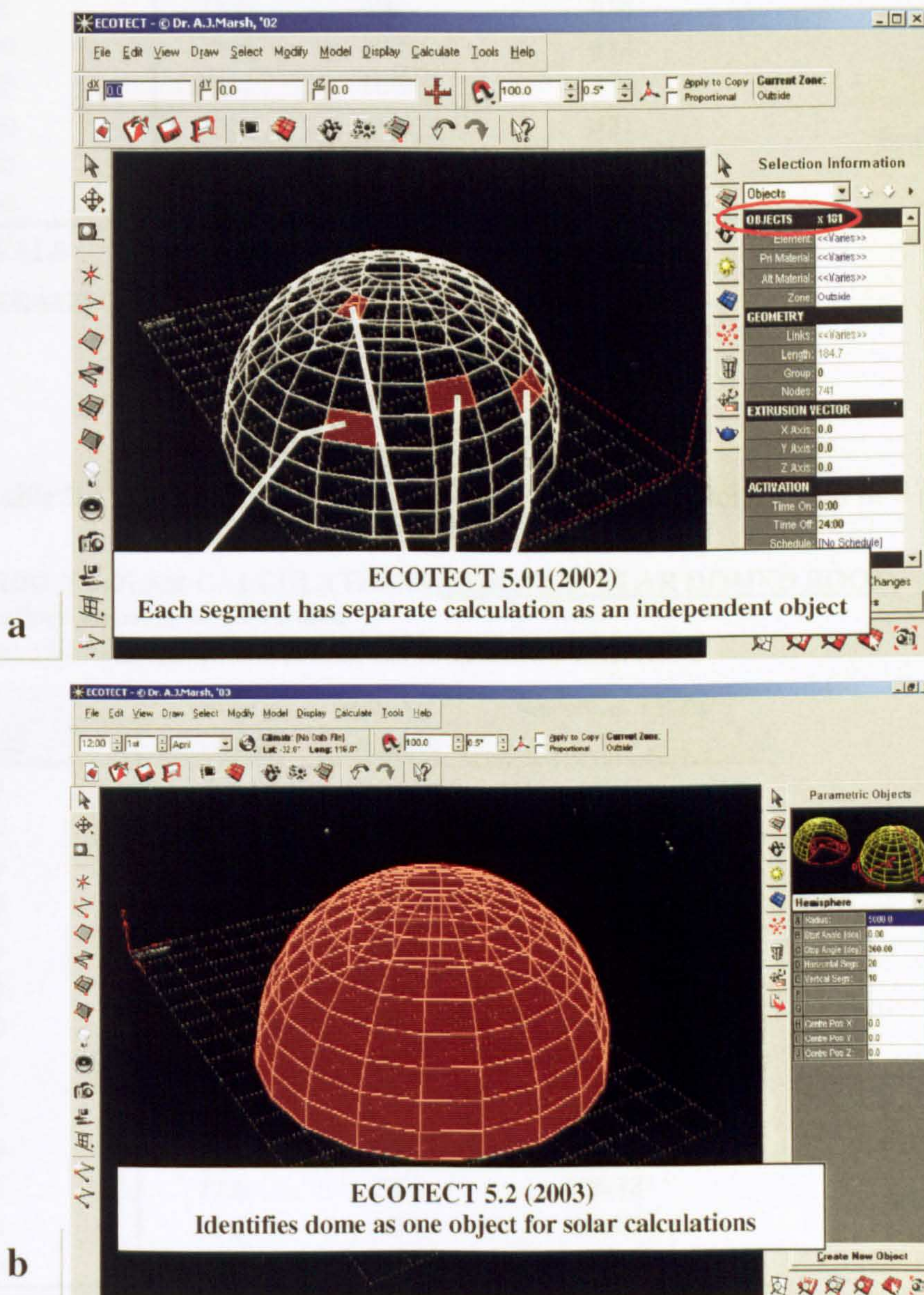


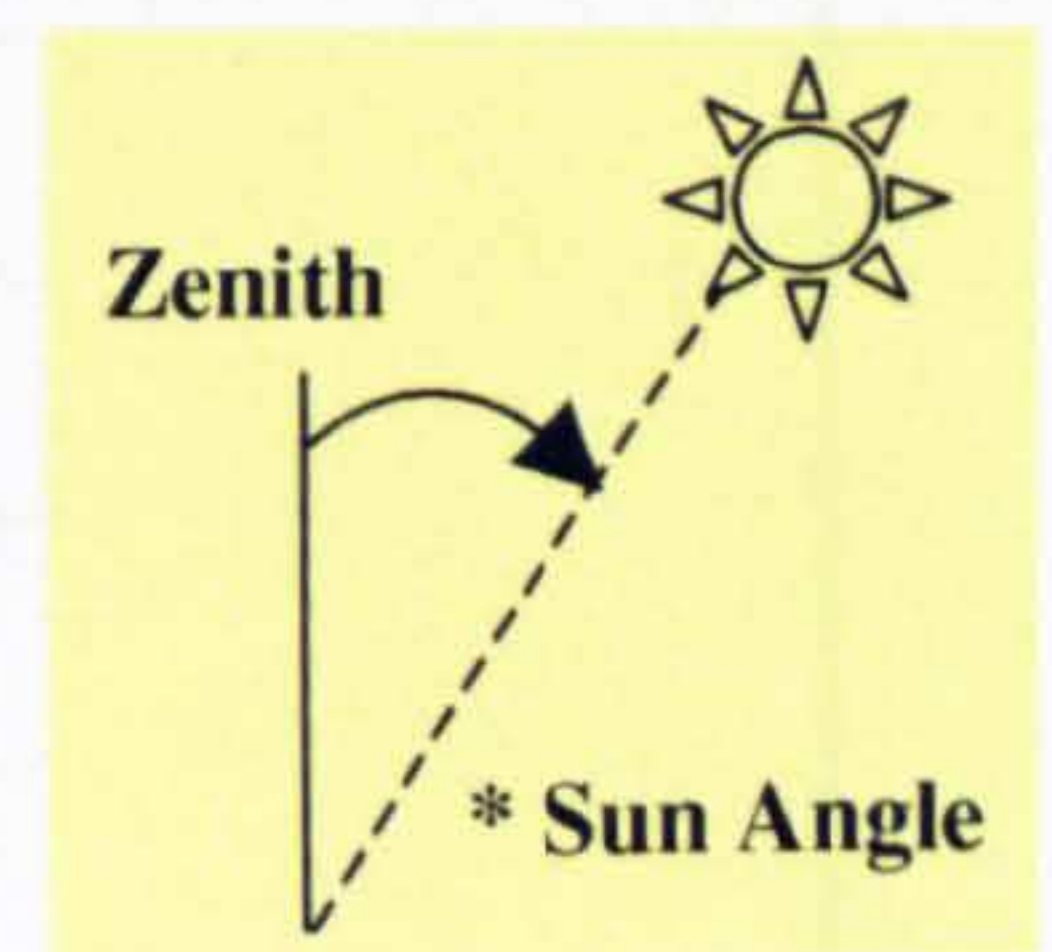
Figure 9-13 (a) ECOTEECT v5.01 (b) ECOTEECT v5.20

Table 9-4 Solar Radiation Intensity W/m^2 Received on Domed-roof in *Summer***HOURLY SOLAR CALCULATIONS (SEMICIRCULAR DOMED ROOF)**

Location: Riyadh, Saudi Arabia

Date: 15th June

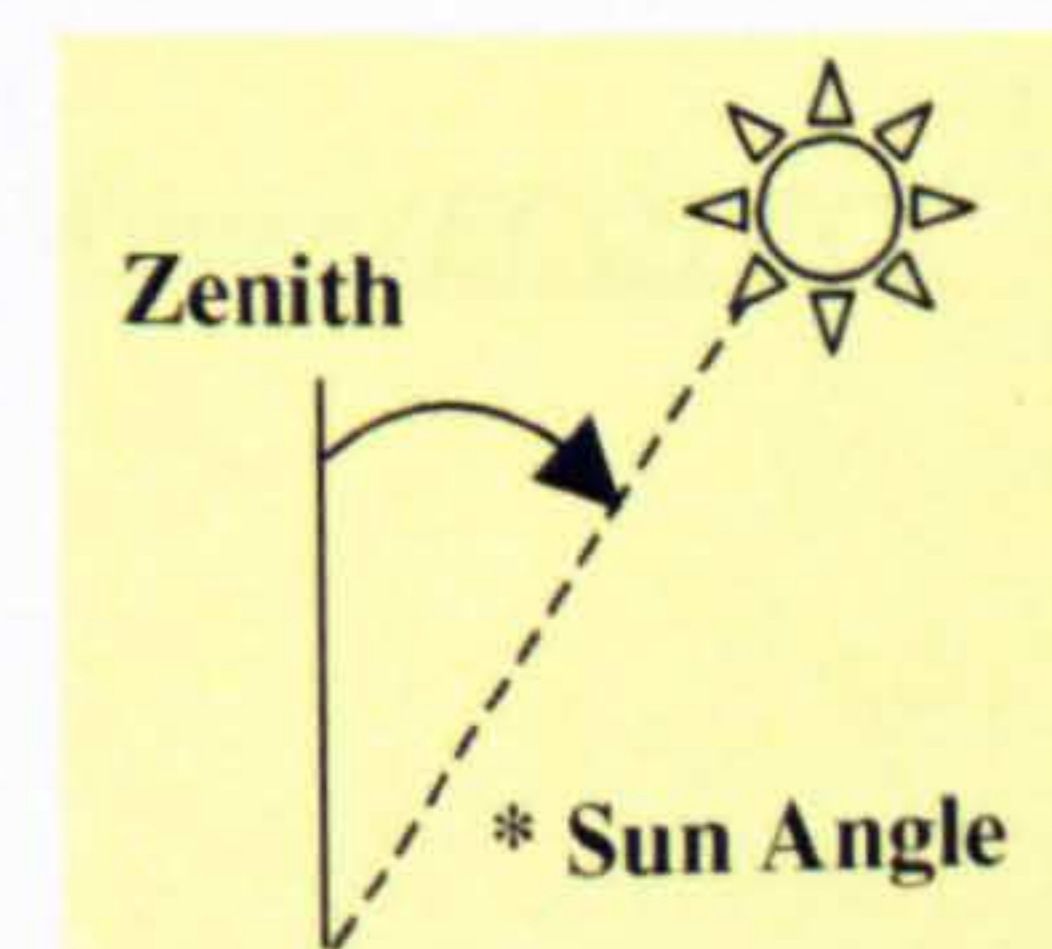
HOUR	*SUN ANGLE	SOLAR SHADE	Received (W/m^2)
06:00	79.2	39%	100
07:00	66.2	33%	267
08:00	53.0	23%	421
09:00	39.5	18%	534
10:00	25.9	12%	612
11:00	12.3	6%	658
12:00	2.0	0%	681
13:00	15.3	4%	658
14:00	28.9	10%	612
15:00	42.4	16%	534
16:00	55.9	21%	421
17:00	69.1	30%	267
18:00	81.9	37%	100
TOTALS			5865
AVERAGE			451.54

**Table 9-5** Solar Radiation Intensity W/m^2 Received on Domed-roof in *Winter***HOURLY SOLAR CALCULATIONS (SEMICIRCULAR DOMED ROOF)**

Location: Riyadh, Saudi Arabia

Date: 15th December

HOUR	*SUN ANGLE	SOLAR SHADE	Received (W/m^2)
06:00	86	54%	0
07:00	84.7	4%	68.32
08:00	73.1	67%	226.78
09:00	62.9	0%	359.72
10:00	54.6	0%	451.605
11:00	49.3	0%	506.345
12:00	47.9	0%	524.92
13:00	50.9	0%	506.345
14:00	57.6	0%	451.605
15:00	66.7	0%	359.72
16:00	77.6	2%	226.78
17:00	83.5	4%	68.32
18:00	86.3	4%	0
TOTALS			3750.46
AVERAGE			288.49



9.3.2.3 Comparison Between the Solar Performances Semicircular domed Using Two Different Computer simulation Tools

Fig. (9-14) illustrates the results calculated in the previous two sections, which have been generated using the ECOTECH solar tests on semicircular dome and flat roof. The generated results on both geometries show a number of similarities to the main trends, which have been, concluded from SRSM results for curved roofs in chapter 6 and 7. Moreover, $I_{(HTCS)}$ distribution-curves look identical to the $I_{(HTCS)}$ ones for Dome_{1(std)} (A=B) semicircular dome in chapter 8.

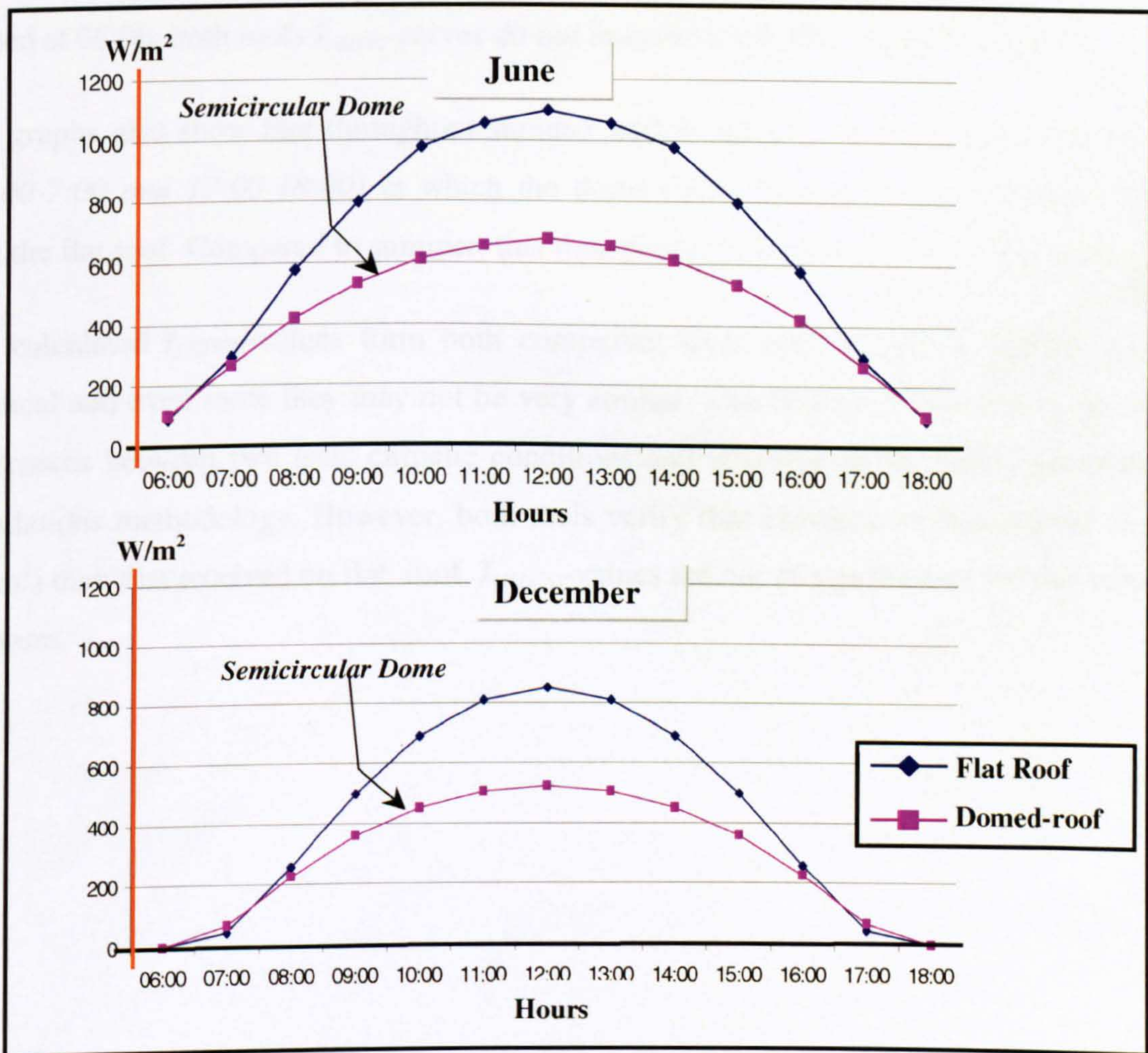


Figure 9-14 $I_{(HTCS)}$ W/m² on Semicircular Dome and Flat Roofs In Summer & Winter (ECOTECH v5.20 Results)

As the previous graphs show, ECOTECH $I_{(HTCS)}$ -values and distribution forms on flat and domed roofs in summer and winter are symmetrical around midday-axis and have the same main features at both seasons, which are generated previously by SRSM. In summer and winter, the maximum received solar radiation on both roofs takes place at midday, both $I_{(HTCS)}$ -curves have similar characteristics, which ascend differently at each roof geometry after 06:00 in the morning where both curves are not intersected.

In both seasons both $I_{(HTCS)}$ -curves get very close during 08:00 and before reaching their maximum at midday. During the afternoon, each roof $I_{(HTCS)}$ -curve descends differently till the two curves get very close again around 17:00, where they become intersected. As they started at 06:00, both roofs $I_{(HTCS)}$ -curves do not intersect each other at 18:00.

The graphs also show that throughout summer and winter day there are two time periods (06:00-7:00 and 17:00-18:00) in which the dome receives more solar radiation intensity than the flat roof. Compared to summer, this time period is slightly different in winter

The calculated $I_{(HTCS)}$ -values from both computing tools (ECOTECH & SRSM) are not identical and even more they may not be very similar. This believed to be due to the slight differences between two tests climatic conditions and also due to the nature of each tool calculations methodology. However, both tools verify that curved roof receives less $I_{(HTCS)}$ (W/m^2) than that received on flat roof. $I_{(HTCS)}$ -values are not of significance for this research purposes.

Finally, to compare graphically between the two models $I_{(HTCS)}$ findings (SRSM and ECOTECH), Fig. (9-15) presents the SRSM $I_{(HTCS)}$ results, which have been calculated previously in Chapter 8 for three domed-roofs with different curvatures. Dome_{1(std)} is the semicircular dome, where A=B. roof. $I_{(HTCS)}$ distribution-curves of the semicircular dome in Fig. (9-15) look very similar to these in Fig. (9-14).

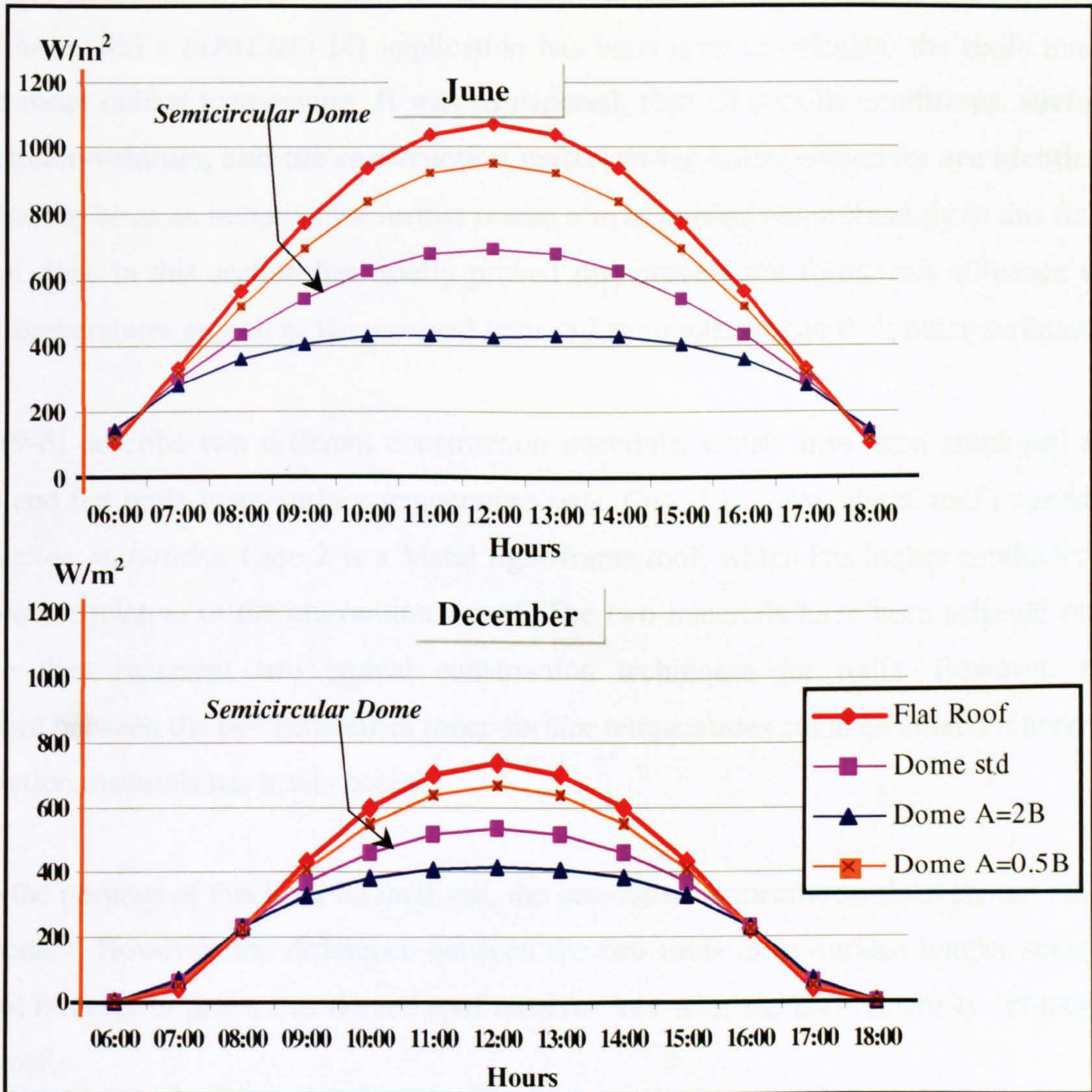


Figure 9-15 $I_{(HTCS)}$ W/m² on Three Domes and Flat Roof In Summer & Winter
(SRSM Results)

9.3.3 Curved-Roofs Indoor Thermal Analysis

In order to provide more validations for SRSM and ECOTECT general findings, this section reviews the findings of a brief indoor thermal analysis for semicircular dome and flat geometries. Therefore, the test is undertaken only to provide evidence of the lower indoor temperature that can be achieved using domed-roof. However, the effect of a curved roof on the indoor temperature seems to be complex due to the peculiar geometries such inner-spaces have. IES's (*APACHE*) [8] application has been used to calculate the roofs inner-surface mean radiant temperature. **It was considered, that all outside conditions, surface areas, inner-volumes, and the construction materials for both geometries are identical.** It is meant to be as an initiative for further research to be carried out profoundly in this field. The test done in this section has briefly proved that curved-roof forms can influence the indoor temperatures as well as the received solar radiation intensity on their outer-surfaces.

Table (9-6) describe two different construction materials, which have been employed for domed and flat roofs inner-surface temperature tests. Case 1 is conventional roof (*standard construction materials*). Case 2 is a Metal light-frame roof, which has higher conductivity and U-value relative to the conventional roof. The two materials have been selected only because they represent two typical construction techniques for roofs. However, the difference between the two geometries inner-surface temperatures could be altered if another construction materials has been chosen.

Due to the purpose of this brief thermal test, the generated temperature-values are not taken into account. However, the difference between the two roofs inner-surface temperatures is essential in order to prove that domed roof receives less solar radiation intensity compared to flat roof.

Table 9-6 Two Construction Materials For Domed and Flat roofs [8]

	Case 1 Conventional Roof Construction (<i>Stone/ Bitumen/Ceiling Tiles//Air Gap/Fibre</i>)	Case 2 Metal Light Roofing Frame
CIBSE U-value	0.25 W/m ² K	2.01

Generally, the amount of heat gained by radiation (*absorbed radiation G*) can be transferred from the roof by three ways; free convection to the surrounding, radiation from the roof and conduction through the roof to the indoor [10]. This can be expressed as:

$$G = q_c + q_r + q_k \quad [10] \qquad \text{Equation 9-1}$$

Where q is the heat transfer from the roof per unit area, c is denoted for convection, r is denoted for radiation and k is denoted for conduction.

It has been demonstrated previously that flat roof receive more solar radiation intensity (W/m^2) than the curved one. Therefore, the flat roof is expecting to conduct more heat than the curved one and this may cause indoor discomfort in hot climates. Among other factors, the resulting variations in the external solar intensities above flat and curved roofs outer-surfaces creates indoor temperature differences. The test noticed that there is a constant difference in the hourly temperature throughout the daytime-period at each case. Fig. (9-16) only compares between the day-average (*daytime hours average*) inner-surface temperatures of the two geometries (dome and flat) at the two cases in summer and winter.

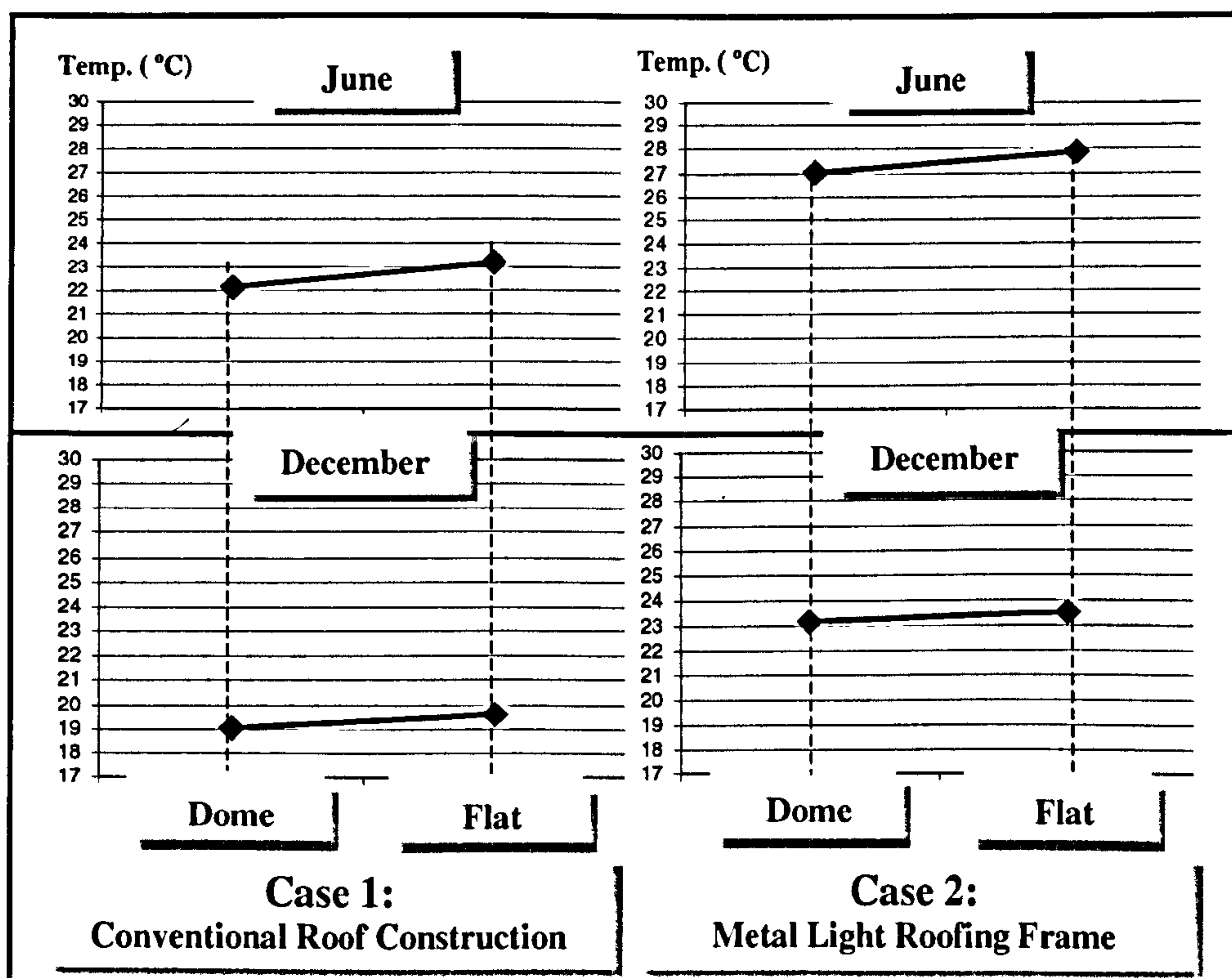


Figure 9-16 Day-average inner-surface temperature of Domed and Flat roofs

9.4 VALIDATION OF THE RESEARCH WORK AND MAIN FINDINGS

Comparison with Independent Recently Published Research on Curved-roofs Solar Performance

As it has been mentioned previously in this thesis and earlier in this chapter, there are some references that addressed the topic of solar radiation on inclined surfaces with different orientations. However, at the time of commencing this research, a limited number of published-work touched the solar performances of curved-roofs in hot-arid or tropical regions. This part reviews very recent independent research some of which was published while preparing this thesis for submission, it compares between the research main findings and generated results. Each one of these research attempts tested the solar and thermal performance of one particular curved-roof form.

Research work has been carried out by Gomez-Munoz, et al, it has been published in December 2003 [11]. The term “hemispherical vault roof” has been used by the author of this publication instead of hemispherical or semicircular dome, as it only tests the solar performance of a semicircular dome. “Vault” in architecture is a single curved structure, or an expanded curved cross section as this thesis used to identify, therefore, vaulted form has not been tested in this paper. However, its main findings are validating the results of this thesis.

The paper looked mainly at the solar performance of a semicircular domed-roof (hemisphere). It employed a computer program that was developed to calculate the solar radiation intensity at each of the rectangular planes, which covered the entire surface of the dome. A 40×60 rectangle grid was selected and occurrence of solar incidence was determined for a given time, day and latitude for each grid point's rectangle. In general, the paper compared between the solar performance of domed and flat roof using similar methodology to the one presented in this thesis of sloped planar segments.

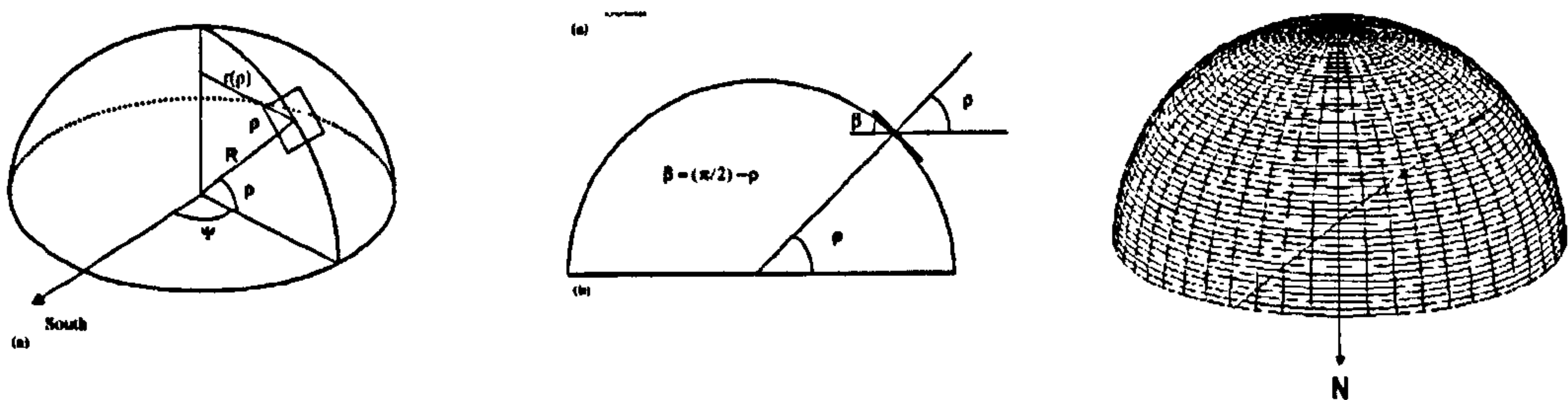


Figure 9-17 Geometrical Methodology (Gomez-Munoz) [11]

For hot-arid climates, the paper provided concluding remarks, which show similar trends of that concluded in the thesis for domed-roof solar performance. The paper also mentioned the self-shaded capabilities of curved-roof. The term “Auto-shading” has been used by the paper’s author instead of self-shaded. The paper has pointed out that self-shaded is one particular characteristic of the dome-type roof, which occurs most of the day except possibly at noon. Fig. (9-18) compares between the main results of the work carried out by Gomez-Munoz (et al) (Fig. (9-18) (a)) and the work carried out in this thesis (Fig. (9-18) (b)). Also see Fig.(9-14) For ECOTECH Results (carried out in this thesis).

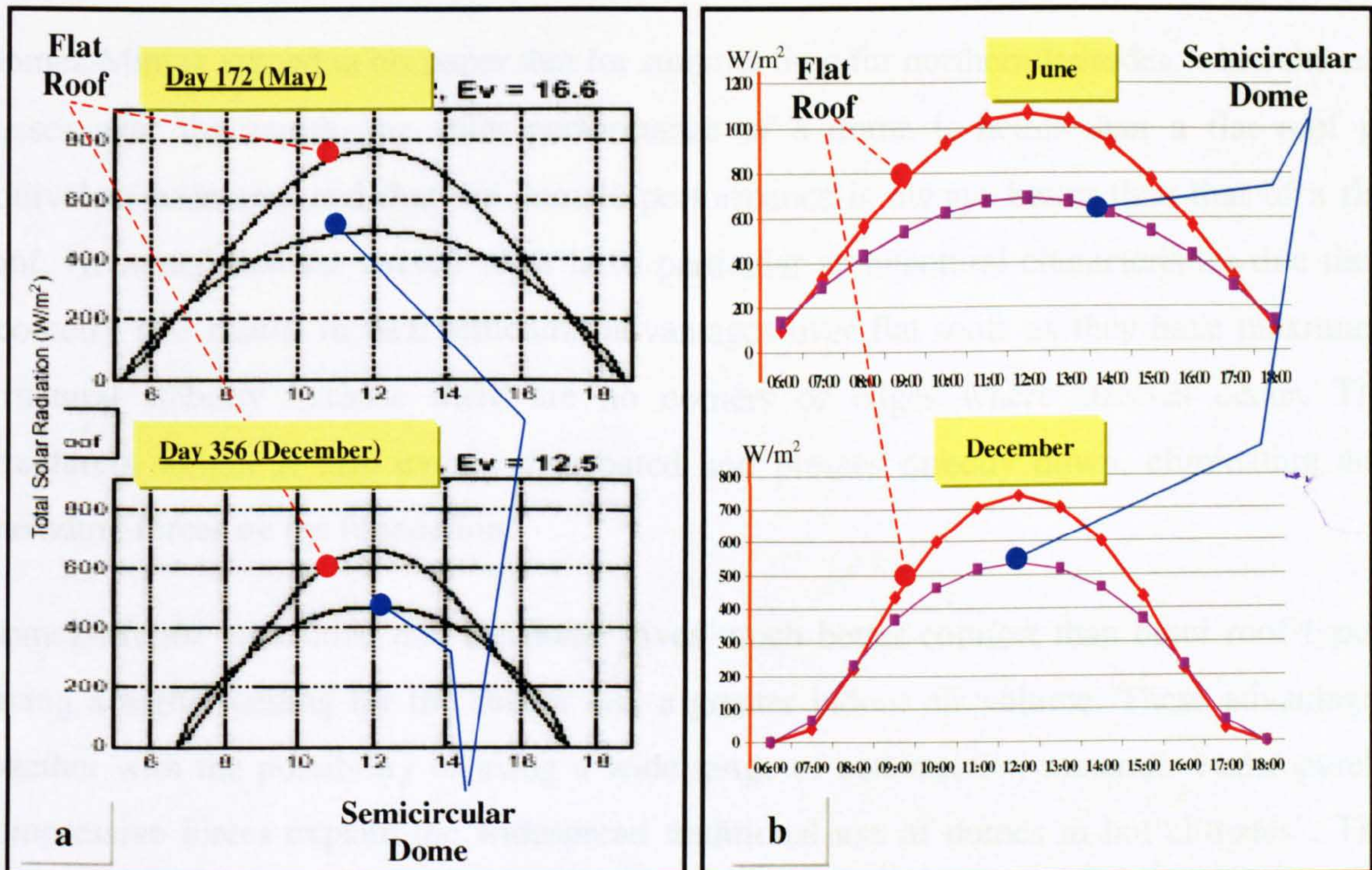


Figure 9-18 Graphical Comparison Between The Main Findings

(a) Work carried out by Gomez-Munoz (et al) (b) Work carried out in this thesis

Gomez-Munoz (et al) [11] stated “The hemispherical vault roof has some solar advantages over other types of roofs due to its self-shading property, which diminishes the received solar energy, especially when the sun is out of the zenith, also because at any time, the solar energy strikes the dome normally at only one point on the surface. A third reason he pointed out that the exposed surface of the dome is the largest among roofs with regular geometry (flat, tilted, gable, hipped, pavilion hipped, barrel vault, etc.), for the same height and equivalent base area, which results in the solar radiation intensity being spread over a larger area and heat transmission to the interior is reduced”.

Gomez-Munoz (et al) [11] added that for most of the day, part of the roof is shaded from the sun, and thus at that time it can act as a radiator, absorbing heat from the sunlit part of the roof and the internal air, and transmitting it to the cooler outside air in the roof's shade. He stated that *"this effect is particularly effective for roofs domed in the form of a hemisphere since at least part of the roof is always shaded except at noon when the sun is directly overhead"*. The former properties are better understood as a function of solar elevation angle, since the solar radiation received by the hemispherical vault roof is independent of the azimuth".

Gomez-Munoz argued in his paper that for summer time for northern latitudes, when the sun passes near the zenith, the solar performance of a dome is better than a flat roof of equivalent base area and that the dome's performance is always better than that of a flat roof. He added that the curved roofs have particular architectural characteristics due their geometry that results in their structural advantages over flat roofs as they have maximum structural stability because there are no corners or edges where stresses occur. The structure's weight is also evenly distributed and presses directly down, eliminating any spreading forces on the foundation.

Gomez-Munoz concluded that the dome gives much better comfort than other roof types, giving a higher ceiling for the shelter and a greater indoor air volume. These advantages together with the possibility of using a wide range of construction materials under purely compressive forces explain the widespread traditional use of domes in hot climates". The conclusion drawn by Gomez-Munoz in his research on curved roofs solar performance agrees to a large extent to the work presented in this thesis.

Another research work has been carried out by Runsheng, et al at *Desert Architecture and Urban Planning Unit Ben-Gurion University of the Negev*, it was published in 2003 [12,13]. Runsheng, et al pointed out to the fact that very little quantitative research exists in the literature of the use of domed and vaulted roofs in the hot arid regions, although many other studies focused on climate related issues [12].

The work discussed the technique used to predict heat transfer through domed or vaulted roof. It is based on a three-dimensional heat transfer equation and solar geometry and compares between the thermal behaviour of curved and flat roofs in terms of heat flux and daily heat flow through them into an air-conditioned building under different climatic conditions.

Runsheng concluded that that the results of their numerical calculations under hot climatic conditions shows that the heat flux and the daily heat flow through the curved roofs are unaffected by the roof radius, thickness and thermal properties, but are notably influenced by the half rim angle of both domed and vaulted roofs and the ambient temperature [12]. Runsheng's research pointed out that in order to reduce the heat gains through a vaulted roof building it should be oriented towards the north-south, this was the same results that was found in the research undertaken in this thesis (Chapter 6 & 7).

It is worth noting that the model used in that research only addressed heat flux and heat flow through the roofs assuming an air-conditioned building. It has not taken into account the effect of curves roof on indoor temperature of a passive building design due to the complexity of heat transfer between curved roofs and the indoor air. The same research unit has carried out another attempt in 2003 [13]. This research analysed the absorbed radiation by domed and vaulted roofs compared to flat roofs.

Finally, most of the main findings and results of the above research work can be also drawn from the research done in this thesis. The work done in this thesis is believed to be comprehensive and extensive from the architectural point of view findings and conclusions. All these attempts and others prove that there is an urging necessity in carrying out more research in this area looking at the thermal performance of spaces enclosed by curved roofs (vaulted and domed).

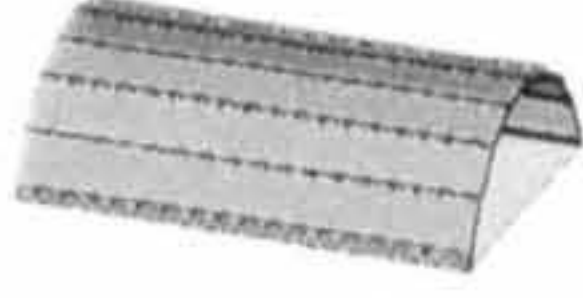

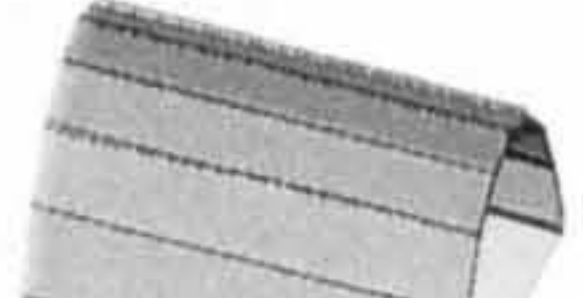
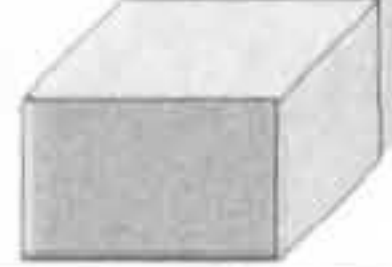
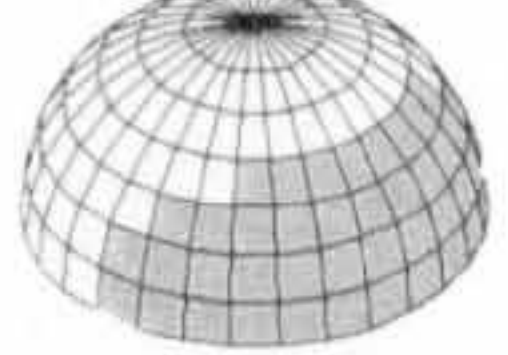

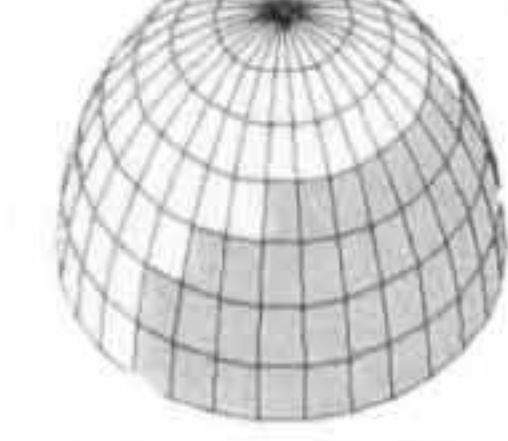
9.5 NOVEL CONTRIBUTION AND AIMS FULFILLMENT

This part presents a concluded discussion of a number of the main research findings and roof-form comprehensive solar investigation outputs presented in the thesis. These findings are believed to be novel contribution to the architectural practice and roof-design process in architecture. It compares between the solar performances of a number of different curved-roofs in a way that can be easily used as design guidelines and tools for curved-roofs architecture in hot-arid regions.

9.5.1 Solar Performance of Flat and Curved-roofs with Different Forms, Curvatures, and Orientations

Table (9-8) summarises a number of solar findings to be maintained within the architectural context in order to provide guidance to the roofs design, form, curvature and orientation in such climatic regions for summer and winter conditions.

Table 9-8 The Average Daily Received $I_{(HTCS)}$ on Different Curved Roof Forms and Curvatures in Summer and Winter and Their Ratios % to that on Flat Roof

Roof Geometry (Form & Orientation)		Day Average $I_{(HTCS)}$ W/m ²			$\frac{I_{(HTCS) \text{ CCS}}}{I_{(HTCS) \text{ flat roof}}} \%$			
		June	Dec.	Form Seasonal Ratio %	June	Dec.		
Extended CCS (Vaulted Roof)	 1 (A=B)	N-S	449	306	68.2	69.6	83.8	
		E-W	512	292	57	76.9	80.1	
		NW-SE	480	294	61.3	72.9	80.6	
		NE-SW	480	294	61.3	72.9	80.6	
	 2 (A=0.5B)	N-S	587	341	58.1	89.1	93.4	
		E-W	604	339	56.1	91.7	93	
		NW-SE	596	339	56.9	90.4	92.9	
		NE-SW	596	339	56.9	90.4	92.2	
	 3 (A=2B)	N-S	280	270	96.4	42.5	74	
		E-W	392	236	60.2	59.5	64.7	
		NW-SE	345	242	70.1	52.3	66.4	
		NE-SW	344	243	70.1	52.2	66.5	
	 (A=B=0)	659	365	55.4				
Rotated CCS (Domed Roof)	 4 (A=B)		471	294	62.4	71.47	80.54	
		 5 (A=0.5B)		597	340	57	90.59	93.15
			 6 (A=2B)		348	250	71.8	52.80

The percentage of the received $I_{(HTCS)}$ on a curved roof form to that received by the flat roof is displayed in Table (9-8). For each orientation of the extended CCS, the minimum received $I_{(HTCS)}$ in summer and winter is recorded on the extended CCS curvature where $A=2B$. For all extended CCS facing the (N-S), the curvature where $A=2B$ receives the minimum $I_{(HTCS)}$ (280 W/m^2), this represents 42.5% from the received $I_{(HTCS)}$ by the flat roof (659 W/m^2). The other (N-S) oriented curvatures, which have flatter profiles (*less concavity*) (*form no. 1 and no. 2*) receive more $I_{(HTCS)}$ with the comparison to form no.3, Table (9-8). In summer, the (N-S) orientation records the minimum $I_{(HTCS)}$ with the comparison to the other tested directions at each geometry. Whereas, the (N-S) orientation receives the maximum $I_{(HTCS)}$ in winter with the comparison to the other directions. This concludes that the (N-S) direction is the most preferable orientation for the extended CCS (vaulted roofs) in both summer and winter.

The semicircular curvature ($A=B$) receives about 449 W/m^2 in summer when it faces (N-S) (*69.6 % from that received by the flat*), while it receives 512 W/m^2 when it faces (E-W) in summer (*76.9% from that received by the flat*). The same geometry receives 480 W/m^2 when the curvature becomes orientated towards (NE-SW) or (NW-SE) in summer (*72.9% from that received by the flat*). This concludes that the secondary orientations are more energy efficient compared to the (E-W)-facing direction in summer. While in winter, the semicircular curvature that faces (N-S) receives the maximum $I_{(HTCS)}$ as same as the other curvatures when they face (N-S), Table (9-8).

The domed form solar behaviours are similar to the vaulted roof behaviours in summer and winter. Form no. 6 where $A=2B$ receives the minimum $I_{(HTCS)}$ in summer and winter compared to the other curvatures, which have flatter profiles (*less concavity*) (*form no. 4 and no. 5*). It is concluded that vaulted roof form is more preferable than domed ones in order to receive less $I_{(HTCS)}$ in summer and winter. The table also computes the “Form Seasonal Ratio %”, which represents the ratio between the received $I_{(HTCS)}$ in winter to that in summer for each form. It verifies that curved roof forms in general are more preferable than the flat form in summer and winter. Where all curved roof form-seasonal-ratios are closer to 1 (100%) from the flat seasonal ratio (55.4%), Table (9-8).

9.5.2 Design Guidelines of Solar Performance of Flat and Curved Roofs Form and Orientation in Hot-arid Regions

The research has generated seasonal contour-indexes for roof solar performances in summer and winter. The comparability of these indexes is presented in this section.

9.5.2.1 Flat and Vaulted Roofs in Summer and Winter

Fig (9-19) illustrates seasonal contour-indexes for solar performances of vaulted-roof outer-surfaces with different curvatures and orientations in summer.

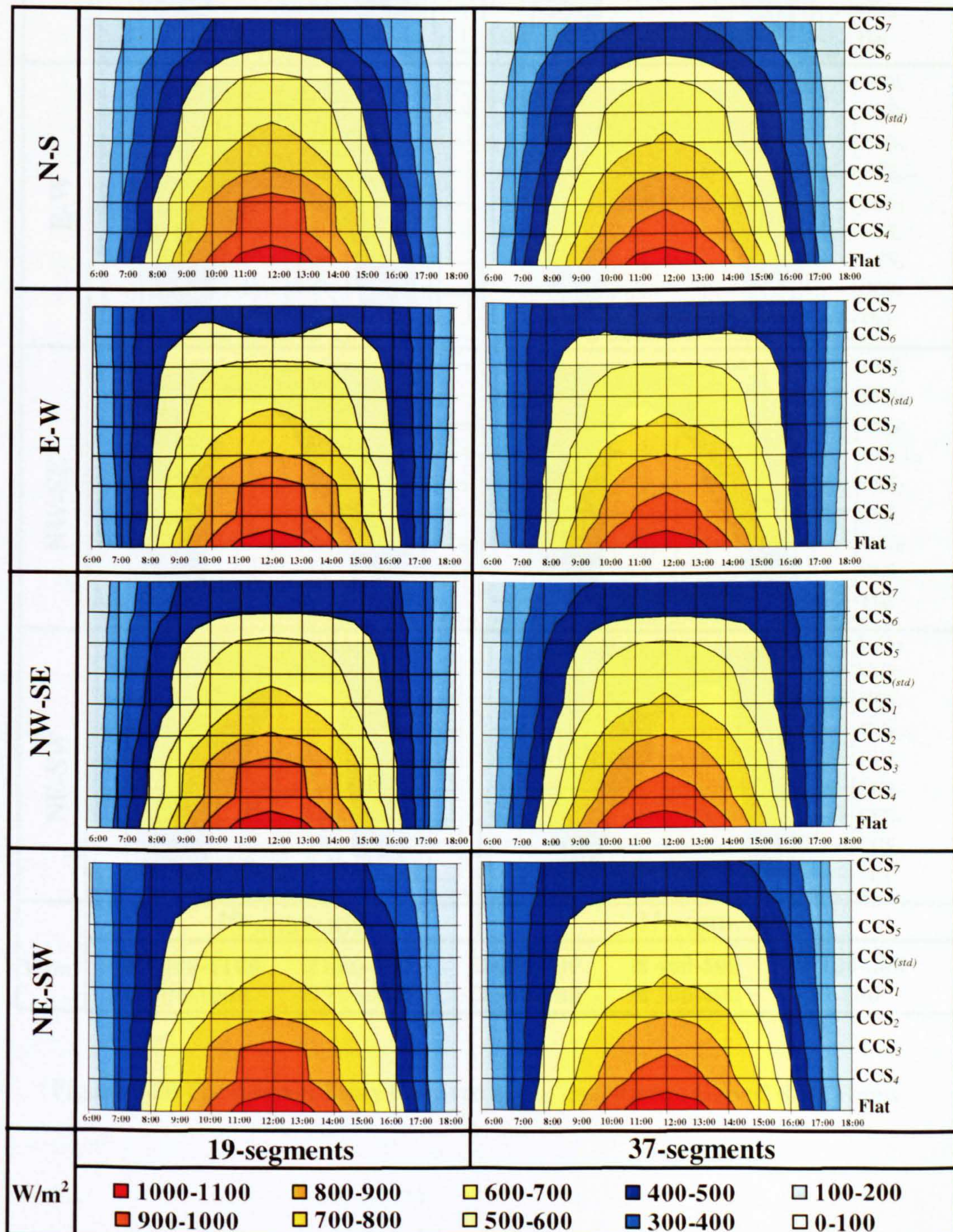


Figure 9-19 The Average Daily Received $I_{(HTCS)}$ on Different Curved Roof Forms

Fig (9-20) illustrates these indexes for the previous vaulted-roofs with the same orientations in winter.

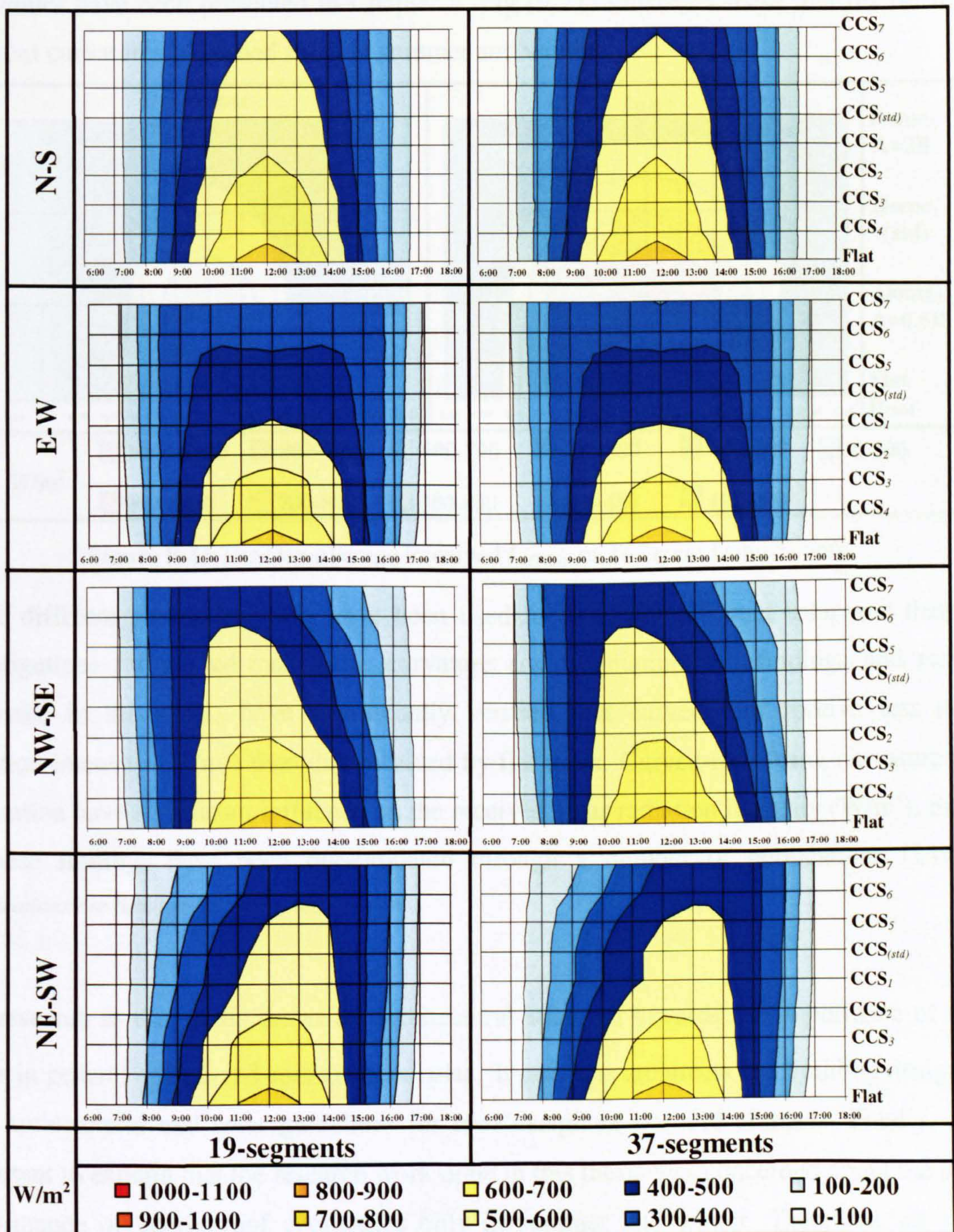


Figure 9-20 The Average Daily Received $I_{(HTCS)}$ on Different Curved Roof Forms

9.5.2.2 Flat and Domed Roofs in Summer & Winter

Seasonal contour-indexes for solar performances of domed-roof outer-surfaces in summer and winter have been presented in Chapter 8. Fig (9-21) illustrates these indexes for three different curvatures of domed roofs in summer and winter.

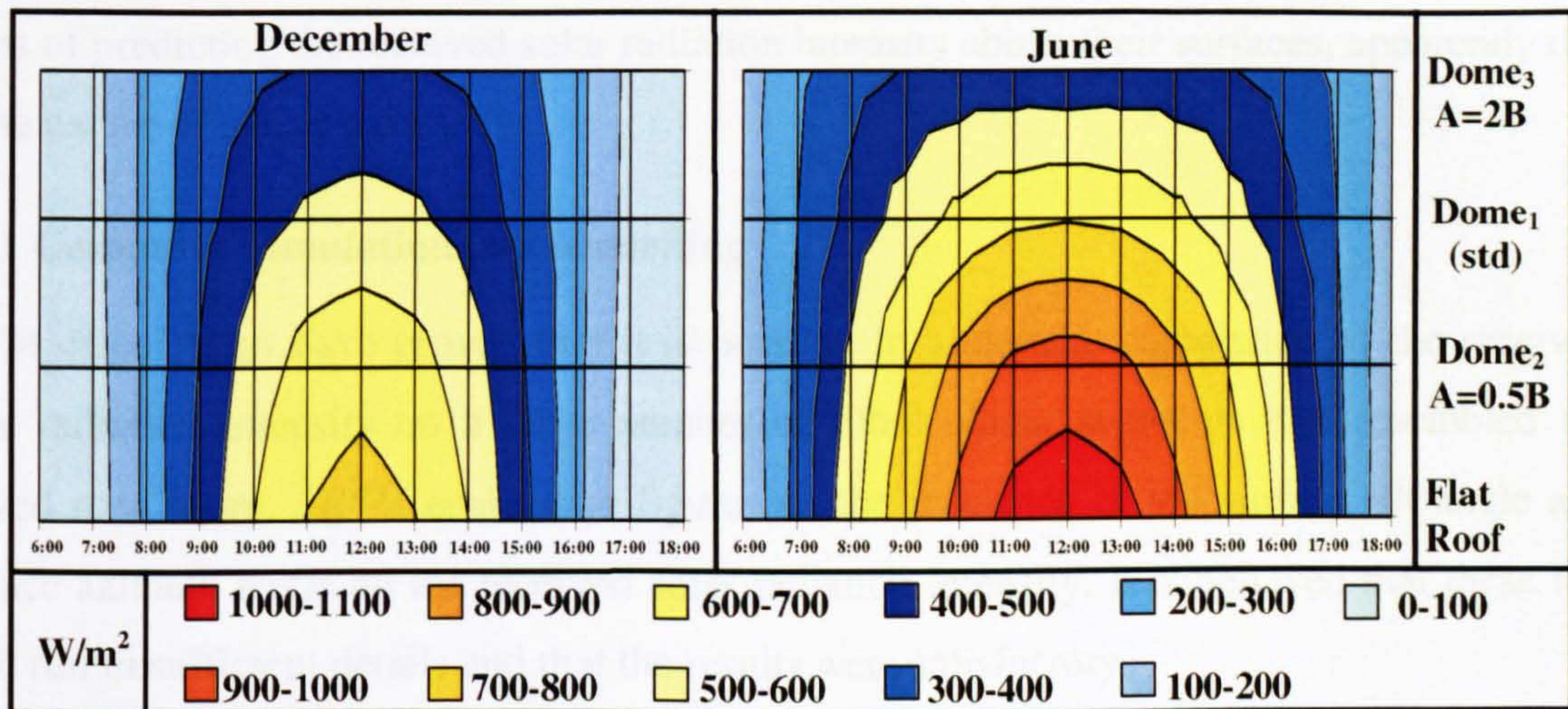


Figure 9-21 The Day-average Received $I_{(HTCS)}$ on Different Domed-roofs

Three different simulation tools have been used to carry out different solar and thermal investigations for curved-roof form, curvature and orientation. All findings and results discussed in this thesis have significantly verified that curved roof receive less solar radiation intensity (W/m^2) than that received by flat roofs. Curved-roof form, curvature and orientation have significant influence on the received solar radiation intensity (W/m^2). Some of these findings have been disseminated through a number of publications [14-18]. (Publications are listed at the end of this chapter).

The research in this thesis draws an architectural attention towards the importance of roof forms in general and curved-roofs in particular. It provides architects and building designers with architectural and solar guidelines for roof design in hot-arid climates. Finally, it is important to explain that the research work done in this thesis was concerned about the solar performance of curved-roof geometries only in summer and winter. Therefore, all solar calculations for flat and curved roofs have been carried out only in June and December, which represent summer and winter respectively. Moreover, the design for these two seasons is more crucial than the rest of the year, especially for hot-arid climates and geographical latitudes. However, designing for peaks and day-averages either in summer or winter is more essential than the rest of day hours.

9.6 RECOMMENDATIONS FOR FURTHER RESEARCH WORK

Extensive theoretical and experimental investigations have been conducted to predict the solar and thermal performances of planar surfaces (*horizontal and oblique*). However, it is not an easy task to define the solar and thermal performances of curved-roofs, especially in terms of predicting the received solar radiation intensity above their surfaces, apparently due to the nature of their geometries.

9.6.1 Computer Simulation and Modelling

SRSM calculations have proved that it is possible to undertake calculation of the received solar radiation intensity on a large number of tilted planar segments that resembled the curved roof forms. *SRSM* enabled to figure out the influence of the surface tilt angle and surface azimuth angle on the received solar radiation intensity. It is believed that these test were run in sufficient details and that the results were satisfactory.

Therefore, it is recommended that future computer simulation studies take into consideration more climatic parameters, internal and external surface convection heat transfer calculations and generate more detailed indoor thermal findings of curved roof geometries. Therefore, calculate indoor air temperature and mean radiant temperature throughout the day in summer and winter. This will facilitate the thermal and environmental prediction of spaces enclosed by curved forms, and thus increase their wider acceptance for different applications in hot arid regions.

Curved-forms geometrical configurations are not well defined in most of 2D and 3D drawing tools and model builders of these packages. It has been found that these configurations are not well linked with the indoor thermal calculations, which is proved by the relatively small differences in indoor temperatures between the two tested geometries, investigated in the present research. (*flat and dome*).

For carrying out further research in this field, it is recommended that computer simulation packages identify the geometrical parameters of such curved forms in more details. The influences of such forms on the indoor temperatures and their external surface convection heat transfer calculations need to be well established.

9.6.2 Monitoring of Full-Scale Models

Despite their availability and viability, physical scale models in artificial skies are restricted to the conditions of laboratories simulation and their validation results. Moreover, such experiments always face a number of difficulties through building up the physical model and their artificial environment preparations. Furthermore, computer simulation is very similar in concept to the experimental tests in terms of having a number of assumptions and simulations, which may not be similar to the real situation. Besides providing relative less time and effort to run, computer simulation is more accurate than the experimental work and easy to control the input conditions, which is not an easy task to provide in physical models and lab work.

Scaling is also one of the limitations of both computer simulation and experimental lab tests. However, in computer simulation some of these limitations are overcome due to the fact that it employs real dimensions and sizes for tested objects and spaces. On the other hand, predicting the intensity of received solar radiation on curved forms by different solar radiation calculation tools and simulation software was very satisfactorily performed with the proper geometrical resemblance into infinitesimal inclined planar-segments.

Consequently, full-scale models can be built in real climatic conditions to avoid the previous disadvantages and difficulties of experimental lab tests. Likewise, monitoring a number of existing buildings with employing advanced measurements and tools or run a very limited number of experimental base tests are expensive and time consuming. The suggested solar and thermal investigations have to be carried out using various full-scale curved roof curvatures (*cross-section-ratio CCSR*). The proposed full-scale model may represent an extended curved roof cross-section (vault) or a rotated one (dome) with test cells placed along the model outer surface.

The purpose of such full-scale study is to facilitate better understanding of solar performance of curved roof outer surfaces and to compare the simulated findings. It may also test the curved roofs thermal performances. Therefore, this section discusses number of recommendations for such tests.

As discussed previously in many parts of the thesis, other factors like roof colour, roof layers components and thickness and thermal properties of roof construction-materials can significantly influence the amount of gained solar heat by roof surface. Therefore, all full-scale models features and components have to be taken into account throughout experiment phases (i.e. full-scale models must be erected from similar materials and colours).

Firstly, it is recommended to investigate the direct impact of curvature morphology on the received solar radiation intensity above the roof surface by measuring the solar intensity at several points (*different locations and inclinations*) along variety of cross-sections) using radiation sensors [19] as the (*Pyranometer*) [10]. The inner-surface and indoor temperatures are influenced by difference in solar intensity along the curved-roof outer surface. Fig. (9-22) sketches a proposed full-scale model for solar and thermal tests in hot climates.

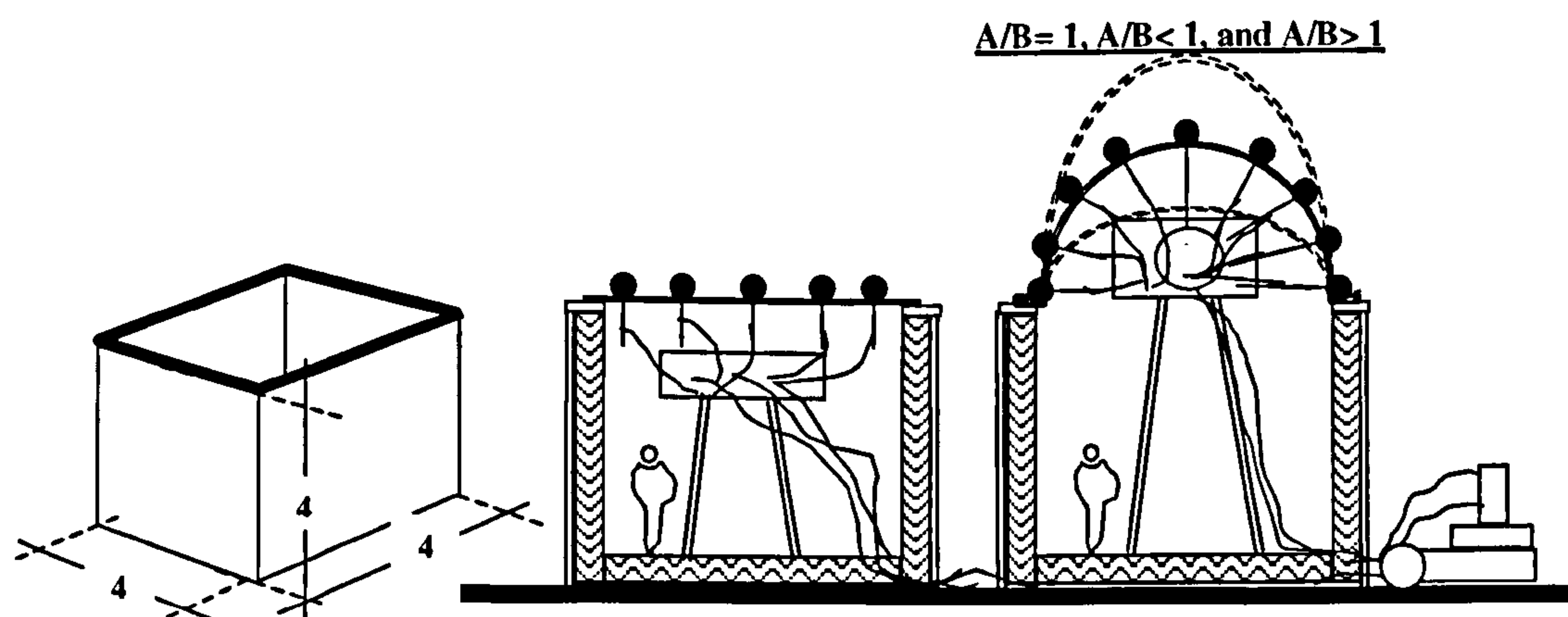


Figure 9-22 Full-scale Model Sketches

For indoor thermal measurements, well-insulated walls are required for monitoring the effect of roof curvatures on the indoor temperature and mean radiant temperature. Only roofs can be without insulation. It is also recommended to avoid creating wall openings in order to eliminate ventilation effects and to make the inner volume sealed as much as possible. This, however, could require special materials and fixed indoor conditions during the measurement process.

Finally, beside the full-scale investigations, the research suggests number of enhancement ideas, which could be incorporated into such developed further work. Example of these ideas are summarised below:

- Solar and thermal performances of traditional vaulted and domed roofs can be enhanced when they integrate with other architectural elements. This has been proved in traditional architecture and other related research work. Gadi (2000) [20] tested the use of domed-roof, pitched-roof and open courtyard in buildings. He concluded that domed-roof achieves relatively high ventilation ratios in comparison to the other tested cases. He justified that a top-opened dome provides air suction. He added that dome with a higher profile can increase this ratio. This creates a continuous indoor airflow, which is very essential for indoor thermal comfort in dense urban areas in hot-arid regions [20]. Further studies on the effect some architectural elements such as a small opening in the apex of different curved-roof forms, a doubled layer curved-roof, or both elements together as shown in Fig. (9-23), can be integrated within the thermal investigation of vaulted and domed roofs in hot arid regions.

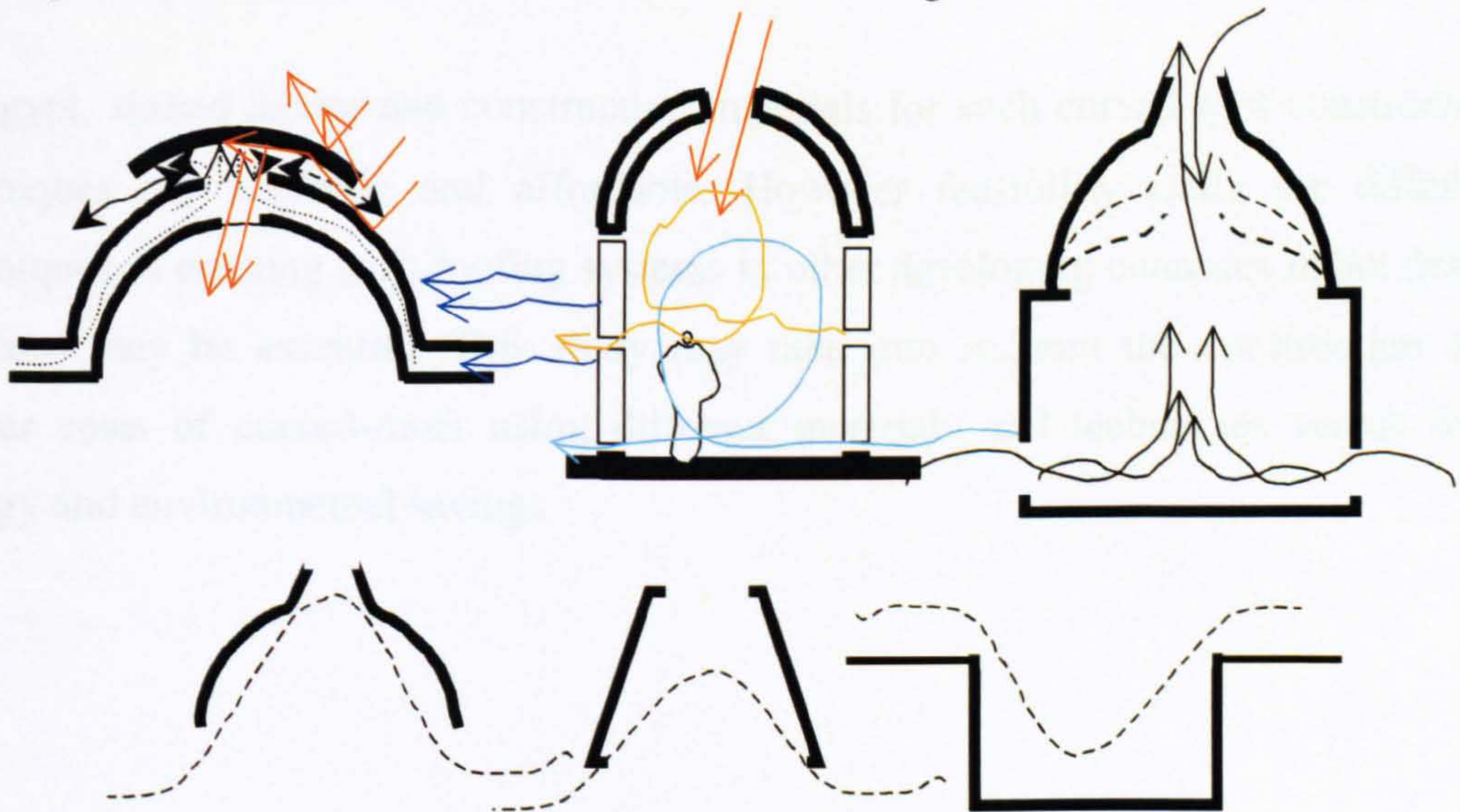


Figure 9-23 Schematic Sketches for some Ideas to be investigated in Further Research

- The architectural characteristics of curved-roof enclosed spaces can have a great effect on the overall indoor thermal performance of this type of roofs. The higher ceiling of curved roofs creates larger volumes than the flat, this may provide different ventilation and airflow patterns, as shown in Fig. (9-23). Another effect of higher ceilings, which requires further investigations, is its relation with the human view factor (Keeping in mind that the human view factor influences the irradiative heat transfer between the roof and the space occupants).
- Simulation of airflow patterns and velocity around the external curved roof surfaces in order to test the influence of the CCS orientation and curvature on the convection heat loss.
- Monitoring the solar behaviour above existing buildings roofs in hot-arid climates, especially those with curved roof forms (*Vaults and Domes*) to be compared with the full-scale and computer simulation results. This helps to have a better understanding of the behaviour and the effects of these forms in the built environment and can be useful for post occupancy evaluation.
- In Egypt, skilled labour and construction materials for such curved-roof construction techniques are available and affordable. However feasibility study for different techniques of erecting such roofing systems in other developing countries in hot desert climates may be essential. This study may take into account the construction and labour costs of curved-roofs using different materials and techniques versus their energy and environmental savings.

Reference List

1. Bahadori, M. N. and Haghghat, F. Passive Cooling in Hot, Arid Regions in Developing Countries by Employing Domed Roofs and Reducing the Temperature of Internal Surfaces. *Building and Environment* 1985;Vol. 20(No. 2):pp:103-13.
2. Monolithic Dome Institute. Monolithic Dome Homes [Web Page]. Available at <http://www.monolithic.com/gallery/homes/index.html>.
3. Muneer, T. *Solar Radiation & Daylight Models for the Energy Efficient Design of Buildings*. Oxford, UK: Butterworth-Heinemann, 1997.
4. Stasinopoulos, T. N. *Geometric Forms & Insolation; An analytical Study of the Influence of Shape on Solar Irradiation* [Dept. of Architecture - : National Technical University of Athens, Athens, 1999. Doctoral Dissertation .
5. Laouadi, A. and Atif, M. R. Natural convection heat transfer within multi-layer domes. *International Journal of Heat and Mass Transfer* 2001;Vol. 44:pp 1973-81.
6. Laouadi, A. and Atif, M. R. Prediction Models of Optical Characteristics for Domed Skylights under Standard and Real Sky Conditions. Proceedings of the 7th International IBPSA Conference. 2001 Aug 13-2001 Aug 15; Rio de Janeiro, Brazil. Institute of Research in Construction, National Research Council Canada, NRC-CNRC.
7. Laouadi, A. and Atif, M. R. Transparent Domed Skylights: *Optical Model for Predicting Transmittance, Absorptance and Reflectance*. *International Journal of Lighting Resrarch and Technòlogy* 1998;Vol. 30(No. 3):pp. 111-8.
8. IES (Ve Version 4.1) [Licensed Software University Package].
9. ECOTECH V5 [The complete building design & environmental analysis tool. Square One's flagship software. It features a designer-friendly 3D modelling interface fully integrated with acoustic, thermal, lighting, solar and cost functions.].
10. Duffie, J. and Beckman, W. *Solar Energy Laboratory University of Wisconsin-Madison, Solar Engineering of Thermal Processes*, 2nd ed., New York: John Wiley & Sons, 1991.
11. Gomez-Munoz, V. M., Porta-Gandara, M. A. and Heard, C. Solar Performance of Hemispherical Vault Roofs. *Building and Environment* 2003 Dec;Vol.38(No.12):pp: 1431-8.
12. Runsheng, T., Meir, I. A. and Etzion, Y. Thermal Behaviour of Buildings with Curved Roofs as Compared with Flat Roofs. *Solar Energy* 2003 May;74:pp: 273-86.
13. Runsheng, T., Meir, I. A. and Etzion, Y. An Analysis of Absorbed Radiation by Domed and Vaulted Roofs as Compared with Flat Roofs. *Energy and Buildings* 2003;Vol. 35:pp: 539-48.
14. Elseragy A. A. and Gadi M. B., Computer Simulation of Solar Radiation Received by Curved Roof in Hot-Arid Regions, Proceedings of the Building Simulation 2003, 2003 Aug 11-2003 Aug 14; EINDHOVEN, Netherlands.

15. Elseragy, A. A. and Gadi M. B. Traditional Architecture, Energy Consciousness and Sustainability, *An approach to affordable and thermally comfortable buildings in hot-arid climates with special reference to Egypt*. Proceedings of the Second World Conference on Technology Advances for Sustainable Development & Workshop on Renewable Energy & Development of Remote Areas. 2002 Mar 11-2002 Mar 14; Cairo, Egypt.
16. Elseragy, A. A. and Gadi M, B. Roof Geometric Forms and Solar Irradiation Intensity In Hot-Arid Climates. Proceeding of the ISES Solar World Congress 2003, ISES 2003, Solar Energy for a Sustainable Future. 2003 Jun 14-2003 Jun 19; Svenska Mässan Congress Centre, Göteborg, Sweden.
17. Elseragy, A. A and Gadi M. B. Sustainable Potentialities of Traditional Roofs Geometries in Egypt and Hot-Arid Climates, An Analytical Study of Traditional Curved Roof Forms Towards More Energy Efficient Architecture. Proceedings of Passive And Low Energy Architecture 20th International Conference PLEA 2003. Santiago, Chile: 2003.
18. Elseragy, A. A. and Gadi M. B. The Solar Performance of Vaulted Roof Geometry and Orientation. Proceedings of the Seminar on Renewable Energy and the Sustainable Urban Environment. Nottingham, UK. University of Nottingham: 2003: pp: 61-8.
19. KIPP & Zonen. Radiation Sensors (Including Special Sensor Design and Calibration services). Oldenzaal, Holland.
20. Gadi, M. B. Design and simulation of a new energy conscious system, (Basic Concept). Applied Energy 2000; Vol. 65:pp. 349-53.

BIBLIOGRAPHY

Bibliography

- Abbideen K. Aspects of Passive Cooling and The potential Savings in Energy, Money and Atmospheric Pollutants Emissions in Existing Air Conditioned Mosques. Edinburgh, UK: University of Edinburgh; 1996. Ph.D Thesis.
- Abel, Chris. Architecture and Identity: responses to cultural and technological change //with a foreword by Suha Ozkan. 2nd ed. Oxford: Architectural Press; 1994.
- ADAUA. Site Visit to Rosso, Mauritania. In Reading the Contemporary African City. Singapore: Concept Media/The Aga Khan Award for Architecture; 1983. (Brian Brace Taylor (ed)).
- Ahmed A. M. Roofs in the Hot Dry tropics. UK: London University; 1975. Ph.D Thesis.
- Al-Motawake M. K. Solar Energy Applications in the Yemen Arab Republic. UK: Cranfield University; 1986. Ph.D. Thesis.
- Al-Sanea S. A. Thermal Performance of Building Roof Elements. Building and Environment, 2002; Vol. 37: pp 665-75.
- Al- Sanea SA. Thermal Performance of Building Roof Elements. Building and Environment, Vol. 37: pp. 665-75.
- Alawadhi S. A. A. ; Sayigh A. M. The History of Building materials in Kuwait and its Sustainability to local Climate.
- Ali Z. F.; Mallick F. H.; GURKULA at Nadia, India, An environmental friendly village, Environmentally Friendly Cities - *Proceedings of PLEA 98 Passive and Low Energy Architecture*, 1998 Jun; Lisbon, Portugal.
- Alia F. Hasan. ArchNet: An Online Resource on Islamic Architecture. [Web Page] 2002; <http://www.suite101.com/article.cfm/4205/90695> [Accessed Jun 2002].
- Alia F. Hasan. Contemporary Egyptian Architects. [Web Page] 2001; www.suite101.com/article.cfm/4205/84003
- Anderson, B. Solar Energy: *Fundamental Building Design* (1973).
- ArchNet Digital Architectural Library. [Web Page]; <http://www.archnet.org> [Accessed Jul 2003].
- Argyro Nicolakeas. Passive Solar Design For Mediterranean Buildings; The Greek Case. Manchester: University of Manchester; 1989 Sep.
- ASHRAE Handbook 2000: Heating, Ventilating, and Air-Conditioning Systems and Equipment. SI ed. Atlanta, Ga.: American Society of Heating, Refrigeration and Air-Conditioning Engineers; 2000.
- Bahadori M. N, Haghightat F., Passive Cooling in Hot, Arid Regions in Developing Countries by Employing Domed Roofs and Reducing the Temperature of Internal Surfaces. Building and Environment 1985; Vol. 20(No. 2):pp:103-13.
- Baird G., The Architectural Expression of Low Energy Architecture World Renewable Energy Congress VII (WREC 2002) 2002: Elsevier Science Ltd.
- Baker, N. Energy and Environment in Architecture *A Technical Design Guide*. (2000).
- Bancroft J. Editor's Note: The New Crop of Energy-Efficient Building Materials. Arid Land News Letter, 1994 (Fall-Winter); ALN No. 36.

- Bansal, N. K.: *Passive Building Design - A Hand of Natural Climatic Control*. Amsterdam, The Netherlands: Elsevier Science B.V., (1994).
- Boake MT. Sustainability & Construction Technology: An Attitude in Support of Quality. *Architronic*, Vol. 5 (No. 2).
- Boake MT. Passive Versus Active Solar Design: Opposing Strategies in Support of a New Sustainable Vernacular. *Architronic: In Support of a New Sustainable Vernacular* Vol. 4 (NO. 3): p. 2.
- Boas M. V., Environmental criteria and design principles for a new community in Brasilia, *Environmentally Friendly Cities - Proceedings of PLEA 98 Passive and Low Energy Architecture*, 1998 Jun; *Lisbon, Portugal*.
- Bouchlaghem N. Optimizing the Design of Building Envelopes for Thermal Performance. *Automation in Construction*; 2000; Vol.10: pp101-12.
- Bourges, B. and Scharmer, K. The New European Solar Radiation Atlas: A Tool for Designers, Engineers and Architects. Information System for Renewable Energy (WIRE), International Solar energy Society ISES Publication <http://wire0.ises.org>
- Britten JR. What is a Satisfactory House? A Report of Some Household's Views, BRE Current; Paper 26, 1987.
- Cartes I. A. Traditional Architecture, Building Materials and Appropriate Modernity in Chilean Cities. *Renewable Energy* 1998; Vol. No. 15: pp. 283-6.
- Chalfoun N. V., Using CALPAS 3 as a tool to optimise the design of passive solar desert houses in North TAHRIR, *Proceedings of Egypt 12th Passive solar conference, Solar' 87* (The American solar energy society & the solar energy society of Canada) 1987 Jul.
- Chown G. A. Roof Function, Requirements and Components, *Construction Practice*. [Web Page]; http://www.nrc.ca/irc/practice/roo1_E.html
- CIBSE Guide A, Design Data, London, UK: The Chartered Institute of Building Services Engineers, (1999).
- Coach H. Chapter 4- Bioclimatism in Vernacular Architecture. *Renewable Sustainable and Energy Reviews*, 1998; Vol. No. 2: pp 67-87.
- Cook J. Architecture Indigenous to Extreme Climates. *Energy and Building*, 1996; Vol. No.23: pp. 277-91.
- Cook J., Sustainable suburbs for the American desert, *goals and models*, *Environmentally Friendly Cities - Proceedings of PLEA 98 Passive and Low Energy Architecture; Lisbon, Portugal*. 1998.
- D., Barnett; W., Browning. "A primer on Sustainable Building", A report Colorado. Rocky Mountain Institute.
- Davidson, Cynthia C. Great Mosque of Riyadh and Old City Centre Redevelopment. In *Architecture Beyond Architecture*. London: Academy Editions: 1995. (Cynthia C. Davidson, and I. S. e., editor).
- Davidson CC. Kaedi Regional Hospital. *Architecture Beyond Architecture*, London: Academy Editions 1995; Cynthia C. Davidson, and Ismail Serageldin, eds.
- Davidson, Cynthia C. e. Tuwaiq Palace. In *Legacies for the Future: Contemporary Architecture in Islamic Societies*. London: Thames and Hudson: 1998. (Cynthia C. Davidson (ed)).

- De Wilde P.; van der Voorden M.; Brouwer J.; Augenbroe G. and Kann H.; The Need for Computational Support in Energy-Efficient Design Projects in the Netherlands; Proceedings of the 7th International IBPS Conference 2001 Aug 13-2001 Aug 15; Rio de Janeiro, Brazil.
- Depecker P, Menezo C, Virgone J and Lepers S.; Design of Building Shape and Energetic Consumption. *Building and Environment*, 2001; Vol.36: pp.627-35.
- Donn M.; Amor R. and Harrison D.; A Design for an Internet Based Simulation Quality Control Tool.
- Doshi, Balkrishna. Toward an Appropriate Living Environment: Questions on Islamic . Development. In *Places of Public Gathering in Islam*. Philadelphia: Aga Khan Award for Architecture: 1980. (Linda Safran (ed).
- Duffie, J.; Beckman W; Solar Energy Laboratory, University W. M.; Solar Engineering of Thermal Processes. 2nd ed. New York: John Wiley & Sons; 1991.
- Edited by M., Santamouris; D., Asimakopoulos. *Passive Cooling of Buildings*. European Commission (Directorate General xvii for Energy); (1996).
- Edwards B. *Sustainable Architecture - European Directives & Building Design*, (1999).
- Ellipse and Circle Java Applets, Edwards, Paul; Barry, Colin and Edwards, Peter; School of Design Engineering and Computing, Bournemouth University.
- El Jack K. An Agricultural training Centre: Case Study in Nianing, Senegal. *Changing Rural Habitat*, 1982; Vol. I: Case Studies.
- Elgazayerly, F E. Study of Planning and Design Regulations and Principles for the Urban Settlements in the Egyptian Desert. Cairo, Egypt: Institute of Urban and Building Research, Ministry of Housing, Infrastructure and Urban Settlements; 2000 Jun. Report No.: 3: Planning and Design Recommendations.
- Elseragy, A. A.; Gadi, M. B., Computer Simulation of Solar Radiation Received by Curved Roof in Hot-Arid Regions, Proceedings of the Building Simulation 2003 2003 Aug 11-14, 2003, EINDHOVEN, Netherlands.
- Elseragy, A. A.; Gadi, M. B. Roof Geometric Forms and Solar Irradiation Intensity In Hot-Arid Climates Proceeding of the ISES Solar World Congress 2003, ISES 2003, Solar Energy for a Sustainable Future 2003 Jun 14-19, 2003; Svenska Mässan Congress Centre, Göteborg, Sweden.
- Elseragy, A. A.; Gadi, M. B., Traditional Architecture, Energy Consciousness and Sustainability, *An approach to affordable and thermally comfortable buildings in hot-arid climates with special reference to Egypt*, Proceedings of the Second World Conference on Technology Advances for Sustainable Development & Workshop on Renewable Energy & Development of Remote Areas 2002 Mar 11-2002 Mar 14; Cairo, Egypt.
- Energy in Architecture - The European Passive Solar Handbook*.
- Etzio Y. A Bio-Climatic Approach to Desert Architecture. *Arid Land News Letter* 1994 Fall-1994 Winter; ALN No. 36.
- Etzion Y., Pearlmutter D., Erell E., Meir I. A. Adaptive Architecture: *Integrating Low-energy Technologies for Climate Control in the Desert*. 1997; Vol. 6: pp 417-25.
- Evans, M. *Housing Climate and Comfort*. London: Architectural Press; 1980.
- Exell R.H.B., A program in BASIC for calculating solar radiation in tropical climates on small computers. *Renewable Energy Review Journal*, 1986 Dec; Vol. 8(No. 2).

- Fathy H. Architecture and Environment. Arid Land News Letter 1994 Fall-1994 Winter; ALN No. 36.
- Fathy, H. Architecture for the poor *An Experiment in Rural Egypt*. [Web Page] (1973).
- Fathy H. Natural Energy and Vernacular Architecture, *principles and examples with reference to hot -arid climates*. Chicago & London: Published for United Nations University by the university of Chicago press ; 1986. (EDITED BY WALTER SHEARER; Abdel-Rahman; Ahmed Sultan.
- Filippin C., Beascochea EA, Derosa C. CL, Estelrich D. A passive building for ecological research in Argentina: The first two years experience. Solar Energy 1998; Vol. 63 (No. 2): pp. 105-15.
- Gadi M. B. Design and simulation of a new energy conscious system, (Basic Concept). Applied Energy 2000; Vol. 65: pp. 349-53.
- Gadi M. B. Design and simulation of a new energy conscious system, (Ventilation and thermal performance simulation). Applied Energy 2000; Vol. 65: pp. 355-66.
- Gan G., A parametric Study of Trombe Walls for Passive Cooling of Buildings. Energy and Buildings 1998; Vol.27: pp.37-43.
- Garcia-Chavez J. R, Towards a new sustainable ecological community, *Principles, Strategies, and Applications (Integration of sustainable technology into architectural design and regional planning)* Environmentally Friendly Cities - Proceedings of PLEA 98 Passive & Low Energy Architecture, 1998 Jun; Lisbon, Portugal.
- Garden G. K. [Web Page]; www.nrc.ca/irc/cbd/cbd070e.html
- Givoni, B. Man, Climate And Architecture, 2nd Edition, Applied Science Publishers, London, 1976.
- Griffiths, I. D., Field Studies of Thermal Comfort in Passive Solar Buildings 2nd European Conference on Architecture 1989; Paris.
- Hamdy, I. F. Architectural Approach to The Energy Performance of Buildings in a hot-dry climate, with special reference to Egypt. Bath: University of Bath; (1986). Ph.D. Thesis.
- Hamza N., Elsafty A., Dudek S., Integrated Double-Skin-Solar Cooling System for Office Building Facades in Hot Arid Regions. World Renewable Energy Congress VII (WREC 2002), Elsevier Science Ltd. 2002.
- Holod, Renata; Darl Rastorfer. Halawa House. In Architecture and Community. New York: Aperture. 1983. (Renata Holod ; Darl Rastorfer, eds, editors.
- Hottel H. C, Woertz, B. B. Performance of Flat Plate Solar Heat Collectors. Transactions of the American Society of Mechanical Engineers 1942; Vol. 64, (91).
- IHVE Guide Book A. London, UK: The Institution of Heating and Ventilating Engineers; (1970).
- Ilana Frie., Methods for Climate Control in Arid Zones. Housing in Arid Lands - *Design and Planning*. London: The Architectural Press; 1984. (GOLANY, G.)
- India: Vault and Dome Structures At The Indian Institute of Technology, *New Delhi*. Mimar, 2002 Jul; Vol. 41.
- Jan de Rooden. The fired Mudbrick House. [Web Page]; <http://www.johnnyrolfjanderooden.nl/firedmuho.htm>. [Accessed Aug 2003].
- Jan de Rooden. The Fired Mudbrick House (Jan de Rooden). [Web Page]; www.johnnyrolfjanderoodenceramicart.com/firedmuho.htm

Jasmina Radosavljevic, Amelia Dordevic, Defining of the Intensity of Solar Radiation on Horizontal and Oblique Surfaces on Earth. FACTA UNIVERSITATIS, Series: Working and Living Environmental Protection, Vol. 2 (No. 1): pp. 77-86.

Jones, D. L., Architecture and the Environment - *Bio-climatic Building Design*. [Web Page], (1998).

Jones, D. L., Architecture and the Environment. London; (1998).

Kassarjian J. B.; Ardalan N., The Iran Centre for Management Studies in Tehran, Iran. Higher Education facilities, Aga Khan Program for Islamic Architecture. [Web Page] 1982; <http://archnet.org/library>. [Accessed Apr 2002].

Khan H-U. National Commercial Bank. Mimar 16: Architecture Development 1985.

Khodabakhshi Sh., Sustainable Construction and Vernacular Architecture of Iran, World Renewable Energy Congress VII (WREC 2002) 2002: Elsevier Science Ltd.

KIPP & Zonen, Radiation Sensors (Including Special Sensor Design and Calibration services). Oldenzaal, Holland.

Koenigsberger, O. H.; (et al). Manual of Tropical housing and Building - *Part one: Climatic Design*. (1973).

Kremers, Jack. "Defining sustainable Architecture" Architronic. [Web Page] (1995); <http://www.saed.kent.edu/v4n3/v4n3.02.html> .

Laouadi A, Atif M.R., Comparison between Computed and Field Measured Thermal Parameters in an Atrium Building. Building and Environment 1999 Mar; Vol. 34 (no: 2): pp. 129-38.

Laouadi A., Atif M. R. Natural convection heat transfer within multi-layer domes. International Journal of Heat and Mass Transfer 2001; Vol. 44: pp 1973-81.

Laouadi A. ; Atif M. R., Prediction Models of Optical Characteristics for Domed Skylights under Standard and Real Sky Conditions Proceedings of the 7th International IBPSA Conference 2001 Aug 13-2001 Aug 15; Rio de Janeiro, Brazil. Institute of Research in Construction, National Research Council Canada, NRC-CNRC.

Laouadi A., Atif M. R. (Institute of Research in Construction, National Research Council Canada NRC-CNRC). Transparent Domed Skylights: *Optical Model for Predicting Transmittance, Absorptance and Reflectance*. International Journal of Lighting Research and Technology 1998; Vol. 30(No. 3): pp. 111-8.

LCHS(Lund Centre for Habitat Studies) , Norton J. Woodless Construction. 1997; Vol. 9 (No. 2).

Littlefair, P. J. e. a. Environmental site layout planning: solar access, microclimate and passive cooling in urban areas. London: construction Research Communications; 2000.

Lunde J. Peter. Solar Thermal Engineering. Canada: John Wiley and Sons, Inc.; 1980.

Makachia A. P. Control of Energy in Offices in Nairobi- *A study of Fenestration in a Tropical Highland Climate*.

Mallick FH. Thermal Comfort and Buildings Design in The Tropical Climates. Energy and Buildings 1996; Vol.23: pp. 161-167.

Minke, G. Earth Construction Handbook, *The Building Material Earth in Modern Architecture*. Southampton, Boston. WIT Press; 2000.

- Mohamed A. M. The Thermal Performance of Concrete Roofs and Reed Shading Panels Under Arid summer Conditions. *Overseas Building Notes-Information on Housing and Construction in Tropical and Sub-Tropical Countries* 1975 Oct; Vol.164.
- Monolithic Dome Institute. Monolithic Dome Homes [Web Page]. Available at <http://www.monolithic.com/gallery/homes/index.html>.
- Moor, F. Environmental Control Systems - *Heating Cooling Lighting*. (1993).
- Mosquera G. Energy Performance and traditional neighborhood design, Environmentally Friendly Cities - *Proceedings of PLEA 98 Passive and Low Energy Architecture* 1998 Jun; Lisbon, Portugal.
- Muhaisen, Ahmed S. Influence of Building Form on its Solar Energy Potential in Different Climates and Latitudes. Nottingham: University of Nottingham; 2001 Sep. Msc Dissertation.
- Mukhatar Y. A. An investigation into the Thermal Performance of Roofs in Hot Dry Climates. Newcastle, UK: University of Newcastle; 1996. Ph.D. Thesis.
- Mukhtar Y. A. Roofs in Hot Dry Climates, *with special reference to northern Sudan*. *Overseas Building Notes-Information on Housing and Construction in Tropical and Sub-Tropical Countries*; 1978, Oct (No. 182).
- Muneer T., Solar Radiation & Daylight Models for the Energy Efficient Design of Buildings. Oxford, UK: Butterworth-Heinemann, 1997.
- Nahar N. M., Sharam P and Purohit M. M.; Studies on Solar Passive Cooling Techniques for arid areas. *Energy Conversation and Management* 1999; Vol.40 (No.3/4): pp.89-95.
- National Climatic Data Centre. [Web Page]; <http://www.ncdc.noaa.gov/>.
- Nicolakeas A. Passive Solar Design for Mediterranean Buildings the Greek Case. Manchester, UK: University of Manchester, 1989. M.Phil Thesis.
- Nini G. Thermal Effect of Roof on Comfort in Classrooms in Constantine. *World Renewable Energy Congress VII (WREC 2002)*, Elsevier Science Ltd 2002; ElSayigh, A.A. M. ed.
- Nohad A. Toulan., Climatic Considerations in the Design of Urban Housing in Egypt. *Housing in Arid Lands - Design and Planning*. London: The Architectural Press; 1984. (GOLANY, G.
- Norton J. Woodless Construction-1: An Overview. Building Advisory Service and Information Network 1995 Aug.
- Norton J. Woodless Construction: Unstabilised Earth Brick Vault Dome Roofing Without Formwork. *Building Issues* 1997; Vol: 9(No.2): pp:3-26.
- Nubian Vault Construction in Mexico using straw/ Clay blocks. [Web Page]; www.caeloproject.com [Accessed Jul 2002].
- O'Callaghan, P. W. *Building For Energy Conservation*, Pergamon Press, London, 1978.
- O'Sullivan P. Passive Solar Energy in Buildings; (1988). Report No.: *Watt Committee Report No. 17*.
- Olgay, V. *Design with climate: Bioclimatic Approach to architectural Regionalism*. New York: Some chapters based on cooperative research with Aladar Olgay, Van Nostrand Reinhold; 1992.
- Organisation for Economic Cooperation and Development OECD. Energy Statistics. [Web Page]; <http://www.oecd.org> .

Ozdeniz M.B., Bekleyen A., Gonul I. A. Vernacular Domed Houses of Harran in Turkey. *Habitat International* 1998; Vol.22 (No. 4): pp 477-85.

Pearlmutter D.; Erell E.; Etzion Y., (et al). Refining the use of evaporation in an experimental down-draft cool tower. 1996.

Pearson D. *Earth to Spirit - In Search of Natural Architecture*. Gaia books Ltd; 1994.

Peter Stead. *Lessons in Traditional and Vernacular Architecture in Arid Zones. Housing in Arid Lands - Design and Planning*. London: The Architectural Press; 1984. (GOLANY, G.

Physical modeling for thermal analysis of the urban built environment, *12th Passive solar conference proceedings, Solar' 87* (The American solar energy society & the solar energy society of Canada) 1987 Jul.

Profile: El-Wakil. *MIMAR 1: Architecture in Development* 1981; Singapore: Concept Media Ltd.

Promotion of Woodless Construction in Burkina Faso: Mali, and Niger Building and Social Housing Foundation; World Habitat Awards.

Raeissi S., Taheri M. Skytherm; an approach to year-round thermal energy sufficient houses. *Renewable Energy* 2000; Vol.19:pp. 527-43.

Raeissi Soona, Taheri M. Cooling Load Reduction of Buildings Using Passive Roof Options. *Renewable Energy* 1996; Vol. 7 (No. 3): pp. 301-13.

Rastorfer, Darl. *The Late Houses*. In Hassan Fathy. Singapore: Concept Media; 1985. (Hasan-Uddin Khan) ed.

Report by The Egyptian Research Housing Institute. Cairo, Egypt; (2000) (*In Arabic Language*).

Report by The Ministry of Housing. *Urban Planning & New Settlements Division*. Cairo, Egypt; (1999) (*In Arabic Language*).

Roland Stulz. *Roofing Primer; A Catalogue of Potential Solutions*. 1st ed. Switzerland: SKAT; 2000. (Karl Wehrle; Daniel Schwitter and SKAT, editors).

Runsheng Tang, Meir I. A., Etzion Y., Thermal Behaviour of Buildings with Curved Roofs as Compared with Flat Roofs. *Solar Energy* 2003 May;74:pp: 273-86.

Runsheng Tang, Meir I.A., Etzion Y., An Analysis of Absorbed Radiation by Domed and Vaulted Roofs as Compared with Flat Roofs. *Energy and Buildings* 2003; Vol. 35:pp: 539-48.

Salah El Din, O., Abdul Hamid, A. A., etal. *The Usage of Efficient Construction Techniques in Urban Settlements in the Desert areas*, Cairo, Egypt: Institute of Urban and Building Research, Ministry of Housing, Infrastructure and Urban Settlements; 1999 Dec. Report No.:1.

Saleh M. *Habitat International*, 1998; Vol. 22 (No. 4): pp 571-89.

Santelli, Serge; Rasem Badran; William Curtis, et al. *On Creativity, Imagination, and the Design Process, In Space for Freedom*, London: Butterworth Architecture; 1989. (Isma'ail Serageldin, ed..

Sayigh A. A. M., *Solar Energy Application in Buildings*, Academic Press, Inc 1979.

Sharah A., Shalabi B., Rousan A. and Tashtoush B. Effects of Absorptance of External Surfaces on Heating and cooling Loads of Residential Buildings in Jordan. *Energy Conversation and Management*, 1998; Vol.39 (No.3/4): pp. 273-84.

Solar Energy Application in Buildings, Edited by A.A.M. Sayigh.

- Sophia and Stefan Behling in Collaboration with Bruno Schindler Foreword by Norman Foster. *Solar Power The Evolution of Sustainable Architecture* 2000.
- Southern AER. *Earth Sun Geometry. A Quarterly Activity Bulletin of The South Carolina Department of Natural Resources-Southeast Regional Climate Center* 2001 Spring; Volume 7 (No. 1).
- Stasinopoulos, T. N. *Form Insolation Form Index; notes on the relation of geometric shape and solar irradiation, Environmentally Friendly Cities - Proceedings of PLEA 98 Passive and Low Energy Architecture; Lisbon, Portugal.* 1998.
- Stasinopoulos, T. N. *Geometric Forms & Insolation; An analytical Study of the Influence of Shape on Solar Irradiation*, Dept. of Architecture: National Technical University of Athens, Athens; 1999 Mar. Doctoral Dissertation.
- Steel J. *Sustainable Architecture - principles, paradigms, and case Studies* (1997).
- Steele J. *The Complete Architecture of Balkrishna Doshi - Rethinking Modernism for the Development*, London: Thames and Hudson Ltd.; 1998.
- Steele, James. *An Architecture for People: The Complete Works of Hassan Fathy*. London, United Kingdom: Thames and Hudson; 1997.
- Steele, James. *The Hassan Fathy Collection. A Catalogue of Visual Documents at the Aga Khan Award for Architecture*, Bern, Switzerland: The Aga Khan Trust for Culture, 54; 1989.
- Steele, James, *The Hassan Fathy Collection, A Catalogue of Visual Documents at the Aga Khan Award for Architecture*. Bern, Switzerland: The Aga Khan Trust for Culture, 84; 1989.
- Steele, James. *The Hassan Fathy Collection. All ArchNET Articles and Publications have been taken from: A Catalogue of Visual Documents at the Aga Khan Award for Architecture*. Bern, Switzerland: The Aga Khan Trust for Culture. 1984.
- Summerfield A. J. Hayman S., *On Capturing Context in Architecture*.
- Tabet Aoul K. *Bioclimatic Potentialities of Contemporary Housing- Architecture, Energy and Comfort in Algeria*.
- Taylor B. B. *Ramses Wissa Wassef Museum. MIMAR 35: Architecture in Development*. London, Concept Media Ltd 1990.
- The International American Agency for Development. *Solar Radiation Atlas for Egypt, Renewable Energy Authorisation: Ministry of Electricity and Energy*, Cairo; 1990.
- Tillman Lyle, John, *Regenerative Design for Sustainable Development*. New York, Wiley & Sons Inc.; (1994).
- Urban Settlements Authorisation. *Urban Structural and Texture planning for the Toshka Region*. 1st Edition, Cairo, Egypt: Ministry of Housing, Infrastructure and Urban Settlements; 1999.
- Victor M. Gomez-Munoz, Miguel Angel Porta-Gandara, Christopher Heard. *Solar Performance of Hemispherical Vault Roofs*. *Building and Environment* 2003 Dec; Vol.38(No.12):pp: 1431-8.
- Waewsak J., Hirunlabh J., Khadari J., Zeghamti B. *A Bio-Climatic Roof design for Hot and Humid Climate: Design Approach*. *World Renewable Energy Congress VII (WREC 2002)*, Elsevier Science Ltd. 2002.
- Weisstein, Eric W. *Circle - From Mathworld*. [Web Page] 1999; <http://mathworld.wolfram.com/ArcLength.html>. [Accessed 28 Aug 2002].

West S. Improving the sustainable development of building stock by the implementation of energy efficient and climate control technologies. *Building and Environment* 2001; Vol.36: pp 281-289.

World resources Institute "Dimensions of Sustainable Development". Washington, Dc: Report, WRI. (1990).

Yannas, S. & M. E. Environmentally Friendly Cities: *Proceedings of PLEA 98 Passive and Low Energy Architecture*. [Web Page] Jun 1998.

Zakaria N. Z., Woods P. Roof Design and Thermal Performance of Houses in Equatorial Climates. World Renewable Energy Congress VII (WREC 2002), Elsevier Science Ltd. 2002; ElSayigh, A. A. M. ed.

Abdel-Mone'im, Nagla M., Egypt Architecture Online. [Web Page] Jan 2001; <http://www.geocities.com/egyptarchitecture/> [Accessed 2 Mar 2002].

Aga Khan Award in Architecture. [Web Page]; <http://www.akaa98.org>

Agni-Jata. *Economic Earth Construction Designed by Ray Meeker* [Web Page]; www.auroville.org/thecity/architecture/angijata.htm [Accessed Jan 2001].

ARCHICAD 7.0 [A Comprehensive tool for Architecture, enables users to harness the power of integrated 3D modeling.].

Building Efficient Livable Houses. [Web Page] <http://www.aloha.net/~directarchitect.html>

Building Performance Simulation at The Start of The 3rd Millennium. *Building and Environment*. 2002; Vol. 37: pp 756-67.

Climatic Design of Buildings: An Over View. *BA (Arch studies) Year 1 Course No. 65156-Environmental science (Lecture 65156.7)*, www.arch.hku.hk/~cmhui/teach/

Earth Sun Geometry Applet. [Web Page]; <http://cwx.prenhall.com/bookbind/pubbooks/lutgens3/medialib/earthsun/earthsun.html>. [Accessed 11 Jan 2002].

Hassan Fathy main page and Biography, [Web Page]; www.geocities.com/egyptarchitect1/hasanfathi/hfmain.htm

History of Roofs *A Matter of Time*. [Web Page]; www.roofsindia.com/newhistoryofroofs.htm

ECOTECH V5 [The complete building design & environmental analysis tool. Square One's Flagship Software. It features a designer-friendly 3D modeling interface fully integrated with acoustic, thermal, lighting, solar and cost functions.

IES (VE Version 4.1) [Licensed Software University Package] Integrated Environmental Solutions Ltd. 2001.

Online World Atlas (2003 Maps.com): [Web Page]; www.maps.com/explore/atlas/ [Accessed 8 Aug 2002].

"SRSM" Solar Radiation Simulation Model for Quick Basic, Exell, R. H. B., Regional Energy Resources Information Center, Asian Institute of Technology, Bangkok. <http://www.jgsee.kmutt.ac.th/exell/Solar/SolradJS.htm>

SOM Architects. [Web Page]; <http://www.som.com> [Accessed Mar 2001].

APPENDICES

APPENDIX: A

- **Solar Radiation Simulation Model (*Inputs and Outputs*)**
SRSM
 - **Example Spreadsheets (*Vaults and Domes*)**
- **Other Generated Tables For Vaulted Roofs With Different Curvatures and Orientations**

This appendix reviews the Solar Radiation Simulation Model **SRSM** and gives some detailed information, which have been found within the model web site. <http://www.jgsee.kmutt.ac.th/exell/Solar/SolradJS.htm> [1].

This **Solar Radiation Simulator** is a program in *JavaScript* for generating numerical data with the same properties as real solar radiation data in the tropics. It is based on the **Solar Radiation Simulation Model for Quick Basic**.

The Solar Radiation Model for QuickBasic is an upgraded version of the program described in:

R. H. B. Exell [2], A program in BASIC for calculating solar radiation in tropical climates on small computers. *Renewable Energy Review Journal*, Vol. 8, No. 2, December 1986, Regional Energy Resources Information Center, Asian Institute of Technology, Bangkok.

The program can be copied as a text file and used with Microsoft QBasic software (Qbasic.exe and Qbasic.hlp) [1].

The data input values for each surface geometry (slope and orientation) has to be determined for the program in terms of angles (surface azimuth angle and tilt angle). The selected outputs (*the required*) also need to be identified before running the calculations as shown in Fig. (A-1). The generated data file then appears in a separate window as shown in the figure.

Data inputs:

1. Latitude (deg):

The selected latitude must be within the interval +25 deg (north of the equator) to -25 deg (south of the equator) because the model is correct only for the tropics. **The selected geographical location:** Aswan, Egypt (latitude 23.58N°).

2. Mean daily solar irradiation on a horizontal surface each month (MJ/m²):

Collected Solar Data (Aswan 23.58N°) [3]

Month	Collected Data			SRSM Calculations	
	1	2	3	4	5
	KWh/m2	MJ/m2	MJ/m2	MJ/m2	MJ/m2
Jan	4.7	16.92	12.69	18.4	13.8
Feb	5.65	20.34	15.255	21.8	16.35
Mar	6.61	23.796	17.847	25.7	19.275
Apr	7.41	26.676	20.007	28.8	21.6
May	7.68	27.648	20.736	30.4	22.8
Jun	8.02	28.872	21.654	30.8	23.1
Jul	7.94	28.584	21.438	30.5	22.875
Aug	7.45	26.82	20.115	29.3	21.975
Sep	6.76	24.336	18.252	26.8	20.1
Oct	5.81	20.916	15.687	23.2	17.4
Nov	7.96	28.656	21.492	19.5	14.625
Dec	4.39	15.804	11.853	17.4	13.05
(1)& (2): Clear Sky Irradiance "Collected Data"					
(3): 0.75 of Clearness Conditions (2)					
(4): Calculated Values from the Solar Radiation Simulator					
(5): 0.75 of Clearness Conditions (4)					
Unreliable Collected Data					

Table (A-1)

3. Orientation of tilted surface:

The *Azimuth (deg W)* is the angle between south (= zero degrees) and the direction in which the tilted surface is facing, measured towards the west. For example, west is 90 degrees, north is 180 degrees, and east is -90 degrees. The *Tilt angle (deg)* is the angle between the surface and the horizontal plane, which is the same as the angle between the normal to the surface and the zenith.

4. Days of the Year

You can do the calculation for the whole year (365 days), or for selected days at regular intervals. Day #1 is 1 January, day #2 is 2 January, day #365 is 31 December. The numbers which appear initially in the form compute data from day #17 to day #365 with daily step 30; in other words, one day in the middle of each month: 17 Jan, 16 Feb, 18 Mar, 17 Apr, 17 May, 16 Jun, 16 Jul, 15 Aug, 14 Sep, 14 Oct, 13 Nov, 13 Dec. Enter the first and last day, and the number of days in each interval step, to get data for the days you want.

Copyright © 1999 by R. H. B. Exell

Latitude of place for which simulation is to be done:
 Latitude (deg): Latitude must be in the range -25 to 25. *To be Provided from Table (A-1)*
 The latitude of central Thailand is shown. Change this to the latitude of your location.

Mean daily solar irradiation on a horizontal surface each month (MJ/m²):
 Jan: Feb: Mar: Apr: May: Jun:
 Jul: Aug: Sep: Oct: Nov: Dec:

Typical values for central Thailand are shown. Change them to the values for your location.

Orientation of tilted surface:
 Azimuth (deg W from S): Tilt angle (deg):
 The angles for a surface facing south tilted 15 degrees are shown. Change these angles to the angles for your surface.

Days of the year for which simulation is to be done:
 Compute data from day # to day # with daily step

Computation and Outputs:

Select simulated data to be included in file:

Day in the year.
 Daily clear sky global irradiation (MJ/m²). Mean daily global irradiation (MJ/m²).
 Hourly position of the sun:
 Azimuth of the sun (deg W from S). Zenith angle of the sun (deg).
 Hourly clear sky irradiance (W/m²):
 Global. Beam. Diffuse. Total on tilted surface.
 Mean hourly irradiance (W/m²):
 Global. Beam. Diffuse. Total on tilted surface.
 Random hourly irradiance (W/m²):
 Global. Beam. Diffuse. Total on tilted surface.

(Hourly values are at 6:00, 7:00, ..., 17:00, 18:00 apparent solar time.)

One Output For One Month (June)

```

16.7
95,82,69,57,46,39,36,39,46,57,69,82,95
0,136,409,660,851,973,1015,973,851,660,409,136,0
17.7
93,79,66,52,41,31,28,31,41,52,66,79,93
0,168,452,706,903,1030,1073,1030,903,706,452,168,0
19.1
90,76,62,47,34,22,16,22,34,47,62,76,90
0,202,485,736,935,1062,1105,1062,935,736,485,202,0
18.4
87,73,59,44,30,15,5,15,30,44,59,73,87
22,221,489,727,918,1039,1078,1039,918,727,489,221,22
17.8
85,71,57,43,29,15,4,15,29,43,57,71,85
32,224,472,695,874,987,1024,987,874,695,472,224,32
17.0
84,71,57,43,29,16,8,16,29,43,57,71,84
36,222,460,673,845,953,989,953,845,673,460,222,36
16.3
85,71,57,43,29,16,6,16,29,43,57,71,85
34,222,463,679,854,964,1000,964,854,679,463,222,34
16.0
86,72,58,43,29,15,1,15,29,43,58,72,86
27,221,478,707,891,1007,1045,1007,891,707,478,221,27
15.5
89,75,60,46,32,19,11,19,32,46,60,75,89
9,209,484,727,921,1044,1085,1044,921,727,484,209,9
16.2
92,78,64,50,38,27,23,27,38,50,64,78,92
0,182,464,714,910,1037,1080,1037,910,714,464,182,0
16.8
95,81,68,55,44,36,33,36,44,55,68,81,95
0,147,423,674,866,989,1032,989,866,674,423,147,0
16.3
96,83,70,58,48,41,38,41,48,58,70,83,96
0,126,394,643,831,951,993,951,831,643,394,126,0
End of Data File
                
```

```

0,136,409,660,851,973,1015,973,851,660,409,136,0
0,168,452,706,903,1030,1073,1030,903,706,452,168,0
0,202,485,736,935,1062,1105,1062,935,736,485,202,0
22,221,489,727,918,1039,1078,1039,918,727,489,221,22
32,224,472,695,874,987,1024,987,874,695,472,224,32
36,222,460,673,845,953,989,953,845,673,460,222,36
34,222,463,679,854,964,1000,964,854,679,463,222,34
27,221,478,707,891,1007,1045,1007,891,707,478,221,27
9,209,484,727,921,1044,1085,1044,921,727,484,209,9
0,182,464,714,910,1037,1080,1037,910,714,464,182,0
0,147,423,674,866,989,1032,989,866,674,423,147,0
0,126,394,643,831,951,993,951,831,643,394,126,0
End of Data File
                
```

(December)

More than One Output For One Month (June)

As mentioned in the thesis chapters, along side with using the model results for sloped surfaces, the author had to develop a large number of Microsoft Excel Spreadsheets in order to supplement the evaluation of the solar behaviour of different curved-roof, forms, curvatures and orientations. Due to the oversize of these spreadsheets, Appendix (A) are illustrates only samples of these spreadsheets. The following pages of this appendix show spreadsheets for vaulted-roof with different curvatures facing (N-S) in summer. Each curved-roof cross-section is resembled with 19-planar-segments, however, similar spreadsheets for 37-planar-segments have been generated for the same tested curved-roof curvatures. A key for vaulted-roof spreadsheets is presented below.

	6:00	7:00	8:00	9:00	10:00	11:00	12:00	13:00	14:00	15:00	16:00	17:00	18:00	Day Av.	
Planar Segment Slope Angles (South facing Half)	83.37	26	45	55	59	118	165	181	165	118	59	55	45	26	
	75.33	29	50	62	149	241	300	320	300	241	149	62	50	29	
	64.79	33	57	141	279	395	470	495	470	395	279	141	57	33	
	55.04	36	63	229	392	528	614	643	614	528	392	229	63	36	
	46.09	36	132	335	527	684	784	817	784	684	527	335	132	36	
	35.11	42	177	391	590	753	856	889	856	753	590	391	177	42	
25.39	44	228	456	665	834	940	975	940	834	665	456	228	44		
14.5	69	278	515	727	898	1004	1039	1004	898	727	515	278	69		
6.5	90	310	548	757	925	1030	1064	1030	925	757	548	310	90		
0	106	332	567	772	935	1037	1070	1037	935	772	567	332	106	659	
6.5n	121	351	580	778	934	1031	1062	1031	934	778	580	351	121		
14.5n	138	368	587	772	917	1007	1036	1007	917	772	587	368	138		
25.39n	157	380	579	741	867	944	969	944	867	741	579	380	157		
35.11n	170	382	556	692	798	861	882	861	798	692	556	382	170		
46.09n	179	371	512	616	694	740	754	740	694	616	512	371	179		
55.04n	183	354	464	538	592	623	632	623	592	538	464	354	183		
64.79n	182	326	400	440	466	479	482	479	466	440	400	326	182		
75.33n	176	287	319	321	316	310	307	310	316	321	319	287	176		
83.37n	169	251	251	224	196	175	167	175	196	224	251	251	169		
CCS_s	105	280	397	528	636.4	704	725	704	636.4	528	397	280	105	459	
82.16	26	45	56	63	137	186	202	186	137	63	56	45	26		
67.34	32	55	117	248	289	420	454	420	289	117	55	32			
53.17	37	73	246	413	552	641	670	641	552	413	246	73	37		

Hourly Curved-roof $I_{(HTCS)}$ W/m^2 throughout daytime hours

Day-average of $I_{(HTCS)}$ W/m^2 received on Curved-roof

$I_{(HTCS)}$ W/m^2 received on Curved-roof at particular hour

Column presents the solar behaviour of different parts of the curved roof during particular hour

Vaulted-roof Spreadsheet Key

Spreadsheet Example For Vaults

$I_{(HTCS)}$ W/m² on 19 Joint Planar Segments CCS₁-CCS₇

(ASWAN 23.58°N) June (Vault Full Cross- Section) (N-S)

	6:00	7:00	8:00	9:00	10:00	11:00	12:00	13:00	14:00	15:00	16:00	17:00	18:00	Day Av.
83.37	26	45	55	59	118	165	181	165	118	59	55	45	26	
75.33	29	50	62	149	241	300	320	300	241	149	62	50	29	
64.79	33	57	141	279	395	470	495	470	395	279	141	57	33	
55.04	36	63	229	392	528	614	643	614	528	392	229	63	36	
46.09	36	132	335	527	684	784	817	784	684	527	335	132	36	
35.11	42	177	391	590	753	856	889	856	753	590	391	177	42	
25.39	44	228	456	665	834	940	975	940	834	665	456	228	44	
14.5	69	278	515	727	898	1004	1039	1004	898	727	515	278	69	
6.5	90	310	548	757	925	1030	1064	1030	925	757	548	310	90	
0	106	332	567	772	935	1037	1070	1037	935	772	567	332	106	659
6.5n	121	351	580	778	934	1031	1062	1031	934	778	580	351	121	
14.5n	138	368	587	772	917	1007	1036	1007	917	772	587	368	138	
25.39n	157	380	579	741	867	944	969	944	867	741	579	380	157	
35.11n	170	382	556	692	798	861	882	861	798	692	556	382	170	
46.09n	179	371	512	616	694	740	754	740	694	616	512	371	179	
55.04n	183	354	464	538	592	623	632	623	592	538	464	354	183	
64.79n	182	326	400	440	466	479	482	479	466	440	400	326	182	
75.33n	176	287	319	321	316	310	307	310	316	321	319	287	176	
83.37n	169	251	251	224	196	175	167	175	196	224	251	251	169	
CCS₁	105	250	397	528	636.4	704	725	704	636.4	528	397	250	105	459

82.16	26	45	56	63	137	186	202	186	137	63	56	45	26	
67.34	32	55	117	248	358	430	454	430	358	248	117	55	32	
53.13	37	73	246	413	552	641	670	641	552	413	246	73	37	
42.27	40	136	337	525	680	779	811	779	680	525	337	136	40	
32.6	43	190	409	611	776	880	914	880	776	611	409	190	43	
24.39	44	233	462	671	841	947	982	947	841	671	462	233	44	
16.35	64	270	506	718	889	996	1031	996	889	718	506	270	64	
11.08	78	293	530	742	911	1017	1052	1017	911	742	530	293	78	
5.13	93	315	553	761	928	1032	1066	1032	928	761	553	315	93	
0	106	332	567	772	935	1037	1070	1037	935	772	567	332	106	659
5.13n	118	347	578	777	935	1033	1065	1033	935	777	578	347	118	
11.08n	131	361	585	776	926	1019	1049	1019	926	776	585	361	131	
16.35n	141	371	587	768	911	998	1027	998	911	768	587	371	141	
24.39n	155	380	580	745	873	951	976	951	873	745	580	380	155	
32.6n	167	382	563	707	818	885	906	885	818	707	563	382	167	
42.27n	176	376	529	645	733	785	802	785	733	645	529	376	176	
53.13n	182	358	475	556	615	649	659	649	615	556	475	358	182	
67.34n	181	317	381	412	431	439	441	439	431	412	381	317	181	
82.16n	170	257	262	239	214	196	189	196	214	239	262	257	170	
CCS₂	104	268	438	587	708.6	784	809	784	708.6	587	438	268	104	507

	6:00	7:00	8:00	9:00	10:00	11:00	12:00	13:00	14:00	15:00	16:00	17:00	18:00	Day Av.
68.15	32	55	109	238	347	417	440	417	347	238	109	55	32	
45.36	39	119	312	495	646	742	774	742	646	495	312	119	39	
32.17	43	192	412	614	779	884	918	884	779	614	412	192	43	
24.34	44	233	462	672	841	984	983	984	841	672	462	233	44	
15.75	66	273	509	721	892	999	1034	999	892	721	509	273	66	
13.05	73	284	522	734	904	1010	1045	1010	904	734	522	284	73	
9.18	83	300	538	749	918	1023	1058	1023	918	749	538	300	83	
6.24	91	311	549	758	926	1030	1064	1030	926	758	549	311	91	
4.14	96	319	556	764	930	1034	1068	1034	930	764	556	319	96	
0	106	332	567	772	935	1037	1070	1037	935	772	567	332	106	659
4.14n	116	344	576	777	936	1034	1067	1034	936	777	576	344	116	
6.24n	120	350	580	778	934	1031	1063	1031	934	778	580	350	120	
9.18n	127	357	584	777	930	1025	1056	1025	930	777	584	357	127	
13.05n	135	365	586	774	921	1031	1042	1031	921	774	586	365	135	
15.75n	140	370	587	769	913	1001	1030	1001	913	769	587	370	140	
24.34n	155	380	580	745	873	952	977	952	873	745	580	380	155	
32.17n	166	382	564	709	821	889	911	889	821	709	564	382	166	
45.36n	179	372	515	622	702	749	764	749	702	622	515	372	179	
68.15n	181	314	375	403	419	426	428	426	419	403	375	314	181	
CCS₃	105	297	499	677	819.3	910	936	910	819.3	677	499	297	105	581

68.88	13	54	103	229	336	405	429	405	336	229	103	54	13	
43.94	40	127	323	509	662	759	791	759	662	509	323	127	40	
28.95	43	209	433	639	806	912	946	912	806	639	433	209	43	
19.77	55	255	489	700	870	977	1012	977	870	700	489	255	55	
14.03	70	280	517	729	900	1006	1041	1006	900	729	517	280	70	
10.82	79	294	531	743	912	1018	1053	1018	912	743	531	294	79	
7.35	88	307	545	755	923	1028	1062	1028	923	755	545	307	88	
5.84	92	313	550	759	927	1031	1065	1031	927	759	550	313	92	
3.75	97	320	557	765	931	1034	1068	1034	931	765	557	320	97	
0	106	332	567	772	935	1037	1070	1037	935	772	567	332	106	659
3.75n	115	343	576	776	936	1035	1067	1035	936	776	576	343	115	
5.84n	119	349	579	778	935	1032	1064	1032	935	778	579	349	119	
7.35n	123	353	582	778	933	1029	1060	1029	933	778	582	353	123	
10.82n	130	361	585	776	927	1020	1050	1020	927	776	585	361	130	
14.03n	137	367	587	772	919	1009	1038	1009	919	772	587	367	137	
19.77n	147	375	585	760	897	981	1008	981	897	760	585	375	147	
28.95n	162	382	572	725	844	917	940	917	844	725	572	382	162	
43.94n	178	374	522	633	716	766	782	766	716	633	522	374	178	
68.88n	181	312	370	395	409	415	416	415	409	395	370	312	181	
CCS ₄	104	300	504	684	827.3	916	945	916	827.3	684	504	300	104	586

	6:00	7:00	8:00	9:00	10:00	11:00	12:00	13:00	14:00	15:00	16:00	17:00	18:00	Day Av.
86.74	24	42	52	56	67	108	122	108	67	56	52	42	24	
81.94	26	46	56	66	140	189	206	189	140	66	56	46	26	
74.45	29	51	63	160	254	315	335	315	254	160	63	51	29	
66.5	32	56	125	258	370	443	467	443	370	258	125	56	32	
57.66	35	61	206	363	493	577	605	577	493	363	206	61	35	
47.78	39	104	292	470	618	712	743	712	618	470	292	104	39	
35.38	42	175	389	588	750	853	887	853	750	588	389	175	42	
22.16	48	243	475	686	856	962	997	962	856	686	475	243	48	
6.82	89	309	547	757	924	1029	1063	1029	924	757	547	309	89	
0	106	332	567	772	935	1037	1070	1037	935	772	567	332	106	659
6.82n	122	351	581	778	934	1030	1062	1030	934	778	581	351	122	
22.16n	151	378	583	753	885	966	992	966	885	753	583	378	151	
35.38n	170	382	555	691	796	859	879	859	796	691	555	382	170	
47.78n	180	368	504	602	676	719	733	719	676	602	504	368	180	
57.66n	183	347	447	513	559	585	593	585	559	513	447	347	183	
66.5n	182	320	387	421	442	452	455	452	442	421	387	320	182	
74.45n	177	290	326	331	329	325	322	325	329	331	326	290	177	
81.94n	170	258	264	242	218	199	193	199	218	242	264	258	170	
86.74n	164	235	222	183	145	118	108	118	145	183	222	235	164	
CCS ₅	104	229	350	457	547	604	623	604	547	457	350	229	104	400

87.32	24	42	52	55	58	98	112	98	58	55	52	42	24	
84.67	24	44	54	58	98	143	158	143	98	58	54	44	24	
81.46	27	46	57	72	148	198	214	198	148	72	57	46	27	
77.19	28	49	60	126	212	269	288	269	212	126	60	49	28	
71.09	31	53	82	202	304	370	392	370	304	202	82	53	31	
64.35	33	57	145	284	401	477	502	477	401	284	145	57	33	
53.81	37	69	240	406	543	631	661	631	543	406	240	69	37	
37.82	41	162	371	567	727	828	861	828	727	567	371	162	41	
13.89	71	281	518	730	900	1007	1042	1007	900	730	518	281	71	
0	106	332	567	772	935	1037	1070	1037	935	772	567	332	106	659
13.89n	136	367	587	773	919	1009	1038	1009	919	773	587	367	136	
37.82n	172	380	546	676	775	834	853	834	775	676	546	380	172	
53.81n	182	356	471	549	607	640	650	640	607	549	471	356	182	
64.35n	182	327	403	444	472	486	489	486	472	444	403	327	182	
71.09n	179	303	353	370	378	379	379	379	378	370	353	303	179	
77.19n	175	279	304	299	289	279	275	279	289	299	304	279	175	
81.46n	171	260	268	248	225	208	201	208	225	248	268	260	171	
84.67n	167	245	240	208	176	153	145	153	176	208	240	245	167	
87.32n	164	232	217	175	136	108	98	108	136	175	217	232	164	
CCS ₆	103	204	291	369	437	482	496	482	437	369	291	204	103	328

	6:00	7:00	8:00	9:00	10:00	11:00	12:00	13:00	14:00	15:00	16:00	17:00	18:00	Day Av.
89.1	23	41	50	54	56	67	80	67	56	54	50	41	23	
85.6	25	43	53	57	84	127	142	127	84	57	53	43	25	
82.7	26	45	56	60	129	176	193	176	129	60	56	45	26	
79.8	27	47	58	93	173	226	243	226	173	93	58	47	27	
75.13	29	50	62	152	244	304	324	304	244	152	62	50	29	
68	32	55	111	240	349	419	443	419	349	240	111	55	32	
59.9	35	60	185	337	463	544	571	544	463	337	185	60	35	
44.3	40	125	320	506	658	755	787	755	658	506	320	125	40	
15.94	65	272	508	720	891	998	1033	998	891	720	508	272	65	
0	106	332	567	772	935	1037	1070	1037	935	772	567	332	106	659
15.94n	140	370	587	769	912	1000	1029	1000	912	769	587	370	140	
44.3n	178	374	520	630	713	762	777	762	713	630	520	374	178	
59.9n	183	341	433	491	531	553	559	553	531	491	433	341	183	
68n	181	315	376	405	421	429	430	429	421	405	376	315	181	
75.13n	177	287	321	323	319	313	311	313	319	323	321	287	177	
79.8n	172	267	282	268	250	236	230	236	250	268	282	267	172	
82.7n	169	254	257	233	206	187	179	187	206	233	257	254	169	
85.6n	166	240	232	197	162	137	128	137	162	197	232	240	166	
89.1n	161	223	201	153	108	78	66	78	108	153	201	223	161	
CCS ₇	102	197	273	340	400	439	452	439	400	340	273	197	102	304

The following pages of this appendix show spreadsheets for domed-roof curvatures. Each domed-roof geometry is resembled by 18 rings, each ring has the same tilted angle and comprises of 24-plabnar-segments with different orientations (*different azimuth angles*). A key for domed-roof spreadsheets is presented below.

	06:00	07:00	08:00	09:00	10:00	11:00	12:00	13:00	14:00	15:00	16:00	17:00	18:00	
0	23	40	49	53	56	64	57	64	56	53	49	40	23	48.23
15	23	40	49	53	56	57	64	111	128	116	78	40	23	64.46
30	23	40	49	53	56	57	64	130	165	166	135	77	23	79.85
45	23	40	49	53	56	57	62	213	330	379	404	336	173	167.3
60	23	40	49	53	56	57	61	250	406	507	536	468	257	212.5
75	23	40	49	53	56	57	59	274	458	585	635	570	325	244.9
90	23	40	49	53	56	57	57	283	483	628	649	637	372	260.5
105	23	40	49	53	56	57	57	277	478	631	709	662	369	266.2
120	23	40	49	53	56	57	57	255	445	595	679	646	349	254.2
135	23	40	49	53	56	57	57	220	385	523	607	588	367	232.7
150	23	40	49	53	56	57	57	174	303	418	496	493	316	195
165	65	58	49	53	56	57	57	120	204	288	355	367	246	151.9
180	160	218	193	142	95	62	57	62	95	142	193	218	160	138.2
-165	246	367	355	288	204	120	57	57	56	53	49	58	65	151.9
-150	265	456	460	377	257	123	58	58	56	53	49	39	21	174.8
-135	367	588	607	523	385	220	57	57	56	53	49	40	23	232.7
-120	394	646	679	595	445	255	57	57	56	53	49	40	23	257.6
-105	396	662	709	631	478	277	57	57	56	53	49	40	23	268.3
-90	372	637	694	628	483	283	57	57	56	53	49	40	23	264
-75	325	570	635	585	458	274	59	57	56	53	49	40	23	244.9
-60	257	468	536	507	406	250	61	57	56	53	49	40	23	212.5
-45	173	336	404	397	330	213	62	57	56	53	49	40	23	168.7
-30	79	184	248	263	235	166	63	57	56	53	49	40	23	116.6
-15	23	40	78	116	128	111	64	57	56	53	49	40	23	64.46
R1	141	236	258	237	191	127	59.1	128	190	234	253	233	137	186
0	25	44	54	58	93	137	152	137	93	58	54	44	25	74.92
15	25	44	54	58	60	79	152	196	205	178	123	48	25	95.6
30	25	44	54	58	60	62	152	251	311	325	292	209	86	148.4

24 Azimuth Angles

Ring with particular slope angle. The ring comprises of 24 planar-segments

Day-average of $I_{(HTCS)}$ W/m^2 received on one ring
Each Dome comprises of 18 rings

Domed-roof Spreadsheet Key

Spreadsheet Example For Domes

(ASWAN 23.58°N) Dome ₁ (A=B) June														
	06:00	07:00	08:00	09:00	10:00	11:00	12:00	13:00	14:00	15:00	16:00	17:00	18:00	
0	23	40	49	53	56	64	57	64	56	53	49	40	23	48.23
15	23	40	49	53	56	57	64	111	128	116	78	40	23	64.46
30	23	40	49	53	56	57	64	130	165	166	135	77	23	79.85
45	23	40	49	53	56	57	62	213	330	379	404	336	173	167.3
60	23	40	49	53	56	57	61	250	406	507	536	468	257	212.5
75	23	40	49	53	56	57	59	274	458	585	635	570	325	244.9
90	23	40	49	53	56	57	57	283	483	628	649	637	372	260.5
105	23	40	49	53	56	57	57	277	478	631	709	662	369	266.2
120	23	40	49	53	56	57	57	255	445	595	679	646	349	254.2
135	23	40	49	53	56	57	57	220	385	523	607	588	367	232.7
150	23	40	49	53	56	57	57	174	303	418	496	493	316	195
165	65	58	49	53	56	57	57	120	204	288	355	367	246	151.9
180	160	218	193	142	95	62	57	62	95	142	193	218	160	138.2
-165	246	367	355	288	204	120	57	57	56	53	49	58	65	151.9
-150	265	456	460	377	257	123	58	58	56	53	49	39	21	174.8
-135	367	588	607	523	385	220	57	57	56	53	49	40	23	232.7
-120	394	646	679	595	445	255	57	57	56	53	49	40	23	257.6
-105	396	662	709	631	478	277	57	57	56	53	49	40	23	268.3
-90	372	637	694	628	483	283	57	57	56	53	49	40	23	264
-75	325	570	635	585	458	274	59	57	56	53	49	40	23	244.9
-60	257	468	536	507	406	250	61	57	56	53	49	40	23	212.5
-45	173	336	404	397	330	213	62	57	56	53	49	40	23	168.7
-30	79	184	248	263	235	166	63	57	56	53	49	40	23	116.6
-15	23	40	78	116	128	111	64	57	56	53	49	40	23	64.46
R1	141	236	258	237	191	127	59.1	128	190	234	253	233	137	186
0	25	44	54	58	93	137	152	137	93	58	54	44	25	74.92
15	25	44	54	58	60	79	152	196	205	178	123	48	25	95.92
30	25	44	54	58	60	62	152	251	311	325	292	209	86	148.4
45	25	44	54	58	60	62	150	298	406	458	448	360	180	200.2
60	25	44	54	58	60	62	149	335	481	567	580	491	263	243.8
75	25	44	54	58	60	62	147	359	533	646	678	594	331	276.2
90	25	44	54	58	60	62	146	368	558	689	737	660	378	295.3
105	25	44	54	58	60	62	144	361	553	692	752	689	401	299.6
120	25	44	54	58	60	62	142	340	520	656	722	669	400	288.6
135	25	44	54	58	60	62	141	305	461	583	650	611	373	263.6
150	25	44	54	58	60	62	140	259	379	479	539	516	322	225.9
165	25	44	54	58	60	89	139	206	280	349	399	391	252	180.5
180	167	243	237	204	171	148	139	148	171	204	237	243	167	190.7
-165	252	391	399	349	280	206	139	89	60	58	66	83	72	188
-150	322	516	539	479	379	259	140	62	60	58	54	44	25	225.9
-135	378	611	650	583	461	305	141	62	60	58	54	44	25	264
-120	400	669	722	656	520	340	142	62	60	58	54	44	25	288.6
-105	401	689	752	692	553	361	144	62	60	58	54	44	25	299.6
-90	378	660	737	689	558	368	146	62	60	58	54	44	25	295.3
-75	331	594	678	646	533	359	147	62	60	58	54	44	25	276.2
-60	263	491	580	567	481	335	149	62	60	58	54	44	25	243.8
-45	180	360	448	458	406	298	150	62	60	58	54	44	25	200.2
-30	86	209	292	325	311	251	152	62	60	58	54	44	25	148.4
-15	25	48	123	178	205	196	152	79	60	58	54	44	25	95.92
R2	145	250	284	272	234	179	146	179	234	272	284	252	147	221
0	27	47	58	90	170	222	240	222	170	90	58	47	27	112.9
15	27	47	58	62	65	165	240	280	280	240	168	73	27	133.2
30	27	47	58	62	65	112	239	334	385	385	335	232	93	182.6
45	27	47	58	62	65	67	238	381	479	516	489	382	185	230.5
60	27	47	58	62	65	67	237	417	553	625	619	512	268	273.6
75	27	47	58	62	65	67	235	441	605	702	716	613	335	305.6
90	27	47	58	62	65	67	233	450	629	744	774	678	381	324.2
105	27	47	58	62	65	67	231	443	625	748	789	704	404	328.5
120	27	47	58	62	65	67	230	422	592	712	760	687	402	317.8
135	27	47	58	62	65	73	228	388	533	640	688	630	376	293.5
150	27	47	58	62	65	120	227	343	452	537	579	537	326	260
165	27	47	58	62	65	120	227	343	452	537	579	537	326	260
180	172	266	280	265	247	232	226	232	247	265	280	266	172	242.3
-165	257	412	440	409	354	290	227	174	137	116	111	108	79	239.5
-150	326	537	579	537	452	343	227	120	65	62	58	47	27	260
-135	376	630	688	640	533	388	228	73	65	62	58	47	27	293.5
-120	402	687	760	712	592	422	230	67	65	62	58	47	27	317.8

-105	404	704	789	748	625	443	231	67	65	62	58	47	27	328.5
-90	381	678	774	744	629	450	233	67	65	62	58	47	27	324.2
-75	335	613	716	702	605	441	235	67	65	62	58	47	27	305.6
-60	268	512	619	625	553	417	237	67	65	62	58	47	27	273.6
-45	185	382	489	516	479	381	238	67	65	62	58	47	27	230.5
-30	93	232	335	385	385	334	239	112	65	62	58	47	27	182.6
-15	27	73	168	240	280	280	240	165	65	62	58	47	27	133.2
R3	148	262	306	304	276	235	233	239	283	312	314	270	153	256
0	29	50	62	153	245	306	326	306	245	153	62	50	29	155.1
15	29	50	62	67	140	249	326	362	354	300	211	98	29	175.2
30	29	50	62	67	70	197	325	416	457	442	375	255	99	218.8
45	29	50	62	67	70	153	324	462	548	571	526	401	189	265.5
60	29	50	62	67	70	119	323	497	622	677	654	529	270	305.3
75	29	50	62	67	70	98	321	520	672	753	749	628	336	335
90	29	50	62	67	70	92	319	529	696	795	806	692	382	353
105	29	50	62	67	70	101	318	523	692	798	821	717	404	357.8
120	29	50	62	67	70	124	316	502	659	763	792	701	403	349.1
135	29	50	62	67	70	160	315	468	602	693	722	645	376	327.6
150	29	50	62	67	110	206	314	424	522	591	615	553	328	297.8
165	85	133	156	178	213	259	313	372	427	466	478	431	259	290
180	177	288	322	325	321	316	313	316	321	325	322	288	177	293.2
-165	259	431	478	466	427	372	313	259	213	178	156	133	85	290
-150	328	553	615	591	522	424	314	206	110	67	62	50	29	297.8
-135	376	645	722	693	602	468	315	160	70	67	62	50	29	327.6
-120	403	701	792	763	659	502	316	124	70	67	62	50	29	349.1
-105	404	717	821	798	692	523	318	101	70	67	62	50	29	357.8
-90	382	692	806	795	696	529	319	92	70	67	62	50	29	353
-75	328	553	615	591	522	424	314	206	110	67	62	50	29	297.8
-60	270	529	654	677	622	497	323	119	70	67	62	50	29	305.3
-45	189	401	526	571	548	462	324	153	70	67	62	50	29	265.5
-30	99	255	375	442	457	416	325	197	70	67	62	50	29	218.8
-15	29	98	211	300	354	362	326	249	140	67	62	50	29	175.2
R4	152	273	324	334	320	307	319	315	328	341	330	276	152	290
0	31	54	92	215	320	387	410	387	320	215	92	54	31	
15	31	54	66	78	217	333	410	442	425	358	254	123	31	
30	31	54	66	71	124	282	409	494	525	497	413	275	104	
45	31	54	66	71	75	239	408	539	614	622	560	418	192	
60	31	54	66	71	75	206	407	574	686	725	684	542	271	
75	31	54	66	71	75	186	405	596	735	799	777	638	335	
90	31	54	66	71	75	180	404	604	758	839	833	701	379	
105	31	54	66	71	75	188	402	598	754	843	847	725	401	
120	31	54	66	71	75	211	400	578	722	809	819	709	400	
135	31	54	66	71	99	245	399	546	666	740	750	655	374	
150	31	54	66	101	188	290	398	502	589	642	646	565	327	
165	91	157	200	240	288	342	397	452	496	520	513	447	261	
180	180	308	361	382	393	397	397	397	393	382	361	308	180	
-165	261	447	513	520	496	452	397	342	288	240	200	157	91	
-150	327	565	646	642	589	502	398	290	188	101	66	54	31	
-135	374	655	750	740	666	546	399	245	99	71	66	54	31	
-120	400	709	819	809	722	578	400	211	75	71	66	54	31	
-105	401	725	847	843	754	598	402	188	75	71	66	54	31	
-90	379	701	833	839	758	604	404	180	75	71	66	54	31	
-75	335	638	777	799	735	596	405	186	75	71	66	54	31	
-60	271	542	684	725	686	574	407	206	75	71	66	54	31	
-45	192	418	560	622	614	539	408	239	75	71	66	54	31	
-30	104	275	413	497	525	494	409	282	124	71	66	54	31	
-15	31	123	254	358	425	442	410	333	217	78	66	54	31	
R5	154	286	350	374	377	392	404	392	377	374	350	286	154	328
0	33	57	139	276	392	466	491	466	392	276	139	57	33	
15	33	57	70	144	293	414	491	520	493	414	294	147	33	
30	33	57	70	75	203	365	491	569	590	548	448	294	109	
45	33	57	70	75	129	323	490	613	676	668	590	432	194	
60	33	57	70	75	79	291	488	646	745	768	710	551	270	
75	33	57	70	75	79	272	487	668	792	840	799	644	331	
90	33	57	70	75	79	266	485	676	814	878	853	704	374	
105	33	57	70	75	79	274	484	670	810	881	866	728	396	
120	33	57	70	75	110	296	482	651	780	849	839	713	394	
135	33	57	70	75	179	329	481	619	726	782	773	660	369	
150	33	57	88	166	265	373	480	577	652	687	673	574	324	
165	96	180	242	300	361	423	479	529	562	570	545	460	260	
180	182	325	398	437	463	476	479	476	463	437	398	325	182	
-165	260	460	545	570	562	529	479	423	361	300	242	180	96	

-150	324	574	673	687	652	577	480	373	265	166	88	57	33	
-135	369	660	773	782	726	619	481	329	179	75	70	57	33	
-120	394	713	839	849	780	651	482	296	110	75	70	57	33	
-105	396	728	866	881	810	670	484	274	79	75	70	57	33	
-90	374	704	853	878	814	676	485	266	79	75	70	57	33	
-75	331	644	799	840	792	668	487	272	79	75	70	57	33	
-60	270	551	710	768	745	646	488	291	79	75	70	57	33	
-45	194	432	590	668	676	613	490	323	129	75	70	57	33	
-30	109	294	448	548	590	569	491	365	203	75	70	57	33	
-15	33	147	294	414	493	520	491	414	293	144	70	57	33	
R6	154	293	370	409	431	471	485	471	431	409	370	293	154	365
0	35	60	185	336	462	542	569	542	462	336	185	60	35	
15	35	60	74	209	367	492	569	593	558	467	333	171	35	
30	35	60	74	97	281	445	569	641	651	595	480	311	113	
45	35	60	74	79	210	405	568	682	733	710	616	442	194	
60	35	60	74	79	158	375	566	714	799	805	730	556	267	
75	35	60	74	79	129	357	565	735	844	874	816	645	326	
90	35	60	74	79	126	351	564	743	865	911	867	703	367	
105	35	60	74	79	147	359	562	737	861	914	880	725	387	
120	35	60	74	79	192	380	561	719	833	882	854	711	385	
135	35	60	74	115	258	412	559	688	781	819	791	661	362	
150	35	62	137	230	340	453	558	649	710	728	695	578	318	
165	101	202	284	358	432	500	558	602	624	616	573	469	257	
180	183	341	432	490	529	551	558	551	529	490	432	341	183	
-165	257	469	573	616	624	602	558	500	432	358	284	202	101	
-150	318	578	695	728	710	649	558	453	340	230	137	62	35	
-135	362	661	791	819	781	688	559	412	258	115	74	60	35	
-120	385	711	854	882	833	719	561	380	192	79	74	60	35	
-105	387	725	880	914	861	737	562	359	147	79	74	60	35	
-90	367	703	867	911	865	743	564	351	126	79	74	60	35	
-75	326	645	816	874	844	735	565	357	129	79	74	60	35	
-60	267	556	730	805	799	714	566	375	158	79	74	60	35	
-45	194	442	616	710	733	682	568	405	210	79	74	60	35	
-30	113	311	480	595	651	641	569	445	281	97	74	60	35	
-15	35	171	333	467	558	593	569	492	367	209	74	60	35	
R7	153	299	389	443	495	547	564	547	495	443	389	299	153	401
0	36	63	229	393	528	615	644	615	528	393	229	63	36	
15	36	63	97	273	439	567	643	663	620	517	370	193	36	
30	36	63	78	167	357	523	643	708	707	638	509	326	116	
45	36	63	78	83	290	485	642	747	785	747	637	450	193	
60	36	63	78	83	241	457	641	777	847	837	745	558	262	
75	36	63	78	83	214	439	639	797	890	902	826	642	318	
90	36	63	78	83	210	434	638	804	910	937	875	696	356	
105	36	63	78	83	231	441	637	799	906	939	887	717	376	
120	36	63	78	94	273	461	635	781	879	910	863	704	374	
135	36	63	78	184	335	491	634	753	830	850	803	656	352	
150	36	90	184	293	413	530	633	715	763	764	712	578	311	
165	105	222	323	414	501	575	633	671	682	658	597	475	253	
180	183	354	464	538	592	623	632	623	592	538	464	354	183	
-165	253	475	597	658	682	671	633	575	501	414	323	222	105	
-150	311	578	712	764	763	715	633	530	413	293	184	90	36	
-135	352	656	803	850	830	753	634	491	335	184	78	63	36	
-120	374	704	863	910	879	781	635	461	273	94	78	63	36	
-105	376	717	887	939	906	799	637	441	231	83	78	63	36	
-90	356	696	875	937	910	804	638	434	210	83	78	63	36	
-75	318	642	826	902	890	797	639	439	214	83	78	63	36	
-60	262	558	745	837	847	777	641	457	241	83	78	63	36	
-45	193	450	637	747	785	747	642	485	290	83	78	63	36	
-30	116	326	509	638	707	708	643	523	357	167	78	63	36	
-15	36	193	370	517	620	663	643	567	439	273	97	63	36	
R8	151	304	406	478	560	619	638	619	560	478	406	304	151	436
0	38	91	273	447	591	683	713	683	591	447	273	91	38	
15	38	66	149	335	507	638	713	728	677	563	404	214	44	
30	38	66	81	236	432	597	713	770	759	677	534	338	119	
45	38	66	81	156	369	562	712	806	831	779	654	454	191	
60	38	66	81	100	323	535	711	835	889	863	755	555	255	
75	38	66	81	87	297	519	709	853	929	923	831	634	307	
90	38	66	81	87	294	514	708	860	948	956	876	685	344	
105	38	66	81	107	313	521	707	855	945	958	888	705	362	
120	38	66	81	168	353	539	705	839	919	931	865	692	360	
135	38	66	111	252	411	567	704	812	874	875	809	648	339	
150	38	118	230	354	483	604	704	777	811	795	724	575	301	


165	108	242	360	467	565	646	703	735	735	695	616	478	247	
180	181	364	492	583	651	691	703	691	651	583	492	364	181	
-165	247	478	616	695	735	735	703	646	565	467	360	242	108	
-150	301	575	724	795	811	777	704	604	483	354	230	118	38	
-135	339	648	809	875	874	812	704	567	411	252	111	66	38	
-120	360	692	865	931	919	839	705	539	353	168	81	66	38	
-105	362	705	888	958	945	855	707	521	313	107	81	66	38	
-90	344	685	876	956	948	860	708	514	294	87	81	66	38	
-75	307	634	831	923	929	853	709	519	297	87	81	66	38	
-60	255	555	755	863	889	835	711	535	323	100	81	66	38	
-45	191	454	654	779	831	806	712	562	369	156	81	66	38	
-30	119	338	534	677	759	770	713	597	432	236	81	66	38	
-15	44	214	404	563	677	728	713	638	507	335	149	66	38	
R9	149	308	422	516	621	687	708	687	621	516	422	308	149	470
0	39	121	315	499	650	746	778	746	650	499	315	121	39	
15	39	68	200	395	573	705	778	788	729	606	436	234	52	
30	39	68	100	304	503	667	777	827	805	710	556	348	121	
45	39	68	84	229	445	634	777	860	872	805	667	456	188	
60	39	68	84	178	402	610	776	886	925	882	760	549	247	
75	39	68	84	152	379	594	774	903	962	938	830	622	295	
90	39	68	84	155	376	590	773	910	980	968	872	669	328	
105	39	68	84	185	393	596	772	905	977	971	882	687	345	
120	39	68	84	241	430	613	771	890	953	945	861	675	344	
135	39	68	165	318	484	639	770	865	911	894	810	634	325	
150	42	145	275	413	551	673	769	833	853	819	731	567	289	
165	111	259	395	517	626	712	768	795	783	728	631	478	239	
180	178	373	517	624	705	753	768	753	705	624	517	373	178	
-165	239	478	631	728	783	795	768	712	626	517	395	259	111	
-150	289	567	731	819	853	833	769	673	551	413	275	145	42	
-135	325	634	810	894	911	865	770	639	484	318	165	68	39	
-120	344	675	861	945	953	890	771	613	430	241	84	68	39	
-105	345	687	882	971	977	905	772	596	393	185	84	68	39	
-90	328	669	872	968	980	910	773	590	376	155	84	68	39	
-75	295	622	830	938	962	903	774	594	379	152	84	68	39	
-60	247	549	760	882	925	886	776	610	402	178	84	68	39	
-45	188	456	667	805	872	860	777	634	445	229	84	68	39	
-30	121	348	556	710	805	827	777	667	503	304	100	68	39	
-15	52	234	436	606	729	788	778	705	573	395	200	68	39	
R10	140	297	421	539	651	720	743	720	651	540	421	298	140	483
0	41	149	354	547	704	804	837	804	704	547	354	149	41	
15	41	71	250	453	634	767	837	842	776	644	465	252	60	
30	41	71	159	370	570	732	837	877	845	739	574	356	123	
45	41	71	88	302	518	702	836	908	906	825	674	454	183	
60	41	71	87	255	479	680	835	932	955	895	759	539	237	
75	41	71	87	232	458	666	834	947	988	946	823	605	280	
90	41	71	87	234	455	662	833	953	1004	974	861	647	311	
105	41	71	87	262	471	668	832	949	1001	976	870	664	326	
120	41	71	133	312	504	683	831	935	980	953	851	653	325	
135	41	74	218	383	553	707	830	913	941	906	804	616	307	
150	51	171	319	469	614	738	829	883	889	838	733	555	275	
165	113	275	428	563	683	773	829	848	825	755	642	474	230	
180	175	379	538	661	755	811	828	811	755	661	538	379	175	
-165	230	474	642	755	825	848	829	773	683	563	428	275	113	
-150	275	555	733	838	889	883	829	738	614	469	319	171	51	
-135	307	616	804	906	941	913	830	707	553	383	218	74	41	
-120	325	653	851	953	980	935	831	683	504	312	133	71	41	
-105	326	664	870	976	1001	949	832	668	471	262	87	71	41	
-90	311	647	861	974	1004	953	833	662	455	234	87	71	41	
-75	280	605	823	946	988	947	834	666	458	232	87	71	41	
-60	237	539	759	895	955	932	835	680	479	255	87	71	41	
-45	183	454	674	825	906	908	836	702	518	302	88	71	41	
-30	123	356	574	739	845	877	837	732	570	370	159	71	41	
-15	60	252	465	644	776	842	837	767	634	453	250	71	41	
R11	142	310	454	604	730	808	833	808	730	604	454	310	142	533
0	42	177	392	591	754	857	891	857	754	591	392	177	42	
15	42	92	299	507	691	823	890	890	818	678	490	269	67	
30	42	73	218	433	634	792	890	922	879	763	588	362	123	
45	42	73	154	373	587	766	889	949	934	839	677	449	177	
60	42	73	112	331	553	746	889	970	977	902	753	525	225	
75	42	73	95	310	534	734	888	984	1007	948	810	583	264	
90	42	73	104	312	531	730	887	989	1021	972	844	622	291	
105	42	73	138	337	545	735	886	985	1019	974	852	636	305	

120	42	73	195	382	575	749	885	973	1000	953	835	627	304	
135	42	110	270	445	619	770	884	953	965	911	793	594	288	
150	59	197	360	521	673	797	883	927	918	851	730	539	259	
165	115	290	457	606	734	829	883	896	861	777	649	467	219	
180	169	382	556	693	799	862	883	862	799	693	556	382	169	
-165	219	467	649	777	861	896	883	829	734	606	457	290	115	
-150	259	539	730	851	918	927	883	797	673	521	360	197	59	
-135	288	594	793	911	965	953	884	770	619	445	270	110	42	
-120	304	627	835	953	1000	973	885	749	575	382	195	73	42	
-105	305	636	852	974	1019	985	886	735	545	337	138	73	42	
-90	291	622	844	972	1021	989	887	730	531	312	104	73	42	
-75	264	583	810	948	1007	984	888	734	534	310	95	73	42	
-60	225	525	753	902	977	970	889	746	553	331	112	73	42	
-45	177	449	677	839	934	949	889	766	587	373	154	73	42	
-30	123	362	588	763	879	922	890	792	634	433	218	73	42	
-15	67	269	490	678	818	890	890	823	691	507	299	92	42	
R12	137	310	474	642	776	860	887	860	776	642	474	310	137	560
0	43	204	427	631	798	903	937	903	798	631	427	204	43	
15	43	130	346	558	743	874	937	932	854	707	512	284	74	
30	43	75	275	494	694	847	937	960	907	781	597	365	123	
45	43	75	220	441	653	824	936	984	955	848	675	441	170	
60	43	75	183	405	623	806	936	1002	993	903	742	507	212	
75	43	75	168	387	606	796	935	1014	1019	942	791	558	246	
90	43	75	176	388	604	792	934	1018	1031	963	820	591	269	
105	43	75	205	410	616	797	933	1015	1029	965	828	604	281	
120	43	79	255	449	642	809	932	1005	1012	947	813	596	280	
135	43	145	321	504	680	827	932	987	982	911	777	567	267	
150	67	221	399	571	728	851	931	964	941	858	721	519	241	
165	116	302	484	644	781	879	931	937	892	793	651	456	206	
180	163	382	570	720	837	908	931	908	837	720	570	382	163	
-165	206	456	651	793	892	937	931	879	781	644	484	302	116	
-150	241	519	721	858	941	964	931	851	728	571	399	221	67	
-135	267	567	777	911	982	987	932	827	680	504	321	145	43	
-120	280	596	813	947	1012	1005	932	809	642	449	255	79	43	
-105	281	604	828	965	1029	1015	933	797	616	410	205	75	43	
-90	269	591	820	963	1031	1018	934	792	604	388	176	75	43	
-75	246	558	791	942	1019	1014	935	796	606	387	168	75	43	
-60	212	507	742	903	993	1002	936	806	623	405	183	75	43	
-45	170	441	675	848	955	984	936	824	653	441	220	75	43	
-30	123	365	597	781	907	960	937	847	694	494	275	75	43	
-15	74	284	512	707	854	932	937	874	743	558	346	130	43	
R13	131	308	498	676	818	905	934	905	818	676	498	308	131	585
0	44	230	458	667	836	943	978	943	836	667	458	230	44	
15	44	167	390	606	790	918	978	968	884	731	531	297	80	
30	44	114	330	551	748	895	977	991	929	794	603	366	122	
45	44	76	283	506	714	876	977	1011	969	850	669	430	162	
60	44	76	253	475	688	861	976	1027	1001	897	725	486	197	
75	44	76	240	460	674	852	976	1037	1023	930	767	529	226	
90	44	76	246	462	672	849	975	1040	1033	948	791	557	246	
105	44	81	271	480	683	853	974	1038	1032	949	798	568	256	
120	44	124	313	513	705	863	973	1029	1017	934	785	561	255	
135	44	180	369	559	737	879	973	1014	992	903	754	536	243	
150	75	244	435	616	777	899	972	995	957	859	708	496	222	
165	116	312	507	678	822	922	972	972	916	804	648	443	192	
180	156	380	579	742	869	947	972	947	869	742	579	380	156	
-165	192	443	648	804	916	972	972	922	822	678	507	312	116	
-150	222	496	708	859	957	995	972	899	777	616	435	244	75	
-135	243	536	754	903	992	1014	973	879	737	559	369	180	44	
-120	255	561	785	934	1017	1029	973	863	705	513	313	124	44	
-105	256	568	798	949	1032	1038	974	853	683	480	271	81	44	
-90	246	557	791	948	1033	1040	975	849	672	462	246	76	44	
-75	226	529	767	930	1023	1037	976	852	674	460	240	76	44	
-60	197	486	725	897	1001	1027	976	861	688	475	253	76	44	
-45	162	430	669	850	969	1011	977	876	714	506	283	76	44	
-30	122	366	603	794	929	991	977	895	748	551	330	114	44	
-15	80	297	531	731	884	968	978	918	790	606	390	167	44	
R14	125	309	519	705	853	945	975	945	853	705	519	309	125	606
0	54	254	487	698	869	976	1011	976	869	698	487	254	54	
15	45	203	432	649	832	956	1011	996	907	750	546	309	87	
30	45	160	384	604	798	937	1011	1015	944	801	604	364	120	
45	45	127	346	568	770	922	1010	1031	976	846	658	416	152	
60	45	107	321	543	749	910	1010	1044	1002	884	703	461	181	

75	45	102	311	531	738	902	1009	1052	1020	911	737	496	204	
90	45	111	316	532	736	900	1009	1055	1028	926	757	519	220	
105	45	133	336	547	745	903	1008	1053	1027	927	762	528	228	
120	45	168	370	574	762	912	1007	1045	1015	914	752	522	228	
135	50	213	415	611	788	924	1007	1033	995	889	727	502	218	
150	82	265	468	657	821	940	1007	1018	967	854	689	469	201	
165	115	321	526	707	857	959	1006	999	933	809	641	426	177	
180	148	376	585	759	896	979	1006	979	896	759	585	376	148	
-165	177	426	641	809	933	999	1006	959	857	707	526	321	115	
-150	201	469	689	854	967	1018	1007	940	821	657	468	265	82	
-135	218	502	727	889	995	1033	1007	924	788	611	415	213	50	
-120	228	522	752	914	1015	1045	1007	912	762	574	370	168	45	
-105	228	528	762	927	1027	1053	1008	903	745	547	336	133	45	
-90	220	519	757	926	1028	1055	1009	900	736	532	316	111	45	
-75	204	496	737	911	1020	1052	1009	902	738	531	311	102	45	
-60	181	461	703	884	1002	1044	1010	910	749	543	321	107	45	
-45	152	416	658	846	976	1031	1010	922	770	568	346	127	45	
-30	120	364	604	801	944	1015	1011	937	798	604	384	160	45	
-15	87	309	546	750	907	996	1011	956	832	649	432	203	45	
R15	118	315	536	729	882	978	1009	978	882	729	536	315	118	625
0	68	276	513	725	895	1002	1037	1002	895	725	513	276	68	
15	46	238	471	687	867	987	1037	1017	924	764	557	318	92	
30	45	205	434	653	841	973	1037	1031	952	802	601	360	118	
45	45	181	406	626	820	961	1036	1044	976	837	642	399	142	
60	45	166	387	607	805	952	1036	1053	996	865	676	433	164	
75	45	161	379	598	796	946	1036	1059	1010	886	701	460	181	
90	45	168	383	599	795	945	1035	1062	1016	897	717	477	193	
105	45	185	398	610	801	947	1035	1060	1015	897	721	483	200	
120	45	212	424	630	815	953	1034	1055	1006	888	713	479	199	
135	64	246	458	659	834	963	1034	1046	991	869	694	464	192	
150	89	285	498	693	859	975	1034	1034	969	842	665	439	179	
165	114	327	542	731	887	989	1033	1020	944	808	629	407	161	
180	139	368	587	771	915	1005	1033	1005	915	771	587	368	139	
-165	161	407	629	808	944	1020	1033	989	887	731	542	327	114	
-150	179	439	665	842	969	1034	1034	975	859	693	498	285	89	
-135	192	464	694	869	991	1046	1034	963	834	659	458	246	64	
-120	199	479	713	888	1006	1055	1034	953	815	630	424	212	45	
-105	200	483	721	897	1015	1060	1035	947	801	610	398	185	45	
-90	193	477	717	897	1016	1062	1035	945	795	599	383	168	45	
-75	181	460	701	886	1010	1059	1036	946	796	598	379	161	45	
-60	164	433	676	865	996	1053	1036	952	805	607	387	166	45	
-45	142	399	642	837	976	1044	1036	961	820	626	406	181	45	
-30	118	360	601	802	952	1031	1037	973	841	653	434	205	45	
-15	92	318	557	764	924	1017	1037	987	867	687	471	238	46	
R16	111	322	550	748	905	1003	1035	1003	905	748	550	322	111	640
0	81	297	535	746	915	1021	1055	1021	915	746	535	297	81	
15	66	271	507	720	896	1011	1055	1031	935	772	565	325	97	
30	54	249	482	698	879	1001	1055	1041	953	798	594	353	114	
45	46	233	463	680	865	993	1055	1049	970	821	621	379	131	
60	46	223	450	667	854	987	1055	1055	983	840	644	402	145	
75	46	220	445	661	849	984	1055	1059	992	854	661	420	157	
90	46	224	448	661	848	983	1054	1061	996	861	672	431	165	
105	52	236	458	669	852	984	1054	1060	995	862	674	436	169	
120	64	254	475	682	861	988	1054	1056	990	855	669	433	169	
135	79	276	498	702	874	995	1053	1050	979	843	656	423	164	
150	95	303	525	725	891	1003	1053	1042	965	825	637	406	156	
165	112	331	555	750	909	1012	1053	1033	948	802	613	385	143	
180	128	359	584	777	929	1023	1053	1023	929	777	584	359	128	
-165	143	385	613	802	948	1033	1053	1012	909	750	555	331	112	
-150	156	406	637	825	965	1042	1053	1003	891	725	525	303	95	
-135	164	423	656	843	979	1050	1053	995	874	702	498	276	79	
-120	169	433	669	855	990	1056	1054	988	861	682	475	254	64	
-105	169	436	674	862	995	1060	1054	984	852	669	458	236	52	
-90	165	431	672	861	996	1061	1054	983	848	661	448	224	46	
-75	157	420	661	854	992	1059	1055	984	849	661	445	220	46	
-60	145	402	644	840	983	1055	1055	987	854	667	450	223	46	
-45	131	379	621	821	970	1049	1055	993	865	680	463	233	46	
-30	114	353	594	798	953	1041	1055	1001	879	698	482	249	54	
-15	97	325	565	772	935	1031	1055	1011	896	720	507	271	66	
R17	105	328	560	761	922	1022	1054	1022	922	761	560	328	105	650
0	94	316	553	762	929	1033	1066	1033	929	762	553	316	94	
15	86	303	539	749	919	1027	1066	1038	938	775	568	330	102	

30	80	292	527	738	910	1023	1066	1042	948	788	583	344	110	
45	76	283	517	729	903	1019	1066	1047	956	799	596	357	119	
60	73	278	511	722	898	1016	1066	1050	963	809	608	368	126	
75	73	277	508	719	895	1014	1066	1052	967	816	617	377	132	
90	73	277	508	719	895	1014	1066	1052	967	816	617	377	132	
105	79	285	514	723	897	1014	1066	1052	969	820	623	385	138	
120	85	294	523	730	901	1016	1066	1050	966	817	620	384	138	
135	93	305	535	739	908	1019	1065	1047	961	810	614	379	136	
150	101	319	548	751	916	1023	1065	1043	954	801	604	371	131	
165	109	333	563	764	926	1028	1065	1038	945	790	592	360	125	
180	118	347	578	777	935	1033	1065	1033	935	777	578	347	118	
-165	125	360	592	790	945	1038	1065	1028	926	764	563	333	109	
-150	131	371	604	801	954	1043	1065	1023	916	751	548	319	101	
-135	136	379	614	810	961	1047	1065	1019	908	739	535	305	93	
-120	138	384	620	817	966	1050	1066	1016	901	730	523	294	85	
-105	131	371	604	801	954	1043	1065	1023	916	751	548	319	101	
-90	136	383	622	820	969	1053	1066	1013	895	719	509	279	75	
-75	132	377	617	816	967	1052	1066	1014	895	719	508	277	73	
-60	126	368	608	809	963	1050	1066	1016	898	722	511	278	73	
-45	119	357	596	799	956	1047	1066	1019	903	729	517	283	76	
-30	110	344	583	788	948	1042	1066	1023	910	738	527	292	80	
-15	102	330	568	775	938	1038	1066	1027	919	749	539	303	86	
R18	105	331	565	769	931	1033	1066	1033	933	770	567	332	106	657

Tables (A-2) – (A-9) display the generated results of $I_{(HTCS)}$ on Vaulted Roofs (37- Planar-segments)
 (The 19- planar- Segments tables are not included in this Appendix)



(ASWAN 23.58°N) (N-S) JUNE




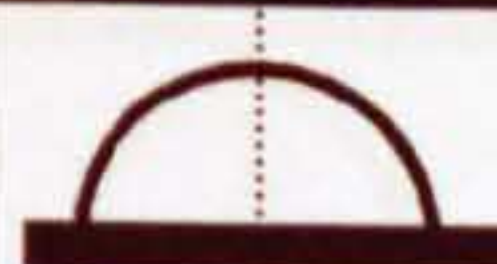


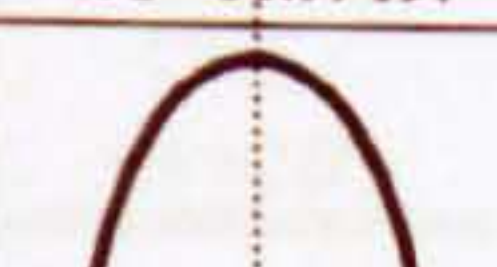
CCSR ₍₃₇₎		Solar Radiation Intensity W/m ²														C/H %
		06:00	07:00	08:00	09:00	10:00	11:00	12:00	13:00	14:00	15:00	16:00	17:00	18:00	Day Av.	
A < B	Flat Roof	106	332	567	772	935	1037	<u>1070</u>	1037	935	772	567	332	106	659	100
	 CCS4 (A=0.5B)	105	301	505	685	828	918	<u>947</u>	918	828	685	505	301	105	587	89.1
	 CCS3 (A=0.6B)	104	287	477	643	778	861	<u>888</u>	861	778	643	477	287	104	553	83.9
	 CCS2 (A=0.8B)	104	267	435	583	703	778	<u>803</u>	778	703	583	435	267	104	503	76.4
A = B	 CCS1 (A=B)	105	246	389	517	622	687	<u>709</u>	687	622	517	389	246	105	449	68.2
A > B	 CCS5 (A=1.25B)	104	225	342	447	534	589	<u>607</u>	589	534	447	342	225	104	391	59.4
	 CCS6 (A=1.67B)	103	202	285	361	426	470	<u>484</u>	470	426	361	285	202	103	321	48.8
	 CCS7 (A=2B)	101	189	254	310	363	398	<u>410</u>	398	363	310	254	189	101	280	42.4

Table (A-2)



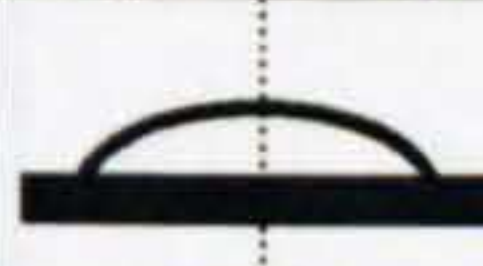




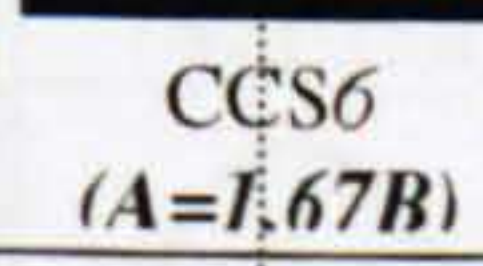
CCSR ₍₃₇₎		Solar Radiation Intensity W/m ²													C/H %	
		06:00	07:00	08:00	09:00	10:00	11:00	12:00	13:00	14:00	15:00	16:00	17:00	18:00		Day Av.
A < B	 Flat Roof	0	40	224	434	600	704	<u>740</u>	704	600	434	224	40	0	365	100
	 CCS4 (A=0.5B)	0	46	220	408	556	648	<u>680</u>	648	556	408	220	46	0	341	93.4
	 CCS3 (A=0.6B)	0	48	218	398	537	624	<u>654</u>	624	537	398	218	48	0	331	90.7
	 CCS2 (A=0.8B)	0	51	218	385	511	591	<u>618</u>	591	511	385	218	51	0	318	87.1
A = B	 CCS1 (A=B)	0	53	218	374	489	561	<u>585</u>	561	489	374	218	53	0	306	83.8
A > B	 CCS5 (A=1.25B)	0	55	217	362	466	531	<u>553</u>	531	466	362	217	55	0	293	80.3
	 CCS6 (A=1.67B)	0	56	215	348	441	498	<u>516</u>	498	441	348	215	56	0	279	76.5
	 CCS7 (A=2B)	0	56	212	338	425	477	<u>495</u>	477	425	338	212	56	0	270	74

Table (A-3)





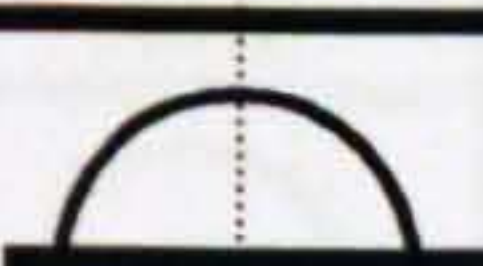
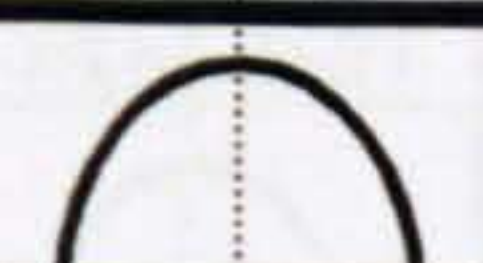
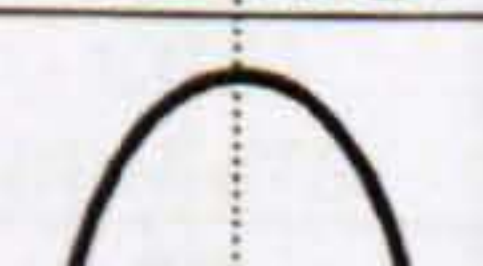
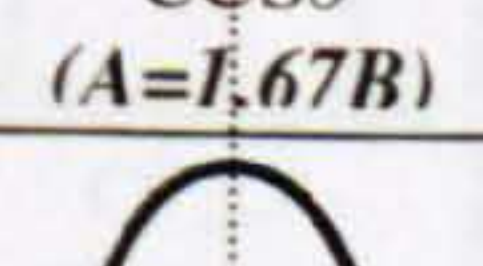
CCSR ₍₃₇₎		Solar Radiation Intensity W/m ²														C/H %
		06:00	07:00	08:00	09:00	10:00	11:00	12:00	13:00	14:00	15:00	16:00	17:00	18:00	Day Av.	
		106	332	567	772	935	1037	<u>1070</u>	1037	935	772	567	332	106	659	100
A < B	 CCS4 (A=0.5B)	132	336	532	701	834	918	<u>947</u>	918	834	701	532	336	132	604	91.7
	 CCS3 (A=0.6B)	143	339	519	670	790	864	<u>888</u>	864	790	670	519	339	143	580	88
	 CCS2 (A=0.8B)	157	345	501	626	724	783	<u>803</u>	783	724	626	501	345	157	544	82.6
A = B	 CCS1 (A=B)	168	352	486	583	654	696	<u>710</u>	696	654	583	486	352	168	507	76.9
A > B	 CCS5 (A=1.25B)	178	356	476	541	585	604	<u>609</u>	604	585	541	476	356	178	467	70.9
	 CCS6 (A=1.67B)	187	359	452	493	503	<u>492</u>	483	<u>492</u>	503	493	452	359	187	419	63.6
	 CCS7 (A=2B)	190	358	440	467	459	<u>430</u>	410	<u>430</u>	459	467	440	358	190	392	59.5

Table (A-4)









CCSR ₍₃₇₎		Solar Radiation Intensity W/m ²														C/H %
		06:00	07:00	08:00	09:00	10:00	11:00	12:00	13:00	14:00	15:00	16:00	17:00	18:00	Day Av.	
A < B	 Flat Roof	0	40	224	434	600	704	<u>740</u>	704	600	434	224	40	0	365	100
	 CCS4 (A=0.5B)	0	59	237	410	544	627	<u>657</u>	627	544	410	237	59	0	339	93
	 CCS3 (A=0.6B)	0	65	242	401	519	592	<u>617</u>	592	519	401	242	65	0	327	89.7
	 CCS2 (A=0.8B)	0	72	252	389	483	540	<u>559</u>	540	483	389	252	72	0	310	85
A = B	 CCS1 (A=B)	0	78	261	380	448	484	<u>496</u>	484	448	380	261	78	0	292	80.1
A > B	 CCS5 (A=1.25B)	0	83	268	370	414	427	<u>428</u>	427	414	370	268	83	0	273	74.8
	 CCS6 (A=1.67B)	0	89	274	357	374	358	<u>344</u>	358	374	357	274	89	0	250	68.5
	 CCS7 (A=2B)	0	91	275	349	352	320	<u>293</u>	320	352	349	275	91	0	236	64.7

Table (A-5)

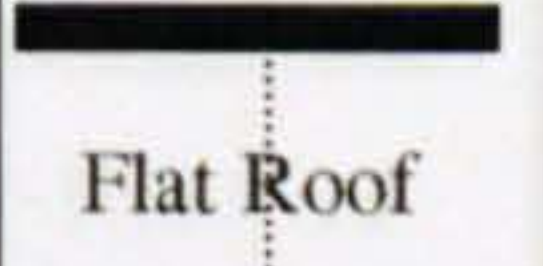


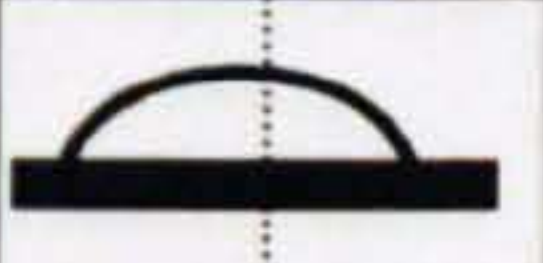

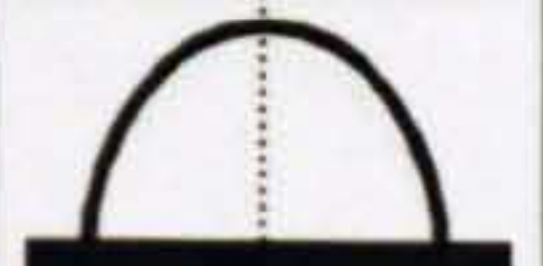

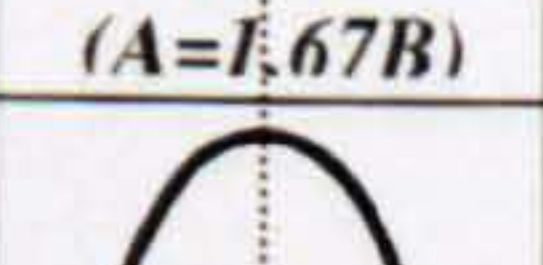
CCSR ₍₃₇₎		Solar Radiation Intensity W/m ²														C/H %
		06:00	07:00	08:00	09:00	10:00	11:00	12:00	13:00	14:00	15:00	16:00	17:00	18:00	Day Av.	
A < B	 Flat Roof	106	332	567	772	935	1037	<u>1070</u>	1037	935	772	567	332	106	659	100
	 CCS4 (A=0.5B)	106	308	513	689	831	918	<u>947</u>	918	832	696	526	331	131	596	90.4
	 CCS3 (A=0.6B)	106	298	489	654	783	862	<u>888</u>	862	785	661	509	331	142	567	86
	 CCS2 (A=0.8B)	107	284	455	599	712	780	<u>803</u>	780	716	612	485	334	155	525	79.7
A = B	 CCS1 (A=B)	108	271	420	542	636	691	<u>709</u>	691	642	562	456	338	166	480	72.9
A > B	 CCS5 (A=1.25B)	108	258	386	485	557	597	<u>609</u>	598	566	513	443	338	176	433	65.7
	 CCS6 (A=1.67B)	108	243	347	417	462	480	<u>484</u>	481	476	457	419	340	185	377	57.2
	 CCS7 (A=2B)	107	234	326	381	409	414	411	417	<u>428</u>	427	404	338	188	345	52.3

Table (A-6)




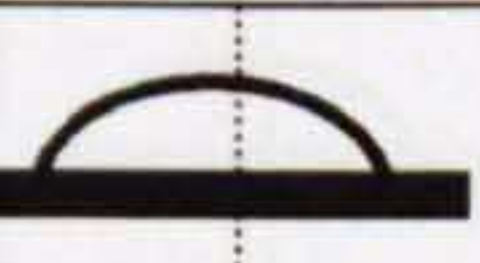
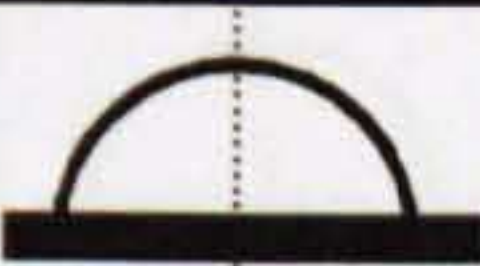


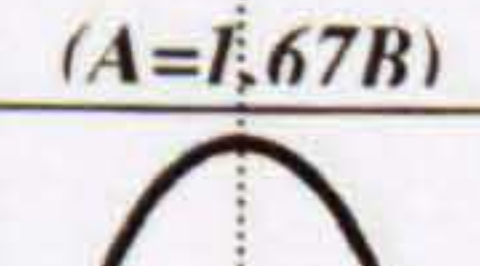
CCSR ₍₃₇₎		Solar Radiation Intensity W/m ²													C/H %	
		06:00	07:00	08:00	09:00	10:00	11:00	12:00	13:00	14:00	15:00	16:00	17:00	18:00		Day Av.
A < B	 Flat Roof	0	40	224	434	600	704	<u>740</u>	704	600	434	224	40	0	365	100
	 CCS4 (A=0.5B)	0	60	247	428	563	646	<u>668</u>	628	543	387	203	42	0	339	92.9
	 CCS3 (A=0.6B)	0	67	258	427	549	621	<u>636</u>	599	503	365	194	43	0	328	89.8
	 CCS2 (A=0.8B)	0	75	274	429	531	585	<u>590</u>	545	459	332	180	44	0	311	85.2
A = B	 CCS1 (A=B)	0	82	287	431	516	553	<u>545</u>	494	410	296	166	45	0	294	80.6
A > B	 CCS5 (A=1.25B)	0	87	297	432	501	<u>520</u>	500	443	359	258	165	45	0	278	76.2
	 CCS6 (A=1.67B)	0	93	309	431	482	<u>484</u>	448	382	297	210	136	46	0	255	69.9
	 CCS7 (A=2B)	0	95	312	426	<u>470</u>	463	420	349	263	182	127	45	0	242	66.4

Table (A-7)

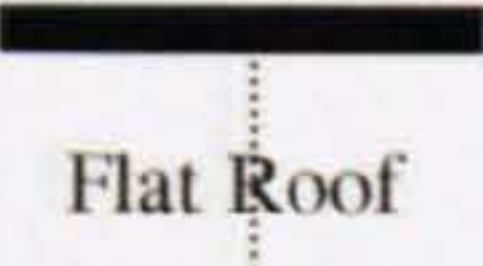


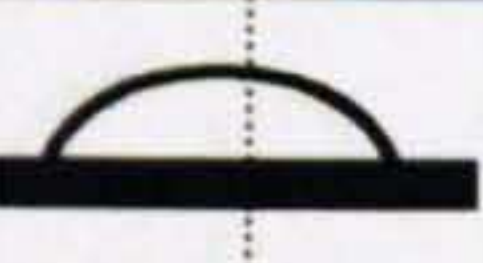
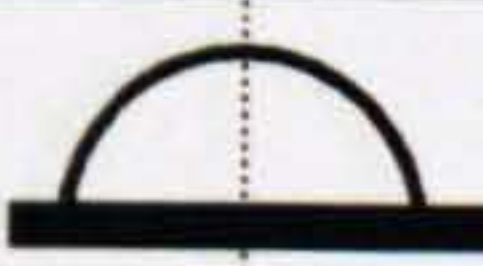

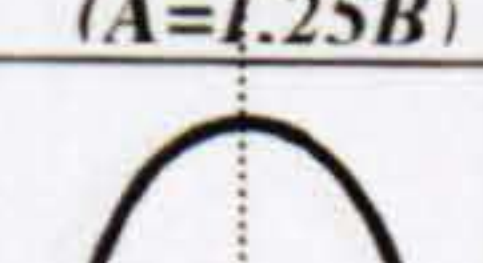
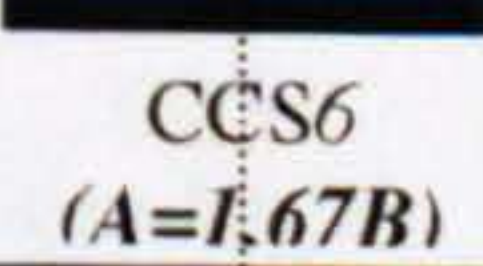
CCSR ₍₃₇₎		Solar Radiation Intensity W/m ²														C/H %
		06:00	07:00	08:00	09:00	10:00	11:00	12:00	13:00	14:00	15:00	16:00	17:00	18:00	Day Av.	
	 Flat Roof	106	332	567	772	935	1037	1070	1037	935	772	567	332	106	659	100
A < B	 CCS4 (A=0.5B)	131	331	526	696	832	918	947	918	830	690	513	308	106	596	90.4
	 CCS3 (A=0.6B)	142	330	509	661	785	862	888	862	783	655	488	298	106	567	86
	 CCS2 (A=0.8B)	155	334	485	612	716	781	803	780	712	599	455	284	107	525	79.6
A = B	 CCS1 (A=B)	166	338	464	562	642	689	709	694	636	542	420	271	108	480	72.8
A > B	 CCS5 (A=1.25B)	176	339	443	513	566	598	609	597	557	485	386	258	108	434	65.8
	 CCS6 (A=1.67B)	185	340	419	457	476	481	484	480	462	417	347	243	108	377	57.2
	 CCS7 (A=2B)	188	338	405	417	427	416	409	414	410	381	326	234	107	344	52.2

Table (A-8)

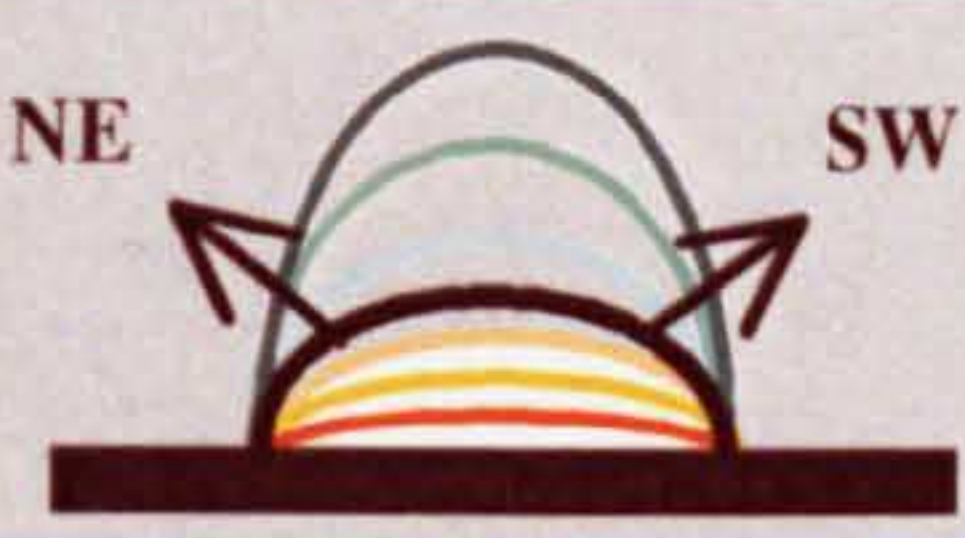




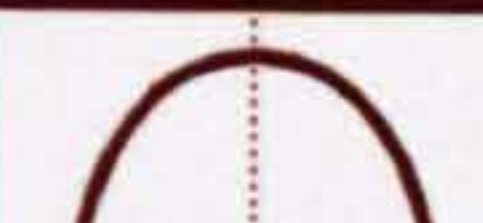

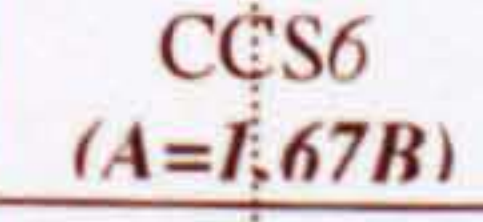
 (ASWAN 23.58°N) (NE-SW) DECEMBER																
CCSR ₍₃₇₎	Solar Radiation Intensity W/m ²														C/H %	
	06:00	07:00	08:00	09:00	10:00	11:00	12:00	13:00	14:00	15:00	16:00	17:00	18:00	Day Av.		
Flat Roof	0	40	224	434	600	704	<u>740</u>	704	600	434	224	40	0	365	100	
A < B	 CCS4 (A=0.5B)	0	42	203	387	534	629	<u>668</u>	645	562	428	247	60	0	339	92.9
	 CCS3 (A=0.6B)	0	43	194	365	503	595	<u>636</u>	621	549	427	258	67	0	328	89.8
	 CCS2 (A=0.8B)	0	44	180	332	459	547	<u>591</u>	585	531	429	274	75	0	311	85.3
A = B	 CCS1 (A=B)	0	45	166	296	410	495	<u>545</u>	553	516	431	287	82	0	294	80.6
A > B	 CCS5 (A=1.25B)	0	45	153	258	359	443	500	<u>520</u>	501	432	299	87	0	277	75.8
	 CCS6 (A=1.67B)	0	46	136	210	297	382	448	<u>484</u>	482	431	308	93	0	255	69.9
	 CCS7 (A=2B)	0	45	127	182	263	349	420	463	<u>470</u>	427	312	96	0	243	66.5

Table (A-9)

APPENDIX: B

Integrated Environmental Solutions IES

(Virtual Environment VE. (VE. 4.0 & 4.1))

This appendix reviews some information about the Integrated Environmental Solutions *IES* (VE Version 4.0 & 4.1)[4].

“The **Virtual Environment-VE 4.1** is an integrated suite of applications linked by a Common User Interface (CUI) and a single Integrated Data Model (IDM). This means that all the applications have a consistent “look and feel” and that data input for one application can be used by the others. It has number of modules such as “**Apache-sim**”[4] for thermal simulation, “**Radiance**”[3] for lighting simulation, and “**SunCast**”[4] for solar shading analysis. “**ModelIT**”[4] is the application used for input of 3D geometry used to describe the model”.

The appendix also review some slides of the *APACHE* and the *SUNCAST* solar investigations, which have been used to find out the exposed and the self-shaded areas and ratios on three dome curvatures (*Shade-analysis study in Chapter 8*). On each dome geometry, day no. 15 at each month has been chosen to represents each month throughout the year, figure B.1a. (*any other day can be chosen*). Figure B.1b shows the shade analysis outputs for one segment (*segment no. 597*), where the dome geometry is composed of 600 segments to find out the exposed and the self-shaded patterns. Each dome has been resembled into 100 segments to calculate the self-shaded and the exposed area ratios and number of segments.

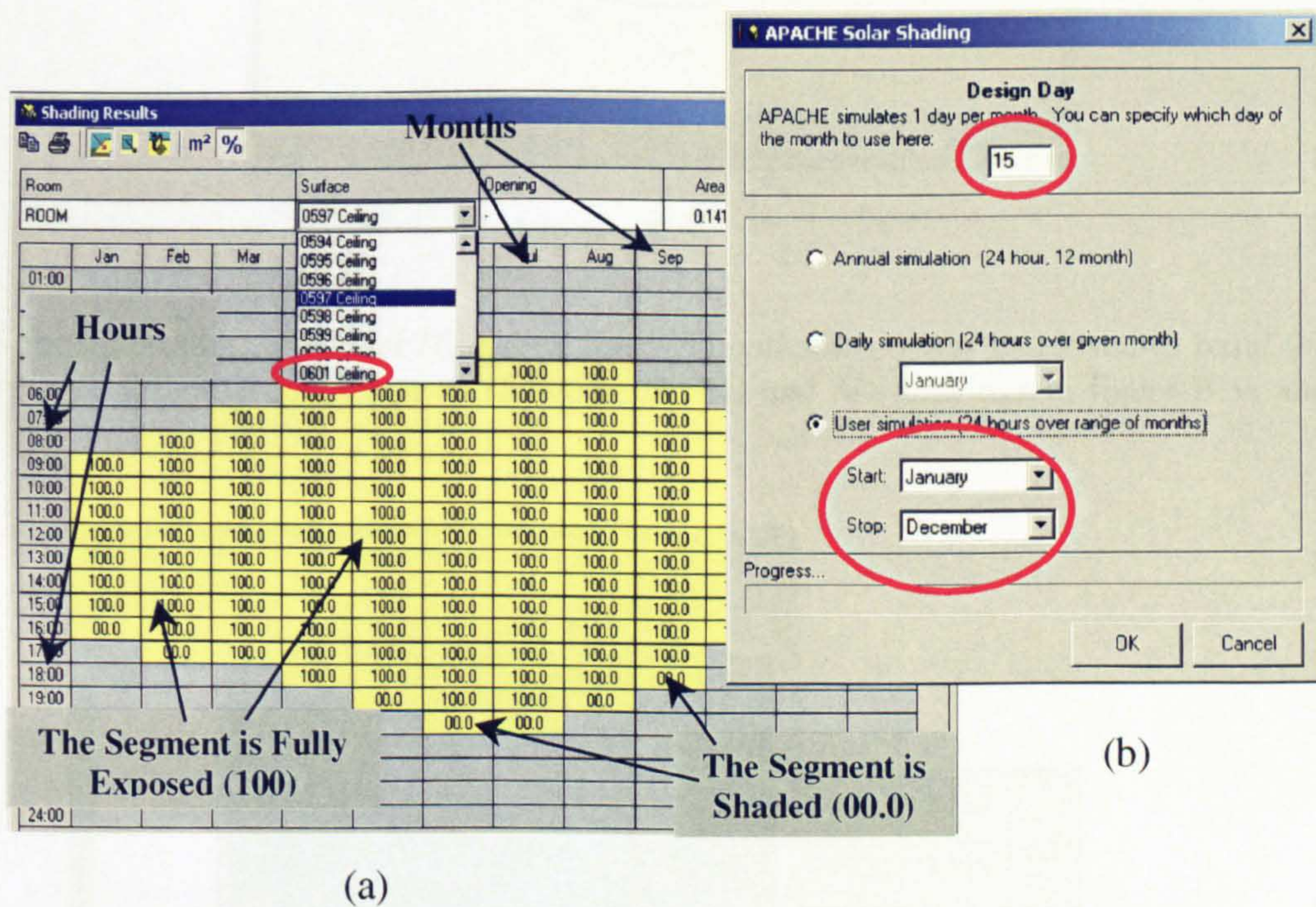


Figure B-1



The IES also includes a Sunpath application, which can generate sunpath diagram for particular geographical latitude, figure B.2.

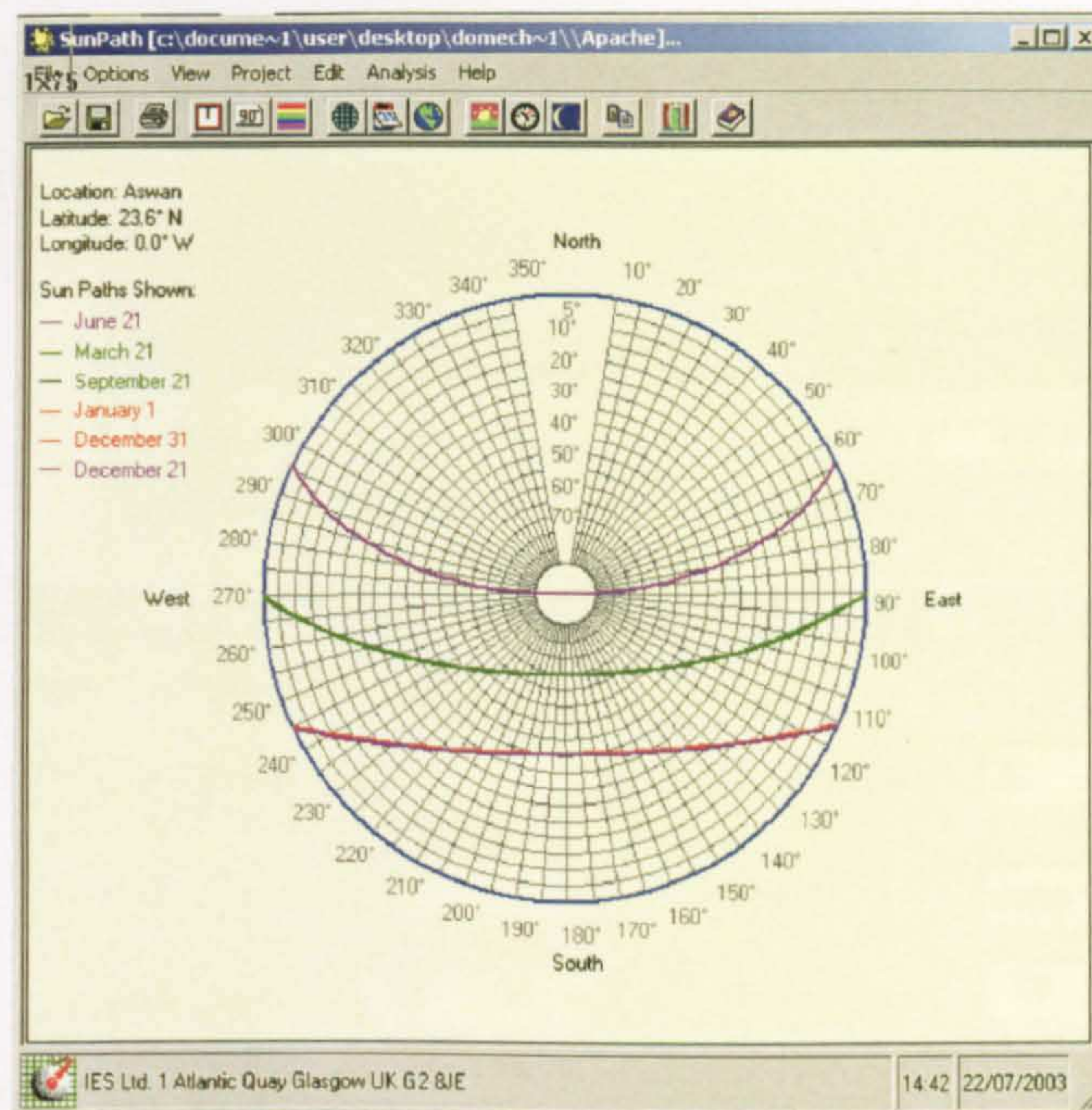


Figure B-2

The IES model builder or (*Model IT, one of the IES applications*) was employed to build the geometry with different curvatures as shown in the 2D and 3D drawings in figure B.3a and B.3b.

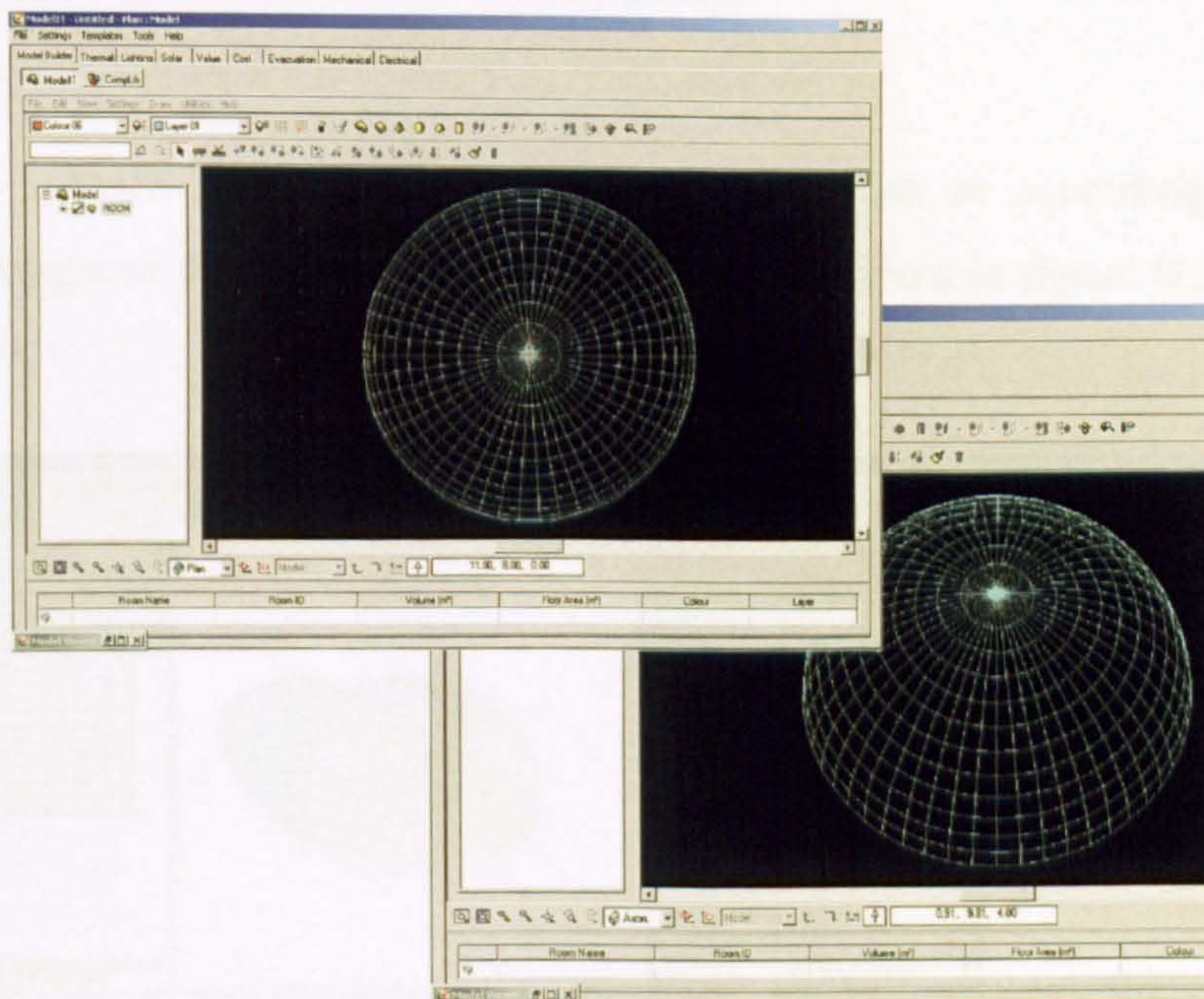


Figure B-3

For hourly images by the *SUNCAST* application, the start and the finish time for creating images have to be identified. The interval of creating images throughout the

day has been identified every 60 minutes. As figure B.4 depicts, the Eye Azimuth and Eye Altitude control the generated-image view angles (*plan or 3D view*).

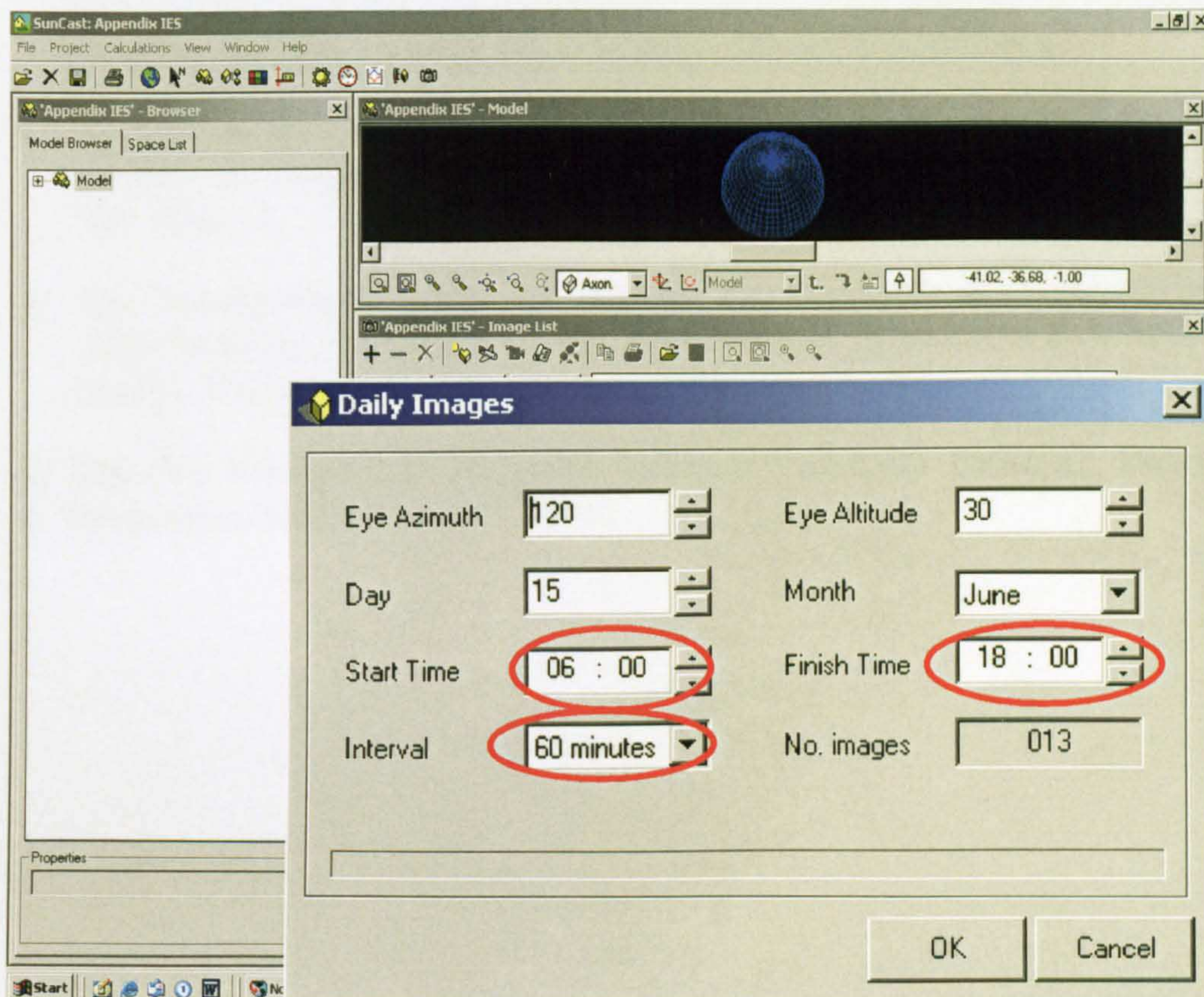


Figure B.4

The hourly images have been generated for each hour or according to the chosen interval throughout the day for a particular month as shown in figure B.5a & B.5b.

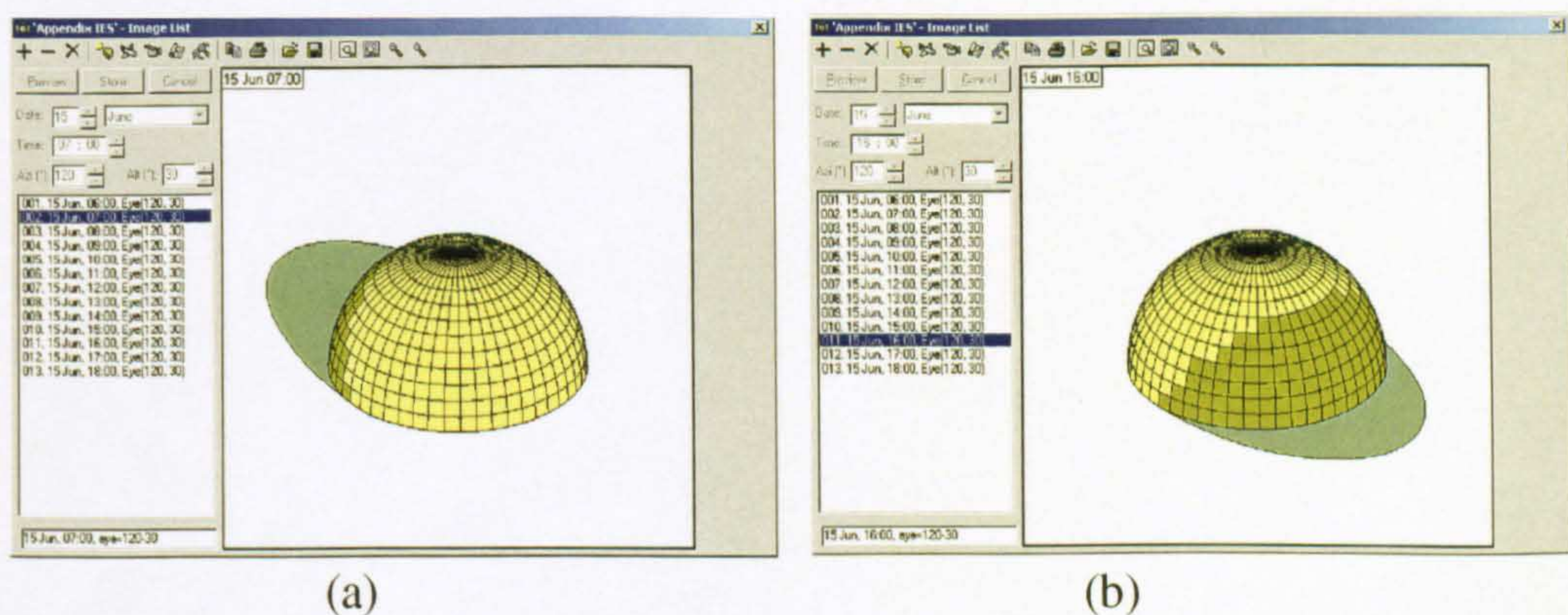


Figure B.5

Reference List

1. **"SRSM" Solar Radiation Simulation Model for Quick Basic**, Exell, R. H. B. Regional Energy Resources Information Centre, Asian Institute of Technology, Bangkok. <http://www.jgsee.kmutt.ac.th/exell/Solar/SolradJS.htm> .
2. **Exell, R. H. B.** A program in BASIC for calculating solar radiation in tropical climates on small computers. *Renewable Energy Review Journal*, 1986 Dec; Vol. 8(No. 2).
3. **The International American Agency for Development.** Solar Radiation Atlas for Egypt, Renewable Energy Authorisation - Ministry of Electricity and Energy, Cairo , 1990.
4. **IES (Ve Version 4.1)** [Licensed Software University Package]. Integrated Environmental Solutions Ltd. 2001.